SURVEILLANCE OF GROUNDWATER QUALITY IN RELATION TO GEOCHEMISTRY IN SELECTED DISTRICTS OF KERALA, WITH SPECIAL REFERENCE TO FLUORIDE AND ARSENIC CONTAMINATION

Thesis submitted to
The University of Calicut in partial fulfillment of
the requirement for the Degree of

DOCTOR OF PHILOSOPHY IN ENVIRONMENTAL SCIENCES

SHEEJA K. M.

DEPARTMENT OF BOTANY
DIVISION OF ENVIRONMENTAL SCIENCE
UNIVERSITY OF CALICUT
JULY, 2023

DECLARATION

I hereby declare that the thesis, titled **Surveillance of Groundwater Quality in Relation to Geochemistry in Selected Districts of Kerala, with Special Reference to Fluoride and Arsenic Contamination**, submitted to the University of Calicut in partial fulfillment of the requirements for the award of the Degree of Doctor of Philosophy in Environmental Sciences, is a record of original research work carried out by me under the guidance and supervision of Pro. (Dr.) C. C. Harilal, Professor, Division of Environmental Science, Department of Botany, University of Calicut, and the thesis has not formed the basis for the award of any Degree, Diploma, Fellowship, or any other similar title, to any candidate in any University. It is also affirmed that all corrections and modifications suggested by the adjudicators have been fully incorporated into the thesis.

Calicut University Campus **Sheeja K.M**
Date :

UNIVERSITY OF CALICUT
DEPARTMENT OF BOTANY
Division of Environmental Science
P.O. Calicut University, Malappuram District, Kerala – 673635
contact: 9447956226; ccharilal22@gmail.com

Dr. C.C. Harilal
Professor &
Dean, Faculty of Science

This is to certify that the thesis titled **Surveillance of Groundwater Quality in Relation to Geochemistry in Selected Districts of Kerala, with Special Reference to Fluoride and Arsenic Contamination**, submitted to the University of Calicut by Ms. Sheeja K.M., in partial fulfillment of the award of the Degree of Doctor of Philosophy in Environmental Sciences, is a bona-fide record of research work carried out by her under my guidance and supervision in the Division of Environmental Science, Department of Botany, University of Calicut.

No part of the present work has previously formed the basis for the award of any other Degree, Diploma, Fellowship, or similar title, to any candidate in any University. The modifications suggested by the Research Advisory Committee of the University of Calicut have been incorporated into the thesis. It is also affirmed that all corrections and modifications suggested by the adjudicators have been fully incorporated into the thesis.

Calicut University Campus
Date

C. C. Harilal
(Research Guide and Supervising Teacher)

ACKNOWLEDGEMENT

On the completion of this thesis work, I feel immense pleasure in expressing my deep sense of gratitude to my thesis supervisor, Prof. (Dr.) C.C. Harilal, Division of Environmental Science, Department of Botany, University of Calicut, for his precious supervision, inspiring guidance, excellent support, and constant encouragement. His positive criticism, constructive suggestions, and philosophical mentoring helped me complete this thesis. He has been an inspiring human being and an interactive teacher.

I express my thanks to Prof. (Dr.) Jos T. Puthur, Professor and Head, Department of Botany; Prof. (Dr.) V.V. Radhakrishnan; Prof. (Dr.) Santhosh Nampy; Dr. John E. Thoppil, Senior Professor; and Prof. (Dr.) M. Sabu former Heads for providing various facilities during the tenure of work.

I express my sincere thanks to former doctoral committee members Prof. (Dr.) K. V. Mohanan. Patron Department of Botany, Gregor Mendel Foundation, Calicut University, Prof. (Dr.) P. Manimohan, Mycology Division, Department of Botany, University of Calicut, and the present doctoral committee members for their corrections and suggestions.

Prof. (Dr.) A. Yusuf, Department of Botany and Director, Inter University Centre for Plant Biotechnology, University of Calicut, is greatly acknowledged for his timely help and providing lab facilities.

I wish to thank Dr. A. K. Pradeep, Assistant Professor; Dr. P. Sunojkumar, Associate Professor; Dr. Manju C. Nair, Associate Professor; Dr. C. Pramod, Assistant Professor; Dr. M. Shamina, Assistant Professor; Dr. L. Resmi, Assistant Professor; and Dr. K.P. Deepna Latha, Assistant Professor, for their support and suggestions.

My heartfelt thanks to the Director and staff of the Central Instrumentation Facility, University of Calicut, for their technical and instrumental assistance during my work.

I am indebted to my M.Phil. guide, Dr. A.A. Mohamed Hatha, Professor, School of Marine Sciences,Cochin University of Science and Technology, Cochin, and my teacher, Dr. E. V. Ramaswamy, Professor, Mahatma Gandhi University, Kottayam, for their suggestions and motivations.

I take this opportunity to express my deep sense of gratitude to Dr. K. V. Ajayan and Dr. Roni M., UGC-DSK Post-Doctoral Fellows, Division of Environmental Science, Department of Botany, University of Calicut, and Dr. Panneer Selvam, Assistant Professor, Department of Biology, Faculty of Science, University of Tabuk, Saudi Arabia, for the technical assistance and support rendered during the course of study.

Also, it is my pleasure to acknowledge the sincere advice, suggestions, and support extended by all my friends and lab mates. I really appreciate the support given by Dr. E. S. Hareesh, Ms. Jasmine P. J., Ms. Sashna N. C., Ms. Aparna Sreekumar, Ms. Jiji P. V., Ms. Swetha K., Ms. Naseefa P. K., Mr. Bassam Ahmed Mohammed Alghfori, Mr. Nandakumar M. K., and Ms. Snehaprabha M.

With a deep sense of gratitude, I express my faithfulness to my senior researchers, Dr. Hidayath R. M., Dr. Snisha S., Dr. Bindhumol G.P., Dr.Sajith U., Dr. Neethu G. Pillai, and Dr. Karthika S. Menon, for their constant support.

I wish to place on record my gratitude to Dr. P. S. Harikumar, Senior Principal Scientist (Rtd), and Dr. Madhavan Komath, Scientist (Rtd), CWRDM, Calicut, for their valuable guidance and technical support.

Thanks to Dr.Sreeja R., Assistant Professor, Department of Geology, University of Calicut for her precious suggestions and advice in mineralogical studies. I thank my colleagues, Dr. Rathy M. C., Dr. Shanti T. R., Ms. Shamili V. K., and Dr. Anju Jose, Assistant Professors, and the non-teaching staffs of Department of Environmental Science, for their friendly recommendations and support. I am grateful to all my students from the Department of Environmental Science.

My hearty thanks to the office staffs and Librarians Department of Botany, the University of Calicut, and the Department of Botany for their constant support and encouragement rendered for the successful completion of the thesis work.

Gratitude in all its forms goes to my Husband Mr. Arunkumar R. S., Amma, Vallyamma, Sister (Sheeba K M), and brother (Rajesh K M), who helped me during the sampling process and always stood by my side with constant support and emotional backing during all these years.

Special appreciation to my daughter Amiyaa and son Ayansh, their smiles filled me with much energy and inspiration during all my tough times. Though my Acha and father-in-law are no longer physically present in this world, I believe their blessings remain constantly with me. I am grateful to my Mother-in-law, Brother-in-laws, Sister-in-laws, Nieces and Nephews, and entire extended family for their unwavering support in helping me achieve everything that has transpired in my life to date.

My thanks to my friends Raseena Moolamgottu, Sarath G. Nair, Habeeb K. C., Jishin T. S., Lins Simon, Maya R., Jiji P., Santhosh Kumar, Jeomol, and all other friends from Botany Department for their timely help with my research work are greatly acknowledged.

All of my friends and well-wishers who have supported me on the journey acknowledge the assistance provided by everyone, directly or indirectly, for the successful completion of my Doctor of Philosophy Degree.

Above all, my thanks go to the Almighty God for granting me wisdom, health, and strength for the successful completion of my thesis.

Sheeja K M

Dedicated to

My Children
Amiyaa & Ayansh
I love you beyond all reason.

CONTENT

LIST OF TABLE

LIST OF FIGURE

ABBREVIATIONS

OW	-	Open Well
BW	-	Bore well
MCM	-	Million Cubic Meter
Pr	-	Pre-monsoon
Mo	-	Monsoon
Po	-	Post-monsoon
Avg.	-	Average
Fig.	-	Figure
Figs.	-	Figures
SD	-	Standard Deviation
Temp.	-	Temperature
EC	-	Electrical Conductivity
TDS	-	Total Dissolved Solids
TSS	-	Total Suspended Solids
TS	-	Total Solids
TAc.	-	Total Acidity
TA	-	Total Alkalinity
TH	-	Total Hardness
Ca	-	Calcium
Mg	-	Magnesium
Na	-	Sodium
K	-	Potassium
Cl	-	Chloride
SO_4	-	Sulphate
NO_3	-	Nitrate
PO_4	-	Phosphate

F	-	Fluoride
DO	-	Dissolved Oxygen
T. coli	-	Total Coliform
E. coli	-	Escherichia coli
Fe	-	Iron
Cu	-	Copper
Cd	-	Cadmium
Pb	-	Lead
Ni	-	Nickel
As	-	Arsenic
Mn	-	Manganese
Zn	-	Zinc
EW	-	Excellent Water
GW	-	Good Water
PW	-	Polluted Water
VPW	-	Very Polluted Water
UD	-	Unsuitable for Drinking
IDW	-	Inverse Distance Weighted
WQI	-	Water Quality Index
HPI	-	Heavy Metal Pollution Index
AAHPI	-	Annual Average Heavy Metal Pollution Index
MI	-	Metal Index
AAMI	-	Annual Average Metal Index
CS	-	Core Sample
XRD	-	X-ray Diffraction analysis
XRF	-	X-ray Fluorescence analysis

ABSTRACT

Groundwater is considered the safest source of drinking water, and 89% of the world's population relies on it. India is one of the largest consumers of groundwater worldwide, accounting for around one-fourth of the global share and exceeding 230 km^3/annum. Globally, and particularly in India, arsenicosis and fluorosis are two emerging health problems linked to groundwater. Fluoride and Arsenic are present in the earth's crust, but elevated concentrations in the groundwater are the result of human-triggered activities. The combination of Fluoride and Arsenic may cause health consequences. Fluoride, Arsenic, salinity, and heavy metals were assessed quantitatively and qualitatively in this study under various climatic, geological, and topographical circumstances. This study evaluated the occurrence and distribution pattern fluoride, arsenic, salinity, and heavy metals in distinct climatic, geological, and topographical conditions. The study also focused on the quantitative availability of groundwater reserves in the two Districts.

The groundwater availability in Palakkad District is 434.17 MCM and 249.32 MCM in Malappuram District during the study period. Fluoride contamination is severe in the eastern part of the Palakkad District and south eastern part of the Malappuram District. Arsenic pollution is also dominant in these regions. In contrast to the coastal system, the inland system has a higher salinity. Mg-Ca-HCO_3 type water predominates due to rock-water interaction in the Palakkad District, while precipitation-induced calcium sulphate type water predominates in the Malappuram District. Heavy metal contamination was severe in both Districts, and Cd and Pb pollution were dominant. The mean heavy metal pollution index (HPI) indicates that the highest heavy metal incidence occurred in the Pr period and the least during the Po period in the study area. Cd, Pb, and Ni have concentrated in urban areas in the study area, whereas iron-mediated issues are higher in coastal region associated with fluvial deposits. The metal index was high in Malappuram and highly concentrated along the coastal line. WQI indicates 48% of the groundwater is poor in Palakkad,

while the majority of the Malappuram groundwater is of good quality. 11% of the groundwater in Palakkad is unsuitable for irrigation.

High Mg ion concentration, high alkalinity, and a lengthy groundwater residence period in the aquifer are the factors that enhanced the solubility of Fluoride. Silicon oxide is the dominant component in mineral samples. The XRD and XRF data reveal that the hornblende-biotite gneiss is indicative of the Fluoride source. Moreover, the trace amounts of Fluorite and Arsenic in the mineral sample are indicative of these contaminants in the study area. The mineralogical study of Fluoride and Arsenic contaminated areas demonstrated that the causes of Fluoride and the majority of Arsenic contaminations were geological in nature.

GENERAL INTRODUCTION

Groundwater is one of the most precious and exploitable natural resources on Earth. It sustains life and assures food security. The global distribution of water shows that 96.5% of it is primarily saline and is associated with the oceans, 1% forms saline groundwater, and the remaining 2.5% is fresh water. However, all the freshwater is not available for usage. About 68.7% of it forms the ice caps and glaciers, 29.9% is held up in the ground, and the remaining 1.4% forms the surface and other water resources (Shiklomanov 1993; Trenberth et al. 2007). The groundwater is not dispersed uniformly in all regions of the world and its occurrence, mobility, and availability are based on geology, geography, structure, and disposition, which vary with places and at varying depths (Lone and Mir 2021). These attributes, along with the geohydrological settings and hydrometeorological variables are the quantitative components of groundwater regulation (Urrutia et al. 2019).

Access to clean water is a fundamental need and human right. It is critical to human development from the standpoint of health and socioeconomic development, especially in the era of accelerated climate change. Groundwater is considered the safest drinking water source and approximately 89% of the world's population relies on it for drinking and domestic purposes (Martnez-Santos 2017). Still, in developing nations, up to 844 million people continue to live without essential water services (Bayu et al. 2020). The availability of surface water is a major factor that determines groundwater abstraction demand.

Groundwater is expected to become more strategically important for global water and food security as climate change increases the frequency and intensity of climate extremes like droughts and floods and increases precipitation variability. Once again, this is exacerbated by improved and cheaper drilling and pumping equipment that provides rapid access to groundwater. Groundwater is also threatened by urbanization and rising populations. Due to this, groundwater abstraction has increased beyond limits in the last 50 years (Nowak and Lawniczak-Maliska 2019). As many as 36 countries throughout the world are considered to be "water-limited"

(Reig et al. 2013). From a public health point of view, the advantages of developing groundwater are substantial, but much-expanded groundwater dependence has drawbacks as well.

The quality, quantity, and over-extraction of groundwater have become major global concerns. Groundwater availability and quantity vary with location and are influenced by the composition of aquifer material and groundwater storage (Thomas and Famiglietti 2019). Groundwater quality is mostly determined by its physical, chemical, and biological characteristics. Both natural and man-made factors can contribute to a decline in the quality of groundwater. According to WHO and BIS, all criteria in standards for drinking water, irrigation, and industrial consumption must have permissible limits. Consuming water above this threshold limit is hazardous to individuals, organisms, and the environment. These attributes make water significantly scarcer in various developing nations (Adimalla 2020b).

India is one of the largest consumers of groundwater, worldwide. The availability of groundwater throughout the year has made it the principal source of potable water. According to estimates, the country utilizes 230 km^3 of groundwater annually, which is around one-fourth of the global total (Central Groundwater Board 2011; Chinnasamy and Agoramoorthy 2015). The majority of the nation's growing use of groundwater during the past four decades has been for agricultural purposes (Narayanamoorthy 2011). Water security is ensured for millions of communities and farmers through decentralized access to groundwater. But, there are an estimated 30 million groundwater structures in India, and overexploitation has caused the groundwater table to decline (Chinnasamy et al. 2013). According to the assessment of the World Bank (2012), the country would have a severe groundwater crisis in 2032. The quality of groundwater has also changed substantially. Around 347 Districts, or 59% of all Districts in India lack access to clean drinking water (Shankar et al. 2011). Six to eight million people die annually as a result of drinking contaminated water (Nazir et al. 2020). Approximately 80% of infections in India are waterborne (Abedin et al. 2019).

Salinity problems are becoming more widespread in the arid/semiarid regions of India. About 6.73 million hectares (ha) of salt-affected soils (SAS) are scattered across 15 States and 13 agroclimatic zones in India. Salt-affected areas are distinguished by groundwater with a high pH, sodium carbonate and bicarbonate concentrations, and sodium adsorption ratio (SAR) (Mandal 2019). The water used by most of the Indian States is of poor quality, and 25% of the groundwater sources are sodic or salty (Singh 2009). Salinity-affected regions are induced by the weathering of rocks and minerals rich in sodium. The salinity is also accelerated by canal irrigation, which increases the concentration of sodium carbonate and bicarbonate ions in groundwater. This type of salinity is more prevalent in inland areas. In contrast, salty zones in coastal areas are also generated by salinity intrusion from creeks and lakes (Mandal et al. 2018). Significant portions of the country are already saturated with water and salinized in the majority of canal-served Districts. The overuse of aquifers contributed to a further increase in salinity in groundwater (Nath et al. 2021b). The salinity of water reflects the total amount of salt dissolved in it. Consuming such salinity-contaminated water results in a variety of disorders, including hypertension and cardiovascular diseases (Shammi et al. 2019). Yet, this is not the only issue linked to groundwater.

The combination of F and As may have serious health consequences for humans (Jha and Tripathi 2021). Fluorosis caused by ingesting fluoridated water has been recorded in numerous nations, particularly in low-income nations such as India, Argentina, Mexico, China, Tanzania, and South Africa (Wang et al. 2012; Adimalla and Li 2019; He et al. 2020). F and As is a major concern in the groundwater of the Indian subcontinent. In India, excessive skeletal fluorosis is a severe health issue that is endemic to certain regions and affects the poor (Chakraborti et al. 2016b). According to reports, six million people in India are paralyzed due to fluorosis (Singh et al. 2014). Andhra Pradesh, Tamil Nadu, Uttar Pradesh, Karnataka, Gujarat, Rajasthan, Maharashtra, Telangana, Bihar, Haryana, and Kerala are significantly affected States in India. F-affected groundwater is more prevalent in dry tropical hard rock and metamorphic terrains (Mandal and Sanyal 2019; Bera et al. 2021). It

is reported that the groundwater in volcanic residual sites has a high F concentration (Jha and Tripathi 2021).

The limits assigned to F range from 0.7 mg/L in warm regions to 1.2 mg/L in cold climates, with a threshold level of 1.5 mg/L. (WHO 2004; Ali et al. 2016). The Bureau of Indian Standards (2012) suggests the limit of F as 1.0 mg/L for drinking water. Globally, the optimum concentration for preventing dental caries is fixed at 0.7 and 1.2 mg/L. (Health US Do 2015). Approximately half of the daily F intake is absorbed by teeth and bones, with a significant fraction also deposited in the kidneys. Additionally, F impacts the cardiovascular and nervous systems (Han et al. 2021b).

Arsenic, the most toxic heavy metal, is a looming menace to humanity on a global scale, affecting an estimated 500 million people (Chakraborti et al. 2013). It is interesting due to its health implications. Arsenic in the human body is primarily derived through the ingestion of contaminated drinking water. Rock-water interactions are reportedly the primary source of As pollution (Singh et al. 2022). WHO stipulated that its concentration in drinking water should not exceed 10 µg/L. All naturally occurring forms of As are exceedingly dangerous, as they are carcinogens, teratogens, and mutagens. Diseases such as keratosis, melanosis, and skin malignancies are connected to As exposure. Additionally, it damages internal organs (Kumar et al. 2021a).

Arsenicosis is a serious environmental disease affecting people all over the world due to overexposure to As. More than 20 nations, including India, Bangladesh, Thailand, China, Chile, Argentina, USA, Canada, and Mexico, have documented drinking water arsenicosis (Smedley and Kinniburgh 2002; Chung et al. 2014; He et al. 2020). Extensive research on As contamination in northern India, particularly in the Ganga basin, has been published (Saha and Sahu 2016; Rahman et al. 2021; Shah 2012). In 2018, the Central Ground Water Board reported that 10 Indian States have issues related to As. Recent reports, however, indicate that As has affected 20 States and 4 Union Territories, including Jharkhand, UP, West Bengal, Himachal Pradesh, Tripura, Manipur, Nagaland, Bihar, Assam, Gujarat, Haryana, Punjab,

Arunachal Pradesh, Madhya Pradesh, Odisha, Chhattisgarh, Karnataka, Telangana, Andhra Pradesh, and Tamil Nadu, that have Alluvial land which is a primary source of As, followed by hard rock terrain (Shaji et al. 2021). Arsenic pollution in Indian States is related to arsenopyrite, and the volcanic Kotri lineament (Bhattacharya et al. 2019).

Other than As a few other heavy metals also reach the water resources as a result of natural processes or human causes. These are the elements of higher atomic weight and densities, which are five times greater than water (Banfalvi et al. 2011). 50 elements are identified as heavy metals and 17 of them are highly toxic (Seema et al. 2011). The non-biodegradability and the bio-magnification potential of heavy metals such as Cd, Pb, and Hg through the food chain are making them more hazardous (Malyan et al. 2019). Nickel (Ni) and Mn (Mn) are well known for their carcinogenic effects. Cu, Fe, and Zn are the essential elements that are desirable in very limited quantities in a healthy diet, but in excess leads to several health issues (Gaur and Agnihotri 2019).

Owing to drastic industrialization, urbanization, and modernization of agricultural practices, the accumulation of heavy metals in the environment, particularly in developing nations, has increased dramatically in recent years (Adimalla et al. 2020a). Various research on heavy metal contamination has been undertaken in south India, with only a few in Kerala. The geo-accumulation of Cu, Pb, Ni, Zn, and Fe found in the Kabani river basin in South India is attributed to industrial inputs (Hejabi and Basavarajappa 2013). Heavy metals such as Fe, Mn, Ni, Cr, Pb, Cd, and Zn were identified in high amounts in groundwater near the Kalpakkam region of south India (Chidambaram et al. 2012). Also, there are reports regarding the presence of heavy metals in a deep well sample close to disposal sites in Chennai, South India (Parameswari and Mudgal 2014). The contamination of groundwater in the District of Viruthanagar in Tamil Nadu with heavy metals in the order Zn > Mn > Pb > Cu > Hg > Cr > Cd is attributed to both anthropogenic and natural inputs (Muthulakshmi et al. 2012). In the Krishnagiri District of Tamil Nadu, 2% of the stable hard rock aquifers are contaminated with toxic heavy metals such as Pb, Zn,

As, and Cd (Manikandan et al. 2019). The health concerns posed by heavy metals in samples of groundwater from the Tamiraparani river basin in southern India were evaluated (Magesh et al. 2017). High quantities of Pb, Fe, and Cu were detected in groundwater near a sewage farm in the District of Thiruvananthapuram, Kerala (Varghese and Jaya 2014). There have been reports of chronic exposure to As and Pb in drinking water sources from the Alappuzha, Kottayam, Pathanamthitta, and Ernakulam Districts of Kerala (Jose and Ray 2018). The concentration of trace elements in groundwater is determined by natural variables such as the kind of aquifer, the quality of infiltrating water, the weathering of minerals inside the aquifers, and the length of residence (Singh et al. 2011; Voutsis et al. 2015; Mora et al. 2020).

In South India, water treatment or purification is restricted to specialized sectors, while the rural populace is forced to use untreated water due to the exorbitant pricing associated with water treatment. There are numerous ways in which water can become contaminated. Infiltration causes widespread contamination of groundwater, affecting rural and urban drinking water sources (Shamrukh and Abdel-Wahab 2011; Kurwadkar et al. 2020). Infiltration from polluted agricultural soils, leaching from industrial effluents and tailing ponds, urban sewage dumping, and contaminated surface water and groundwater interaction are anthropogenic sources of groundwater contamination (Balderacchi et al. 2013; Rajendiran et al. 2015). Furthermore, mining activities are the major contributors to groundwater As and F concentrations (Chandio et al. 2021).

According to reports, F, and a few toxic trace metals, including As are naturally occurring components, and the primary source of these elements in groundwater is the interaction between rock and water. Fluorite, biotite, amphiboles, and apatite are fluorine-bearing minerals that, upon interaction with water, generate a high F concentration in groundwater (Tossou et al. 2021). Pyrite, an As-bearing mineral in rocks and sediments, contributes to high As levels in groundwater. Furthermore, important factors that contribute to the enrichment of As and F include unique climatic conditions and distinct geological environments (He et al. 2020). Hence,

monitoring the occurrence and the pattern of mobilization of F, As and heavy metals in groundwater sources is crucial from a health standpoint. To identify how to minimize and prevent pollution from a multitude of sources, it is necessary to design and implement numerous evaluation tools.

In these contexts, the present study was carried out with the following objectives:

- To assess the magnitude of groundwater sources of two Districts of Kerala representing both coastal (Malappuram) and inland systems (Palakkad).
- To evaluate the physicochemical characteristics of groundwater with special reference to contaminants like arsenic, fluoride, salinity, and heavy metals.
- To find out the influence of geochemical and environmental factors responsible for the obilisation/distribution of water contaminants such as arsenic, fluoride, salinity, and heavy metals in the groundwater pertaining to the two Districts.
- To propose management measures for overcoming issues related to groundwater contamination in the two Districts.

The thesis is summarized in two chapters. The first chapter comprises the first and second objectives and it includes the quantitative status of groundwater in both Districts, along with an assessment of 30 water quality parameters, including the hydrochemical studies, heavy metals, and biological parameters. This chapter comprehensively analyzed 66 groundwater samples from both Palakkad and Malappuram Districts in three distinct seasons, such as pre-monsoon (Pr), Monsoon (Mo), and Post Monsoon (Po). The introduction, review (regarding groundwater scenarios, groundwater potential studies, groundwater status of the study area, tools for hydrochemical studies, water quality index, heavy metal pollution index and metal index, GIS interpolation studies, hydro-geochemical studies in India and Kerala, health impacts and the sources of F, and heavy metals), materials and methods, results and discussion, summary and conclusion are included in the first chapter.

In the second chapter, the third and fourth objectives are addressed. This chapter focused primarily on the mineralogical analysis, its interpretations, and recommendations for resolving groundwater issues identified in the study area.

Chapter 1
Groundwater Availability and Geochemistry in Palakkad and Malappuram Districts.

1.1. INTRODUCTION

The groundwater resources are declining in both quality and quantity due to several reasons, including insufficient or erratic precipitation, urbanization, population expansion, and unscientific land developments. All these are depleting the groundwater and may also cause seawater intrusion in the coastal aquifers (Sappa et al. 2015; Jia et al. 2019). The geology of an area has the greatest impact on groundwater quality and various anthropogenic activities, including waste dumps also pose significant threats (Houria et al. 2020). It is quite difficult to restore groundwater to its original purity, once it has been contaminated.

F and As concentrations in groundwater are significantly impacted by their sources and activating factors (Handa 1975). The primary sources of these contaminants are rocks and minerals with which groundwater comes into contact, and the dissolution activating factors include pH, alkalinity, salinity, and redox state (Alarcon-Herrera and Gutierrez 2022; Chandrajith et al. 2020). Geogenic mineral ions develop as a prominent contaminant of groundwater sources due to the greater reliance on it, expanding drilling activity, and deeper excavations for the retrieval of groundwater sources. In addition, point and non-point sources of human activity are developing as hazards to freshwater sources. The toxicity of these water contaminants is strongly related to co-occurring elements, the dissolving rate, and the complexity of aquifer constituents (Pi et al. 2015).

Arsenicosis and fluorosis can result from prolonged exposure to these elements, primarily through drinking water. Drinking water fluorosis is the most predominant of the three (drinking water fluorosis, burning coal fluorosis, and drinking tea fluorosis) types of fluorosis (Choi et al. 2012). It is a global health concern that typically manifests as endemic fluorosis, which is prevalent in several regions of the world. Arsenic is a heavy metal profoundly found in the earth's crust, frequently occurring as arsenates, sulphides, or metal arsenides (Smedley et al. 2005). It is widely distributed in the environment and its inorganic form is extremely poisonous. In groundwater, arsenate (+5) is the predominant form, but in anoxic conditions, the more poisonous arsenite (+3) is likely to be present (WHO 2017).

1.1.1 The Conceptual Framework and Selection of study area

In recent times, F, As, and heavy metal contamination are reported to be the most persistent issues related to groundwater (Madhav et al. 2020). Several researchers have observed F contamination of groundwater in southern India, except for a few isolated incidents in Kerala (Raj and Shaji 2017; Shaji et al. 2018; Mukherjee and Singh 2022). Worldwide, As is regarded as a growing lethal pollutant. Recently, pollution due to As and other heavy metals has been reported in a few regions in southern India (Shaji et al. 2021).

Kerala State, falling in the southwestern part of India is also reported to have groundwater issues in many of its Districts. To prevent further depletion of groundwater supplies, it is essential to comprehend the origin and mechanisms of pollution reach and the salinization process. However, limited work has been attempted in the area of seasonal ionic concentrations in groundwater and F and heavy metals including As release related to geological formations in Kerala State. To understand the geochemistry of groundwater in different seasons and different climatic, and topographic conditions, Palakkad and Malappuram Districts of Kerala were selected for the study, which are representative of inland and coastal regions.

Palakkad District encompasses a tropical region, extending from the gaps of the Western Ghats. It covers an area of 4,478 km². This region has diverse climatic conditions, ranging from semiarid conditions in the east to moist and humid conditions in the west, due to its unique topography, which is attributed to an altitude ranging from 0 to 2258 m above MSL (Shaji et al. 2007). According to the 2011 census, the population density is 627 and 400 people/km² in urban and rural areas, respectively. Groundwater from dug wells and bore wells forms the major source of drinking water in this region.

Malappuram is known to be the land of hills and valleys, and the altitude ranges from -2 to 2554 m above MSL. This District falls on the coastline of Kerala and covers an area of 3546.20 km². It is unique with a higher population density of 1,742/km² as against the national average of 464/km² (https://www.census2011.co.in

/census/District/275-Malappuram.html). A tropical humid climate with moderate temperature is generally experienced in this region.

This chapter analyzed the quantity of groundwater available throughout the study period, using 30 water quality criteria, including F and heavy metals, in an extensive manner. With adequate tools, the study also analyzed the genesis and distribution patterns of various elements. The GEC-recommended methodology was used to evaluate groundwater availability during the study period. Using several approaches, each water quality parameter was discussed individually and in detail. The statistical tool, the Piper plot, the Chadha diagram, the Wilcox plot, and the Gibbs plot have been utilized to comprehend the relationships between physicochemical characteristics, geochemistry, and the source of pollutants especially the F enrichment mechanism in groundwater. In a single-value technique, the WQI, HPI, and MI indices have been utilized to understand pollution levels. Rainfall and temperature in the study area are statistically analyzed in connection with water quality parameters to determine their influence on those parameters. The generation of different kinds of maps for easier interpretation has been facilitated by a GIS tool. To correlate the results with geology, maps of mineral groups are created for the study area. To examine the topographical factors a digital elevation model of GIS has been used. To understand the distribution pattern of various contaminants, a GIS interpolation model has been used. The approaches made in this study will be useful in assessing the anthropogenic as well as geo-environmental reasons underlying the release of F, As, and other heavy metals in the groundwater sources of other similar environments across the world and in formulating management plans for their control. The study gains significance as it is a comprehensive one in the area of the geochemistry of F, As, and heavy metal pollution in the primary drinking water sources of the study area.

1.2. Review of Literature

1.2.1. Groundwater

Water is a very important resource for all forms of life to exist. Groundwater is the water that seeps through rocks and soil to form a subsurface reservoir. The material in which the groundwater is stored is called an aquifer (Mandel 2012). It includes rock, sand, gravel, sandstone, limestone, etc. Water moves beneath the earth's surface through the porous media depending on the hydraulic conductivity of the saturated material and the hydraulic gradient (Mbonimpa et al. 2002). Thus the conductivity is a physical property that varies with aquifer material and hydraulic gradient and is measured at the right angle to the direction of flow (Sudicky et al. 2010). It is expressed in the unit of feet/day or meter/hour. Permeability is the ability of a material to allow a fluid to pass through it. The region where water wets and fill the aquifer minerals is called the saturated zone. The upper layer of the saturated zone is called the water table. The water table can be as shallow as a foot below the earth's surface or it can be serval hundred feet below according to the geological and hydrological settings of an area (Sloan 1972).

1.2.2. Groundwater Scenario of World

Groundwater is considered the principal stock of available freshwater resources in the world and one-third of the world's population depends on groundwater for domestic use (Richts and Vrba 2016). Only less than 1% of the total water reserve of the earth is available for use, out of which 96% is groundwater (USGS 2020; NASA 2020). Groundwater forms the major source of drinking water supply in urban and rural areas of semi-arid and tropical regions with great economical value (Burness and Brill 2001; Groenfeldt and Schmidt 2013; Kumari and Rai 2020). On the contrary, it is a freely available common resource for all (Aulenbach 1967). Due to this reason, individuals or corporates are making a profit out of over-abstraction (Barlow and Clarke 2017). This over-exploitation of groundwater has severely threatened and headed to premature depletion of these reserves (Custodio 2002). The exhaustion of common resources can be referred to as the ‘tragedy of commons’, where we fail to allocate the resource for the optimal use of an individual or group

(Hardin 1968). Besides this, the growing world population accelerated the demand for water for domestic purposes. A high share of the world's agricultural irrigation is dependent on groundwater (Dalin et al. 2017). Many countries started groundwater-based developmental activities to meet the water demand that affected critically in sustaining streams lakes and wetlands (Hiscock 2011). The overuse of groundwater and encroachment in groundwater recharge areas led to the decline in the water table which escalated the geogenic contamination (Bondu et al. 2016; Shaji et al. 2021). Moreover, the consumeristic approach of humans made all the water resources more contaminated all over the world and has compromised the ability of groundwater to resolve the emerging water management crisis in the 21st century (De Nicola et al. 2015).

1.2.3. Groundwater Scenario in India and Kerala

In India, 86% of the rural water supply, 50% of the urban water supply, and 60% of the irrigation supply is based on groundwater sources (Malyan et al. 2019; Maheshwari et al. 2014; Varua et al. 2016). The hydrological setting of India can be broadly classified into two, the alluvial aquifer system in the Indo-Gangetic plain and the hard rock aquifer system in peninsular India (Suhag 2016). As of 2015, the total water availability in India is 1,869 Billion Cubic Meters (BCM)/year but the usable water is 1,123 BCM/year. About 690 BCM/year of surface water and 433 BCM/year of groundwater together form usable water (CWC 2015). Taking account of the natural discharge of groundwater of 35 BCM, the net annual groundwater availability for the entire country is 398 BCM (CGWB). In the past 50 years, the groundwater abstraction rate in India has increased 10-fold to meet the demand of the increasing population (Margat and Van der Gun 2013). Nowadays more erratic type of rainfall is observed in India and hence farmers depend on groundwater for agricultural use (Chinnasamy et al. 2018). Also, industrial and urban demand for groundwater had become a stress on these resources, and the continual use led to the lowering of the water table (Chinnasamy et al. 2013). Groundwater depletion study using NASA gravity recovery and climate experiment satellites 3 and hydrological modeling system 4 estimated a mean rate of 4.0 ± 1.0 cm yr-1 of depletion of

groundwater in India (Rodell et al. 2009). Some reports depict that the groundwater pumping has exceeded the rainfall recharge (Shah 2008). As a result, the open wells in the unconfined aquifers, surface streams, and ponds are dried out and have been used for other purposes (Heath 1998). This has led to the intensification of bore wells in deeper semi-confined and confined aquifers in semi-arid and tropical regions of India (Raizada et al. 2018; Shah 2010). The groundwater development in Haryana, Delhi, Panjab, and Rajasthan exceeded more than 100%, which implies that groundwater consumption is more than the annual recharge (CWC 2015). The unsustainable use of groundwater for various purposes has led to complex issues in the area of sustainability of this resource in India, (Chinnasamy and Agoramoorthy 2015).

The major source of groundwater in Kerala is precipitation and infiltration. Kerala has 120-140 rainy days with an annual average rainfall of 3070 mm. Kerala receives the highest rainfall during the southwest monsoon (70%) and the surplus water infiltrates down to form the saturated zone (Vishnu et al. 2020). The infiltration rate depends on several factors and the major causes are surface earth material, permeability, and porosity of aquifer material (Brunke and Gonser 1997). The highest infiltration occurs in the coastal region while the lowest is in the highland (Canora et al. 2008; Ranjan et al. 2006). The occurrence and availability of groundwater vary from place to place due to diversified aquifer formations, lithological and tectonic formations, and climatological variations (Tiwari and Pai 2021). Kerala has 88% of a crystalline rock surface which does not permit water to percolate through it. The shallow aquifers are mostly weathered, disintegrated and thick weathered types are seen through the midland. On the contrary, a thin layer of weathered crystalline is in the highland region (Varma 2017). The aquifer materials in Kerala are diversified from the oldest Archean to the recent alluvium deposit (Jha and Sinha 2009). The annual mean depth in which water is found in this aquifer is 2-16 mbgl, which yields from 2-10 M^3 per day. Similarly, crystalline fractures are usually seen at the depth of 60- 175 mbgl, with a yield ranging from 1-35 liters per second (GEC 2012). The water level decline was assessed to be 10-20 cm per year in Kerala with various hydrogeological patterns (GEC 2012). The water demand has

exponentially increased over decades, for example, from 0.5 Km^3/Year in 1960 to 1.5 Km^3/ year in 2001 (Wada et al. 2011). Therefore the groundwater development in Kerala is in progress from 47% in 2011(CGWB).

1.2.4. Groundwater potential studies in India

Groundwater studies in India have started since 1979. Groundwater monitoring over time and space are very essential to gather information on groundwater level and quality by analyzing the representative samples (Kulmatov et al. 2020). Groundwater level monitoring in extreme weather conditions is very essential to understand the variability in water potential as well as the water quality status (Khan et al. 2015). However, groundwater monitoring is a time-consuming and costly affair and hence it is essential to optimize as possible (El Bedawy 2014). The selection of wells for quantity and quality monitoring of groundwater in an area is known as the groundwater monitoring network and this network of wells can be used for the continuous observation of groundwater (Kavusi 2020).

Singh and Singh (2002) highlighted the groundwater situation in India. The over-exploitation of groundwater for intensive irrigation caused a 1-2 meter/year decline of the water table in unirrigated parts of India and at the same time, irrigated areas showed an increase of 1 meter /year. Groundwater variation was worked out in Mo and Po seasons in the granitic aquifer region, Andhra Pradesh, India using a variogram (Kumar and Ahmed 2003). Two years of groundwater level data (2002-03) and the GIS interpolation method were used to estimate the groundwater potential of Himalayan foothill regions in India. The result shows that a high-relief area has poor groundwater potential than the low elevated region (Israel et al. 2006). Shekhar et al. (2006) assessed future groundwater availability in South West District of NCT, Delhi, India, using GEC (2012) methodology and categorized groundwater into different microzones according to its thickness. This study estimated 481 million $m^{3\ of}$ fresh groundwater in the District in 2006 and would reduce this to 176 million m^3 in 2022.

Panda et al. (2007) evaluated the influence of drought and anthropogenic influence in the Indian State of Orissa using GEC 2012 methodology. The study concluded

that rainfall has a significant influence on groundwater levels in semi-consolidated and consolidated aquifers in all seasons. Sreekanth et al. (2009) proposed a groundwater level forecast using Artificial Neutral Network (ANN) from monthly groundwater level, rainfall, relative humidity, and temperature data. Chatterjee and Purohit (2009) have assessed the groundwater recharge potential and groundwater availability in India from monthly groundwater level estimates and rainfall data. In India, 433 billion cubic meters of water can be refillable, and 399-meter cubes as annual availability. Bekesi et al. (2009) monitored groundwater levels to evaluate groundwater storage and groundwater demand in different seasons. They allocated groundwater in the Gnangara region of Western Australia in a sustainable manner.

The groundwater level with rainfall availability was estimated in the Palamu District of Jharkhand State using the water below-ground level method (bgl). The highest decline up to 8-10 m was observed during May during the study period (Shalini et al. 2012). Over-exploitation of groundwater leads to water table decline as well as water quality deterioration in the Deccan trap basaltic terrain of Maharashtra, India. This study reported a decline of groundwater by 0.03 to 0.04 m/year WR watershed (Pophare et al. 2014).

According to Tiwari et al. (2016a), the groundwater level is highly related to slope, elevation, geology, soil, and drainage pattern. Panda and Wahr (2016) estimated groundwater storage in the Ganges basin and Panjab State in India using hydro-climatic data from the GRACE satellite established in 2002 by NASA. Similar observations were made by Bhanja et al. (2019) in 12 major river basins in India using groundwater level data. Chinnasamy et al. (2018) used a combination of water balance and water table fluctuation methods to estimate the specific yield in the semi-arid hard-rock region of Rajasthan in India. Urbanization-induced land cover changes reduced groundwater level depletion in Howrah Municipal Corporation of the Indian State of West Bengal (Patra et al. 2018). Shaji et al. (2018) assessed the Pr hydrology of the Chittur Block of Palakkad District, Kerala, India. The water level in the dug wells of this region ranged between 1.18 mbgl to 11.93 mbgl. The yield of wells was found to be 5 m^3 /hour to 10 m^3 /hour. The monthly groundwater

level along with temperature and rainfall data were collected for aquifer assessment in Ganjimatta, Karnataka State of India using a multi-layer perception neural network model and algorithm method (Javadinjad 2020). The groundwater potential zone of the Vaigai sub-basin in India has been evaluated using GIS by Pothiraj and Rajagopalan (2013). They have given different weightage for the thematic maps like geology, land use, geomorphology, soil, and hydrology and overlaid to understand the groundwater potential zones.

1.2.5. Groundwater status of Palakkad and Malappuram District

According to the study by the Central Ground Water Board (CGWB), the groundwater potential of Palakkad District has increased from 626 mm^3 in 1989 to 795 mm^3 in 2009. At the same time, due to the increased demand, groundwater development increased from 9% to 61%. Out of 13 Block Panchayats in the Palakkad District, Chittur is overexploited, Malampuzha is in a critical stage and Pattambi and Thrithala Blocks are in semi-critical conditions. The valley fills/ alluvium, weathered /fractured crystalline, and laterite constitutes major aquifers in the Palakkad District (Shaji et al. 2007). The hard rock province covers around 80% of the District and the groundwater is occupied in the weathered or fractured portion of the rock under a semi-confined or confined state. The depth of weathering ranges between 10 to 23 mbgl and the water table ranges between 5-10 mbgl. The yield of the open wells is reported to be 5 -25 m^3/day and that of bore wells is 43 to 1650 m3/day (Varma 2017). A decline in the water table was reported in the eastern part of the Palakkad District of around 0.4 m /year and the yield of the well in the Palakkad gap was site-specific (Kumar at al. 2016c). In the rest of the region, the water table decline was reported to be 0.2-0.3 m/year. A rising trend in the water table was reported in the central-western region of the Palakkad District (Varma 2017).

The study by CGWB from 1989 to 2009 revealed that the groundwater potential of the Malappuram District has decreased from 582 mm^3 to 484 mm^3. Similarly, groundwater development increased from 12% in 1989 to 58% in 2009. 3 Block Panchayats out of 14 are in semi-critical condition. The aquifer system consists of

weathered or fractured crystalline, laterite, alluvium, and tertiaries (Nair et al. 2017). The weathered zone of Malappuram varies from 15-20 meters and the groundwater development is mostly through dug wells. Laterite is the most important lithological unit of the Malappuram District and is widely seen in the midland region of the District (Sreekumar and Aslam 2010). Laterite is seen as a thin layer of 1- 3 meters over charnokite and as thick as 15 to 20 meters over hornblende gneiss. Tertiary sediments are lateralized at the top and seen over the alluvium layer along the coastal line (Varma 2017).

1.2.6. Tools for the hydrogeochemical studies of groundwater

The hydrochemistry of groundwater is dynamic and generally controlled by its medium of contact. Hydrochemistry directly defines the quality of water for various purposes. Hence, the surveillance and assessment of groundwater quality are very essential for the current century (Kumar 2013). Water chemistry was first described by Hill (1940) using a trilinear diagram. This study worked out the geochemical pattern in the Coachella Valley of California and grouped water into four major categories: common salt group, alkali group, bittern group, and hardness group. However, these categories don't attain much popularity due to their complexity and applicability. The Piper diagram, proposed by Piper (1944), is the most popular and widely used trilinear diagram for interpreting groundwater water types and hydrochemistry. This hydrochemical diagram was aimed at facilitating the interpretation of the evolutionary trends of groundwater. The Piper plots consider six ion groups, such as calcium, magnesium, and sodium plus potassium cations, and sulphate, chloride, and carbonates plus bicarbonates. Durov (1948) modified the piper plot and its needed software application for the depiction. Chadha (1999) proposed a hydrochemical diagram consisting of eight subfields. The percentage of mill equivalence of calcium plus magnesium (representing alkaline earth) and sodium and potassium (representing alkali metals) reacting values are plotted on the "X" axis, and the percentage of mill equivalence of carbonates plus bicarbonates (weak acid anions) and sulphate plus chloride reaction values are plotted on the "Y" axis. To scientifically justify the proposed hydrochemical diagram, Chadha collected

groundwater from different geological formations in Karnataka State, India. Gibbs (1970) proposed a boomerang plot to understand the process of groundwater chemistry. According to the Gibbs plot, the three major mechanisms of water chemistry can be defined by atmospheric precipitation, rock dominance, and the evaporation of crystalline processes.

1.2.7. Important Tools for the groundwater quality assessment

1.2.7.1. Water Quality Index (WQI)

Approaches for determining water quality have advanced from simple comparisons of water chemistry with standards to the practice of sophisticated data-intensive models. The WQI is a widely used method for assigning weights to various ions in the water and calculating the suitability index, developed by Horton (1965) and in 1970 Brown et al. created a general Water quality index (WQI). Steinhart et al. (1982) proposed a novel environmental quality index to summarise methodical information on the status and trends in the Great Lakes ecosystem. The water quality index was calculated using several physicochemical and bacteriological parameters. However, the estimation of water quality indices seeks a single value that reduces a large number of parameters and represents data in a simple manner (Wali et al. 2020). Various kinds of water quality indices are being used worldwide; for example, the British Columbia Water Quality Index (BCWQI), the Canadian Council of Ministers of the Environment Water Quality Index (CCMEWQI), River Status Index (RSI), the National Sanitation Foundation Water Quality Index (NSFWQI), the Overall Index of Pollution (OIP), Oregon Water Quality Index (OWQI), the Dinius Water Quality Index (DWQI), the EPA's Contamination Index (CI), Bhargava Method Water Quality Index (BMWQI), Malaysia Water Quality Index (MWQI), Water Contamination Index (WCI), Vaal Water Quality Index (Vaal WQI) and the Recreational Water Quality Index (RWQI) (Bhargava 1985; Rocchini and Swain 1995; Zandbergen and Hall 1998; Sargaonkar and Deshpande 2003; Cude 2001). CCME WQI is used by many countries around the world, and it was endorsed by the United Nations Environmental Program (UNEP) in 2007 as a model for the Global Drinking Water Quality Index (GDWQI). Dissolved oxygen, pH,

turbidity, total dissolved solids, nitrates, phosphates, and metals are among the most commonly used parameters in WQI (Lumb et al. 2011). The majority of the WQI model components were created using expert opinions and local guidelines (Sutadian et al. 2016). WQI models normally comprise four sequential stages: (1) the selection of water quality parameters, (2) the generation of sub-indices for each parameter, (3) the calculation of parameter weighting values, and (4) the aggregation of sub-indices to compute the overall water quality index (Uddin et al. 2021).

1.2.7.2. Heavy Metal Pollution (HPI) and Metal Index (MI)

Heavy metals are one of the most serious contaminants, posing a global problem due to their long-term persistence in soils and water, increasing geo-ecological risks and disrupting natural biogeochemical cycles (Chabukdhara and Nema 2012). Heavy metals, both essential and non-essential, have ecotoxicological effects on living organisms (Ali and Khan 2019). Monitoring heavy metal pollution in the environmental matrix in ground and surface waters is important in the context of human health (Hashmi et al. 2014). The HPI is a method of rating and comparing values that shows the combined influence of each heavy metal on overall water quality (Prasanna et al. 2012). The rating is based on the relative importance of each heavy metal on water quality and was calculated as the inverse proportional of the recommended standard. The method of indexing based on the weighted arithmetic quality mean is developed in two basic steps: establishing a rating scale for each selected quality characteristic and assigning weightage to it, and selecting pollution parameters on which the index is to be based (Mohan et al. 1996). HPI is a vital tool to evaluate groundwater quality (Varghese and Jaya 2014; Chidambaram et al. 2012; Sajil Kumar et al. 2012; Mohana and Velmurugan 2020). The Metal Index is another important indexing for metal pollution in drinking water (Bakan et al. 2010; Sanaei et al. 2021), which takes into account the potential additive effect of heavy metals on human health and allows for a quick evaluation of the overall quality of drinking water (Morais et al. 2012). It only considers the concentration and standard value of the heavy metals (Tamasi and Cini 2004).

1.2.8. GIS

Groundwater location is heavily influenced by geology, geomorphology, lineaments, soil, land use, drainage, and slope (Srivastava and Bhattacharya 2006). Topographic features of the study area are usually described, and interpreted in terms of structural geology and geomorphology using digital elevation models (DEM) in GIS (Jordán et al. 2005). Morphometry is the measurement and mathematical analysis of the configuration of the earth's surface, as well as the shape and dimension of its landforms (Agarwal 1998). Morphometric analysis of a watershed gives a quantitative explanation of the drainage system, which is a key aspect of watershed characterization (Strahler 1964). Evaluating various terrain and morphometric parameters of drainage basins and watersheds provides a flexible environment and a powerful tool for the manipulation and analysis of spatial information (Ali and Khan 2013). Traditional methods such as field observations and topographic maps can be used to distinguish drainage networks in a watershed or advanced methods such as DEMs can be used (Ozdemir and Bird 2009). DEMs can be used to extract drainage networks that contain all exterior links (Martz and Garbrecht 1992).

GIS-based groundwater adulteration mapping can assist decision-makers with proper land use and water resource management. This will allow the analysis to include groundwater protection and a health impact assessment (Lee et al. 2007). The Geographical Information System (GIS) has been widely used in risk mapping (Parveen and Kumar 2012; Aghajani et al. 2017; Aravinthasamy et al. 2020). Time and cost constraints reduce the amount of in situ data collection and field investigation (Wagner 1995). Thus surface interpolation methods in GIS are extremely powerful tools for predicting the spatial distribution of groundwater contamination (Gong et al. 2015). Geostatistics is a discipline that offers very useful methods for dealing with spatially distributed data such as groundwater contamination (Arslan 2012; Mirzaei and Sakizadeh 2016). Interpolation analysis, which recognizes spatial patterns and interpolates values at unsampled locations, plays a critical role in the sustainable management of groundwater systems by providing estimated input parameters at consistent grid points from measurements

taken at random locations (Srivastava et al. 2012; Kazemi et al. 2021). Interpolation methods such as inverse distance weighting (IDW) and kriging have seen extensively used in groundwater investigations and pollution mapping (Mirzaei and Sakizadeh 2016; Elumalai et al. 2017b). In predicting some contaminant levels in groundwater, the inverse distance weighted (IDW) method outperformed the kriging (Gaussian, spherical, and cokriging) approach (Gong et al. 2014). Geostatistical interpolation techniques depend on both statistical and mathematical methods to generate surfaces and assess prediction uncertainty (Johnston et al. 2001).

1.2.9. Hydrogeochemical studies of groundwater in different regions of India

Lakshmanan et al. (2003) evaluated the hydrochemical process of groundwater in Kancheepuram District, Tamil Nadu State, India as falling into two categories: Ca^{2+} -HCO_3 and Ca^{2+} -Cl^- -HCO_3^- type. The Ca^{2+} -HCO_3^- type is due to rainfall recharge having low ion content and a high concentration of chloride ions indicating the irrigation return flow, contaminated river recharge to nearby wells, and evaporation processes. Kumar et al. (2009) classified the groundwater of the Manimuktha River basin in Tamil Nadu, India, into two types: Ca^{2+} -HCO_3 and Ca^{2+} -Na^+ -HCO_3^-. This study discloses that silicate and carbonate weathering are the mechanisms that constitute Cl, Ca^{2+}, Mg^{2+}, and K^+ in the groundwater. Excess concentrations of NO_3^-, NO_2^-, and PO_4^{3-} are due to anthropogenic pollution and irrigation return flow.

The geochemistry of the Neyveli basin of Cuddalore District, Tamil Nadu State, India has been studied by Prasanna et al. (2011). The correlation among anions and cations like Ca^{2+} -Mg^{2+}, Cl^- -Ca^{2+} -Mg^{2+}, Na^+ -K^+, and F^- -K^+ indicates that weathering along with the leaching process constitutes these chemicals in the groundwater system. Ramesh and Elango (2012) used the Piper plot to classify the groundwater of the Tondair River basin, Tamil Nadu State, India. The major water types delineated for irrigation and drinking purposes were Ca^{2+} -HCO_3^-, Ca^{2+} -Mg^{2+} -Cl^-, and Na^{2+} -Cl^-. The geochemical processes controlling groundwater chemistry in the Adyar River basin, Tamil Nadu, India, were identified by Brindha

et al. (2014). The Chadha and Schoeller diagrams show that the key processes that control the groundwater chemistry in that region are evaporation and ion exchange.

Srinivas et al. (2014) identified mixed Ca–Mg–Cl and Na–Cl as the major water types in the groundwater of Agasteeswaram Taluk of Kanyakumari District, Tamil Nadu State, India. Variation of ionic constituents was observed in Pr and Po groundwater samples. The rock-water interaction, the ion exchange process, and surface runoff are the major factors influencing groundwater chemistry in this region. The higher concentration of Na and Cl may be derived from halite dissolution, saltpan development, and saltwater intrusion. Ca–Cl, mixed Ca–Mg–Cl, and Na–Cl types of water with medium to very high salinity were observed in the coastal zone from Tiruchendur to Koodamkulam area. This region is severely affected by seawater intrusion, saltpan deposits, and beach placer mining activities (Chandrasekar et al. 2014). A study conducted in the coastal area of South Chennai, India States that Na–Cl is the dominant type of water, and the higher (> 1) molar ratios of Cl/HCO_3 and Mg/Ca indicate seawater intrusion (Kumar et al. 2014a). The alkaline water with $-HCO_3^-$ ions is the principal ion observed in various lithological units in the Madurai region of Tamil Nadu State, India, and the alkali-carbonate type of water indicates the rock weathering in these regions (Adithiya et al. 2016; Thivya et al. 2013).

A comprehensive study on the hydrogeochemical processes of the coastal aquifer of Thiruvalluvar District, Tamil Nadu State, India has been conducted by Senthilkumar et al. (2018). The major causes of salinization of groundwater are irrigation return flow, domestic wastes, ion exchange processes, silicate weathering, and evaporation. Na–Cl-type hydrochemical characteristics are reflected in the aquifer of the coastal region of the Cuddalore District of Tamil Nadu. The $Cl/ (Cl + HCO_3)$ ratio indicates that these regions have been subjected to saltwater intrusion (Chidambaram et al. 2018). $Na^+ -HCO_3^- > Ca^{2+} -Mg^{2+} -HCO_3^- > Ca^{2+} - Mg^{2+} SO_4^{2-} Cl^- > Na^+ -Cl^-$ is the dominant groundwater type in the Peddagavu region of central Telangana, India, which enhanced the F toxicity (Adimalla et al. 2018).

The hydrochemical evaluation of groundwater in the Chittoor District, Andhra Pradesh, South India reveals the water type in the order of Na^+ -HCO_3^- >Ca^{2+} -HCO_3^- >Mg^{2+} -HCO_3^- . Mafic silicate, felsic silicates, and soluble minerals as the main factors responsible for chemical undulations in groundwater (Nagaraju et al. 2018). The groundwater of Prakasam District, Andhra Pradesh, India was found to be alkaline and is characterized by Na^+ -HCO_3^- and Na^+ Cl^- facies. The main factors that influence groundwater chemistry are rock weathering and are subsequently changed by anthropoid activities, which are supported by genetic geochemical evolution and hydrogeochemical relations (Rao 2018). The geochemical and statistical evaluation of groundwater in shallow aquifers in Agra city, India, revealed that the major cations were $Na^+ > Ca^{2+} > Mg^{2+} > K^+$, while the anions were $HCO_3^- > Cl^- > SO_4^{2-}$ and $NO_3 > F^-$ (Yadav et al. 2018).

The shallow groundwater possesses higher concentrations of Ca, Na, K, and SO_4 than deep water, in a study reported in Madura City, Western Uttar Pradesh, India (Ahamad et al. 2019). But a high concentration of trace elements like As, Mo, Sr, and Zn ions are more dominant in the deep aquifer. The major water types include Na-K-Cl-SO_4 and Ca-Mg-Cl-SO_4 in the shallow aquifer and Ca-Mg-Cl-SO_4 type in the deep aquifer in the Po season of 2017. The groundwater of the Hindon River basin of Ghaziabad, India was characterized by the Na^+ - HCO_3^- type in the pre and Po seasons with an elevated concentration of nitrate, making 89% of samples unsuitable for drinking purposes. The aquifer chemistry is mainly driven by rock weathering (Ahmed and Khurshid 2019). Similarly, groundwater in the quaternary aquifers of Unnao District, Uttar Pradesh, India is reported to be slightly alkaline with Ca^{2+} -Mg^{2+} -HCO_3^- and Na^+ -K^+ -HCO_3^- in both Pr and Po seasons (Ansari and Umar 2019). The major hydrogeochemical facies and geochemical evaluation of groundwater of Kangayam Taluk, Tirupur District are evaluated by Duraisamy et al. (2019). Ca-Mg-Cl>Ca-Cl>Na-Cl type water is predominant in this region due to the presence of ion exchange processes between groundwater and biotite, hornblende, feldspars, and ferromagnesian minerals in hard rocks.

Groundwater chemistry of a semi-arid alluvial region in Panipat District, Haryana, India, showed the inter-ionic relationship between $Ca^{2+} + Mg^{2+}$ and $SO_4^{2-} + HCO_3^-$. It specified that carbonate and silicate weathering were consistently dominant in this region and the Piper diagram depicted the water as Ca^{2+} -Mg^{2+} -SO_4^{2-} -HCO_3^- type (Kaur 2019). The hydrogeochemical processes of surface water and groundwater in the Barak Valley of NE India are chiefly controlled by silicate weathering and ion exchange processes. The Gibbs and scatter plot were used to assess the hydrochemical processes in this region and the main hydro facies identified are the Ca-Mg-HCO_3 type of surface water and different types of groundwater such as Na-HCO_3, Ca-Mg-HCO_3 -Cl, Na-Cl and Ca-Mg-HCO_3 (Khangembam and Kshetrimayum 2019). The hydrogeochemical pattern of groundwater in Coimbatore District, South India exhibited an alkaline nature in all seasons with the dominance of $CaHCO_3$ and Ca–Na–HCO_3 types of water and the steady increase of NO_3 in the samples indicating anthropogenic influences (Kumar and James 2019).

Long-time rock water interaction and precipitation are the chief factors that influence the groundwater geochemistry of Chamba City (HP), northwest Himalaya, India. Carbonate weathering is more prevalent than silicate weathering, which results in alkali metals in groundwater, and the water is characterized by Ca^{2+} -Mg^{2+} -Cl^-, Na^+ -HCO_3^-, and Ca^{2+} -Mg^{2+} -HCO_3^- with temporary or permanent hardness (Kumar et al. 2019). A study on hydrogeochemical characteristics, and salinization processes in a coastal area of the Puri District of Odisha, on the southeastern coast of India, clearly showed that the groundwater facies is changing from Na-K-HCO_3 to Na-Mg-Cl type due to the mixing of saline water into freshwater aquifers. The chemical weathering of rock-forming minerals in the aquifer zones, aided by the evaporation processes, is the leading hydrogeochemical process controlling the groundwater composition in this coastal zone (Mohanty and Rao 2019).

The evaluation of hydrogeochemical fingerprints of groundwater in Jirania Block, west District of Tripura, India reveals that Ca-HCO_3 is the major water type and is

slightly acidic, which enhanced weathering, mineral dissolution, and ion exchange reactions (Paul et al. 2019). The groundwater geochemistry of the sub-urban area of Visakhapatnam, Andhra Pradesh, India, primarily categorized as $Ca^{2+} > Na^{+} > Mg^{2+} > K^{+}$: $HCO_3^{-} > Cl^{-} > SO_4^{2-} > NO_3$ facies indicates that the largest contamination is from natural sources and the groundwater quality is characterized by fresh to brackish and hard types (Rao and Chaudhary 2019). Likewise, a study conducted in Y.S.R District, Andhra Pradesh, India, evaluated the hydrogeochemistry of groundwater using a Piper plot states that water is of mixed Ca Mg Cl type that directs the geogenic and anthropogenic sources of pollution (Sunitha and Reddy 2019).

The major water types of the hard rock region of the Nalgonda District of south India are characterized by Ca^{2+} -Mg^{2+} -HCO_3^{-} and Ca-Mg-Cl^{-} with a slightly alkaline nature, having nitrate and F contamination (Adimalla et al. 2020c). Similarly, silicate weathering is reported to be the source of ionic concentration in the Nanganur region in South India. Ca^{2+} -Mg^{2+} -SO_4^{2-} , and Na^{+} -Cl^{-} -SO_4^{2-} hydro facies were dominant in the region (Adimalla et al. 2020b). The dominant hydro facies of the Kudal town of Sindhudurg District of coastal Maharashtra, India, were reported to be alkaline earth (Ca + Mg) greater than alkalis (Na + K) in both pre and Po. However, strong acids (SO_4 + Cl) exceed weak acids (CO_3 + HCO_3). The Gibbs plots suggest rock-water interaction and evaporation-crystallization are the major processes controlling aquifer chemistry in this region (Gaikwad et al. 2020). The groundwater of the Shanmuganadhi River basin exhibited 72% of samples in the mixed Ca^{2+} -Mg^{2+} - Cl type, indicating the transition state of freshwater to brackish water. The chief geochemical processes that control the groundwater chemistry in this region are silicate weathering, carbonate dissolution, and reverse ion exchange (Karunanidhi et al. 2020).

The geochemical appraisal of groundwater in the Maneswar Block of Odisha, India, revealed that the $Ca^{2+} > Na^{+} > Mg^{2+} > K^{+}$ cations and $HCO_3^{-} > Cl^{-} > SO_4^{2-} > CO_3^{2-}$ anions are dominant in these regions, and Chada's Trilinear Diagram suggests that alkaline earth exceed alkali. According to the Gibbs plot, the

aquifer characteristics and the geochemistry of this region are mainly influenced by rock and evaporation crystallization (Mahanta et al. 2020). The major water type in central Tamil Nadu, India, is Na-HCO_3 in all the seasons that indicate weathering and ion exchange are the major processes controlling geochemistry (Pillai et al. 2020). According to a study in Wanaparthy, Telangana, India, the majority of the groundwater is Ca^{2+} -HCO_3^-, Na^+ -Cl^-, and mixed types, with alkaline in nature, and the Gibbs plot indicates that the groundwater chemistry is predominantly controlled by rock-water interaction (Rao et al. 2020).

A study conducted in the semi-arid region of the Gujarat State indicates that the water is Ca^{2+} -Mg^{2+} - HCO_3^- type and the main controlling factors of the hydrogeochemistry of the region are rock weathering and rock–water interaction. It also showed the high F and NO_3 contamination in this region (Shirke et al. 2020). Na, Mg, Ca, and K are the major ionic components of the groundwater of agriculture-dominated Taluks of Jalandhar District, Punjab. The major facies in this region are Ca^{2+} -Mg^{2+} -HCO_3^- followed by Ca^{2+} -Mg^{2+} -Cl^- -SO_4^{2-}, indicating rock weathering, silicate and carbonate dissolution, and ion exchange processes as factors controlling the aquifer chemistry (Singh et al. 2020). A Piper plot analysis of the hydrochemical evolution in a shallow coastal alluvial aquifer in the Ramanathapuram District of Tamil Nadu, India, demonstrates that reverse ion exchange and seawater intrusion are the main processes that determine groundwater characteristics (Sivakarun et al. 2020). The groundwater quality of the industrial centers (i.e., Vellore) of south India is evaluated by Venkatesan et al. (2020). The major water types are Ca-Cl and mixed Ca-Mg-Cl, and the groundwater is highly polluted with NO_3, and the health risk assessment was also high.

The groundwater of the coastal tract of Tamil Nadu and Puducherry exhibited an acidic to alkaline nature with $Na^+ > Ca^{2+} > K^+ > Mg^{2+}$ and $Cl^- > HCO_3^- > SO_4^{2-}$ ions. The trilinear piper plot indicates $CaHCO_3$, $NaHCO_3$, $CaCl_2$, mixed $CaNaHCO_3$, and NaCl due to the rock and water interaction in the coastal aquifers (Khan et al. 2021). In both the pre-and Po seasons, the piper plot of groundwater from the semi-arid region of the Shivganga river basin, Pune, Maharashtra, India,

expressed mixed water and Ca–Mg–Cl type. This indicates that alkaline earth (Ca^{2+} & Mg^{2+}) considerably exceeds the alkalis (Na^{+} & K^{+}) and weak acids (HCO_3^{-} & CO_3^{2-}) and surpasses the strong acids (Cl^{-} & SO_4^{2-}) (Kadam et al. 2021).

1.2.10. Hydrogeochemical studies of groundwater in Kerala

Hydrogeochemistry was used to tackle concerns about the origin and attenuation of diffuse pollution from intensive agriculture, waste disposal, and point source pollution from urban and industrial sources. However, few studies have been reported in Kerala concerning hydrogeochemical studies of groundwater and are reviewed here.

A study on groundwater samples from the weathered and fractured aquifers in the Precambrian charnockite aquifers in Kerala State, India, observed that groundwater in both the aquifers is generally basic, with a decreasing concentration of Cl with increasing depth, together with an increase in HCO_3 +SO_4 , and is indicative of the ion exchange process and lack of manmade pollution in deep aquifers (Nandakumaran and Balakrishnan 2020).

The hydrochemistry of groundwater in the Kazhakuttam Block of Trivandrum District, Kerala was evaluated by Kumar and Divya (2012). The major ions in the order of $Na^{+} > Ca^{2+} > Mg^{2+} > K^{+}$ and $Cl^{-} > HCO_3^{-} > SO_4^{2-} > NO_3^{-} > PO_4^{3-}$ indicate the dominance of alkaline earth and weak acids. The Na-Mg-Cl facies during the Pr changed to Na-Cl facies in the Po, and the high concentration of nitrate and acidic nature of groundwater makes it unsuitable for drinking. A study in the Thettiyar watershed, Thiruvananthapuram District, Kerala shows that the nature of groundwater is acidic (strong acid exceeds weak acid) as most of the samples are sodium chloride and mixed types in both Pr and Mo seasons. The rock type of this region is characterized by the khondalite group along with charnockite, migmatite complex, and laterite patches (Nath et al. 2021a). Groundwater characterization in the laterite aquifer of Eruthavoor in Thiruvananthapuram District, Kerala, India, indicates $Na^{+} + K^{+} > Ca^{2+} > Mg^{2+}$ and $HCO_3^{-} > Cl^{-} > SO_4^{2-} > NO_3^{-}$ as the major ions and Gibbs plots suggest that the aquifer nature is mainly influenced by

precipitation (Rejith et al. 2021). A hydrogeochemical study of the hard rock terrain of the Kallada River basin, Kollam, has been extensively studied by Aju et al. (2021). The dominant groundwater type in the Kallad river basin is observed to be Ca^{2+} -Mg^{2+} - Cl^- type in Pr and Na^+ - Cl^- type during the Po, but the Na^+ - Cl^- type is dominant in deeper wells in all the seasons.

A shift of water type from Ca^{2+} -Mg^{2+} - Cl^- - SO_4^{2-} in Pr to Na^+ - K^+ - Ca^{2+} HCO_3 in the Po season was observed due to the addition of Na^+ and HCO_3 through leaching of crystalline rock in the phreatic zone in the Muvattupuzha region of Cochin (Laluraj et al. 2006). Hydro-geochemical characteristics of groundwater in phreatic aquifers in Cochin City exhibited major water types in the order of Na-Ca-Cl-HCO_3 >Ca-Na-Mg-HCO_3 -Cl > Ca-Na-HCO_3 -Cl as per the Hill-Piper plot (Priju et al. 2012). Similarly, Sajeev et al. (2020) reported the predominant water types around the Vembanadu Lake of Cochin as Ca-HCO_3 , Na-Cl, and mixed Ca-Na-HCO_3 . Strong linkage between the host rock and groundwater quality specified significant rock-water interaction in this area. Evaluation of groundwater quality in the coastal stretch of Alappuzha District, Kerala Stated that the water is hard to very hard and the predominant facies are Ca–Mg–HCO_3 types, using a Piper diagram (Prasanth et al. 2012). The hydrochemical investigation of the groundwater in the Meenachil River Basin, Kerala, showed the majority (51.2%) of samples in the Ca-Mg-HCO_3 -Cl type in the Pr and Po periods, and dominance of Ca-Na-Mg-HCO_3 -Cl type due to dissolution/precipitation, cation exchange, and mixing with agricultural return flow (Vincy et al. 2015).

The groundwater of the phreatic zone in the Alappuzha District has been studied and the high concentration of electrical conductivity, Ca^{2+} , and Cl^- directs its saline nature. The correlation coefficient between EC and Na^+ , Cl^- , SO_4^{2-} is significant in this region as it indicates the tidal inlets and or contribution from marine aerosols (Shaji et al. 2009). The major factors that control the geochemistry in the tropical coastal regions of the Alappuzha region were found to be the weathering of carbonate and silicate minerals as well as the interaction between groundwater and the aquifer matrix. Groundwater recharge of this region by rain and lake water

intrusion caused the domination of Ca-Mg-HCO type in the Mo season, whereas Ca-Mg-Cl and mixed cations-Cl types due to weathering of carbonate and silicate minerals (Tm et al. 2017) in the Pr season.

The shallow aquifer groundwater quality in the paddy-dominated agriculture river basin in Chittur was observed to have Na-Ca-HCO_3 and Na-HCO_3 types of water, and Gibbs plots suggested that rock weathering is the dominant process that controls the groundwater chemistry (Kannan and Joseph 2009). Similarly, the Na-Ca-CO_3 - HCO_3 -Cl type facies are dominant in groundwater collected from the shallow hard rock aquifer system in the Pudunagaram Panchayat of Palakkad District, and the rock-dominated process is a major controlling factor of water chemistry (Kumar et al. 2016c). Groundwater studies in igneous terrains in the Chittur Block of Palakkad District revealed that the major facies are Mg-Ca-Na-HCO_3 primarily due to the silicate weathering. The Ca^{2+} ions rapidly precipitate into calcite which enhances the Na^{+} and F ions in groundwater, thus sequentially increasing the alkalinity (Shaji et al. 2018). The results of the hydrochemical investigation of groundwater and surface water of the Thuthapuzha Sub- basin of Kerala, State that river water and groundwater are dominated by alkaline earth and weak acids (Ca-HCO_3 type) and a small percentage of the open well samples belong to NaCl, mixed Ca-Mg-Cl, and mixed Ca-Na-HCO_3 types. The groundwater chemistry of the Thuthapuzha Sub- basin is controlled by weathering and rock water interaction (Manjula and Warrier 2019).

The hydrogeochemical status of the shallow aquifer in the Kalanad Basin, Kasaragod, Kerala, India shows that 50% of the samples are Na-Cl> mixed > Mg-HCO_3 types, which indicates seawater intrusion (Anoop et al. 2021).

1.2.11. Health Impact of Fluoride and its Source in Groundwater

More than 200 million people are subjected to skeletal and dental fluorosis in 28 countries and remarkably, 66 million people are affected by the fatal disease of fluorosis in India (Narsimha and Sudarshan 2017). More than 177 Districts in 22 States in India are reported to have F contamination in groundwater (Adimalla et al. 2019). Fatal F concentrations in groundwater have been extensively studied in South

India and reported by several authors (Brindha et al. 2011; Shaji et al. 2018; Subba Rao et al. 2020; Narsimha and Sudarshan 2018; Narsimha and Rajitha 2018; Adimalla and Li 2019; Mukherjee and Singh 2018). People are seriously affected by fluorosis which is well documented in several reports (Acharya 2005; Ramesh et al. 2014; Krishnan et al. 2015; Reddy et al. 2017) as 50% of urban and 85% of rural domestic water requirements in India are met through groundwater sources (Ayoob and Gupta 2006).

F ions in drinking water are easily absorbed from both the stomach and small intestine through diffusion processes (Whitford 1994). However, F absorption in the human body is influenced by several factors, including stomach pH, the chemical nature of F consumed, the presence of food in the stomach, interactions with other dietary constituents in the gastrointestinal tract, and the presence of aluminium, calcium, and magnesium compounds (Yang and Liang 2011). Half of the absorbed F is rapidly assimilated into developing bones and teeth, and the excess F is expelled through urine (Cerklewski 1997). Rapid accumulation of F in bones and skeletons is taking place in children and it declines with age (Nagendra Rao 2003). Once F has been assimilated into hard tissues, it is a very slow process to retrieve it (Spencer et al. 1975; Doull et al. 2006). Varying degrees of F illness, such as dental fluorosis, skeletal fluorosis, non-skeletal fluorosis, calcification of ligaments, and challenging joint movements, would occur according to the quantity and period of ingestion (Whitford 1996). Additionally, high levels of F can affect the functions of the liver, heart, lungs, kidney, brain, chromosomes, nervous systems, thyroid glands, and reproductive abilities (Iano et al. 2014; Chen et al. 2002; Nakamoto and Rawls 2018; Aydin et al. 2003; Dharmaratne 2019; Zuo et al. 2018; Valdez-Jiménez et al. 2011). According to Wang et al. (2022), F exposure has a positive relationship with behavioral problems, particularly psychosomatic problems in schoolchildren. Similarly, F affects the growth, mental ability, and intelligence of schoolchildren (Kundu et al. 2015; Xiang et al. 2003; Trivedi et al. 2007; Seraj et al. 2012; Wang et al. 2007; Rocha-Amador et al. 2007).

F is the most electronegative of all the elements and has a significant tendency to gain a negative charge and form F ions in solution (Hem 1989). It has the same charge and radius as hydroxide ions, and they may substitute for one another through ion exchange processes (Raghav et al. 2019). Minerals that contain fluorides such as fluorite (CaF_2), muscovite [$(KF)_2$ $(Al_2 O_3)_3$ $(SiO_2)_6$ $(H_2 O)$], biotite [K $(Mg,Fe)_3$ Al Si_3 O_{10} F_2], cryolite (Na_3 AlF_6), villiamite (NaF) and fluorapatite (Ca_5 $(PO_4)_3$ F), on dissolution and ion exchange, causes elevated F in groundwater (Todd 1980; Adimalla and Venkatayogi 2017; Kraynov et al. 1969; Narsimha and Sudarshan 2017). Temperature, pH, the type of geological formation, and the length of time the water is in contact with it will contribute to the concentration of F in natural waters.

Excessive F levels in groundwater are a major issue for those living in arid and semi-arid areas with high evaporation and low rainfall (Adimalla and Li 2019). Low rates of groundwater recharge may cause lower solubility of $CaCO_3$ minerals, which reduces the Ca concentration and enriches the F content in the groundwater (Vithanage and Bhattacharya 2015). Excessive evaporation of groundwater under tropical conditions causes a decrease in Ca activity with increasing Na/Ca ratios, resulting in higher F levels (Battaleb-Looie et al. 2012; Dissanayake and Chandrajith 2019; Mukherjee and Singh 2020). F levels as high as 650 mg/kg of F can be found in silicate minerals in the earth's crust (Chandrajith et al. 2012; Raju 2017). Few clay minerals (illite, chlorite, and smectites) have good anion exchange medium and can release considerable amounts of F into groundwater (Boyle 1992).

Most of the people in Kerala rely on groundwater for their drinking needs, without any pre-treatment. General groundwater quality studies have been carried out in different parts of the State. However, limited work has been attempted in the area of seasonal release of F and other ionic constituents in the groundwater. The work related to F incidence, particularly in Kerala State, has been reviewed here.

Fluoride concentrations in the groundwater of phreatic aquifers in the Muvattupuzha river basin were found to be within allowable limits (Laluraj and Gopinath 2006). Alleppey, a coastal District with backwater tourism activity was reported to

have a very poor water quality index and F pollution (Raj and Shaji 2017). An average value of 25.88 mg kg^{-1} F was reported in the soil of the Kuttanad region in Kerala (Roshni and Harikumar 2021).

Shaji et al. (2007) reported high F concentrations in shallow and deep aquifers in the Koppanur and Chinnamoolathara regions of the Chittur Block in Palakkad District. According to Kukillaya and Narayanan (2014), the groundwater in the Korayar River basin in the eastern part of the Palakkad District was characterized by high alkalinity, which rapidly precipitated calcium carbonate and promoted F concentration. Sajeeve and Gupta (2017), reported that geogenic factors are responsible for the F contamination in groundwater in Kollengode and Chittur Taluks of Palakkad District. A high degree of weathering is responsible for the changes in the groundwater chemistry of this region. Nitrate and F pollution is relevant in the Chittur Block of the Palakkad District (Gandhi et al. 2008; Shaji et al. 2018). Similarly, Arumugam et al. (2019) reported the prevalence of F in Chittur and Kollengode Blocks of the Palakkad District. The predominance of F with high alkalinity and hardness was observed in groundwater samples around clay mines in the Kannur District (Manoj et al. 2020). The prevalence of dental fluorosis among school children in Malappuram District, Ambalapuzha Taluk of Alappuzha District, and Eruthenpathy Panchayat of Palakkad has been reported by Abraham et al. (2016), Gopalakrishnan et al. (1999) and Diljo et al. (2013), respectively.

1.2.12. Health impact of heavy metals and their source in groundwater

1.2.12.1. Arsenic (As)

Arsenic poisoning attributed to drinking water is one of the world's biggest environmental disasters documented in the last century (Mandal and Suzuki 2002; Wang and Wai 2004). Groundwater pollution is one of the most common routes for humans to be exposed to inorganic As (Chung et al. 2014). Higher concentrations of As have been reported from various parts of the world, and the most significantly affected countries belong to South American and South Asian regions (Kapaj et al. 2006). In Asia, severely affected countries include India, China, Bangladesh, and Pakistan (Shaji et al. 2021). In India, As-related diseases affected millions of people

in West Bengal, who ingest water with more than 10 g/L As (Das et al. 1996; Das et al. 2012; Chakraborti et al. 2016b). Further, the As concentration is dangerously above the permitted levels in drinking water sources of the Indian States such as West Bengal (Acharyya and Shah 2010; Hoque et al. 2012; Dey et al. 2014; Ghosal et al. 2015), Manipur (Chakraborti et al. 2008; Oinam et al. 2011; Chandrashekhar et al. 2014), Uttar-Pradesh (Acharyya et al. 1999; Shah 2010; Yasunori et al. 2012; Srivastava and Sharma 2013; Namrata et al. 2015), Chatisgarh (Patel et al. 2006; Shukla et al. 2010; Patel et al. 2017), Bihar (Saha 2009; Chakraborti et al. 2016a; Singh et al. 2014b; Thakur and Gupta 2019; Kumar and Ghosh 2021), Assam (Chetia et al. 2011; Sailo and Mahanta 2014; Mahanta et al. 2016; Kumar et al. 2016a), Jharkhand (Bhattacharjee et al. 2005; Nayak et al. 2008; Alam et al. 2016; Tirkey et al. 2016), Gujarat (Shirke and Pawar 2015; Wu at al. 2021), Panjab (Hundal et al. 2007; Kumar and Singh 2020). Karnataka (Mamatha and Rao 2010; Mohan et al. 2012a) Madhya Pradesh (Chakraborti et al. 1999; Singh et al. 2020; Bage et al. 2021), Hariyana (Yadav et al. 2020b), Tripura (Bhattacharya et al. 2020), Arunachal Pradesh, Nagaland, and Manipur (Singh 2004; Devi et al. 2009; Shah 2015).

When As contaminates groundwater, it enters the human body and causes serious health problems. The most poisonous inorganic form of As, As (III) enters the body mainly through drinking water. Even As (V) reaches cell membranes, it is reduced to As (III) (Sarkar and Paul 2016). 95% of the ingested As (III) is absorbed through the gastrointestinal tract and most of this toxic inorganic form is converted to organic methylated As by the liver and excreted through urine. The rest of the As is absorbed by the bloodstream and transported to other parts of the body (Saha et al. 1999). Skin illnesses such as pigmentation and hyperkeratosis, as well as skin cancer, are the most prevalent indications of chronic As exposure (Col et al. 1999). Lung cancer, black foot disease, heart, vascular, and renal diseases are among the other health concerns connected to chronic As poisoning (Tseng 2005; Balakumar and Kaur 2009; Ratnaike 2003; Singh et al. 2011a).

The As contamination risk is much greater in groundwater than in surface water (Ayers et al. 2017). Weathering, erosion, and leaching from geogenic sources are the primary sources of As in groundwater (Bhattacharya et al. 1997; Mukherjee et al. 2019; Wang et al. 2021b). It is mostly associated with rocks with high iron oxides, clays, and sulphide mines (Acharyya and Shah 2007; Garelick et al. 2009; Cheng et al. 2009; Jerzykowska et al. 2014). High levels of inorganic As are the characteristics of the groundwater extracted from the sedimentary aquifers (Das et al. 1996; Anawar et al. 2003; Kumar et al. 2016b). Reductive dissolution, alkali desorption, sulphide oxidation, and geothermal conversion are the four main mechanisms of As mobilization to water resources (Ravenscroft et al. 2009; Herath et al. 2016). In the humid, tropical Bengal delta, the As-bearing rocks of the Himalayas are the primary source of As in groundwater, and the mechanism that enhances it is the reductive dissolution of biochemical reactions fueled by the huge organics in the delta (Alam et al. 2002; Mladenov et al. 2010; Chen et al. 2016; Verma et al. 2016; Raessler 2018). Arsenic also enters the atmosphere through anthropogenic activities. The use of As is in industrial activities, metal processing, wood preservatives, weedicides, pesticides, fertilizers, animal feed additives, metal alloys, corrosion inhibitors, semiconductors, and glass manufacture. The majority of As is used in agriculture and as a wood preservative (Han et al. 2003; Wrye 2008; Neumann et al. 2010).

1.2.12.2. Iron (Fe)

Fe is the fourth most prevalent element in the earth's crust, accounting for 5.6 percent (Schmitz Jr 2005). The groundwater contamination of Fe may be from geogenic sources, industrial effluents, or domestic waste (Subba Rao 2008). Fe is required for the formation of hemoglobin, myoglobin, and a variety of enzymes (Sánchez et al. 2017). A shortage of Fe causes anemia and a deterioration in health (Guralnik 2005). It also causes serious health problems such as fatigue, joint pain, hemosiderosis, diabetes, liver cancer, hepatocellular carcinomas, heart disease, liver cirrhosis, and infertility (Mobarra et al. 2016; Palmer et al. 2018). Water with higher

Fe content affects color, taste, and odor, stains on garments, and corrodes water pipelines (Behera et al. 2012; Chaturvedi et al. 2014; Yadav et al. 2019).

Fe contamination of groundwater has been reported in several nations throughout the world, including India (Thakuria and Godboley 2016). High Fe concentrations in groundwater can be found in Bangladesh, Cambodia, China, Egypt, Kenya, Nigeria, several States in the USA, and European countries including the Netherlands and Ireland (Hossain et al. 2013; Ngah and Nwankwoala 2013). Over 1.1 lakh habitations in India have been found to have Fe-contaminated groundwater (Mehta and Srivastava 2012). It has been reported in Assam, Chattisgarh, Karnataka, Orissa, and West Bengal. Confined pockets are detected with Fe contamination in groundwater in Bihar, Uttar Pradesh, Punjab, Rajasthan, Maharashtra, Madhya Pradesh, Jharkhand, Tamil Nadu, Kerala, and in the north-eastern States (Rajmohan and Elango 2005; Kshetrimayum and Hegeu 2016; Subba Rao 2008).

The major source of Fe in groundwater is geogenic (Kushawaha and Aithani 2021). In soils and sediments, especially below 20 cm depth, pyrite is the source of a substantial concentration of free Fe (non-silicate Fe) (Otero et al. 2009). Similarly, laterite contains rich Fe, which may be formed from the degradation of mafic igneous rocks and immature sedimentary rocks such as greywackes (Widdowson 2009). Laterites are formed by severe weathering of aluminosilicate rocks in the World's intertropical zones (Bhukte 2020). Bauxite, an ore of Fe is formed by the weathering of numerous parent rocks, including Khondalite, Deccan Trap basalt, Granite gneiss, Charnockite, and others (Babu et al. 2021). India has vast bauxite deposits and is ranked fifth in the world and the majority of bauxite deposits are found in the eastern ghat region (Bhukte et al. 2021). However, lateritic bauxite deposits can be found in the Indian States of Odisha, Andhra Pradesh, Chhattisgarh, Madhya Pradesh, Maharashtra, Jharkhand, Gujarat, Goa, Karnataka, Kerala, Tamil Nadu, Uttar Pradesh, Rajasthan, and union territory of Jammu & Kashmir (Banerjee 1975; Bhukte et al. 2017; Fortier et al. 2019). Raymahashay et al. (1987) discovered laterite soil deposits near Calicut in Kerala with remarkable flexibility and cation-exchange capability. Other anthropogenic sources such as industries, mining and

related activities, and fertilizer application are reported to be the sources of Fe contamination of groundwater (Elumalai et al. 2017a).

1.2.12.3. Cadmium (Cd)

Cd is classified as carcinogenic to humans by the International Agency for Research on Cancer (IARC) (Satoh et al. 2002). Due to its bio-accumulative property and delayed exhaustion from the body with a half-life range of 20–30 years, it is one of the most dangerous metals providing major health concerns to humans (Rani et al. 2014; Filipic 2012). The Cd comes into the human body via food and water, dermal interaction, smoking, and occupational exposure through inhalation, and ingestion, however, food and water is the important exposure route (Wu et al. 2016; Rehman et al. 2018). Drinking cadmium-contaminated water over time can cause Cd to accumulate in a variety of vital organs and tissues, including the liver, kidneys, immune system, bone, and reproductive organs, but mostly in the kidney cortex, and if cumulative exposure is high enough, it can harm kidneys and bones, as well as cause cancer and cardiovascular disease (Rahimzadeh et al. 2017; Qasemi et al. 2019). The well-known trauma *itai itai* disease in Japan was caused by long-term Cd ingestion through drinking water, and Cd-induced renal tubular dysfunction is still common, progressive, and irreversible in those born between 1914 and 1939 (Inaba et al. 2005; Aoshima 2016). Parkinson's disease, Alzheimer's disease, and Huntington's disease are among the neurodegenerative disorders triggered by Cd (Okuda et al. 1998; Johnson 2001; Panayi 2002).

Cd is a non-essential trace element for humans and other living organisms, and is widely distributed in the earth's crust at low concentrations (1 mg/kg) (Beyer et al. 2000). It is found in trace amounts in different types of rocks, and in coal and petroleum in association with Zn (Thornton 1986; Tabelin et al. 2018; Dickson et al. 2020). The origin of groundwater contamination of Cd in association with soft water is mainly from geo-genic sources (Cui et al. 2016). Its concentration is likely to increase in mining and smelting areas (Hiatt and Huff 1975; Du et al. 2020; Xing et al. 2020). Cd is an uncommon metal, and the mineral greenockite (CdS) and otavite ($CdCO_3$) are the most common types (Thornton 1986; Ye et al. 2012). It is mostly

seen in association with Zn and polymetallic ores, primarily lead-zinc and copper-lead-zinc complexes, with the Cd concentration in the range between 0.3 and 1% (Hiatt and Huff 1975; Schwartz 2000). The anthropogenic sources of Cd pollution include agriculture runoff, industrial emissions, and transportation (Chopra et al. 2009; Li et al. 2016; Vardhan et al. 2019). A higher concentration of Cd, of up to 300 mg/L is present in the phosphate fertilizer (McLaughlin et al. 1995; Al-Shawi and Dahl 1999; Roberts 2014). The high concentration of Cd in the shallow aquifer is due to waste dumps and urbanization, which are well documented (Amadi and Nwankwoala 2013; Shaharoona et al. 2019).

1.2.12.4. Lead (Pb)

Pb enters the biota through a variety of routes, including inhalation of Pb-laden dust, oral consumption of Pb through contaminated water, and ingestion of Pb-infected food and soil (Cao et al. 2011; Levin et al. 2021). Pb can have a variety of harmful effects due to its widespread distribution in the body. However, the skeleton, blood, and soft tissues attain the highest percentage of ingested Pb and form the total Pb burden in the body (Rabinowitz 1991; Babayigit et al. 2016; Goyer and Clarkson 2001). Health effects due to Pb are similar in all age groups, from mild effects such as irritation, eye burn, vomiting, diarrhea, pulmonary irritation, headaches, dizziness, fatigue, and nausea, to more serious difficulties such as allergic dermatitis, occupational asthma, painters' syndrome, lung cancer, reproductive damage, kidney and liver damage (Patocka and Cerny 2003; Matovic et al. 2015; Boskabady et al. 2018; Balasubramanian et al. 2020; Lal et al. 2020). Pb harms physiology, and in some circumstances, human exposure levels have been connected to the development of diabetes and metabolic diseases (Leff et al. 2018). Patients with a blood Pb level of 30 to 80 g/dl experience severe gastrointestinal problems. Similarly, Pb ingestion is the main cause of hepatotoxic effects (Mudipalli 2007). The accumulation of Pb in the tissues of livestock from abandoned mine areas is well documented, and its meat and other food products may also pose a risk to human health (Rumbeiha et al. 2001; Sharpe and Livesey 2005).

Pb is found as a mineral in combination with other elements such as sulphur (PbS, galena) and $PbSO_4$ (anglesite)) and oxygen ($PbCO_3$ (cerussite) (Elizondo-Alvarez et al. 2020). Pb pollution is caused by mining activity in numerous places in the world. For example, in Zamfara State in northern Nigeria, Pb poisoning from artisanal gold mining resulted in the deaths of over 300 people, due to an average concentration of 1270 mg/L Pb in local river water (Mejia 2015). High levels of Pb contamination in groundwater have also been linked to previous magmatic activity and the existence of intrusive and extrusive rocks (Frei 1992; Etuk et al. 2008). In south-eastern China, high Pb concentrations were found in connection with climatic conditions (Wang et al. 2019a). In the Ishiagu zone of south-eastern Nigeria, shale rocks contain about 1.70 mg/L Pb (Odika et al. 2020). Anthropogenic sources such as solid waste incineration emit massive amounts of Pb, particularly in urban areas (Tian et al. 2012). Storage batteries, solders, bearings, cable coverings, ammunition, plumbing, pigments, caulking, and sound and vibration absorbers are made of this metal (Al Hagibi et al. 2018). Pb is well-known as an occupational hazard resulting from the smelting, combustion, production, and disposal of lead-based gasoline, insecticides, glass, and ceramics (Wuana and Okieimen 2011; Gautam et al. 2016; Balasubramanian et al. 2020). Pb pollution in groundwater is reported in several parts of India due to rock-water interaction (Négrel et al. 2010), mining activities (Patel et al. 2006; Nagaraju et al. 2014), waste disposal (Buragohain et al. 2010), diesel fuel (Khan et al. 2010), seawater intrusion due to intensive pumping for agriculture (Vetrimurugan et al. 2017), pesticides (Malyan et al. 2019), and leachate from landfill (Maiti et al. 2016).

1.2.12.5. Nickel (Ni)

Ni is a widely distributed metal, and other than occupational exposure sources it enters the human body mainly through water and food (Duda-Chodak and Blaszczyk 2008). It causes allergies, heart problems, lung fibrosis, kidney problems, and respiratory cancer (Yeganeh et al. 2013). McDermott et al. (2015) reviewed strong associations with birth weight for babies whose mothers were exposed to Ni. Chashschin et al. (1994) noted an elevation in relative risk for both cardiovascular and musculoskeletal defects with Ni exposure. Guo et al. (2010) established a negative association between the placental concentration of Ni and gestational age.

Huang et al. (2011) established a positive link between Ni and neural tube defects. Roberts et al. (2014) found a link between Ni and autism spectrum disorder.

Ni is one of many trace metals that are broadly distributed in the environment. They are being released from both natural and anthropogenic sources and are also from both static and mobile causes (Das et al. 2008). Ni is the 24th most plentiful element in the Earth's crust, accounting for about 3% of the Earth's composition (Barceloux and Barceloux 1999). It is the fifth most abundant element by weight, after iron, oxygen, magnesium, and silicon (Klein et al. 2010). Nickel and its compound have several commercial and industrial uses such as metallurgical, chemical, and food processing (Genchi et al. 2020). Other major uses of Ni are Ni-Cd batteries, electronics, and computers (Sarvi and Masoum 2008). The commercially important Ni compounds are Ni chloride, sulphate, nitrate, carbonate, hydroxide, acetate, and oxide (Barceloux and Barceloux 1999). Ni mainly enters the atmosphere as a result of the combustion of coal and petroleum fuels as well as the incineration of waste and sewage, which gradually enters the soil and groundwater (Navratil and Minarik 2005). Two commercial classes of Ni origin are sulphide ores and silicate oxide (Whittington and Muir 2000). Wind-blown dust derived from the weathering of rocks and soils, volcanic emissions, forest fires, and vegetation are all natural sources of Ni levels in the atmosphere (Cempel and Nikel 2006). Ni laterite deposits are formed by the prolonged and pervasive weathering of Ni silicate-bearing ultramafic rocks, generally in tropical to subtropical climates (Gleeson et al. 2003). It is most abundant in igneous rocks (approximately 0.01%) (Delong 1974; Lightfoot 2016). Pentlandite (FeNi)S, a mineral rich in pyrrhotites and chalcopyrite, provides 90 percent of the world's Ni (Holwell et al. 2017). Ni is also a naturally occurring impurity in some types of asbestos, particularly chrysotile (Gualtieri et al. 2019).

1.2.12.6. Manganese (Mn)

Manganese is a useful metal for human health at a trace level in the diet (Silva et al. 2019). Mn supports the synthesis of amino acids as well as the metabolism of carbohydrates, glucose, and cholesterol. It also helps in bone development and avoids blood clots, and functions as a cofactor in arginase (a key enzyme in urea formation in the liver), pyruvate carboxylase, superoxide dismutase, and

gluconeogenesis (Keen et al. 2000). However, Mn overexposure above 0.10 mg/L in drinking water induces neuron associated dysfunction, leading in emotional instability, cardiovascular toxicity, Parkinson's-like symptoms, hallucinations, and speech disturbance (Afzali et al. 2005; Frisbie et al. 2012; Rutchik et al. 2012; Tuschl et al. 2013). Mn accumulates in bones, with a half-life of about 8–9 years in human bones (O'Neal and Zheng 2015). However, an individual's age, gender, ethnicity, genetics, and pre-existing medical disorders have been shown significant impact on Mn toxicities (Crossgrove and Zheng 2004). Excessive intake of Mn may harm human health (Freeland-Graves et al. 2016; Bowler et al. 2007), with the young and unborn being particularly susceptible (Hafeman et al. 2007; Spangler and Spangler 2009; Wasserman et al. 2011; Bouchard et al. 2011).

The most common source of Mn in the groundwater is the Mn-bearing minerals and rocks in the earth's crust (Devic et al. 2014). Mn exists in two states: Mn (II) is widespread and soluble, and Mn (IV) is more insoluble. Acidic, moist, anaerobic, and organic soil environments favor Mn (IV) reduction to Mn (II) (Sparrow et al. 2014; Jones et al. 2018). Carbonates are very sensitive to weathering in acidic environments, and metals primarily housed by carbonates, such as Mn, are also heavily leached (Butt et al. 2000). Mn(IV/III)-oxides are found as a coat on mineral surfaces and in pore spaces in ultramafic and associated rock sediments and soils (Oze et al. 2007). High Mn enrichment in groundwater was reported in various places in southern China in conjunction with tributary and mainstream floodplains, organic matter-enriched lacustrine sediments, oxbow lake facies, and aquifers with muck or peat (Jia et al. 2018). Domestic sewage, vehicular emissions, metallurgy, pesticides, and atmospheric deposition are all anthropogenic sources of Mn (Fuge 2013). The surface water of the Ganga River near Kolkata, West Bengal, was noted to have a significant concentration of Mn, particularly during the rainy season, at several sites (Aktar et al. 2010). According to Chakrabarty and Sarma (2011), Mn contamination was found in a large number of groundwater sources in the Kamrup District of Assam, India. The CGWB (Central Ground Water Board 2010) of India also observed elevated Mn concentrations in groundwater in West Bengal, Orissa, Andhra Pradesh, Assam, and Telangana.

1.2.12.7. Copper (Cu)

Cu is an essential element for human health and it is generally regarded as nontoxic (Uriu-Adams and Keen 2005). It is the constituent of metalloenzymes, which acts as an electron donor or acceptor (Snyder et al. 2019). It is also necessary for infant development, iron transport, bone strength, host defense mechanisms, red and white cell maturation, cholesterol and glucose metabolism, myocardial contractility, and brain development (Olivares and Uauy 1996). Anemia, neutropenia, and bone abnormalities are the most common clinical manifestations of acquired Cu deficiency (Lazarchick 2012). Other symptoms like hair hypopigmentation, hypotonia, impaired growth, an increased incidence of infections, changes in neutrophil phagocytic capacity, and abnormalities in cholesterol and glucose metabolism are also caused due to the deficiency of Cu. Long long-term exposure to high concentrations can cause other health problems in humans (Olivares et al. 2000; Dietrich et al. 2004; Kisa and Arslan 2021). Higher Cu concentrations cause a variety of hepatic and neurodegenerative disorders as a result of disrupted Cu homeostasis in the body (Gaetke et al. 2014). Wilson's disease is an autosomal recessive genetic disorder in which elevated Cu exposure alters the structure and function of the liver and brain due to Cu accumulation in these organs (Bandmann et al. 2015). According to Desai and Kaler (2008), excess Cu in the human body causes brain injury, mitochondrial damage, DNA breaks, Alzheimer's disorders, and a variety of other neurological disorders.

Cu in groundwater comes from a variety of sources, which include both natural and manmade. The natural sources of Cu are the weathering of rocks and soils, volcanoes, and forest fires (Tabelin et al. 2018). Cu (II) or cupric ion is the most common oxidation state of Cu, forming a coordination bond with six water molecules in a solution (Graddon 2017). The naturally occurring and abundant form of Cu is Cu sulphate (Flemming and Trevors 1989). The concentration of Cu in groundwater depends on several factors, and its dissolution decreases with high pH, clay content, and soil organic carbon (Uchimiya and Bannon 2013).

Mining, refinery, fossil fuel combustion, waste incineration, traffic, fertilizers, and soil amendments are the major anthropogenic sources of Cu (Yetişsin and Kardeş 2021). It has a variety of uses, such as the preservation of wood, agricultural, and

leather products by acting as fungicides (Humphrey 2002). Cu is widely used in electrical equipment, building materials, and as a constituent of many alloys used in jewelry, coins, dental products, and cosmetics such as sterling silver, cupronickel, and constantan (Kumar et al. 2021b). Cu levels in soil profiles and sediments have risen as a result of rapid industrialization and urbanization (Yang et al. 2014). The use of inorganic fertilizers and manure in agriculture increased the amount of Cu in the soil (Dogra et al. 2020). Cu contamination was reported in the nearby groundwater of the Valiathura sewage farm in Kerala (Varghese and Jaya 2014), Nedumkandam Panchayat in the Idukki District of Kerala (Rejith et al. 2009), and the Kadinamkulam estuary region in the Trivandrum District of Kerala (Sasidharan and Jaya 2021).

1.2.12.8. Zinc (Zn)

Zn is a trace element (micronutrient) that is required in minute quantities but in critical limits in both plants and animals (including humans). It functions as a catalyzer during enzyme activity and regulates gene expression (Chasapis et al. 2012). It is a structural component of many enzymes and proteins, including metabolic enzymes, transcription factors, and proteins involved in cellular signaling (Stefanidou et al. 2006). Excessive Zn exposure can result in gastrointestinal symptoms, headaches, and impaired immune function (Fosmire 1999). Similarly, Zn deficiency also causes oligospermia in males, decreased serum testosterone in males, hyperammonemia, and impaired neuropsychological functions (Prasad 2004). The zn concentration of groundwater in many studies conducted in India was reported to be below the detectable level to within the standard limits prescribed by the BIS (Borah et al. 2009; Rajappa et al. 2010; Singh et al. 2012; Krishan et al. 2021). However, a higher concentration of Zn, which exceeded the EPA's allowable limit, was noticed in the groundwater in the Palar and Cheyyar river basins in south India, during the Pr period (Rajmohan and Elango 2005). The elevated concentration of Zn in leachate from the cement factory (Egbe et al. 2017; Raja et al. 2021; Ipeaiyeda and Obaje 2017) and the sewage sludge (Singh and Agrawal 2008; Kang et al. 2011) are also reported to cause groundwater contamination. Hydroxyl-containing FeZi-Mg-silicates are important host minerals for Zn in granites and gneisses (Heinrichs

et al. 1980). It is commonly found in conjunction with Mn, Co, and Ni (Vodyanitskii 2009).

1.3. Materials & Methods

1.3.1. Study area

1.3.1.1. Palakkad

Palakkad District of Kerala State, India, lies between 10° 24′ N and 11° 14′ N latitudes and 76° 02′ E and 76° 54′ E longitudes. It covers an area of 4,478 km^2 and lies between the gaps of the Western Ghats, a mountain chain, and encompasses a vast expanse of plains with intermittent hills and mountains. Physiography of the District includes high land, midland, and low land, extending to 48, 33, and 19%, respectively. Major land-use types include cultivated areas (46.5%), forests (31%), areas of non-agricultural use (12%), and others (10.5%) (Source: www.ecostat.kerala.gov.in). Bharathapuzha, the largest river in the State, flows through the District from east to west.

Kerala, referred to as the 'Gateway of the south-west monsoon to India' experiences three seasons; Pre-monsoon (Pr), monsoon (Mo), and post-monsoon (Po). The Pr extends from February to May, during which the rainfall will be less (361.5 mm in 2019) and the temperature reaches its highest record (40°C in 2019) (IMD). The Po season spans from October to January and during this period the average rainfall will be moderate (491.6 mm in 2019) and the temperature will be the lowest (34°C in 2019), which is below the monsoon temperature (35°C). The normal monsoon, extending from June to September, is with an average rainfall of 2049 mm (Pai and Nair 2009).

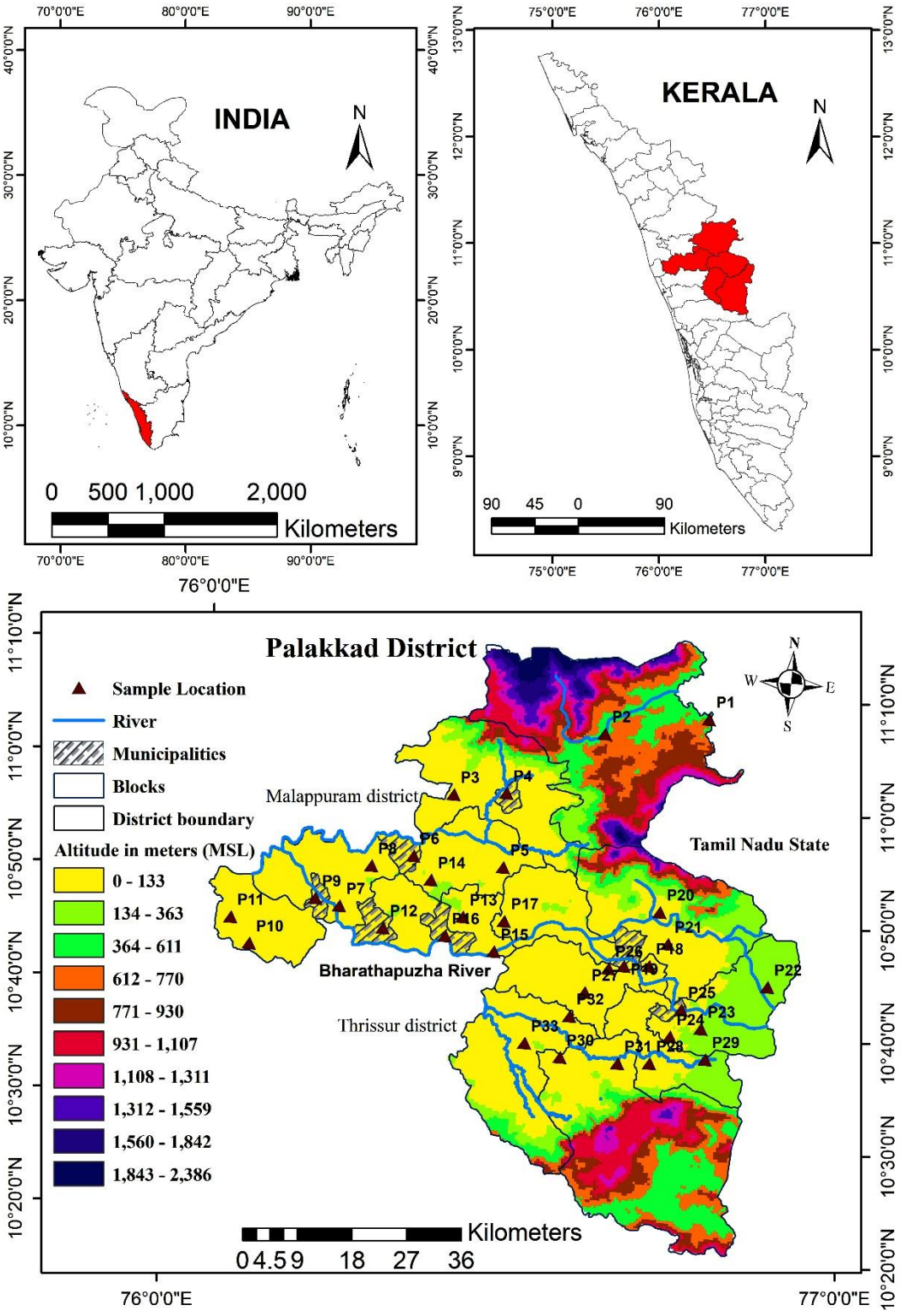

Fig. 1.3.1 Map of Palakkad District showing terrain, altitude, demographic demarcations, sampling sites, and major Rivers and streams

The District also experiences two micro-climatic conditions, which are humid towards the west and semi-humid to dry towards the east. The dry climate of the District is attributed to the gap in the Western Ghats mountain chain and the influence of semi-arid climatic conditions of Tamil Nadu State, situated in the east (Gunnell 1997). The ambient temperature recorded in the study area was 20°C to 45°C. The rainfall pattern shows wide variation in the District, with high rainfall (7000 mm) in the west to low (700 mm) in the east (Satish Kumar et al. 2016). The average annual rainfall from 2014 to 2018 was 2069.98 mm and 1951.8 mm in the study period (2017–2018) (IMD). Similar to rainfall patterns, groundwater availability is higher in the western and lower in the eastern part of the District (Shaji et al. 2018). Land slopes from northeast to west as well as from southeast to west forming the Barathapuzha river basin at the center of the District, which in turn flows from east to west. The highest elevated places are the Anginda Peak of Silent valley mountain ranges (2258 Meters from MSL) in the northern region and the Padagiri Peak in the eastern part of the District. The lowest altitude is found in the south-western stretch of the Bharathapuzha River basins (Fig. 1.3.1)

1.3.1.2. Malappuram

Malappuram District is the land of hills and valleys that lies between 10º 40¹N and 11º 32¹N and latitudes and 75º 50¹ E and 76º 36¹ E longitudes. This District covers a geographical area of 3554.34 km² with three major Rivers; the Chaliyar River which marks the northern border of the District, the Bharathapuzha River at the southern border, and the Kadalundi River which drains through the middle of the District (Fig. 1.3.2). The District has a total forest area of 758. 8684 km², in which 325.3261 km² is reserve forests and the rest is vested forest distributed in Nilambur, Wandoor, and Perinthalmanna Block Panchayats in the Western Ghats. Physiography of the District includes low land (3%), midland (80%), and high land (17%). Major land-use types include cultivated areas (50.6%), forests (21.3%), areas of non-agricultural use (12.7%), and others (15.4%) (Source: www.ecostat.kerala.gov.in).

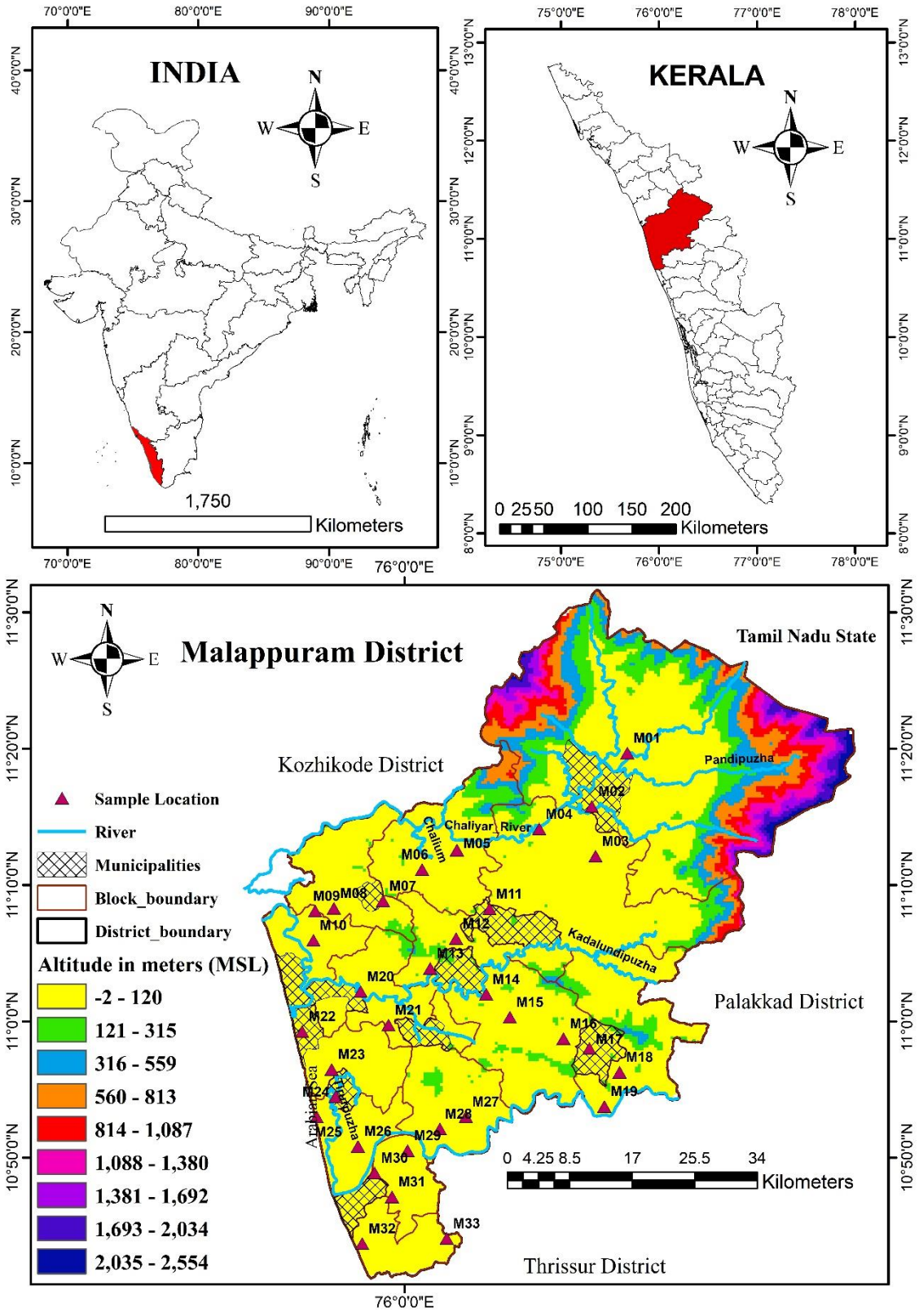

Fig. 1.3.2 Map of Malappuram District showing terrain, altitude, demographic demarcations, sampling sites, and major Rivers and streams

Tropical humid with moderate temperature and heavy rainfall during Mo is the general climatic condition in Malappuram District. There are three monsoonal seasons, which are Pr (February to May), Mo (June- September), and Po (October-January) (Pai and Nair, 2009). The maximum ambient temperature in the study area recorded from 2014 to 2018 was 38ºC during February and March and the minimum temperature recorded was 18ºC during December-January (2014-2018). Similarly, the average annual rainfall from 2014 to 2018 was 2640.62 mm. and the highest rainfall occurred was 3658.5 mm in 2018 (Source: https://mausam.imd.gov.in/). The rainfall recorded during the study period was 2450.9 mm.

The base map of the area has been prepared using toposheets and satellite imageries from Geo-portal Bhuvan. Digitization and thematic map preparations were carried out in ArcMap.10.3.1. The two Districts are found to be ideal for the study of the overall groundwater quality in terms of terrain and climatic conditions as they are representatives of inland and coastal land masses. Also, a comprehensive study on the physicochemical and biological properties of groundwater with special reference to Flouride, Arsenic, and other heavy/trace metals with special reference to the monsoonal pattern was carried out. This would be of great interest in terms of public health, as they form the primary source of drinking water. Also, GIS interpolation models to represent groundwater pollution indices related to these regions are limited. Hence the study is highly helpful for an in-depth understanding of the groundwater quality of the two Districts and in proposing management measures for their conservation.

1.3.2. Selection of sampling networks in Palakkad and Malappuram Districts.

To make an exact representation of samples from the entire District, stratified random sampling was adopted. Different Block Panchayats and Municipalities were considered as different strata and unbalanced stratified random samples were collected from each strata. Thirty-three sources from each District were selected as sampling sites. Accordingly, a total of 66 groundwater sources were selected from Palakkad and Malappuram Districts. The coordinates of collection and monitoring sites were marked with GPS essential software.

1.3.3. Measurement of groundwater table fluctuation

To assess the fluctuation in the water table within the monitoring network, open wells were selected. Accordingly, 15 open wells from the Palakkad District and 27 from the Malappuram District were monitored. Bore wells were eliminated from such investigations as water level measurements were practically difficult. The water level concerning such regions was measured with the help of available groundwater-yielding structures known as 'kokkarni'. Two-time observations were made in each season and accordingly, 6 observations (March & May in Pr, July & September in Mo, and November & January in Po) were made in the year-round monitoring. The groundwater levels were measured with a graduated rope with a weight at the end. Utmost care was taken while measuring the groundwater level using the graduated rope, as sensible observations were needed to assess the point at which the weight at the other end of the rope touches the bottom of the well. Accordingly, measurements concerning the total depth of the well from the ground level, the depth of water level from the ground level, the collar height, the depth of the water column, and the diameter of the well were made.

1.3.4. Groundwater resource assessment

Groundwater assessment helps to identify and estimate the groundwater potential zones of an area. Groundwater Estimation Committee (GEC) constituted by Central Ground Water Board (CGWB) established a refined methodology for evaluating the groundwater level in India. Various government agencies and research institutes follow this standard methodology to evaluate groundwater levels. It is expressed as meters below ground level (mbgl). In the present study, open wells are considered for water level monitoring which is in the unconfined aquifers/semiconfined aquifers in the study area. To assess the water level in bore well-dominated areas, water table measurements were taken from water harvesting structures such as "Kokkarni", a wide, deep, square-shaped open well mainly used for irrigating agriculture areas. As per GEC 2012, the assessment of groundwater resources in semi-confined and confined aquifers is similar. Henceforth the assets accessible under tension are just considered as the groundwater potential for the semi-confined aquifer. The change

or dynamics of the groundwater can be assessed as the product of i) Area of the semi-confined aquifer (m^2) 'A' ii) Specific yield, 'S' iii) Fluctuation in the piezometric head between the Pr 'hPr' and Po 'hPo' seasons. The specific yield is usually represented in percentages (Table 1.3.1).

Table 1.3.1: The specific yield based on the type of geological material in percentage (Kumar and Seethapathi 2002).

Sl. No	Formation	Recommended Value (%)	Minimum Value (%)	Maximum Value (%)
(a)	**Alluvial areas**			
	Sandy alluvium	16.0	12.0	20.0
	Silty alluvium	10.0	8.0	12.0
	Clayey alluvium	6.0	4.0	8.0
(b)	**Hard rock areas**			
	Weathered granite, gneiss, and schist with low clay content	3.0	2.0	4.0
	Weathered granite, gneiss, and schist with significant clay content	1.5	1.0	2.0
	Weathered or vesicular, jointed basalt	2.0	1.0	3.0
	Laterite	2.5	2.0	3.0
	Sandstone	3.0	1.0	5.0
	Quartzite	1.5	1.0	3.0
	Limestone	2.0	1.0	3.0
	Karstified limestone	8.0	5.0	15.0
	Phyllites, Shales	1.5	1.0	2.0
	Massive poorly fractured rock	0.3	0.2	0.5

Accordingly, groundwater availability for both Palakkad and Malappuram was calculated. For computational purposes, the block panchayat and municipal area (m^2) were considered as a single unit. The average piezometric head of each unit in Pr and Po in MSL (Mean Sea Level) was considered for the calculation. About 19 water table measurements from Palakkad and 29 from Malappuram District were taken during the Pr and Po seasons. The type of soil and rock in the study area was noted during the field visit. Secondary data from the published source was also used to estimate the major mineral type in the study area and was noted to be Gneiss-type, which includes charnokite gneiss and biotite gneiss. Hence 3% was considered the standard value for specific yield for charnokite gneiss and biotite gneiss, as recommended by Kumar and Seethapathi (2002).

Change in groundwater storage in the semi-confined area (ΔY) = SA (hPr - hPo)

1.3.5. Collection and preservation of water sample

A bimonthly collection of water samples from both Palakkad and Malappuram District, representing the Pr, Mo, and Po seasons of the year (2017-18) were carried out. 33 groundwater samples (16 dug wells and 17 bore wells) from Palakkad and 33 from (28 dug wells and 5 bore wells) Malappuram District were collected. From each site, samples were collected in two 1L capacity PET bottles, previously washed in acidic water, followed by distilled water, and further rinsed with the sample, before collection. Raw water was collected in one bottle. Another bottle was acidified with nitric acid (pH < 2) immediately after the collection of the sample to lower the pH to arrest the bacterial action, minimize precipitation, and avoid adsorption on the walls of the PET bottle. Samples for dissolved oxygen estimation were collected in DO bottles and reagents were added on the spot to fix the DO. For the microbial estimation, samples were collected in a sterilized plastic bottle of 25ml capacity and it was stored in an ice box. Proper labeling was given on the samples such as name and location, type of well, date and time of sample collection, etc.

1.3.6. Estimation of physicochemical and biological parameters

Electrical Conductivity (EC), pH, and Total Dissolved Solids (TDS) were assessed onsite using a Eutech cyber scan (PCD, 650). The rest of the physicochemical parameters were analyzed in the laboratory, within the time limit as prescribed in APHA. Heavy metals such as Cu, Cd, Pb, As, Ni, Mn, and Zn were estimated by atomic absorption spectroscopy (Shimadzu AA 7000). All the samples were subjected to the analysis of quality parameters, following APHA – AWWA- WPCF (1998) as given below.

1.3.6.1. pH (Electrometric method)

pH is the measure of the intensity of acidity and alkalinity and measures the concentration of hydrogen ions in a solution.

The pH was measured in a Systronics MK IV model device. The instrument was calibrated with buffer solutions of pH 4 and pH 9 before sample measurement. The probe was rinsed with distilled water, blotted dry, and immersed in the sample and the reading from the digital display was noted in the data book.

1.3.6.2. Turbidity

It is an optical property of a liquid that either scatter or absorb light rather than transmitting it in a straight line due to the presence of suspended and dissolved solids in it. The scattering and absorption are directly proportional to the suspended and dissolved solids in it. Nephelometer (Systronics, Model 341) was used to measure the turbidity and expressed in NTU.

Preparation of turbidity standard solution

1 g of hydrazine sulphate was dissolved in double distilled water and made up to 100 ml (a). 10 g of hexamethylenetetramine was dissolved in distilled water to prepare 100 ml of solution (b). Then 5 ml of each of the above solutions (a & b) were mixed in a 100 ml standard flask and kept for 24 hours at 23°C. Then it was made up to 100 ml to make 400 NTU solution having a one-month shelf life.

Standardization and measurement

The instrument was standardized with 40 NTU solutions by appropriate dilution of the standard solution. The sample was shaken thoroughly and kept for a while to eliminate air bubbles. The sample was then taken in a nephelometer sample tube and kept for instrumental reading.

1.3.6.3. Temperature

The temperature of the water samples was measured at the collection site. A digital thermometer with an accuracy of ±0.01°C was used to measure the temperature.

1.3.6.4. Electrical conductivity (EC)

It is the measure of the capacity of the aqueous solution to convey the electrical current. EC is directly proportional to the dissolved minerals in the water. The electrical conductivity is highly influenced by the temperature of the aqueous solution.

The EC was measured on-site with a Eutech cyber scan water quality analyzer (Eutech PCD 650). The instrument was calibrated in the laboratory before experimentation. The probe was well-rinsed with distilled water and blotted to dry and inserted into the sample. The reading was taken from the digital display when it became stable. The results are represented as micro Siemens (µS) per unit area.

1.3.6.5. Salinity

It is the measure of all the salts that are dissolved in the water. Salinity influences the quality and taste of water. At high concentrations, it exhibits scaling in pipes, vessels, and utensils. The salinity of the present study was measured on-site using a Eutech cyber scan water quality analyzer (Eutech PCD 650). The results are represented in ppm.

1.3.6.6. Total Solids (TS) (Gravimetric analysis)

Total solids are the residue left after evaporation and drying of the unfiltered sample at a definite temperature. Total solids include both suspended as wells and dissolved. The groundwater contains mostly mineral matter in dissolved conditions.

50 ml of thoroughly mixed unfiltered sample was pipetted in a pre-weighed porcelain dish. The content was dried in an oven at 105°C and weighed.

Calculation

$$\text{Total Solids (mg/L)} = \frac{(B - A) * 1000 * 1000}{\text{Volume of sample}}$$

Where, A = pre- weight of empty dish in gram

B = weight after drying and cooling the sample residue + dish in gram

1.3.6.7. Total Dissolved Solids (TDS) (Gravimetric analysis)

TDS is determined as the residue left after the evaporation of the filtered sample. TDS is directly proportional to the mineral content of the water. The amount of dissolved solids present in water is a consideration for its suitability for use. It determines the taste of drinking water.

The sample was filtered through Whatman No. 1 filter paper. 50 ml of the filtered sample was taken in a pre-weighed porcelain dish. The content was dried at 105°C and weighed after cooling in a desiccator.

Calculation:

$$\text{TDS (mg/L)} = \frac{(B - A) * 1000 * 1000}{\text{Volume of sample}}$$

Where, A = pre- weight of empty dish in gram

B = weight after drying and cooling the sample residue + dish in gram

1.3.6.8. Total Suspended Solids (TSS) (Gravimetric analysis)

TSS represents the suspended particles present in the water sample. Generally, these impurities are organic. The difference between Total Solids (TS) and Total Dissolved Solids (TDS) determines TSS.

TSS (mg/L) = TS-TDS

1.3.6.9. Acidity (Titrimetric Analysis)

It is the measure of the capacity of water to neutralize hydroxyl ions and it is expressed in terms of calcium carbonate. In natural water, acidity is mainly caused by the free carbon dioxide. Mineral acids such as sulphuric, Iron, and aluminum salts hydrolyze in water to release acidity. Surface and groundwater attain acidity through humic acid either from natural sources or industrial and domestic wastes.

Reagents

Phenolphthalein indicator

Sodium hydroxide (0.02 N)

4 grams of AR sodium hydroxide is dissolved in distilled water and made up to 100 ml in a standard flask to get 1N NaOH. 20 ml of this 1N solution was taken in a 1000ml standard flask and diluted up to the mark to prepare 0.02 N NaOH. It was standardized with oxalic acid for accurate normality.

To 50 ml of a sample taken in a conical flask, 2 drops of phenolphthalein were added and titrated against standard NaOH (0.02N) until the color turned pink.

Calculation

$$\text{Acidity as CaCO3 (mg/L)} = \frac{\text{V NaOH} * \text{N NaOH} * 1000 * 50}{\text{Volume of sample}}$$

Where V is the Volume and N is the Normality

1.3.6.10. Alkalinity (Titrimetric Analysis)

Alkalinity is the measure of the total capacity of water to neutralize the strong acid. The alkalinity is imparted by salts of carbonates, bicarbonates, phosphates, nitrates, and silicates together with hydrogen ions in the state.

Reagents

1. Sulphuric acid (0.02 N)

2.8 ml concentrated sulphuric acid was taken in a 100 ml standard flask and gradually added carbon-dioxide-free distilled water and made exactly up to the mark. 20 ml of this 1N H_2SO_4 was taken in a 1000 ml standard flask and made to obtain 0.02N H_2SO_4. It was standardized against a 0.02 N sodium carbonate solution.

2. Mixed Indicator

20 mg methyl red and 100 mg Bromo cresol green are dissolved in 100 ml 95% of the ethyl or isopropyl alcohol.

To 50 ml of the sample in a conical flask, 4 drops of the mixed indicator were added and titrated against standard sulphuric acid (0.02N) (to pH 4.6) to a light pink color.

Calculation

$$\text{Alkalinity as CaCO3 (mg/L)} = \frac{(\text{V} * \text{N}) \text{ of Sulphuric acid } * 1000 * 50}{\text{Volume of sample}}$$

Where V is the Volume and N is the Normality

1.3.6.11. Hardness (Titrimetric Analysis)

The capacity of water to reduce or destroy the lather of soap is known as hardness. In natural water, hardness is caused by the accumulation of salts from the soil and geological formations or natural sources. Hardness is generally caused by calcium and magnesium ions. Polyvalent ions of some other metals like strontium, iron, aluminum, zinc, and Mn can also precipitate soap. However, these ions are generally

less in natural water, and hence hardness is generally measured as the concentration of calcium and magnesium. In an alkaline medium, EDTA reacts with Ca^{2+} and Mg^{2+} ions to form a soluble chelated complex of wine-red color with EBT at a pH of about 10.

Reagents

1. EDTA solution (0.01M)

3.723g of EDTA was dissolved in distilled water and made up to 1000 ml. It was then stored in the pyrex bottle.

2. Buffer Solution

16.9 g of ammonium chloride was dissolved in 143 ml of concentrated ammonium hydroxide. 1.179 g of disodium salts of EDTA and 0.78g of $MgSO_4$ $7H_2O$ was dissolved in 50 ml of distilled water. These two solutions were mixed and made to 250 ml with double distilled water.

2. Eriochrome Black T (EBT) indicator

0.4g of EBT was ground well with 100g NaCl and stored in a moisture-free container.

To 50 ml of water sample in a clean conical flask, 1 ml of buffer solution was added and followed by a pinch of EBT indicator. It was immediately titrated against standard EDTA (0.01M) until the color turned from wine red to blue. The whole titration was completed in 5 minutes after the addition of the buffer.

Calculation

$$\text{Hardness (mg/L)} = \frac{\text{V EDTA} * \text{M EDTA} * 100 * 1000}{\text{V sample}}$$

Where V is the Volume and M is the Molarity

1.3.6.12. Calcium (Titrimetric Analysis)

The source of calcium in natural water is geological deposits like limestone, dolomite, gypsum, and other gypsiferous materials. Calcium and magnesium are the major scale-forming minerals in the groundwater. To estimate calcium, the sample has to have a sufficiently high pH (12-13) to precipitate magnesium. Therefore only calcium is allowed to react with EDTA in the presence of a murexide indicator.

Reagents

1. Sodium hydroxide 1N: 4 g of NaOH was dissolved and made to 100ml.
2. Murexide (Ammonium purpurate): 200 mg of murexide was ground well with 100g of solid sodium hydroxide
3. EDTA (0.01M)

2 ml of sodium hydroxide solution was poured into 50 ml of the sample taken in a conical flask to attain a pH of 12-13. A pinch of murexide indicator was added and immediately titrated with the standard EDTA taken in a burette. The endpoint showed the color change from pink to purple.

Calculation

$$\text{Calcium (mg/L)} = \frac{\text{V EDTA} * \text{M EDTA} * 100 * 1000}{\text{V sample}}$$

Where V is the Volume and M is the Molarity

1.3.6.13. Magnesium

Magnesium salts occur in significant concentrations in natural waters, especially in groundwater. Similarly, sea and estuary water contains a high concentration of magnesium. The industrial and commercial use of magnesium is numerous and therefore the occurrence of magnesium in industrial wastewater is common. It was determined by finding the difference between the total hardness and calcium.

$$\text{Magnesium as CaCO3 (mg/L)} = \text{Total hardness (mg/L)} - \text{Calcium hardness (mg/L)}$$

1.3.6.14. Chloride (Argentometric method)

It is a common anion present in groundwater. The concentration of chloride in natural water varies from a few milligrams to several thousand milligrams. Higher concentrations of chloride in groundwater may be due to seawater intrusion, industrial effluents, sewage, and brines. Silver nitrate reacts with chloride ions to form a silver chloride complex which precipitates rapidly. In the completion of this reaction, silver nitrate reacts with potassium chromate to form the silver chromate complex, which is brick red.

Reagents

Standard silver nitrate (0.0141N)

2.396 g of silver nitrate is dissolved and made to 1000 ml in a volumetric flask. Standardized it against standard sodium chloride solution (0.0141N). It was then stored in an amber bottle to avoid the reaction with light.

Potassium chromate indicator

25 g of potassium chromate was dissolved in 100 ml of distilled water. A few drops of silver nitrate were added until a red precipitate is formed and it was kept for about 12 hours and filtered and the filtrate was made to 500ml.

To 50 ml of the sample taken in a porcelain basin, 0.5 ml of potassium chromate was added as an indicator. The content was titrated against the standard silver nitrate (0.0141N) to the endpoint. The content was stirred vigorously during the titration to avoid the clumping of the precipitate. A blank titration with distilled water was also conducted.

Calculation

$$\text{Chloride (mg/L)} = \frac{(\text{V silver nitrate for sample} - \text{V silver nitrate for blank}) * \text{N silver nitrate} * 35.45 * 1000}{\text{V sample}}$$

Where V is the Volume and N is the Normality

1.3.6.15. Sodium and potassium (Flame photometric method)

Sodium and potassium (Flame photometric method)

Sodium ions in natural water are ubiquitous. It is present in natural water from negligible to significant quantities. Its combination with other anions such as chloride, sulphate, and F in excess quantities makes the natural water unpalatable. Potassium ranks seventh most abundant element on the earth, but its concentration in natural water is trivial.

Reagents

Stock sodium solution (1000 mg/L) - AR sodium chloride was preheated at 140°C for an hour and 2.524 g was accurately weighed and dissolved in deionized water and made to 1000ml in a volumetric flask. From this Intermediate sodium solution (100 mg/L) and Standard sodium solution (10 mg/L) were prepared.

Stock potassium solution (1000 mg/L) – Dissolve 11.9070 g of dry potassium chloride in 250 ml. of deionized water. Dilute to 1000 ml in a volumetric flask with deionized water. From this intermediate potassium solution (100 mg/L) and standard potassium solution (10 mg/L) were prepared.

The flame photometer (Systronics, 128) was calibrated with the lower and higher concentration of standard sodium/ potassium solutions. The sodium and potassium in the samples were estimated after the calibration of the instrument. The results were noted from the digital display.

1.3.6.16. Sulphate (Turbidimetric method)

Sulphate occurs in natural water as a result of leaching from gypsum and other minerals. Sulphates are added to the water sources through various treatment processes. It contributes total solids in water. Sulphate ions are precipitated as barium sulphate crystals of uniform size. The light absorbed by the precipitate is measured using a spectrophotometer.

Reagent

Conditioning reagent: 75 g of sodium chloride was dissolved in 300 ml distilled water followed by 30 ml of concentrated HCl, 100 ml of 95% ethyl alcohol, and 50 ml of glycerol were added and mixed it well.

Barium chloride: crystal of 20 to 30 mesh.

Standard sulphate solution: 0.1479 g of Na_2SO_4 was dissolved in distilled water and diluted to 1000 ml in a standard flask (1 ml = 100 µg of sulphate). A set of standard sulphate solutions was prepared by diluting it to yield 0.0, 2.5, 5.0, 10.0, 15.0, 20.0, and 30.0 mg/L of sulphate.

To 100 ml of standard sulphate solution and samples, 5 ml of conditioning reagents were added and mixed well using a magnetic stirrer. The speed of the stirrer was maintained the same for standards and samples. While stirring 0.5 g of barium chloride was added and continued stirring for exactly a minute. The spectrophotometer was calibrated using a blank before taking the measurements at 420 nm. Standard solutions followed by blank were poured into an absorption cell of the calibrated spectrophotometer and the optical density was measured at 30-minute intervals for 4 minutes to get the maximum turbidity value. A calibration curve was plotted based on the optical density of the standard solution. The concentration of sulphate in samples was measured from the standard curve.

1.3.6.17. Nitrate (Brucine method)

Nitrate is the end product of the aerobic stabilization of organic nitrogen and it occurs generally in trace quantities in surface water but may attain high concentration in some groundwater. Waste from chemical fertilizer manufacturing factories and fertilizer application in agricultural land may leach from the cesspool to contribute to the nitrate n the groundwater. Nitrate ions react with brucine in the strong sulphuric acid solution to form yellow color which can be measured at 410 nm.

Reagent

Nitrate stock solution - Dissolved 722 mg of KNO_3 (previously dried at 105°C for 24 hours) in distilled water and diluted with 1000 ml in double distilled water (1ml= 0.1 mg nitrate)

Nitrate standard solution - 10 ml of the stock solution was diluted to 100 ml with double distilled water to yield 10 mg/L nitrate solution.

Brucine sulphanilic acid solution -1 g brucine sulphate and 100 mg sulphanilic acid were dissolved in 70 ml hot distilled water and 3 ml con. HCl was added and cooled and diluted to 100 ml with distilled water.

Sulphuric acid solution – To 75 ml of distilled water, 500 ml of concentrated sulphuric acid was added and cooled at room temperature.

To a series of 50 ml beakers pipetted 0.5, 1.0, 1.5, 2.0, 2.5, 3.0, 3.5, 4.0, 4.5, 5.0 ml of nitrate standard solution and each standard solution was diluted with 5 ml distilled water. 5 ml of distilled water was taken as the blank. 5 ml of samples were taken in a 50 ml beaker. 1 ml of brucine sulphanilic acid solution was added to blank, standards, and samples and mixed well. 10 ml of sulphuric acid solution was taken in the second series of 50 ml beakers and the first series beaker with blank, standard, and samples were transferred to the second series. This process was repeated 4 to 6 times and ensured the complete mixing. The beakers were kept for 10 ±1 minutes in the dark. 10 ml of distilled water was added and cooled in the dark for about 20 – 30 minutes. After calibrating the instrument with blank. The standard and samples were measured at 410 nm. A calibration curve was prepared using the absorbance value of standards and the concentration of unknown samples was derived.

1.3.6.18. Inorganic Phosphate (Stannous chloride method)

Phosphate may occur in both groundwaters and surface water as a result of leaching from mineral ores, agricultural run-off, municipal sewage, or industrial discharge. The phosphate in water occurs in different forms; orthophosphate (soluble form),

condensed phosphate, and organic phosphate. The orthophosphate and condensed phosphate together form inorganic phosphate.

Reagents

Ammonium molybdate solution – 25 g ammonium molybdate was dissolved in 200 ml distilled water. In 400 ml distilled water 280 ml of con. Sulphuric acid was carefully added and cooled. In this diluted acid solution, molybdate solution was carefully added and diluted to 1000 ml.

Stannous chloride solution – Dissolved 2.5 g fresh stannous chloride solution in 100 ml glycerol and kept in a water bath and mixed with a glass rod.

Phenolphthalein indicator

Sulphuric acid- nitric acid solution – Carefully add 75 ml of concentrated sulphuric acid to 150 ml distilled water and cool. 1 ml of concentrated nitric acid was added and diluted to 250 ml.

Phosphate stock solution – To 1000 ml volumetric flask, 439 mg of potassium dihydrogen phosphate (KH_2PO_4) was added and made up to 100 m to yield 100 mg/L phosphates.

Standard phosphate solution – 10 ml phosphate stock solution was pipetted to a volumetric flask and diluted to 1000 ml to yield 1 mg/L of phosphate.

Preparation of standard curve

A series of the working range up to 20 µg phosphate and a blank was taken in a 100 ml Nessler tube and diluted to 100 ml.

100 ml of clear sample was taken in a beaker and a drop of phenolphthalein was added to check for the alkalinity. In the presence of alkalinity, it was neutralized with the addition of sulphuric acid-nitric acid solution. 1ml excess of this reagent was added and gently boiled for about 90 minutes and the volume was kept between 25-50 ml during boiling. The sample was cooled and neutralized with a 6N sodium

hydroxide solution using phenolphthalein as an indicator. Made up the content volume to 100 ml.

To the blank, standard, and sample, 4 ml ammonium molybdate solution and 0.5 ml stannous chloride solution were added and mixed well and kept for 10 minutes. Just after 10 minutes and before 12 minutes it was measured at 690 nm in a spectrophotometer. Prepared the calibration curve and inorganic phosphate was calculated.

1.3.6.19. Fluoride (SPADNS METHOD)

F contributes to any combination of elements containing F ions. In its elemental form, fluorine is a pale yellow, highly toxic, and corrosive gas. In nature, fluorine is found combined with minerals as F.

Reagents

1. Stock F solution (100 mg F-/L): 221 mg anhydrous sodium F (NaF) was dissolved in distilled water and diluted to 1000 ml.
2. Standard F solution: (10 mg F-/L): 100 ml of the F solution pipetted out and diluted to 1000 ml.
3. SPANDS solution: 958 mg SPADNS (Sodium 2 (Para Sulphophynylazo) -1, 8-dihydroxy 3, 6-naphthalene disulphonate) was dissolved in distilled water and diluted to 500 ml.
4. Zirconyl-acid reagents: 133 mg zirconyl chloride octahydrate ($ZrOCl_2$ $8H_2O$) was dissolved in about 25 ml distilled water.
5. Acid zirconyl- SPADNS reagents: Equal volumes of SPADNS solution and zirconyl-acid reagents were mixed thoroughly.
6. Reference solution: 10 ml SPADNS solution was added to 100 ml distilled water. 7 ml concentrated HCl was diluted to 10 ml and added to the diluted SPADNS solution.

Preparation of standard curve: A set of standard F solutions were prepared in the range of 0 to 2.0 mg F-/L by diluting appropriate quantities of standard F solution with distilled water in a 50 ml Nessler tube. To each standard 10 ml of acid zirconyl-SPADNS reagents were pipetted and mixed well. The spectrophotometer was set to zero absorbance with the reference solution. Absorbance readings were obtained for all standards at 570 nm and a standard graph was prepared.

Estimation of F: Place 50 ml or an aliquot of the sample diluted to 50 ml with distilled water in a Nessler tube. Add exactly 10 ml of acid zirconyl- SPADNS reagent and mix well. The spectrophotometer was set to zero and the absorbance was taken immediately after the addition of the reagents. Find the F concentration from the standard curve and express it in mg F /L.

1.3.6.20. Dissolved oxygen

Oxygen is dissolved in most water in varying concentrations. The dissolved oxygen present in the groundwater is comparatively much lower than the surface water due to little or lack of contact with atmospheric air. The solubility of the oxygen depends on the temperature, pressure, and salinity of the water. The iodometric and electrometric methods are equally good to estimate oxygen in the water. This iodometric method was used to estimate the dissolved oxygen concentration in groundwater. The basic Winkler method is used to determine the DO.

When manganous sulphate is added to the sample containing alkaline potassium iodide, manganous hydroxide is formed, which is oxidized to the manganic oxide by oxygen present in the sample. This manganic oxide liberates iodine equivalent to the oxygen in the sample with the addition of sulphuric acid.

Reagents

1. Manganese sulphate: 90 g of manganous sulphate monohydrate is dissolved in distilled water filtered and diluted to 250 ml.

2. Alkaline-iodide-azide: 175 g of potassium hydroxide and 37.5 g of potassium iodide were dissolved in distilled water and diluted to 250 ml.

3. Concentrated sulphuric acid

4. Sodium thiosulphate solution (0.025 N): dissolved 24.82 g sodium thiosulphate in boiled and cooled distilled water and made up to 1000 ml (0.01 N) and standardized with 0.01N potassium dichromate. 250 ml of the 0.01N sodium thiosulphate was diluted to 1000 ml to obtain 0.025 N solution.

5. Starch solution: 2 g starch was dissolved in 100 ml distilled water.

To the sample collected in a 300 ml DO bottle, 2 ml of manganous sulphate solution followed by alkali-iodide-azide reagent was added on site. The bottle was stoppered and inverted several times and mixed well and allowed to settle the precipitate. Just before the titration 2 ml of concentrated sulphuric acid was added and assured the complete dissolution of precipitate to liberate the iodine which was titrated with standard sodium thiosulphate using starch as an indicator.

Calculation

$$\text{Dissolved Oxygen (mg/L)} = \frac{Vt * Nt * 8 * 1000}{V2 * (V1 - V)/V1}$$

Where, Vt = Volume of Sodium thiosulphate

Nt = Normality of Sodium thiosulphate

V1 = Total volume of the bottle after stoppering

V2 = Volume of the sample taken

V = Total volume of manganous sulphate and alkali iodide

1.3.6.21. Total Coliforms

Total coliforms in the water samples were enumerated using the spread plate method. MacConkey agar is a selective medium to enumerate lactose-producing coliform bacteria.

The plate, medium, serial dilution tubes, pipettes, and distilled water were autoclaved at 15 lbs pressure and 110°C for about 20 minutes. The medium was plated and cooled inside the laminar airflow chamber. The plates were incubated at 37°C for 24 hours to ensure that no contamination has occurred. 1 ml of sample and 2 sets of the serially diluted samples were poured into the labeled MacConkey agar plate and evenly spread with an 'L' shape rod and kept for a few minutes to absorb the sample in the solid medium. The plate was then incubated at 37°C for 24 – 48 hours. The resultant growth of all colonies on the plates was counted and expressed in the Colony Forming Unit (CFU) / ml of the sample.

Calculation:

$$\text{Total Coliform bacteria (CFU/ml)} = \frac{\text{Number of colonies formed}}{\text{Volume of Sample used}}$$

1.3.6.22. Escherichia coli

Escherichia Coli (*E.coli)* in the water samples was enumerated using the spread plate method. EMB (Eosin Methylene Blue) agar is a selective medium to enumerate *E.coli,* which gives green metallic sheen color.

The plate, medium, serial dilution tubes, pipettes, and distilled water were autoclaved at 15 lbs pressure and 110°C for about 20 minutes. The medium was plated and cooled inside the laminar airflow chamber. The plates were incubated at 37°C for 24 hours. 1 ml of sample and 2 sets of the serially diluted samples were spread on the EMB agar plate. The plates were then incubated at 37°C for 24 – 48 hours. The resultant growth of all colonies on the plates was counted and expressed in the Colony Forming Unit (CFU) / ml of the sample.

$$E.coli\ \text{(CFU/ml)} = \frac{\text{Number of colonies formed}}{\text{Volume of Sample used}}$$

1.3.6.23. Heavy Metals

Heavy metal estimation by Atomic Absorption Spectrometer: The analysis of heavy metals such as cadmium (Cd), copper (Cu), lead (Pb), nickel (Ni), zinc (Zn), and

manganese (Mn) was performed in Atomic Absorption Spectrometer (AAS) (AA-7000 series, Shimadzu) using acetylene gas as fuel (9 psi) and air as the oxidizer. All the working conditions were optimized to attain an accurate result. The certified standard solutions of different heavy metals were used to prepare the standard curve. The preserved samples were filtered with Whatman filter paper and aspirated into the fuel-rich air-acetylene flame. The instrument compares the absorbance value with the standard curve and the concentrations of the metals in the samples were determined and displayed in the monitor connected with the instrument.

Average values of three replicates were taken for each reading. A blank was run between each standard and sample. Deionized double distilled water was used as blank.

1.3.6.24. Arsenic (As)

Arsenic was determined by colorimetric method with test strips and reagent with the help of Arsenic Test Kit (HI Media catalog No. WT025-1NO) with the ppb level precision. The samples were acidified with nitric acid and lowered the pH to 2 and refrigerated to preserve them. These 50 ml of each sample were reduced its volume to 5 ml by evaporation on a hot plate at 110°C. The reaction vessel was filled with 5 ml of sample. The contents of one of the reagents As-1 (Potassium permanganate and Malonic acid) were swirled for a minute and reagent As-2 (zinc powder, zinc dust stabilized, Sodium tungstate) was added to the reaction vessel. Cap was immediately attached to the test strip with the test field of 2 cm inserted into the reaction vessel and swirled to mix. The mixture was allowed to react for 12 minutes and the reaction vessel was swirled intermittently during the reaction period. The yellow color was developed on the test strip, and the intensity of the color increased with the As content in the sample. The strip was removed and washed with distilled water and the colour was compared with the chart on the strip bottle. The color change was equivalent to As content in the sample water. The result was expressed in mg/L.

1.3.6.25. Iron

Natural Fe occurs predominantly as a ferric form because ferrous readily gets oxidized to ferric in the presence of oxygen. The estimation of total Fe is usually

done with colorimetrical or photometrical using the thiocyanate method. Ferric ion combines with thiocyanate ions to form red-colored ferric thiocyanate which is measured colorimetrically or spectrobolometrically.

Reagents

1. Concentrate hydrochloric acid
2. Dilute hydrochloric acid, 50%
3. Potassium permanganate solution (0.2N): Dissolved 600mg of potassium permanganate in 80 ml distilled water and made up to 100 ml.
4. Fe stock solution (100 mg/L): To 20 ml of con. H_2SO_4, 50 ml distilled water was added. Dissolved 0.7022 g of ferrous ammonium sulphate in the prepared acid solution and warm it gently. Potassium permanganate solution was added dropwise until a slight pink color persisted and made up to 1000 ml.
5. Fe standard solution (10 mg/L): Diluted 50 ml stock solution was diluted to 500 ml.
6. Thiocyanate solution: 10 g potassium thiocyanate was dissolved in 80 ml of distilled water and made up to 100 ml.

100 ml of well-shaken sample was placed in a 250 ml beaker and 5 ml of 50% HCl was added. Heated to reduce the volume to 40 ml and cooled. Potassium permanganate solution was added drop by drop until the color persisted for 5 minutes. It was transferred to a 50 mi Nessler tube and diluted up to the mark.

Pipetted a series of concentrations of the Fe standard covering 0.02 mg/L to 0.3 mg/L in a 50 ml Nessler tube. 1 ml of diluted HCl and 2 drops of potassium permanganate were added and mixed well and diluted to the mark with distilled water.

To the standard and samples, 1ml of thiocyanate was added and mixed well. The spectrophotometer was set to zero using a blank and the optical density was

measured at 480 nm. The concentration of the unknown sample was found from the standard curve.

1.3.7. Piper plot

To create a graph with major cations and anions, Piper (1944) suggested one diamond, adjoined by two triangles corresponding with cations and anions. The right triangle represents the anions and the left triangle represents the cations. In an anion triangle, the base axis represents chloride, the left for carbonate and bicarbonate, and the right one for sulphate. The cation one has a calcium base, the left axis for magnesium, and the right for sodium plus potassium. Based on the location of the sample point in the diamond plot, the hydro chemical facies can be identified. Diagrammes.exe software was used to plot the piper diagram to identify the type of water.

1.3.8. Gibb's Plot

Gibbs (1970) first proposed the major mechanism that controls water chemistry. Atmospheric precipitation, evaporation-crystallization, and rock dominance are the factors that determine water characteristics. The scatter plot gives a clear picture of these processes. Sodium/ (calcium + sodium) ratios (x-axis) are plotted against total dissolved solids (salinity) on the y-axis. The boomerang shape which fits on the scatter plot depicts the major factor which influences the hydrochemistry.

1.3.9. Chadha diagram

This diagram is also used to categorize water types and for a better understanding of hydrochemistry. A total of eight fields are mentioned by Chadha (1999); they are: 1. Alkaline earth exceeds alkali metals. 2. Alkali metals exceed alkaline earth. 3. Weak acidic anions exceed strong acidic anions. 4. Strong acidic anions exceed weak acidic anions. 5. Alkaline earth and weak acidic anions exceed both alkali metals and strong acidic anions, respectively. 6. Alkaline earths exceed alkali metals and strong acidic anions exceed weak acidic anions. 7. Alkali metals exceed alkaline earths and strong acidic anions exceed weak acidic anions. 8. Alkali metals exceed alkaline earths and weak acidic anions exceed strong acidic anions. Diagrammes.exe software was used to plot the Chadha diagram.

1.3.10. Wilcox plot

It can be used to determine the feasibility of water for irrigation use (Wilcox, 1955). It is a simple scatter plot of sodium hazard (Sodium Absorption Ratio (SAR)) on the Y-axis verses salinity hazard (Electrical conductivity) on the X-axis. The conductivity is plotted by default in a log scale. It comprises the following zones to categorize the SAR and salinity index. Diagrammes.exe software was used to plot the Wilcox diagram.

Salinity Hazard Zones (μS/cm)

C1 - Low (0-249)

C2 - Medium (250-749)

C3 - High (750-2249)

C4 - Very High (2250-5000)

Sodium Hazard Zones

S1 - Low

S2 - Medium

S3 - High

S4 - Very High

1.3.11. GIS

The digital depiction of the land surface elevation for any reference datum is known as a digital elevation model (DEM). DEM is the most basic type of digital topographic representation. The physiographic and demographic features are mapped and the terrain characteristics are elucidated in Digital Elevation Model (DEM) in GIS application. With a small number of collected data points, IDW interpolation is used to forecast unknown values for chemical concentrations in groundwater. IDW also allows for good and selective interpolation depending on the number of samples and their geographical distribution. The spatial distribution is an algorithmic technique in which an inverse distance weighing of nearby sample

points is given to estimate the variance of each sample. Source and spatial distribution of important water quality parameters such as F, and heavy metals are depicted with the IDW interpolation method in GIS. ArcGIS10.3.1 was used to perform the DEM and IDW interpolation analysis. DEM is a digital elevation model (DEM) that is based on the terrain surface and may be described entirely by a continuous and single-valued representation z.

$$z = f(xy)$$

Here, x and y, respectively, indicate the coordinates in the x direction and y direction, and z is the elevation.

Similarly, the generic equation for IDW interpolation is as follows:

$$Z_0 = \frac{\sum_i^s Zi \frac{1}{d_i^k}}{\sum_i \frac{1}{d_i^k}}$$

Z_0 is the estimated value at point 0

Z_i is the Z value at control point i

d_i is the distance between control point i and control point 0

S is the number of control points used in the estimation

k the specified power.

1.3.12. Statistical analysis

Pearson's correlation coefficient amongst 22 important parameters was estimated for all three seasons using SPSS 16.0 software. The significance level was calculated at * $p < 0.05$ and ** $p < 0.01$. Correlation has also been worked out between the rainfall data and HPI and MI indices. The rainfall data of the study period (February 2017-January 2018) was collected from the website of the India Meteorological Department (IMD).

1.3.13. Water Quality Index (WQI)

It is a very important and useful method for defining the suitability of groundwater for drinking. WQI expresses the overall quality of groundwater and it is used worldwide for the quality check (Wagh et al. 2019). It was proposed by Brown in 1970, and modified by Backman in 1998. It is a reliable method to recognize the impact of each water quality parameter and can be used as a dependable tool for groundwater quality assessment (WHO 2008; Sener et al. 2017). It can be done by four-step processes; including the calculation of relative weight (*Wi*), the quality rating (*qi*), the subindex of the parameter (*SIi*), and the result of WQI.

Step 1: The relative weight (*Wi*)

$$Wi = \sum \frac{wi}{\sum_{i=1}^{n} wi}$$

Where *Wi* is the relative weight of each parameter, *wi* weight of each parameter, and *n* refers to the number of parameters. The weight (*wi*) and relative weight (*Wi*) of each parameter are according to BIS standards (Mishra et al. 2019) (Table 1.3.2).

Step 2: Calculate the quality rating (*qi*); the concentration of the parameter is divided by the respective standard (BIS 2012) and multiplied by 100.

$$qi = \frac{ci}{si} \times 100$$

Where *ci* is the concentration (mg/L) of parameters in the sample and *si* is the limit value (mg/L) of the resultant parameter.

Step 3: The sub-index of the parameter (*SIi)* (Kumar et al. 2017)

$$SIi = Wi \times qi$$

Step 4: WQI of each sample

$$WQI = \sum_{i=1}^{n} SIi$$

Water can be classified according to its WQI into five groups (Khan and Jhariya 2017) and is given in Table 1.3.3.

Table 1.3.2: The weight (*wi*) and relative weight (*Wi*) of each parameter are according to BIS standards (Mishra et al. 2019).

Parameters **	**Units**	**Weight (*wi*)**	**Relative weight (*Wi*)**	**Standard limits**	**Reference**
pH	-	3	0.032967033	6.5-8.5	BIS
EC (µS)	-	3	0.032967033	400	WHO
Salinity	mg/L	3	0.032967033	250	BIS
TDS	mg/L	4	0.043956044	500	BIS
Turbidity	mg/L	4	0.043956044	5	BIS
TA	mg/L	3	0.032967033	200	BIS
TH	mg/L	4	0.043956044	200	BIS
Ca	mg/L	3	0.032967033	75	BIS
Mg	mg/L	3	0.032967033	30	BIS
Na	mg/L	3	0.032967033	200	WHO
K	mg/L	2	0.021978022	82	WHO
Cl	mg/L	4	0.043956044	250	BIS
SO_4	mg/L	3	0.032967033	200	BIS
NO_3	mg/L	4	0.043956044	45	BIS
PO_4	mg/L	3	0.032967033	1	WHO
F	mg/L	5	0.054945055	1	BIS
E.coli	mg/L	4	0.043956044	Nil	BIS
Fe	mg/L	4	0.043956044	0.3	BIS
Cu	mg/L	3	0.032967033	0.05	BIS
Cd	mg/L	5	0.054945055	0.003	BIS
Pb	mg/L	5	0.054945055	0.01	BIS
Ni	mg/L	5	0.054945055	0.02	BIS
As	mg/L	5	0.054945055	0.01	BIS
Mn	mg/L	3	0.032967033	0.1	BIS
Zn	mg/L	3	0.032967033	5	BIS
		Σ *wi* =91	Σ *Wi* = 1		

Table 1.3.3: Showing the classification of water as per WQI

Range (WQI)	**Type of groundwater**
<50	Excellent
50 ≤ WQI ≥ 100	Good
100 ≤ WQI ≥ 200	Poor
200 ≤ WQI ≥ 300	Very poor
> 300	Unsuitable for drinking/irrigation

1.3.14. Heavy metal Pollution Index (HPI)

The heavy metal pollution index is the most powerful tool to evaluate heavy metal contamination (Mohan et al. 1996). It uses multivariate statistics to consider both standard permissible limits (*Si*) and the highest ideal value (*Ii*).

HPI was estimated using an equation proposed by Mohan et al. (1996):

$$\mathrm{HPI} = \sum_{i=1}^{n} Wi\, Qi$$

Where *Wi* and *Qi* are the weightage index and sub-index of the i^{th} parameter respectively and *n* is the number of parameters considered. The Sub-index *Qi* is calculated by:

$$Qi = \sum_{i=1}^{n} \left[\frac{Mi - Ii}{Si - Ii}\right] * 100$$

Wi indicates the relative weight of the i^{th} heavy metal, which is the reciprocal of the *Si* value. *Si* represents the standard permissible limits of the i^{th} parameter in ppm. *Mi* is the monitored value and *Ii* is the highest ideal value of the i^{th} parameter in ppm concentration. The HPI calculation is detailed in Table 1.3.4.

Table 1.3.4 Specimen calculation of HPI using the average concentration of heavy metals in the study area

Metal ions	Monitored Value (Mi)	BIS permissible limits in ppm (Si)	Maximum allowable limits in ppm (Ii)	Wi	Qi	Wi*Qi	HPI=∑Wi*Qi/∑Wi
Fe	0. 384	0.3		3.33	128.12	427.06	
As	0.0159	0.01	0.05	100	85.1	8508.8	
Pb	0.0118	0.01		100	118.27	11827.1	
Cd	0.00257	0.003		333.33	85.85	28619.5	
Ni	0.0179	0.02		50	89.79	4489.7	
Mn	0.0342	0.1		10	34.29	342.94	
Zn	0.076	5	15	0.2	143.29	29.84	
Cu	0.0224	0.05		20	101.8	2037.9	
				616.86		**56282.84**	**91.24087**

1.3.15. Metal index (MI)

MI was first proposed by Tamasi and Cini (2004). It is the treed evaluation of present data. It considers only monitored value and maximum permissible limits.

$$MI = \sum_{i=1}^{n} \frac{Ci}{(MAC)i}$$

Where *MI* is the metal index and *Ci* is the monitored concentration of each element in the i^{th} sample in ppm. MAC is the maximum admissible concentration of each element in ppm. The sample is represented by the subscript *i* (Namaghi et al. 2011). The specimen calculation is given in Table 1.3.5.

Table 1.3.5 Specimen MI calculation for the annual mean concentration of heavy metals

Heavy metal	**Concentration *Ci* *(mg/L)***	**Maximum Allowable Concentration (MAC)**	$MI = \sum_{i=1}^{n} \frac{Ci}{(MAC)i}$
Cd	0.0027	0.003	0.9
Pb	0.014	0.01	1.4
As	0.02	0.01	2
Ni	0.017	0.02	0.85
Fe	0.474	0.3	1.58
Cu	0.026	0.5	0.052
Mn	0.066	0.1	0.66
Zn	0.062	5	0.0124

1.4. Result and Discussion

The quantity and quality of groundwater resources have become a major global concern. The availability of groundwater varies with location and is influenced by the composition of aquifer material and groundwater storage. The quality of groundwater is mostly determined by natural and man-made factors. The present study has assessed the groundwater availability in Palakkad and Malappuram Districts. The study has also undertaken the quality assessment of groundwater from 66 sites in both Districts in three seasons from February 2017 to January 2018. The results are analyzed to reveal the qualitative issues associated with groundwater resources, the causes, and the management measures.

1.4.1. Geology of Palakkad and Malappuram District

The geological sequence of the lithological components in the Palakkad District can be classified into (a) Recent – which includes topsoil, valley fill, and riverine alluvium (b) Sub recent (laterite), and (c) Archean (CGWB). The dominant Archean mineral groups of Palakkad District are presented in Fig. 1.4.1. Hornblende–biotite gneiss is distributed in major parts of the District (~42%), especially in the eastern Palakkad Gap region. The charnokite group (~ 32%) composed of charnokite / charnokite gneiss, mixed with minor intrusive type magnetite quartzite, pyroxene

granulite, and hornblende granulites are distributed throughout the western lowlands. Garnet-sillimanite gneiss of khondalite group, hornblende-schist, and granite gneiss form linear bodies in the northeastern hill region. Metamorphed ultramafic group of talc-chlorite schist, talc-pyroxene-garnet schist, and amphibolite group of hornblende-biotite schist and gneiss with amphibolites bands garnet forms metaultramafite in Attappady Block in the north. Quartz-feldspar gneiss along the tributaries and fluvial alluvium deposit at the cessation of Bharathapuzha River in the western part of the District is prevalent. Hornblende – biotite gneiss is distributed to a great extent in the Chittur, Kollengode, Attappady, Palakkad, Kuzhalmannam, and Nenmmara Blocks along with khondolite group in Chittur and charnochite group in Attappady.

Malappuram District can be separated into two major geological belts based on how different rock types are exposed (a) the charnockite group of rocks, which makes up the majority of the area, and (b) the migmatite complex in the eastern part (Fig.1.4.2). The charnokite (charnockite/charnockite gneiss) is composed of banded magnetite quartzite, pyroxene granulite, amphibolite/hornblende granulite, and pyroxenite, which are all found in descending order of abundance. The migmatite complex is made up of gneiss and quartzo-feldspathic gneiss/garnet-biotite gneiss as well. Small masses of metaultramafites (talc-tremolite schist, talc-pyroxene-garnet schist, banded magnetite quartzite), as well as high-grade schist and gneiss (hornblende-biotite schist and gneiss+garnet with amphibolite band), make up the Wayanad group, which also extends into Tamil Nadu. The rock of the peninsular gneiss complex is represented by granite gneiss and hornblende biotite gneiss distributed near the eastern boundary (Perinthalmanna and Manjeri). Lateralization of more than 10 meters is widespread in the District and more prominent in the Angadippuram region. Clay formations near the coastal region and paleo-marine, fluvial, fluvial-marine, and marine formations are also distributed in the coastal plain (Fig.1.4.2) (www.dmg.kerala.gov.in).

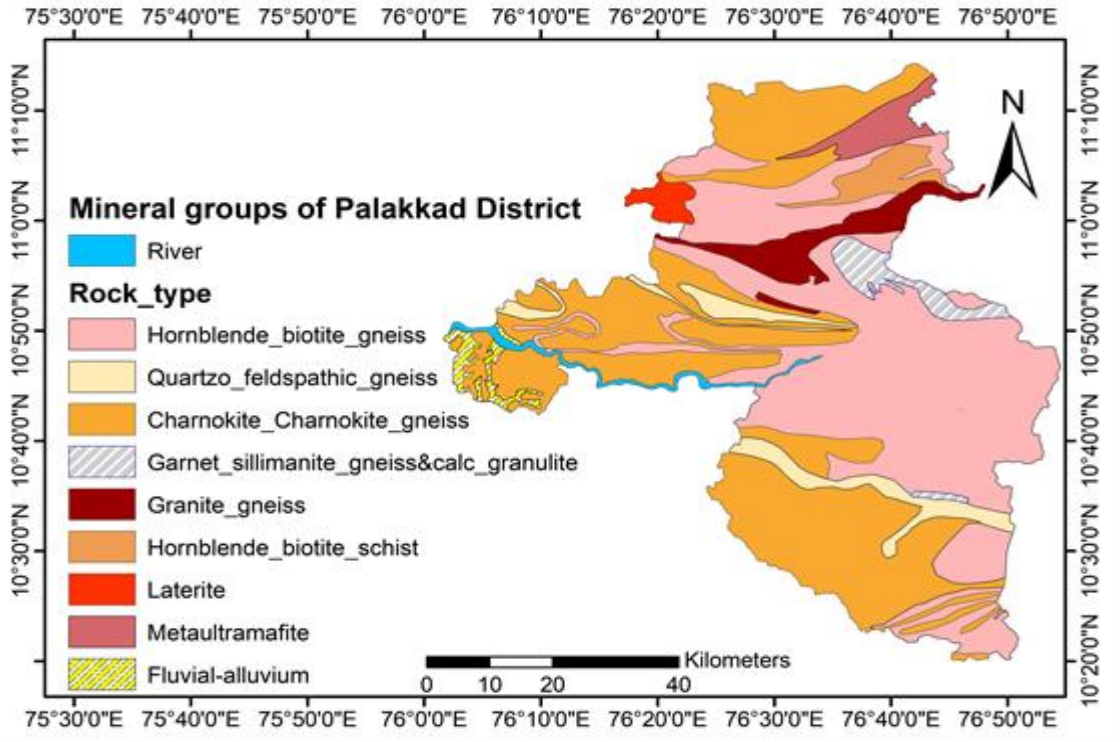

Fig. 1.4.1 The dominant Archean mineral groups of the Palakkad district

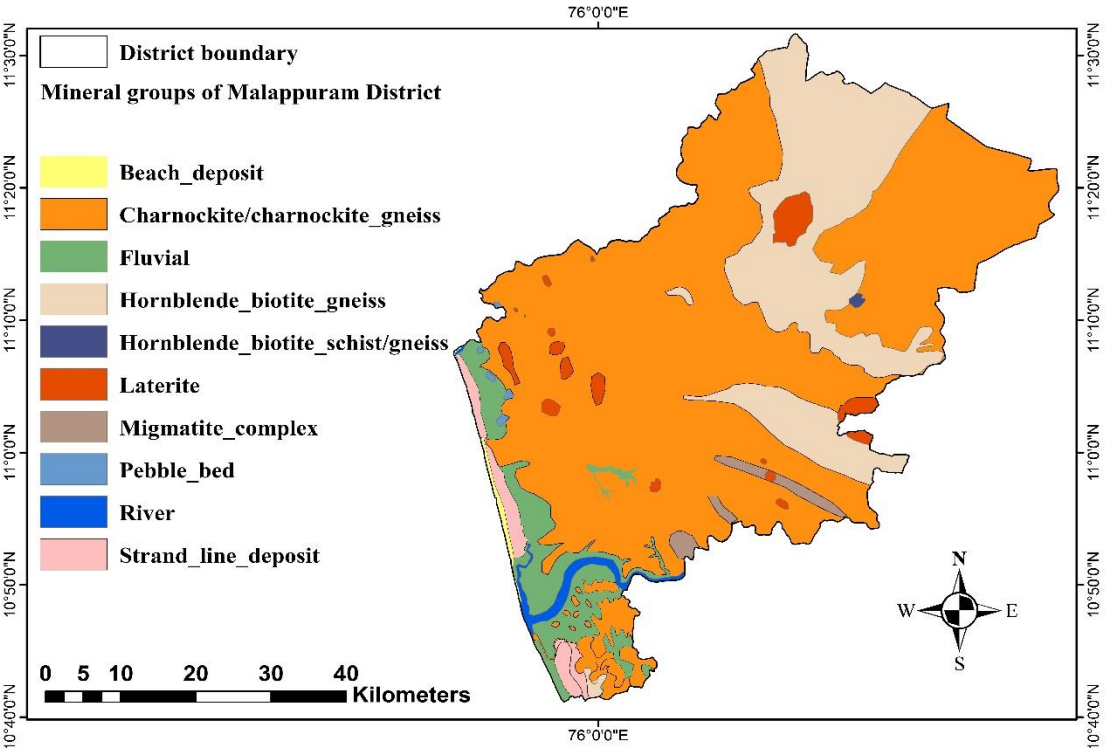

Fig.1.4.2 The dominant Archean mineral groups of the Malappuaram district

1.4.2. Quantitative status of Groundwater in Palakkad & Malappuram Districts.

For quantitative estimation of groundwater sources in Palakkad and Malappuram Districts, details of water table confining to wells and other sources, along with rainfall data were collected. The details of sampling wells of Palakkad and Malappuram Districts are given below:

Table 1.4.1. Details of sampling wells of Palakkad District including sample code, sampling site, administrative units, geographical coordinates, and type and depth of the water source.

Sample ID	Sample Site	Block Panchayat/ Municipality	Coordinates	Type of Well*	Depth of well (mt.)
P1	Sholayur	Attappady	$11^0 07^1 32^{11}$ N, $76^0 44^1 39^{11}$ E	BW	62.48
P2	Agali	Attappady	$11^0 05^1 32^{11}$ N, $76^0 35^1 39^{11}$ E	OW	8.84
P3	Kotoppadam	Mannarkad	$10^0 59^1 28^{11}$ N, $76^0 22^1 36^{11}$ E	BW	94.49
P4	Mannarkad	Municipality	$10^0 59^1 31^{11}$ N, $76^0 27^1 15^{11}$ E	OW	11.43
P5	Kadambazhippuram	Cherppullassery	$10^0 52^1 52^{11}$ N, $76^0 27^1 31^{11}$ E	BW	60.96
P6	Cherppullassery	Municipality	$10^0 53^1 12^{11}$ N, $76^0 19^1 30^{11}$ E	OW	10.67
P7	Ongallur	Pattambi	$10^0 48^1 10^{11}$ N, $76^0 13^1 15^{11}$ E	OW	10.97
P8	Nellaya	Pattambi	$10^0 52^1 00^{11}$ N, $76^0 15^1 51^{11}$ E	BW	76.20
P9	Pattambi	Municipality	$10^0 48^1 42^{11}$N, $76^0 11^1 11^{11}$ E	OW	8.53
P10	Chalissery	Thrithala	$10^0 44^1 13^{11}$N, $76^0 05^1 38^{11}$ E	OW	7.62
P11	Kapur	Thrithala	$10^0 46^1 25^{11}$N, $76^0 03^1 47^{11}$ E	BW	64.01
P12	Shoranur	Municipality	$10^0 46^1 35^{11}$ N, $76^0 17^1 21^{11}$ E	OW	12.19
P13	Ambalappara	Shoranur	$10^0 48^1 10^{11}$ N, $76^0 24^1 20^{11}$ E	OW	10.36
P14	Trikkadiri	Sreekrishnapuram	$10^0 51^1 12^{11}$ N, $76^0 21^1 14^{11}$ E	OW	10.67
P15	Lakkidi	Ottapalam	$10^0 46^1 21^{11}$ N, $76^0 27^1 20^{11}$ E	BW	91.44

P16	Ottapalam	Municipality	$10^0 46^1 22^{11}$ N, $76^0 22^1 55^{11}$ E	BW	85.35
P17	Mannur	Palakkad	$10^0 48^1 07^{11}$ N, $76^0 28^1 02^{11}$ E	OW	10.06
P18	Kodumbu	Palakkad	$10^0 45^1 15^{11}$ N, $76^0 41^1 12^{11}$ E	BW	76.20
P19	Palakkad	Municipality	$10^0 45^1 03^{11}$ N, $76^0 38^1 58^{11}$ E	BW	38.10
P20	Malampuzha	Malampuzha	$10^0 50^1 06^{11}$ N, $76^0 41^1 45^{11}$ E	OW	5.33
P21	Puthussery	Malampuzha	$10^0 47^1 21^{11}$ N, $76^0 42^1 42^{11}$ E	OW	7.80
P22	Eruthenpathy	Chittur	$10^0 44^1 19^{11}$ N, $76^0 51^1 51^{11}$ E	BW	106.68
P23	Perumatti	Chittur	$10^0 40^1 05^{11}$N, $76^0 46^1 16^{11}$ E	OW	21.34
P24	Vandithavalam	Chittur	$10^0 39^1 10^{11}$ N, $76^0 43^1 35^{11}$ E	BW	121.92
P25	Chittur	Municipality	$10^0 41^1 39^{11}$ N, $76^0 44^1 23^{11}$ E	OW	9.14
P26	Kannadi	Kuzhalmannam	$10^0 44^1 44^{11}$ N, $76^0 37^1 39^{11}$ E	OW	6.10
P27	Kuzhalmannam	Kuzhalmannam	$10^0 42^1 27^{11}$ N, $76^0 35^1 42^{11}$ E	OW	4.27
P28	Kollengode	Kuzhalmannam	$10^0 36^1 39^{11}$ N, $76^0 41^1 59^{11}$ E	BW	152.40
P29	Muthalamada	Kuzhalmannam	$10^0 37^1 25^{11}$ N, $76^0 46^1 53^{11}$ E	BW	182.88
P30	Melarkode	Nenmmara	$10^0 36^1 30^{11}$ N, $76^0 34^1 00^{11}$ E	BW	85.35
P31	Elavanchery	Nenmmara	$10^0 36^1 24^{11}$ N, $76^0 39^1 10^{11}$ E	BW	137.16
P32	Erumayur	Alathur	$10^0 40^1 12^{11}$ N, $76^0 34^1 34^{11}$ E	BW	203.00
P33	Vadakkenchery	Alathur	$10^0 37^1 29^{11}$ N, $76^0 30^1 46^{11}$ E	BW	60.96

*Type of wells: OW- Open Well, BW- Bore Well

Table 1.4.2. Details of sampling wells of Malappuram District including sample code, sampling site, administrative units, geographical coordinates, and type and depth of the water source.

Sample ID	Sample Site	Block Panchayat /Municipality	Coordinates	Type of well	Depth of well (mt.)
M01	Chungathara	Nilambur	11°19'40.66"N, 76°16'21.01"E	OW	10.52
M02	Nilambur	Municipality	11°15'45.39"N, 76°13'44.92"E	OW	12.19
M03	Wandoor	Wandoor	11°12'06.78"N, 76°14'01.19"E	OW	11.88
M04	Mambad	Wandoor	11°14'05.98"N, 76° 09'53.13"E	OW	10.97
M05	Kavanur	Areekode	11°12'33.91"N, 76° 03'50.61"E	OW	9.14
M06	Kuzhimanna	Areekode	11°11'07.82"N, 76° 01'17.04"E	OW	10.06
M07	Nediyiruppu	Kondotty	11° 08'49.65"N, 75°58'25.00"E	BW	121.9
M08	Pallikkal	Kondotty	11° 08'16.99"N, 75°54'48.51"E	BW	76.2
M09	Thenhipalam	Tirurangadi	11° 08'05.30"N, 75°53'25.83"E	OW	7.62
M10	Munniyur	Tirurangadi	11° 08'05.30"N, 75°53'25.83"E	OW	7.62
M11	Manjeri	Municipality	11° 08'14.59"N, 76°06'14.22"E	OW	5.49
M12	Pookkottur	Malappuram	11° 06'04.09"N, 76°03'46.91"E	OW	8.53
M13	Oorakam	Malappuram	11° 03'52.54"N, 76°01'53.10"E	OW	6.1
M14	Malappuram	Municipality	11° 01'59.26"N, 76°05'59.88"E	OW	12.19
M15	Makkarapparambu	Mankada	11° 00'17.96"N, 76°07'44.12"E	OW	6.1
M16	Angadippuram	Mankada	10°58'43.45"N, 76°11'40.29"E	OW	9.14
M17	Perinthalmanna	Municipality	10°58'00.32"N, 76°13'34.09"E	OW	10.06
M18	Aliparamba	Perinthalmanna	10°56'15.64"N, 76°15'47.32"E	OW	6.71
M19	Elamkulam	Perinthalmanna	10°53'45.41"N, 76°14'39.94"E	OW	11.58

M20	Vengara	Vengara	11°02'11.12"N, 75°56'46.40"E	OW	10.66
M21	Edarikode	Vengara	10°59'43.27"N, 75°58'49.14"E	BW	73.2
M22	Tanur	Municipality	10°59'14.84"N, 75°52'29.02"E	OW	4.57
M23	Tanalur	Tanur	10°56'27.91"N, 75°54'38.94"E	OW	7.77
M24	Tirur	Municipality	10°54'29.40"N, 75°54'57.39"E	OW	6.7
M25	Vakkad	Tirur	10°52'59.70"N, 75°53'32.63"E	BW	15.2
M26	Trippangode	Tirur	10°50'49.68"N, 75°56'34.87"E	OW	4.57
M27	Valanchery	Municipality	10°53'00.31"N, 76°04'30.07"E	OW	9.14
M28	Athavanadu	Kuttippuram	10°52'06.28"N, 76°02'35.59"E	OW	10.67
M29	Thavannur	Ponnani	10°50'30.66"N, 76°00'13.45"E	OW	7.62
M30	Ponnani	Municipality	10°48'40.44"N, 75°57'35.94"E	OW	6.1
M31	Edappal	Municipality	10°47'07.18"N, 75°59'04.91"E	OW	7.32
M32	Veliyamkode	Perumpadappa	10°43'41.81"N, 75°56'53.53"E	OW	3.96
M33	Alamcode	Perumpadappa	10°44'04.62"N, 76°03'05.47"E	BW	67.4

In Palakkad District, Mo extending from June to September is with an average rainfall of 2049 mm. (Pai and Nair 2009). The District also experiences two micro-climatic conditions, which are humid towards the west and semi-humid to dry towards the east. Severe water scarcity is experienced during the Pr season in the eastern regions of the District, especially in Attappady, Chittur, Kollengode, Nenmmara, and Palakkad Blocks, leading to a higher dependency on bore wells for drinking and agricultural purposes. In the Po season, irrigation canals play a vital role in recharging the surface water resources and shallow aquifers of the regions. The groundwater resources in the rest of the areas are noted to have the availability of water throughout the year. The sample code, sampling site, administrative units, geo coordinates, and the type and depth of wells in Palakkad District are given in

Table 1.4.1. In this region, the total depth i.e. the depth to the bottom of open wells ranged from 4.27 m to 21.34 m and 38.10 m to 203 m for bore wells.

The Malappuram District has a tropical humid climate with moderate temperatures and heavy rainfall during the Mo season. From 2014 to 2018, the average annual rainfall was 2640.62 mm (Source: https://mausam.imd.gov.in/). There is comparatively lesser water scarcity in the Malappuram District than in Palakkad District. However, during the summer months (April and May), water scarcity is limited to a few sampling stations in Nediyiruppu, Pallikkal, and the Alamkode regions, since the availability of water is purely dependent on bore wells. The sample code, sampling site, administrative units, geo coordinates, and the type and depth of wells in the Malappuram District are given in Table 1.4.2. The total depth, that is, the distance from the ground level to the bottom of open wells ranged from 3.96 m to 12.19 m, and bore wells from 15.2 m to 121. 9 m.

Table 1.4.3: Groundwater availability in Palakkad District during the study period (2017-18)

Sl No	Block/ Block+Municipality	Area in KM^2	Major rock type	Sy*	hPo - hPr# in meter	Groundwater availability in Cubic Meters
1	Attappady (Block)	807.23	Hornblende biotite gneiss/schist, Charnokite/ granite gneiss	3%	4.88	118101704.6
2	Mannarkkad (Block + Municipality)	395.75	Hornblende biotite gneiss/schist, charnokite/ granite gneiss & laterite	3%	1.83	21712452.88
3	Sreekrishnapuram (Block + Cherppullassery Municipality)	220.61	Charnokite/ Quartzo feldspathic/granite gneiss	3%	3.315	21937831.3
4	Pattambi (Block + Municipality)	222.83	Hornblende biotite/Charnokite gneiss	3%	2.76	18465167.26
5	Trithala (Block)	171.56	Charnokite gneiss	3%	1.543	7940557.846

6	Ottapalam (Block + Municipality & Shoranur)	231.33	Hornblende biotite/Charnokite gneiss	3%	4.10	28423680.4
7	Palakkad Block + Municipality	231.04	Hornblende biotite/Charnokite gneiss	3%	2.32	16108764.18
8	Malampuzha (Block)	447.05	Hornblende biotite/Garnet sillimanite gneiss	3%	2.11	28308001.31
9	Chittur (Block+ Municipality)	270.34	Hornblende biotite gneiss	3%	5.42	43962266.67
10	Kuzhalmannam (Block)	194.13	Hornblende biotite gneiss	3%	2.67	15554642.9
11	Alathur (Block)	371.82	Hornblende biotite/ Charnokite/ Quartzo feldspathic/gneiss	3%	3.31	36935832.03
12	Kollengode (Block)	175.63	Hornblende biotite/ Charnokite/ Quartzo feldspathic/gneiss	3%	2.75	14495739.8
13	Nenmara (Block)	738.68	Hornblende biotite/ Charnokite/ Quartzo feldspathic/gneiss	3%	2.81	62222540.31
					Total	**434169181.5**
Total groundwater availability in Million Cubic Meters (MCM)						**434.169**

Table 1.4.4: Groundwater availability in Malappuram District during the study period (2017-18)

Sl No	Block/Block+Municipality	Area in KM^2	Major rock type	Sy*	hPo - $hPr^{\#}$ in meter	Groundwater availability in Cubic Meters
1	Nilambur (Block+Municipality)	1127.74	Hornblende biotite/ charnokite gneiss & Laterite	3%	2.50	84489315.33
2	Wandoor (Block)	413.18	Hornblende biotite/ charnokite gneiss	3%	3.63	44959993.47

3	Mankada (Block)	241.47	Hornblende biotite/ charnokite gneiss	3%	2.25	16309555.07
4	Perinthalmanna (Block + Municipality)	241.86	Hornblende biotite/ charnokite gneiss	3%	2.43	16558879.25
5	Malappuram (Block + Municipality)	188.02	Charnokite gneiss	3%	2.39	11081264.64
6	Areekode (Block + Manjeri Municipality)	289.996	Charnokite gneiss	3%	2.05	14615680.51
7	Kondotty (Block + Municipality)	162.04	Charnokite gneiss	3%	1.80	8750077.741
8	Thirurangadi (Block + Municipality)	143.07	Charnokite gneiss & Laterite	3%	1.12	4791351.51
9	Vengara (Block)	117.28	Charnokite gneiss & Laterite	3%	1.45	5094027.397
10	Kuttipuram (Block + Valanchery Municipality)	162.43	Charnokite gneiss	3%	1.35	6564931.413
11	Tanur (Block)	124.87	Fluvial & strandline deposit	6%	2.04	15271824.97
12	Tirur (Block + Municipality)	120.61	Fluvial & strandline deposit	6%	2.13	13299322.17
13	Ponnani (Block + Municipality)	104.99	Fluvial & strandline deposit	6%	1.31	6249087.56
14	Perumbadappu (Block)	93.78	Fluvial & strandline deposit	6%	0.23	1286321.392
					Total	249321632.4
Total groundwater availability in Million Cubic Meters (MCM)						**249.32**

*Specific Yield # Peizometric height in Po (MSL) - Peizometric height in Pr (MSL)

Water level measurements in wells provide the most basic indicator of the condition of the groundwater resource and are critical for groundwater quantification evaluations. Water level measurements from observation wells are the primary source of information about an aquifer's hydrological environment. The groundwater

potential and availability during the study period were assessed as per GEC (2012), from the changes in groundwater storage (ΔY) in the Pr and Po seasons. During the pre and Po seasons, 19 water table measurements were taken in Palakkad and 29 in Malappuram Districts. For calculation, the Block and the adjacent Municipality were treated as a single unit. The area was consolidated into 13 units from Palakkad and 14 units from Malappuram, and the water table was averaged accordingly. The major rock type of each unit, their specific yield, and the total area have been considered for the calculation of groundwater availability during the study period (2017 February to 2018 January) (Table 1.4.3 &1.4.4).

There is an estimated 434.169 million cubic meters (MCM) of groundwater availability in Palakkad and 249.32 MCM in Malappuram. According to the groundwater department (Government of Kerala), the net availability of groundwater in Palakkad in 2009, 2013, and 2017 was 795.25, 648.93, and 591.49 MCM, respectively. Similarly, the net groundwater availability in Malappuram District in 2009, 2013, and 2017 was 484.31, 516.87, and 470.53 MCM, respectively. When these values are compared with the observed data, it is clear that there is a significant decrease in groundwater availability. The groundwater storage in an aquifer is dependent on several factors, such as climate, groundwater abstraction, and land use (Bekesi et al. 2009), as well as the specific yield of the aquifer material and its total area (Kumar and Seethapathi 2002). Any groundwater abstraction would deplete storage in a groundwater system. This depletion of storage is equivalent to aquifer discharge (including abstraction) at rates greater than aquifer recharge (Doll et al. 2014; Wada et al. 2010). Rising groundwater levels, on the other hand, indicate increased storage and recharge exceeding discharge from the groundwater system (Kourakos et al. 2019). The storage factor can be used to compute the changes in volumetric storage (Scanlon et al. 2012).

Hard rocks underpin approximately 65 percent of the country in India (Saraf and Choudhury 1998). Secondary porosity caused by fracturing of the underlying rocks governs the occurrence and movement of groundwater in a hard rock terrain watershed (Subba Rao 2006). Groundwater location is influenced by geology,

geomorphology, lineaments, soil, land use, drainage, and slope (Srivastava and Bhattacharya 2006). Groundwater resources in India are under constant threat of depletion. From 2002 to 2008, the rate of depletion in groundwater resources in the north Indian States in the Indo-Gangetic plains was approximately 109 km^2, with a mean annual depletion of 4.0 ± 1.0 cm $year^1$ (Rodell et al. 2009). It has also been reported that in many parts of India, the decline in the water table is at the rate of 1-2 m/year (Singh and Singh 2002). It has led to groundwater pollution, saltwater encroachment, drying of aquifers, water logging, and salinity intrusion (Basharat 2019).

1.4.3. Hydro geochemical studies of groundwater during different monsoonal Periods (Pr, Mo, Po)

The mean value and standard deviation of water quality parameters such as pH, temperature (°C), EC (µS), salinity (mg/L), TDS (mg/L), TSS (mg/L), TS (mg/L), Turbidity (NTU), TAc. (mg/L), TA (mg/L), TH (mg/L), Ca (mg/L), Mg (mg/L), Na (mg/L), K (mg/L), Cl (mg/L), SO_4 (mg/L), NO_3 (mg/L), PO_4 (mg/L), and DO as well as biological parameters such as total coliforms and *E.coli* in Pr, Mo, and Po seasons were given in the annexure from 1 to 22. The bimonthly concentration of F, its seasonal mean value, and the standard deviations of each sample are given in annexure 23. The statistical summary of each parameter in Pr, Mo, and Po and the proportion of samples exceeding the optimal concentration of drinking water, as prescribed by WHO and BIS in Palakkad and Malappuram Districts, are presented in tables 1.4.5 and 1.4.6 respectively. The bimonthly concentration of heavy metals (Fe, Cu, Cd, Pb, Ni, As, Zn, and Mn) and their seasonal mean value and standard deviations are specified in annexures 23-31. The statistical summary of the eight heavy metals as well as the proportion of samples exceeding the optimal concentration of drinking water standards, prescribed by WHO and BIS, are presented in tables 1.4.7 and 1.4.8 respectively. The correlation of hydro-chemical parameters, including heavy metals of Pr, Mo, and Po of Palakkad and Malappuram Districts is given in tables 1.4.9, 1.4.10, and 1.4.11 as well as 1.4.12, 1.4.13, and 1.4.14 respectively.

Table 1.4.5. Statistical summary of the physicochemical and biological factors of groundwater samples collected in different seasons from Palakkad District.

Parameters **	WHO	BIS	Pr						Mo						Po					
			Min	Max	Mean	SD	%DWS	%DBS	Min	Max	Mean	SD	%DWS	%DBS	Min	Max	Mean	SD	%DWS	%DBS
pH	6.5–9.5	6.5-8.5	4.85	8.53	6.81	0.81	30	32	4.3	8.52	6.84	1.06	30	32	4.75	8.68	6.96	1.03	32	33
Temp.	-	-	27	33.5	30.79	2.06	-	-	20.50	29.40	28.11	1.12	-	-	27	29.50	28.32	0.50	-	-
EC (µS)	400	300*	55	1989	570	435	59	62	77.5	2385	676	508	62	70	76.8	2110	663	488	64	71
Salinity	250	250	34	999	297	227	42	42	12	1360	333	289	53	53	39.9	1004	309	230	50	50
TDS	300	500	28	1011	304	225	36	15	47	1237	353	275	48	29	47	1926	421	340	56	33
TSS	-	-	0.80	843.9	148.67	158.69	-	-	0.80	536.2	108	118.29	-	-	8.30	994	142.89	173.77	-	-
TS	-	-	40	1800	449.59	326.64	-	-	60	1580	464.91	317.07	-	-	80	2920	563.39	449	-	-
Turbidity	5	5	0	18	2.24	3.42	13.64	13.64	0	19.70	3.51	4.06	18.18	18.18	0	27	2.14	4.12	9.09	9.09
TAc	-	-	0	394	29.37	64.05	-	-	0	120	14.28	19.9	-	-	0	160	25.67	34.23	-	-
TA	300	200	4	500	159	120	17	29	6	412	112	94	6	14	8	920	211	187	27	41
TH	180	200	20	1216	279	233	56	53	BDL	504	186	135	51.5	48.5	14	504	190.2	128	53	50
Ca	75	75	4	184	80	44.8	52	52	BDL	218	75.18	51.59	44	44	6	202	69.2	51.8	35	35
Mg	50	30	2	1040	199	208	70	77	BDL	434	110.93	95.99	62	70	4	454	119.4	120.7	61	62
Na	200	-	2.3	389	81	82	12	-	5.9	415.5	85.01	80.52	9.1	-	15.2	441	97.7	95.09	12.2	-
K	82	-	3.4	60	14	9	0	-	BDL	53.8	10	11.06	0	-	BDL	54	11.46	10.28	0	-
Cl	250	250	12.3	496	82	84.5	8	8	12	357	82	78	8	8	12	296	71	66	5	5
SO_4	250	200	BDL	153.9	30	38	0	0	2.1	158.2	33	39	0	0	BDL	246	36	43	0	1.5
NO_3	10	45	BDL	6.74	1.39	1.8	0	0	BDL	8.8	1.89	2.11	0	0	BDL	9.24	1.78	2.34	0	0
PO_4	1 ^	-	0.0112	0.337	0.087	0.062	0	-	0	0.773	0.043	0.104	0	-	0.005	0.412	0.069	0.067	0	-
F	1.5	1	0.6	1.8	1.28	0.23	9	88	0.6	1.8	1.08	0.23	3	52	0.3	2.2	1.3	0.27	7.6	88
DO	-	-	0.41	10.75	3.32	2.21	-	-	0.41	10.13	3.38	2.33	-	-	0.41	6.90	2.89	1.80	-	-
T.coli	-	10/100ml	0	2690	730.14	875.76	-	74	0	2400	784.39	759.77	-	87	0	8700	1483	1811	-	90.9
E.coli	Nil	Nil	0	1750	83.91	244.79	43.94	43.94	0	1015	96.06	179.75	62.12	62.12	0	3280	434.09	775.97	71.21	71.21

** All parameters are in mg/L except pH and EC, *Water quality standard of ICMR, 1975; ^Swaziland Water Services Corporation (SWSC, 2014); [#] Deviation of water quality standards from WHO; [$] Deviation of water quality standards from BIS

Table 1.4.6. Statistical summary of the physicochemical and biological factors of groundwater samples collected in different seasons from Malappuram District.

Parameters#	WHO	BIS	Pr						Mo						Po					
			Min	Max	Mean	SD	% DWS	% DBS	Min	Max	Mean	SD	% DWS	% DBS	Min	Max	Mean	SD	% DWS	% DBS
pH	6.5–9.5	6.5-8.5	4.32	8.41	5.79	0.72	86.36	86.36	3.36	8.65	5.76	0.92	77.27	77.27	3.11	8.45	5.90	0.90	77.27	77.27
Temp.	-	-	27.50	33.50	31.05	1.74	-	-	25.90	29.20	27.60	0.94	-	-	27.00	29.50	28.05	0.65	-	-
EC (µS)	400	300*	40.66	985	214	186	12.12	19.7	42.7	1121	242.14	215.1	15.15	27.23	60.8	1100	241.6	207.6	19.70	27.27
Salinity	250	250	13.60	578.30	132.55	127.96	9.06	9.09	28.45	510.10	113.63	96.67	9.09	9.09	33.5	505.40	114.36	99.25	10.61	10.61
Turbidity	5	5	0	26.4	2.66	3.95	18.18	18.18	0	51.30	4.41	6.63	50	50	0	48.50	2.69	7.91	10.61	10.61
TDS	300	500	23.85	491.4	109.7	84	3	0	29.14	667.6	150.32	130.15	12.12	3	36.82	665.7	143	125	16.7	1.5
TSS	-	-	0.06	807.75	110.85	149.04	-	-	0.12	500.19	90.29	97.19	-	-	1.70	236.36	58.40	58.08	-	-
TS	-	-	40	1120	256.85	216.89	-	-	60	840	240.61	166.41	-	-	40	680	207.58	136.45	-	-
TA	300	200	0	196	45.33	48.9	0	0	0	212	32.	48.48	0	1.52	4	472	73.58	98.94	4.55	12.12
TAc	-	-	0	137.9	26.39	23.16	-	-	0	72	33.61	19.45	-	-	0	96	44.85	22.34	-	-
TH	180	200	0	428	86.15	89.30	10.6	9.1	0	250	64.27	64.16	7.57	6.06	6	244	54.30	56.05	4.54	3.03
Ca	75	75	0	324	44.98	58.98	20	20	0	210	36.84	42.46	18.18	18.18	4	148	27.8	28.75	7.57	7.57
Mg	50	30	0	200	41.2	38.38	34.84	50	0	166	27.48	28.93	15.15	25.76	2	152	22.6	26.45	13.64	21.21
Na	200	-	0.70	121.20	35.61	30.73	0	-	1	138.3	38.95	30.5	0	-	0.7	148.5	38.57	34.49	0	-
K	82	-	1.3	15.2	12.16	2.83	0	-	0	133.8	8.07	21.56	3.04	-	0	141.5	6.97	18.41	1.5	-
Cl	250	250	3.55	124.08	30.22	22.23	0	0	5	157.45	32.57	25.63	0	0	4	107.97	26.64	18.28	0	0
SO_4	250	200	1.38	34.80	8.02	7.92	0	0	1.15	44.40	9.99	10.23	0	0	1.5	55.41	10.24	13.76	0	0
NO_3	10	45	0.06	7.68	2.37	2.03	0	0	0.06	8.30	2.46	2.24	0	0	0	8.02	2.43	2.17	0	0
PO_4	1^	-	0	0.65	0.10	0.10	-	0	0	0.28	0.04	0.06	-	0	0	1.56	0.08	0.19	-	1.52
F	1.5	1	0.94	1.8	1.19	0.18	4.55	69.70	0.37	1.20	0.88	0.16	0	10.61	0.16	1.9	1.15	0.20	4.55	71.21
DO	-	-	0.57	7.29	3.41	1.88	-	-	0	8.10	3.60	1.72	-	-	0.20	8.51	3.03	1.81	-	-
TC	-	10/100 ml	0	2920	388.98	620.91	-	80.30	0	2500	736.51	711.53	-	87.88	0	2870	405.99	583.13	-	75.76
EC	Nil	0/100 ml	0	1050	67.82	163.69	-	57.58	0	570	69.09	108.58	-	69.7	0	1190	119.49	221.27	-	81.82

** All parameters are in mg/L except pH and EC, *Water quality standard of ICMR, 1975; ^ Swaziland Water Services Corporation (SWSC, 2014); # Deviation of water quality standards from WHO; $ Deviation of water quality standards from BIS

Table 1.4.7. Statistical summary of the heavy metals of groundwater samples collected in different seasons from Palakkad District.

Parameters	WHO	BIS	Pr						Mo						Po					
			Min	Max	Mean	SD	% DWS	% DBS	Min	Max	Mean	SD	% DWS	% DBS	Min	Max	Mean	SD	% DWS	% DBS
OP	0.01	0.010	0.0000	0.0500	0.0139	0.018	21.21	21.21	0.0000	0.1000	0.0256	0.03	36.40	36.40	0.0000	0.1000	0.0224	0.03	31.82	31.82
Fe	0.3	0.30	0.0311	4.4500	0.5226	0.77	56.0	56.0	0.0146	3.3700	0.3625	0.54	28.79	28.79	0.0220	3.6389	0.4418	0.64	43.94	43.94
Cd	0.003	0.003	0.0005	0.0070	0.0032	0.002	53.0	53.00	0.0004	0.0060	0.0026	0.002	34.85	34.85	0.0000	0.0068	0.0023	0.00	34.85	34.85
Pb	0.01	0.01	0.0033	0.0367	0.0158	0.01	60.6	60.60	0.0000	0.1207	0.0139	0.022	34.84	34.84	0.0000	0.0484	0.0133	0.014	40.90	40.90
Ni	0.07	0.020	0.002	0.0467	0.0184	0.01	0.00	39.39	0.0000	0.0458	0.0174	0.01	0.00	37.88	0.0061	0.0303	0.0182	0.006	0.00	37.88
Mn	0.4	0.1	0.0000	0.7823	0.0812	0.11	1.5	22.28	0.0050	0.5550	0.0542	0.08	1.5	13.64	0.0059	0.6427	0.0636	0.10	1.5	16.67
Cu	2	0.05	0.0161	0.0411	0.0226	0.004	0.00	0.00	0.0128	0.0574	0.0243	0.01	0.00	1.52	0.0000	0.0318	0.0137	0.01	0.00	0.00
Zn	3	5	0.0000	0.7484	0.0504	0.13	0.00	0.00	0.0009	1.2617	0.0752	0.21	0.00	0.00	0.0061	0.8847	0.0604	0.15	0.00	0.00

Table 1.4.8. Statistical summary of the heavy metals of groundwater samples collected in different seasons from Malappuram District.

	WHO	BIS	Pr						Mo						Po					
			Min	Max	Mean	SD	% DWS	% DBS	Min	Max	Mean	SD	% DWS	% DBS	Min	Max	Mean	SD	% DWS	% DBS
As	0.01	0.01	0	0.050	0.006	0.009	7.58	7.58	0	0.050	0.017	0.020	27.27	27.27	0	0.050	0.025	0.021	39.39	39.39
Fe	0.3	0.30	0.005	5.579	0.414	0.904	24.24	24.24	0.015	6.582	0.346	0.888	19.70	19.70	0.026	5.139	0.393	0.941	19.7	19.7
Cd	0.003	0.003	0.0004	0.0064	0.0028	0.0015	43.94	43.94	0	0.052	0.0033	0.006	34.85	34.85	0	0.024	0.002	0.003	25.76	25.76
Pb	0.01	0.01	0	0.03	0.014	0.007	60.6	60.6	0	0.052	0.007	0.011	22.7	22.7	0	0.065	0.015	0.015	45.45	45.45
Ni	0.07	0.020	0	0.049	0.019	0.010	0	45.45	0.0012	0.0297	0.169	0.007	0	34.85	0.005	0.030	0.018	0.006	0	37.87
Mn	0.4	0.1	0	0.158	0.0234	0.0243	0	1.5	0.006	0.551	0.040	0.077	1.5	9.1	0.007	0.163	0.039	0.037	0	7.58
Cu	2	0.05	0.0161	0.0419	0.0231	0.005	0	0	0.0112	0.1324	0.263	0.016	0	3	0	1.796	0.045	0.219	0	4.55
Zn	3	5	0	1.245	0.118	0.254	0	0	0	0.518	0.061	0.101	0	0	0.005	0.366	0.050	0.078	0	0

Table 1.4.9. Pearson's correlation coefficient among the selected physicochemical parameters of groundwater samples of Palakkad District during Pr

	pH	EC	TDS	TA	TH	Ca	Mg	Cl	F-	Na+	K+	SO4	NO3	PO4	Fe	Cd	Pb	NI	As	Mn	Cu	Zn
pH	1	.648**	.648**	.682**	.699**	.617**	.659**	0.34	.393*	.563**	.368*	.682**	-0.311	-0.251	-0.04	-.536**	.371*	-0.156	0.046	-0.046	0.315	0.060
EC		1	.997**	.913**	.946**	.595**	.945**	.740**	.694**	.940**	.792**	.803**	-0.237	-0.111	-0.10	-0.283	.539**	0.000	0.241	0.126	.501**	0.280
TDS			1	.924**	.949**	.593**	.949**	.753**	.700**	.944**	.801**	.793**	-0.222	-0.088	-0.10	-0.274	.508**	0.002	0.253	0.144	.493**	0.253
TA				1	.887**	.528**	.892**	.628**	.733**	.869**	.721**	.693**	-0.337	-0.059	-0.04	-0.255	0.326	0.003	0.163	0.172	.501**	0.165
TH					1	.716**	.986**	.685**	.644**	.834**	.699**	.782**	-0.288	-0.158	-0.08	-0.295	.461**	0.000	0.305	0.176	.412*	0.178
Ca						1	.610**	.402*	0.159	.428*	0.211	.557**	-0.226	-0.137	-0.14	-0.267	.397*	-0.025	0.197	0.195	0.175	-0.156
Mg							1	.701**	.695**	.841**	.760**	.787**	-0.268	-0.144	-0.06	-0.299	.436*	0.010	0.318	0.177	.402*	0.245
Cl								1.00	.452**	.746**	.671**	.497**	0.094	0.042	-0.03	-0.244	.457**	0.137	0.210	0.276	0.269	0.186
F-									1	.684**	.656**	.608**	-.359*	-0.236	-0.04	-0.091	0.173	-0.098	0.153	0.085	0.193	0.191
Na+										1	.817**	.717**	-0.070	-0.073	-0.11	-0.260	.503**	-0.028	0.223	0.073	.554**	0.300
K+											1	.647**	-0.044	-0.053	-0.02	-0.184	0.303	0.005	0.284	0.049	0.249	0.339
SO4												1	-0.229	-0.316	-0.07	-.386*	.521**	-0.142	0.213	-0.195	0.243	0.293
NO3													1	0.077	-0.10	0.120	-0.030	-0.138	0.100	-0.138	0.088	-0.025
PO4														1	0.02	0.096	-0.150	0.229	0.034	.538**	0.145	0.034
Fe															1	0.288	-0.046	-0.080	-0.225	0.116	-0.134	-0.123
Cd																1	-.372*	0.103	-0.036	0.072	-0.087	-0.309
Pb																	1	0.032	-0.003	-0.094	0.225	0.224
NI																		1	0.133	0.172	-0.032	0.335
As																			1	0.063	0.031	0.262
Mn																				1	0.018	-0.165
Cu																					1	0.330
Zn																						1

**. Correlation is significant at the 0.01 level (2-tailed).

*. Correlation is significant at the 0.05 level (2-tailed).

Table 1.4.10. Pearson's correlation coefficient among the selected physicochemical parameters of groundwater samples of Palakkad District during Mo

	pH	EC	TDS	TA	TH	Ca	Mg	Cl	F-	Na+	K+	SO4	NO3	PO4	Fe	Cd	Pb	Ni	As	Mn	Cu	Zn
pH	1	.592**	.605**	.472**	.715**	.659**	.678**	0.337	0.238	.425*	0.25	.559**	-.387*	0	0.005	0.146	0.013	0.027	-.395*	0.030	-0.060	0.000
EC		1	.994**	.914**	.909**	.689**	.938**	.813**	.660**	.921**	.316	.769**	-.344*	0.09	-.069	.100	.037	.270	-.073	.218	.200	0.106
TDS			1	.915**	.895**	.682**	.922**	.807**	.656**	.934**	0.317	.775**	-0.328	0.102	-0.041	0.058	0.029	0.256	-0.073	0.210	0.209	0.104
TA				1	.742**	.509**	.793**	.751**	.639**	.924**	0.343	.662**	-0.208	0.045	-0.062	0.097	0.111	0.260	-0.006	0.126	0.278	0.139
TH					1	.879**	.970**	.705**	.567**	.702**	0.319	.710**	-.46**	0.105	-0.057	0.260	0.084	0.305	-0.187	0.327	0.164	0.079
Ca						1	.736**	.601**	0.277	.440*	0.292	.416*	-.375*	0.133	-0.002	0.196	0.041	0.209	-.359*	.442*	0.210	-0.017
Mg							1	.693**	.664**	.771**	0.304	.795**	-.46**	0.081	-0.081	0.269	0.098	0.326	-0.081	0.237	0.126	0.121
Cl								1	.434*	.797**	0.20	.418*	-0.17	0.067	0.098	0.027	-0.043	0.077	-0.048	.507**	.425*	-0.026
F-									1	.650**	0.14	.588**	-0.26	-0.066	-0.058	0.235	0.121	.431*	.364*	0.077	0.008	0.236
Na+										1	0.29	.695**	-0.19	0.081	0.003	-0.119	-0.008	0.175	0.058	0.122	0.213	0.173
K+											1	0.24	-0.21	0.216	0.018	0.111	.713**	0.069	-0.032	0.060	0.267	-0.188
SO4												1	-.360*	-0.034	-0.095	0.109	0.068	0.339	-0.096	-0.046	-0.003	0.118
NO3													1	0.216	-0.203	-0.224	-0.143	-0.256	0.286	-0.208	-0.037	-0.034
PO4														1	-0.151	-0.226	0.110	0.000	-0.164	-0.051	0.192	-0.017
Fe															1	-0.100	-0.077	-0.168	-0.171	.434*	0.335	-0.163
Cd																1	0.296	0.117	0.172	0.116	-0.098	-0.007
Pb																	1	0.057	0.165	-0.137	0.109	-0.090
Ni																		1	-0.049	0.069	-0.015	0.087
As																			1	-0.153	-0.194	0.084
Mn																				1	.601**	-0.132
Cu																					1	-0.001
Zn																						1

**. Correlation is significant at the 0.01 level (2-tailed).

*. Correlation is significant at the 0.05 level (2-tailed).

Table 1.4.11. Pearson's correlation coefficient among the selected physicochemical parameters of groundwater samples of Palakkad District during Po

	pH	EC	TDS	TA	TH	Ca	Mg	Cl	F-	Na+	K+	SO4	NO3	PO4	Fe	Cd	Pb	Ni	As	Mn	Cu	Zn
pH	1	.718**	.677**	.704**	.849**	.557**	.691**	.417*	.571**	.472**	.348*	.605**	-.377*	0.202	0.008	0.177	0.128	0.219	-0.132	0.066	0.085	-0.029
EC		1	.975**	.858**	.936**	0.151	.950**	.862**	.778**	.919**	.440*	.781**	-0.273	0.156	-0.063	-0.033	0.045	0.272	-0.065	0.083	0.29	-0.117
TDS			1	.808**	.911**	0.121	.933**	.906**	.723**	.889**	.380*	.688**	-0.273	0.229	-0.08	-0.025	-0.008	0.202	-0.045	0.062	0.306	-0.123
TA				1	.792**	0.221	.773**	.636**	.724**	.807**	.418*	.678**	-.348*	0.046	-0.038	-0.067	-0.022	0.294	-0.127	0.027	0.094	-0.056
TH					1	.376*	.927**	.735**	.706**	.727**	.358*	.756**	-.363*	0.137	-0.059	0.065	0.054	0.322	-0.158	0.115	0.203	-0.144
Ca						1	0.007	0.012	-0.134	-0.113	-0.065	0.175	-0.227	-0.005	-0.038	0.228	-0.214	0.058	-0.107	-0.007	-0.305	-0.301
Mg							1	.775**	.822**	.831**	.410*	.748**	-0.294	0.154	-0.053	-0.035	0.135	0.33	-0.109	0.134	0.339	-0.029
Cl								1	.559**	.850**	0.272	.521**	-0.16	0.216	-0.035	-0.05	-0.133	0.083	0.025	0.124	0.333	-0.175
F-									1	.732**	.381*	.673**	-0.184	0.017	0.072	-0.11	0.245	0.315	-0.096	0.134	.376*	0.104
Na+										1	.451**	.730**	-0.141	0.113	-0.096	-0.137	0.027	0.184	0.042	-0.004	0.311	-0.033
K+											1	0.275	-0.078	0.121	-0.061	0.272	0.28	0.138	-0.183	-0.109	0.168	-0.125
SO4												1	-0.311	0.015	-0.05	-0.09	0.208	0.336	0.011	-0.127	0.188	-0.069
NO3													1	-0.18	-0.205	-0.163	-0.166	-.48**	0.264	-0.064	0.251	0.159
PO4														1	-0.079	0.092	0.063	0.024	0.196	0.019	0.286	-0.135
Fe															1	-0.283	0.043	-0.012	-0.114	0.327	-0.057	-0.042
Cd																1	0.214	0.232	0.081	-0.145	0.096	0.143
Pb																	1	0.036	-0.063	-0.06	0.1	0.148
Ni																		1	-0.092	0.174	-0.061	-0.035
As																			1	0.143	0.066	-0.044
Mn																				1	0.221	-0.156
Cu																					1	0.291
Zn																						1

**. Correlation is significant at the 0.01 level (2-tailed).

*. Correlation is significant at the 0.05 level (2-tailed).

Table 1.4.12. Pearson's correlation coefficient among the selected physicochemical parameters of groundwater samples of Malappuram District during Pr

	pH	EC	TDS	TA	TH	Ca	Mg	Cl	F	Na	K	SO4	NO3	PO4	Fe	Cd	Pb	Ni	As	Mn	Cu	Zn
pH	1	.483**	.493**	.760**	.721**	.656**	.677**	0.33	.373*	.596**	-0.26	.405*	-0.28	0.05	.434*	-0.099	0.079	0.156	0.321	-0.015	0.068	-0.216
EC		1	.982**	.417*	.632**	.576**	.591**	.383*	.466**	.681**	-0.21	0.23	0.25	.369*	0.129	-0.11	0.18	0.321	0.052	-0.093	0.181	-0.032
TDS			1	.421*	.668**	.632**	.567**	.425*	.462**	.696**	-0.27	0.27	0.23	0.32	0.181	-0.096	0.135	0.285	0.027	-0.095	0.156	-0.056
TA				1	.833**	.759**	.778**	0.26	0.31	.534**	-0.09	0.29	-0.20	-0.01	.424*	0.104	0.043	0.245	.438*	0.101	0.132	-0.062
TH					1	.971**	.782**	.520**	0.32	.753**	-0.21	.390*	0.14	-0.02	.473**	0.055	0.131	.370*	0.169	0.094	0.136	0.027
Ca						1	.609**	.569**	0.26	.725**	-0.24	0.33	0.16	-0.03	.559**	0.011	0.094	.367*	0.045	0.174	0.075	0.056
Mg							1	0.24	.358*	.602**	-0.06	.440*	0.05	0.02	0.111	0.152	0.189	0.267	.440*	-0.14	0.253	-0.056
Cl								1	0.20	.639**	-.52**	0.13	0.25	0.00	0.191	0.097	0.135	0.166	-0.083	0.082	0.099	0.206
F									1	0.31	-0.33	0.13	-0.21	0.13	0.064	-0.127	-0.037	0.079	-0.022	-.346*	-0.109	-0.039
Na										1	-.392*	.401*	0.25	0.12	0.093	0.014	.349*	0.316	0.155	-0.043	0.106	0.133
K											1	-0.20	-0.02	0.02	0.051	0.073	-0.076	0.105	0.14	0.145	0.028	0.07
SO4												1	0.01	-0.03	-0.073	0.144	0	0.22	0.038	-0.251	-0.01	-0.059
NO3													1	-0.01	-0.131	-0.068	0.198	0.094	-0.201	0.207	0.327	.411*
PO4														1	0.023	0.188	-0.148	0.16	-0.023	0.189	0.244	0.029
Fe															1	-0.214	-0.059	-0.066	-0.013	0.168	-0.208	-0.077
Cd																1	-0.257	0.14	0.169	0.265	0.292	0.34
Pb																	1	0.076	0.246	-0.13	-0.193	0.245
Ni																		1	-0.058	0.04	0.048	0.049
As																			1	-0.183	.354*	-0.085
Mn																				1	0.316	.485**
Cu																					1	0.073
Zn																						1

**. Correlation is significant at the 0.01 level (2-tailed).
*. Correlation is significant at the 0.05 level (2-tailed).

Table 1.4.13. Pearson's correlation coefficient among the selected physicochemical parameters of groundwater samples of Malappuram District during Mo

	pH	EC	TDS	TA	TH	Ca	Mg	Cl	F	Na	K	SO4	NO3	PO4	Fe	Cd	Pb	Ni	As	Mn	Cu	Zn
pH	1	.690**	.681**	.833**	.797**	.757**	.699**	0.22	0.22	.550**	0.32	.644**	0.02	0.004	0.278	-0.009	-0.167	-0.11	-0.073	0.051	0.044	-0.152
EC		1	.992**	.810**	.888**	.815**	.821**	.760**	0.00	.893**	.778**	.666**	0.34	-0.043	0.279	0.141	-0.141	-0.252	0.148	0.225	0.084	-0.072
TDS			1	.790**	.883**	.813**	.812**	.777**	0.01	.906**	.775**	.654**	.348*	-0.025	0.269	0.136	-0.111	-0.228	0.136	0.282	0.069	-0.091
TA				1	.850**	.840**	.696**	0.29	0.13	.607**	.407*	.572**	-0.08	0.055	.499**	0.059	-0.14	-0.121	0.084	0.095	-0.034	-0.143
TH					1	.949**	.878**	.525**	0.12	.741**	.562**	.674**	0.24	-0.024	.450**	0.099	-0.192	-0.259	0.169	0.268	-0.012	-0.108
Ca						1	.682**	.457**	0.14	.685**	.412*	.533**	0.21	-0.008	.610**	0.016	-0.205	-0.22	0.122	0.337	-0.033	-0.124
Mg							1	.522**	0.08	.678**	.678**	.757**	0.22	-0.044	0.118	0.208	-0.136	-0.271	0.209	0.11	0.023	-0.063
Cl								1	0.00	.847**	.763**	.422*	.560**	-0.032	0.071	0.136	-0.095	-0.216	0.107	.427*	0.106	-0.03
F									1	-0.01	-0.14	0.05	0.03	.351*	0.182	0.017	0.176	0.246	-0.106	0.098	0.037	-0.135
Na										1	.653**	.487**	.380*	-0.144	0.108	0.026	-0.192	-0.273	-0.048	.344*	0.135	-0.039
K											1	.610**	.401*	0.054	-0.063	0.26	0.064	-0.108	.369*	-0.012	-0.029	-0.032
SO4												1	0.18	-0.167	0.196	0.311	-0.21	-0.319	0.252	0.09	-0.013	-0.214
NO3													1	-0.198	-0.013	0.019	0.004	-.378*	-0.097	0.169	.377*	-0.012
PO4														1	0.008	0.25	.403*	.733**	0.339	-0.05	-.380*	-0.168
Fe															1	-0.011	-0.089	-0.195	0.065	.373*	-0.061	-0.129
Cd																1	0.107	0.182	.436*	0.182	-0.069	0.23
Pb																	1	0.31	-0.136	-0.187	-0.165	0.083
Ni																		1	0.26	-0.093	-.355*	0.134
As																			1	-0.014	-0.235	0.109
Mn																				1	-0.015	-0.023
Cu																					1	-0.087
Zn																						1

**. Correlation is significant at the 0.01 level (2-tailed).

*. Correlation is significant at the 0.05 level (2-tailed).

Table 1.4.14. Pearson's correlation coefficient among the selected physicochemical parameters of groundwater samples of Malappuram District during Po

	pH	EC	TDS	TA	TH	Ca	Mg	Cl	F	Na	K	SO4	NO3	PO4	Fe	Cd	Pb	Ni	As	Mn	Cu	Zn
pH	1	.607**	.623**	.859**	.669**	.614**	.551**	0.06	0.22	.591**	0.243	.547**	-0.161	-0.002	.368*	0.16	-0.202	0.08	.438*	0.13	-0.01	-0.054
EC		1	.804**	.753**	.760**	.668**	.469**	.518**	.456**	.724**	0.118	.432*	0.168	0.214	.459**	-0.065	-0.135	-0.17	.381*	.354*	-0.11	-0.02
TDS			1	.850**	.892**	.766**	.745**	.575**	.412*	.867**	.576**	.582**	0.238	0.243	.397*	-0.072	-0.097	-0.1	.509**	0.295	-0.16	-0.055
TA				1	.862**	.795**	.715**	.346*	0.34	.798**	.384*	.643**	-0.086	0.033	.487**	0.066	-0.055	-0	.533**	0.264	-0.09	-0.189
TH					1	.814**	.671**	.558**	0.28	.697**	.472**	.614**	0.192	0.022	.530**	-0.019	-0.06	-0.07	.477**	0.193	-0.11	-0.133
Ca						1	.682**	.406*	0.27	.666**	.411*	.519**	0.097	-0.023	.623**	-0.107	0.007	-0.15	.466**	0.256	-0.12	-0.067
Mg							1	.352*	0.22	.699**	.718**	.654**	0.204	-0.024	0.099	-0.045	-0.043	-0.23	0.342	0.09	-0.07	-0.154
Cl								1	0.13	.542**	0.302	0.254	.433*	-0.141	0.152	-0.131	-0.062	-0.19	0.327	.503**	0.149	-0.194
F									1	0.309	0.031	0.189	0.122	.434*	0.216	0.035	0.078	-0.13	0.333	-0.088	0.004	0.07
Na										1	.465**	.499**	0.294	-0.021	0.149	-0.117	-0.011	-0.01	.506**	.347*	-0.15	-0.096
K											1	.429*	0.208	0.069	-0.03	-0.022	-0.004	0.08	0.238	-0.127	-0.14	-0.089
SO4												1	-0.118	0.044	-0.002	0.064	-0.165	-0.02	0.27	0.137	0.159	-0.106
NO3													1	-0.124	-0.174	-0.236	0.116	-0.26	0.045	-0.027	-0.06	-0.014
PO4														1	0.225	0.26	-0.099	0.042	-0.125	-0.107	-0.17	0.281
Fe															1	-0.1	0.016	-0.18	0.265	0.112	-0.05	-0.019
Cd																1	0.114	.591**	-0.137	-0.126	-0.22	-0.088
Pb																	1	0.186	-0.097	-0.097	-0.09	0.183
Ni																		1	-0.141	-0.192	-.46**	0.233
As																			1	0.24	0.192	0.16
Mn																				1	0.131	-0.118
Cu																					1	-0.093
Zn																						1

**. Correlation is significant at the 0.01 level (2-tailed).
*. Correlation is significant at the 0.05 level (2-tailed).

1.4.3.1. pH

The pH of water is a fundamental quality parameter that determines the solubility and biological availability of chemical constituents such as nutrients and heavy metals. During the study period, pH measurements in the Palakkad District ranged from 4.85 to 8.53 in Pr, 4.3 to 8.52 in Mo, and 4.75 to 8.68 in Po (Table 1.4.5). Excessively high and low pH levels can be harmful to the living systems. BIS (2012) recommends the pH of drinking water to be within 6.5-8.5 and, accordingly, 32% of Pr and Mo samples and 33% of Po samples of Palakkad were outside the standard limit (Table 1.4.5). Samples from P04, P06, P09, P14, P16, and P20 were in the acidic range, and a high acidic pH was observed in Mo samples (Annexure 1), which were mostly drawn from open wells. The acidic pH of groundwater can happen due to the recharge and leaching of organic acids into shallow aquifers (Knutsson et al. 1994). Rainfall with a pH of 5.56 is reported in the Silent Valley region of the Palakkad District, which may also cause acidic pH in groundwater (ENVIS; Samarghandi et al. 2016). Water samples from bore wells noticed an alkaline pH.

In the studies on groundwater quality in the Malappuram District, 86.36% of the Pr and 77.27% of the Mo and Po samples are not within the permissible limits of pH (6.5-9.5) specified by the WHO and BIS (Table 1.4.6). The acidic nature of groundwater was noticed in the majority of the samples collected from this area. 85% of the water samples are from open wells and they are considered shallow aquifers (Bennett et al. 2010). The infiltration and leaching of organic acids can also contribute to the acidity of groundwater, particularly in shallow aquifers (Samarghandi et al. 2016). Also, lithological characteristics have a profound influence on water quality (Ahmed et al. 2022). Most of the regions in the Malappuram District are covered by the charnockite and charnockite gneisses types of mineral groups (Fig.1.4.2). Acidic types of charnockite gneiss at the boundary of the Western Ghats massif can subside to low pH in the groundwater (Gunnel 1997).

1.4.3.2. Temperature

Groundwater temperatures, particularly in shallow aquifers, are affected by ground surface temperatures, which are dependent on land cover and climatic conditions. High water temperatures were observed during Pr, followed by Po and Mo in the Palakkad District (Table 1.4.5). The least water temperature of about 20.50°C was observed in a groundwater sample collected from a bore well at a depth of 121.9 meters (P24) in the Mo season. In contrast, a higher temperature was also observed in the sample collected from the bore well (P22) at a depth of 106.68 meters in the Pr season. This difference is mainly attributed to the ambient climatic conditions as well as the land use pattern of this region. In Malappuram District, the lowest temperature of 25.9°C was observed in M14 in the Mo season and the highest of 33.5°C (M14 & M21) in the Pr season (Table 1.4.6). The highest fluctuation of groundwater temperature was observed in the shallow aquifer of the urban region (M14) (Annexure 2). Climate change and urbanization influence groundwater temperatures (Taylor and Stefan 2009). Seasonal temperature cycles penetrate the ground to depths of 10 -15 meters in northern temperate climate regions (Bucci et al. 2017). Groundwater temperatures affect microbial activity in aquifers, and also cause oxygen depletion (Danielopol et al 2003).

1.4.3.3. EC, TDS, and Salinity

Electrical conductivity (EC) is an important indicator of water quality as it measures the total charged particles in water (Tutmez et al. 2006). Total dissolved solids (TDS) and salinity are proportional to EC as it increases charged particles in water (Wilcox 1948; Harilal 2005). The Indian Council of Medical Research (ICMR) limits 300 µS EC for drinking water (ICMR, 1975). Also, WHO states that the EC in water meant for drinking purposes must not exceed 400 µS. The EC of samples was higher than the ICMR standards in Po (71%), followed by Mo (70%) and Pr (62%) in Palakkad District (Table 1.4.5). Conductivity was found to be higher in confined aquifer samples than in shallow aquifers (P01, P19, P22, P24, P26, P28, P29, P30, and P31) (Annexure 3). In the Malappuram District, 22.73% of the Po and 27.27% of the Mo and Pr samples exceeded this limit (Table 1.4.6).

Salinity may impart a salty taste to water if it goes beyond 250 mg/L (Kumar and Puri 2012). In the Palakkad District, salinity levels in groundwater samples were higher in Mo (53%) and Po (50%) seasons (Table 1.4.5), whereas from Malappuram, the salinity was slightly higher in the Po season and 10.6% of the samples exceeded the standard limits of BIS and WHO for drinking purposes (Table 1.4.6). Elevated levels of salinity were observed mostly in bore well samples and the samples collected from the coastal areas (P01, P18, P19, P22, P24, P26, P28, P29, P30, P31, M07, M25, M30, and M32) (Annexure 4).

WHO recommends a TDS value of < 300 mg/L for drinking water sources (Fawell and Ong 2012), and BIS suggests a value of < 500 mg/L. High levels of TDS in drinking water may cause an objectionable taste and have a laxative effect. The present study in the Palakkad District showed a higher TDS value (> 500 mg/L) during Po (33%), Mo (29%), and Pr (15%) seasons (Table 1.4.5). High TDS was observed in the samples drawn from bore wells mostly constructed in confined aquifers (P01, P19, P21-22, and P28-P31 (Annexure 5). In the samples from Malappuram, the dissolved constituents were very low, and only Mo samples (3%) and Po samples (1.5%) exceeded the BIS limit of 500 mg/L. However, 16.7% of Po samples, 12.1% of Mo, and 3% of Pr samples were above the permissible limits of WHO standards for drinking water (>300mg/L) (Table 1.4.6). Several factors contribute to the enrichment of dissolved minerals in groundwater. The highest number of samples from Malappuram that exceeded the standard limits of TDS was from the coastal plains in the Po season (M25, M30, and M32). A salty taste of water is associated with seawater or brackish water, but it can also be related to high total dissolved solids (TDS) (Burlingame et al. 2007). The TDS levels vary greatly depending on the source of the water and the geology of the area (Van der Aa 2003)

The elevated levels of EC, TDS, and salinity during the Mo and Po seasons can be attributed to soluble salts in rocks and soils, with which groundwater is associated (Srinivas et al. 2014). The rainwater that infiltrates through the rocks and soils can enrich the minerals in the shallow or confined aquifers (Sharma and Chhipa 2016). A strong positive correlation between EC and TDS was observed in all seasons in

both Districts, as it also exhibited a strong positive correlation with most of the cations and anions, especially Na, Mg, Cl, SO_4, and F (Table 1.4.9–14). The mineral components of soluble salts and relative soluble salts in water and soil have the characteristics of transportation and symbiotic aggregation (Tunstall 2005). Therefore, the solubility and transport of minerals in rocks and soils may be affected by subsurface inflow, drainage pattern, and topography of the land (Xu et al. 2014).

1.4.3.4. Turbidity, TS, and TSS

Turbidity is the measure of cloudiness or light penetration of water. Undissolved substances which scatter light in all directions give the measure of turbidity (Daigavaneet al. 2017). Knowledge of turbidity allows an estimate to be made of the concentration of the suspended solids (Patil et al. 2011). The presence of colloidal impurities and other fractions of solids of both organic and inorganic origins contributes to the turbidity in natural water (Jiang 2001). Total solids are the combined weight of both total dissolved solids and suspended solids. The major dissolved solids are Ca, Mg, Na, K, Cl, SO_4 , NO_3 , PO_4 , Fe, F, silica, carbonates, and bicarbonates (Ali et al. 2019a). Silt, planktons, organic particles, and domestic or industrial waste are all examples of suspended solids. Suspended solids are visible and can be removed by filtration, whereas dissolved solids are a major concern and require a more sophisticated facility for their removal (Garcia-Segura et al. 2017).

BIS and WHO prescribe that the maximum limit of turbidity should not exceed 5 NTU for drinking water. The results of the samples from Palakkad revealed that 18.2% of Mo, 13.6% of Pr, and 9.1% of Po samples exceeded the standard limits (Table 1.4.5). High turbidity was observed throughout the year in most samples collected from the bore wells (P01, P18, P19, P22, P24, P28-31) in the Palakkad District (Annexure 8). The reason for this is attributed to the presence of dissolved Fe in groundwater, which is immediately oxidized when it comes in contact with the air and forms a brown precipitate (Verschoor and Molot 2013). Elevated levels of turbidity are observed in the samples collected from the Malappuram District, particularly in Mo (50%), followed by Pr (18.2%) and Po (10.6%) seasons (Table

1.4.6). Similar to that of the Palakkad District, Fe contamination contributed to turbidity in water samples collected from the bore wells (M8, M25, and M30) (Annexure 8) in all seasons. Seasonal turbidity due to heavy rainfall is higher in the open well samples (shallow aquifer) of the Malappuram District than in Palakkad (Goransson et al. 2013). Algae and other suspended particles might have attributed turbidity in the open well samples (M15, M26, M30) (Annexure 8) of the Malappuram District throughout the year (Bilotta and Brazier 2008).

There are no limits recommended by WHO or BIS for TS and TSS in drinking water. Turbidity, on the other hand, can be measured indirectly because suspended solids and precipitates of dissolved solids contribute to it. The highest TS was found in a sample collected from a bore well in the Palakkad District (P01, P18, P19, P22, P24, P28-31), (Annexure 7). In contrast, both suspended and dissolved solids contributed to TS in the Malappuram District (M08, M15, M25, M26, M30, and M33) (Annexures 5, 6, 7). Turbidity has no health consequences, but it can interfere with disinfection and provide a medium for microbial growth (Chahal et al. 2016). Turbidity in water may indicate the presence of disease-causing organisms. Suspended solids never settle to the bottom, and hence can transport pesticides and microbes (Walker et al. 2019).

1.4.3.5. TAc and TA

High seasonal fluctuations of acidity were observed in the open well samples from the western Palakkad region (P9, P10, and P17) (Annexure 9), whereas less variation was noted in the samples from the Malappuram District. The mean value of total acidity in Malappuram District was higher, particularly in the Mo and Po seasons (Table 1.4.6). High acidity is observed in the shallow aquifers in both Districts. The reasons for the total acidity are attributed to three factors. The first is that the leachate of organic acids from the waste dumps can reach the shallow aquifer (Knutson et al. 1994), acid rain (Samargandhi et al. 2016), and geological sources like the acidic type of charnockite gneiss predominantly in the Malappuram District (Gunnel 1997). A high concentration of CO_2 in the atmosphere is easily dissolved in shallow open wells and can also contribute to acidity in groundwater

(Apps et al. 2010). A significant negative correlation between pH and NO_3 in samples from Palakkad, in Mo and Po, indicates an anthropogenic input of total acidity. Whereas in Malappuram, samples show no significant negative correlation between pH and NO_3 , showing a geogenic source of acidity (Gunnel 1997). Acidity in groundwater can have long-term effects on health, the environment, and the economy. The acidity will increase the dissolution of Fe, As, Cd, Pb, and Ni, causing significant health problems (Velusamy et al. 2021). It exacerbates corrosion issues, resulting in high maintenance costs. Furthermore, groundwater interaction with surface water bodies may cause acidification of streams and other surface water bodies, resulting in environmental consequences (Takem et al. 2015).

Total alkalinity (TA) is a measure of the concentration of all alkaline substances dissolved in water. In Palakkad District, 27% of Pr, 14% of Mo, and 42% of Po samples exceeded the desirable limits (> 200 mg/L) of BIS, while in Malappuram District, it was only 1.5% of Mo and 12.12% of Po samples (BIS 2012). Subsequent reductions in alkalinity with increased total acidity in both Districts were observed. Total alkalinity was comparatively higher in the samples collected from the eastern region of the Palakkad District (P22, P23, P25, P26, P28-30, and P32) (Annexure 10).

Groundwater flowing through carbonate-rich rocks typically has a pH greater than 7. (Umar et al. 2013). This apparent seasonal variation in alkalinity in the Palakkad District could be attributed to chemical processes in groundwater and alkaline soils, as well as the influence of rainfall (Ekere et al. 2019). Bicarbonate is said to be the dominant anion in Palakkad and Chittur Blocks (Kannan et al. 2021). The dissolution of crystalline limestone in the Palakkad Gap region is responsible for the majority of the alkalinity (Soman 1997). Furthermore, alkalinity correlates positively with pH (Table 1.4.9, 1.4.10, and 1.4.11), indicating the geological causes of high alkalinity in the Palakkad District. At pH levels 6.3–8.3, bicarbonate is the dominant species, and it is coupled with the cations sodium, calcium, magnesium, and potassium (Deutsch 2020).

1.4.3.6. TH, Ca, Mg, Cl, and SO_4

Calcium and magnesium are the dominant cations, imparting hardness to water. It is specified as milligrams of calcium carbonate equivalent per liter and is considered very hard if the value is greater than 180 mg/L (Wasana et al. 2017). Carbonates cause temporary hardness, and bicarbonates (sulphate and chloride) are the basis of permanent hardness in water. TH, calcium, and magnesium hardness recorded were higher in Sholayur (P01), Puthussery (P21), Eruthenpathy (P22), Perumatti (P23), Chittur (P25), Kollengode (P28), Muthalamada (P29), and Erumayur (P33) regions of the Palakkad District. Also, 53.3% of Pr, 50% of Po, and 48.5% of Mo samples were above the acceptable limits of TH (200 mg/L). The essential quantity of calcium in drinking water is 75 mg/L and magnesium is 30–50 mg/L (BIS 2012; WHO 2009). However, 52% of Pr, 44% of Mo, and 35% of Po samples from the Palakkad District exhibited calcium concentrations higher than the standard limit, and 77% of Pr, 70% of Mo, and 62% of Po samples had magnesium above 30 mg/L (Table 1.4.5).

Hard water is rare in the Malappuram District. Only 10.6% of the Pr, 6.06% of Mo, and 3.03% of the Po samples exceeded the BIS standard limits of 200 mg/L. The calcium concentration in the samples exceeded the BIS (2012) limits by 21.21%, 18.18%, and 12.12%, in the Pr, Mo, and Po samples respectively, and 46.96% of the Pr, 15.15% of the Mo, and 19.7% of the Po samples exceeded the BIS limits for magnesium (Table 1.4.6).

Chloride and sulphate in groundwater are mostly considered as anthropogenic inputs (Khatri and Tyagi 2015), but they also get into groundwater as a result of rock-water interaction (Logeshkumaran 2015). Chloride alters the taste of water if it exceeds the level of 250 mg/L (BIS 2012). In the study region, the chloride content of groundwater fluctuated with the season. The Palakkad District recorded a minimum of 12.3 mg/L to a maximum of 496 mg/L in Pr, 12 mg/L to 357 mg/L in Mo, and 12 mg/L to 296 mg/L in Po seasons. The chloride concentration of Pr (8%), Mo (8%), and Po (5%) samples remained high above the standard limit in the samples from the Palakkad District (>250 mg/L) (Table 1.4.5). Chloride contamination was observed

both in open wells (P21) and bore wells (P22, P28, and P31). The chloride contagion of the shallow aquifer (P21) is attributed to be an anthropogenic source such as the mixing of septic and sewage system (Venkatesan and Swaminathan 2009). Similarly, the deep well water with high chloride is ascribed to be the reason for mineral sources like gneiss and granite in the study area. Gneiss contains up to 48 mg of soluble chloride per kilogram of rock, and granite contains up to 300 mg Cl/kg of rock (Bucher and Stober 2002). The higher correlation of TH with chloride, calcium, and magnesium (Tables 1.4.9-13) in samples from the study area in all seasons explains the possibility of permanent hardness in groundwater due to $CaCl_2$ and $MgCl_2$ (WHO 2009).

Water with a high sulphate concentration has laxative properties (Bashir et al. 2012). The sulphate values of the samples were within the standard limits, except for Eruthenpathy village in Po (1.5%) season in Palakkad. Chloride and sulphate concentrations in the groundwater of Malappuram District are within the BIS standard limits for drinking water (Table 1.4.6). Sulphate too showed a moderate to strong correlation with Ca and Mg, respectively, specifying the permanent hardness of groundwater. However, chloride and sulphate hardness were not in equal proportion, and chloride-dominated hardness was prominent. Alkalinity is an indirect measure of the amount of carbonates and bicarbonates in water (Wurts 2002). TH and TA had a strong positive connection (Table 1.4.9-13) in all seasons, specifying the transitory nature of hardness. As a result, both temporary and permanent hardness prevail in the study area.

Calcium had a weak positive (Pr & Mo) and negative (Po) correlation with F, while TH, magnesium, chloride, and sulphate had a strong positive correlation with F in the Palakkad District (Tables 1.4.9, 1.4.10, and 1.4.11). In the Malappuram District Mg exhibited a significant positive correlation with the F only in the Pr season (Tables 1.2.12). The higher concentration of magnesium and a lower concentration of calcium in groundwater favors the entry of F into it (Handa 1975). Calcium in water gradually precipitates the F, and hence the presence of calcium is more important to reduce F concentration in groundwater (McCann 1968). A strong

relation between Na and Cl (Tables 1.4.9, 1.4.10, and 1.4.11) in the study area indicates rock-water interaction, likely from calcium and magnesium silicate weathering, which enhanced the hardness of groundwater (Srinivas et al. 2014).

1.4.3.7. Na & K

Sodium concentrations in groundwater range from 2.3 to 389 mg/L, with a mean of 81mg/L during the Pr, 5.9 to 415.5mg/L with a mean of 85mg/L in Mo, and 15.2 to 441 mg/L with a mean of 97.7mg/L in Palakkad District (Table 1.4.5). Sodium can affect the taste of drinking water at levels higher than 200 mg/L (WHO 2004), but only 12% of Pr, Po, and 9.1% of Mo samples in the Palakkad District (Table 1.4.5) exceeded this standard limit, while no sample in Malappuram (Table 1.4.6). The samples collected from the eastern rather than the western regions of the Palakkad District had a higher concentration of sodium. Malappuram showed the maximum mean value of sodium during Mo (38.9 mg/L) and Po (38.5 mg/L) seasons (Table 1.4.6).

Sodium is abundantly found in water from both natural sources and from the wide use of domestic and industrial purposes. Mineral waters contain more than 200 mg/L of sodium. (Van der Aa 2003). A higher sodium percentage in drinking water causes serious health issues such as hypertension, congenital illnesses, kidney disorders, and nervous system abnormalities (Qian 2018; Narsimha et al. 2017). To minimize salt intake for persons on a low-sodium diet who are concerned about hypertension, the US Environmental Protection Agency (USEPA) recommends that sodium not exceed 30–60 mg/L (Advisory 2003). When this element is taken into account, groundwater from Palakkad with a mean value of Na above 81 mg/L in all seasons (Table 1.4.5) suggests that the water is unfit for consumption by people who follow a low-sodium diet. A significant positive correlation between Na and Cl (Tables 9, 10 & 11) in the study area indicates rock water interaction more precisely from the igneous rocks which are abundantly present in the study area (Srinivas et al. 2014; Reddy et al. 2019). The relatively high sodium concentration may have a detrimental effect on soil structure and permeability, resulting in alkaline soils as Na has a strong relation with TA in all seasons (Tables 9, 10 & 11) (Gupta 2015).

The WHO (2004) recommends a potassium limit of 82 mg/L in drinking water, although just 3% of Mo and 1.5% of Po samples in the Malappuram District surpassed this limit (Table 1.4.6). The samples taken from the Palakkad District were within the standard limit in all seasons, and the highest mean value obtained was 14 mg/L in the Po season (Table 1.4.5). Potassium is nearly as common as sodium in igneous and metamorphic rocks. Its concentration in groundwater is one-tenth or even one-hundredth of that of sodium. Potassium scarcity in groundwater is produced by two reasons, the first of which is the resistance of potassium minerals to weathering and dissolution and the other is potassium fixation in clay minerals (Goldich 1938; Simonsson et al. 2009).

1.4.3.8. NO_3 and PO_4

The nitrate in groundwater has prime importance due to its health impact. The maximum permissible limit of nitrate in drinking water prescribed by BIS is 45 mg/L, whereas the WHO prescribes 10 mg/L. Nitrates are rarely found in geological formations, and pollution from these ions is mostly caused by man-made sources such as sewage and fertilizers. Nitrate is produced naturally by microbes (Juncher Jorgensen et al. 2009). The highest occurrence of nitrate was found in the Mo season in both Districts (Table 1.4.5 and 6). A high concentration of nitrate was observed in shallow wells (P02, P04, P13, P17, P20, P25, M01, M05, M23, M27, and M29) in Palakkad and Malappuram Districts (Annexure 18). However, samples from both Districts were found to be within the permissible limits of BIS and WHO standards (Tables 1.4.5 and 6). A significant positive correlation between nitrate and sulphate levels in the Palakkad District during the Mo season (Table 1.4.10) indicates its point source (Sajilkumar et al. 2014). Similarly, the negative correlation between NO_3 and SO_4 has been attributed to the cause of denitrification processes (Tang et al. 2004; Fang et al. 2015). Septic tanks (McQuillan 2004), animal and human waste (Suthar et al. 2009), and agricultural fields may also be the source of nitrate in groundwater (Stigter et al. 1998; Agrawal et al. 1999). The substantial positive connection of NO_3 with Cl in the Mo and Po seasons in the Malappuram District (Table 1.4.13 and 14) suggests that the above-mentioned sources may be the cause of nitrates in shallow aquifers. The strong positive correlation between NO_3 and K in Malappuram during the Mo season (Table 1.4.13) confirms that the nitrate

contamination is from an agricultural source, as fertilizers are a good supplier of these ions (Sajikumar et al. 2014).

Phosphorus is one of the most important elements required for plant and animal growth. Natural sources of phosphorus in groundwater and surface water include the natural breakdown of rocks and minerals, weathering of soluble inorganic elements, decaying biomass, deposition from air, runoff, and sedimentation (USGS 2005). Anthropogenic sources include fertilizers, detergents, industrial discharge, wastewater and septic system effluent, animal wastes, phosphate mining, synthetic material, drinking water treatment, and forest fires (Smil 2000). There are three types of phosphate found: orthophosphate, met-pho sulphate, and organically bound phosphate. Natural processes produce ortho-form, which is seen in domestic sewage. On degradation to polyform of phosphates in detergents and insecticides, they can covert to ortho form. Phosphorus in elemental form is extremely hazardous and can accumulate in the body (Fadiran et al. 2008). Phosphate levels naturally present in surface and groundwater bodies are not detrimental to human health, animals, or the environment. Extremely high phosphate levels, on the other hand, can create digestive issues.

The World Health Organization (WHO) and the Bureau of Indian Standards (BIS) do not specify any phosphate limits for drinking water. To combat eutrophication, the USEPA has imposed phosphorous limits. These are that total PO_4 must be 0.05 mg/L for streams that discharge into reservoirs, total PO_4 levels in reservoirs must be maintained at 0.025 mg/L, and streams should not be allowed to flow into reservoirs or lakes if total PO_4 is 0.1 mg/L. According to the Swaziland Water Service Corporation (SWSC 2014), the maximum allowable concentration of PO_4 in drinking water must be 1 mg/L. Samples from Palakkad and Malappuram were within the permissible limits of SWSC, except for Po samples (1.52%) of Malappuram District. However, it has high eutrophication potential as 24% Pr, 11% Mo, and 17% Po samples of the Palakkad District and 27% Pr, and 12% Mo and Po samples of the Malappuram District exceeded the limits of 0.1 mg/L. The phosphate in groundwater is usually found in trace quantities. The higher concentration of phosphate in groundwater represents anthropogenic sources of pollution from agriculture run-off and domestic waste dumps (Khatri and Tyagi 2015). It can reach the groundwater through infiltration and percolation processes, especially in shallow

aquifers. A significant positive correlation between PO_4 and EC was observed in Pr samples of Malappuram District (Table 12). A strong correlation between PO_4 and F was observed in the Mo and Po seasons in the Malappuram District (Tables 13 and 14). Phosphate fertilizers contain small quantities of F as impurities (Sharma and Sharma 2004). The use of phosphate fertilizer and the precipitation and leaching of these ions in shallow aquifers in the Mo and Po seasons may be the reason for the significant correlation of these ions (Sujatha 2003; Kundu and Mandal 2009).

1.4.3.9. Dissolved Oxygen (DO)

Dissolved oxygen is a colorless, tasteless gas that is dissolved in water and has no adverse effects on human health. The Palakkad District has a minimum of 0.41–10.75 mg/L in Pr with a mean of 3.32 mg/L, 0.4–10.13 mg/L with a mean of 3.38 mg/L in Mo, and 0.41–6.90 mg/L with a mean of 2.89 mg/L in Po season (Table 1.4.5). In the Malappuram District, Pr was 0.57 mg/L with a mean value of 3.14 mg/L, Mo was 0-8.10 mg/L with a mean value of 3.6 mg/L, and Po was 0.20-8.5 mg/L with a mean value of 3.03 mg/L (Table 1.4.6). DO is used to assess the stability of trace metals, radionuclides, hazardous anionic complexes, and organic pollutants in groundwater. The atmosphere is the primary source of dissolved oxygen in the water. Atmospheric oxygen is rapidly used by microbes in soil and unsaturated zones for their respiration and decomposition of organic matter (Refsgaard et al. 1991). Groundwater is typically considered anoxic since it is present below the water table and has little opportunity to mix with oxygen. Also, oxygen mixing is exactly proportional to the hydrostatic pressure, and depth (Cox 2003). The most important geochemical oxidant of ferrous silicate is oxygen (White and Yee 1985). The concentration of dissolved ions in water is mostly influenced by dissolved oxygen. In the presence of dissolved oxygen, Fe rapidly precipitates as oxyhydroxide. These oxyhydroxides are important heavy metal adsorbents (Le et al. 2019).

When the groundwater is contaminated by dissolved organic carbon from landfill leachate, the microorganisms rapidly utilize the DO to decompose the organic matter (Ma et al. 2021). Therefore, the DO is likely absent in contaminated shallow groundwater. Hence, site-specific verification of DO is very important. As many metals have multiple oxidation states and are thus susceptible to DO, the

concentration of many hazardous metals in groundwater is determined by DO (Duruibe et al. 2007). For example, in anoxic circumstances, As is insoluble (Sadiq 1990). Iron and Mn, on the other hand, are insoluble in oxygenated water (Yarincik et al. 2000).

1.4.3.10. Total coliforms and *E.coli*

Biological contamination in drinking water is a major public health issue in underdeveloped and developing countries. According to the WHO, over 1.1 billion people worldwide drink contaminated water, resulting in 88 percent of diarrhea cases (Osiemo et al. 2019). Gastrointestinal infection cases have been recognized as a result of E. coli contamination due to sewage in recreational waters (USEPA 1986). The survival pattern of fecal coliforms is comparable to that of other bacterial pathogens (Nowicki et al. 2021). As a result, E. coli was used as a biomarker of fecal contamination in water samples (USEPA 1986). Warm-blooded animal feces may contain a range of pathogenic intestinal microbes. *Escherichia coli* contains both commensal and pathogenic strains that cause a variety of human diseases, resulting in more than 2 million deaths every year (Kaper et al. 2004). These pathogenic *E.coli* enters the water resources through sewage, septic tanks, and animal wastes (Pandey et al. 2014). The growth and survival of E. coli in natural habitats are influenced by both biotic and abiotic factors (Rochelle-Newall et al. 2015). Availability of water and nutrients, temperature, pH, and solar radiation are examples of abiotic variables. Biotic factors like the presence of other microorganisms and the competition with these organisms also influence the survival of *E.coli* (Jang et al. 2017).

Total coliform contamination was highest in the Palakkad District during Po (90.9%) followed by Mo (87%) and Pr (74%) as it exceeds the BIS (2012) standard limits of 10 CFU/100 ml. Similar trends of E. coli contamination were observed in the Palakkad as samples were above the standard limits by 71.2% in Po, 63.1% in Mo, and 43.9% in Pr season. In the case of Malappuram District the total coliform infection in groundwater was higher than the standard limit in the order of 87.88% in Mo>80% in Pr >75.7% in Po season, but, the *E.coli* contamination was highest in Po (81.8%) followed by Mo (69.7%) and 57.88% in Pr. Both the bore wells and open wells were highly contaminated with coliforms and *E.coli* in Palakkad and

Malappuram Districts (Annexures 21 and 22). The maximum microbial contamination level observed in Mo and Po seasons is attributed to the precipitation and washing down of solid and liquid waste and ultimately reaching the groundwater system as a result of infiltration and groundwater recharge. The population density of Kerala is much higher and hence most of the distance norms concerning the construction of septic and sewage treatment systems are not been followed due to space constraints, resulting in higher microbial contamination in surface and groundwater sources.

Table 1.4.15. Pr correlation of microbiological parameters with pH and temperature in Palakkad District

	Temperature	pH	T .coli	*E.coli*
Temperature	1			
pH	0.088	1		
T .coli	.596**	0.063	1	
E.coli	.283*	0.024	.265*	1

**. Correlation is significant at the 0.01 level (2-tailed). *. Correlation is significant at the 0.05 level (2-tailed).

Table 1.4.16. Mo correlation of microbiological parameters with pH and temperature in Palakkad District

	Temperature	pH	T .coli	T .coli
Temperature	1			
pH	0.175	1		
T .coli	-0.061	0.052	1	
E.coli	-0.171	-0.081	.340**	1

**. Correlation is significant at the 0.01 level (2-tailed).

Table 1.4.17. Po correlation of microbiological parameters with pH and temperature in Palakkad District

	Temperature	pH	T .coli	T .coli
Temperature	1			
pH	0.006	1		
T .coli	0.02	-0.053	1	
E.coli	-.310*	0.053	0.179	1

*. Correlation is significant at the 0.05 level (2-tailed).

Table 1.4.18. Pr correlation of microbiological parameters with pH and temperature in Malappuram District

	Temp	pH	T.coli	*E.coli*
Temp	1			
pH	0.236	1		
T.coli	.362**	0.22	1	
E.coli	.329**	0.107	.276*	1

**. Correlation is significant at the 0.01 level (2-tailed). *. Correlation is significant at the 0.05 level (2-tailed).

Table 1.4.19. Mo correlation of microbiological parameters with pH and temperature in Malappuram District

	Temp	pH	T.coli	*E.coli*
Temp	1			
pH	0.234	1		
T.coli	-0.077	0.015	1	
E.coli	-0.004	-0.14	.283*	1

*. Correlation is significant at the 0.01 level (2-tailed).

Table 1.4.20. Po correlation of microbiological parameters with pH and temperature in Malappuram District

	Temp	pH	T.coli	*E.coli*
Temp	1			
pH	-0.238	1		
T.coli	-0.071	0.166	1	
E.coli	-0.181	0.151	.538**	1

**. Correlation is significant at the 0.01 level (2-tailed).

A significant positive correlation between total coliforms and E. coli with water temperature was observed in the summer season (Pr) in both Districts (Table 1.4.15 and 1.4.18). In contrast, no significant or negative relationship between water temperature and microbial pollution was exhibited in the Mo and Po seasons (Table 1.4.16-17, 1.4.19-20). A few studies found a positive relationship between water temperature and bacterial concentrations due to the coincidence of high summer temperatures with periods of significant precipitation and discharge (Schilling et al. 2009; Islam et al. 2017). Investigations have already reported the luxuriant growth of intestinal bacteria in waterbodies in tropical temperatures (Winfield and

Groisman 2003; Tiefenthaler et al. 2009). In the study area, the infiltration of contaminated storm water might have contributed to microbial contamination in the groundwater sources in both Districts. Extreme weather events, especially heavy rainfall, and flood situations, are common occurrences in Kerala. Increased runoff from agricultural fields and urban areas, leakages from drains and sewers, sediment resuspension etc. are positively connected with microbial contamination of groundwater. Some other studies (Vermeulen and Hofstra 2013; Duvert et al. 2019; Wiesner-Friedman et al. 2022) reveal similar causes for positive relationships between microbial concentrations and precipitation. However, the net effect of environmental variables (temperature, precipitation, and salinity) on pathogen concentration and growth fluctuations is unknown (Vermeulen and Hofstra 2013).

1.4.3.11. Fluoride

The WHO recommends that the F concentration in drinking water should not exceed 1.5 mg/L. Also as per BIS (2012), the desirable concentration of F in drinking water should be 1 mg/L. Tables 1.4.5 and 1.4.6 provide a statistical summary of the F concentrations in samples from the Palakkad and Malappuram Districts. F levels in the groundwater samples in the Palakkad District ranged from 0.6 to 1.8 mg/L with a mean of 1.28 mg/L in Pr, 0.6 to 1.8 mg/L with a mean value of 1.08 mg/L in Mo, and 0.3 to 2.2 mg/L in Po, with a mean of 1.3 mg/L (Table 1.4.5). The F concentration of samples collected from the Malappuram District ranged from 0.94 to 1.8 mg/L with a mean value of 1.19 mg/L in Pr, 0.37 to 1.2 mg/L with a mean value of 0.88 mg/L in Mo, and 0.16 to 1.9 mg/L in the Po season. However, 88% of the Pr, Po, and 52% of the Mo samples were above the desirable limits of BIS (1 mg/L) in the Palakkad District (Table 1.4.5). Similarly, 69.7% of Pr, 10.6% of Mo, and 71.2% of Po from the Malappuram District exceeded the BIS drinking water standard limits (Table 1.4.6).

F and pH had a strong positive correlation during Pr ($r = 0.393$) and Po ($r = 0.57$) in the Palakkad District (Tables 1.4.9 to 11). Additionally, EC, TDS, TA, TH, and Mg revealed a strong positive correlation with F in all seasons in the Palakkad District (Tables 1.4.9 to 11). Likewise, a significant correlation of F with pH was observed in the samples from the Malappuram District during the Pr season ($r = 0.393$) (Table 1.4.12). A strong positive correlation of F was observed with EC, TDS, and a

positive correlation with TA and TH in the Pr season, followed by the Po season in the Malappuram District (Tables 1.4.12 to 14). A strong correlation of F with Mg was observed in the Po season in the samples from Malappuram (Table 1.4.12). In contrast, Ca, Fe, and NO_3 had a weak positive or negative correlation with F in both Districts during all seasons (Table 1.4.9 to14).

The strong relation of F with EC and TDS indicates that F contamination in the study area is associated with a higher concentration of bicarbonates, especially magnesium and sodium (Valdez-Alegría et al. 2019). This, together with the close connection of F and hydroxyl groups in silicate minerals, supports a more widespread role for F in increasing the electrical conductivity of various silicate minerals (Li et al. 2017). A strong relation of Na with Cl (Tables 1.4.9 to 11) also indicated rock-water interaction, likely from calcium and magnesium silicate weathering, which enhanced the hardness of groundwater (Srinivas et al. 2014). The groundwater drawn from Attappady (P01, P02), Chittur (P22-25), and Kollengode (P28 and P29) Blocks of the Palakkad District revealed high alkalinity, hardness, as well as F content, especially in the samples from bore wells (Annexure 10 and 11). The significant positive correlation of pH, TA, and TH indicates that alkalinity and hardness are the most important factors influencing F desorption from rocks and soils to groundwater (Saxena and Ahmed 2001; Alagumuthu and Rajan 2008). The increase in F with an increase in alkalinity may be due to the higher dissolution of F-bearing minerals in alkaline conditions (Jha et al. 2013).

The strong correlation of F with Mg and the weak correlation with Ca was noted in the Palakkad District throughout the year (Table 1.4.9 to 11) and in the Pr season in Malappuram (Table 1.4.12). The higher concentration of magnesium and a lower concentration of calcium in groundwater favors the entry of F into it (Handa 1975). Calcium in water gradually precipitates the F, and hence the presence of calcium is more important to reduce F concentration in groundwater (McCann 1968). Fe exhibited a negative correlation with TA, TH (Pr, Mo, and Po), and F (Pr & Mo) in the Palakkad District (Table 1.4.9 to 11). A dissolved form of iron (Fe (OH) 3 (aq)), which causes hardness, exists at pH below 6.5 or 10 and above (Hem 1977; Das et al. 2007). There were no samples with a pH greater than 10 in the Palakkad District, and only a few samples from the western stretch were slightly acidic, indicating that Fe contributed hardness is insignificant. The Fe estimated from the samples can be

its ionic species such as Fe^{+++}, $FeOH^{++}$, $Fe(OH)^{+2}$, Fe^{++}, and $FeOH^{+}$. Moreover, the presence of Fe in groundwater points to the drop in actual F content in that system due to its adsorption by Fe (Vithanage et al. 2012).

In the case of Malappuram, however, the majority of the samples have an acidic pH with soft water (86.36% of Pr and 77.27% of Mo and Po samples) (Annexure 1), and the hardness contributed by Ca and Mg is very low. Additionally, the lateritic topsoil is found widely all over the District, which has an abundant concentration of Fe and aluminium (Das et al. 2007). The laterite deposit with acidic soil contributes to the Fe concentration in groundwater (Schellmann 1994). Groundwater is generally deprived of oxygen and so has a high content of reduced Fe. Fe exists in solution in the ferrous state, usually as ferrous bicarbonate. It can only remain in solution in the absence of oxygen and generally when the pH is below 6.5 (Hem 1977; Das et al. 2007). Hence it is ascribed that the trace amount of alkalinity might have been contributed by the dissolved Fe in the samples from Malappuram.

There is no attribution from external sources of pollution, as nitrate and F showed a negative correlation with each other in all seasons (Adimalla et al. 2019) in the Palakkad District. However, F contamination (1.6 mg/L) in shallow wells of acidic pH range was also observed in one sample (Pattambi region (P9)) in Mo in Palakkad District (Annexure 1 and 23) and samples of Malappuram District in Pr season (M21, M27, and M33) (Annexure 1 and 23). It may be due to oxidation-reduction reactions as part of the geochemical process, which plays an important role in the leaching of F from the rocks and soil. The organic acids present in the shallow wells can easily dissolve the F from hornblende–biotite gneiss and mica (Kularatne and Pitawala 2012). The intensive use of phosphate fertilizers for agriculture activity can also impart F to groundwater through precipitation and infiltration processes as F exhibited a strong positive correlation with PO_4 in Mo and Po seasons in Malappuram District (Table 1.4.13 and 1.4.14) (Sujatha 2003; Kundu and Mandal 2009). This is due to the presence of F in trace quantities as an impurity in phosphate fertilizers (Sharma and Sharma 2004). F pollution in groundwater is highly associated with the geological and hydrological conditions of the area (Ramamohana et al. 1993).

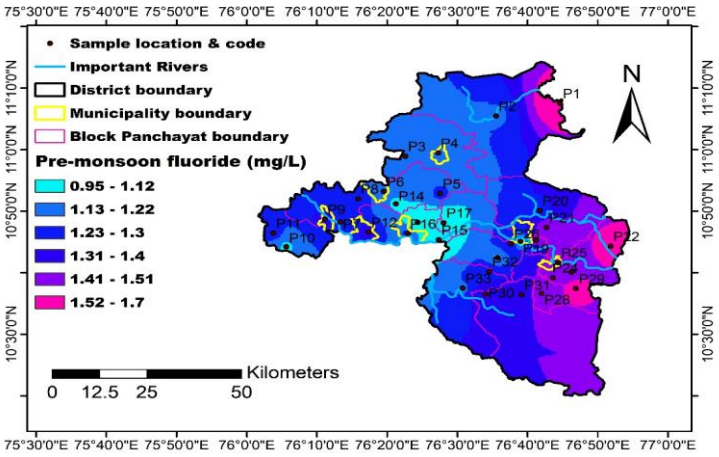

(a) Spatial distribution of Fluoride in pre-monsoon

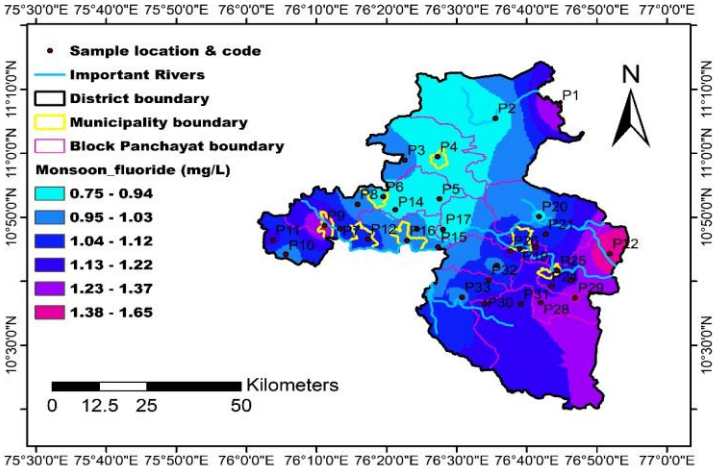

(b) Spatial distribution of Fluoride in monsoon

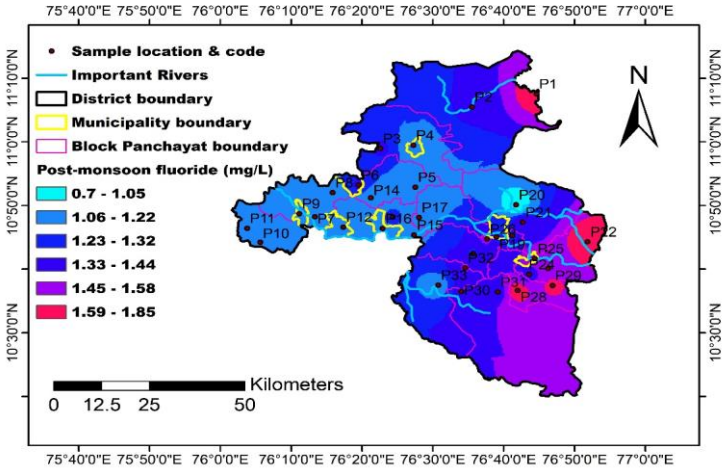

(c) Spatial distribution of Fluoride in post- monsoon

Fig.1.4.3 IDW interpolation of groundwater Fluoride in different seasons in Palakkad District

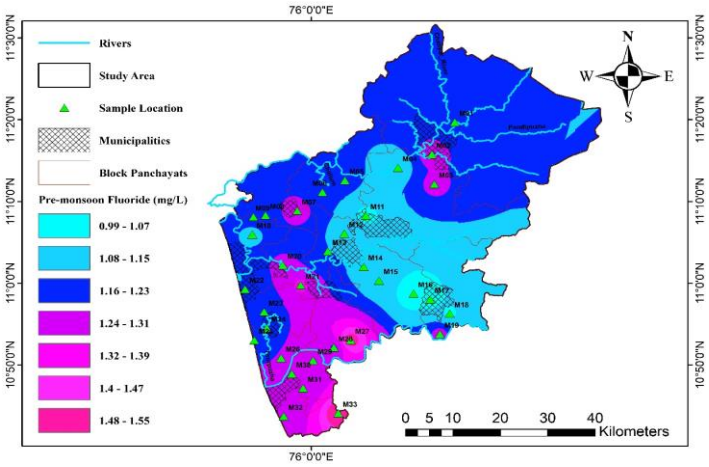

(a) Spatial distribution of Fluoride in pre-monsoon.

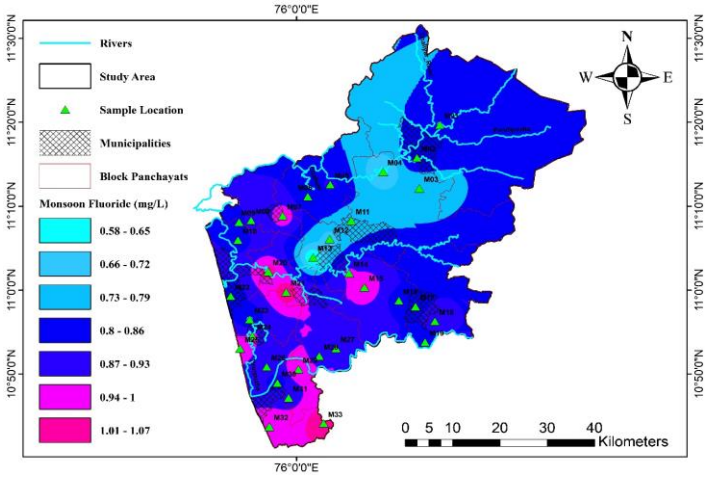

(b) Spatial distribution of Fluoride in monsoon.

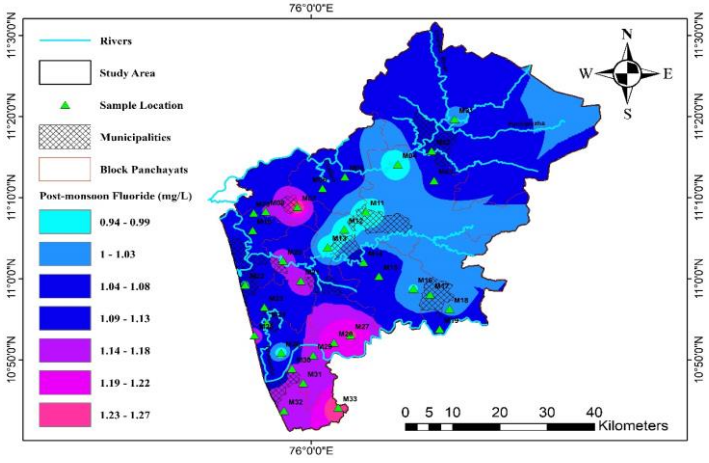

(c) Spatial distribution of Fluoride in post-monsoon.

Fig.1.4.4 IDW interpolation of groundwater Fluoride in different seasons in Malappuram District

1.4.3.11.1. Spatial analysis of Flouride

ArcMap was used for the spatial analysis. The spatial analysis of seasonal F was developed for the Palakkad (Fig.1.4.3) and Malappuram Districts (Fig.1.4.4). The maximum F prevalence was recorded in the Palakkad area during the Po season (Fig.1.4.3 (c)). The Attappady (P01), Chittur (P22), and Kollengode (P29) Blocks, which are located in the easternmost section of the District, are the most severely damaged regions. The Pattambi Municipality, situated in the western part of the District, also exhibited high F contamination in the Mo season (Fig.1.4.3 (b)). It can be seen that the F is mostly connected with hornblende biotite gneiss when the spatial F concentration is compared with the mineral groups of the Palakkad District. The Pr season had the maximum F occurrence in the Malappuram District (Fig.1.4.4 (a)). F levels in groundwater are especially high in the southeastern area (Fig.1.4.4). The F distribution and interpolation analyses show that the primary sources of F are minerals of the charnokite/charnokite gneiss type.

Many studies across the world have noted similar findings. Biotite-hornblende-gneisses contributed F to the groundwater of Bagalkot, Kolar, and Tumkur Districts of Karnataka; Guntur District of Andhra Pradesh; and Gharbar Village of Dhanbad District, Jharkhand (Tirumalesh et al. 2007; Mamatha et al. 2010; Subba Rao et al. 2013; Patolia and Sinha 2017). Specifically because of the hornblende biotite gneisses, north-central and north-western Sri Lanka are impacted by F in groundwater (Young et al. 2017). High F levels in groundwater are caused by igneous, charnockite, and gneissic rocks in significant portions of Tamil Nadu, Telungana, and Karnataka States (Manikandan et al. 2014; Thivya et al. 2017; Sajil Kumar et al. 2014; Chidambaram et al. 2014; Brinda et al. 2016).

1.4.4. Heavy metals

Industrial, agricultural, and urbanization with poor waste management practices have triggered heavy metal contamination in diverse environments of developing countries (Gowd 2010; Wang et al. 2018). The source and distribution pattern of

heavy metals such as As, Cd, Pb, Cu, Fe, Ni, Mn, and Zn and their correlation with other physicochemical parameters of groundwater samples are evaluated. The pollution index, metal index, and spatial distribution of pollutants are assessed, as well as the geo-environmental factors responsible for the persistence of heavy metals. The impact of precipitation on the mobilization of heavy metals was also evaluated. The statistical summary of heavy metals analyzed in the groundwater samples of the Palakkad District is given in Table 1.4.7, and Malappuram District is given in Table 1.4.8.

1.4.4.1. Arsenic (As)

Arsenic is a known carcinogen, which is also recognized as the king of poison. The As contamination of drinking water has been documented in numerous areas around the world, particularly in South Asia (Hassan et al. 2017; Palit et al. 2019; Sahoo et al. 2020). It has been reported in the groundwater of the Indian State of West Bengal (Mandal and Suzuki 2002). Water is the primary route for As to enter the human body (Khairul et al. 2017). Millions of people in China, India, Bangladesh, Pakistan, and Taiwan, consume As-contaminated groundwater (Rahman et al. 2009: Kim et al. 2011). According to BIS (2012) and WHO, its concentration in drinking water should not exceed 0.01mg/L.

The As concentrations in the Palakkad samples ranged from below detectable levels (0.000 mg/L) to 0.050 mg/L in Pr, 0.00 to 0.10 mg/L in Mo, and 0.00 to 0.10 mg/L in Po seasons. The extent of As contamination was highest during the Mo (36.4%) and Po (31.8%) seasons, with samples exceeding the drinking water standard limits of 0.01 mg/L, with the least occurring during the Pr season (21.1%) in Palakkad District (Table 1.4.7). Pattambi (OW), Ongallur (OW), Ambalappara (OW), Mannnur (OW), Palakkad (BW), Puthussery (OW), and Kuzhalmannam (OW) regions are highly affected places (Annexure 24).

Arsenic-contaminated aquifers are characterized by high alkalinity and carbonate content (Jain et al. 2018), since a positive correlation of As with TA, TH (0.305),

and Mg (0.318) was observed in the Pr season (Table 1.4.9). In the Pr season, a strong negative correlation of As with Fe and a positive correlation with sulphate (Table 1.4.9) indicates that the Fe-As sulphate precipitation (Chitsazan et al. 2009) imparts low As to the groundwater, which is attributed to the low incidence of As in the Palakkad District. This relation weakened during the Mo and Po seasons (Tables 1.4.10 and 1.4.11), and the As incidence was at its maximum during this period (Table 1.4.7). Under the influence of rain in the Mo season, As showed a significant negative correlation with pH during this period. Moreover, in the Palakkad District, the groundwater of the eastern region is characterized as alkaline, while the western part is slightly acidic, and the highest arsenic incidence was observed in the open wells from the central and western parts of the District, except for one bore well sample from the Palakkad Municipality. Arsenic pollution in the Palakkad District can therefore be attributed to the oxidative dissolution of As in a shallow aquifer. This is supported by Harvey et al. (2006), who demonstrated that scorodite, an As-containing mineral, dissolves between 2 and 6 pH. Anawar et al. (2003) indicate that oxidative dissolution of As is responsible for As pollution in the Bengal Delta, and vertical profiling of As occurrence reveals that the As concentration is detected up to 41 meters from the subsurface.

The concomitant ions in the water body either facilitate or inhibit the adsorption of As. Many scientific studies have shown that cations facilitate adsorption while anions inhibit it (Zhang et al. 2017). As showed a strong positive correlation with anions in the Pr season and negative or weak correlations during the Mo and Po seasons (Table 1.4.9 to 11). Moreover, As exhibited a significant negative correlation with Ca in the Mo season (Table 1.4.10). The fact that As also observed a significant positive relationship with F (0.364) in Mo indicates its geogenic attribution. Also, an acidic pH will inhibit the adsorption of As on Fe and Mn ions (Anawar et al. 2003), since As exhibited a weak correlation with Fe and Mn during the Mo and Po seasons in Palakkad District.

The concentration of As in the Malappuram District ranged from below the detectable level to 0.05 mg/L (Table 1.4.8). A similar trend of As incidents were noticed in Malappuram District. It showed the highest sustenance (39.34%) of As during the Po and Mo (27.27%) and the least during the Pr season (7.58%), which is above 0.01 mg/L, the BIS standard limit for drinking water. However, none of the samples showed an As value above the maximum acceptable level of 0.05 mg/L as per the BIS standards.

In the Pr season, the As exhibited a considerable positive association with TH and Mg, as well as a strong positive correlation with pH. (Table 1.4.12). As demonstrated a poor association with the majority of parameters during Mo, except for K, PO_4 , and Cd, which exhibited substantial positive correlations, and NO_3 , which exhibited a high positive correlation (0.399). (Table 1.4.13). Concentrations of Cd as an impurity in phosphate fertilizers range from 0.009 to 2.58 mg/kg (Yang et al. 2005). Cd is present in inorganic fertilizers such as nitrate and potash (Huang et al. 2007). Sodium arsenate, calcium arsenate, and lead arsenate are additionally utilized as insecticides and herbicides (Bhattacharya et al. 2007). All of the data suggest that agricultural sources are the primary cause of As contamination in Malappuram District. During the Po season, As exhibited, a significant positive connection with pH, EC, TA, TH, Ca, and Na, as well as a high association with Mg, Cl, and F (> 0.325). (Table 1.4.14). The high alkaline groundwater (> 8) also induces As seepage from rocks with which it comes into contact. The Po correlation pattern indicates that alkalinity promotes As release in the groundwater sources of Malappuram (Anawar et al. 2003; Guo et al. 2003; Mushtaq et al. 2018). During the Po season, samples from Malappuram have a mean pH of 5.90. The As contamination in the Malappuram District is also suspected to be caused by the decrease in groundwater quality resulting from landfill leachate penetration (Hua et al. 2020).

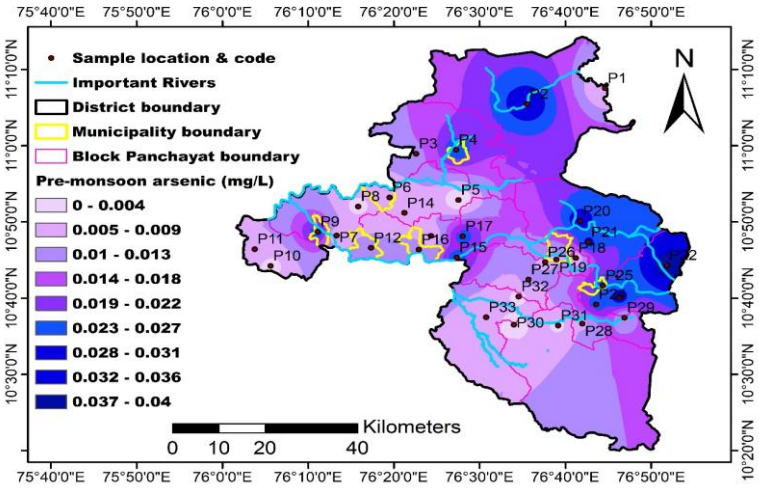

(a) Spatial distribution of Arsenic in pre-monsoon

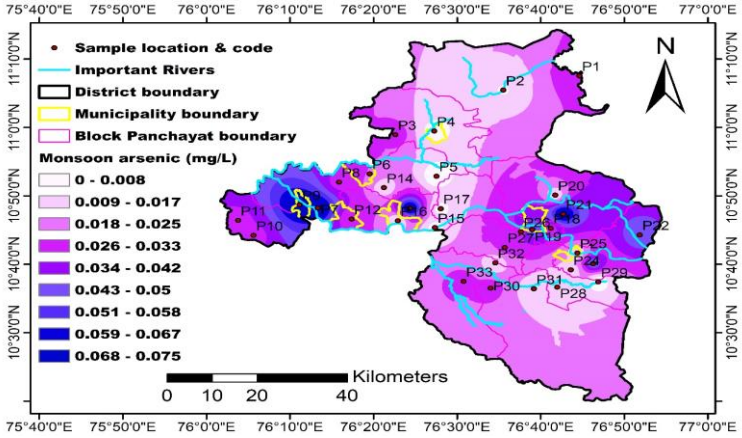

(b) Spatial distribution of Arsenic in monsoon

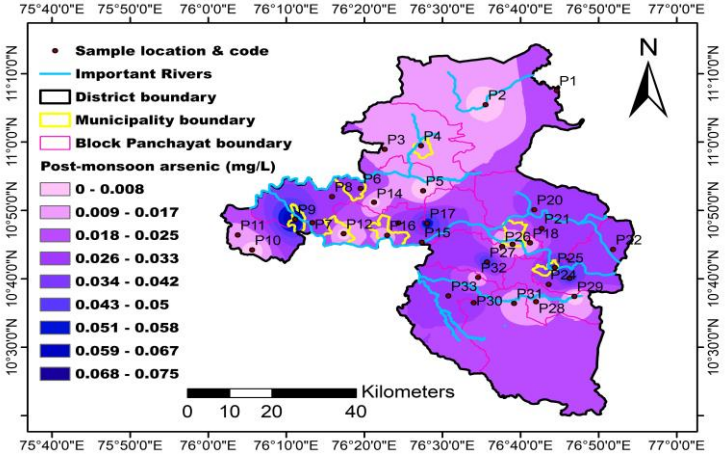

(c) Spatial distribution of Arsenic in post-monsoon

Fig.1.4.5 IDW interpolation of groundwater Arsenic in different seasons in Palakkad District

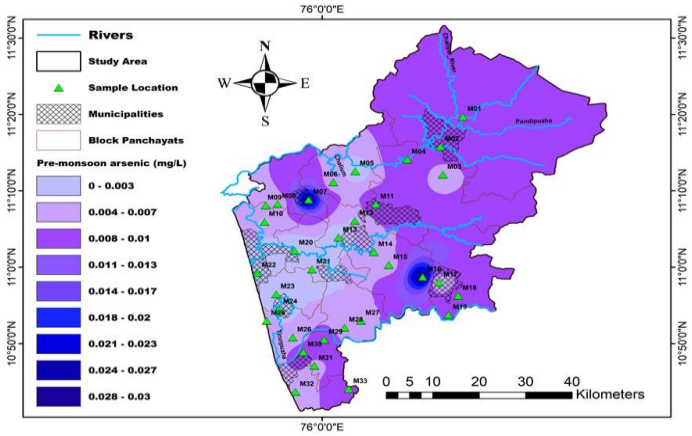

(a) Spatial distribution of Arsenic in pre-monsoon

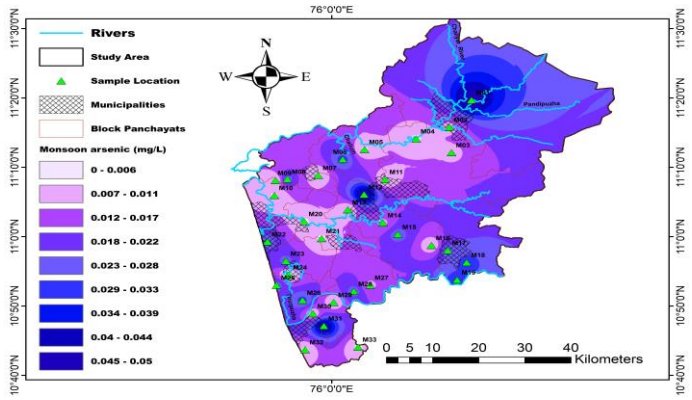

(b) Spatial distribution of Arsenic in monsoon

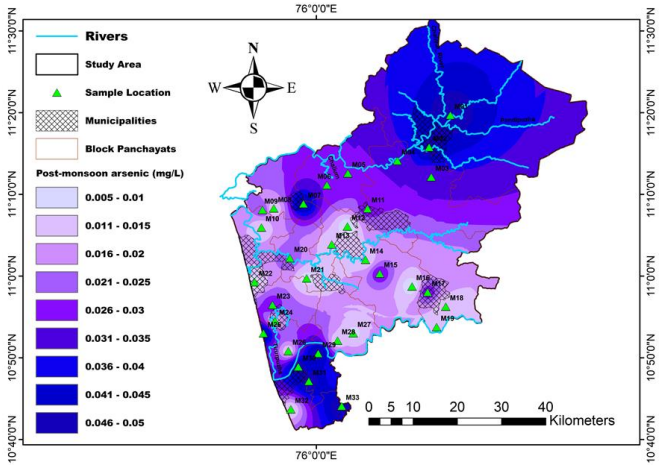

(c) Spatial distribution of Arsenic in post-monsoon

Fig.1.4.6 IDW interpolation of groundwater arsenic in different seasons in Malappuram District

1.4.4.1.1. Spatial analysis of Arsenic

The interpolation model in the Arc Map software was used for the spatial analysis. The As contamination in different seasons for Palakkad and Malappuram Districts is presented in Figs. 1.4.5 and 1.4.6, respectively. During the Pr season, the As concentration is spread across the eastern part of the Palakkad District, including the Blocks of Attapady (P2), Malampuzha (P20, 21), Chittur (22, 25), Palakkad (P17), Ottapalam (P15), and Pattambi (P9). However, the Pr average was up to 0.04 mg/L (Fig.1.4.5 (a)). During the Mo season, considerable As pollution was detected in the Pattambi (P09), Ambalappara (P13), and Puthussery (P21) regions, with the seasonal average reaching up to 0.075 mg/L (Fig.1.4.5 (b)). Pattambi (P09), Mannur (P17), Perumatti (P23), and Kuzhalmannam (P27) had the highest As concentrations in the Po season (Fig.1.4.5 (c)). In Malappuram, only the Nediyiruppu (M07) and Angadippuram (M16) regions have the highest prevalence of As during the Pr season. However, during the Mo and Po seasons, there was a greater spread (Fig.1.4.6). On the banks of the Chaliar River (M01 and M02), the Bharathapuzha River (M29, 30 31, and 33), and the Tirur River (M26), the prevalence of As was significantly higher.

The spatial spread was observed in the upstream part of Palakkad District during the Pr season (Fig.1.4.5 (a)). When referring to the As contamination with the mineral group map of the study area, the As contamination was highly associated with the fluvial alluvium and hornblende biotite gneiss type (Figs.1.4.1 and 1.4.5) in Palakkad and the fluvial deposit, migmatite complex, and charnockite/charnockite gneiss in Malappuram District (Figs. 1.4.1 and 1.4.6). The As contamination was severe in the Mo and Po seasons in the study area. The area associated with river banks and fluvial deposits has a high concentration of As in both Districts. Smedley and Kinniburgh (2002) reported the average concentration of As in the alluvial sand and muds of Bangladesh as 2.9 mg/kg and 6.5 mg/kg, respectively. Granite (0.2–15 mg/Kg), limestone (0.1–20 mg/Kg), and marine mudstone/shale (3–15 mg/Kg) also contain As in a substantial amount. The sedimentary and hydrogeological cycles of these materials can also lead to the formation of As-rich sediments and soils. Source,

speciation, mineralogy, biological relations, and geochemical panels all influence the distribution of As in the environment (Bowell et al. 2014).

1.4.4.2. Fe

Fe is the second most abundant element in the earth's crust and is very essential for living organisms in trace quantities (WHO 1996). High Fe content in drinking water produces minor toxicity. The concentration of Fe in drinking water needs to be within 0.3 mg/L (BIS 2012). But, 56% of Pr, 44% of Po, and 29% of Mo samples in Palakkad District exceeded this limit (Table 1.4.5). Also, Fe exhibited a negative correlation with TA, TH (Pr, Mo, and Po), and F (Pr and Mo) (Table 1.4.9 and 1.4.10), indicating that Fe contributed alkalinity and hardness is minor when compared to other ions. The Fe estimated from the samples may be Fe^{+++}, $FeOH^{++}$, $Fe(OH)^{+2}$, Fe^{++}, and $FeOH^{+}$. All these indicate that the Fe contamination in the groundwater is not geogenic in Palakkad District. Furthermore, the presence of Fe in groundwater indicates a decrease in the real F level in that system due to Fe adsorption (Vithanage et al. 2012). Fe content in natural waterways is often ferrous (Fe^{2+}) or ferric (Fe^{3+}), depending on pH and dissolved oxygen levels (Raju 2006).

In Malappuram District, the concentration of total Fe ranged between 0.005 to 5.57 mg/L in Pr, 0.015 to 6.58 mg/L in Mo, and 0.026 to 5.13 mg/L in Po season. The samples exceeded the BIS standard limit in the order of 24% in Pr followed by 19.7% Mo and Po seasons (Table 1.4.6). The elevated levels of Fe in the groundwater are more prominent in the coastal belts and are associated with the fluvial deposits in the Malappuram District. In groundwater, divalent types of Fe and Mn (Fe^{2+} and Mn^{2+}) cause pollution, as they have organoleptic properties (Ellis et al. 2000). Fe and Mn showed a significant positive correlation during Mo. Fe also showed a strong positive correlation with pH, TH, and TA (Tables 1.4.12 to 14) in all the seasons. Additionally, the lateritic topsoil is found widely all over the District, which has an abundant concentration of Fe and aluminum (Das et al. 2007). The laterite deposit with acidic soil contributes to the Fe concentration in groundwater (Schellmann 1994). Groundwater is generally deprived of oxygen and

so has a high content of reduced Fe. Fe exists in solution in the ferrous state, usually as ferrous bicarbonate. It can only remain in solution in the absence of oxygen and generally when the pH is below 6.5 (Hem 1977; Das et al. 2007). Hence it is ascribed that the trace amount of alkalinity might have been contributed by the dissolved Fe in the samples from Malappuram District. Fe oxide is one of the important elements that contribute to the hardness and alkalinity of groundwater (Malakootian et al. 2010). Weathering of Fe-bearing minerals such as feldspars, pyroxenes, epidote, and hornblende present in the aquifer matrix, as well as the dissolution of Fe pipes and their components, can also result in high Fe levels in groundwater (Dill et al. 2013; Rao and Latha 2019).

1.4.4.3 Cadmium (Cd)

Cd (Cd) is a trace element that is found in abundance in the environment. Cd concentrations in soils and groundwater can be increased by both geogenic and anthropogenic causes, which is critical for ensuring healthy and safe drinking water (Kubier et al. 2019). Cancer is caused by high Cd dosages (Lee et al. 2005). The BIS and WHO drinking-water quality guidelines set a recommendation value of 0.003 mg/L for Cd. The highest concentration of Cd occurred during the Pr (0.007 mg/L) and Po (0.0068 mg/L) seasons in Palakkad District (Table 1.4.7). However, the magnitude of pollution was higher during Pr (53%) than Mo (34.85%) and Po (34.85%) in Palakkad District, as it exceeded the standard limit. Cd showed a significant negative correlation with pH in the Pr season (-.536) (Table 1.4.9). In Malappuram District, the highest concentration of Cd occurred during the Pr (0.0064 mg/L) and Mo (0.0061 mg/L) seasons. The Pr (43.93%), Mo (34.85%), and Po (27.76%) samples exceeded the limit of WHO and BIS (2012) (Table 1.4.8). It showed either a negative or a weak positive correlation with pH, EC, and TDS in all the seasons (Table 1.4.12 to 14). Similar trends of Cd contamination were reported in the Karur region of South India (Ahamed and Loganathan 2017).

Cd remains in solution at pH 6.5 and it enhances mobility at a lower pH (Charlatchka and Cambier 2000). Thus, the toxicity and dissolution of Cd are highly dependent on the pH of water. Cd is a highly mobile heavy metal in the environment

(Kubier et al. 2019). It is chemically similar to Zn and occurs naturally with Zn in sulphide ores (Wang et al. 2011). Cd exhibited a strong negative correlation with Zn, and sulphate during Pr and a weak correlation in other seasons in Palakkad (Table 1.4.9 to 11), which indicate that Cd contamination is not associated with natural sources. However, it has a positive correlation with Pb and Ni in the Mo and Po seasons, which points out that automobile waste can be the source of Cd (Nisa and Sujatha 2020). Similar results were observed in the Malappuram District, as a strong relation between Cd and As (.436) was observed during the Mo season as well as Ni (.591) in the Po season (Table 1.4.13 and 1.4.14). A high concentration of Cd was observed in the samples taken from urban than suburban areas in the Palakkad District as well as a higher concentration of Cd was observed in the samples adjoining motorable roads of the Malappuram District (Annexure 25). The high Cd contamination in urban environments is reported in various research studies (Sekabira et al. 2010; Mohan et al. 2012b; Castillo-Nava et al. 2020). Thus, the Cd concentration in the groundwater samples of the study area is not only geo-genic but also anthropogenic**.**

1.4.4.4. Lead (Pb)

Lead poisoning is one of the most serious public health hazards due to the persistence of Pb in the environment. The BIS and WHO prescribe that the maximum permissible limit of Pb in drinking water should not exceed 0.01 mg/L. During the Pr season, Pb concentrations ranged from 0.0033–0.0367 mg/L, BDL–0.1207 mg/L in Mo, and BDL–0.0484 mg/L in Po in the Palakkad District (Table 1.4.7). Pollution is prominent during Pr as 60.6% of the samples were above the permissible limits of drinking water and the least pollution was observed during the Mo (34. 84%) season in Palakkad District (Table 1.4.7). Pb showed a significant positive correlation with pH, EC, TDS, sulphate, and chloride in the Palakkad District in the Pr season (Table 1.4.9) (Mamabolo et al. 2009). At high pH, Pb forms a complex with bicarbonates, sulphates, and chlorides and forms an insoluble complex (Mann 1980). However, during Mo, rainwater with an acidic pH can dissociate these complexes when groundwater gets recharged with precipitation. Thus, Pb exhibited a weak correlation with pH, sulphate, and chloride during the Mo

and Po seasons (Table 1.4.10 and 1.4.11). Hence, the highest concentration of Pb in samples was observed in the Mo season (P27-0.1207 mg/L) in Palakkad District. These pollutants get into groundwater by diffusion through soil solution (Milivojevic et al. 2016). However, the pH is not the sole factor that determines the Pb contamination, because the Pb contamination in the groundwater was seen in both acidic and alkaline samples (Ebrahimi et al. 2010; Alghamdi et al. 2021)

A similar trend of contamination was observed in Malappuram District. The Pb concentration in the samples was most conspicuous in Pr (60.6%) and lowest in Mo (22.7%). Though the level of pollution was higher during Pr, an elevated concentration of Pb was observed in samples of the Po season and is attributed to the dissociation of Pb complexes (Table 1.4.8). As most of the samples showed acidic pH in the Malappuram District, it showed a weak correlation between Pb and pH in all seasons (Table 1.4.12 to 14). The solubility of Pb is based on several factors, like acidic pH and temperature (Li et al. 2013). Pb showed a significant positive correlation with Na during the Pr season in both Palakkad and Malappuram Districts, indicating the intensification of Na with the lowering of the water table (Table 1.4.9 and 1.4.12). The weak (negative or positive) correlation between Pb and Na in other seasons in both the Districts (Tables 1.4.10, 1.4.11, 1.4.13, and 1.4.14) ascribes to the increased accumulation of anthropogenic ionic components (Pb) and dissipation of geogenic ions (Na) in Mo. The present study showed an uneven distribution of Pb as the samples collected from nearby highways and junctions of townships of both the Districts (Palakkad -P6, P7, P9, P26, P27, P28, P32, P33, and Malappuram - M2, M10, M13, M14, M16, M21, M23, M24, and M32), had a higher concentration of Pb when compared to the samples collected from rural areas with less traffic (Annexure 26). It reveals that automobile exhaust waste and urban waste are also acting as sources of Pb contamination (Prabhakar et al. 2019). A high concentration of Pb in the surface soil of the industrialized area of Palakkad was reported by Nisa and Sujatha (2020). Groundwater can also be contaminated by agricultural activities and landfill leachate (Yang et al. 2018).

1.4.4.5. Nickel (Ni)

Ni is the 24th most plentiful element in the earth's crust and comprises approximately 3% of the earth's composition. As a member of the transition metal

series, it is resistant to corrosion by water, air, and alkali and is thus widely used in the steel and metal industries; batteries; electroplating; forging; mineral processing; paint formulation; and steam-electric power plants (Campbell et al. 2006; Raval et al. 2016). A low level of Ni in the environment cannot be avoided, and it may not be hazardous to the human population. But high doses of Ni have their own toxico-kinetics and carcinogenic activity (Kasprzak 2003).

The concentration of Ni in the groundwater samples of the Palakkad District was in the range of 0.002 to 0.0467 mg/L in Pr, 0.00 to 0.0458 mg/L in Mo, and 0.006 to 0.0303 mg/L in Po seasons. According to BIS (2012), the acceptable limit of Ni in drinking water is 0.02 mg/L, but the sample exceeded the permissible limits by 39.0% in Pr and 38.0% in Mo and Po seasons (Table 1.4.7). The concentration of Ni was highest during Pr and gradually decreased its concentration as the intensity of rain and infiltration increased during the Mo and Po seasons (Table 1.4.7). In Malappuram District, the Ni concentration was observed in the range of 0.00 to 0.049 mg/L in Pr, 0.0012 to 0.029 mg/L in Mo, and 0.005 to 0.0300 mg/L in Po seasons. The highest percentage of samples that deviated from the BIS standard limit is in the Pr season (45.45%) followed by Po (37.87%) and Mo (34.85%) (Table 1.4.8).

The pH, normally less than 6.5, favors the dissolution of Ni (Galvin 1996). Ni showed a negative correlation with pH in the Pr season in Palakkad District, which indicates the highest dissolution at acidic pH (Heikkinen 2003) (Table 1.4.9). It also exhibited a strong positive correlation with TH, Mg, and F in Mo and Po seasons in the Palakkad District, pointing towards its geogenic attribution (Table 1.4.10 and 1.4.11). Ni is found as a trace element in a wide range of minerals, notably those containing high levels of magnesium and Fe, such as olivine and pyroxenes (Ringwood 1955; Veter et al. 2017). In particular, Ni exhibited more or less a weak positive or negative correlation with nitrate, phosphate, and chloride throughout the study period (Table 1.4.9 to 11).

In the case of the Malappuram District, Ni exhibited a strong positive correlation with TH, Ca, and Na, indicating that the source of Ni is from the mineral sources in the Pr season (Table 1.4.12) (Hoang et al. 2004). Ni is a common metal normally found with lateritic stores (Kasprzak et al. 2003). In Malappuram District, lateritic

outcrops are seen in the majority of areas. In the Mo season, Ni showed a strong negative correlation with TH, Ca, and Mg as well as a significant positive correlation with NO_3 and PO_4, which specifies the entry of Ni from the anthropogenic sources along with rain water recharge (Table 1.4.13). Cd showed a similar trend of concentration in groundwater samples of the Malappuram District as these ions exhibited strong relations during the Po season, which indicates their common source (Bhuyan et al. 2017). A significant negative correlation between Ni and Cu was observed in the Mo and Po seasons in the Malappuram District (Table 1.4.13 and 14).

1.4.4.6. Manganese (Mn)

Mn is a mineral abundantly found in rock, soil, and water (Nganje et al. 2021). Mn is considered non-carcinogenic but may cause many health issues (Williams et al. 2012). The excess intake of Mn will damage motor function and affect the lungs, nerves, and may cause Parkinsonism and impotency (Zoni et al. 2007). Mn significantly affected the cognitive skills of children in Bangladesh, who consumed an excess quantity of Mn in drinking water (Sultana et al. 2017). In groundwater, the divalent form of Mn (Mn^{2+}) causes contamination, as they possess organoleptic properties (Ellis et al. 2000).

Mn levels in the Palakkad District ranged from below detectable to 0.7823 mg/L in Pr, 0.005 to 0.555 mg/L in Mo, and 0.006 to 0.64 mg/L in Po (Table 1.4.7). As per BIS (2012), the desirable limit of Mn in drinking water should not exceed 0.01 mg/L, but the prevalence of Mn was highest during Pr (22.72%), followed by Po (16.67%) and Mo (13.64%) in Palakkad District. A significant positive correlation between Mn and PO_4 was observed in the Pr season. It exhibited a significant positive correlation with chloride in the Mo seasons, expressing their ascription to man-made water contamination. Mn showed a significant positive correlation and a strong positive relation with Fe during the Mo and Po seasons, respectively (Johnson et al. 2018). These ions showed a similar trend of correlation with pH, EC, and TDS (Tables 1.4.9 to 11). Mn showed a significant positive correlation with phosphate in Pr and chloride during the Mo season, attributing multiple sources of pollution from agricultural and urban waste.

The incidence of Mn was highest during the Mo period in the Malappuram District, as 9.1% of the samples exceeded the national standard limits (BIS 2012) (Table 1.4.12). Though these elements are non-carcinogenic, they are likely to cause other health issues (Williams et al. 1999; Da Silva et al. 2017). In groundwater, divalent type Mn (Mn^{2+}) causes pollution as it has organoleptic properties (Ellis et al. 2000). Mn and Fe had a significant positive correlation during the Mo season as well as a positive correlation during the Pr. It is generally considered that the Mn and Fe in groundwater are from geogenic sources, but a high concentration is attributed to anthropogenic sources (Rusydi et al. 2021). Mn exhibited a significant positive correlation with Na and Cl in the Mo and Po seasons. High salinity is suspected of causing the dissolution of Mn^{2+} and Fe^{2+} in groundwater from rocks and soil through ion-exchange reactions (Wen 2012).

1.4.4.7. Cu and Zn

Copper levels in drinking water should not exceed 0.05 mg/L, according to the BIS (2012) limit. The concentration of Cu in the groundwater of Palakkad ranged from 0.0161 to 0.0411 mg/L in Pr, 0.128 to 0.014 mg/L in Mo, and below detectable limits to 0.0318 mg/L in the Po season. Only 1.5% of the Mo samples were above the standard limits. Cu concentrations in groundwater in the Malappuram District ranged from 0.016 to 0.0419 mg/L in the pr season, 0.0112 to 0.1324 mg/L in the mo season, and below detectable limits to 1.796 mg/L in the po season. Mo samples (3%) and Po samples (4.55%) from this area exceeded the standard limits. In groundwater, only a small amount of copper is dissolved (Cu^{2+}), while the rest is complexed with organic and inorganic ligands or exists as a colloidal phase (Lage et al. 1996). It has also been found that sewage contributes significant amounts of Cu to water resources (Bergbäck et al. 2001).

The significant positive correlation of Cu with F in Po and the positive correlation in the Pr season in the samples from Palakkad indicate the geogenic origin of Cu (Tables 1.4.9 and 1.4.11). Similarly, a substantial positive correlation between Cu and Mg as well as Cu and Na was observed in the Pr season (Table 1.4.9). It is also observed that there is a high correlation between Cu and Cl as well as Cu and Mg in

Mo in the Palakkad District (Table 1.4.10). A significant positive correlation of Cu with NO_3 in Mo samples from Malappuram is attributed to the agricultural source of pollution. However, a strong negative correlation was observed between the Cu and PO_4 in the Mo samples, which indicates that the Cu might be from the copper nitrate-based pesticides. A significant negative correlation was also observed between Cu and Ni in the samples from Malappuram Districts (Table 1.4.13).

BIS (2012) prescribes 5 mg/L as the desirable limit of Zn in drinking water. Zn concentrations in groundwater samples ranged from BDL to 0.748 mg/L in Pr, 0.0004 to 1.262 mg/L in Mo, and 0.0061 to 0.885 mg/L in Po season (Table 1.4.7). Similarly, the Zn concentration in the samples from Malappuram ranged from BDL to 1.245 mg/L in Pr, BDL to 0.518 mg/L in Mo, and 0.005 to 0.366 mg/L in the Po season (Table 1.4.8). The samples were within the desirable limits in both Districts. In the Pr samples of Malappuram, there was a significant positive correlation with Mn and NO_3 (Table 1.4.12). No significant correlation between Zn and other minerals was observed in the samples from Palakkad.

1.4.5. Water type

1.4.5.1. Piper Plot

Fig. 1.4.7 depicts the seasonal characteristics of groundwater in the Palakkad District as represented by the relationship between Na^+ , K^+ , Ca^{2+} , Mg^{2+} , CO_3 , HCO_3^- , Cl^- , and SO_4^{2-} ions. Sample points are distributed along the mixing lines in the piper plot. During Pr, 45% of samples were grouped under magnesium bicarbonate hydrofacies, 7.5% as calcium chloride type, and the rest came under mixed type. These facies switched to 21% calcium chloride, 9% salinity, 3% magnesium chloride, and a 67% mixed type in Mo. In Po, 60.6% is characterized by magnesium bicarbonate, 33.3% as the mixed type, and 6% as the salinity type. Throughout the year, the anionic array was $HCO_3^- > Cl^- > SO_4^{2-} > NO_3^-$, and the cationic array was $Mg^{2+} > Na^+ > Ca^{2+} > K^+$. Magnesium-type water was dominated throughout the Pr and Po seasons.

In the Malappuram District, the major cations studied in the groundwater samples are Ca^{2+} , Mg^{2+} , Na^{+} , and K^{+} and the anions are Cl^{-} , $SO_4{}^{2-}$, $NO_3{}^{-}$ and $PO_4{}^{2-}$ (Table 1.4.6). The cations and anions are represented in a piper plot (Fig.1.4.8), which defines the type and characteristics of water (Srinivas et al. 2014). There were no dominant cations in all the seasons, but calcium and sulphate types of water were dominant throughout the Mo and Po seasons. During the Pr season, the majority of samples were characterized as mixed types. The piper plot indicates that the water is calcium chloride and sulphate type (Fig.1.4.8). The sulphates in water are found to be related to gypsum stores (Sharma and Kumar 2020). Alkali chloride fluid inclusions in massive charnockite have been reported in South India (Newton et al. 2019). The majority of the land area in Malappuram is covered with the charnockite types of rocks (Fig.1.4.2). Occasionally, chloride and sulphate act as amphoteric ions, which acidify the water resources (Quina et al. 2009). Additionally, the lateritic topsoil, which is found widely all over the District, can also impart acidity to groundwater (Ghosh 2019). This is recognized to be the reason for the acidic nature of groundwater resources in this region.

It is evident from this illustration that magnesium and sodium predominate in groundwater in the Palakkad District. These cations increase the solubility of F from parent rock and the concentration of F in groundwater (Gizaw et al. 2014; Kumar et al. 2014b). Similarly, the presence of As in aquifers is indicated by the alkalinity, high bicarbonate level, and magnesium type of water. In addition, in Palakkad, As displayed a high positive association with Mg and F and a considerable negative correlation with Ca. The geological configuration and water type, particularly the Ca and Fe content, disfavor F and As in the groundwater of Malappuram District. However, increased F in a few samples, notably those connected with samples from bore wells, has been linked to the charnockite gneiss type in the Malappuram District. The highest As concentration reported in the Malappuram District was 0.05 mg/L, and the Mo and Po seasons had a significant prevalence. The significant correlation of As with TA and Ca in Malappuram indicates the release of As into the groundwater. The hydrofacies of groundwater in this study vary with the seasons and are strongly impacted by geology and precipitation (Saji Kumar et al. 2019).

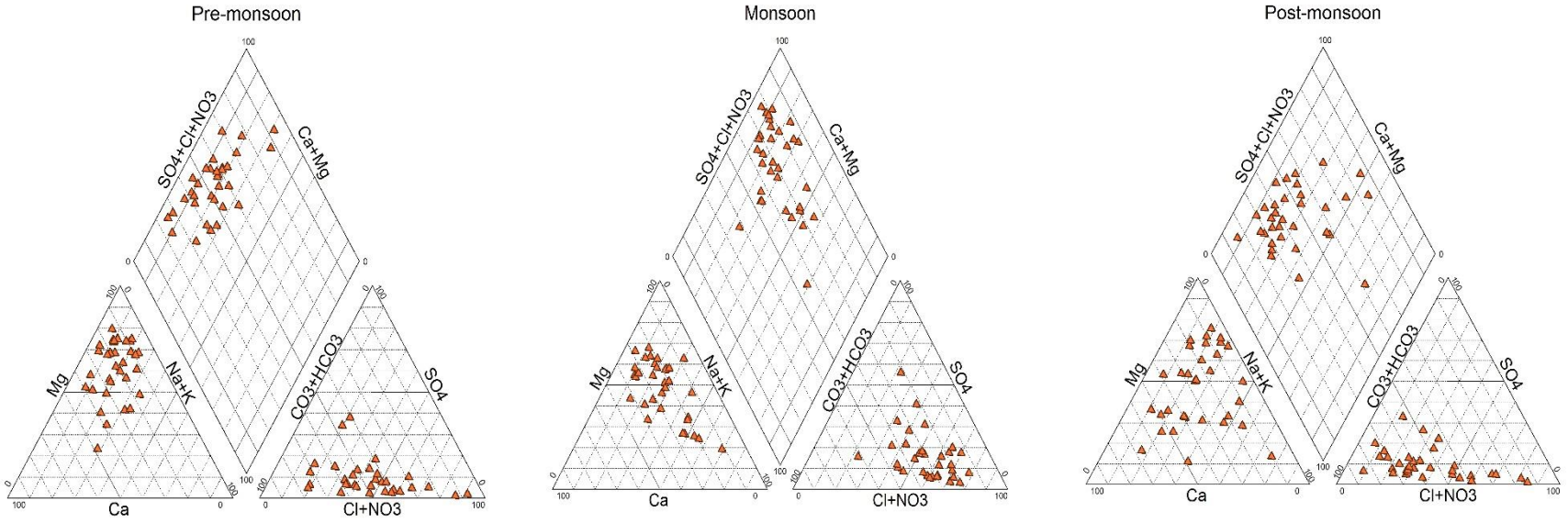

Fig.1.4.7 Piper diagram showing hydro facies in different seasons in Palakkad District

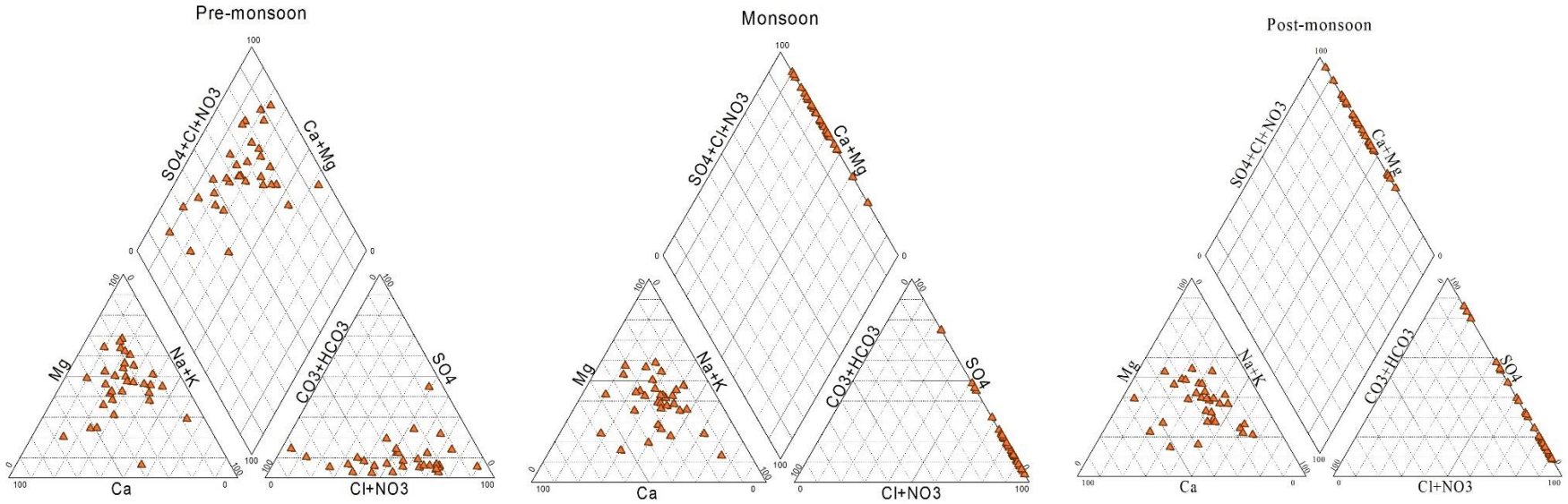

Fig.1.4.8 Piper diagram showing hydro facies in different seasons in Malappuram District

1.4.5.2. Chadha diagram

It is a modified form of the Piper plot. It represents a square or rectangular field that describes the general ion distribution and the properties of groundwater to show the hydrochemical processes and geochemical classification of groundwater. The difference in mill equivalent percentage between alkaline earth (Ca + Mg) and alkali metals (Na + K) is plotted on the X axis, in terms of percentage reacting value. The difference between weak acidic anions (CO_3 + HCO_3) and strong acidic anions (Cl + SO_4) is plotted on the Y axis. One of the four probable sub-fields of the proposed figure would correspond to the mill equivalent percentage differences between weak acidic anions and strong acidic anions, as well as between alkaline earth and alkali metals. The sample exhibited different water types according to different monsoonal seasons.

The Pr samples of the Palakkad District come under the Ca-Mg-Cl and Ca-HCO_3 types (Fig.1.4.9 (a)). During the Mo season, the majority of the samples (97%) are Ca-Mg-Cl (Fig.1.4.9 (b)), but 61% of the Po samples are Ca-HCO_3 , 33% are Ca-Mg-Cl, and only 6% are Na-Cl (Fig.1.4.9(c)). In the Malappuram District, the majority of Pr samples (66.7%) come under the Ca-Mg-Cl type, only 6% are Na-Cl type, and the rest fall under the Ca-HCO_3 type (Fig1.4.10 (a)). A similar trend was observed in the Mo season, but 82% of it came under the Ca-Mg-Cl type (Fig.1.4.10 (b)). The Ca-HCO_3 type of water (60%) is most predominant in the Po season (Fig.1.4.10 (c)). The dominance of bicarbonate-type water forms as a result of weathering and recharge. The Ca-Mg-Cl type water indicates the major hydrochemical process is reverse ion exchange, and the Na-Cl type mainly results from evaporation (Rashid et al. 2019).

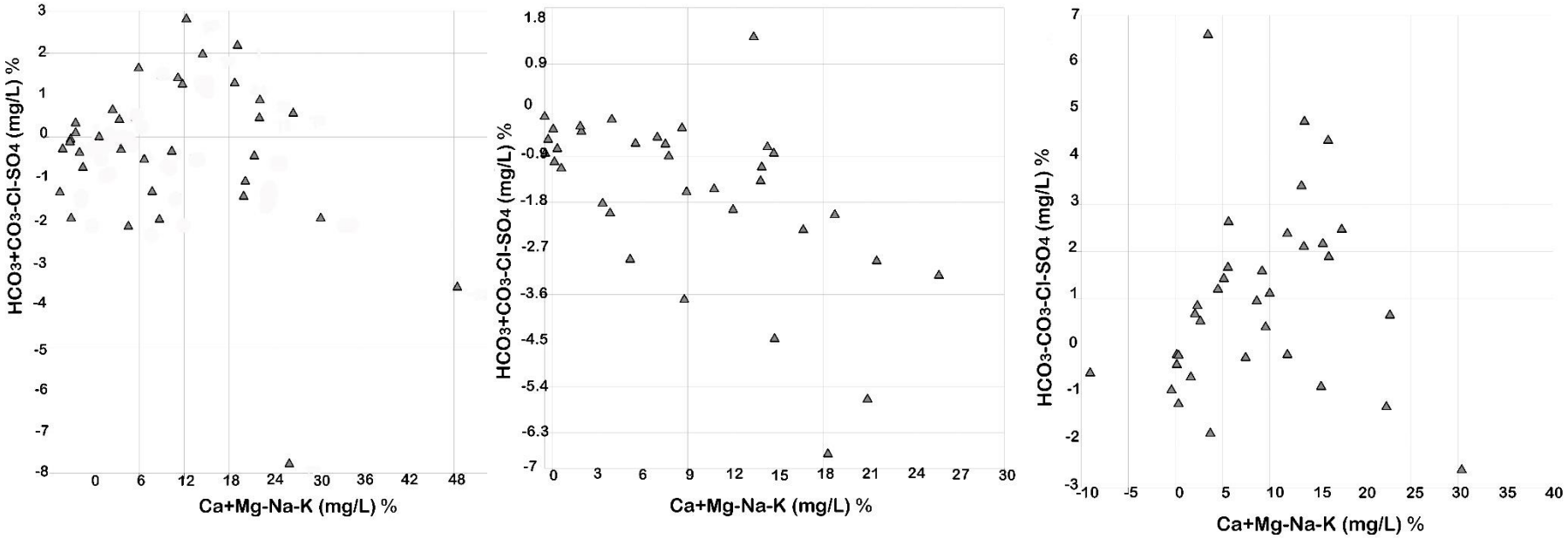

(a) Pre-monsoon (b) Monsoon (c) Post-monsoon

Fig.1.4.9 Chadha diagram showing the geochemical classification of groundwater in different seasons in Palakkad District

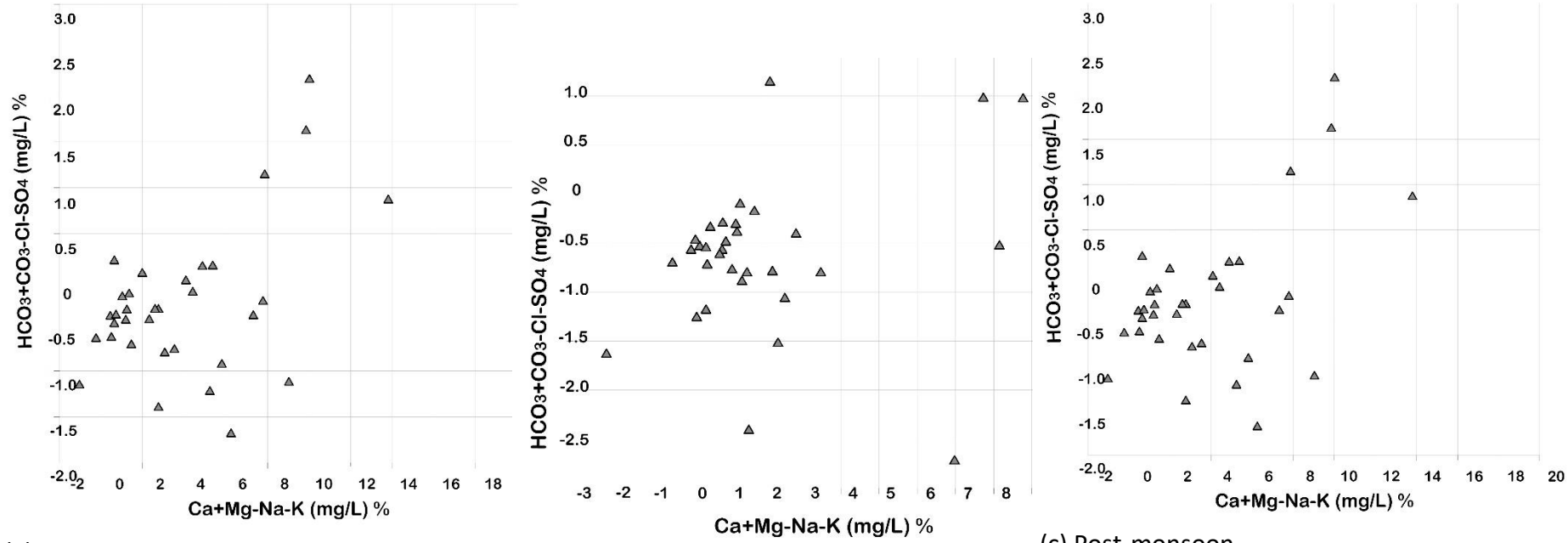

(a) Pre-monsoon

(b) Monsoon

(c) Post-monsoon

Fig.1.4.10 Chadha diagram showing the geochemical classification of groundwater in different seasons in Malappuram District.

1.4.6. Wilcox plot

Wilcox (1955) suggested a classification system for evaluating irrigation waters based on soluble sodium percentage. It is used to plot the electrical conductivity and sodium percentage values of the samples under study. According to this, water can be classified into excellent, good, admissible, tolerable, and bad for irrigation purposes. The higher number indicates that the water is problematic for irrigation and the lower number indicates good quality (USDA 1954). From the analysis, it is observed that the majority of the Pr samples of the Palakkad District fall under the excellent to good category, and only 9% are tolerable and 3% come under the bad category (Fig.1.4.11 (a)). Much better water quality was observed during the Mo and Po seasons, with 3% of Mo and 12% of the Po samples coming under the tolerable category (Fig.1.4.11 (b &c)). Samples from Malappuram showed excellent and good in all seasons (Fig.1.4.12 (a, b & c)). The proportion of salt is crucial for irrigation purposes as sodium reacts with the soil to decrease permeability (Hwang et al. 2017).

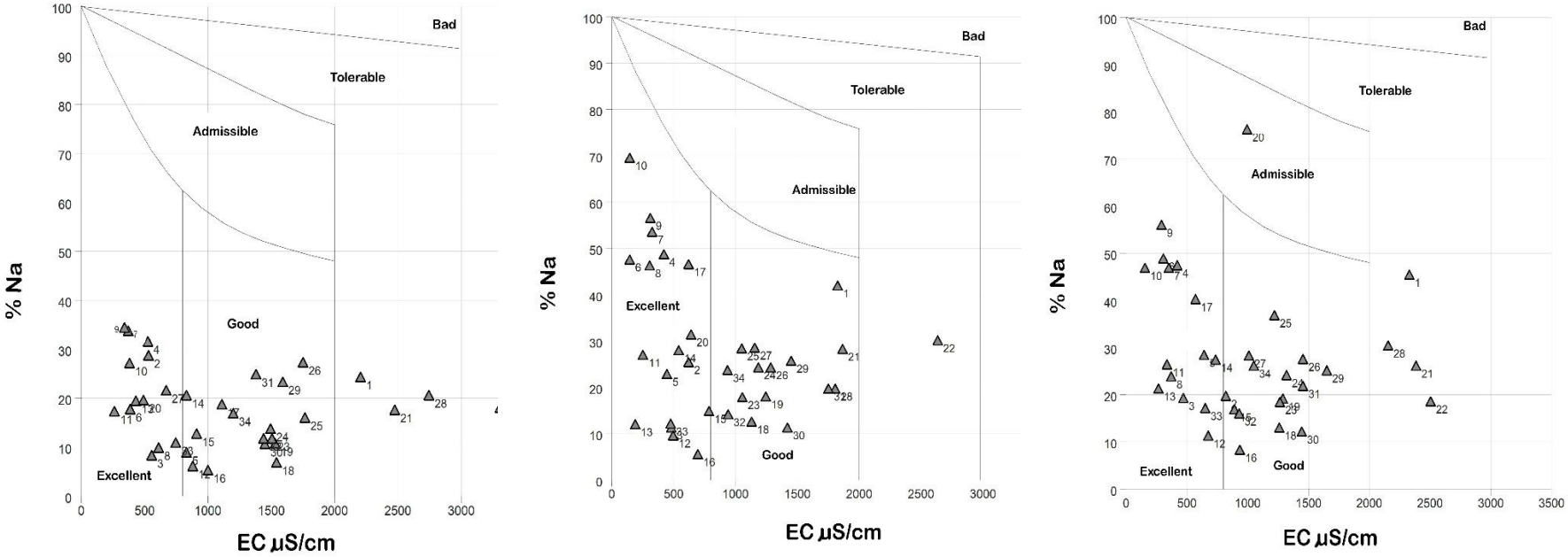

(a) Pre-monsoon (b) Monsoon (c) Post-monsoon

Fig.1.4.11 Conductivity and sodium percentage link for ranking of irrigation water quality in the Palakkad District in different season.

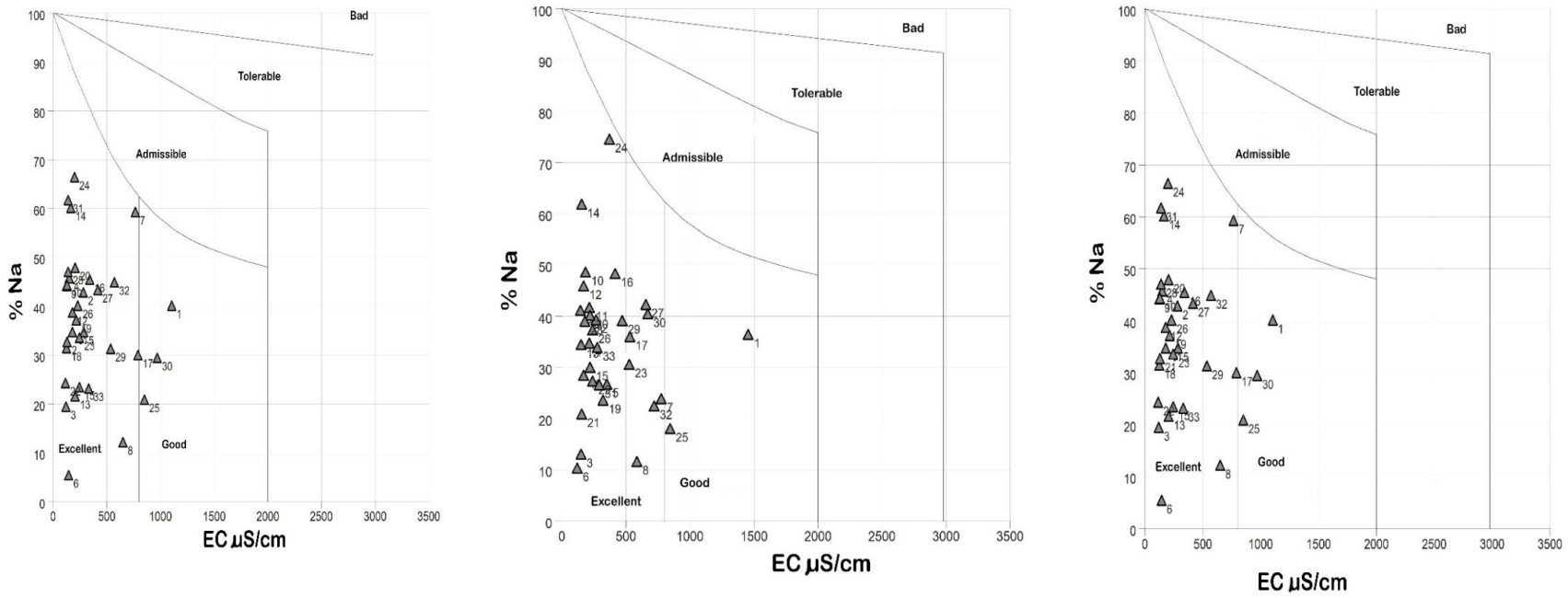

(a) Pre-monsoon (b) Monsoon (c) Post-monsoon

Fig.1.4.12 Conductivity and sodium percentage link for ranking of irrigation water quality in the Malappuram District in different season.

1.4.7. Gibbs plot

To understand the process of groundwater chemistry, the Gibbs boomerang was used. It serves as a representation of the origin of groundwater's chemical elements, such as precipitation, rock, and evaporation dominance (Gibbs 1970). An annual average of both anions and cations was calculated for the Gibbs plot. From the observations, it is clear that salinity and F concentrations are mainly dominated by rock water interactions in the Palakkad District (Fig.1.4.13). Precipitation and evaporation also play a role in the F enhancement of groundwater in a few regions. Moreover, the hydro-chemical analysis also indicates that F contamination is geogenic in the Palakkad District. Precipitation-enhanced salinity is more dominant in the Malappuram District (Fig.1.4.14). Rock-water interaction also played a dominant role in the mineralization of water in a few places in the Malappuram District. This view is supported by several research reports. The mineral contamination of groundwater is predominantly due to its contact with rocks (Usham et al. 2018). Weathering liberates F from F-bearing minerals such as apatite, biotite gneiss, titanite hornblende-schist, and khondolite (Marghade et al. 2020). Fluorites, amphiboles, and micas can also act as sources of F contamination in groundwater (Kumar et al. 2013).

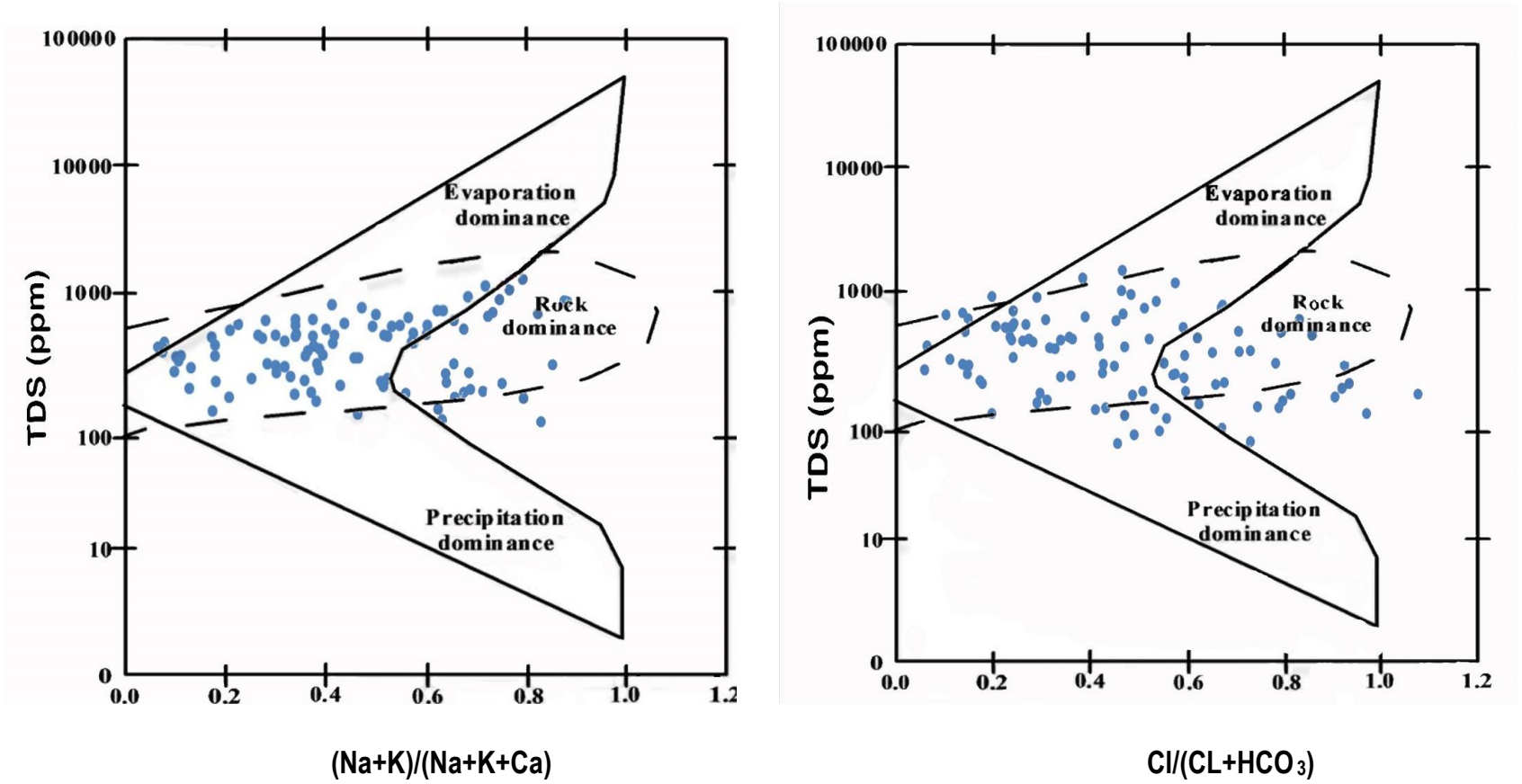

Fig.1.4.13 Governing mechanism of groundwater chemistry in Palakkad district.

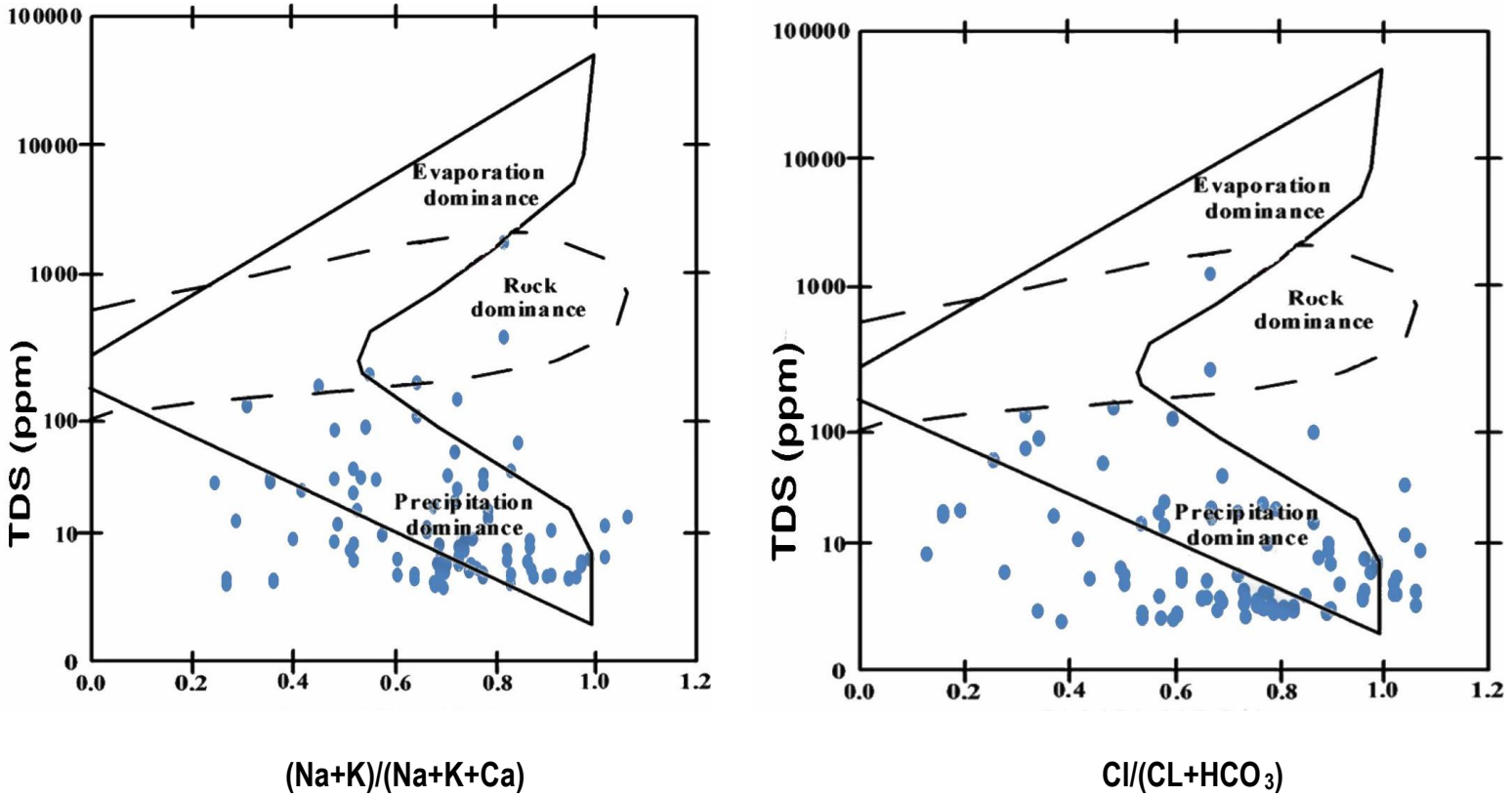

Fig.1.4.14 Governing mechanism of groundwater chemistry in Malappuram district.

1.4.8. Water Quality Index (WQI)

The significance of the water quality index is the need to consistently share and communicate with the public about monitoring ambient water. The need for a systematized process for assessing and rating various bodies of water around the region is addressed in a second way. A comprehensive analysis of multiple factors is attempted to be condensed into a single claim in the index. Five categories make up the Water Quality Index: excellent (0-50), good (50-100), poor (100-200), very poor (200-300), and unsuitable for drinking (>300). The value of WQI varies with biological parameters such as E. coli and total coliforms. Therefore, WQI is calculated in two different ways; one is inclusive of biological parameters and the other is exclusive of biological parameters.

The relative weight of the WQI inclusive of biological parameters is given in table 1.4.21, and the correspondent results for Palakkad District and Malappuram are given in tables 1.4.22 and 1.4.23. The WQI, inclusive of biological parameters in the Palakkad District ranges from 54 to 6218 in Pr, 44 to 4576 in Mo, and 59 to 10913 in Po. Similarly, in the Malappuram District, the WQI ranges from 44 to 3990 in Pr, 43 to 2235 in Mo, and 94 to 5610 in the Po season. The Po season has declining water quality, whereas the Mo season has better water quality. The precipitation, which diluted the metal ions in the water, is thought to be one of the reasons why the water quality improved during the Mo season. The chlorination of wells during the Mo period is attributed to the other reason, which reduced bacterial contamination. During the Pr and Po seasons, there was no excellent water in the Palakkad District, and only 3% of the Mo sample was excellent. 12.12% of the Pr, 15.15% of Mo, and 9.09% of the Po samples of the Palakkad District fall under the "good" category. Most of the samples from Palakkad, including 45% of the Pr, 58% of Mo, and 76% of the Po samples, were grouped as unsuitable for drinking. The rest of the sample either falls into the poor or very poor category. In the case of the Malappuram District, 3% of the Pr and Mo samples were excellent, and 15.5% of the Pr, 18.18% of Mo, and 3.03% of the Po samples were of good type. The majority of the samples from Malappuram, like 45%, 48%, and 52% of the Pr, Mo, and Po, respectively,

were classified as unfit for drinking. The remaining are either poor or unfit to drink (Table 1.4.24).

Table 1.4.21. The Relative Weight of Physicochemical and biological parameters selected for WQI

Parameters	**Weight (wi)**	**Relative Weight (Wi)**	**Desirable Limit**	**Reference**
pH	2	0.029	6.5-8.5	BIS
Conductivity	2	0.029	400	WHO
TDS	3	0.043	500	BIS
TH	3	0.043	200	BIS
TA	1	0.014	200	BIS
Ca	3	0.043	75	BIS
Mg	3	0.043	50	WHO
Na	2	0.029	200	WHO
Cl	2	0.029	250	BIS
NO_3	5	0.072	45	BIS
SO_4	3	0.043	250	BIS
PO_4	3	0.043	1	BIS
F	5	0.072	1	BIS
Fe	4	0.058	0.3	BIS
Pb	5	0.072	0.01	BIS
Cd	5	0.072	0.003	BIS
Ni	5	0.072	0.02	BIS
Cu	2	0.029	0.05	BIS
As	5	0.072	0.01	BIS
Zn	1	0.014	5	BIS
E.coli	5	0.072	0	BIS
	Σ wi = 69	Σ Wi = 1.000		

Table 1.4.22. Water Quality Index (WQI) inclusive of biological parameters for individual groundwater samples of Palakkad District in the different monsoonal period

Sample	Pr		Mo		Po	
	WQI	**Type**	**WQI**	**Type**	**WQI**	**Type**
P01	125	PW	590	UD	10373	UD
P02	76	GW	54	GW	3685	UD
P03	565	UD	86	GW	10913	UD
P04	112	PW	149	PW	9285	UD
P05	102	PW	44	GW	59	GW
P06	362	UD	64	GW	1530	UD
P07	1107	UD	383	UD	3313	UD
P08	139	PW	3257	UD	1120	UD
P09	1680	UD	148	PW	827	UD
P10	1403	UD	1787	UD	1004	UD
P11	54	GW	229	VPW	60	GW
P12	788	UD	66	GW	60	GW
P13	64	GW	1075	UD	142	PW
P14	1143	UD	190	UD	4564	UD
P15	371	UD	404	UD	223	VPW
P16	186	PW	60	UD	162	PW
P17	2361	UD	1386	UD	908	UD
P18	1026	UD	367	UD	160	UD
P19	127	PW	358	UD	1202	UD
P20	1782	UD	598	UD	1988	UD
P21	278	VPW	363	UD	2202	UD
P22	350	UD	248	VPW	6476	UD
P23	1144	UD	930	UD	5041	UD
P24	109	PW	1859	UD	12203	UD
P25	6418	UD	375	UD	5143	UD
P26	184	PW	850	UD	2556	UD
P27	140	PW	214	VPW	2927	UD
P28	152	PW	2470	UD	651	UD
P29	110	PW	105	PW	5310	UD
P30	172	PW	930	UD	514	UD
P31	370	UD	4576	UD	8152	UD
P32	115	PW	127	PW	208	VPW
P33	66	GW	1403	UD	3139	UD

Table 1.4.23. Water quality index (WQI) inclusive of biological parameters for individual groundwater samples of Malappuram District in the different monsoonal period

Sample	Pr		Mo		Po	
	WQI	Type	WQI	Type	WQI	Type
M01	3990	UD	110	PW	5610	UD
M02	331	UD	269	VPW	299	VPW
M03	151	PW	43	EW	299	VPW
M04	406	UD	113	PW	288	VPW
M05	405	UD	289	VPW	451	UD
M06	268	VPW	263	VPW	1459	UD
M07	317	UD	795	UD	106	PW
M08	520	UD	80	GW	4643	UD
M09	791	UD	559	UD	217	VPW
M10	76	GW	1646	UD	174	PW
M11	1357	UD	1114	UD	1338	UD
M12	188	PW	773	UD	628	UD
M13	1864	UD	1013	UD	681	UD
M14	219	VPW	388	UD	197	PW
M15	141	PW	220	VPW	892	UD
M16	102	PW	2164	UD	1283	UD
M17	831	UD	90	GW	114	PW
M18	1397	UD	369	UD	240	VPW
M19	62	GW	88	GW	2513	UD
M20	171	PW	70	GW	732	UD
M21	163	PW	2235	UD	94	GW
M22	44	EW	141	PW	297	VPW
M23	82	GW	187	PW	461	UD
M24	210	VPW	373	UD	202	VPW
M25	391	UD	756	UD	627	UD
M26	60	GW	890	UD	179	GW
M27	305	UD	73	GW	1494	UD
M28	103	PW	452	UD	198	GW
M29	128	PW	281	VPW	388	UD
M30	1352	UD	621	UD	1525	UD
M31	124	PW	1624	UD	285	VPW
M32	1506	UD	65	GW	2692	UD
M33	85	GW	223	VPW	142	GW

Table 1.4.24. Water type based on WQI range inclusive of biological parameters of groundwater samples of Palakkad and Malappuram District in the different monsoonal period

WQI Range	Water Type	Pr%		Mo%		Po%	
		Pkd.	Mlp.	Pkd.	Mlp.	Pkd.	Mlp.
<50	Excellent	0	3	3	3	0	0
50-100	Good	12	15	15	18	9	3
100-200	Poor	39	27	15	12	9	21
200-300	Very poor	3	9	9	18	6	24
>300	Unsuitable for drinking	45	45	58	48	76	52

Pkd. = Palakkad; Mlp. = Malappuram

The relative weight of the WQI excluding biological parameters is given in table 1.4.25, and the WQI for Palakkad and Malappuram is presented in tables 1.4.26 and 1.4.27 respectively. The value of WQI excluding biological parameters varies from 58 to 222 in the Pr, 39 to 179 in the Mo, and 35 to 171 in the Po season in Palakkad. The WQI of the samples from Malappuram ranged from 37 to 178 in the Pr, 34 to 175 in the Mo, and 37 to 212 in the Po seasons. A major percentage of samples from the Palakkad District fall into the good and poor category (Table 1.4.28), whereas samples from Malappuram fall into the excellent and good category (Table 1.4.28). In the Palakkad District, the Pr season was characterized by 48.48% good and 48.48% poor; in the Mo season, it was 9.09% excellent, 45.45% good, and 45.45% poor; and in the Po season, it was 6.06% excellent, 48.48% good, and 45.45% poor. Excellent kinds of water are predominant in the Malappuram District in all seasons, like 27.27% of Pr samples, 30.30% of Mo samples, and 9.09% of Po samples. The water characterized by good type was 66.66% in Pr, 60.60% in Mo, and 72.72% in the Po season. The rest of the samples from Malappuram District fall into the poor category (Table 1.4.28).

Table 1.4.25. The relative weight of physicochemical parameters selected for WQI

Parameters	Weight (wi)	Relative Weight (Wi)	Desirable Limit	Reference
pH	2	0.031	6.5-8.5	BIS
EC	2	0.031	400	WHO
TDS	3	0.047	500	BIS
TH	3	0.047	200	BIS
TA	1	0.016	200	BIS
Ca	3	0.047	75	BIS
Mg	3	0.047	50	WHO
Na	2	0.031	200	WHO
Cl	2	0.031	250	BIS
NO_3	5	0.078	45	BIS
SO_4	3	0.047	250	BIS
PO_4	3	0.047	1	BIS
F	5	0.078	1	BIS
Fe	4	0.063	0.3	BIS
Pb	5	0.078	0.01	BIS
Cd	5	0.078	0.003	BIS
Ni	5	0.078	0.02	BIS
Cu	2	0.031	0.05	BIS
As	5	0.078	0.01	BIS
Zn	1	0.016	5	BIS
	Σ wi = 64	Σ Wi =1.000		

Table 1.4.26. Water quality index (WQI) exclusive of biological parameters for individual groundwater samples of Palakkad District in the different monsoonal period

Sample	Pr		Mo		Po	
	WQI	Type	WQI	Type	WQI	Type
P01	135	PW	132	PW	122	PW
P02	82	GW	59	GW	72	GW
P03	124	PW	93	GW	123	PW
P04	71	GW	64	GW	55	GW
P05	71	GW	48	EW	64	GW
P06	69	GW	69	GW	78	GW
P07	68	GW	122	PW	79	GW
P08	151	PW	116	PW	121	PW
P09	65	GW	122	PW	116	GW
P10	58	GW	64	GW	35	EW
P11	58	GW	72	GW	65	GW
P12	93	GW	72	GW	65	GW
P13	69	GW	91	GW	75	GW
P14	76	GW	50	GW	50	GW
P15	98	GW	67	GW	86	GW
P16	84	GW	65	GW	78	GW
P17	109	PW	39	EW	87	GW
P18	117	PW	124	PW	95	GW
P19	137	PW	134	PW	93	GW
P20	86	GW	63	GW	67	GW
P21	183	PW	120	PW	143	PW
P22	222	VPW	170	PW	171	PW
P23	127	PW	110	PW	117	PW
P24	118	PW	83	GW	96	GW
P25	128	PW	75	GW	111	PW
P26	121	PW	160	PW	117	PW
P27	74	GW	134	PW	129	PW
P28	164	PW	121	PW	120	PW
P29	119	PW	113	PW	117	PW
P30	128	PW	110	PW	128	PW
P31	108	PW	121	PW	134	PW
P32	125	PW	98	GW	108	PW
P33	71	GW	77	GW	86	GW

Table 1.4.27. Water Quality Index (WQI) exclusive of biological parameters for individual groundwater samples of Malappuram District in the different monsoonal period

Sample	Pr					
	WQI	Type	WQI	Type	WQI	Type
M01	79	GW	119	PW	110	PW
M02	66	GW	58	GW	109	PW
M03	54	GW	46	EW	70	GW
M04	57	GW	45	EW	78	GW
M05	48	GW	40	EW	59	GW
M06	44	GW	51	GW	60	GW
M07	109	PW	62	GW	96	GW
M08	76	GW	86	GW	77	GW
M09	38	EW	39	EW	59	GW
M10	44	EW	48	EW	71	GW
M11	55	GW	56	GW	65	GW
M12	48	EW	76	GW	37	EW
M13	50	GW	44	EW	55	GW
M14	50	GW	49	EW	57	GW
M15	55	GW	121	PW	69	GW
M16	79	GW	63	GW	64	GW
M17	89	GW	77	GW	84	GW
M18	71	GW	68	GW	45	EW
M19	67	GW	56	GW	50	GW
M20	37	EW	36	EW	110	PW
M21	60	GW	61	GW	62	GW
M22	48	EW	55	GW	68	GW
M23	70	GW	66	GW	70	GW
M24	52	GW	34	EW	43	EW
M25	178	PW	175	PW	212	VPW
M26	64	GW	67	GW	58	GW
M27	85	GW	60	GW	58	GW
M28	41	EW	61	GW	72	GW
M29	60	GW	51	GW	88	GW
M30	99	GW	49	EW	131	PW
M31	57	GW	82	GW	75	GW
M32	71	GW	50	EW	69	GW
M33	92	GW	66	GW	115	PW

Table 1.4.28. Water type based on WQI range exclusive of biological parameters of groundwater samples of Palakkad and Malappuram Districts in the different monsoonal period

WQI Range	Water Type	Pr%		Mo%		Po%	
		Palakkad	Malappuram	Palakkad	Malappuram	Palakkad	Malappuram
<50	Excellent	0	27	9	30	6	9
50-100	Good	48	67	45	61	48	73
100-200	Poor	48	6	45	9	45	15
200-300	Very poor	3	0	0	0	0	3
>300	Unsuitable for drinking	0	0	0	0	0	0

1.4.8.1. Spatial representation of the WQI

The spatial difference of WQI excluding biological factors is demonstrated for Palakkad (Fig. 1.4.15) and Malappuram (Fig. 1.4.16). Due to high evaporation rates and mineral concentrations in groundwater, the water quality in the Palakkad area was significantly affected during the Pr season. The east and south-eastern parts of the District are found to be the hotspot, as the water quality is found to be very poor in this region in all seasons. Due to the leaching of pollutants and minerals from the upstream area, high WQI is also present in the western region, which is the downstream area. The central and western border regions of the Palakkad District showed much better WQI in all seasons. A heterogeneous type of water quality is observed in Malappuram District. Due to the mineral deposits in the coastal plains, the southwestern area of the Malappuram District is distinguished by poor water quality. The majority of the Malappuram area receives excellent or good-quality water throughout the year. During the Po season, precipitation and the resulting rock-water interaction have a significant negative impact on the water quality (Wagh et al. 2019). Water quality indices (WQIs) are intended to be useful and persuasive instruments for the management of water quality and the sustainable development of water resources (Uddin et al. 2021).

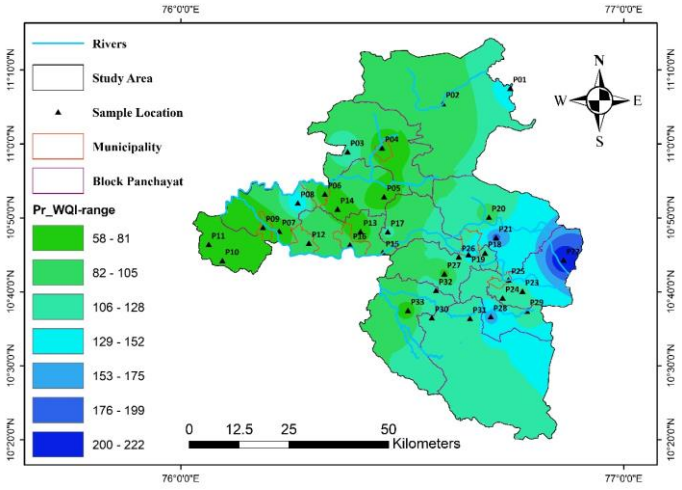

(a) The spatial difference of WQI in pre-monsoon

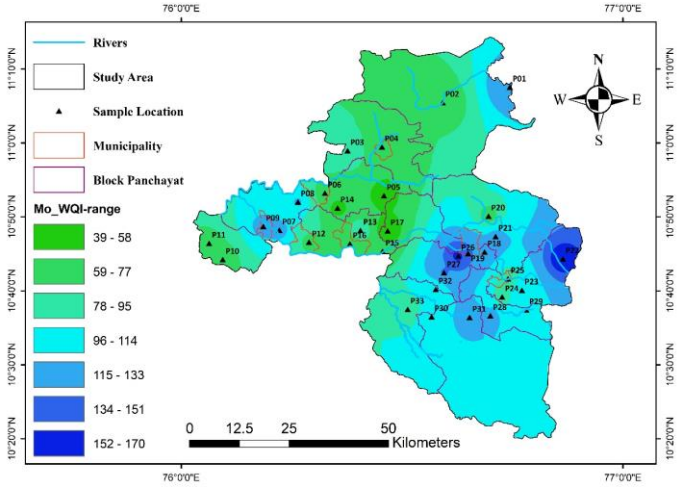

(b) **(b)** The spatial difference of WQI in monsoon

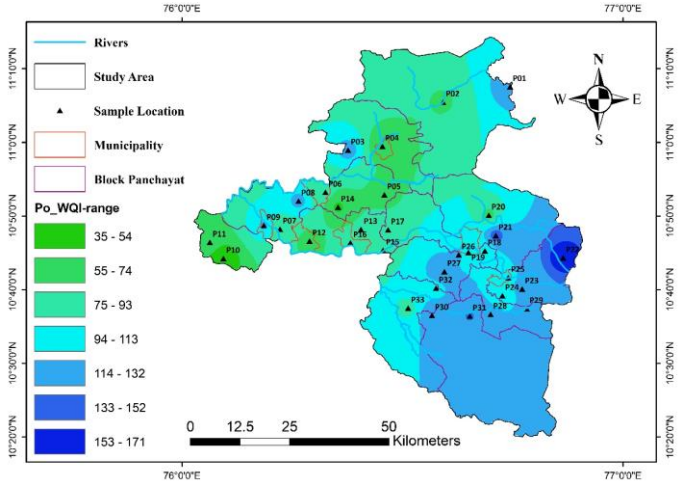

(c) The spatial difference of WQI in post-monsoon

Fig.1.4.15 The spatial difference of WQI excluding biological factors in different seasons in Palakkad District.

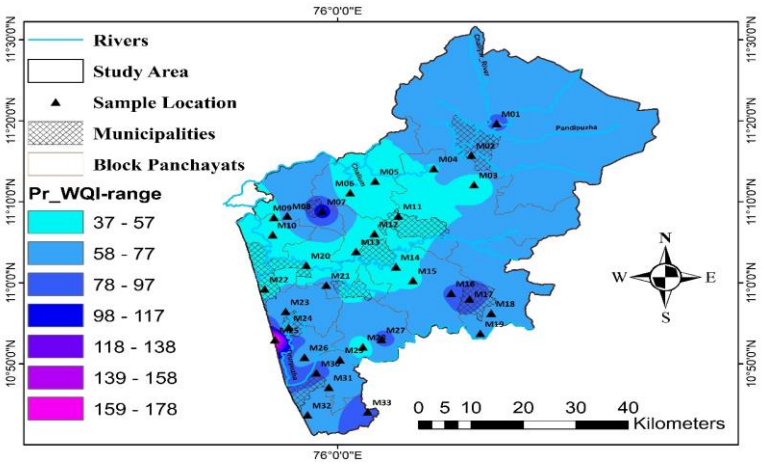

(a) The spatial differences of WQI in pre-monsoon

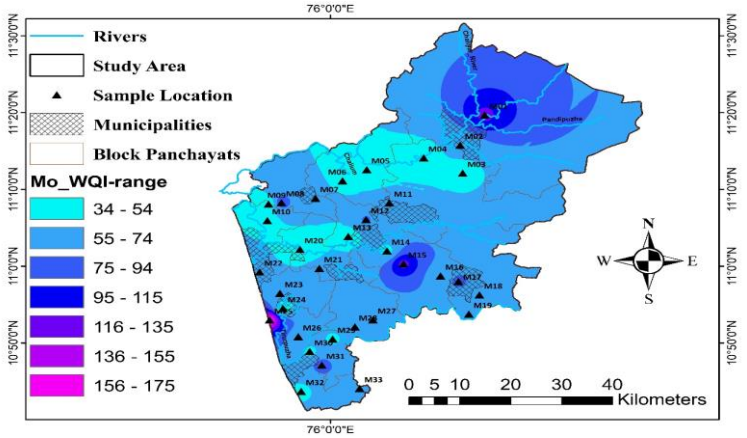

(b) The spatial differences of WQI in monsoon

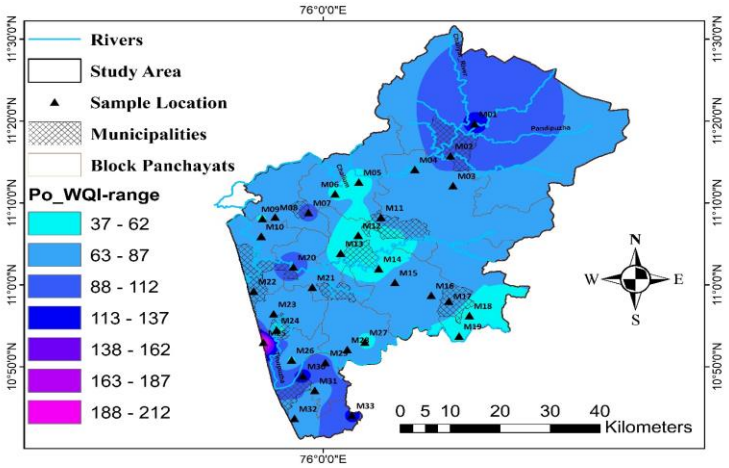

(c) The spatial differences of WQI in post-monsoon

Fig.1.4.16 The spatial difference of WQI excluding biological factors in different seasons in Malappuram District.

1.4.9. Heavy Metal Pollution (HPI) and Metal Index (MI)

Calculating the heavy metal pollution index (HPI) is a standard method for assessing groundwater pollution affected by excessive heavy metal concentrations (Mohan et al. 1996). HPI evaluates the cumulative effect of each heavy metal on the overall water quality status. The HPI was calculated in ppm concentration and the specimen calculation is given in Table 1.4.29 (Eldaw 2020). HPI was observed separately for selected sampling points for the different seasons, such as Pr, Mo, and Po. The Annual Average Heavy Metal Pollution Index (AAHPI) was also calculated by taking the average HPI for the three seasons. The HPI classification of samples has been done based on the AAHPI values. The Metal index is the most widely used index for heavy metal pollution assessment. MI was calculated in the same manner as HPI. The detailed specimen calculation for MI is given in Table 1.4.30. The Annual Average Metal Index (AAMI) was calculated by taking the average of MI for the three seasons (Pr, Mo, and Po). The annual mean of MI is expressed as AAMI. Water quality based on MI can be classified into six groups (Lyulko et al. 2001). The seasonal mean value of HPI and its annual mean (AAHPI), MI, and its annual mean for the Palakkad and Malappuram Districts were given in Tables 31 and 34. The seasonal rainfall from both Districts was correlated with the HPI and MI.

The high levels of heavy metal contamination in the Palakkad area were recorded during the Pr season (mean HPI = 110), although they decreased with rains during the Mo season (mean HPI = 90). In the Palakkad District, the HPI index classed 70%, 33%, and 58% of the Pr, Mo, and Po samples as poor. The rest of the samples are grouped into excellent and good. The seasonal rain data of Palakkad, such as 251.9 mm in Pr, 1524 mm in Mo, and 176.9 mm in Pr is correlated with the seasonal mean HPI. It exhibited negative results also (-0.31), affirming the dilution of heavy metals during the Mo season. The AAHPI indicates that 3% and 54.5% of the samples were excellent and good respectively, and 42.5% were poor. Likewise, MI was highest during the Pr season as most of the metal ion concentrations were highest in this season (Table 1.4.32). Since MI exhibited a negative correlation with rainfall (-0.213) in the Palakkad District. The majority of the samples fall into the good category; a small percentage of the samples are classified as slightly affected; and no samples were in the category of moderately, strongly, or seriously affected in

all the seasons (Table 1.4.33). The uppermost metal indices were observed from the samples taken from bore wells (P3, P8, and P31) (Table 1.4.31). The AAMI exhibited that only 3% of the groundwater samples were found to be very pure and the majority (88%) of the groundwater came under the good category. Only 3% of the samples were slightly affected (Table 1.4.33). The rest of the samples are slightly polluted with heavy metals from multiple sources such as natural, transportation, urbanization, and agricultural pollution.

Malappuram District had similar outcomes. The Pr exhibited the highest levels of heavy metal pollution, with a seasonal mean of 104. The HPI decreased in the Mo period (Mean HPI = 84), while the Po period (Mean HPI = 78) had the lowest degree of contamination (Table 1.4.34). Based on the HPI value, 12% of the Mo and Po samples were excellent types; 42% of the Pr, 62% of Mo, and 64% of the Po samples were good; and 58% of the Pr, 27% of Mo and 24% of the Po samples were poor. The HPI's annual mean (AAHPI) exhibited that 70% of the samples were good and 30% of the samples were poor (Table 1.4.35). The Malappuram District received rainfall of 178.9 mm in the Pr, 1928.2 mm in the Mo, and 353.8 mm in the Po seasons throughout the research period. In the Malappuram District, a negative relationship between HPI and rainfall (-0.31) was noted. The average MI was similar in the Pr (0.50) and Po (0.51) seasons, but it dropped to 0.46 in the Mo season (Table 1.4.34). Based on the MI index, the majority of the Pr (79%), Mo (67%), and Po (70%) samples were observed to be in the good category. 18%, 30%, and 24% of the Pr, Mo, and Po samples fall in the very pure category. Only 3% of the Po samples were slightly affected and the remaining 3% of the Pr, Mo, and Po samples were moderately affected (Table 1.4.36). The reduction of average MI in Mo is attributed to the dilution of groundwater by precipitation (1928.2 mm) since the MI exhibited a negative correlation with rainfall (-0.96). The highest MI was noticed in the samples from coastal regions (M25, M30, and M33), which are connected with Fe deposits (Muhammad et al. 2021). The Annual Average Metal Index (AAMI) estimates that in the present condition, only 3% of samples are moderately affected, 12% are found to be very pure, and the rest are good for consumption (Table 1.4.36).

Heavy metal pollution is severe in both Districts during the Pr season and minimal during the Po season. Tiwari et al. (2016b) also reported groundwater having the highest HPI during Pr and least during Po in the Bokaro coalfield in Jharkhand, India. Evaporation, concentration, groundwater extraction, human activity, and surface water recharge all have an impact on groundwater (Zhu et al. 2020). Metal concentrations are higher in areas close to industrial and coal mining facilities (Mahato et al. 2016). High HPI was observed in urbanized and township areas, which recognize that urban waste and transportation are assumed to be the real causes of heavy metal pollution. Heavy metals of natural existence are much more stable and have lower bioavailability than anthropogenic sources. On the other hand, anthropogenic sources of heavy metals act as potent pollutants (Jin et al. 2019; Arslan et al. 2021).

Table 1.4.29. Specimen calculation of HPI using the average concentration of heavy metals in the study area

Metal ions	**Monitored value in mg/L (Mi)**	**BIS Permissible in mg/L (Si)**	**Maximum allowable limits in mg/L (Ii)**	**Wi**	**Qi**	**Wi***Qi	**HPI**=∑Wi*Qi/∑Wi
Fe	0. 384	0.3		3.33	128.12	427.06	
As	0.0159	0.01	0.05	100	85.1	8508.8	
Pb	0.0118	0.01		100	118.27	11827.1	
Cd	0.00257	0.003		333.33	85.85	28619.5	
Ni	0.0179	0.02		50	89.79	4489.7	
Mn	0.0342	0.1		10	34.29	342.94	
Zn	0.076	5	15	0.2	143.29	29.84	
Cu	0.0224	0.05	1.5	20	101.8	2037.9	
				616.86		**56282.84**	**91.24087**

Table 1.4.30. Specimen calculation of MI

Heavy metal	**Concentration *Ci* *(mg/L)***	**Maximum Allowable Concentration (MAC)**	$MI = \sum_{i=1}^{n} \frac{Ci}{(MAC)i}$
Cd	0.0027	0.003	0.9
Pb	0.014	0.01	1.4
As	0.02	0.01	2
Ni	0.017	0.02	0.85
Fe	0.474	0.3	1.58
Cu	0.026	0.5	0.052
Mn	0.066	0.1	0.66
Zn	0.062	5	0.0124

Table 1.4.31. Seasonal HPI, MI, and Annual Average of HPI and MI of the samples in the Palakkad District.

Sl No	HPI (Pr)	HPI (Mo)	HPI (Po)	Mean AHPI	MI (Pr)	MI (Mo)	MI (Po)	Mean AMI
P1	107	57	86	83	0.51	0.76	0.49	0.59
P2	107	96	103	102	0.34	0.27	0.28	0.29
P3	150	125	136	137	1.23	1.24	1.49	1.32
P4	160	102	104	122	0.40	0.35	0.37	0.37
P5	79	50	65	65	0.74	0.46	0.58	0.59
P6	127	99	101	109	0.54	0.49	0.40	0.47
P7	141	116	137	131	1.86	0.65	0.41	0.97
P8	154	137	147	146	1.99	1.24	1.22	1.48
P9	111	110	101	108	0.24	0.52	0.44	0.40
P10	109	86	67	87	0.42	0.27	0.24	0.31
P11	100	89	93	94	0.46	0.46	0.43	0.45
P12	130	103	108	113	0.59	0.42	0.26	0.43
P13	70	23	79	57	0.82	0.35	0.47	0.55
P14	96	51	41	63	0.43	0.38	0.23	0.35
P15	106	87	64	86	0.43	0.32	0.18	0.31
P16	101	78	67	82	0.39	0.30	0.35	0.35
P17	118	45	35	66	0.55	0.26	0.21	0.34
P18	123	126	99	116	0.48	0.67	0.42	0.52
P19	125	90	95	103	1.01	0.66	0.50	0.72
P20	101	77	60	80	0.53	0.44	0.30	0.42
P21	141	98	86	108	1.21	0.46	0.25	0.64
P22	63	42	63	56	0.57	0.35	0.43	0.45
P23	95	38	36	57	0.60	0.42	0.89	0.64
P24	94	75	60	77	0.38	0.42	0.26	0.36
P25	59	44	22	41	0.64	0.38	0.49	0.50
P26	133	215	139	163	0.49	1.22	0.61	0.77
P27	109	185	96	130	0.59	1.04	0.69	0.77
P28	121	96	69	96	0.75	0.59	0.54	0.63
P29	122	75	96	98	0.52	0.38	0.68	0.53
P30	93	77	74	81	0.49	0.46	0.60	0.51
P31	91	101	82	91	1.09	1.25	1.42	1.25
P32	123	130	141	131	0.75	0.76	0.80	0.77
P33	75	58	80	71	0.40	0.49	0.53	0.47
Mean	110	90	86	95	0.68	0.57	0.53	0.59

Table 1.4.32. Seasonal and annual water type based on HPI classification in Palakkad District

HPI	Character	Pr		Mo		Po		AAHPI	
		Classification of samples based on HPI value	Total % samples	Classification of samples based on HPI value	Total % samples	Classification of samples based on HPI value	Total % samples	Classification of samples based on AAHPI value	Total % samples
<50	Excellent	NIL	0	P13, P17, P22-23, P25	15	P14, P17, P23, P24	12	P25	3%
50-100	Good	P5, P13, P14, P22-25, P30-31, P33	30	P1-2, P5-6, P10-11, P14-16, P19-21, P24, P28-30, P33	52	P1, P5, P10, P11, P13, P15-16, P18-22, P27-31, P33	30	P1, P5, P10, P11, P13, P14, P15, P16, P20, P22, P23, P24, P28, P29, P30, P31, P32	54.50%
>100	Poor	P1-4, P6-12, P15-22, P25, P29, P32	70	P3-4, P7-9, P12, P18, P26-27, P31-32	33	P2-4, P6-9, P12, P26, P32	58	P2, P3, P4, P6, P7,P8, P9, P12, P18, P19, P21, P26, P24, P32	42.50%

Table 1.4.33. Seasonal and annual water type based on MI classification of samples in Palakkad District

MI Class	Character	Pr		Mo		Po		AAMI	
		Classification of samples	Total % samples	Classification of samples	Total % samples	Classification of samples	Total % samples	Classification of |samples	Total % samples
< 0.3	Very pure	P9	3	P2, P10, P17	9	P2, P10, P12, P14-15, P17, P21, P24	24	P2	3%
> 0.3 - 1.0	Good	P1-2, P4-6, P10-18, P20, P22-30, P32-33	79	P1, P4 -7, P9 , P11-16, P18-25, P28-P30, P32-33	76	P1, P4 -7, P9 , P11, P13, P16, P18-20, P22-23, P25-30, P32-33	67	P1, P4 to P7, P9 to P30, P32, P33	88%
> 1.0 - 2.0	Slightly affected	P3, P7-8, P19, P21, P31	18	P3, P8, P26-27, P31	15	P3, P8, P31	9	P3, P8, P31	9%
>2.0 - 4.0	Moderately affected		0	0	0	0	0	Nil	0
> 4.0 – 6.0	Strongly affected		0	0	0	0	0	Nil	0
> 6.0	Seriously affected		0	0	0	0	0	Nil	0

Table 1.4.34. Seasonal HPI, MI, and Annual Average of HPI (AAHPI) and MI (AAMI) of the samples in the Malappuram District

Heavy Metal Index					Metal Index			
Sample Code	Pr	Mo	Po	AAHPI	Pr	Mo	Po	AAMI
M1	154	109	67	110	0.41	0.28	0.35	0.35
M2	140	125	113	126	0.47	0.41	0.73	0.54
M3	118	95	87	100	0.42	0.37	0.42	0.40
M4	101	85	105	97	0.48	0.39	0.58	0.48
M5	71	50	34	52	0.38	0.29	0.22	0.30
M6	95	47	61	67	0.29	0.26	0.28	0.28
M7	113	78	80	90	0.52	0.25	0.36	0.38
M8	146	116	77	113	0.39	0.53	0.38	0.43
M9	63	75	63	67	0.29	0.31	0.36	0.32
M10	68	86	110	88	0.37	0.44	0.61	0.47
M11	121	123	66	103	0.34	0.49	0.32	0.38
M12	99	67	67	78	0.37	0.31	0.25	0.31
M13	101	77	109	95	0.40	0.48	0.53	0.47
M14	104	93	68	88	0.30	0.35	0.44	0.36
M15	125	115	90	110	0.28	0.29	0.25	0.28
M16	106	128	116	117	0.39	0.56	0.69	0.55
M17	159	126	87	124	0.77	0.63	0.34	0.58
M18	138	112	93	115	0.69	0.33	0.21	0.41
M19	98	42	112	84	0.42	0.29	0.30	0.34
M20	66	65	47	59	0.24	0.25	0.42	0.30
M21	103	117	115	112	0.49	0.63	0.68	0.60
M22	109	78	58	82	0.41	0.30	0.25	0.32
M23	123	75	54	84	0.50	0.30	0.41	0.40
M24	77	46	52	58	0.55	0.28	0.28	0.37
M25	73	78	62	71	2.42	2.34	2.46	2.41
M26	98	92	94	95	0.59	0.39	0.59	0.52
M27	113	97	78	96	0.32	0.76	0.41	0.50
M28	84	51	59	64	0.28	0.46	0.71	0.48
M29	94	83	47	75	0.27	0.41	0.17	0.28
M30	113	60	88	87	0.89	0.30	0.80	0.66
M31	117	78	66	87	0.33	0.27	0.32	0.31
M32	75	50	100	75	0.45	0.25	0.495	0.40
M33	70	49	38	52	0.94	0.95	1.087	0.99
Mean	104	84	78	89	0.50	0.46	0.51	0.49

Table 1.4.35. Seasonal and annual water type based on the HPI classification of samples in Malappuram District

HPI	Character	Pr		Mo		Po		AAHPI	
		Classification of samples based on HPI value	Total % samples	Classification of samples based on HPI value	Total % samples	Classification of samples based on HPI value	Total % samples	Classification of samples based on AAHPI value	Total % samples
<50	Excellent	NIL	0	M6, M19, M24, M33	12	M5, M20, M29, M33	12	Nil	0
50-100	Good	M5-6, M9-10, M12, M19-20, M25-26, M28-29, M32-33	42	M3-5, M7, M9-10, M12-14, M20, M22-23, M25-32	61	M1, M3, M6-9, M11-12, M14-15, M17-18, M22-28, M30-31	64	M4, M5, M6, M7, M9, M10, M12, M13, M14, M19, M20, M22, M23, M24, M25, M26, M27, M28, M29, M30, M31, M32, M33	70
>100	Poor	M1-4, M8, M11. M13-18, M21-23, M27, M30-31	58	M1-2, M8, M11, M15-18, M21	27	M2, M4, M10, M13, M16, M19, M21, M32	24	M1, M2, M3, M8, M11, M15, M16, M17, M18, M21	30

Table 1.4.36. Seasonal and annual water type based on the MI classification of samples in the Malappuram District

MI Classification	Character	Pr		Mo		Po		AAMI	
		Classification of samples	Total % samples	Classification of samples	Total % samples	Classification of samples	Total % samples	Classification of samples	Total % samples
< 0.3	Very pure	M6, M9, M15, M20, M28-29	18	M1, M6-7, M15, M19-20, M24, M31-32	30	M5-6, M12, M15, M18, M22, M24, M29	24	M5, M6, M15, M29	12%
> 0.3 - 1.0	Good	M1-5, M7-8, M10-14, M16-19, M21-24, M26-27, M30-33	79	M2-5, M8-14, M16-18, M21-23, M26, M30, M33	67	M1-4, M7-11, M13-14, M16-17, M19-21, M23, M26-28, M30, M32	70	M1, M2, M3, M4, M7, M8, M9, M10, M11, M12, M13, M14, M16, M17, M18,M19, M20, M21, M22, M23, M24,M25, M26, M27, M28, M30, M31, M32, M33	85%
> 1.0 - 2.0	Slightly affected	NIL	0	NIL	0	M33	3	Nil	0%
>2.0 - 4.0	Moderately affected	M25	3	M25	3	M25	3	M25	3
> 4.0 – 6.0	Strongly affected	NIL	0	NIL	0	NIL	0	Nil	0
> 6.0	Seriously affected	NIL	0	NIL	0	NIL	0	Nil	0

1.4.9.1 Spatial analysis of HPI and MI

The Inverse Distance Weighted (IDW) interpolation analysis tool in GIS can be used to assess heavy metal spatial distribution and identify pollution sources (Hou et al. 2017; Bux et al. 2021). The HPI index interpolation in different seasons for Palakkad and Malappuram is given in Fig.s 1.4.17 and 1.4.18, respectively. The present study shows that the highest heavy metal pollution occurred during the Pr period in both Districts. During the Pr season, HPI is more prevalent in municipal and adjacent areas such as Kottopadam (P03), Mannarkkad (P04), Cherppullassery (P07), Nellaya (P08), Pattambi (P09), Shoranur (P12), Kodumbu (P18), Palakkad (19), Kannadi (P26), and Kuzhalamannam (P27) in the Palakkad District (Fig.1.4.17 (a)). Most of these regions are also low-lying. In the Mo period, heavy metals were also observed in the southern part of the Palakkad District (Fig.4.17 (b)). A comparable trend in HPI was exhibited in both the Pr and Po seasons in the Palakkad District. A similar tendency was also observed in Malappuram District. Heavy metal contamination was severe in the municipal area and other townships including Chungathara (M01), Nilambur (M02), Pallikkal (M08), Perinthalmanna (M17), and Aliparamba (M18) in Pr season Fig.1.4.18 (a)). In addition to these impacted regions, Manjeri (M11) and Edarikode also exhibited significant HPI throughout the Mo season Fig.1.4.18 (b)). The most elevated levels of contamination have occurred during the Pr and their spread during the Mo season. IDW gives a visual interpretation of pollution sources as it is directly based on surrounding measured values (Srivastava et al. 2011). This method is used to predict the value of unmeasured sites (Chowdhury and Maiti 2016).

Digital terrain can be best represented by the DEM method in Geographical Information Systems (represented as a study area). It is a three-dimensional morphometric depiction of a geographical area based on measurements and mathematical analysis (Zhao 2020). Compared with interpolation analysis, the DEM reveals that the heavy metals are more concentrated in samples collected from low-lying areas, predominantly near streams in the Palakkad District (Fig.1.4.17).

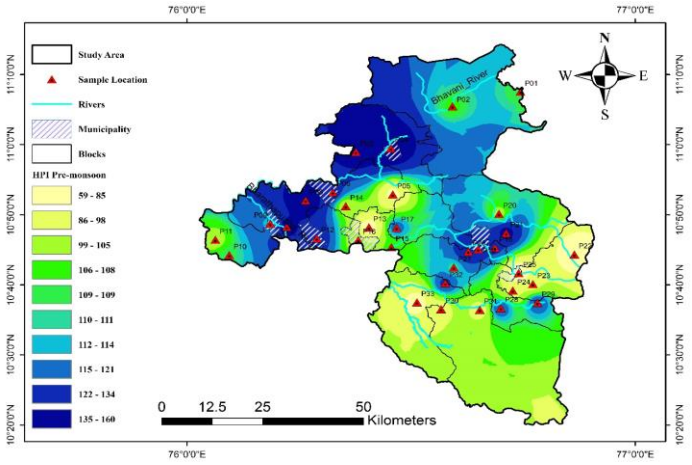

(a) Spatial spread of heavy metal pollution in pre-monsoon

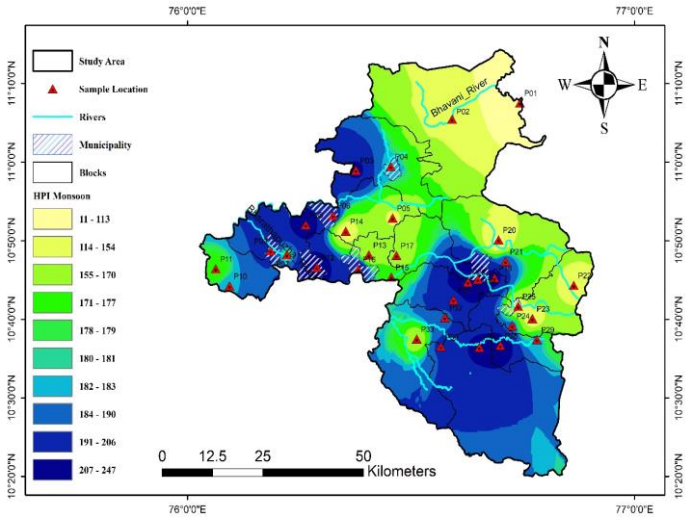

(b) Spatial spread of heavy metal pollution in monsoon

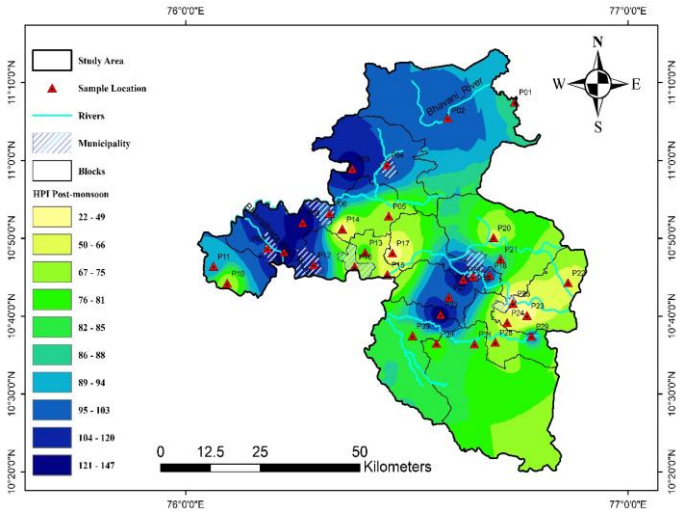

(c) Spatial spread of heavy metal pollution in post-monsoon

Fig.1.4.17 HPI in different monsoonal period in Palakkad district.

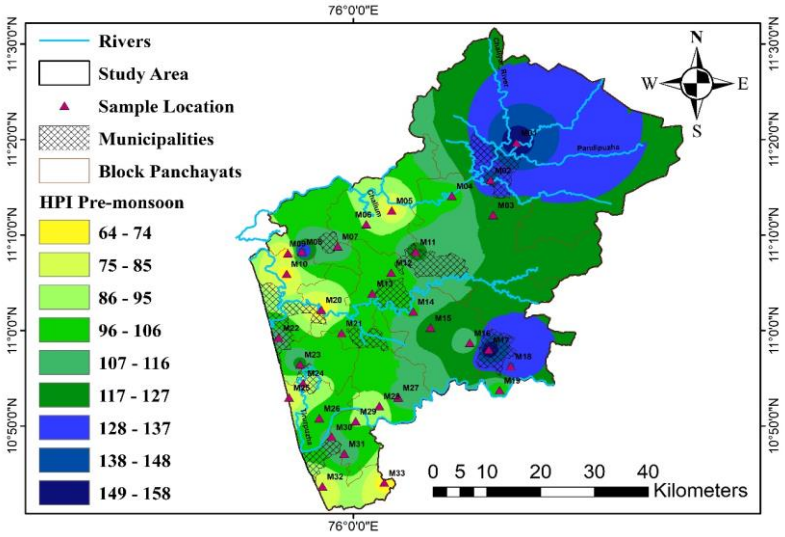

a. Spatial spread of heavy metal pollution in pre-monsoon

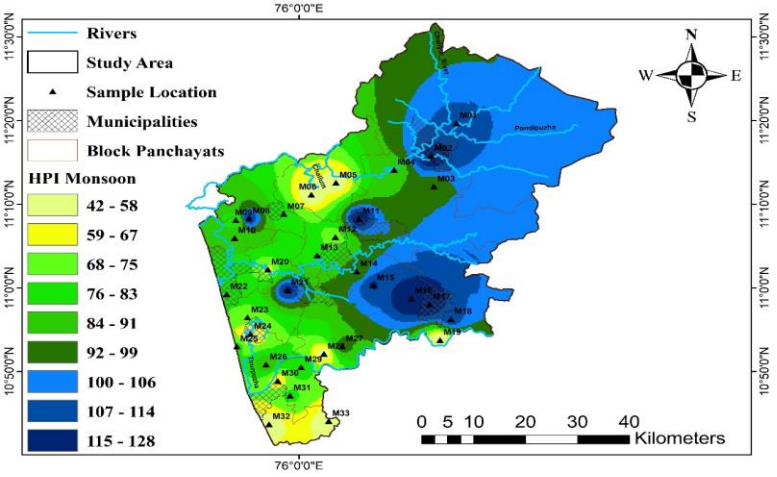

b. Spatial spread of heavy metal pollution in monsoon

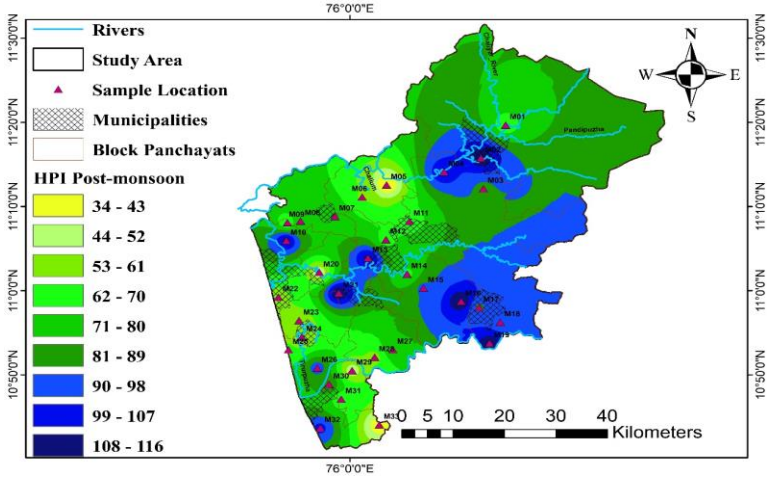

c. Spatial spread of heavy metal pollution in post-monsoon

Fig.1.4.18 HPI in different monsoonal period in Malappuram district.

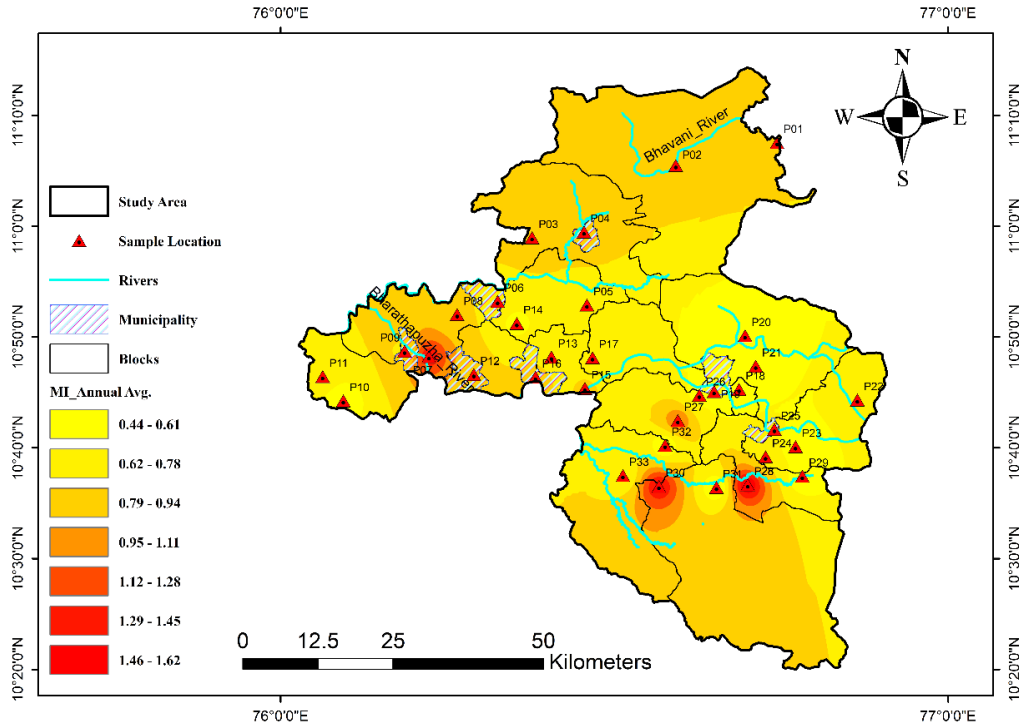

Fig.1.4.19 The spatial distribution of the annual average of the metal index in Palakkad District.

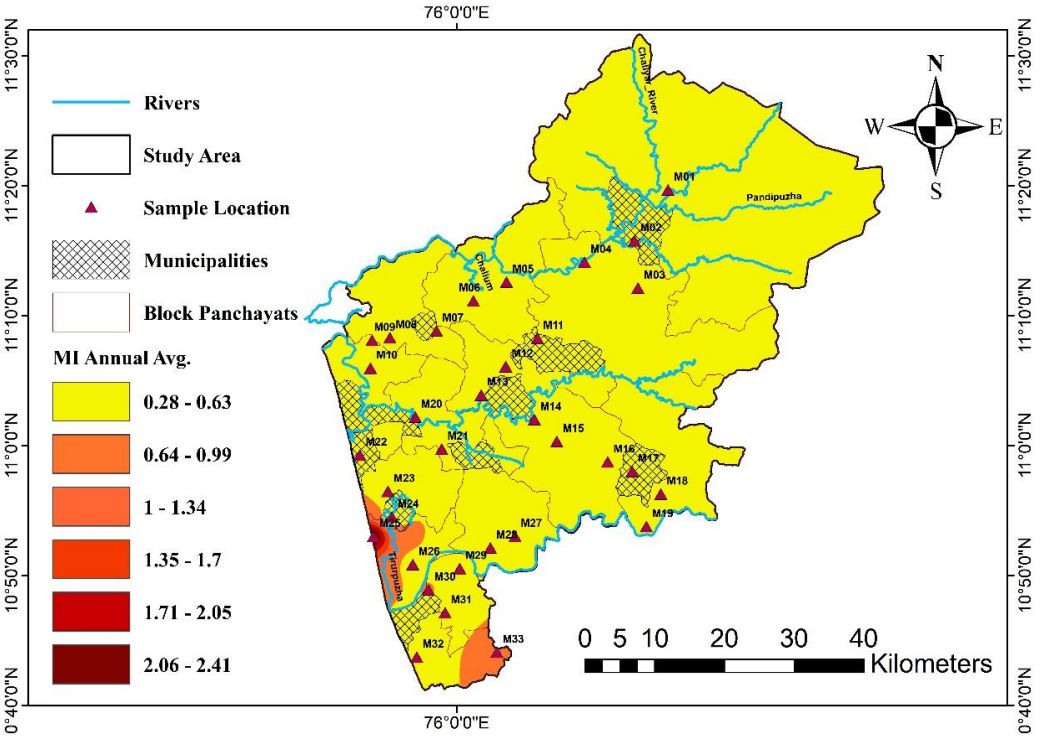

Fig.1.4.20 The spatial distribution of the annual average of the metal index in Malappuram District.

The heavy metal contamination in Malappuram was found in highland and midland urban areas rather than the coastal plains. More precisely it is concentrated in the valleys of highlands and midlands in the Malappuram District. The concentrations of heavy metals were found in open wells and bore wells in both Districts at all seasons, but primarily during the Pr season. Improper solid waste management and runoff from agricultural and industrial sites may enter shallow groundwater, which concentrates during Pr as the groundwater table declines (Kale et al. 2010). Hydraulic interaction of confined aquifers with nearby streams will also lead to heavy metal contamination in them because the precipitation and runoff will give pollution load to the streams (Barlow et al. 2000). Rainfall, wind, and drainage patterns have a high significance in the accumulation of heavy metals in the environment (Harikumar et al. 2009; Gowd et al. 2010).

Spatial analysis of the annual average metal index of Palakkad and Malappuram is given in Figs. 1.4.19 and 1.4.20 respectively. The spatial analysis of the metal index was performed using the IDW interpolation method. The Kollengode, Nenmmara, and Ongallur portions of the Palakkad District showed elevated metal concentrations in groundwater (Fig.1.4.19). In the coastal belt of the Malappuram District, MI is elevated and linked to fluvial deposits along the coast (Fig.1.4.20).

1.5. Summary

This research involves a comprehensive assessment of groundwater resources and the hydrochemical and biological characteristics of groundwater, with particular attention to fluoride (F), arsenic (As), other heavy metals, and salinity in the inland and coastal regions. By examining the influence of geochemical and environmental factors on the mobilization of these contaminants, this study aims to uncover the underlying mechanisms affecting groundwater quality. The summary of this work is as follows:

The annual rainfall of Palakkad District during the study period was 1951.8 mm. The ambient temperature recorded a minimum of 20°C and a maximum of

45°C. Hornblende–biotite gneiss is distributed in major parts of the Palakkad District, especially in the eastern Palakkad Gap region and charnokite gneiss along the western lowlands. The annual rainfall of Malappuram District during the study period was 2450.9 mm. The atmospheric temperature recorded was a minimum of 18°C and a maximum of 38°C in this District. There are two geological belts: I the charnockite group of rocks, which makes up the majority of the area; and II the migmatite complex, in the easternmost corner of the District. Clay, fluvial, and marine deposits are along the coastal belts of the Malappuram District.

The depth of open wells and bore wells in the Palakkad District varied from 4.27 m to 21.34 m and 38.10 m to 203 m, respectively. Open wells in the Malappuram District have a depth range of 3.96 m to 12.19 m, whereas bore wells have a depth range of 15.2 m to 121. 9 m. During the period of the study, the total groundwater availability in the Malappuram District was 249.32 million cubic meters, while it was 434.17 million cubic meters in the Palakkad District.

The samples from the western region of the Palakkad District were in the acidic range, and the majority of the samples from the Malappuram District were also acidic. In the study area, acidity dominates in open well samples. The water samples had their maximum temperatures during the Pr season, and a minimum during Mo, with a lowest of 20.5 °C, which was reported from a bore well sample (P24). The bore well samples had higher EC, TDS, and salinity values than the open wells. However, the addition of salinity to groundwater is also influenced by geological attribution. High turbidity and solid content of the samples were observed in the bore well samples due to the presence of dissolved Fe, which readily oxidized when it came into contact with the air (P01, P18-P19, P22, P24, P26, P28-30, and P32). Similarly, total hardness, calcium, and magnesium hardness were highest in Sholayur (P01), Puthussery (P21), Eruthenpathy (P22), Perumatti (23), Chittur (P25), Kollengode (P28), Muthalamada (P29), and Erumayur (P33). The samples from the Palakkad District had higher levels of hardness, whereas the samples from the Malappuram District had the lowest.

Both open wells and bore wells were found to be contaminated with chloride. The sulphate concentration in the samples is within the permitted range, except for P22 (Eruthenpathy) during the Po season. 12% of the Pr, Po, and 9.1% of the Mo samples from the Palakkad area had sodium levels over the recommended limits, however, there was no sodium contamination in the samples from Malappuram. In contrast, the Malappuram region showed low levels of potassium contamination (3% in Mo and 1.5% in Po samples), while there was none in the Palakkad District. Nitrates and phosphates are within the BIS-mandated acceptable levels (2012). Phosphates in the sample, however, had significant potential for eutrophication because they were above the 0.1 mg/L limit. In the Po and Mo seasons, levels of both total and E. coli were high. Microbial growth was present in samples from both bore wells and open wells.

The study area is highly contaminated with F. The majority of the samples were above the desired limits of 1 mg/L, including 88% of the Pr and Po and 52% of the Mo samples from Palakkad. In the same way, these limits were exceeded in 69.7% of the Pr, 10.6% of the Mo, and 72% of the Po samples. 9, 3, and 7.6% of the Pr, Mo, and Po samples respectively from Palakkad, exceeded the permitted limits when compared to the maximum acceptable limit of 1.5 mg/L. In the Malappuram District, it is 4.5% of the Pr, 0% of the Mo, and 4.5% of the Po samples. F and pH were shown to be strongly correlated in the study area during the Pr and Po seasons. Additionally, there was a high association between F, EC, TDS, TH, and Mg and a negative correlation between F, Ca, Fe, and nitrate. F incidence was higher in the Palakkad District compared to the Malappuram District, and Attapady (P1), Chittur, and Kollengode Blocks of Palakkad have extremely high F throughout the year. During the Mo season, Pattambi Block also had a high F incidence. F levels in the Malappuram District were found to be excessive in the southeast.

The highest As contamination was observed in Mo (36.4%), followed by Po (31.8%), and Pr (21.1%) in Palakkad, and the highest incidence observed in Malappuram was in the Po (39.34%) season, followed by Mo (27.27%) and Pr

(7.58%). As showed a strong positive correlation with F and a negative correlation with calcium in the Mo season in Palakkad District. Additionally, it has been noted that in the Palakkad District, there is a negative correlation between As and Fe as well as As and Mn. Because As shows a strong correlation with Na and Cd, both anthropogenic and natural sources of As in groundwater have been recognized in the Malappuram District. In the research area, As can be found in both acidic and alkaline circumstances. In the Mo and Po seasons, the prevalence of As is high. Fluvial alluvium in the study area is strongly related to the geographical distribution of As in the study area.

Heavy metal contamination by Cd, Pb, and Ni was severe in both Districts. 53% of the Pr, 34.85% of the Mo and Po samples of Palakkad, and 43.94% of the Pr, 34.85% of Mo, and 25.76% of the Po samples of Malappuram District were above the permissible limits of Cd prescribed by BIS (2012). The dissolution of Cd in groundwater was inversely correlated with pH, showing that an acidic pH facilitated its dissolution. Additionally, a strong association with Pb and Ni suggested that the source of the Cd was likely from automobiles. Pb contamination in the order of Pr (60.6%) >Po (40.9%)>Mo (34.84%) in the Palakkad District and Pr (60.6%) >Po (45.45%)>Mo (22.7%) in the Malappuram District were noticed. High Pb was seen both in acidic and alkaline water. The sample collected from nearby areas of the highway shows a high concentration of Pb. Ni incidences were higher in Malappuram, compared to Palakkad District. Ni concentration was above the permissible limits of BIS and was in the order of Pr (39%) > Mo and Po (38%) in Palakkad District and Pr (45.45%) > Po (37.87) > Mo (34.84%) in Malappuram. The geogenic source of Ni is more apparent in Palakkad, whereas in Malappuram District, both geogenic and agricultural sources are prevalent.

In comparison to other heavy metals, the Mn contamination is relatively low. The incidence is Pr (22.72%)> Po (16.67%)> Mo (13.64%) in Palakkad and Mo (9.1%)>Po (7.58%)>Pr in the Malappuram District. Multiple sources of pollution are attributed to the cause of Mn pollution in the study area. Both Districts had the lowest levels of Cu contamination. Only 1.5% of the Mo samples from the District

of Palakkad and 4.5% and 3% of the Po and Mo samples respectively from the District of Malappuram were below the acceptable range.

The piper plot indicated that the cationic array in the Palakkad District was Mg^{2+} > Na^{+} > Ca^{2+} > K^{+} , and the anions were in the order: HCO_3^{-} > Cl^{-} > SO_4^{2-} > NO_3^{-} . In the Palakkad region, magnesium-type water predominated throughout the Pr and Po seasons. In Malappuram District, no dominant cations were observed in Pr, but the Mo and Po seasons were dominated by calcium and sulphate types of water. During the Pr season, the majority of the samples were mixed types. Chadha's diagram depicts most of the samples falling under the Ca-Mg-Cl and Ca-HCO_3 types, and only a small percentage of samples fall into the Na-Cl type in the study area. According to Wilcox plots, 97% of the samples from Palakkad are excellent, good, or tolerable for irrigation, while only 3% are poor for irrigation. Samples from Malappuram, however, are an excellent and good category for irrigation. According to Gibb's plot, precipitation-induced salinity in the Malappuram District and rock-water interaction in the Palakkad District are the main causes of F and water salinity, respectively. In both areas, the Pr season has a high frequency of Fe, followed by Po and Mo. Fluvial deposits in the coastal belts and laterite reserves in other areas are linked to the majority of the Fe incidence.

The Water Quality Index (WQI) has been calculated in two different ways, i.e., including biological variables and excluding biological components. In the WQI, including the biological parameter, the majority of the water samples from both Districts are rated as poor or unfit for drinking. Only 3% of Mo samples were found to be excellent, while 12% of Pr, 15% of Mo, and 9% of Po samples came into the good and the remaining samples from all three seasons fell into the unfit for drinking category in the Palakkad District. In the Malappuram District, based on the WQI, taking into consideration biological factors, only 3% of the Pr and Mo samples were excellent, 15.15% of the Pr, 18.18% of Mo, and 3% of the Po samples were good, and rest of the samples fell into the category of being unfit for drinking. Water quality excluding biological parameters indicates that no water is in the range of unsuitable for drinking and most of the samples fall into good or

poor categories in the study area. In the Palakkad District, 48% of the Pr samples, 45% of the Mo samples, and 48% of the Po samples were found to be good, whereas 48% of the Pr samples, 45% of the Mo samples, and 45% of the Po samples were classified as poor. The Malappuram District had 27%, 30%, and 9% of the Pr, Mo, and Po samples that were excellent, respectively. 6%, 9%, and 15% of the Pr, Mo, and Po samples fall into the poor category, while 47%, 61%, and 73% of the Pr, Mo, and Po samples go into the good category. Additionally, 3% of the Po samples from Malappuram fall into the category of very poor.

The central and western regions of the Palakkad District are distinguished by better water quality year-round, according to the spatial analysis of the WQI. The District's eastern region has significantly degraded water quality. The southwestern part of the Malappuram District is notable for having poor water quality. However, most of the samples are of excellent or good quality.

Following HPI and MI, the Palakkad District experienced the highest pollution during the Pr season and the least during the Mo season. In the District of Palakkad, the HPI index categorized 70%, 33%, and 58% of the Pr, Mo, and Po samples as poor. According to the AAHPI, 42.5% of the samples were bad, 3% were excellent, and 54.5% were good. The samples from bore wells had the highest metal indices (P3, P8, and P31). According to AAMI, 3% of the samples from the Palakkad District were very pure. In the Malappuram District, the Pr exhibited the highest levels of heavy metal pollution, with a seasonal mean of 104. The HPI decreased in the Mo period (Mean HPI = 84), while the Po period (Mean HPI = 78) had the lowest degree. 58% of the Pr, 27% of the Mo, and 24% of the Po samples were poor. AAHPI exhibited that 70% of the samples were good and 30% of the samples were poor. The average MI was similar in the Pr (0.50) and Po (0.51) seasons, but it dropped to 0.46 in the Mo season in the Malappuram District. The highest MI was noticed in the samples from coastal regions, which are connected with Fe deposits (M25, M30, and M33). The Annual Average Metal Index (AAMI) estimates that in the present condition, only 3% of samples are moderately affected. Rainfall was shown to be negatively correlated with HPI and MI in both Districts.

IDW analysis provides a visual model that shows HPI is more widespread in township areas of both districts. Spatial analysis of the annual average metal index shows that the Kollengode, Nenmmara, and Ongallur regions of the Palakkad District showed elevated metal concentrations in groundwater. In the coastal belt of the Malappuram District, MI is elevated and linked to fluvial deposits.

Conclusion

The present study elucidated the groundwater stores and their trends of salinity, F, and heavy metal concentrations during different monsoonal periods in the Palakkad (inland) and Malappuram (coastal) Districts of Kerala, India. The following findings are drawn from this study: The east and southern regions of the Palakkad District, in particular, depend largely on bore wells for the year-round availability of drinking water. Open wells are the primary source of drinking water in the western portion of the Palakkad District and most of the Malappuram District. The groundwater availability in the Palakkad District is 434.17 MCM and 249.32 MCM in the Malappuram District.

The correlation analysis was found to be a reliable approach for determining the relationship between the hydrochemical parameters and their origin. The majority of samples taken from shallow aquifers in the Malappuram District and the western half of the Palakkad District show that the groundwater is acidic. Alkaline water is a distinctive feature of the groundwater in the eastern part of the Palakkad District. Sulphate and chloride pollution is comparatively low in the study area. In all the seasons, TH and TA had a significant positive association.

Na concentration was higher in the eastern region of Palakkad than in the coastal District of Malapuram, although it remained within acceptable limits. Similarly, the concentration of potassium is higher in the coastal District (Malappuram) than in the inland (Palakkad). The samples from open wells that were taken during the Mo season showed the highest nitrate incidence. However, the nitrate levels in the study area were within acceptable ranges. A strong positive correlation between NO_3 and K in Malappuram samples is an indicator of pollution from the agricultural source. Both the Palakkad and Malappuram Districts found evidence of

PO_4 contamination, particularly in samples taken from shallow aquifers, which is likely from agricultural sources.

High levels of *E. coli* and total coliforms were observed in the samples collected from both open wells and bore wells in the study area. In both Districts during the Pr season, there was a substantial positive association between total coliforms, E. coli and water temperature that points to the ability of coliforms to survive in tropical conditions.

Heavy metal contamination is more prominent in both Districts. The Pb, Cd, As, Ni, Fe, and Mn in groundwater exceeded the standard limit. Cd and Pb exhibited a severe extent of contamination. Cd pollution in both Districts is associated with anthropogenic sources, as this element is naturally found in association with Zn in sulfide ores. No incidence of Zn was found in the study area, and Cd exhibited a strong negative correlation with Zn and sulfate. There is a significant positive correlation with the As and Ni points that Cd from anthropogenic sources. The samples collected from nearby highways show a high concentration of Pb in the Mo season, which traces its source to highway transportation.

The prevalence of Fe contamination is high during Pr and Po seasons in the Palakkad District as it is not from geogenic sources because iron-related alkalinity and hardness are not present in the Palakkad District. On the other hand, the considerable positive association between the TA and TH with Fe in the Malappuram samples indicates that iron-infused alkalinity and hardness are common in this region. The geogenic iron contamination in the Malappuram District is closely related to the river deposits along the coastal belts and the laterite deposits in other areas.

Water sources in the current study site are also at risk of Ni and Mn contamination. In both Districts, Ni contamination showed a similar pattern to As contamination. The correlation analysis of the parameters in Malappuram reveals that Ni is from both geogenic and anthropogenic sources, however, it was observed that Ni in the Palakkad District is of natural origin. Multiple sources of contamination of Mn are attributed in both Districts because Mn showed a significant positive correlation

with PO_4 , Cl, and Fe in Palakkad as well as Fe, Na, and Cl in Malappuram District in different seasons. Only 1.5% of the Mo samples from Palakkad and 3% of Mo and 4.5% of the Po samples from Malappuram District had Cu levels that were higher than the acceptable limits. Most samples in the study area had Cu and Zn levels that are below the thresholds for detection. All heavy metals under consideration, excluding Pb and Cu, are found to have enhanced solubility in an acidic pH.

In the Palakkad District, Mg-Ca-HCO_3-type water predominated throughout the Pr and Po seasons. Calcium and sulphate types of water predominated in the Malappuram District during the Mo and Po seasons. The majority of the samples in the study area are represented in Chadha's diagram as belonging to Ca-Mg-Cl and Ca-HCO_3 types. The Wilcox plot indicates that 3% of the Palakkad samples were unsuitable for irrigation while 9% are tolerable. In the Malappuram District, all of the water samples were excellent for irrigation. In brief, the Palakkad District has more salinity in its groundwater than Malappuram District.

Widespread F contamination was observed in the Palakkad District. The Pr season had the maximum levels of F pollution in the upstream area (Attappady, Chittur, and Kollengode Blocks). In the Mo season, the western part of the Palakkad District (Pattambi Block) also showed high F concentrations in groundwater due to precipitation and induced leaching processes. Although F pollution in the Palakkad area during the Po season is similar to that during the Pr season, the elevated F concentration in the Po sample indicates an accumulative trend of F with rising temperatures and falling groundwater levels. The F contamination in Malappuram has similar trends as in Palakkad District. F levels in the Malappuram sample, however, are not as high as they are in the Palakkad area. It was discovered that the Malappuram District's southeast, which borders the Palakkad District, has a high F concentration.

The rock-water interaction with evaporation-induced F contamination was observed in major parts of the Palakkad District, such as the Attapady (P1), Chittur (P22–P25), and Kollengode (P28 and P29) Blocks. The alkalinity, magnesium, and NaCl

were higher in the groundwaters of the Palakkad District, while the Fe and calcium levels were low. Precipitation-induced F contamination was dominant in the Malappuram District. Higher concentrations of Fe and calcium and the acidic nature of the groundwater might have prevented the dissolution of F in samples from Malappuram District. Moreover, the Hornblende biotite gneiss is widely spread in the Palakkad District and is the main source of F, whereas the charnockite group is predominant in the Malappuram District. The groundwater in the study area is of the calcium chloride and sulphate types, indicating acidity. Other geogenic inputs like laterite, charnockite, and charnockite gneiss types of minerals also contribute acidity to groundwater, as evident in the Malappuram District. High alkalinity is caused by the hornblende biotite gneiss that contributes to the magnesium bicarbonate type of groundwater. Thus, the rock type in an aquifer determines its water quality.

Arsenic in water is a serious concern, beyond the optimal limit of 0.01 mg/L, as recommended by the BIS and WHO. Arsenic was shown to have a strong relationship with TH and Mg in the samples from both regions. A higher association of As and F in the water samples from the Palakkad region suggests that As is geogenic. It has also been assumed that As in the Malappuram District is both geogenic and anthropogenic due to the extensive connection between As and Cd during the Mo season. As pollution is characterized by high amounts of alkalinity and carbonate in groundwater, especially during the Pr season. Extreme As pollution occurred throughout the Mo and Po seasons, and was concentrated in the downstream regions of both Districts. The contamination from As was higher in open wells than in bore wells. According to the spatial analysis, samples from a nearby river showed a substantial concentration of As in the study region, which is related to alluvial deposits. Upon comparison of the geographical distribution of As contamination with mineral groups, it is noted to be associated with Hornblende-biotite gneiss (P20-23) and Charnockite / Charnockite gneiss (M07).

The WQI, HPI, and MI are excellent tools to evaluate the overall water quality and heavy metal contamination in the study area. The intensity and spatial distribution

of the WQI, HPI, and MI in various seasons are well described using IDW interpolation. The inclusion of biological parameters in WQI makes most of the samples either poor or unsuitable for drinking purposes. In Palakkad District, considering WQI, the majority of the samples are categorized into the poor (about 45%) and the good (about 45%) categories in all seasons (excluding biological characteristics). In a similar perspective, in Malappuram, the majority of the samples are categorized into the good category. In Palakkad, excellent water is scarce, although it is common in the Malappuram area.

The mean heavy metal pollution index (HPI) indicates that the highest heavy metal incidence occurred in the Pr period and the least during the Po period in the study area. The high HPI in the Pr period can be attributed to the lowering of the groundwater table, which concentrates the available mineral ions. In the Palakkad District, high HPI was noted in urban areas, townships, and low-lying areas, whereas in the Malappuram District, it was noted in highland and midland valleys. There is a considerable dilution of the Metal Index (MI) from Pr to Po in the Palakkad District. Samples from Malappuram revealed dilution during the Mo season and a comparable MI profile during the Pr and Po seasons. Cd, Pb, and Ni have concentrated in urban areas in the study area, whereas Fe-mediated issues are higher in coastal region associated with fluvial deposits. In addition, transportation, solid waste dumps, and agricultural runoff also pose heavy metal pollution in the areas under study. The drainage pattern of the land was also noted to have an important role in the accumulation of heavy metals.

Chapter 2.
The Mineralogical aspects of the contaminated sites

2.1 Introduction

Geochemistry has a considerable influence on the composition and mobilization of elements in groundwater. Unweathered and weathered rocks are intricately linked to groundwater in an aquifer. Typically, the unconfined and semiconfined aquifer zones are noticed between 40 and 45 meters below the surface (Malleshwaram 2014). The semiconfined aquifer even reaches up to 60 meters, whereas the confined aquifer extends from 60 to 240 meters in depth (Wu et al. 2015a; Su et al. 2020). Bore wells or deep wells are often made in semiconfined or confined aquifers, while open wells are typically built in unconfined or perched aquifers (Fenta et al. 2020).

The residence period of water in the surface and subsurface layers impacts the concentration of dissolved minerals in the groundwater (Jesubek et al. 2013). At relatively shallow depths, water might have been retained for a few hours, but at moderate depths, it may be decades old, and even at higher depths or after flowing a considerable distance from its source, it will be several thousand years old (Muller et al. 2016). Numerous reports affirm that the residence time of groundwater is directly related to the quantity of dissolved minerals (Richards et al. 2022; Han et al. 2015; Vinnarasi et al. 2020; Ezaki et al. 2020; Marghade et al. 2020). The inorganic rock is composed of a variety of major and minor/trace elements, which can attribute to a wide range of chemical components in the associated matrix. Thus the nature and type of rock to which the water is linked has a greater influence on various attributes of the groundwater. This includes both metals and non-metals (Balaram et al. 2019; Khan et al. 2022). The dissolution of minerals in water is further influenced by other variables, including temperature and pH (Riedel 2019; Chen et al. 2020). Thus, an inventory of rocks, soils, and associated mineralogy will provide inputs for a systematic elucidation of the geochemistry and mechanisms of rock-water interactions.

The previous chapter dealt with an inventory of the quality of groundwater confining to Palakkad and Malappuram Districts of Kerala, in the perspective of contamination by As, F, and other heavy metals. The present study is aimed to get an in-depth knowledge of the geochemical conditions of the subsurface aquifers confined to the study areas; assess the quantities of F and As in the rock samples from contaminated regions, and establish the relationships of F and As in the groundwater with sub-

surface mineralogy. The results have been statistically validated to derive conclusions regarding the geogenic or anthropogenic release of F and As and to provide sustainable management solutions to overcome the effects of these contaminants in the impacted regions. A review of the mineralogy of soil components, the methodology used, and the resultant impacts of minerals on groundwater, especially F and As is given below:

2.2. Review of literature

Groundwater is the primary source of drinking water, especially in tropical regions. The contamination of groundwater reserves by toxic elements from geogenic sources such as rocks and soils is a serious issue in almost all nations (Chandrajith et al. 2020; Raju 2022). Iron, As, and other trace metals are natural and inseparable components of the Earth's crust (Pais and Jones 1997). The concentrations of F and As in groundwater are determined by the parent rock, its weathering status, and its physicochemical properties (Wagh et al. 2016; Yadav et al. 2020a; Moghtaderi et al. 2020). This session reviews the earlier studies and reports on the petrological attribution of F and As in groundwater sources and its after-effects. The present review also included the research undertaken on the elemental composition of geological reserves related to groundwater using XRD and XRF studies.

2.2.1. Fluoride on Earth

The thirteenth most prevalent element on Earth is fluorine (Harsanyi and Sandford 2015). Being electronegative, it reacts easily with other elements. It is estimated that 625 mg F/kg of soil is present in the earth's crust (Vithanage and Bhattacharya 2015; Edmunds and Smedley 2013). F concentrations vary with the rock type, ie. from 1300 mg/kg for marine shale to 1000 mg/kg for alkaline igneous rocks and 100 mg/kg for ultramafic rocks (Ozsvath 2009; BalconeBoissard et al. 2009).

F is widespread in soils, plants, and animals, including humans. Several variables influence the F concentration in soil (Weinstein and Davison 2004). The F concentration is commonly low in soil (407 mg/kg) due to strong mobility (Zhu et al. 2007), while the upper continental crust averages 557 mg/kg (Enalou et al. 2018). The application of phosphate fertilizer can enhance the F concentration in soil to 123% (Loganathan et al. 2001; Ramteke et al. 2018). The F addition by agricultural

practices is due to the dissolution of F metal complexes, which are accelerated by acidic pH (Gan et al. 2021). F mobility is also governed by alkalinity and temperature (Ali et al. 2016).

F migration may also result from its interaction with clay, other anionic chemicals, and organic molecules (Dash and Rath 2020). F concentration is lower in soils with rich organic matter and low clay minerals (Zhu et al. 2007). Clay minerals with sesquioxides (Fe_2O_3 and Al_2O_3) on their surface absorb the F in the following pattern: $FeOH^{-\frac{1}{2}} + F^{-1} \leftrightarrow FeF^{-\frac{1}{2}} + OH_1$ (Zelazny et al. 1986; Roshni and Harikumar 2021). Due to their comparable charges and ionic sizes, hydroxide ions and F ions are rapidly exchanged in soil (Cai et al. 2001; Saxena and Ahmed 2001). Kaolinite and illite were more efficient than montmorillonite in absorbing F (Agarwal et al. 2002). Fe and Al oxides in the aqueous phase on the surface of the clay contain plenty of hydroxyl ions (OH), which facilitate the sorption of F ions (Sujana et al. 2009; Liang et al. 2013; Kang et al. 2013). F may also be adsorbed and precipitated by organic materials with a high concentration of Ca ions (Tumer et al. 2005; Wang et al. 2021d).

The weathering of F-bearing rocks is the primary natural source of F enrichment in groundwater (Mukherjee and Singh 2018; Adimalla 2020; Tiwari et al. 2020). Volcanic eruptions and marine aerosols are the secondary natural sources recognized (Farooqi et al. 2009; Edmunds and Smedley 2013). Fluorite (CaF) and apatite ($Ca_5(PO_4)_3$ (F, Cl, OH) are the two most prevalent F-containing minerals (Zhou et al. 2017). The main sources of F are amphiboles and micas, which are found in a variety of sedimentary rock types (Handa 1975). F is further generated from fluorspar, topaz, and cryolite in the soil (Durrani and Farooqi 2021; Wang et al. 2021a; Alferyeva et al. 2022).

The illite, chlorite, villiaumite, cryolite, and fluorapatite-containing aquifer have a high F content (Deshmukh et al. 1995; Kumar et al. 2015). Churchil et al. (1948) estimated the highest concentration of F in coal (295 ppm). F is present in minute levels in calcrete and dolocrete (Jacks et al. 2005). Granitic rocks include F-rich minerals such as biotite, hornblende, amphiboles, and muscovite (Mukherjee and Singh 2018; Vural and Gundogdu 2020). According to the findings, large levels of F are also associated with the minerals syenites, granites, quartz monzonites,

granodiorites, and felsic and biotite gneisses inside metamorphic crystalline igneous rocks (Ozsvath 2006; Valenzuela-Vasquez et al. 2006; Ludington et al. 2009; Manikandan et al. 2014). Basalt, limestone, sandstone, and shale also release F into groundwater under optimal circumstances (Saxena and Ahmed 2003; Dubey et al. 2021).

On a global scale, regions with large sedimentary rocks, crystalline igneous and metamorphic rocks, volcanic activity, and arid and semi-arid regions are associated with high F (Shahin 2002; Edmunds and Smedley 2013; Zango et al. 2019). Cryolite (54 wt. %), fluorite (48 wt. %), topaz (11.5 wt. %), fluorapatite (3.8 wt. %), biotite, and muscovite, which contain around 1 wt. % F, is said to have the highest F concentrations by weight (Maria and Laura 2015).

2.2.2. Arsenic on Earth

Arsenic has been in use since ancient times with the turn of the 20^{th} century, As compounds with vivid hues have been used to create imaginable works of art (Emsley 2006). As is prevalent in several sedimentary minerals and solid phases (Huyen et al. 2019; Schuh et al. 2019). As is found to occur as oxides and hydroxides of Mn, Al, and Fe (Penke et al. 2020; Zhang et al. 2020). Pyrite [$Fe(S, As)_2$] is the most prevalent As-containing mineral source (Savage et al. 2000; Paktunc 2008; Abbott et al. 2017; Saunders et al. 2018; Xing et al. 2019; Fakhreddine et al. 2021). It is also found as arsenides and arsenites (O'Day 2006; Rae 2020). Common sulphide forms include arsenopyrite (FeAsS), realgar (AsS), and orpiment ($As_2 S_3$) (Lengke et al. 2009; Marc et al. 2018). Under anaerobic conditions, pyrites are stable, but when exposed to air, they oxidize to generate iron oxide and As (Sun et al. 2012; Wang et al. 2020b; Dong et al. 2020). Foley and Ayuso (2008) categorized As sources as primary minerals, such as pyrrhotite, niccolite, realgar, glaucodot, lollingite, arsenopyrite-cobaltian, cobaltite, Ni-pyrite, and gersdorffite; and secondary minerals, which serve as an intermediate reservoir of As, which include claudetite, orpiment, scorodite, secondary arsenopyrite, goethite, natrojarosite, ferrihydrite, melanterite, rosenite, and Mn-hydroxide coatings.

The release of As into groundwater is affected by pH, redox conditions, the presence of microorganisms, and organic matter (Han et al. 2019; Patel et al. 2019). In a desired scenario, the metal oxides (Fe, Mn, and Al) in groundwater absorb the As (Ali et al. 2019b). Particularly, reductive dissolution of MnOOH and FeOOH mediated by anaerobic bacteria has been recognized as one of the sources of As release into groundwater (Martin et al. 2015; Guo et al. 2019). Both oxidized and reduced forms of As are discharged into groundwater (Alarcon-Herrera et al. 2013; Huyen et al. 2019). Under reducing circumstances, the redox chemistry of metal oxides alters, releasing As into the water body (Smedley et al. 2002). The mobilization of As in groundwater is caused by the redox cycling of Fe(III)-SO_4 caused by periodic irrigation (Xie et al. 2015). Additionally, it adsorbs into metal hydroxides and is the principal cause of As contamination in the groundwater system (Smedley and Kinniburgh 2002).

As-enriched regions show a regular pattern of distribution. As is also enriched in the aquifers of foreland basins created around mountain belts as a result of the convergence of tectonic margins (Mukherjee et al. 2019; Coomar et al. 2019; Zhang et al. 2022). As in groundwater is closely connected to volcanic materials derived from orogenic subduction zones (Mukherjee et al. 2014; Raychowdhury et al. 2014). Many of these sedimentary basins are regarded tectonically as foreland basins that formed as a result of lithospheric flexure during mountain formation (Ingersoll 1988; Garcia-Castellanos 2002). Magma gases are discharged as hydrothermally loaded gases from hot springs, which are also carried into foreland basins by streams, glacial erosion, or wind (Tapia et al. 2022). Under favorable circumstances, the solid As in the aquifer matrix dissolves into the groundwater (Chakraborty et al. 2015). According to reports, evaporation-induced enrichment causes dry and semiarid regions to have high As concentrations in groundwater (Nicolli et al. 2010). Sedimentary aquifers in arid and semi-arid areas have high concentrations of As due to irrigation by high As-enriched water (Xie et al. 2012). Additionally, As-enriched groundwater is a distinguishing feature of alluvial zones (Ahmed et al. 2004; Huq et al. 2018).

2.2.3. The invention and subsequent development of XRD techniques

High-energy electromagnetic waves with a wavelength between 10^{-3} and 10^{1} nm are X-rays (Norgard and Best 2017). When X-ray photons contact with materials, a variety of interactions may occur, resulting in various absorption and scattering effects (Ren and Zuo 2018). As a result, X-ray photons striking all atoms inside an irradiated region scatter in every direction (Noyan and Cohen 2013). Due to the periodic nature of a crystalline structure, constructive or destructive scattered radiation will arise, resulting in specific diffraction patterns that may be examined to determine the crystal structure of a material (Epp 2016).

Since the beginning of the 20^{th} century, X-ray diffraction has been used in a variety of scientific disciplines, including geology, environmental science, material science, engineering, and biology, to evaluate various mineral types (Davey 1925; Sponsler 1925; Wyckoff et al. 1926; Bowen et al. 1926; Murdock 1930; Warren 1940; Mooney 1950; Koehler et al. 1960; Calvert et al. 1989; Bunaciu et al. 2015; Hillier 2000; Ward 2016; Uvarova et al. 2020). Laue, Friedrich, and Knipping started the use of XRD for the characterization of crystals in 1912, which gave rise to new study avenues in the field of material science (Epp 2016). Powder X-ray Diffraction (XRD) analysis is a useful instrument for mineral prospecting in geological materials (Chauhan and Chauhan 2014). Using XRD data, the Raman Laser Spectrometer's findings on the composition of ultramafic rocks on Mars were verified (Rull et al. 2017; Lalla et al. 2020; Veneranda et al. 2020). It is used for identifying novel crystalline substances (Bunaciu et al. 2015). Singh et al. (2016) used XRD to determine the mineral compositions of clay. According to Lodh et al. (2022), XRD-based measurements have their benefits for measuring the residual strain matrix components in crystalline materials.

Powdered XRD techniques are commonly used to measure the extent of F and As in rock samples (Creelman and Ward 1996; Farooqi et al. 2009; Raju et al. 2017). According to XRD data, biotite is the principal geologic source of F in the groundwater of Gaya District, Bihar State, India (Ranjan and Yasmin 2019). F removal in groundwater was evaluated using the XRD technique, which revealed the sanorthite, melilite, and labradorite (Sandoval et al. 2019). Using the XRD technique, the F content of granitic soil was determined, and the author identified

fluorite, biotite, quartz, albite, and microcline as the principal F donors to groundwater (Abdelgawad et al. 2009).

2.2.4. The invention and subsequent development of XRF techniques

Hevesy pioneered the use of X-ray fluorescence (XRF) for chemical analysis in 1927 (Thomsen 2006; Plebow 2016; Ebel 1986; Kaulich 2009). Henke (1962) analyzed the low atomic number of elements from phosphorus to sodium using this approach. Henke postulated in 1963 the significance of soft X-ray excitation sources including multilayer crystals, collimators, and detectors for the detection of fluorine, nitrogen, boron, carbon, and sodium using mass absorption coefficients for low energy XRF (0.4–4.4 nm). Thatcher and Campbell (1965) emphasized the significance of the X-ray tube, which facilitates the detection of long-wave X-ray spectra from light elements, such as fluorine. Luke (1968) used an indirect technique to determine lanthanum in lanthanum F precipitates, therefore overcoming the limitations of traditional XRF (Plebow 2013). Norrish (1969) proposed the XRF settings for the investigation of Mg, Al, Si, P, K, Ca, Ti, Mn, and Fe. Sato et al. (1979) employed a high vacuum (~10^{-6} torr) XRF approach to determine the amount of fluorine in slag, with the slag transformed into glass beads, and the X-ray F Kα(1.83 nm) was used.

Leoni et al. (1982) quantified F, Cl, and S in 32 rock samples using XRF techniques with a F detection limit of 500 ppm. Later, synthetic multilayers were used to enhance the reflectivity of XRF in soft X-rays (Huang et al. 1989; De Boer and Chauvineau 1994). XRF was used by Figi (1995) to conduct a semiquantitative investigation of F, Pb, Cd, Cl, and Br in plastic. Powdered rock samples have been utilized for more exact elemental analysis using the XRF method since 2000 (Pouzar et al. 2001; Klockenkamp and Von Bohlen 2001). Later in 2000, portable XRF analyzers for various elements were introduced (Kalnicky and Singhvi 2001; Melquiades and Appoloni 2004; Karydas 2007; Palmer et al. 2009; Radu and Diamond 2009; Higueras et al. 2012). Jung et al. (2010) enhanced wavelength dispersive X-ray analysis by using synthetic matrix calibration standards for metal and non-metal analysis.

For the exact evaluation of diverse metals and non-metals, the XRF method and sample preparations were significantly modified in 2015. Total reflection XRF

(TXRF) and X-ray fluorescence (XRF) modified with the laser-induced breakdown spectroscopic technique were used for the elemental analysis of a variety of samples (Margu et al. 2013; Pashkova and Revenko 2015; Sitko et al. 2015; Aguirre et al. 2015; Lin et al. 2017; Ullah et al. 2018). Even though these spectral approaches offer a high degree of sensitivity and selectivity, they have limitations. Pytlakowska et al. (2016) used graphite oxide with glycine to preconcentrate chromium, zinc, and copper ions from water samples before their measurement by energy-dispersive X-ray fluorescence spectroscopy (EDXRF). Ryan et al. (2017) developed a handheld, portable XRF for the quantitative analysis of chemical components for surveying applications.

ED XRF was used extensively for the study of As, F, and heavy metals (Chen et al. 2018; Kanwar et al. 2020; Joseph 2021; Saini and Ratan 2022). The fluorine content of the rock sample (phosphate deposits) in Turkey was determined using ED-XRF (Akyuz et al. 2008). This approach was used to calculate the F solubility analysis of ZrF and HfF. (Tarnopolskaia et al. 2021). Using ED-XRF, the fluorine content of a sample of dental enamel was measured (Soares et al. 2015; Eskelsen et al. 2018; Otel et al. 2022). The covering material used in ED-XRF also affects the detection of F in the soil samples (Kuzmina et al. 2022). Using the XRF technique, Fuoco et al. (2022) estimated the rock chemistry of the deep crystalline aquifer and quantified the F- and As-containing minerals, including plagioclase, oligoclase-andesine, biotite, annite-phlogopite-fluorannite-fluorplogopite, muscovite, and fluormuscovit. Chea et al. (2006) assessed the F concentration of the whole rock and biotite using the XRF technique.

EDXRF can analyze As in solids isolated from geological, synthetic, and aqueous substances (Sandoval et al. 2019). Arsenic may be assessed with an interference-free detection limit of up to 40 mg/kg in water samples and 60 mg/kg in soil samples (Melamed 2005). The primary interferences that are recorded are moisture content and particle size (Markowicz et al. 2008; Parsons et al. 2013; Quiniou and Laperche 2014). Alternative procedures require an extraction step that removes a large proportion of the element from the sample before measurement (Ene et al. 2010; Beiyuan et al. 2017).

The ED-XRF method is employed to determine the mineral composition of a variety of samples, including pottery, cement, archaeological, forensic, and geological materials (Wilberforce 2016; Radtke et al. 2017). Having used this approach, Slavk et al. (2012) analyzed soil samples from industrial locations for toxic heavy metals. Using the XRF technique, the heavy metal contamination in polluted zones of a granitic terrain in southern India has been examined (Purushotham et al. 2012). Utilizing the ED-XRF technique, the soil from the vineyard was analyzed for heavy metals (Bhat et al. 2022). Byers et al. (2019) determined the heavy metal concentration of algae by portable ED-XRF. XRF was utilized to identify heavy metal contamination in soil samples from South India's granitic terrain (Purushotham et al. 2012).

The XRD and XRF techniques are frequently used to determine the mineral components of rock particles. X-ray fluorescence (XRF) spectrometer is a potent device for qualitative and quantitative investigation of most elements in diverse solid phase samples (e.g., soil, sediments, and rock) (Bergqvist et al. 2019; Gregory et al. 2019; Yarmohammadi and Wood 2022). The Rietveld (1988) XRD method enables reliable mineralogical analysis of fine-grained rocks. The organic substance functions as an amorphous phase, whereas the minerals produce definite peaks (Gotze et al. 2020; Raudsepp et al. 2022). Thus numerous studies have been undertaken using XRD and XRF techniques to reveal the mineralogical characteristics of rock materials on groundwater quality. The present study in Palakkad and Malappuram Districts has been undertaken from this perspective.

2.3. Materials and methods

2.3.1 Sample location

High Fluoride and Arsenic contaminated sites in the study area were selected for the core sampling (Fig. 2.3.1) and subsequent elucidation of the mineral characteristics. The seasonal mean values of F and As, which is above the maximum permissible limit in the study area are depicted in Chapter 1. The severity of F contamination was more in Chittur and Kollengode Blocks and hence 2 samples each from these Blocks were collected. One sample each from the highly As contaminated sites such as Palakkad and Malampuzha Blocks were also collected. Altogether six core samples were collected from the contaminated areas. The samples were collected

during the drilling of bore wells in these regions. The rock samples from 40 to 100 meters in depth were selected for F-contaminated sites (CS1–CS4) since the high concentration of F is attributed to being present in the deep aquifers. The core samples of As contaminated sites from 5 to 50 meters (CS5 and CS6), as the prevalence of As is in shallow alluvial aquifers (Table 2.3.1).

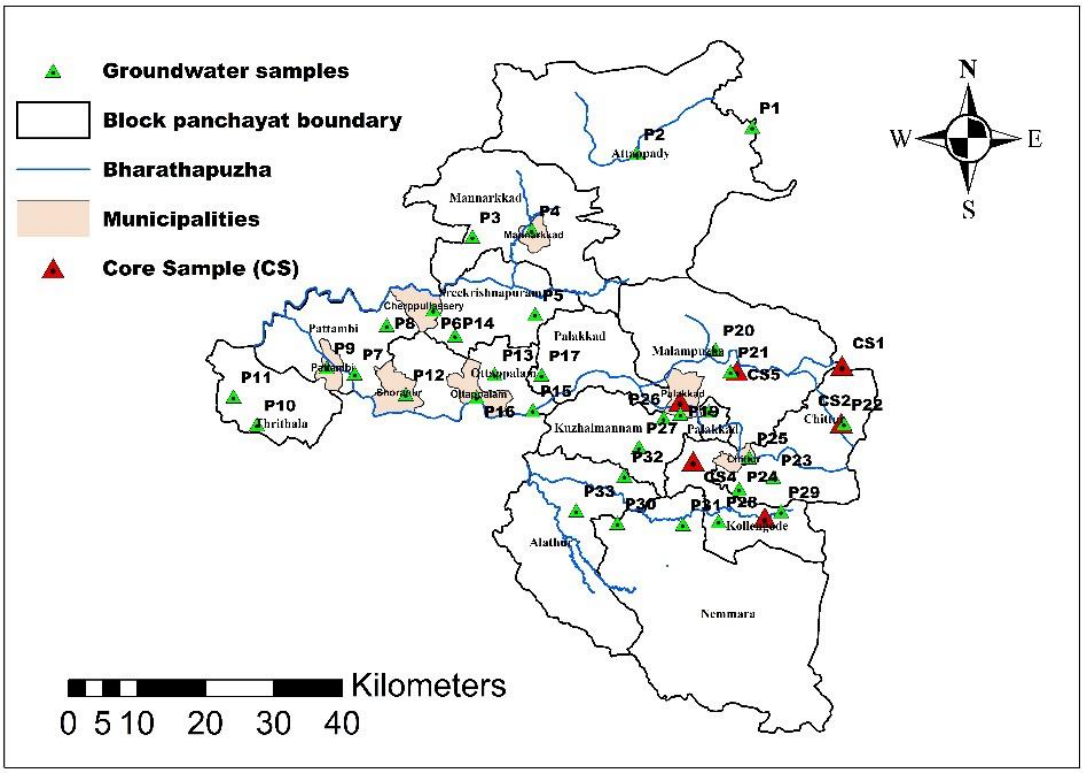

Fig. 2.3.1. The map showing the Core Samples (CS) from Fluoride and Arsenic contaminated sites.

2.3.2. Preparation of the samples

Approximately 5 kg samples, ranging in size from silt to gravel, were collected from respective sites in transparent polythene bags and were labeled properly. The samples were then carefully transported to the laboratory. The samples were then dried in the shade for one week. Following the procedure of coning and quartering, approximately 100 g of the samples were placed in a porcelain dish, oven-dried at 60°C (48 hours) to remove all moisture, and cooled in a desiccator. For XRD and XRF analysis, the dried samples were crushed in an agate mortar and pestle and sieved through a 0.03-mm screen to yield the powdered samples. The materials were then stored in a labeled PET bottle and immediately subjected to analysis.

Table 2.3.1. The details of core sampling sites and the depth of the bore hole drilled

Sample code	Sample site	Block Panchayat	Coordinates	Total depth drilled hole (Meter)
CS1	Velanthavalam	Chittur	10°48' 50.4"N 76°51'43.2"E	134.11
CS2	Eruthenpathy	Chittur	10°44'20.4"N 76°51'39.6"E	100.58
CS3	Muthalamada	Kollengode	10°36'57.6"N 76°45'36"E	82.30
CS4	Koduvayur	Kollengode	10°41'20.4"N 76°39'57.6"E	158.50
CS5	Puthussery	Malampuzha	10°47'20.4"N 76°42'39.6"E	76.2
CS6	Palakkad (Yakkara)	Palakkad Municipality	10°45'39.6"N 76°38'56.4"E	60.96

2.3.3. XRD analysis

A powder X-ray diffractometer from Malvern-Panalytical made with "X'pert3 Powder" was used for the analysis. To generate a smooth and level surface, the sample was placed within the sample holder. The material was then placed within the XRD apparatus to generate a diffractogram for each sample. The diffractogram revealed the peak location and structural intensity of the mineral. All the samples were examined from 5 to 80° 2θ at a 10°/min 2θ scanning speed and a 0.03° 2θ step size. The energy of the X-ray photon was related to the radiation frequency by E=hv, where: h=Planck's constant (6.626 × 10-34J/s or 4.135 × 10-15eV/s) and v=frequency. The wavelength λ was related to the photon energy (λ=1.240 × 10-6/E). PANalytical software provides solutions for dependable chemical and structural analysis of a wide range of materials. This diffractometer is equipped with a versatile prefix module that facilitates optical path modifications. Consequently, a single diffractometer may be used for a variety of applications. OriginPro 8 software was utilized to depict the peak. Also, the peak intensity was compared with JCPDS (The Joint Committee on Powder Diffraction) data file.

2.3.4. XRF analysis

The physical approach of X-ray fluorescence spectrometry allows for quick elemental analysis. It allows the chemical composition of major and trace elements to be determined. It measures the weight proportion (W %) of the constituents. Here, samples were analyzed with a Spectro-Ametek SPECTRO XEPOS-XRF device. This equipment employs the Energy Dispersion X Fluorescence Spectrometer (ED-XRF) method. The operational concept consists of blasting a sample with a sufficient flow of X photons, after which the sample emits numerous X-rays of varying intensities. A semiconductor detector collects the fluorescence radiation in an energy-dispersive XRF sensor. The X-rays generate signals in the detector that are proportional to the incoming radiation's energy. A multichannel analyzer is used to capture the signals. This technique handles each X-ray individually, yet at a rapid rate. This sophisticated XRF detector can process one million counts per second. That makes it a quasi-simultaneous measurement. The spectrum can provide enough data to calculate intensities, which can be used to estimate the sample's composition.

2.4. Result and Discussion

The mineralogical examination assists in determining the chemical composition of the minerals in the bedrock. It provides an accurate depiction of the geochemical condition of every aquifer system. The mineralogical information provides a strong basis for evaluating the chemistry of groundwater, especially concerning toxic minerals. In the present study, six core samples were extracted from locations contaminated with F and As to assess the mineralogical components of the impacted aquifer system. The inputs regarding F and As contamination in the groundwater sources, as outlined in Chapter I have been used for the selection of sites. The powdered rock/soil samples were used for the mineralogical estimation of F and As. This present study utilized XRD and XRF techniques for assessing the chemical composition of the core samples.

Powder XRD is a compact, sophisticated device that is very helpful for mineral characterization (Pabis-Mazgaj et al. 2021). When X-rays strike a piece of rock, they diffract in a pattern indicative of the mineral structure. In powder X-ray diffraction,

the diffraction pattern is formed from a mineral powder rather than a single crystal. It is a simpler and more practical way of analyzing minerals (Rubio 2021). The location of the diffractogram's peak is determined by the wavelength. It was used more often in the reflection configuration (Gonzalez et al. 2020). When Bragg's criteria are met, interactions between the sample and the incoming X-ray beam generate powerful reflected X-rays through constructive interference. This is the connection between incident X-rays, the beam's angle, and the distance between atomic lattice planes (Chala and Emire 2021). Due to its inherent crystal structure, each mineral has a unique X-ray diffraction pattern, enabling the identification of minerals in core samples (Ali et al. 2022).

Fig. 2.4.1 (CS1 and CS2) and Fig. 2.4.2 (CS3 and CS4) show the X-ray diffraction (XRD) of samples from F-contaminated locations such as Chittur Block and Kollengode Block, respectively. Fig. 2.4.3 illustrates the XRD peak of As-contaminated locations, including Malampuzha (CS5) and Palakkad (CS6). The sample was crystalline, as shown by the sharp peaks in the results. Using Malvern Panalytical's XRD program, the F-related minerals and As peaks were recognized. The XRD diffractogram highlighted F-related minerals such as fluorite, biotite, quartz, and plagioclase (albite), as well as As peaks.

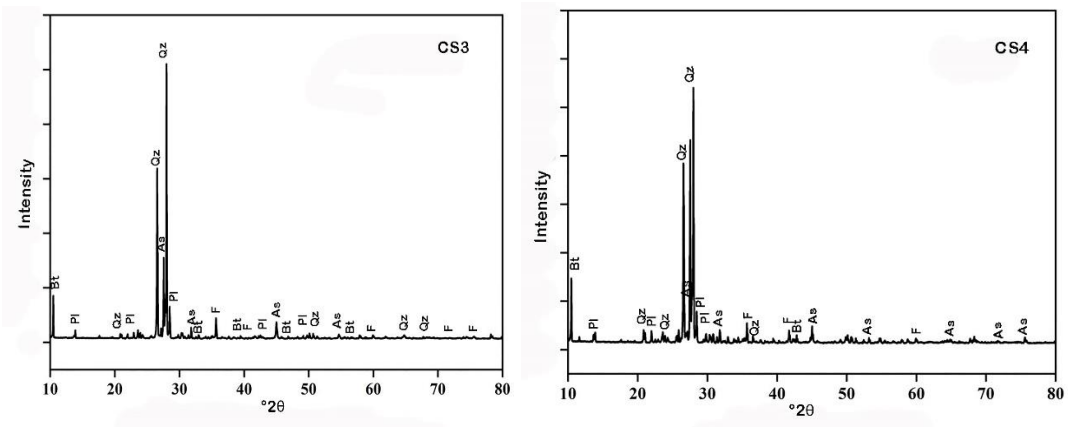

Qz - Quartz, Bt – Biotite, Pl – Plagioclase (Albite), F – Fluorite, As – Arsenic

Fig. 2.4.1. XRD diffractograms of samples from fluoride-contaminated areas (Chittur block)

The XRD spectrum reveals that quartz (SiO_2) contributes to the majority of the rock's mineral content. The core samples also included a greater quantity of plagioclase-derived albite. The mica family mineral biotite is also well characterized on the XRD graph. However, the F mineral fluorite (CaF) is found at lower intensities. The XRD patterns of all samples indicate the presence of As (Fig. 2.4.1 to 3).

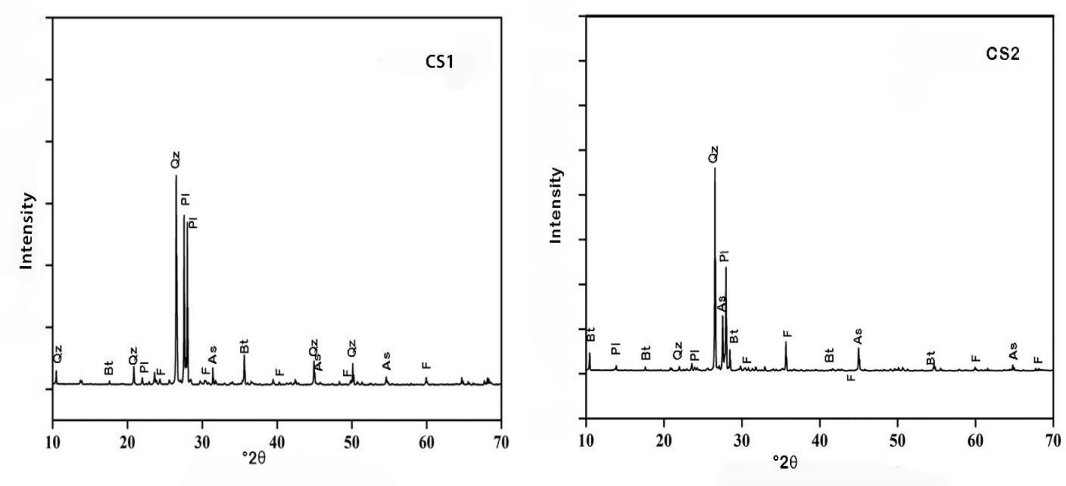

Qz - Quartz, Bt – Biotite, Pl – Plagioclase (Albite), F – Fluorite, As - Arsenic

Fig. 2.4.2. XRD diffractograms of samples from fluoride contaminated areas (Kollengode block)

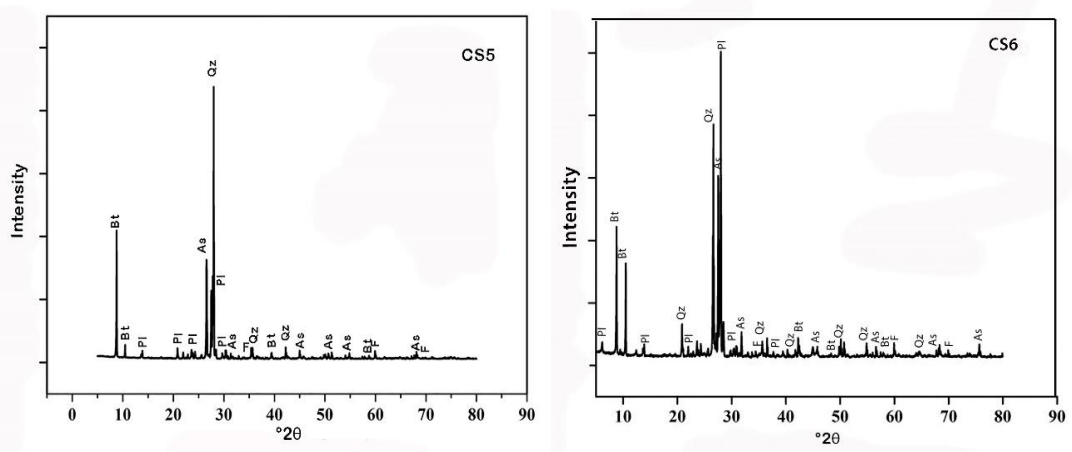

Qz - Quartz, Bt – Biotite, Pl – Plagioclase (Albite), F – Fluorite, As - Arsenic

Fig. 2.4.3. XRD diffractograms of samples from arsenic-contaminated areas (Palakkad and Puthussery Blocks)

The major mineral constituents of the core samples as estimated by the XRF technique are listed in Table 2.4.1 and Fig. 2.4.4. Among the most abundant metal oxides in core samples from the study area, SiO_2 varied from 25.23 to 33.75 w.%, followed by Al_2O_3 and Fe_2O_3 with ranges of 6.9 to 8.9 (w.%) and 2.98 to 4.62 (w.%), respectively. Mg oxides range from 1.93 to 4.34 (w.%) and Ca oxides from 1.17 to 2.34 (w.%), respectively. K_2O, P_2O_5, SO_3, and Mn vary between 1.869 and 3.336 (w.%), 0.4214 and 0.7161 (w.%), 0.09313 and 0.2766 (w.%), and 0.03981 and 0.06596 (w.%), respectively. The mineral composition of the samples includes:

CS1 is in the order $SiO_2 > Al_2O_3 > Fe_2O_3 > MgO > K_2O > CaO > P_2O_5 > Ti > SO_3$;

CS2, it is in the order $SiO_2 > Al_2O_3 > MgO > Fe_2O_3 > K_2O > CaO > P_2O_5 > Ti > SO_3$;

CS3, it is in the order $SiO_2 > Al_2O_3 > MgO > Fe_2O_3 > K_2O > CaO > P_2O_5 > Ti > SO_3$;

CS4 it is in the order $SiO_2 > Al_2O_3 > Fe_2O_3 > K_2O > MgO \cong CaO > P_2O_5 > Ti > SO_3$;

CS5, it is in the order $SiO_2 > Al_2O_3 > Fe_2O_3 > K_2O > MgO \cong CaO > P_2O_5 > Ti > SO_3$;

CS6 it is in the order $SiO_2 > Al_2O_3 > Fe_2O_3 > MgO > K_2O > CaO > P_2O_5 > Ti > SO_3$.

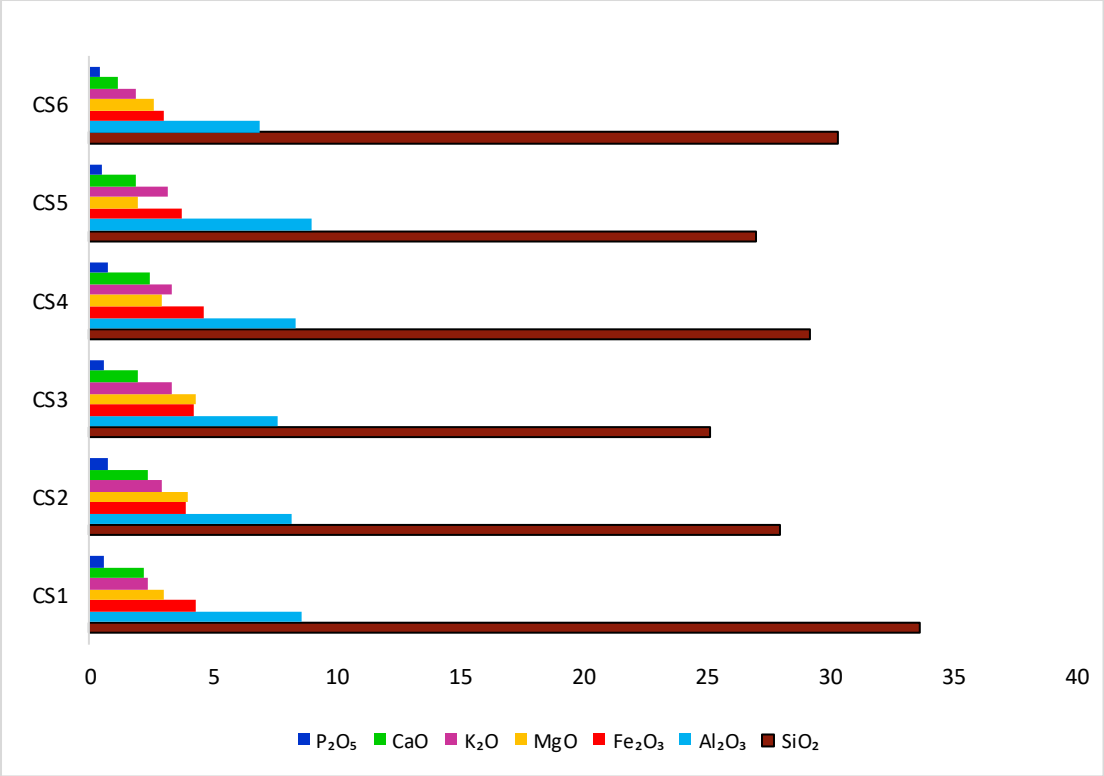

Fig. 2.4.4. The abundance order of minerals in the core samples

Table 2.4.1. Summary of the abundance of major elements in rock samples from fluoride and As contaminated sites of the study area.

Elements (wt. %)	**Samples**					
	CS1	**CS2**	**CS3**	**CS4**	**CS5**	**CS6**
SiO_2	33.72	28	25.23	29.21	27.02	30.41
$Al_2\ O_3$	8.577	8.225	7.66	8.326	8.971	6.941
$Fe_2\ O_3$	4.323	3.887	4.225	4.624	3.711	2.985
MgO	3.046	3.978	4.339	2.968	1.934	2.594
$K_2\ O$	2.396	2.953	3.336	3.323	3.191	1.869
CaO	2.185	2.361	1.934	2.443	1.907	1.17
$P_2\ O_5$	0.5529	0.7145	0.5392	0.7161	0.5208	0.4214
Ti	0.2885	0.3779	0.3544	0.3801	0.2788	0.2723
SO_3	0.09313	0.2673	0.2079	0.2766	0.1212	0.1094
Ba	0.08011	0.05566	0.07733	0.2728	0.09005	0.08047

Mn	0.06596	0.05797	0.06325	0.05241	0.0506	0.03981
Sr	0.02756	0.07851	0.06862	0.08198	0.04924	0.02639
Groundwater F (Max.) in mg/L	2.2	2.2	1.9	1.4	1.3	1.5
Groundwater As (Max.) in mg/L	0.05	0.05	0.05	0.10	0.10	0.10

A total of 14 significant trace elements were in the core samples. F, As, Pb, Cd, Mn, Cu, and Zn in the groundwater of the study area, as described in Chapter 1, are analyzed in the core sample using XRF analysis (Table 2.4.1). Other significant trace elements, including Cr, Hg, Cl, Zr, V, Rb, and Mo, are also evaluated. The F concentration ranges from 67 to 290 mg/kg in the core sample. As concentrations in the samples varied from 0.085 mg/kg to 0.886 mg/kg. Pb, Cd, and Ni concentrations ranged from 7.475 to 22.23 mg/kg, 0.085 to 0.644 mg/kg, and 67.54 to 257.3 mg/kg, respectively.

Table 2.4.2. Summary of the trace elements in rock samples from fluoride and As-contaminated sites of the study area.

Elements (mg/kg)	Samples					
	CS1	CS2	CS3	CS4	CS5	CS6
F	290	250	174	96	85	67
As	0.085	0.085	0.085	0.8858	0.775	0.085
Pb	15.53	21.59	22.23	14.52	17.95	7.475
Cd	0.085	0.085	0.085	0.085	0.085	0.644
Ni	112.3	104.9	257.3	166.2	67.54	127.2
Cu	39.8	26.68	36.45	40.06	23.28	25.05
Zn	62.26	64.9	65.67	66.92	56.26	30.21
Cr	306	286.4	461.9	424.1	194.3	405.2
Hg	0.085	0.085	0.085	0.085	0.085	0.085
Cl	244.7	313.7	296.6	258.4	144.5	105.1
Zr	94.07	134.2	177.1	506.3	137.6	110.1
V	75.27	73.16	77.74	74.14	71.68	60.91
Rb	80.4	54.32	47.79	36.27	52.11	21.29
Mo	1.321	0.6584	2.67	2.61	1.123	0.085
Groundwater F (Max.) in mg/L	2.2	2.2	1.9	1.4	1.3	1.5
Groundwater As (Max.) in mg/L	0.05	0.05	0.05	0.10	0.10	0.10

Table 2.4.2. lists a total of 14 significant trace elements in the core samples. F, As, Pb, Cd, Mn, Cu, and Zn in the groundwater of the study area, as described in Chapter 1, are attempted in the core samples using XRF analysis. Other significant trace elements, including Cr, Hg, Cl, Zr, V, Rb, and Mo, are also evaluated. The F concentration ranged from 67 to 290 mg/kg in the core sample. Arsenic concentrations in the sample varied from 0.085 mg/kg to 0.886 mg/kg. Pb, Cd, and

Ni concentrations ranged from 7.475 to 22.23 mg/kg, 0.085 to 0.644 mg/kg, and 67.54 to 257.3 mg/kg, respectively.

Geologically, the study area is defined by the Peninsular Gneissic Complex (PGC), and granite and granite gneiss are the predominant rock types. Gabbro, dolerite, hornblende, apatite, pegmatite, quartz and epidote veins, and alluvium are younger intrusive minerals. These regions are characterized by migmatite complexes comprised of hornblende biotite gneiss, garnet biotite gneiss, and quartzofelpathic gneiss. Small quantities of quartz veins and pegmatite, limestone, and Kankar (nodular calcium carbonate) are also present in the vicinity. In addition, fluvial sediments are seen along the Bharathapuzha and the coastline of its tributaries.. The migmatite rocks are medium to coarse-grained and well-exposed, while biotite gneisses are typically banded and occur as slabs and inselbergs in low-topographic regions (Sudheer Kumar et al. 2017).

2.4.1. The minerals that contribute fluoride to the groundwater sources

The spatial analysis of groundwater samples reveals that F contamination is prevalent in the eastern part of the District with biotite and quartzofelpathic gneiss-dominated sites with semi-arid climatic conditions. The XRD and XRF studies quantitatively affirmed the presence of F in the core samples (Fig. 2.4.1 to 3 and Table 2.4.2). F is detected in large amounts in CS1, CS2, and CS3. The samples CS1 and CS2 showed F concentrations of 290 and 250 mg/kg F, respectively, representing the groundwater sample from Eruthenpathy panchayat (P22), which had a maximum F value of 2.2 mg/L. With an F concentration of 174 mg/kg, core sample CS3 represented groundwater samples with F concentrations greater than 1.8 mg/L (P28 and P29).

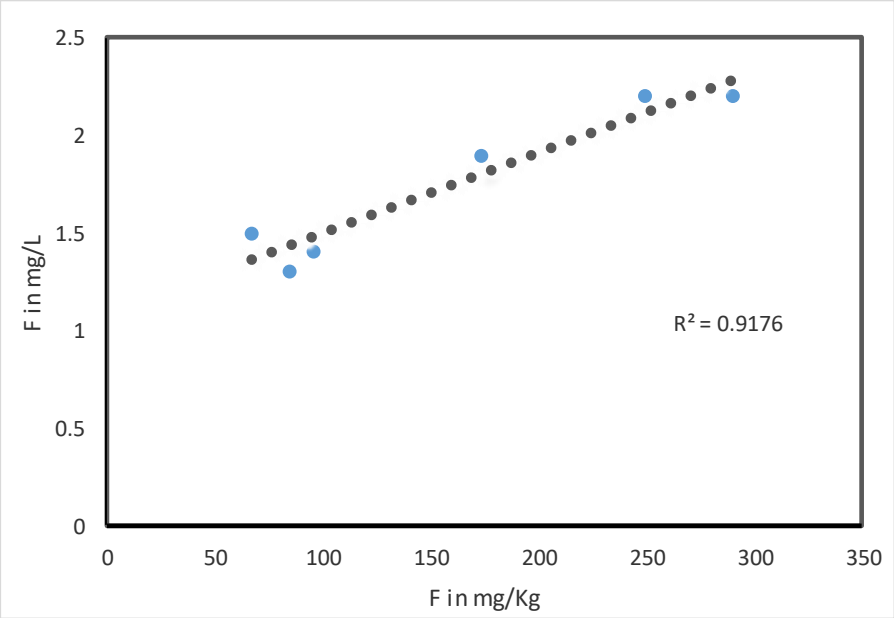

Fig. 2.4.5. The correlation of water (mg/L) and soil (kg/mg) F

F is the most common form of fluorine that occurs in the environment. As stated, silicon dioxide (quarts) is the predominant component in the core sample tested using the XRF. The country rock, hornblende-biotite gneiss, is banded with quartz. It is crystalline and the second-most prevalent mineral in the Earth's continental crust (28%) (Johnson et al. 2021). Quartz contains F as it is a quick F absorber, and it releases F into water under optimal conditions (Webster et al. 1997; Gobindlal et al. 2022). Several research findings suggest that the weathering of silicate minerals may increase the groundwater F content (Su et al. 2019; Elumalai et al. 2019; Younas et al. 2019; Thapa et al. 2019; Chicas et al. 2022). Quarts are a prominent F-contributing silicate mineral from gneiss rock terrains in arid and semi-arid regions (Karunanidhi et al. 2020; Dubey et al. 2021).

$Al_2 O_3$ is the second-largest mineral component associated with the core samples, whereas $Fe_2 O_3$, MgO, and $K_2 O$ alternate for the third-place position. The rock particles are mostly composed of aluminum, and it occurs naturally as the mineral corundum in its crystalline polymorphic phase (McCormick 2018). Corundum is a crystalline form of aluminium oxide, normally containing trace amounts of iron,

titanium, vanadium, and chromium (Litasov et al. 2019; Lytvynov 2019; Baalousha et al. 2021). The aluminosilicates, are the most frequent primary and secondary minerals, which comprise plagioclase feldspars (albite), micas (hornblende-biotite), and clay minerals (kaolin) (Chong 2019; El-Desoky et al. 2022; Vinnarasi et al. 2022). Hornblende and plagioclase are the essential minerals of hornblende and amphibolite schist, while quartz, sphene, sericite, and magnetite are accessory minerals (Rout et al. 2022)

Hematite ($Fe_2\ O_3$) is the form of iron found in the core sample from the study area. Through reductive hydrolysis, iron serves as a secondary source of F (Kern et al. 2008). Since F has a reduced solubility in the pH range of 6.0 to 6.5, F becomes complexed with iron (FeF), aluminium (AlF), and silicon (SiF) at lower pH, and it is then released into groundwater under favorable conditions (Viero et al. 2009; Zhang et al. 2017). The alkaline environment prevents the formation of a complex of F with oxyhydroxide minerals and clay (Mukherjee and Singh 2018). However, ferric (Fe^{3+}) and aluminium (Al^{3+}) ions are rarely complexed with F in groundwater due to their poor solubility and their tendency to precipitate as goethite (FeO(OH)) and gibbsite ($Al(OH)_3$) in the presence of ferrihydrite (complexed iron) (Hua et al. 2015; Cui et al. 2019; Young et al. 2019; Dey et al. 2022). Iron and aluminium ions may play a significant role in very acidic (pH 4) and oxidized environments (Montazeri et al. 2021; Song et al. 2022).

In F-contaminated regions (CS1, CS2, and CS3), the concentration of Ca is lower than the Mg concentration in both water samples (explained in Chapter I) and core samples (Table 2.4.1). In F-contaminated areas, the ionic strength of the groundwater was extremely high, and core samples suggested that the presence of salinity and hardness contributed to minerals, particularly Mg and Ca (Kimambo et al. 2019; Udeshani et al. 2020). Hence, cation exchange and alkalinity are crucial determinants of F enrichment in groundwater (Luo et al. 2021). Both Ca and Mg combine with the F; however, Ca exhibits a high affinity for F (Paudyal et al. 2018). Ca interacts with F to form the unstable ionic species CaF in groundwater (Viero et

al. 2009; Cui and Qin 2022). It also forms carbonate and sulphate salts as well (Liu et al. 2015b; Amarasooriya et al. 2020).

Increased MgO concentrations also reflect the high groundwater F concentration (Adimalla 2019). Magnesium is frequently an important component in the F complexation of groundwater (Zhang et al. 2019). Nevertheless, Mg will be released to groundwater due to cation exchange between Na^+ adsorbed on clay minerals, making the aquifers alkaline. The enrichment of F in groundwater is particularly favored by the alkaline conditions (Wu et al. 2015b; Zabala et al. 2016).

Fluorite and biotite dissolution rate and precipitation are the primary processes that determine the F concentration in groundwater. The SiO_2 concentrations are higher than that of $Fe_2\ O_3$ and MgO concentrations in the core samples and are indicative of the granitic (felsic) origin of the minerals (**Table 2.4.1**) (Patel et al. 2022). Moreover, the negative relationship between SiO_2 and MgO illustrates the effect of silica dilution (Kumar and Saxena 2011). A significant link between $Al_2\ O_3$ and $K_2\ O$ and CaO suggests the existence of illite, which is generated by the weathering of mica and feldspar and regulates the concentration of these minerals (Ghosh et al. 2019; Umbugadu and Igwe 2019). The positive correlation with $Fe_2\ O_3$ and $Al_2\ O$ in the samples implies biotite weathering (Tossou et al. 2021). The presence of TiO_2 , Ni, and Cr verifies the existence of vermiculate resulting from biotite's hydrothermal alteration (Nadeau and Harris 2019).

In the crystalline structures of biotites and amphiboles, fluorine substitutes hydroxyl groups (K_2 (Mg, Fe_4 (Fe, Al)$_2$ [Si_6 Al $O_{2\ 0}$] $(OH)_2$ (F, Cl)$_2$) (Beard et al. 2020). When the bedrock is rich in biotite, weathering transforms it into the principal source of F in groundwater (Berger et al. 2016; Karunanidhi et al. 2021; Vinnarasi et al. 2021; Zango et al. 2021). CaF_2 is also discovered in hydrothermal deposits in igneous settings (Han et al. 2020). The highest solubility of fluorite was recorded at temperatures between 110 and 120 degree celsius (Viero et al. 2009). The breakdown of carbonates, silicates, and sulphates, which liberates calcium, also reduces the concentration of F in groundwater (Devaraj et al. 2020). F dissolution is

increased by the formation of calcium complexes mostly with HCO (Makubalo and Diamond 2020)

2.4.2. *The minerals that contribute arsenic into the groundwater sources*

The spatial analysis of As in groundwater samples reveals that its contamination is linked to alluvial deposits (as detailed in Chapter 1). The XRD and XRF studies of the core samples from the As-contaminated areas conclusively demonstrate the presence and quantity of As in such areas (Figs. 2.4.1 to 3 and Table 2.4.2). As is also found in large amounts in CS5 (0.77 mg/kg) from the alluvial plain of River Korayar, which is downstream to the Walayar reservoir. Similarly, the CS4 sample also had a high As concentration, up to 0.8858 mg/L. This sample site is characterized by valleys and rice fields, irrigation canals, and small streams. It is the down valley area of the Meenkara and Chulliyar reservoirs. Groundwater sample P27 is located in the down-valley position of CS4 and also contains a high concentration of As (0.10 mg/L). The conditions confirm that the As concentration in the groundwater is more related to geogenic sources. A moderate positive correlation between the As content of groundwater with that of the As content of the core samples is indicative of the evidence of a geogenic source (Fig. 2.4.6). The other F-contaminated sites, especially from the village area, showed a minimum value of 0.085 mg of As/kg of soil.

Several minerals include As; the most frequent are metal oxides and hydroxides (Mn, Al, and Fe), elemental As, sulphides, arsenides, and arsenites (Van Herreweghe et al. 2003). As is present both in igneous and sedimentary rocks (Tabelin et al. 2018). Common As bearing minerals found in ore zones include sulphides such as arsenopyrite (FeAsS), cobaltite (Co (AsS), orpiment ($As_2 S_3$), prostite ($Ag_3 As_3 S$), and enagite ($CuAsS_4$); other As carrying minerals include arsonolite (AsO_3), claudidite (AsO_3), and lollingite ($FeAs_2$) (Bari et al. 2020; Wang et al. 2020c; Russell 2021). Arsenian pyrite [$(Fe(S, As)_2$] is the primary mineral source of As, and the most prevalent geogenic cause of As pollution (Voute et al. 2019; Xing et al. 2019).

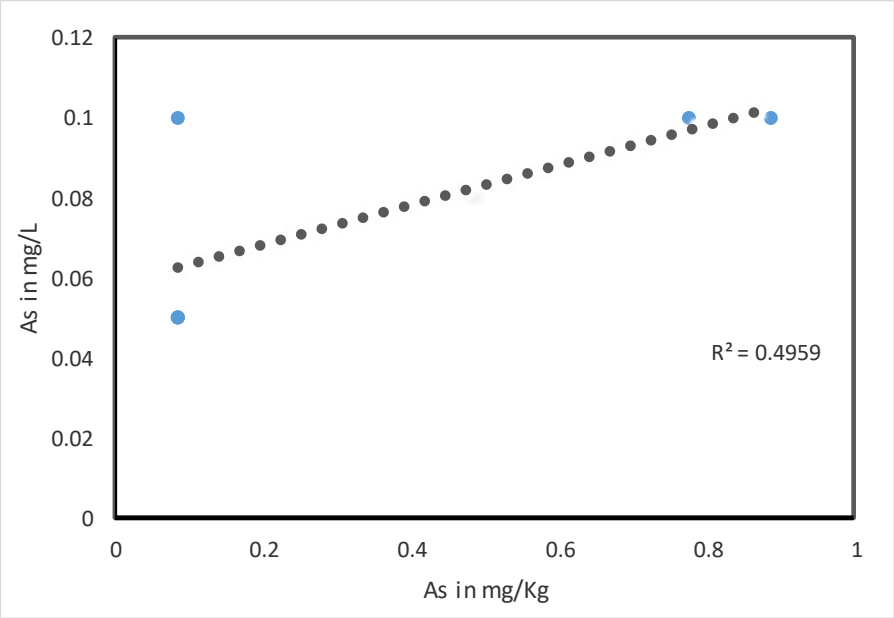

Fig. 2.4.6. The correlation of water (mg/L) and soil (kg/mg) As

Common sources of higher concentrations of As in groundwater include the internal thermal system of the earth, deposits from volcanic eruptions, and alluvial deposits in basins (Das et al. 2018; Yang et al. 2018). When sulphur combines with As-containing Fe compounds, in-situ pyrite is formed (Lu et al. 2021). Pyrite is more stable in reducing than oxidizing environments (Liu et al. 2019; Duverger et al. 2020). During summer paddy cultivation, the rapid withdrawal of groundwater causes the groundwater table to fall, which in turn results in the invasion of atmospheric oxygen and the oxidation of arsenopyrite (Kumarathilaka et al. 2018; Yin et al. 2022). In conclusion, the decomposition of pyrite results in the mobilization of As through the formation of sulphuric acid and iron sulphate (Sanyal 2017). Sedimentary organic matter under anaerobic conditions also releases As due to the decomposition by microbes (Gustave et al. 2018; Wang et al. 2021c).

The correlation statistics demonstrate a strong positive relationship between As and aluminium, iron, and calcium (Table 4). As adsorption onto Fe oxides/hydroxides is a significant contributor to the formation of important As sources (Wang et al. 2016; Zang et al. 2018). Fe (II)-catalyzed iron oxide recrystallization can either liberate As or incorporate it into the oxide structure. Aluminum, copper, iron, lead, magnesium,

manganese, and nickel are the common metallic elements frequently found in As minerals (Liu et al. 2015a; Shakerkhatibi et al. 2019; Fayet-Moore et al. 2020). As is also present in sediments such as aluminium, iron, and calcium arsenates (Osono and Katoh 2021). It is frequently discovered as the arsenides of nickel, cobalt, copper, and iron, which are the apparent constituents of sulphide ores (Kalugin et al. 2021). As well, there is a significant positive relationship between As and Ba. Several scientific reports also suggest that As and barium occur together in natural samples (Planer-Friedrich et al. 2001; Kato et al. 2013; Davis et al. 2014; Nuamah Daniel 2019). A strong positive correlation between As and K suggests the presence of clay constituents (Mueller and Hug 2018). Typically, As is found in clay and sulfur-rich portions (Jelenova et al. 2018; Karayigit et al. 2020). In aquifer sediments, As availability is greater, it is released into the environment more readily (Huq et al. 2020; Kumar et al. 2020).

Both oxidizing and reducing conditions result in the discharge of As into the groundwater (Kumar et al. 2020). In semiarid environments, oxidation processes are more prevalent (Alarcon-Herrera et al. 2013). Adsorption onto metal oxides, particularly Fe, Al, and Mn oxides, is most dominant under reducing conditions (Wang et al. 2020a; Kumar et al. 2020). Although As appears to be a concern in humid and tropical regions due to the enrichment of As through evaporation and formation of As-rich groundwater (He et al 2020; Shaji et al. 2021). In addition, under oxidizing conditions, As is released by the oxidation of As-containing sulphide minerals such as arsenopyrite (FeAsS) (Coudert et al. 2020; Hong et al. 2022). The principal mode of As release in reducing aquifers is reductive hydrolysis of metal (hydr) oxides (Liu et al. 2020; Kumar et al. 2022). As is released in slightly alkaline and highly reducing environments through the adsorptive release of iron oxides (Wang et al. 2019b). It is difficult to categorize aquifers as entirely oxidizing or exclusively reducing; they are typically a hybrid of the two conditions (Das et al. 2018). However, with increasing depth, there is also the prospect of a change from an oxidizing to a reducing state owing to a decreased oxygen flux (Abiye and Bhattacharya 2019; Hussain et al. 2019). Resultantly, oxidation-reduction potential is a crucial factor in regulating the As concentration in groundwater reserves.

Table 2.4.3. Correlation among the element components of the rock samples

	SiO	AlO	FeO	MgO	KO	CaO	PO	Ti	SO?	Ba	Mn	Sr	F	As	Pb	Cd	Ni	Cu	Zn	Cr	Cl	Zr	V	Rb
SiO	**1**																							
AlO	**0.045**	**1**																						
FeO	**0.005**	**0.536**	**1**																					
MgO	**-0.323**	**-0.29**	**0.368**	**1**																				
KO	**-0.692**	**0.527**	**0.669**	**0.287**	**1**																			
CaO	**-0.019**	**0.69**	**.866***	**0.34**	**0.669**	**1**																		
PO	**-0.109**	**0.442**	**0.684**	**0.39**	**0.598**	**.909***	**1**																	
Ti	**-0.41**	**0.052**	**0.615**	**0.701**	**0.652**	**0.706**	**.862***	**1**																
SO	**-0.468**	**0.033**	**0.495**	**0.57**	**0.645**	**0.636**	**.854***	**.975****	**1**															
Ba	**0.057**	**0.162**	**0.542**	**-0.194**	**0.381**	**0.405**	**0.486**	**0.423**	**0.48**	**1**														
Mn	**0.031**	**0.442**	**0.733**	**0.601**	**0.408**	**0.657**	**0.376**	**0.355**	**0.158**	**-0.167**	**1**													
Sr	**-0.623**	**0.203**	**0.549**	**0.515**	**.823***	**0.678**	**.826***	**.937****	**.962****	**0.444**	**0.23**	**1**												
F	**0.448**	**0.096**	**0.232**	**0.538**	**-0.248**	**0.333**	**0.198**	**0.107**	**-0.062**	**-0.498**	**0.712**	**-0.145**	**1**											
As	**-0.192**	**0.545**	**0.324**	**-0.569**	**0.543**	**0.326**	**0.32**	**0.119**	**0.239**	**0.752**	**-0.278**	**0.356**	**-0.719**	**1**										
Pb	**-0.591**	**0.457**	**0.507**	**0.613**	**0.757**	**0.62**	**0.493**	**0.56**	**0.471**	**-0.237**	**0.726**	**0.626**	**0.332**	**-0.063**	**1**									
Cd	**0.246**	**-0.801**	**-.828***	**-0.303**	**-0.807**	**-.882***	**-0.657**	**-0.511**	**-0.417**	**-0.175**	**-0.781**	**-0.573**	**-0.27**	**-0.315**	**-.819***	**1**								
Ni	**-0.418**	**-0.469**	**0.375**	**0.695**	**0.338**	**0.023**	**0.029**	**0.48**	**0.38**	**0.187**	**0.319**	**0.369**	**-0.03**	**-0.218**	**0.267**	**-0.089**	**1**							
Cu	**0.303**	**0.122**	**.840***	**0.382**	**0.25**	**0.527**	**0.357**	**0.396**	**0.241**	**0.513**	**0.624**	**0.197**	**0.306**	**0.041**	**0.119**	**-0.434**	**0.558**	**1**						
Zn	**-0.241**	**0.641**	**.906***	**0.489**	**0.805**	**.929****	**0.764**	**0.695**	**0.587**	**0.275**	**0.806**	**0.69**	**0.319**	**0.236**	**0.805**	**-.963****	**0.271**	**0.575**	**1**					
Cr	**-0.111**	**-0.716**	**0.18**	**0.513**	**-0.015**	**-0.159**	**-0.024**	**0.385**	**0.332**	**0.358**	**-0.019**	**0.204**	**-0.112**	**-0.218**	**-0.186**	**0.285**	**.869***	**0.528**	**-0.053**	**1**				
Cl	**-0.216**	**0.216**	**0.738**	**.846***	**0.566**	**0.788**	**0.754**	**.840***	**0.709**	**0.084**	**0.789**	**0.702**	**0.556**	**-0.197**	**0.764**	**-0.711**	**0.468**	**0.557**	**.853***	**0.234**	**1**			
Zr	**-0.126**	**0.127**	**0.594**	**-0.001**	**0.523**	**0.485**	**0.601**	**0.611**	**0.662**	**.971****	**-0.094**	**0.634**	**-0.474**	**0.705**	**-0.058**	**-0.261**	**0.315**	**0.507**	**0.389**	**0.426**	**0.253**	**1**		
V	**-0.253**	**0.578**	**.882***	**0.523**	**0.759**	**0.8**	**0.558**	**0.554**	**0.409**	**0.141**	**.897***	**0.539**	**0.362**	**0.112**	**.822***	**-.937****	**0.393**	**0.627**	**.959****	**0.008**	**.811***	**0.245**	**1**	
Rb	**0.341**	**0.677**	**0.5**	**0.155**	**0.135**	**0.546**	**0.208**	**-0.057**	**-0.216**	**-0.313**	**.839***	**-0.131**	**0.738**	**-0.199**	**0.503**	**-0.679**	**-0.215**	**0.359**	**0.587**	**-0.482**	**0.44**	**-0.341**	**0.657**	**1**

*. Correlation is significant at the 0.05 level (2-tailed). **. Correlation is significant at the 0.01 level (2-tailed).

2.4.3. Correlation between fluoride and arsenic in the core samples

In the core samples, an inverse relationship between F and As was observed (R2 - 0.719) (Table 2.4.3 and Fig. 2.4.7). Several authors have discussed the negative and positive correlations between F and As co-occurrences in groundwater and core samples. The reason for the co-occurrence has been evaluated because both F and As exhibit a positive correlation with sodium and alkalinity, but there is no direct correlation between As and F (Rango et al. 2010; Barranquero et al. 2017). The other reason for the co-occurrence of these elements is the continuous upward flow of F-rich groundwater from a deeper aquifer that combines with an alkaline, superficial aquifer with a high As concentration (Ahn 2012). Rapid solubility of amorphous silica in vitreous fragments containing As, F, and V allows the co-occurrence of these elements in alkaline aquifers (del Pilar Alvarez and Carol 2019). It has been reported that spring and groundwater samples from a volcanic sedimentary aquifer contain both fluorine and As (Parrone et al. 2020). Vertical discharge of pyrite-oxidized superficial groundwater into the deep aquifer is the cause of F and As co-occurrence in semiarid regions of the Yuncheng Basin in northern China (Li et al. 2022). According to Alarcon-Herrera et al. (2020), silica volcanic rock is prone to emit both As and F. India's northern Tripura State has intermediate, moderately deep, and deep aquifers contaminated with F and As (Bhattacharya et al. 2020). River sediments in the Indian State of Assam are reportedly contaminated with As and have the potential to discharge the element F (Patel et al. 2019).

Geographically diverse scientific studies indicate that reductive hydrolysis is the primary cause of the As contamination of groundwater (Kumar et al. 2014; Singh and Singh 2018; Zhou et al. 2017; Sridharan and Nathan 2018; Jha and Tripathi 2021). Groundwater in the lower Gangetic Plain is reportedly contaminated with both F and As, and a very weak positive correlation was observed between As and F. (De et al. 2022). According to a study conducted in the Brahmaputra flood plain, As contamination is nearer to the river, whereas F contamination appears to have an inverse relationship with river proximity (Das et al. 2016). Different

geological conditions in northern China, according to a study, increase the levels of F and As in groundwater sources. As is liberated during the reductive dissolution of pyrite, and F is liberated during the precipitation dissolution of CaF_2 (Pi et al. 2015). According to Jain et al. (2018), the principal cause of As contamination in the Barpeta District of Assam State in India is reducing conditions induced by large sediment flows and organic matter.

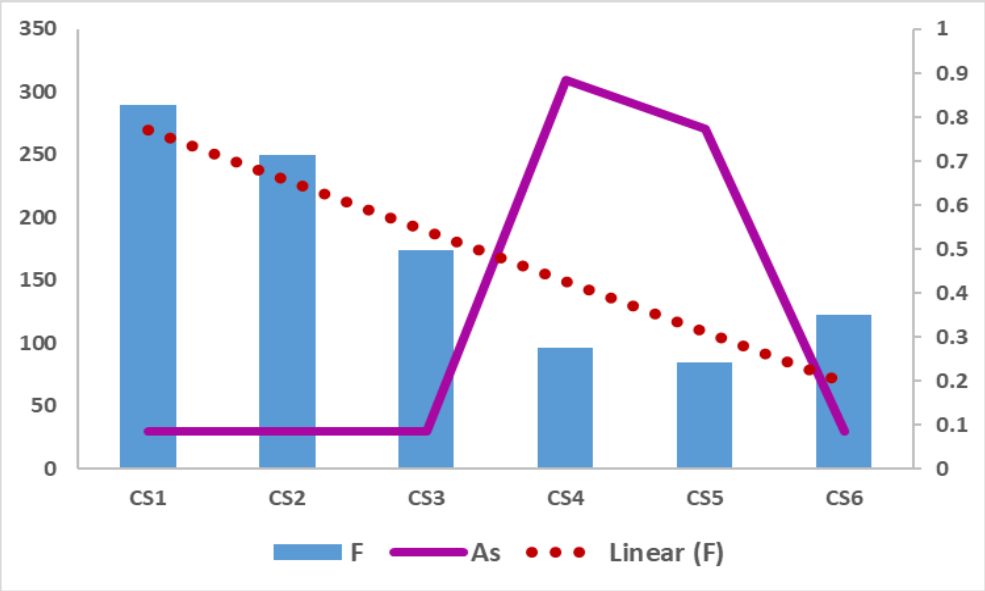

Fig. 2.4.7. The trend of F and As in the core samples

As-enriched littoral Holocene sediment and oxidative weathering are the causes of As contamination in the groundwater sources of Bangladesh (Huq et al. 2020). The principal reason for As contamination in the floodplain region of central-east Bangladesh is the dissolution of Fe–Mn oxyhydroxides (Saha and Rahman 2020). As contamination in the Canadian Shield in western Quebec, Canada is caused by the degradation of As-bearing sulphides present in the oxic/suboxic zone of the aquifer (Bondu et al. 2017). The contamination of As is most prevalent in agricultural and alluvial soils with a high organic matter content, whereas the occurrence of F is strongly associated with an alkaline condition and the presence of fluorite in the deeper aquifer (Bhatt et al. 2022). The widespread use of pesticides, fertilizers, and herbicides in the Amritsar District of Punjab, India, is the primary cause of the region's rising F pollution levels (Virk 2019).

According to several scientific investigations, the F concentration is greater at greater depths than in shallow aquifers (Hayat and Baba 2017; Nizam et al. 2022). The concentration of chloride and sulphate ions in water can also buffer the concentration of F in groundwater, and phosphate mining regions are typically associated with high F concentrations in groundwater and surface water (Chowdhury et al. 2019). The primary causes of F pollution in the western region of the Ordos basin in northwestern China are mineral dissolution (calcite, feldspar, dolomite, and fluorite), cation exchange, and evaporation (Su et al. 2019). Extreme alkalinity causes the precipitation of calcite and the dissolution of F (Reddy et al. 2016; Kumar et al. 2018; Chen et al. 2020). The principal cause of F pollution in Adoni, Kurnool District, Andhra Pradesh, is excessive fertilizer use on agricultural fields (Rahman and Umamahesh 2018). F in the groundwater is caused by the weathering and leaching of F from the minerals (Gouri and Choudhary 2017; Narsimha and Rajitha 2018; Noor et al. 2022). High F concentrations are caused by the mineralization of bedrock; both anthropogenic and natural sources are responsible for F contamination (Sahu et al. 2017; Sahu et al. 2021; Gogoi et al. 2021). Silicate weathering is responsible for the discharge of F into groundwater at high concentrations (Behera and Das 2018; Sahoo et al. 2022). F contamination is the result of alkalinity-mediated rock-water interaction in the presence of elevated HCO_3 and Na^+ (Kumar et al. 2018). The long residence time of water within an igneous or sedimentary confined aquifer, combined with low Ca and high Mg concentrations, facilitates the leaching of F-bearing minerals (Raj and Shaji et al. 2017). The primary sources of F in groundwater are granitic and hard rock terrain (Narsimha and Sudarshan 2017; Munna et al. 2020). F is derived from biotite and apatite in the hard rock terrain of Uttar Pradesh's Bundelkhand massif (Ram et al. 2021). The primary sources of F are alkaline volcanic rock and glass (Gevera and Mouri 2018; Gevera et al. 2020; Tomasek et al. 2022; González-Guzmán et al. 2022). The principal sources of F in the Limpopo Province of South Africa are smectite clays and the muscovite present in the sandstone, greywacke, and basalt (Onipe 2018; Oyebanjo 2020).

According to the aforementioned literature, it is evident that there is no direct correlation between the As and the F. The geological existence of F and As, as well as their release into groundwater, are distinct. In groundwater, it is due to the

reductive dissolution of iron-bearing minerals, oxidation of sulphide minerals, alkali desorption, geothermal activity, microbial action, and organic matter. As contamination is predominantly the result of the reductive dissolution of iron-containing minerals. F contamination is dependent upon the dissolution and precipitation of fluorite. F contamination is most prevalent in deep aquifers containing biotite, igneous granite, volcanic, sedimentary, and limestone deposits, whereas As contamination is more prevalent in shallow aquifers, particularly in alluvial, fluvial, and sedimentary deposits and rocks. F concentration is directly proportional to alkalinity, while As pollution occurs in acidic to mildly alkaline environments. In shallow aquifers, anthropogenic pollution such as the indiscriminate use of fertilizers and pesticides causes both F and As contamination.

In the mineral samples, there is a strong positive correlation between As and zircon (Zr) (Table 4). Zirconium (Zr) is a lithophile element that occurs as silicates or oxides and exhibits a high degree of chemical stability during degradation. After weathering, the majority of this Zr mineral leaches and forms placer or alluvial deposits (Suiekpayev et al. 2010). The correlation analysis displays a substantial positive correlation between the As and the Ba. Barium is only present in trace amounts but is found widely in the earth's crust, especially in shale and sandstone, and occasionally in igneous minerals (Andrew-Oha et al. 2017; Aziz et al. 2017). Extremely reactive, barium does not exist in free form. It is most commonly found as barium sulphate and carbonate, it also occurs as arsenate (Krishna et al. 2020). The strong correlation between these elements is attributed to the presence of barium arsenate ($Ba_3\ (AsO4)_2$) in core samples (Planer-Friedrich et al. 2001).

2.4.4. Correlation among other heavy metals in the core samples

Other than F and As there are a few other elements whose health effects warrant significant concern. The correlation between groundwater samples and their corresponding core samples has been determined for the problematic elements found in the groundwater, which include Fe, Cd, Pb, and Ni. The correlation between the other elements in the core samples has also been identified to comprehend the geochemistry of the region under investigation.

The correlation between the concentrations of Fe in groundwater and the corresponding concentrations in core samples is moderate (Fig. 2.4.8). It indicates

that Fe contamination is both geological and man-made. The weak positive correlation between the concentrations of Cd, Pb, and Ni in groundwater and their corresponding concentrations in core samples confirms the anthropogenic origins of contaminants (Fig. 2.4.9 to 11). The availability and dissolution of these elements are contingent on several factors. In the mineral samples from the study area, a significant correlation between FeO and CaO, Cd, Cu, Zn, Va, and Mo was found. The correlation between FeO and CaO indicates the presence of epidote feldspar in the mineral samples (Afshooni et al. 2013). These correlations between metal concentrations suggest a shared or similar geochemical behavior or origin (Fernandes et al. 2019; Njogu et al. 2020). The correlation between Fe and Cd, Cu, Zn, Va, and Mo suggests granitic rocks (Abdulla 2009; Xu et al. 2021). In the mineral sample, a significant correlation between Mg and Cl was observed (Table 4). Magnesium and chlorite minerals can be found in every dominant rock type, but they are most commonly found in grey hornblende biotite granite gneiss (Basha et al. 2022). Mg has a strong positive correlation with Ti, so it is often linked with silicate or clay minerals (Kimura 1998).

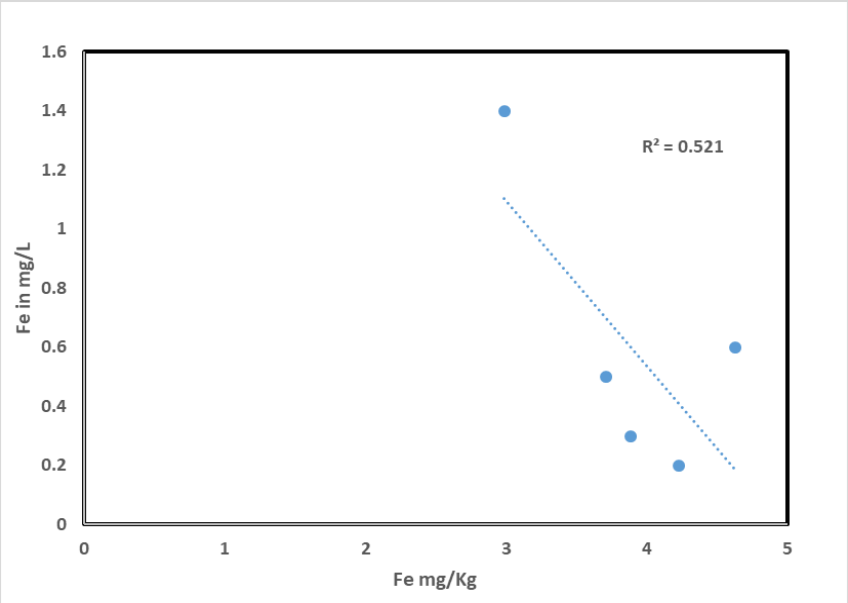

Fig. 2.4.8. The correlation of water (mg/L) and soil (kg/mg) Fe

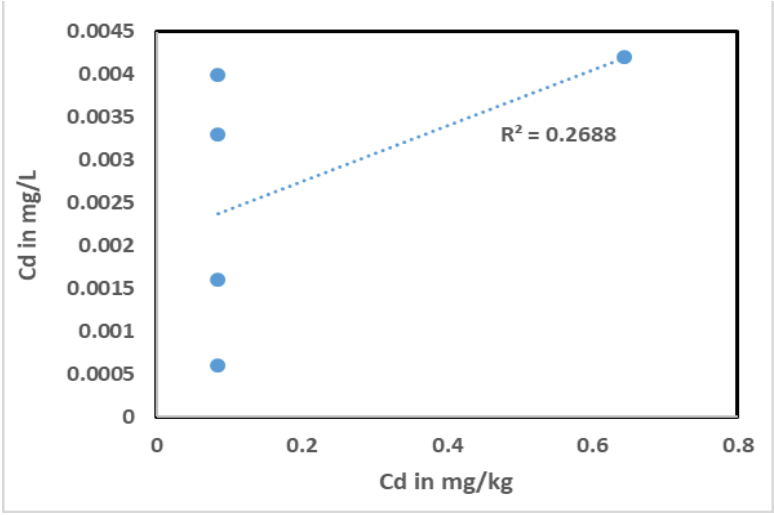

Fig. 2.4.9. The correlation of water (mg/L) and soil (kg/mg) Cd

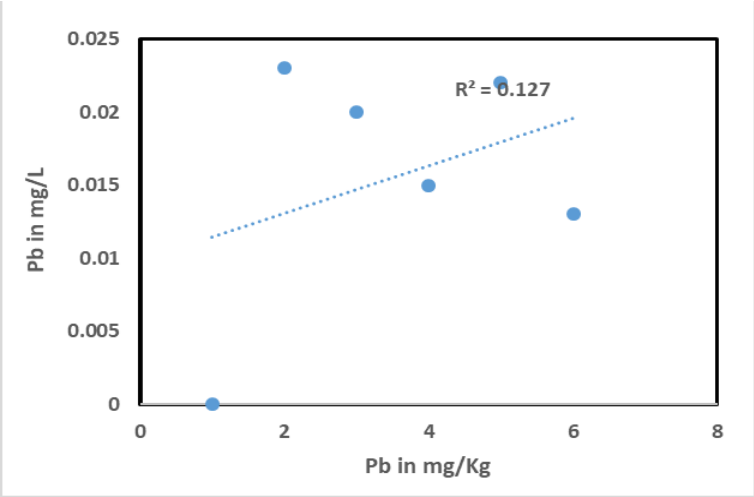

Fig. 2.4.10. The correlation of water (mg/L) and soil (kg/mg) Pb

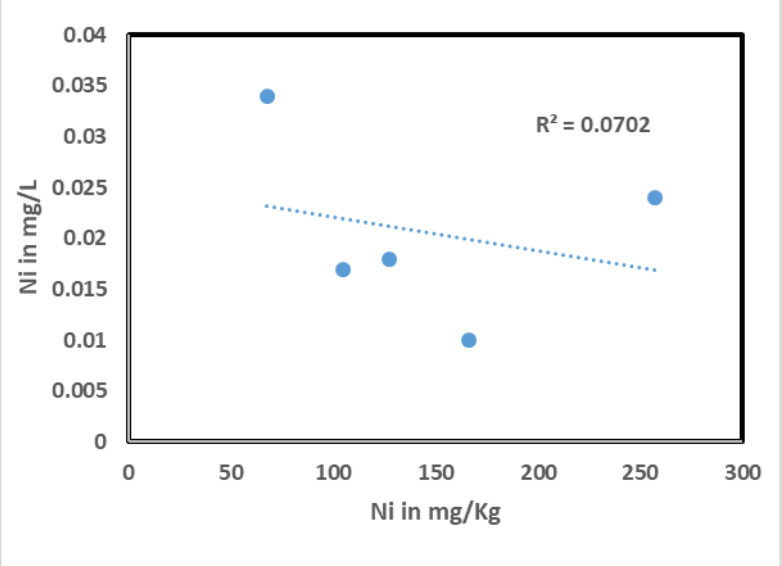

Fig. 2.4.11. The correlation of water (mg/L) and soil (kg/mg) Ni

A significant correlation between K_2 O and Sr was observed in the mineral samples (Table 4). Sr is one of the alkaline earth elements. Ca and Ba share similar chemical properties with strontium. It is considered normal for concentrations up to 600 mg/kg (Wang et al. 2017), and the concentrations in the core samples ranged from 263.9 to 819.8 mg/kg. Potassium feldspar has been associated with strontium, which may explain the strong correlation with K2O (Haider et al. 2020; Gislam et al. 2020). K2O exhibited a negative correlation with F and a positive correlation with As. Potassium feldspar is strongly associated with alluvial deposits in coastal regions (Haider et al. 2020; Irzon et al. 2020). CaO has a strong relationship with P_2 O_5 , Cd, Zn, and V. Calcium and phosphates are common apatite mineral constituents (Piccoli and Candela 2002).

Cadmium is present in all minerals and sediment at a concentration of less than 1 ppm and is always accompanied by zinc (Kakonyi and Ahmed 2020). In the mineral samples, a significant positive correlation between P_2 O_5 and SO_3 , Ti, and Sr was observed (Table 4). Similarly, SO_3 and Sr, and Cl, Ti exhibited a substantial positive correlation (Table 4). Apatite is a minor and pervasive mineral found in the majority of igneous rocks (Harlov 2015; O'Sullivan et al. 2018). Apatite minerals usually contain Cl, P_2 O_5 , SO_3 , and Sr (Hutchinson 2019; Mercer et al. 2020; Pan et al. 2021). Sr also accumulates together with gypsum as a result of the evaporation mechanism, which is the reason for the significant correlation between SO_3 and Sr (Nedobukh and Semenishchev 2020).

A significant positive correlation was observed between Ba and Zr in the study area (Table 4). Very little barium is found in sediment, and is associated with feldspar, and celsian (Magnall et al. 2020). Ba is typically found in igneous rocks (Castillo-Oliver et al. 2017) as barium sulphate or barite, most frequently in pyrite (Xiong et al. 2021; Yao et al. 2022). It is also found in potassium-rich and highly alkaline rocks (Jeske 2013; Pathak et al. 2020). The concentration of barium in the mineral sample varied between 556.6 mg/kg and 2,728 mg/kg. Zr occurs in alkaline igneous rocks and agpaitic granite (Sjoqvist et al. 2017; Wu et al. 2023). Hence, it can be stated that the source of Ba and Zr is alkaline igneous rocks.

In the core sample, Mn displayed a strong positive correlation with F, Zn, and Cl, as well as a substantial positive correlation with V and Rb. Mn generally occurs in combination with quartz, feldspar, and ilmenite (Pharoe 2020). The range of Zn concentration in the sediment core is 10 to 500 mg/kg. Zn is abundant and extensively dispersed in the earth's crust. The Zn concentration varies depending on the type of rock, with igneous minerals comprising 70 mg/kg, limestone 20 mg/kg, and sandstone 10 mg/kg. The Zn concentration in the core sample varies between 30.21 mg/kg and 66.92 mg/kg.

Chlorite is a prevalent component of igneous rocks produced by the hydrothermal alteration of pyroxenes, amphiboles, biotite, and garnet (Ako et al. 2015; Soloviev et al. 2019). Vanadium is a relatively abundant trace element present in numerous earth materials. The vanadium concentration in the core sample was more consistent, ranging from 60.91 to 77.74 mg/kg (Table 3). The average vanadium concentration in the Earth's crust is 97 mg/kg (Schlesinger et al. 2017). Vanadium is present in igneous and sedimentary minerals, where it is identical to zinc (Awan et al. 2010). Rb is a reactive alkali metal (Ballmann et al. 2022), and its significant positive correlation with Mn indicates its source is from pegmatite and it consists of quartz, feldspar, and mica (Camp 2011; Han et al. 2021). Cl demonstrated a considerable positive correlation with Mg, Ti, Zn, and V in core samples. In granite igneous rocks, Cl is typically incorporated with Ti, V, Mg, and Zn (Wilkinson et al. 2015; Feng et al. 2022).

Significant positive correlations were observed between Pb and V, while significant negative correlations were observed between Pb and Cd. In contrast, Cd demonstrated a significant negative correlation with V and a positive correlation with Zn. The Pb concentration in the core sample ranged from 7.475 mg/kg to 22.23 mg/kg (Table 3). The reported concentration of lead in soil range from 2 mg/kg to 200 mg/kg (Ma et al. 1995; Amritphale et al. 1997). Tabelin et al. (2018) report that the Pb and Cd concentrations in igneous rocks are 30 mg/kg and 0.6 mg/kg, respectively. Pb is sparsely soluble but highly soluble in acidic water, and it can substitute for Ca in fluorapatite (Yan et al. 2020). Due to weathering, felsic volcanic

rock discharges a considerable amount of lead (Novoselov et al. 2022). The strong correlation between lead and vanadium indicates the presence of vanadinite ($Pb_5(VO_4)_3Cl$) (lead and vanadium ore) (Silin et al. 2020). It is a secondary mineral that forms from lead ore in semiarid to arid climates (Boni et al. 2007).

The significant relationship between Cd and Zn indicates the presence of peridotite, which is ultramafic due to its low silica content (less than 45%) and high magnesium and iron content (Wang et al. 2016; Pickard et al. 2022). These relationships are supported by the significant positive correlation between zinc and iron oxide and the negative correlation between zinc and silica.

Ni concentrations in the core samples ranged from 67 mg/kg to 257.3 mg/kg. It also exhibited a significant positive correlation with Cr. The average Ni concentration in the earth's crust is 86 mg/kg (Klein and Costa 2022). The nickel concentration in soils around the world fluctuates. The range of Cr concentration in the samples was 194.3 mg/kg to 461.9 mg/kg. The average concentration of Cr in the earth's crust is 100 mg/kg, according to Barnhart (1997). The mobility of Ni is predominantly determined by the acidic pH. Higher Ni and Cr concentrations indicate the presence of ultramafic rocks (Vithanage et al. 2019). Cu has a strong positive correlation with Mo, while Zn has a correlation with Cl and V. Cu concentrations in the samples ranged from a minimum of 23.28 mg/kg to a maximum of 40.06 mg/kg. Copper concentration in igneous minerals ranges between 20 and 200 mg/kg (Liu et al. 2014). The core samples indicated a wide range of Zr concentrations, from 94 mg/kg to 506.3 mg/kg. According to Caricchi et al. (2014), the average Zr concentration in granodiorite magma is between 50 mg/kg and 250 mg/kg. The relationship between these elements suggests that these minerals are derived from intrusive igneous-granitic rocks.

2.5 Conclusion

It is widely accepted that lithology and other climatic conditions have the greatest influence on hydrochemistry, especially on groundwater. This study primarily evaluated the source of F, As, and heavy metals in the groundwater sources of the Palakkad District, which revealed an excessively high concentration of F and As in

the groundwater. To better understand the relationship between groundwater chemistry and the contaminated zone, core mineral samples were collected and analyzed for trace elements at these sites. XRD and XRF are utilized in the evaluation of minerals.

Geologically, the study region is characterized by the Peninsular Gneissic Complex (PGC), and granite and granite gneiss are the predominant rock forms. Silicon dioxide (quartz) is the predominant component in the core samples, as determined by XRF. The hornblende-biotite gneiss country rock is banded with quartz. The dominant mineral group in the study area is aluminosilicates, which consist of plagioclase feldspars (albite), micas (hornblende-biotite), and clay minerals (kaolin). Additionally, there is evidence of a fragmented fluorite deposit in the western part of the Palakkad area. These are the primary sources of F in the region having contaminants. In addition, the Mg concentration in the core samples is high while the Ca concentration is minimal. In the groundwater samples, a similar trend in ionic concentrations was observed. Consequently, cation exchange and alkalinity are crucial determinants of groundwater F enrichment. SiO_2 concentrations in the core samples are greater than those of Fe_2 O_3 and MgO, indicating the granitic (felsic) origin of the minerals with ultramafic enclaves. The XRD analysis reveals that the primary sources of F in the study area are quartz, albite, biotite, and fluorite.

The XRD and XRF results point out the presence and concentration of As in the core samples from the study area. Fluvial deposits are related to the spatial distribution of As in the study location. As is primarily associated with Al, Fe, and Ca, and occurs as arsenate in the sediments of the study area. Furthermore, the correlation between As and K indicates the presence of potassium feldspar and clay in the alluvial deposits. The positive correlation between As and Fe suggests that arsenopyrite is a sulfur-rich source of As. Barite is also associated with the source of As. In the studied locations, both oxidizing and reducing conditions predominate to discharge As into the groundwater. In a reducing environment, As is absorbed by Fe, Al, and Mn due to the semiarid climatic condition that exists in the study area.

There was a moderately positive correlation between the concentration of As in groundwater and As in the mineral sample. The absence of a significant correlation between them, however, is indicative of both geological and anthropogenic causes. As and F have an inverse relationship, which is indicative of their contrary origins. F contamination is more prevalent in the deep granitic aquifer, whereas As contamination exists in both superficial and deep aquifers. Vertical discharge of pyrite-oxidized shallow groundwater into deep aquifers is another reason for the presence of As in deep aquifers.

The poor correlation between groundwater concentration and the concentration of heavy metals in core samples, such as Cd, Pb, and Ni, indicates that the origin of these elements in groundwater is anthropogenic. It is understood that vanadite is responsible for the greatest proportion of lead. The concentration and correlation of trace elements in the core sample indicate the granitic nature of the sample, with quartz constituting the majority of the sample. The elevated concentrations of Mg and Cl indicate the presence of grey hornblende biotite granitic gneiss. In addition, the relationship between high concentration and correlation between Ba and Zr indicates the presence of alkaline igneous minerals. The presence of high concentrations of Ni and Cr in the mineral samples confirms the ultramafic intrusion within the igneous rock.

GENERAL CONCLUSION

The flat inland region (Palakkad District) has a greater groundwater reserve than the undulating coastal region (Malappuram District) accounting for 434.17 million cubic meters and 249.32 MCM respectively. The contamination levels of salinity, as well as As and F, are greater in Palakkad than in Malappuram District. The most significant issues in the coastal District are the acidic pH and iron contamination caused by fluvial sedimentation. The township and transport are highly associated with Cd, Pb, and Ni contamination. According to the Water Quality Index, 45 percent of the groundwater in Palakkad falls into poor quality, whereas the majority of groundwater in Malappuram falls into good quality. In both Districts, the HPI index was high during the pre-monsoon period. F and As contamination are prevalent in the middle and eastern regions of the Palakkad District.

The mineralogical analysis of F- and As-contaminated regions reveals that the source of F contamination was solely geological in origin. Additionally, the vast majority of As contamination is geological in origin. F and As were found to have an inverse relationship in the study area. F and As occur in the study area under different environmental conditions. F occurs in the alkaline hornblende biotite gneiss aquifer in the study region with a low concentration of Ca and a higher concentration of Mg ions. As can be found in relatively shallow aquifers containing sedimentary or alluvial deposits associated with rivers and agricultural fields. The release of As into groundwater is influenced by both oxidation and reduction potentials.

THE MANAGEMENT APPROACHES TO ADDRESS GROUNDWATER POLLUTION ISSUES IN THE TWO DISTRICTS

Based on in-depth observations and scientific data analysis, several management strategies addressing the current issues are discussed. The study area consists of two distinct regions: one is a coastal and hillock region, while the other is a tropical plain with semiarid climate conditions. The characteristics of groundwater depend on its geological settings and climatic conditions. As the climatic conditions and geological settings of the two Districts are dissimilar, groundwater reserves and related issues are distinct. Concerning groundwater issues in the areas under study, certain recommendations are made:

- The combined utilization of surface water and groundwater for all water-intensive activities, a comprehensive strategy for rainwater harvesting, and conservation of excess surface water during the wet season to mitigate excessive groundwater salinity concentrations.

- To control the poor quality of groundwater, large-scale groundwater extraction should be avoided, particularly deep extraction of groundwater.

- By adding and dissolving carbonate substrate materials, which generate alkalinity and utilize protons, the acidity of the groundwater can be neutralized. The dosage can be determined based on the pH level and water volume.

- Reverse osmosis, iron exchange, neutralization filters, artificial wetland construction, acid injection, and aeration ponds can be used to remediate elevated alkalinity and iron concentrations in potable water at the community level.

- A broad variety of adsorbents, such as calcium and calcium-based adsorbents, carbon, oxide, and double hydroxide, as well as a wide variety of nanoparticles and natural materials, can be used to remove F from groundwater at the community or household level.

- Household treatment methods such as chlorination and consuming boiled water can prevent microbiological contamination.

- Arsenic can be removed from potable water using membrane technology, adsorption, and electrocoagulation at the community level. Bioremediation and phytoremediation can be utilized to remove As from contaminated soil.

- It is possible to reduce the excessive use of fertilizers and pesticides through the adoption of improved agricultural practices, such as crop rotation and water-efficient crops, for the management of water resources and soil nutrients.

- Construction of green dams to prevent the loss of runoff water to the ocean and increase groundwater recharge to neutralize salinity; afforestation with drought- and salinity-tolerant plants to acclimatize to the dryness of the arid environment are suggested.

- To make the public and rural sectors more aware of the significance of the quantity and quality of water, its health effects, and the need for water resource development, regular education campaigns should be organized. Periodic and continuous monitoring of all sources of potable water should be ensured before utilization, for which community mobilization is required.

RECOMMENDATIONS

Arsenic (As) and fluoride (F) are the two most obvious pollutants in aquifers across the world, both in terms of distribution and risk. While most research focuses on independent descriptions of their hydrogeochemistry, the current work attempted to bring them together concerning their origin and route. Co-contamination is significantly influenced by local hydrogeochemical processes and seasonality. Co-occurrences of As and F are relatively common but are hidden since one is dominant.

Fluoride pollution is more prevalent in semi-arid environments, whereas arsenic is found in alluvium deposits. Hence the ionic characterization of arsenic and its prevalence in alluvial planes will be further investigated. The epidemiological research suggests that the interface between these two interacting parts of public health is somewhat complex and can be influenced by some unknown variables. Existing hypotheses for As-F interactions are equivocal, especially for antagonistic interactions, which require further investigation. To further understand the occurrence and distribution of fluoride, significant geological research is required. In future research, it is increasingly vital to increase the number of heavy metals employed in hydrochemical analysis, such as mercury, chromium, vanadium, and rubidium, to determine the synergistic impacts of these elements. The exploration of the interactions of co-occurring elements with hazardous elements is critical for addressing the wider issue of freshwater utility and sustainability.

REFERENCES

Abbott, A. P., Al-Bassam, A. Z., Goddard, A., Harris, R. C., Jenkin, G. R., Nisbet, F. J., & Wieland, M. (2017). Dissolution of pyrite and other Fe–S–As minerals using deep eutectic solvents. *Green Chemistry*, *19*(9), 2225-2233.

Abdelgawad, A. M., Watanabe, K., Takeuchi, S., & Mizuno, T. (2009). The origin of fluoride-rich groundwater in Mizunami area, Japan—Mineralogy and geochemistry implications. *Engineering Geology*, *108*(1-2), 76-85.

Abdulla, H. (2009). Bioweathering and biotransformation of granitic rock minerals by actinomycetes. *Microbial ecology*, *58*, 753-761.

Abedin, M., Collins, A. E., Habiba, U., & Shaw, R. (2019). Climate change, water scarcity, and health adaptation in southwestern coastal Bangladesh. *International Journal of Disaster Risk Science*, *10*(1), 28-42.

Abiye, T. A., & Bhattacharya, P. (2019). Arsenic concentration in groundwater: Archetypal study from South Africa. *Groundwater for Sustainable Development*, *9*, 100246.

Abraham, A., Pullishery, F., & Raghavan, R. (2016). Dental caries and calculus status in children studying in Government and Private Schools in Malappuram, Kerala, India. *IAIM*, *3*(3), 35-41.

Acharya, S. (2005). Dental caries, its surface susceptibility and dental fluorosis in South India. *International dental journal*, *55*(6), 359-364.

Acharyya, S. K., & Shah, B. A. (2007). Groundwater arsenic contamination affecting different geologic domains in India—a review: influence of geological setting, fluvial geomorphology and Quaternary stratigraphy. *Journal of Environmental Science and Health, Part A*, *42*(12), 1795-1805.

Acharyya, S. K., Chakraborty, P., Lahiri, S., Raymahashay, B. C., Guha, S., & Bhowmik, A. (1999). Arsenic poisoning in the Ganges delta. *Nature*, *401*(6753), 545-545.

Adimalla, N. (2019). Groundwater quality for drinking and irrigation purposes and potential health risks assessment: a case study from semi-arid region of South India. *Exposure and health*, *11*(2), 109-123.

Adimalla, N. (2020). Assessment and mechanism of fluoride enrichment in groundwater from the hard rock terrain: a multivariate statistical approach. *Geochemistry International*, *58*(4), 456-471.

Adimalla, N., & Li, P. (2019). Occurrence, health risks, and geochemical mechanisms of fluoride and nitrate in groundwater of the rock-dominant semi-arid region, Telangana State, India. *Human and Ecological Risk Assessment: An International Journal*, *25*(1-2), 81-103.

Adimalla, N., & Venkatayogi, S. J. E. E. S. (2017). Mechanism of fluoride enrichment in groundwater of hard rock aquifers in Medak, Telangana State, South India. *Environmental Earth Sciences*, *76*(1), 45.

Adimalla, N., Chen, J., & Qian, H. (2020a). Spatial characteristics of heavy metal contamination and potential human health risk assessment of urban soils: A case study from an urban region of South India. *Ecotoxicology and environmental safety*, *194*, 110406.

Adimalla, N., Qian, H., & Li, P. (2020b). Entropy water quality index and probabilistic health risk assessment from geochemistry of groundwaters in hard rock terrain of Nanganur County, South India. *Geochemistry*, *80*(4), 125544.

Adimalla, N., Qian, H., & Nandan, M. J. (2020c). Groundwater chemistry integrating the pollution index of groundwater and evaluation of potential human health risk: A case study from hard rock terrain of south India. *Ecotoxicology and Environmental Safety*, *206*, 111217.

Adimalla, N., Vasa, S. K., & Li, P. (2018). Evaluation of groundwater quality, Peddavagu in Central Telangana (PCT), South India: an insight of controlling factors of fluoride enrichment. *Modeling Earth Systems and Environment*, *4*(2), 841-852.

Adimalla, N., Venkatayogi, S., & Das, S. V. G. (2019). Assessment of fluoride contamination and distribution: a case study from a rural part of Andhra Pradesh, India. *Applied Water Science*, *9*(4), 1-15.

Advisory, D. W. (2003). Consumer acceptability advice and health effects analysis on sodium. *US Environmental Protection Agency Office of Water (4304T), Health and Ecological Criteria Division, Washington, DC*, *20460*.

Afshooni, S. Z., Mirnejad, H., Esmaeily, D., & Haroni, H. A. (2013). Mineral chemistry of hydrothermal biotite from the Kahang porphyry copper deposit (NE Isfahan), Central Province of Iran. *Ore Geology Reviews*, *54*, 214-232.

Afzali, Darush, Mohammad Ali Taher, Ali Mostafavi, and Sayed Ziae Mohammadi Mobarakeh. (2005). Thermal modified Kaolinite as useful material for separation and preconcentration of trace amounts of manganese ions. *Talanta* 65, 476-480.

Agarwal, C. S. (1998). Study of drainage pattern through aerial data in Naugarh area of Varanasi district, UP. *Journal of the Indian Society of Remote Sensing*, *26*(4), 169-175.

Agarwal, M., Rai, K., Shrivastav, R., & Dass, S. (2002). A study on fluoride sorption by montmorillonite and kaolinite. *Water, air, and soil pollution*, *141*(1), 247-261.

Aghajani, J., Farnia, P., & Velayati, A. A. (2017). Impact of geographical information system on public health sciences. *Biomedical and Biotechnology Research Journal (BBRJ)*, *1*(2), 94.

Agrawal, G. D., Lunkad, S. K., & Malkhed, T. (1999). Diffuse agricultural nitrate pollution of groundwaters in India. *Water science and technology*, *39*(3), 67-75.

Aguirre, M. A., Selva, E. J., Hidalgo, M., & Canals, A. (2015). Dispersive liquid–liquid microextraction for metals enrichment: a useful strategy for improving sensitivity of laser-induced breakdown spectroscopy in liquid samples analysis. *Talanta*, *131*, 348-353.

Ahamed, A. J., & Loganathan, K. (2017). Water quality concern in the Amaravathi River Basin of Karur district: a view at heavy metal concentration and their interrelationships using geostatistical and multivariate analysis. *Geology, Ecology, and Landscapes*, *1*(1), 19-36.

Ahmad, S., & Khurshid, S. (2019). Hydrogeochemical assessment of groundwater quality in parts of the Hindon River basin, Ghaziabad, India: implications for domestic and irrigation purposes. *SN Applied Sciences*, *1*(2), 151.

Ahmad, S., Umar, R., & Arshad, I. (2019). Groundwater quality appraisal and its hydrogeochemical characterization—Mathura City, Western Uttar Pradesh. *Journal of the Geological Society of India*, *94*(6), 611-623.

Ahmed, K. M., Bhattacharya, P., Hasan, M. A., Akhter, S. H., Alam, S. M., Bhuyian, M. H., ... & Sracek, O. (2004). Arsenic enrichment in groundwater of the alluvial aquifers in Bangladesh: an overview. *Applied Geochemistry*, *19*(2), 181-200.

Ahmed, M., Mumtaz, R., Baig, S., & Zaidi, S. M. H. (2022). Assessment of correlation amongst physico-chemical, topographical, geological, lithological and soil type parameters for measuring water quality of Rawal watershed using remote sensing. *Water Supply*.

Ahn, J. S. (2012). Geochemical occurrences of arsenic and fluoride in bedrock groundwater: a case study in Geumsan County, Korea. *Environmental geochemistry and health*, *34*, 43-54.

Aju, C. D., Reghunath, R., Achu, A. L., & Rajaneesh, A. (2021). Understanding the hydrogeochemical processes and physical parameters controlling the groundwater chemistry of a tropical river basin, South India. *Environmental Science and Pollution Research*, 1-17.

Ako, T. A., Vishiti, A., Ateh, K. I., Kedia, A. C., & Suh, C. E. (2015). Mineral alteration and chlorite geothermometry in platinum group element (PGE)-Bearing meta-ultramafic rocks from South east Cameroon. *Journal of Geosciences and Geomatics*, *3*(4), 96-108.

Aktar, W., Paramasivam, M., Ganguly, M., Purkait, S., & Sengupta, D. (2010). Assessment and occurrence of various heavy metals in surface water of Ganga river around Kolkata: a study for toxicity and ecological impact. *Environmental monitoring and assessment*, *160*(1), 207-213.

Akyüz, S., Akyüz, T., Çağlar, H., & Çağlar, N. (2008). FT-IR, EDXRF analysis of the Mardin-Mazidag phosphate deposit of Turkey and relations between phosphate, uranium and fluorine.

Al Hagibi, H. A., Al-Selwi, K. M., Nagi, H. M., & Al-Shwafi, N. A. (2018). Study of Heavy Metals contamination in Mangrove Sediments of the Red Sea Coast of Yemen from Al-Salif to Bab-el-Mandeb Strait. *J Ecology & Natural Resources*, *2*(1), 121.

Alagumuthu, G., & Rajan, M. (2008). Monitoring of fluoride concentration in ground water of kadayam block of Tirunelveli district, India: Correlation with physico-chemical parameters. *Chem*, *1*(4), 757-765.

Alam, M. G. M., Allinson, G., Stagnitti, F., Tanaka, A., & Westbrooke, M. (2002). Arsenic contamination in Bangladesh groundwater: a major environmental and social disaster. *International journal of environmental health research*, *12*(3), 235-253.

Alam, M., Shaikh, W. A., Chakraborty, S., Avishek, K., & Bhattacharya, T. (2016). Groundwater arsenic contamination and potential health risk assessment of Gangetic Plains of Jharkhand, India. *Exposure and Health*, *8*(1), 125-142.

Alarcón-Herrera, M. T., & Gutiérrez, M. (2022). Geogenic Arsenic in Groundwater: Challenges, Gaps and Future Directions. *Current Opinion in Environmental Science & Health*, 100349.

Alarcon-Herrera, M. T., Bundschuh, J., Nath, B., Nicolli, H. B., Gutierrez, M., Reyes-Gomez, V. M., ... & Sracek, O. (2013). Co-occurrence of arsenic and fluoride in groundwater of semi-arid regions in Latin America: Genesis, mobility and remediation. *Journal of Hazardous Materials*, *262*, 960-969.

Alarcón-Herrera, M. T., Martin-Alarcon, D. A., Gutiérrez, M., Reynoso-Cuevas, L., Martín-Domínguez, A., Olmos-Márquez, M. A., & Bundschuh, J. (2020). Co-occurrence, possible origin, and health-risk assessment of arsenic and fluoride in drinking water sources in Mexico: Geographical data visualization. *Science of the Total Environment*, *698*, 134168.

Alferyeva, Y. O., Chevychelov, V. Y., & Novikova, A. S. (2022). Experimental Study of the Crystallization Conditions of Ongonites of the Ary-Bulak Massif (Eastern Transbaikalia). *Petrology*, *30*(2), 212-225.

Alghamdi, A. G., Aly, A. A., & Ibrahim, H. M. (2021). Assessing the environmental impacts of municipal solid waste landfill leachate on groundwater and soil contamination in western Saudi Arabia. *Arabian Journal of Geosciences*, *14*(5), 1-12.

Ali, A., Chiang, Y. W., & Santos, R. M. (2022). X-ray diffraction techniques for mineral characterization: A review for engineers of the fundamentals, applications, and research directions. *Minerals*, *12*(2), 205.

Ali, H., & Khan, E. (2019). Trophic transfer, bioaccumulation, and biomagnification of non-essential hazardous heavy metals and metalloids in food chains/webs—Concepts and implications for wildlife and human health. *Human and Ecological Risk Assessment: An International Journal*, *25*(6), 1353-1376.

Ali, S. A., & Khan, N. (2013). Evaluation of morphometric parameters—a remote sensing and GIS based approach.

Ali, S., Thakur, S. K., Sarkar, A., & Shekhar, S. (2016). Worldwide contamination of water by fluoride. *Environmental chemistry letters*, *14*(3), 291-315.

Ali, W., Mushtaq, N., Javed, T., Zhang, H., Ali, K., Rasool, A., & Farooqi, A. (2019a). Vertical mixing with return irrigation water the cause of arsenic enrichment in groundwater of district Larkana Sindh, Pakistan. *Environmental pollution*, *245*, 77-88.

Ali, W., Rasool, A., Junaid, M., & Zhang, H. (2019b). A comprehensive review on current status, mechanism, and possible sources of arsenic contamination in groundwater: a

global perspective with prominence of Pakistan scenario. *Environmental geochemistry and health*, *41*(2), 737-760.

Al-Shawi, A. W., & Dahl, R. (1999). The determination of cadmium and six other heavy metals in nitrate/phosphate fertilizer solution by ion chromatography. *Analytica chimica acta*, *391*(1), 35-42.

Amadi, A. N., & Nwankwoala, H. O. (2013). Evaluation of heavy metal in soils from Enyimba dumpsite in Aba, southeastern Nigeria using contamination factor and geo-accumulation index.

Amarasooriya, A. A. G. D., & Kawakami, T. (2020). Removal of co-existing fluoride, calcium, magnesium, and carbonates, by non-chemical induced electrolysis system for drinking and industrial purposes. *H2Open Journal*, *3*(1), 10-31.

Amritphale, S. S., Prasad, M., Saxena, S., & Chandra, N. (1999). Adsorption behavior of lead ions on pyrophyllite surface. *Main group metal chemistry*, *22*(9), 557-566.

Anawar, H. M., Akai, J., Komaki, K., Terao, H., Yoshioka, T., Ishizuka, T., ... & Kato, K. (2003). Geochemical occurrence of arsenic in groundwater of Bangladesh: sources and mobilization processes. *Journal of Geochemical Exploration*, *77*(2-3), 109-131.

Andrew-Oha, I., Mosto-Onuoha, K., & Sunday-Dada, S. (2017). Contrasting styles of lead-zinc-barium mineralization in the Lower Benue Trough, Southeastern Nigeria. *Earth Sciences Research Journal*, *21*(1), 7-16.

Anoop, S., Ashwathi, C., Baburaj, V. H., & Pillai, R. S. (2021). Hydrogeochemical status and geoelectrical characteristics of the shallow aquifers of Kalanad Basin, Kasaragod, Kerala, India. *Applied Water Science*, *11*(2), 1-16.

Ansari, J. A., & Umar, R. (2019). Evaluation of hydrogeochemical characteristics and groundwater quality in the quaternary aquifers of Unnao District, Uttar Pradesh, India. *HydroResearch*, *1*, 36-47.

Aoshima, K. (2016). Itai-itai disease: renal tubular osteomalacia induced by environmental exposure to cadmium—historical review and perspectives. *Soil Science and Plant Nutrition*, *62*(4), 319-326.

APHA AWWA, W. P. C. F. (1998). Standard methods for the examination of water and wastewater 20th edition. *American Public Health Association, American Water Work Association, Water Environment Federation, Washington, DC*.

Apps, J. A., Zheng, L., Zhang, Y., Xu, T., & Birkholzer, J. T. (2010). Evaluation of groundwater quality changes in response to CO2 leakage from deep geological storage. *Transport in Porous Media*, *82*(1), 215-246.

Aravinthasamy, P., Karunanidhi, D., Subba Rao, N., Subramani, T., & Srinivasamoorthy, K. (2020). Irrigation risk assessment of groundwater in a non-perennial river basin of South India: implication from irrigation water quality index (IWQI) and geographical information system (GIS) approaches. *Arabian Journal of Geosciences*, *13*(21), 1-14.

Arslan, G., & Burke, J. (2021). Positive education to promote flourishing in students returning to school after COVID-19 closure. *Journal of School and Educational Psychology*, *1*(1), 1-5.

Arslan, H. (2012). Spatial and temporal mapping of groundwater salinity using ordinary kriging and indicator kriging: The case of Bafra Plain, Turkey. *Agricultural water management*, *113*, 57-63.

Arumugam, T., Kunhikannan, S., & Radhakrishnan, P. (2019). Assessment of fluoride hazard in groundwater of Palghat District, Kerala: a GIS approach. *International Journal of Environment and Pollution*, *66*(1-3), 187-211.

Aulenbach, D. B. (1967). Water--Our Second Most Important Natural Resource. *BC Indus. & Com. L. Rev.*, *9*, 535.

Awan, R. S., Liu, C., Yang, S., Wu, Y., Zang, Q., Khan, A., & Li, G. (2021). The occurrence of vanadium in nature: Its biogeochemical cycling and relationship with organic matter—a case study of the early Cambrian black rocks of the niutitang formation, western Hunan, China. *Acta Geochimica*, *40*(6), 973-997.

Aydin, G., Çiçek, E., Akdoğan, M., & Gökalp, O. (2003). Histopathological and biochemical changes in lung tissues of rats following administration of fluoride over several generations. *Journal of Applied Toxicology: An International Journal*, *23*(6), 437-446.

Ayers, J. C., George, G., Fry, D., Benneyworth, L., Wilson, C., Auerbach, L., ... & Goodbred, S. (2017). Salinization and arsenic contamination of surface water in southwest Bangladesh. *Geochemical Transactions*, *18*(1), 1-23.

Ayoob, S., & Gupta, A. K. (2006). Fluoride in drinking water: a review on the status and stress effects. *Critical reviews in environmental science and technology*, *36*(6), 433-487.

Aziz, H. A., Ghazali, M. F., Hung, Y. T., & Wang, L. K. (2017). Toxicity, Source, and Control of Barium in the Environment. In *Handbook of Advanced Industrial and Hazardous Wastes Management* (pp. 463-482). CRC Press.

Baalousha, M., Wang, J., Erfani, M., & Goharian, E. (2021). Elemental fingerprints in natural nanomaterials determined using SP-ICP-TOF-MS and clustering analysis. *Science of The Total Environment*, *792*, 148426.

Babayigit, A., Ethirajan, A., Muller, M., & Conings, B. (2016). Toxicity of organometal halide perovskite solar cells. *Nature materials*, *15*(3), 247-251.Rabinowitz, M. B. (1991). Toxicokinetics of bone lead. *Environmental health perspectives*, *91*, 33-37.

Babu, S. S., Rao, V. P., Satyasree, N., Ramana, R. V., Mohan, M. R., & Sawant, S. (2021). Mineralogy and geochemistry of the sediments in rivers along the east coast of India: Inferences on weathering and provenance. *Journal of Earth System Science*, *130*(2), 1-24.

Backman, B., Bodiš, D., Lahermo, P., Rapant, S., & Tarvainen, T. (1998). Application of a groundwater contamination index in Finland and Slovakia. *Environmental geology*, *36*(1), 55-64.

Bage, G., Meshram, T., Baswani, S. R., Dora, M. L., Talwar, A. K., Kinker, A. O., ... & Randive, K. (2021). Arsenic, from a Woeful Environmental Hazard to a Wishful Exploration Tool: A Case Study of Arsenic Contaminated Groundwater of Chakariya Area, Singrauli District, Madhya Pradesh, India. In *Innovations in Sustainable Mining* (pp. 115-138). Springer, Cham.

Bakan, G., Özkoç, H. B., Tülek, S., & Cüce1T, H. (2010). Integrated environmental quality assessment of the Kızılırmak River and its coastal environment. *Turkish Journal of Fisheries and Aquatic Sciences*, *10*(4).

Balakumar, P., & Kaur, J. (2009). Arsenic exposure and cardiovascular disorders: an overview. *Cardiovascular toxicology*, *9*(4), 169-176.

Balaram, V. (2019). Rare earth elements: A review of applications, occurrence, exploration, analysis, recycling, and environmental impact. *Geoscience Frontiers*, *10*(4), 1285-1303.

Balasubramanian, B., Meyyazhagan, A., Chinnappan, A. J., Alagamuthu, K. K., Shanmugam, S., Al-Dhabi, N. A., ... & Arasu, M. V. (2020). Occupational health hazards on workers exposure to lead (Pb): A genotoxicity analysis. *Journal of infection and public health*, *13*(4), 527-531.

Balcone-Boissard, H., Michel, A., & Villemant, B. (2009). Simultaneous determination of fluorine, chlorine, bromine and iodine in six geochemical reference materials using pyrohydrolysis, ion chromatography and inductively coupled plasma-mass spectrometry. *Geostandards and Geoanalytical Research*, *33*(4), 477-485.

Balderacchi, M., Benoit, P., Cambier, P., Eklo, O. M., Gargini, A., Gemitzi, A., ... & Trevisan, M. (2013). Groundwater pollution and quality monitoring approaches at the European level. *Critical reviews in environmental science and technology*, *43*(4), 323-408.

Ballmann, G. M., Evans, M. J., Gentner, T. X., Kennedy, A. R., Fulton, J. R., Coles, M. P., & Mulvey, R. E. (2022). Synthesis, Characterization, and Structural Analysis of AM [Al (NONDipp)(H)(SiH2Ph)](AM= Li, Na, K, Rb, Cs) Compounds, Made Via Oxidative Addition of Phenylsilane to Alkali Metal Aluminyls. *Inorganic Chemistry*, *61*(49), 19838-19846.

Bandmann, O., Weiss, K. H., & Kaler, S. G. (2015). Wilson's disease and other neurological copper disorders. *The Lancet Neurology*, *14*(1), 103-113.

Banerjee, P. K. (1975). A reconnaissance survey of the distribution of some trace elements in Indian bauxite. *Mineralium deposita*, *10*(2), 177-188.

Bánfalvi, G. (2011). Heavy metals, trace elements and their cellular effects. In *Cellular effects of heavy metals* (pp. 3-28). Springer, Dordrecht.

Barceloux, D. G., & Barceloux, D. (1999). Nickel. *Journal of toxicology: clinical Toxicology*, *37*(2), 239-258.

Bari, A. F., Lamb, D., Choppala, G., Bolan, N., Seshadri, B., Rahman, M. A., & Rahman, M. M. (2020). Geochemical fractionation and mineralogy of metal (loid) s in abandoned mine soils: Insights into arsenic behaviour and implications to remediation. *Journal of Hazardous Materials*, *399*, 123029.

Barlow, M., & Clarke, T. (2017). *Blue gold: The battle against corporate theft of the world's water*. Routledge.

Barlow, P. M., DeSimone, L. A., & Moench, A. F. (2000). Aquifer response to stream-stage and recharge variations. II. Convolution method and applications. *Journal of Hydrology*, *230*(3-4), 211-229.

Barnhart, J. (1997). Occurrences, uses, and properties of chromium. *Regulatory toxicology and pharmacology*, *26*(1), S3-S7.

Barranquero, R. S., Varni, M. R., Vega, M., Pardo, R., & Ruiz de Galarreta, V. A. (2017). Arsenic, fluoride and other trace elements in the Argentina Pampean plain.

Basha, U. I., Rajasekhar, M., Ghosh, S., Das, P., & Suresh, U. (2022). Spatial assessment of groundwater quality using CCME-WQI and hydrochemical indices: a case study from Talupula Mandal, Ananthapuramu district, South India. *Applied Water Science*, *12*(7), 168.

Basharat, M. (2019). Water management in the Indus Basin in Pakistan: challenges and opportunities. In *Indus River Basin* (pp. 375-388). Elsevier.

Bashir, M. T., Ali, S. A., & Bashir, A. D. (2012). Health effects from exposure to sulphates and chlorides in drinking water. *Pakistan J. of medical and health sciences*, *3*, 648-652.

Battaleb-Looie, S., Moore, F., Jafari, H., Jacks, G., & Ozsvath, D. J. E. E. S. (2012). Hydrogeochemical evolution of groundwaters with excess fluoride concentrations from Dashtestan, South of Iran. *Environmental Earth Sciences*, *67*(4), 1173-1182.

Bayu, T., Kim, H., & Oki, T. (2020). Water governance contribution to water and sanitation access equality in developing countries. *Water Resources Research*, *56*(4), e2019WR025330.

Beard, C. D., van Hinsberg, V. J., Stix, J., & Wilke, M. (2020). The effect of fluorine on clinopyroxene/melt trace-element partitioning. *Contributions to Mineralogy and Petrology*, *175*(5), 44.

Behera, B., & Das, M. (2018). Application of multivariate statistical techniques for the characterization of groundwater quality of Bacheli and Kirandul area, Dantewada district, Chattisgarh. *Journal of the Geological Society of India*, *91*(1), 76-80.

Behera, B., Das, M., & Rana, G. S. (2012). Studies on ground water pollution due to iron content and water quality in and around, Jagdalpur, Bastar district, Chattisgarh, India. *Journal of chemical and Pharmaceutical research*, *4*(8), 3803-3807.

Beiyuan, J., Li, J. S., Tsang, D. C., Wang, L., Poon, C. S., Li, X. D., & Fendorf, S. (2017). Fate of arsenic before and after chemical-enhanced washing of an arsenic-containing soil in Hong Kong. *Science of the total environment*, *599*, 679-688.

Bekesi, G., McGuire, M., & Moiler, D. (2009). Groundwater allocation using a groundwater level response management method—Gnangara groundwater system, Western Australia. *Water resources management*, *23*(9), 1665-1683.

Bennett, H. B., Shantz, A., Shin, G., Sampson, M. L., & Meschke, J. S. (2010). Characterisation of the water quality from open and rope-pump shallow wells in rural Cambodia. *Water Science and Technology*, *61*(2), 473-479.

Bera, B., Bhattacharjee, S., Chamling, M., Ghosh, A., Sengupta, N., & Ghosh, S. (2021). Fluoride dynamics in precambrian hard rock terrain of North Singhbhum Craton and effect of fluorosis on human health and society. In *Groundwater and Society* (pp. 319-348). Springer, Cham.

Bergbäck, B., Johansson, K., & Mohlander, U. (2001). Urban metal flows–a case study of Stockholm. Review and Conclusions. *Water, air and soil pollution: Focus*, *1*(3), 3-24.

Berger, T., Mathurin, F. A., Drake, H., & Åström, M. E. (2016). Fluoride abundance and controls in fresh groundwater in Quaternary deposits and bedrock fractures in an area with fluorine-rich granitoid rocks. *Science of the Total Environment*, *569*, 948-960.

Bergqvist, M., Landström, E., Landström, E., & Luth, S. (2019). Access to geological structures, density, minerals and textures through novel combination of 3D tomography, XRF and sample weight. *ASEG Extended Abstracts*, *2019*(1), 1-3.

Beyer, W. N. (2000). Hazards to wildlife from soil-borne cadmium reconsidered. *Journal of Environmental Quality*, *29*(5), 1380-1384.

Bhanja, S. N., Mukherjee, A., Rangarajan, R., Scanlon, B. R., Malakar, P., & Verma, S. (2019). Long-term groundwater recharge rates across India by in situ measurements. *Hydrology and Earth System Sciences*, *23*(2), 711-722.

Bhargava, D. S. (1985). Expression for drinking water supply standards. *Journal of Environmental Engineering*, *111*(3), 304-316.

Bhatt, A. G., Kumar, A., & Singh, S. K. (2022). Hydro-geochemical evolution of groundwater and associated human health risk in River Sone subbasin of Middle-Gangetic floodplain, Bihar, India. *Arabian Journal of Geosciences*, *15*(5), 405.

Bhattacharjee, S., Chakravarty, S., Maity, S., Dureja, V., & Gupta, K. K. (2005). Metal contents in the groundwater of Sahebgunj district, Jharkhand, India, with special reference to arsenic. *Chemosphere*, *58*(9), 1203-1217.

Bhattacharya, A. K., Sarani, C., Kumar Roy, A., Karthik, D., Singh, A., Kumari, S., & Kumar, P. (2019). An analysis of arsenic contamination in the groundwater of India, Bangladesh and Nepal with a special focus on the stabilisation of arsenic-laden sludge from arsenic filters. *Electronic Journal of Geotechnical Engineering*, *24*(1), 1-34.

Bhattacharya, P., Adhikari, S., Samal, A. C., Das, R., Dey, D., Deb, A., ... & Santra, S. C. (2020). Health risk assessment of co-occurrence of toxic fluoride and arsenic in groundwater of Dharmanagar region, North Tripura (India). *Groundwater for sustainable development*, *11*, 100430.

Bhattacharya, P., Welch, A. H., Stollenwerk, K. G., McLaughlin, M. J., Bundschuh, J., & Panaullah, G. (2007). Arsenic in the environment: biology and chemistry. *Science of the total environment*, *379*(2-3), 109-120.

Bhukte, P. G., Daware, G. T., Masurkar, S. P., Chaddha, M. J., & Agnihotri, A. (2021). Beneficiation of Low-Grade Bauxite: A Case Study of Lateritic Bauxite of India. In *Innovations in Sustainable Mining* (pp. 85-98). Springer, Cham.

Bhukte, P. G., Daware, G. T., Masurkar, S. P., Mahendiran, P., Janbandhu, K., Rao, K. R., ... & Agnihotri, A. (2020). Geochemical, mineralogical and petrological characteristics of Lateritic Bauxite deposits formed on Deccan Trap Basalt with reference to high-level and coastal (low level) deposits of Maharashtra. *Journal of the Geological Society of India*, *95*(6), 587-598.

Bhukte, P. G., Puttewar, S. P., & Agnihotri, A. (2017). Evaluation and beneficiation of Lateritic Bauxite deposits of India. *J Geosci Res*, *1*, 251-256.

Bhuyan, M. S., Bakar, M. A., Akhtar, A., Hossain, M. B., Ali, M. M., & Islam, M. S. (2017). Heavy metal contamination in surface water and sediment of the Meghna River, Bangladesh. *Environmental nanotechnology, monitoring & management*, *8*, 273-279.

Bilotta, G. S., & Brazier, R. E. (2008). Understanding the influence of suspended solids on water quality and aquatic biota. *Water research*, *42*(12), 2849-2861.

Bondu, R., Cloutier, V., Rosa, E., & Benzaazoua, M. (2016). A review and evaluation of the impacts of climate change on geogenic arsenic in groundwater from fractured bedrock aquifers. *Water, Air, & Soil Pollution*, *227*(9), 1-14.

Bondu, R., Cloutier, V., Rosa, E., & Benzaazoua, M. (2017). Mobility and speciation of geogenic arsenic in bedrock groundwater from the Canadian Shield in western Quebec, Canada. *Science of the Total Environment*, *574*, 509-519.

Boni, M., Terracciano, R., Evans, N. J., Laukamp, C., Schneider, J., & Bechstädt, T. (2007). Genesis of vanadium ores in the Otavi Mountainland, Namibia. *Economic Geology*, *102*(3), 441-469.

Borah, K. K., Bhuyan, B., & Sarma, H. P. (2009). Heavy metal contamination of groundwater in the tea garden belt of Darrang district, Assam, India. *E-Journal of Chemistry*, *6*(S1), S501-S507.

Boskabady, M., Marefati, N., Farkhondeh, T., Shakeri, F., Farshbaf, A., & Boskabady, M. H. (2018). The effect of environmental lead exposure on human health and the contribution of inflammatory mechanisms, a review. *Environment international*, *120*, 404-420.

Bouchard, M. F., Sauvé, S., Barbeau, B., Legrand, M., Brodeur, M. È., Bouffard, T., ... & Mergler, D. (2011). Intellectual impairment in school-age children exposed to manganese from drinking water. *Environmental health perspectives*, *119*(1), 138-143.

Bowell, R. J., Alpers, C. N., Jamieson, H. E., Nordstrom, D. K., & Majzlan, J. (2014). The environmental geochemistry of arsenic—an overview—. *Reviews in Mineralogy and Geochemistry*, *79*(1), 1-16.

Bowen, N. L., & Wyckoff, R. W. G. (1926). A petrographic and X-ray study of the thermal dissociation of dumortierite. *Journal of the Washington Academy of Sciences*, *16*(7), 178-189.

Bowler, R. M., Roels, H. A., Nakagawa, S., Drezgic, M., Diamond, E., Park, R., ... & Doty, R. L. (2007). Dose–effect relationships between manganese exposure and neurological, neuropsychological and pulmonary function in confined space bridge welders. *Occupational and environmental medicine*, *64*(3), 167-177.

Boyle, D. R. (1992). Effects of base exchange softening on fluoride uptake in groundwaters of the Moncton Sub-Basin, New Brunswick, Canada. In *International symposium on water-rock interaction* (pp. 771-774).

Brindha, K., Rajesh, R., Murugan, R., & Elango, L. (2011). Fluoride contamination in groundwater in parts of Nalgonda District, Andhra Pradesh, India. *Environmental Monitoring and Assessment*, *172*(1), 481-492.

Brindha, K., Vaman, K. N., Srinivasan, K., Babu, M. S., & Elango, L. (2014). Identification of surface water-groundwater interaction by hydrogeochemical indicators and assessing its suitability for drinking and irrigational purposes in Chennai, Southern India. *Applied Water Science*, *4*(2), 159-174.

Brown, R. M., McClelland, N. I., Deininger, R. A., & Tozer, R. G. (1970). A water quality index-do we dare. *Water and sewage works*, *117*(10).

Brunke, M., & Gonser, T. O. M. (1997). The ecological significance of exchange processes between rivers and groundwater. *Freshwater biology*, *37*(1), 1-33.

Bucci, A., Barbero, D., Lasagna, M., Forno, M. G., & De Luca, D. A. (2017). Shallow groundwater temperature in the Turin area (NW Italy): vertical distribution and anthropogenic effects. *Environmental Earth Sciences*, *76*(5), 1-14.

Bucher, K., & Stober, I. (2002). Water-rock reaction experiments with Black Forest gneiss and granite. In *Water-Rock Interaction* (pp. 61-95). Springer, Dordrecht.

Bunaciu, A. A., UdriŞTioiu, E. G., & Aboul-Enein, H. Y. (2015). X-ray diffraction: instrumentation and applications. *Critical reviews in analytical chemistry*, *45*(4), 289-299.

Buragohain, M., Bhuyan, B., & Sarma, H. P. (2010). Seasonal variations of lead, arsenic, cadmium and aluminium contamination of groundwater in Dhemaji district, Assam, India. *Environmental monitoring and assessment*, *170*(1), 345-351.

Bureau of Indian Standards (BIS) (2012), Bur. Indian Stand. IS 10500, 1.

Burlingame, G. A., Dietrich, A. M., & Whelton, A. J. (2007). Understanding the basics of tap water taste. *Journal-American Water Works Association*, *99*(5), 100-111.

Burness, H. S., & Brill, T. C. (2001). The role for policy in common pool groundwater use. *Resource and energy economics*, *23*(1), 19-40.Press.

Butt, C. R., Lintern, M. J., & Anand, R. R. (2000). Evolution of regoliths and landscapes in deeply weathered terrain—implications for geochemical exploration. *Ore Geology Reviews*, *16*(3-4), 167-183.

Bux, R. K., Haider, S. I., Batool, M., Solangi, A. R., Shah, Z., Karimi-Maleh, H., & Sen, F. (2021). Assessment of heavy metal contamination and its sources in urban soils of

district Hyderabad, Pakistan using GIS and multivariate analysis. *International Journal of Environmental Science and Technology*, 1-13.

Byers, H. L., McHenry, L. J., & Grundl, T. J. (2019). XRF techniques to quantify heavy metals in vegetables at low detection limits. *Food Chemistry: X*, *1*, 100001.

Cai, J., Liu, J., Gao, Z., Navrotsky, A., & Suib, S. L. (2001). Synthesis and anion exchange of tunnel structure akaganeite. *Chemistry of Materials*, *13*(12), 4595-4602.

Calvert, C. S., Palkowsky, D. A., & Pevear, D. R. (1989). A combined X-ray powder diffraction and chemical method for the quantitative mineral analysis of geologic samples.

Camp, K. F. (2011). Geochemical Evolution of Pegmatites as Monitored by Select Indicator Elements. In *Earth and Environmental Sciences, University of New Orleans, Slidell, LA. Presentation at AAPG Annual Convention and Exhibition, Houston, Textas, USA.*

Campbell, R., Bakker, M. G., Havrilla, G., Montoya, V., Kenik, E. A., & Shamsuzzoha, M. (2006). Preparation of mesoporous silica templated metal nanowire films on foamed nickel substrates. *Microporous and mesoporous materials*, *97*(1-3), 114-121.

Canora, F., Fidelibus, M. D., Sciortino, A., & Spilotro, G. (2008). Variation of infiltration rate through karstic surfaces due to land use changes: A case study in Murgia (SE-Italy). *Engineering Geology*, *99*(3-4), 210-227.

Cao, X., Ma, L., Liang, Y., Gao, B., & Harris, W. (2011). Simultaneous immobilization of lead and atrazine in contaminated soils using dairy-manure biochar. *Environmental science & technology*, *45*(11), 4884-4889.

Caricchi, L., Simpson, G., & Schaltegger, U. (2014). Zircons reveal magma fluxes in the Earth's crust. *Nature*, *511*(7510), 457-461.

Castillo-Nava, D., Elias-Santos, M., López-Chuken, U. J., Valdés-González, A., de la Riva-Solís, L. G., Vargas-Pérez, M. P., ... & Luna-Olvera, H. A. (2020). Heavy metals (lead, cadmium and zinc) from street dust in Monterrey, Mexico: ecological risk index. *International Journal of Environmental Science and Technology*, *17*(6), 3231-3240.

Castillo-Oliver, M., Giuliani, A., Griffin, W. L., O'Reilly, S. Y., Thomassot, E., & Drysdale, R. N. (2017, September). New constraints on the origin of carbonates in kimberlites integrating petrography, mineral chemistry and in situ stable isotope analysis. In *International Kimberlite Conference: Extended Abstracts* (Vol. 11).

Cempel, M., & Nikel, G. J. P. J. S. (2006). Nickel: a review of its sources and environmental toxicology. *Polish Journal of Environmental Studies*, *15*(3).

Central Ground Water Board (CGWB) website, FAQs, http://www.cgwb.gov.in/faq.html.

Central Groundwater Board, 2011: Ground water scenario in major cities of India. Indian Ministry of Water Resources Rep., 229 pp.

Central Water Commission (CWC), Water and Related Statistics, April 2015, http://www.cwc.gov.in/main/downloads/Water%20&%20Related%20Statistics%20 2015.pdf

Cerklewski, F. L. (1997). Fluoride bioavailability—nutritional and clinical aspects. *Nutrition research*, *17*(5), 907-929.

CGWB (Central Ground Water Board), 2010. Ground Water Quality in Shallow Aquifers of India. Ministry of Water Resources, Govt. of India.

Chabukdhara, M., & Nema, A. K. (2012). Assessment of heavy metal contamination in Hindon River sediments: a chemometric and geochemical approach. *Chemosphere*, *87*(8), 945-953.

Chadha, D. K. (1999). A proposed new diagram for geochemical classification of natural waters and interpretation of chemical data. *Hydrogeology journal*, *7*(5), 431-439.

Chae, G. T., Yun, S. T., Kwon, M. J., Kim, Y. S., & Mayer, B. (2006). Batch dissolution of granite and biotite in water: Implication for fluorine geochemistry in groundwater. *Geochemical Journal*, *40*(1), 95-102.

Chahal, C., Van Den Akker, B., Young, F., Franco, C., Blackbeard, J., & Monis, P. (2016). Pathogen and particle associations in wastewater: significance and implications for treatment and disinfection processes. *Advances in applied microbiology*, *97*, 63-119.

Chakrabarty, S., & Sarma, H. P. (2011). Heavy metal contamination of drinking water in Kamrup district, Assam, India. *Environmental monitoring and assessment*, *179*(1), 479-486.

Chakraborti, D., Biswas, B. K., Chowdhury, T. R., Basu, G. K., Mandal, B. K., Chowdhury, U. K., ... & Rathore, K. C. (1999). Arsenic groundwater contamination and sufferings of people in Rajnandgaon district, Madhya Pradesh, India. *Current science*, *77*(4), 502-504.

Chakraborti, D., Rahman, M. M., Ahamed, S., Dutta, R. N., Pati, S., & Mukherjee, S. C. (2016a). Arsenic contamination of groundwater and its induced health effects in Shahpur block, Bhojpur district, Bihar state, India: risk evaluation. *Environmental Science and Pollution Research*, *23*(10), 9492-9504.

Chakraborti, D., Rahman, M. M., Chatterjee, A., Das, D., Das, B., Nayak, B., ... & Kar, P. B. (2016b). Fate of over 480 million inhabitants living in arsenic and fluoride endemic Indian Districts: Magnitude, health, socio-economic effects and mitigation approaches. *Journal of Trace Elements in Medicine and Biology*, *38*, 33-45.

Chakraborti, D., Rahman, M. M., Das, B., Nayak, B., Pal, A., Sengupta, M. K., ... & Quamruzzaman, Q. (2013). Groundwater arsenic contamination in Ganga–Meghna–Brahmaputra plain, its health effects and an approach for mitigation. *Environmental earth sciences*, *70*(5), 1993-2008.

Chakraborti, D., Singh, E. J., Das, B., Shah, B. A., Hossain, M. A., Nayak, B., ... & Singh, N. R. (2008). Groundwater arsenic contamination in Manipur, one of the seven North-Eastern hill states of India: a future danger. *Environmental Geology*, *56*(2), 381-390.

Chakraborty, M., Mukherjee, A., & Ahmed, K. M. (2015). A review of groundwater arsenic in the Bengal Basin, Bangladesh and India: from source to sink. *Current Pollution Reports*, *1*, 220-247.

Chala, D. B., & Emire, S. A. (2021). X-Ray Diffraction and Patterns: Diffraction Techniques Application for Food Quality Assurance in Bio-Food Industry.

Chandio, T. A., Khan, M. N., Muhammad, M. T., Yalcinkaya, O., Wasim, A. A., & Kayis, A. F. (2021). Fluoride and arsenic contamination in drinking water due to mining activities and its impact on local area population. *Environmental Science and Pollution Research*, *28*(2), 2355-2368.

Chandrajith, R., Diyabalanage, S., & Dissanayake, C. B. (2020). Geogenic fluoride and arsenic in groundwater of Sri Lanka and its implications to community health. *Groundwater for sustainable development*, *10*, 100359.

Chandrajith, R., Padmasiri, J. P., Dissanayake, C. B., & Prematilaka, K. M. (2012). Spatial distribution of fluoride in groundwater of Sri Lanka. *Journal of the National Science Foundation of Sri Lanka*, *40*(4).

Chandrasekar, N., Selvakumar, S., Srinivas, Y., Wilson, J. J., Peter, T. S., & Magesh, N. S. (2014). Hydrogeochemical assessment of groundwater quality along the coastal aquifers of southern Tamil Nadu, India. *Environmental earth sciences*, *71*(11), 4739-4750.

Charlatchka, R., & Cambier, P. (2000). Influence of reducing conditions on solubility of trace metals in contaminated soils. *Water, Air, and Soil Pollution*, *118*(1), 143-168.

Chasapis, C. T., Loutsidou, A. C., Spiliopoulou, C. A., & Stefanidou, M. E. (2012). Zinc and human health: an update. *Archives of toxicology*, *86*(4), 521-534.

Chashschin, V. P., Artunina, G. P., & Norseth, T. (1994). Congenital defects, abortion and other health effects in nickel refinery workers. *Science of the total environment*, *148*(2-3), 287-291.

Chatterjee, R., & Purohit, R. R. (2009). Estimation of replenishable groundwater resources of India and their status of utilization. *Current science*, 1581-1591.

Chaturvedi, N., Ahmed, M., & Dhal, N. K. (2014). Effects of iron ore tailings on growth and physiological activities of Tagetes patula L. *Journal of soils and sediments*, *14*(4), 721-730.

Chauhan, A., & Chauhan, P. (2014). Powder XRD technique and its applications in science and technology. *J Anal Bioanal Tech*, *5*(5), 1-5.

Chen, Jun, Xuemin Chen, Kedi Yang, Tao Xia, and Hong Xie. "Studies on DNA damage and apoptosis in rat brain induced by fluoride." *Zhonghua yu Fang yi xue za zhi [Chinese Journal of Preventive Medicine]* 36, no. 4 (2002): 222-224.

Chen, Q., Hao, D., Gao, Z., Shi, M., Wang, M., Feng, J., ... & Yu, Y. (2020). The enrichment process of groundwater fluorine in sea water intrusion area of Gaomi City, China. *Groundwater*, *58*(6), 882-891.

Chen, S. H., Li, Y. X., Li, P. H., Xiao, X. Y., Jiang, M., Li, S. S., ... & Liu, W. Q. (2018). Electrochemical spectral methods for trace detection of heavy metals: A review. *TrAC Trends in Analytical Chemistry*, *106*, 139-150.

Chen, Z., Wang, Y., Xia, D., Jiang, X., Fu, D., Shen, L., ... & Li, Q. B. (2016). Enhanced bioreduction of iron and arsenic in sediment by biochar amendment influencing microbial community composition and dissolved organic matter content and composition. *Journal of Hazardous materials*, *311*, 20-29.

Cheng, H., Hu, Y., Luo, J., Xu, B., & Zhao, J. (2009). Geochemical processes controlling fate and transport of arsenic in acid mine drainage (AMD) and natural systems. *Journal of hazardous materials*, *165*(1-3), 13-26.

Chetia, M., Chatterjee, S., Banerjee, S., Nath, M. J., Singh, L., Srivastava, R. B., & Sarma, H. P. (2011). Groundwater arsenic contamination in Brahmaputra river basin: a water quality assessment in Golaghat (Assam), India. *Environmental monitoring and assessment*, *173*(1), 371-385.

Chicas, S. D., Omine, K., Prabhakaran, M., Sunitha, T. G., & Sivasankar, V. (2022). High fluoride in groundwater and associated non-carcinogenic risks at Tiruvannamalai region in Tamil Nadu, India. *Ecotoxicology and Environmental Safety*, *233*, 113335.

Chidambaram, S., Anandhan, P., Prasanna, M. V., Thivya, C., Thilagavathi, R., & Sarathidasan, J. (2014). Geochemical evaluation of fluoride contamination of groundwater in the Thoothukudi District of Tamilnadu, India. *Applied Water Science*, *4*(3), 241-250.

Chidambaram, S., Karmegam, U., Prasanna, M. V., & Sasidhar, P. (2012). A study on evaluation of probable sources of heavy metal pollution in groundwater of Kalpakkam region, South India. *The Environmentalist*, *32*(4), 371-382.

Chidambaram, S., Sarathidasan, J., Srinivasamoorthy, K., Thivya, C., Thilagavathi, R., Prasanna, M. V., ... & Nepolian, M. (2018). Assessment of hydrogeochemical status of groundwater in a coastal region of Southeast coast of India. *Applied water science*, *8*(1), 1-14.

Chinnasamy, P., & Agoramoorthy, G. (2015). Groundwater storage and depletion trends in Tamil Nadu State, India. *Water Resources Management*, *29*(7), 2139-2152.

Chinnasamy, P., Hubbart, J. A., & Agoramoorthy, G. (2013). Using remote sensing data to improve groundwater supply estimations in Gujarat, India. *Earth Interactions*, *17*(1), 1-17.

Chinnasamy, P., Maheshwari, B., Dillon, P., Purohit, R., Dashora, Y., Soni, P., & Dashora, R. (2018). Estimation of specific yield using water table fluctuations and cropped area in a hardrock aquifer system of Rajasthan, India. *Agricultural Water Management*, *202*, 146-155.

Chitsazan, M., Dorraninejad, M. S., Zarasvandi, A., & Mirzaii, S. Y. (2009). Occurrence, distribution and source of arsenic in deep groundwater wells in Maydavood area, southwestern Iran. *Environmental geology*, *58*(4), 727-737.

Choi, A. L., Sun, G., Zhang, Y., & Grandjean, P. (2012). Developmental fluoride neurotoxicity: a systematic review and meta-analysis. *Environmental health perspectives*, *120*(10), 1362-1368.

Chong, T. F. (2019). Mineralogy and petrology of a drill core section from Borg, SW Norrköping–fracture fillings and tentative mineral reactions.

Chowdhury, A., & Maiti, S. K. (2016). Assessing the ecological health risk in a conserved mangrove ecosystem due to heavy metal pollution: A case study from Sundarbans Biosphere Reserve, India. *Human and Ecological Risk Assessment: An International Journal*, *22*(7), 1519-1541.

Chowdhury, A., Adak, M. K., Mukherjee, A., Dhak, P., Khatun, J., & Dhak, D. (2019). A critical review on geochemical and geological aspects of fluoride belts, fluorosis and natural materials and other sources for alternatives to fluoride exposure. *Journal of Hydrology*, *574*, 333-359.

Chung, J. Y., Yu, S. D., & Hong, Y. S. (2014). Environmental source of arsenic exposure. *Journal of preventive medicine and public health*, *47*(5), 253.

Churchill, H.V., Rowley, R.J. and Martin, L.N. (1948) Fluorine content of certain vegetation in Western Pennsylvania area. Anal. Chem., 20 (1), 69–71.

Cimbolakova, I., Uher, I., Lakticova, K. V., Vargova, M., Kimakova, T., & Papajova, I. (2020). Heavy metals and the environment. *Environ. Factors Affect. Hum. Heal*, *10*.

Col, M., Çöl, C., Soran, A., Sayli, B. S., & Oztürk, S. (1999). Arsenic-related Bowen's disease, palmar keratosis, and skin cancer. *Environmental Health Perspectives*, *107*(8), 687-689.

Coomar, P., Mukherjee, A., Bhattacharya, P., Bundschuh, J., Verma, S., Fryar, A. E., ... & Thunvik, R. (2019). Contrasting controls on hydrogeochemistry of arsenic-enriched groundwater in the homologous tectonic settings of Andean and Himalayan basin aquifers, Latin America and South Asia. *Science of the Total Environment*, *689*, 1370-1387.

Coudert, L., Bondu, R., Rakotonimaro, T. V., Rosa, E., Guittonny, M., & Neculita, C. M. (2020). Treatment of As-rich mine effluents and produced residues stability: Current knowledge and research priorities for gold mining. *Journal of hazardous materials*, *386*, 121920.

Cox, B. A. (2003). A review of dissolved oxygen modelling techniques for lowland rivers. *Science of the Total Environment*, *314*, 303-334.

Creelman, R. A., & Ward, C. R. (1996). A scanning electron microscope method for automated, quantitative analysis of mineral matter in coal. *International Journal of Coal Geology*, *30*(3), 249-269.

Crossgrove, J., & Zheng, W. (2004). Manganese toxicity upon overexposure. *NMR in Biomedicine: An International Journal Devoted to the Development and Application of Magnetic Resonance In Vivo*, *17*(8), 544-553.

Cude, C. G. (2001). Oregon water quality index a tool for evaluating water quality management effectiveness 1. *JAWRA Journal of the American Water Resources Association*, *37*(1), 125-137.

Cui, H., Fan, Y., Yang, J., Xu, L., Zhou, J., & Zhu, Z. (2016). In situ phytoextraction of copper and cadmium and its biological impacts in acidic soil. *Chemosphere*, *161*, 233-241.

Cui, P., & Qin, B. (2022). Removal and Recycling of Fluoride from Wastewater from a Nonferrous Metallurgy Plant. *JOM*, *74*(8), 3111-3118.

Cui, Y., Chen, J., Zhang, Y., Peng, D., Huang, T., & Sun, C. (2019). pH-dependent leaching characteristics of major and toxic elements from red mud. *International Journal of Environmental Research and Public Health*, *16*(11), 2046.

Custodio, E. (2002). Aquifer overexploitation: what does it mean? *Hydrogeology journal*, *10*(2), 254-277.

Da Silva, A. L. C., Urbano, M. R., Almeida Lopes, A. C. B. D., Carvalho, M. D. F. H., Buzzo, M. L., Peixe, T. S., ... & Paoliello, M. M. B. (2017). Blood manganese levels and associated factors in a population-based study in Southern Brazil. *Journal of Toxicology and Environmental Health, Part A*, *80*(19-21), 1064-1077.

Daigavane, V. V., & Gaikwad, M. A. (2017). Water quality monitoring system based on IoT. *Advances in wireless and mobile communications*, *10*(5), 1107-1116.

Dalin, C., Wada, Y., Kastner, T., & Puma, M. J. (2017). Groundwater depletion embedded in international food trade. *Nature*, *543*(7647), 700-704.

Danielopol, D. L., Griebler, C., Gunatilaka, A., & Notenboom, J. (2003). Present state and future prospects for groundwater ecosystems. *Environmental conservation*, *30*(2), 104-130.

Das, B., Hazarika, P., Saikia, G., Kalita, H., Goswami, D. C., Das, H. B., ... & Dutta, R. K. (2007). Removal of iron from groundwater by ash: A systematic study of a traditional method. *Journal of Hazardous materials*, *141*(3), 834-841.

Das, D., Samanta, G., Mandal, B. K., Roy Chowdhury, T., Chanda, C. R., Chowdhury, P. P., ... & Chakraborti, D. (1996). Arsenic in groundwater in six districts of West Bengal, India. *Environmental Geochemistry and Health*, *18*(1), 5-15.

Das, K. K., Das, S. N., & Dhundasi, S. A. (2008). Nickel, its adverse health effects & oxidative stress. *Indian journal of medical research*, *128*(4), 412.

Das, N., Das, A., Sarma, K. P., & Kumar, M. (2018). Provenance, revalence and health perspective of co-occurrences of arsenic, fluoride and uranium in the aquifers of the Brahmaputra River floodplain. *Chemosphere*, *194*, 755-772.

Das, N., Deka, J. P., Shim, J., Patel, A. K., Kumar, A., Sarma, K. P., & Kumar, M. (2016). Effect of river proximity on the arsenic and fluoride distribution in the aquifers of the Brahmaputra floodplains, Assam, northeast India. *Groundwater for Sustainable Development*, *2*, 130-142.

Das, N., Paul, S., Chatterjee, D., Banerjee, N., Majumder, N. S., Sarma, N., ... & Giri, A. K. (2012). Arsenic exposure through drinking water increases the risk of liver and cardiovascular diseases in the population of West Bengal, India. *BMC public health*, *12*(1), 1-9.

Dash, B., & Rath, S. S. (2020). Density functional theory and molecular dynamics insights into the site-dependent adsorption of hydrogen fluoride on kaolinite. *Journal of Molecular Liquids*, *299*, 112265.

Davey, W. P. (1925). The lattice parameter and density of pure tungsten. *Physical Review*, *26*(6), 736.

Davis, H. T., Aelion, C. M., Lawson, A. B., Cai, B., & McDermott, S. (2014). Associations between land cover categories, soil concentrations of arsenic, lead and barium, and population race/ethnicity and socioeconomic status. *Science of the total environment*, *490*, 1051-1056.

De Boer, D. K. G., & Chauvineau, J. P. (1994). Europhysics Industrial Workshop: Exploiting X-rays at the Nanoscale Continues to Challenge. *Europhysics News*, *25*(1), 13-14.

De, A., Mridha, D., Joardar, M., Das, A., Chowdhury, N. R., & Roychowdhury, T. (2022). Distribution, prevalence and health risk assessment of fluoride and arsenic in groundwater from lower Gangetic plain in West Bengal, India. *Groundwater for Sustainable Development*, *16*, 100722.

Dehbandi, R., Moore, F., & Keshavarzi, B. (2018). Geochemical sources, hydrogeochemical behavior, and health risk assessment of fluoride in an endemic fluorosis area, central Iran. *Chemosphere*, *193*, 763-776.

del Pilar Alvarez, M., & Carol, E. (2019). Geochemical occurrence of arsenic, vanadium and fluoride in groundwater of Patagonia, Argentina: sources and mobilization processes. *Journal of South American Earth Sciences*, *89*, 1-9.

Delong, S. E. (1974). Distribution of Rb, Sr and Ni in igneous rocks, central and western Aleutian Islands, Alaska. *Geochimica et Cosmochimica Acta*, *38*(2), 245-266.

Desai, V., & Kaler, S. G. (2008). Role of copper in human neurological disorders. *The American journal of clinical nutrition*, *88*(3), 855S-858S.

Deshmukh, A. N., Wadaskar, P. M., & Malpe, D. B. (1995). Fluorine in environment: A review. *Gondwana Geol. Mag*, *9*, 1-20.

Deutsch, W. J. (2020). *Groundwater geochemistry: fundamentals and applications to contamination*. CRC press.

Devaraj, N., Chidambaram, S., Vasudevan, U., Pradeep, K., Nepolian, M., Prasanna, M. V., ... & Panda, B. (2020). Determination of the major geochemical processes of groundwater along the Cretaceous-Tertiary boundary of Trichinopoly, Tamilnadu, India. *Acta Geochimica*, *39*, 760-781.

Devi, N. L., Ch, Y. I., & Shihua, Q. I. (2009). Recent status of arsenic contamination in groundwater of northeastern India–a review.

Devic, G., Djordjevic, D., & Sakan, S. (2014). Natural and anthropogenic factors affecting the groundwater quality in Serbia. *Science of the Total Environment*, *468*, 933-942.

Dey, S., Kumar, A., Mondal, P. K., Chopra, D., Roy, R., Jindani, S., ... & Jain, V. K. (2022). Ultrasensitive colorimetric detection of fluoride and arsenate in water and mammalian cells using recyclable metal oxacalixarene probe: a lateral flow assay. *Scientific Reports*, *12*(1), 17119.

Dey, T. K., Banerjee, P., Bakshi, M., Kar, A., & Ghosh, S. (2014). Groundwater arsenic contamination in West Bengal: current scenario, effects and probable ways of mitigation. *International Letters of Natural Sciences*, *8*(1).

Dharmaratne, R. W. (2019). Exploring the role of excess fluoride in chronic kidney disease: a review. *Human & experimental toxicology*, *38*(3), 269-279.

Dickson, A. J., Idiz, E., Porcelli, D., & van den Boorn, S. H. (2020). The influence of thermal maturity on the stable isotope compositions and concentrations of molybdenum, zinc and cadmium in organic-rich marine mudrocks. *Geochimica et Cosmochimica Acta*, *287*, 205-220.

Dietrich, A. M., Glindemann, D., Pizarro, F., Gidi, V., Olivares, M., Araya, M., ... & Edwards, M. (2004). Health and aesthetic impacts of copper corrosion on drinking water. *Water Science and Technology*, *49*(2), 55-62.

Diljo Jose, T., Vidyasagaran, K., & Babu, J. 2014) Fluoride contamination of ground water and fluorosis among school students of Eruthempathy Panchayat, Palakkad District, Kerala, India. Eco. Env. & Cons. 20 (2), 507-510.

Dill, H. G., Kaufhold, S., Lindenmaier, F., Dohrmann, R., Ludwig, R., & Botz, R. (2013). Joint clay–heavy–light mineral analysis: a tool to investigate the hydrographic–hydraulic regime of Late Cenozoic deltaic inland fans under changing climatic conditions (Cuvelai-Etosha Basin, Namibia). *International Journal of Earth Sciences*, *102*(1), 265-304.

Dissanayake, C. B., & Chandrajith, R. (2019). Fluoride and hardness in groundwater of tropical regions-review of recent evidence indicating tissue calcification and calcium phosphate nanoparticle formation in kidney tubules. *Ceylon Journal of Science*, *48*(3), 197-207.

Dogra, N., Sharma, M., Sharma, A., Keshavarzi, A., Minakshi, Bhardwaj, R., ... & Kumar, V. (2020). Pollution assessment and spatial distribution of roadside agricultural soils: a case study from India. *International journal of environmental health research*, *30*(2), 146-159.

Doll, P., Mueller Schmied, H., Schuh, C., Portmann, F. T., & Eicker, A. (2014). Global-scale assessment of groundwater depletion and related groundwater abstractions: Combining hydrological modeling with information from well observations and GRACE satellites. *Water Resources Research*, *50*(7), 5698-5720.

Dong, Y., Zeng, W., Lin, H., & He, Y. (2020). Preparation of a novel water-soluble organosilane coating and its performance for inhibition of pyrite oxidation to control acid mine drainage at the source. *Applied Surface Science*, *531*, 147328.

Doull, J., Boekelheide, K., Farishian, B. G., Isaacson, R. L., Klotz, J. B., Kumar, J. V., ... & Webster, T. F. (2006). Fluoride in drinking water: a scientific review of EPA's standards. *National Academies, Washington*, 205-223.

Du, B., Zhou, J., Lu, B., Zhang, C., Li, D., Zhou, J., ... & Zhang, H. (2020). Environmental and human health risks from cadmium exposure near an active lead-zinc mine and a copper smelter, China. *Science of The Total Environment*, *720*, 137585.

Dubey, M., Deshpande, S., Gaikwad, S., Gaikwad, G., & Dongre, A. (2021). Lithological controls on the groundwater fluoride enrichment in central India. *Arabian Journal of Geosciences*, *14*, 1-19.

Duda-Chodak, A., & Blaszczyk, U. (2008). The impact of nickel on human health. *Journal of Elementology*, *13*(4), 685-693.

Duraisamy, S., Govindhaswamy, V., Duraisamy, K., Krishinaraj, S., Balasubramanian, A., & Thirumalaisamy, S. (2019). Hydrogeochemical characterization and evaluation of groundwater quality in Kangayam taluk, Tirupur district, Tamil Nadu, India, using GIS techniques. *Environmental Geochemistry and Health*, *41*(2), 851-873.

Durov, S. A. (1948). Natural waters and graphic representation of their composition. In *Dokl Akad Nauk SSSR* (Vol. 59, No. 3, pp. 87-90).

Durrani, T. S., & Farooqi, A. (2021). Groundwater fluoride concentrations in the watershed sedimentary basin of Quetta Valley, Pakistan. *Environmental Monitoring and Assessment*, *193*(10), 1-18.

Duruibe, J. O., Ogwuegbu, M. O. C., & Egwurugwu, J. N. (2007). Heavy metal pollution and human biotoxic effects. *International Journal of physical sciences*, *2*(5), 112-118.

Duverger, A., Berg, J. S., Busigny, V., Guyot, F., Bernard, S., & Miot, J. (2020). Mechanisms of pyrite formation promoted by sulfate-reducing bacteria in pure culture. *Frontiers in Earth Science*, *8*, 588310.

Duvert, C., Priadi, C. R., Rose, A. M., Abdillah, A., Marthanty, D. R., Gibb, K. S., & Kaestli, M. (2019). Sources and drivers of contamination along an urban tropical river (Ciliwung, Indonesia): Insights from microbial DNA, isotopes and water chemistry. *Science of the Total Environment*, *682*, 382-393.

Ebel, H. (1986). X-Ray Fluorescence Analysis (XRP) in Europe. *Advances in X-Ray Analysis*, *30*, 7-11.

Ebrahimi, A., Ehrampoush, M. H., Ghaneian, M. T., Davoudi, M., Hashemi, H., & Behzadi, S. (2010). The survey chemical quality of ground water in the vicinity of sanitary landfill of Yazd in 2008.

Edmunds, W. M., & Smedley, P. L. (2013). Fluoride in natural waters. In *Essentials of medical geology* (pp. 311-336). Springer, Dordrecht.

Egbe, E. R., Nsonwu-Anyanwu, A. C., Offor, S. J., Usoro, C. A. O., Etukudo, M. H., & Egbe, D. I. (2017). Element content of surface and underground water sources around a cement factory site in Calabar, Nigeria. *Iranian Journal of Toxicology*, *11*(1), 19-25.

Ekere, N. R., Agbazue, V. E., Ngang, B. U., & Ihedioha, J. N. (2019). Hydrochemistry and Water Quality Index of groundwater resources in Enugu north district, Enugu, Nigeria. *Environmental monitoring and assessment*, *191*(3), 1-15.

El Bedawy, R. (2014). Water resources management: alarming crisis for Egypt. J. Mgmt. & Sustainability, 4, 108.

Eldaw, E., Huang, T., Elubid, B., Khalifa Mahamed, A., & Mahama, Y. (2020). A Novel approach for indexing heavy metals pollution to assess groundwater quality for drinking purposes. *International Journal of Environmental Research and Public Health*, *17*(4), 1245.

El-Desoky, H. M., Tende, A. W., Abdel-Rahman, A. M., Ene, A., Awad, H. A., Fahmy, W., ... & Zakaly, H. M. (2022). Hydrothermal alteration mapping using landsat 8 and ASTER data and geochemical characteristics of Precambrian rocks in the Egyptian shield: A Case Study from Abu Ghalaga, Southeastern Desert, Egypt. *Remote Sensing*, *14*(14), 3456.

Elizondo-Álvarez, M. A., Uribe-Salas, A., & Nava-Alonso, F. (2020). Flotation studies of galena (PbS), cerussite (PbCO3) and anglesite (PbSO4) with hydroxamic acids as collectors. *Minerals Engineering*, *155*, 106456.

Ellis, D., Bouchard, C., & Lantagne, G. (2000). Removal of iron and manganese from groundwater by oxidation and microfiltration. *Desalination*, *130*(3), 255-264.

Elumalai, V., Brindha, K., & Lakshmanan, E. (2017a). Human exposure risk assessment due to heavy metals in groundwater by pollution index and multivariate statistical methods: a case study from South Africa. *Water*, *9*(4), 234.

Elumalai, V., Brindha, K., Sithole, B., & Lakshmanan, E. (2017b). Spatial interpolation methods and geostatistics for mapping groundwater contamination in a coastal area. *Environmental Science and Pollution Research*, *24*(12), 11601-11617.

Elumalai, V., Nwabisa, D. P., & Rajmohan, N. (2019). Evaluation of high fluoride contaminated fractured rock aquifer in South Africa–Geochemical and chemometric approaches. *Chemosphere*, *235*, 1-11.

Emsley, J. (2006). *The elements of murder: a history of poison*. Oxford University Press.

Enalou, H. B., Moore, F., Keshavarzi, B., & Zarei, M. (2018). Source apportionment and health risk assessment of fluoride in water resources, south of Fars province, Iran: Stable isotopes (δ18O and δD) and geochemical modeling approaches. *Applied Geochemistry*, *98*, 197-205.

Ene, A., Bosneaga, A., & Georgescu, L. (2010). Determination of heavy metals in soils using XRF technique. *Rom. Journ. Phys*, *55*(7-8), 815-820.

Epp, J. (2016). X-ray diffraction (XRD) techniques for materials characterization. In *Materials characterization using nondestructive evaluation (NDE) methods* (pp. 81-124). Woodhead Publishing.

Eskelsen, E., Catelan, A., Hernades, N. M. A. P., Soares, L. E. S., Cavalcanti, A. N., Aguiar, F. H. B., & Liporoni, P. C. S. (2018). Physicochemical changes in enamel submitted

to pH cycling and bleaching treatment. *Clinical, cosmetic and investigational dentistry*, *10*, 281.

Etuk, E. U., Igbokwe, V., Ajagbonna, O. P., & Egua, M. O. (2008). Heavy Metals and Microbial Contaminants in a Commercial Polyherbal Product in Nigeria. *Nigerian Journal of Basic and Applied Sciences*, *16*(2), 197-202.

Ezaki, S., Gastmans, D., Iritani, M. A., Santos, V. D., & Stradioto, M. R. (2020). Geochemical evolution, residence times and recharge conditions of the multilayered Tubarão aquifer system (State of São Paulo–Brazil) as indicated by hydrochemical, stable isotope and 14C data. *Isotopes in Environmental and Health Studies*, *56*(5-6), 495-512.

Fadiran, A. O., Dlamini, S. C., & Mavuso, A. (2008). A comparative study of the phosphate levels in some surface and ground water bodiesof Swaziland. *Bulletin of the Chemical Society of Ethiopia*, *22*(2).

Fakhreddine, S., Prommer, H., Scanlon, B. R., Ying, S. C., & Nicot, J. P. (2021). Mobilization of arsenic and other naturally occurring contaminants during managed aquifer recharge: a critical review. *Environmental Science & Technology*, *55*(4), 2208-2223.

Fang, Y., Koba, K., Makabe, A., Takahashi, C., Zhu, W., Hayashi, T., ... & Yoh, M. (2015). Microbial denitrification dominates nitrate losses from forest ecosystems. *Proceedings of the National Academy of Sciences*, *112*(5), 1470-1474.

Farooqi, A., Masuda, H., Siddiqui, R., & Naseem, M. (2009). Sources of arsenic and fluoride in highly contaminated soils causing groundwater contamination in Punjab, Pakistan. *Archives of environmental contamination and toxicology*, *56*(4), 693-706.

Fawell, J., & Ong, C. N. (2012). Emerging contaminants and the implications for drinking water. *International Journal of Water Resources Development*, *28*(2), 247-263.

Fayet-Moore, F., Wibisono, C., Carr, P., Duve, E., Petocz, P., Lancaster, G., ... & Blumfield, M. (2020). An analysis of the mineral composition of Pink Salt available in Australia. *Foods*, *9*(10), 1490.

Feng, Y., Chu, G., Xiao, B., Li, R., Deng, C., Li, G., & Shi, H. (2022). Chlorite mineralogy, geochemistry and exploration implications: A case study of the Xiaokelehe porphyry Cu-Mo deposit in NE China. *Ore Geology Reviews*, *140*, 104568.

Fenta, M. C., Anteneh, Z. L., Szanyi, J., & Walker, D. (2020). Hydrogeological framework of the volcanic aquifers and groundwater quality in Dangila Town and the surrounding area, Northwest Ethiopia. *Groundwater for Sustainable Development*, *11*, 100408.

Fernandes, L. L., Kessarkar, P. M., Rao, V. P., Suja, S., Parthiban, G., & Kurian, S. (2019). Seasonal distribution of trace metals in suspended particulate and bottom sediments of four microtidal river estuaries, west coast of India. *Hydrological Sciences Journal*, *64*(12), 1519-1534.

Figi, R., Lienemann, P., & Richner, P. (1995). Determination of traces of fluorine, chlorine, bromine, cadmium and lead in plastic materials. *Toxicological & Environmental Chemistry*, *52*(1-4), 35-44.

Filipič, M. (2012). Mechanisms of cadmium induced genomic instability. *Mutation Research/Fundamental and Molecular Mechanisms of Mutagenesis*, *733*(1-2), 69-77.

Flemming, C. A., & Trevors, J. T. (1989). Copper toxicity and chemistry in the environment: a review. *Water, air, and soil pollution*, *44*(1), 143-158.

Foley, N. K., & Ayuso, R. A. (2008). Mineral sources and transport pathways for arsenic release in a coastal watershed, USA. *Geochemistry: Exploration, Environment, Analysis*, *8*(1), 59-75.

Fortier, S. M., Hammarstrom, J. H., Ryker, S. J., Day, W. C., & Seal, R. R. (2019). USGS critical minerals review. *Mining Engineering*, *71*(5), 35-47.

Fosmire, G. J. (1990). Zinc toxicity. *The American journal of clinical nutrition*, *51*(2), 225-227.

Freeland-Graves, J. H., Mousa, T. Y., & Kim, S. (2016). International variability in diet and requirements of manganese: causes and consequences. *Journal of Trace Elements in Medicine and Biology*, *38*, 24-32.

Frei, R. (1992). *Isotope (Pb, Rb-Sr, S, O, C, U-Pb) geochemical investigations on Tertiary intrusives and related mineralizations in the Serbomacedonian Pb-Zn, Sb+ Cu-Mo metallogenetic province in northern Greece* (Doctoral dissertation, ETH Zurich).

Frisbie, S. H., Mitchell, E. J., Dustin, H., Maynard, D. M., & Sarkar, B. (2012). World Health Organization discontinues its drinking-water guideline for manganese. *Environmental Health Perspectives*, *120*(6), 775-778.

Fuge, R. (2013). Anthropogenic sources. In *Essentials of medical geology* (pp. 59-74). Springer, Dordrecht.

Fuoco, I., et al. "Use of reaction path modelling to investigate the evolution of water chemistry in shallow to deep crystalline aquifers with a special focus on fluoride." *Science of the Total Environment* 830 (2022): 154566.

Gaetke, L. M., Chow-Johnson, H. S., & Chow, C. K. (2014). Copper: toxicological relevance and mechanisms. *Archives of toxicology*, *88*(11), 1929-1938.

Gaikwad, S. K., Kadam, A. K., Ramgir, R. R., Kashikar, A. S., Wagh, V. M., Kandekar, A. M., ... & Kamble, K. D. (2020). Assessment of the groundwater geochemistry from a part of west coast of India using statistical methods and water quality index. *HydroResearch*, *3*, 48-60.

Galvin, R.M. (1996). Occurrence of metals in waters: An overview. Water SA. 22:7–18

Gan, C. D., Gan, Z. W., Cui, S. F., Fan, R. J., Fu, Y. Z., Peng, M. Y., & Yang, J. Y. (2021). Agricultural activities impact on soil and sediment fluorine and perfluorinated compounds in an endemic fluorosis area. *Science of the Total Environment*, *771*, 144809.

Gandhi, K. Parimala. "Analysis of water quality parameters in selected areas of palakkad district." *Current World Environment* 3.2 (2008): 283.

Garcia-Castellanos, D. (2002). Interplay between lithospheric flexure and river transport in foreland basins. *Basin Research*, *14*(2), 89-104.

Garcia-Segura, S., Eiband, M. M. S., de Melo, J. V., & Martínez-Huitle, C. A. (2017). Electrocoagulation and advanced electrocoagulation processes: A general review about the fundamentals, emerging applications and its association with other technologies. *Journal of Electroanalytical Chemistry*, *801*, 267-299.

Garelick, H., Jones, H., Dybowska, A., & Valsami-Jones, E. (2009). Arsenic pollution sources. *Reviews of Environmental Contamination Volume 197*, 17-60.

Gaur, S., & Agnihotri, R. (2019). Health effects of trace metals in electronic cigarette aerosols—a systematic review. *Biological trace element research*, *188*(2), 295-315.

Gautam, P. K., Gautam, R. K., Banerjee, S., Chattopadhyaya, M. C., & Pandey, J. D. (2016). Heavy metals in the environment: fate, transport, toxicity and remediation technologies. *Nova Sci Publishers*, *60*, 101-130.

Gayathri, S., Krishnakumar, A., Chandana, K. D., Antony, S., Dev, V. V., Arun, V., & Krishnan, K. A. (2021). Multivariate statistical tools in assessing the quality of water resources in Netravati River Basin, Karnataka, India. In *Groundwater Resources Development and Planning in the Semi-Arid Region*, Springer International Publishing. (pp. 315-334).

GEC (2012). Dynamic Groundwater Resources of Kerala (2008-09). Report by Groundwater Estimation Committee (GEC), Kerala. Central Ground Water Board, Thiruvananthapuram. 269p.

Genchi, G., Carocci, A., Lauria, G., Sinicropi, M. S., & Catalano, A. (2020). Nickel: Human health and environmental toxicology. *International journal of environmental research and public health*, *17*(3), 679.

Gevera, P. K., Cave, M., Dowling, K., Gikuma-Njuru, P., & Mouri, H. (2020). Naturally occurring potentially harmful elements in groundwater in Makueni County, south-eastern Kenya: Effects on drinking water quality and agriculture. *Geosciences*, *10*(2), 62.

Gevera, P., & Mouri, H. (2018). Natural occurrence of potentially harmful fluoride contamination in groundwater: an example from Nakuru County, the Kenyan Rift Valley. *Environmental earth sciences*, *77*, 1-19.

Ghosal, U., Sikdar, P. K., & McArthur, J. M. (2015). Palaeosol control of arsenic pollution: the Bengal Basin in West Bengal, India. *Groundwater*, *53*(4), 588-599.

Ghosh, G. K. (2019). Red and Lateritic Soils and Agri-Productivity: Issues and Strategies. *Journal of the Indian Society of Soil Science*, *67*(4 (S)).

Ghosh, S., Mukhopadhyay, J., & Chakraborty, A. (2019). Clay mineral and geochemical proxies for intense climate change in the permian gondwana rock record from eastern india. *Research*, *2019*.

Gibbs, R. J. (1970). Mechanisms controlling world water chemistry. *Science*, *170*(3962), 1088-1090.

Gislam, H., Burnside, N. G., Brolly, M., Deribe, K., Davey, G., Wanji, S., ... & Le Blond, J. S. (2020). Linking soils and human health: geospatial analysis of ground-sampled soil data in relation to community-level podoconiosis data in North West Cameroon. *Transactions of The Royal Society of Tropical Medicine and Hygiene*, *114*(12), 937-946.

Gizaw, M., Molla, M., & Mekonnen, W. (2014). Trends and risk factors for neonatal mortality in Butajira District, South Central Ethiopia,(1987-2008): a prospective cohort study. *BMC pregnancy and childbirth*, *14*(1), 1-6.

Gleeson, S. A., Butt, C. R. M., & Elias, M. (2003). Nickel laterites: a review. *SEG Discovery*, (54), 1-18.

Gobindlal, K., Zujovic, Z., Jaine, J., Weber, C. C., & Sperry, J. (2022). Solvent-Free, Ambient Temperature and Pressure Destruction of Perfluorosulfonic Acids under Mechanochemical Conditions: Degradation Intermediates and Fluorine Fate. *Environmental Science & Technology*.

Gogoi, R. R., Khanikar, L., Gogoi, J., Neog, N., Deka, D. J., & Sarma, K. P. (2021). Geochemical sources, hydrogeochemical behaviour of fluoride release and its health risk assessment in some fluorosis endemic areas of the Brahmaputra valley of Assam, India. *Applied Geochemistry*, *127*, 104911.

Goldich, S. S. (1938). A study in rock-weathering. *The Journal of Geology*, *46*(1), 17-58.

Gong, G., Mattevada, S., & O'Bryant, S. E. (2014). Comparison of the accuracy of kriging and IDW interpolations in estimating groundwater arsenic concentrations in Texas. *Environmental research*, *130*, 59-69.

Gong, J., Geng, J., & Chen, Z. (2015). Real-time GIS data model and sensor web service platform for environmental data management. *International Journal of Health Geographics*, *14*(1), 1-13.

Gonzalez, V., Cotte, M., Vanmeert, F., de Nolf, W., & Janssens, K. (2020). X-ray Diffraction Mapping for Cultural Heritage Science: a Review of Experimental Configurations and Applications. *Chemistry–A European Journal*, *26*(8), 1703-1719.

González-Guzmán, R., Weber, B., Elabd, M. A., Solís, C., Bernard-Romero, R., Velasco-Tapia, F., & Marín-Camacho, P. (2022). Petrogenesis of holocene siliceous sinters from the Los Geysers geothermal field, northern Trans-Mexican Volcanic Belt. *Journal of Volcanology and Geothermal Research*, *431*, 107640.

Gopalakrishnan, P., Vasan, R. S., Sarma, P. S., Ravindran Nair, K. S., & Thankappan, K. R. (1999). Prevalence of dental fluorosis and associated risk factors in Allappuzha district, Kerala. *National Medical Journal of India*, *12*, 99-102.

Göransson, G., Larson, M., & Bendz, D. (2013). Variation in turbidity with precipitation and flow in a regulated river system–river Göta Älv, SW Sweden. *Hydrology and Earth System Sciences*, *17*(7), 2529-2542.

Gotze, J., Mockel, R., & Pan, Y. (2020). Mineralogy, geochemistry and genesis of agate—A review. *Minerals*, *10*(11), 1037.

Gouri, K., & Choudhary, S. K. (2017). Fluoride Contamination in Groundwater Sources of Bhagalpur Municipal Corporation Area, Bhagalpur, Bihar. *IOSR Jour. Environ. Sci., Toxicology and Food Technology (IOSRJESTFT)*, *11*(1), 45-49.

Gowd, S. S., Reddy, M. R., & Govil, P. K. (2010). Assessment of heavy metal contamination in soils at Jajmau (Kanpur) and Unnao industrial areas of the Ganga Plain, Uttar Pradesh, India. *Journal of hazardous materials*, *174*(1-3), 113-121.

Graddon, D. P. (2017). *An Introduction to Co-Ordination Chemistry: International Series of Monographs in Inorganic Chemistry*. Elsevier.

Gregory, B. R., Patterson, R. T., Reinhardt, E. G., Galloway, J. M., & Roe, H. M. (2019). An evaluation of methodologies for calibrating Itrax X-ray fluorescence counts with ICP-MS concentration data for discrete sediment samples. *Chemical Geology*, *521*, 12-27.

Groenfeldt, D., & Schmidt, J. J. (2013). Ethics and water governance. *Ecology and Society*, *18*(1).

Gualtieri, A. F., Lusvardi, G., Zoboli, A., Di Giuseppe, D., & Gualtieri, M. L. (2019). Biodurability and release of metals during the dissolution of chrysotile, crocidolite and fibrous erionite. *Environmental research*, *171*, 550-557.

Gunnell, Y. (1997). Relief and climate in South Asia: the influence of the Western Ghats on the current climate pattern of peninsular India. International journal of climatology: a journal of the Royal Meteorological Society, 17(11), 1169-1182.

Guo, H., Li, X., Xiu, W., He, W., Cao, Y., Zhang, D., & Wang, A. (2019). Controls of organic matter bioreactivity on arsenic mobility in shallow aquifers of the Hetao Basin, PR China. *Journal of Hydrology*, *571*, 448-459.

Guo, H., Wang, Y., Shpeizer, G. M., & Yan, S. (2003). Natural occurrence of arsenic in shallow groundwater, Shanyin, Datong Basin, China. *Journal of Environmental Science and Health, Part A*, *38*(11), 2565-2580.

Guo, Y., Huo, X., Li, Y., Wu, K., Liu, J., Huang, J., ... & Xu, X. (2010). Monitoring of lead, cadmium, chromium and nickel in placenta from an e-waste recycling town in China. *Science of the total environment*, *408*(16), 3113-3117.

Gupta, S. K. (2015). Assessing the hazards of high SAR and alkali water: a critical review. *Journal of Soil Salinity and Water Quality*, *7*(1), 1-11.

Guralnik, J. M., Ershler, W. B., Schrier, S. L., & Picozzi, V. J. (2005). Anemia in the elderly: a public health crisis in hematology. *ASH Education Program Book*, *2005*(1), 528-532.

Gustave, W., Yuan, Z. F., Sekar, R., Chang, H. C., Zhang, J., Wells, M., ... & Chen, Z. (2018). Arsenic mitigation in paddy soils by using microbial fuel cells. *Environmental Pollution*, *238*, 647-655.

Haider, S. W., Mehmood, T., & Siddiqui, S. (2020). Major, minor and trace elements existence in surface sediments from Gwadar to Jiwani Coastal areas of Pakistan. *International Journal of Economic and Environmental Geology*, *11*(2), 37-45.

Han, B. B., Shang, P. Q., Gao, Y. Z., Jiao, S., Yao, C. M., Zou, H., ... & Zheng, H. Y. (2020). Fluorite deposits in China: Geological features, metallogenic regularity, and research progress, China Geology, 3, 473-489.

Han, D., Cao, G., McCallum, J., & Song, X. (2015). Residence times of groundwater and nitrate transport in coastal aquifer systems: Daweijia area, northeastern China. *Science of the Total Environment*, *538*, 539-554.

Han, F. X., Su, Y., Monts, D. L., Plodinec, M. J., Banin, A., & Triplett, G. E. (2003). Assessment of global industrial-age anthropogenic arsenic contamination. *Naturwissenschaften*, *90*(9), 395-401.

Han, J., Chen, H., Hollings, P., Wang, J., Zhang, D., Zhang, L., ... & Ai, Y. (2021a). Efficient enrichment of Rb during the magmatic-hydrothermal transition in a highly evolved granitic system: Implications from mica chemistry of the Tiantangshan Rb-Sn-W deposit. *Chemical Geology*, *560*, 120020.

Han, J., Kiss, L., Mei, H., Remete, A. M., Ponikvar-Svet, M., Sedgwick, D. M., ... & Soloshonok, V. A. (2021b). Chemical aspects of human and environmental overload with fluorine. *Chemical Reviews*, *121*(8), 4678-4742.

Han, Y. S., Park, J. H., Kim, S. J., Jeong, H. Y., & Ahn, J. S. (2019). Redox transformation of soil minerals and arsenic in arsenic-contaminated soil under cycling redox conditions. *Journal of hazardous materials*, *378*, 120745.

Handa, B. K. (1975). Geochemistry and genesis of Fluoride-Containing ground waters in India. *Groundwater*, *13*(3), 275-281.

Hardin, G. (1968). The Tragedy of the Commons.

Harikumar, P. S., Nasir, U. P., & Rahman, M. M. (2009). Distribution of heavy metals in the core sediments of a tropical wetland system. *International Journal of Environmental Science & Technology*, *6*(2), 225-232.

Harilal, C. C. (2005). Phytoplankton diversity of two rivers of Kerala with special reference to aquatic nutrients. *Pollution Research*, *24*(4), 773.

Harlov, D. E. (2015). Apatite: A fingerprint for metasomatic processes. *Elements*, *11*(3), 171-176.

Harsanyi, A., & Sandford, G. (2015). Organofluorine chemistry: applications, sources and sustainability. *Green chemistry*, *17*(4), 2081-2086.

Harvey, M. C., Schreiber, M. E., Rimstidt, J. D., & Griffith, M. M. (2006). Scorodite dissolution kinetics: implications for arsenic release. *Environmental science & technology*, *40*(21), 6709-6714.

Hashmi, M. Z., Yu, C., Shen, H., Duan, D., Shen, C., Lou, L., & Chen, Y. (2014). Concentrations and Human Health Risk Assessment of Selected Heavy Metals in Surface Water of the Siling Reservoir Watershed in Zhejiang Province, China. *Polish Journal of Environmental Studies*, *23*(3).

Hassan, F. I., Niaz, K., Khan, F., Maqbool, F., & Abdollahi, M. (2017). The relation between rice consumption, arsenic contamination, and prevalence of diabetes in South Asia. *EXCLI journal*, *16*, 1132.

Hayat, E., & Baba, A. (2017). Quality of groundwater resources in Afghanistan. *Environmental monitoring and assessment*, *189*, 1-16.

He, X., Li, P., Ji, Y., Wang, Y., Su, Z., & Elumalai, V. (2020). Groundwater arsenic and fluoride and associated arsenicosis and fluorosis in China: occurrence, distribution and management. *Exposure and health*, *12*, 355-368.

Health US Do. (2015). Human Services Federal Panel on Community Water F: US Public Health Service Recommendation for Fluoride Concentration in Drinking Water for the Prevention of Dental Caries. *Public Health Rep (Washington, DC: 1974)*, *130*(4), 318-331.

Heath, R. C. (1998). *Basic ground-water hydrology* (Vol. 2220). US Department of the Interior, US Geological Survey.

Heikkinen, T., & Järvinen, A. (2003). The common cold. *The Lancet*, *361*(9351), 51-59.

Heinrichs, H., Schulz-Dobrick, B., & Wedepohl, K. H. (1980). Terrestrial geochemistry of Cd, Bi, Tl, Pb, Zn and Rb. *Geochimica et Cosmochimica Acta*, *44*(10), 1519-1533.

Hejabi, A. T., & Basavarajappa, H. T. (2013). Heavy metals partitioning in sediments of the Kabini River in South India. *Environmental monitoring and assessment*, *185*(2), 1273-1283.

Hem, J. D. (1977). Reactions of metal ions at surfaces of hydrous iron oxide. *Geochimica et Cosmochimica Acta*, *41*(4), 527-538.

Hem, J. D. (1989) Study and interpretation of the chemical characteristics of natural water. Water supply paper 2254, 3rd edn. US Geological survey, Washington, DC

Henke, B. L. (1962). Sodium and magnesium fluorescence analysis—Part I: Method. *Advances in X-ray Analysis*, *6*, 361-376.

Henke, B. L. (1963). X-ray fluorescence analysis for sodium, fluorine, oxygen, nitrogen, carbon, and boron. *Advances in X-ray Analysis*, *7*, 460-488.

Herath, I., Vithanage, M., Bundschuh, J., Maity, J. P., & Bhattacharya, P. (2016). Natural arsenic in global groundwaters: distribution and geochemical triggers for mobilization. *Current Pollution Reports*, *2*(1), 68-89.

Hiatt, V., & Huff, J. E. (1975). The environmental impact of cadmium: an overview. *International Journal of Environmental Studies*, *7*(4), 277-285.

Higueras, P., Oyarzun, R., Iraizoz, J. M., Lorenzo, S., Esbrí, J. M., & Martínez-Coronado, A. (2012). Low-cost geochemical surveys for environmental studies in developing countries: Testing a field portable XRF instrument under quasi-realistic conditions. *Journal of Geochemical Exploration*, *113*, 3-12.

Hill RA (1940). Geochemical patterns in the Coachella valley, California. Trans Am Geophys Union 21: 46–49

Hillier, S. (2000). Accurate quantitative analysis of clay and other minerals in sandstones by XRD: comparison of a Rietveld and a reference intensity ratio (RIR) method and the importance of sample preparation. *Clay minerals*, *35*(1), 291-302.

Hiscock, K. M. (2011). Groundwater in the 21st century–meeting the challenges. In *Sustaining Groundwater Resources* (pp. 207-225). Springer, Dordrecht.

Hoang, T. C., Tomasso, J. R., & Klaine, S. J. (2004). Influence of water quality and age on nickel toxicity to fathead minnows (Pimephales promelas). *Environmental Toxicology and Chemistry: An International Journal*, *23*(1), 86-92.

Holwell, D. A., Adeyemi, Z., Ward, L. A., Smith, D. J., Graham, S. D., McDonald, I., & Smith, J. W. (2017). Low temperature alteration of magmatic Ni-Cu-PGE sulfides as a source for hydrothermal Ni and PGE ores: A quantitative approach using automated mineralogy. *Ore Geology Reviews*, *91*, 718-740.

Hong, J., Liu, L., Zhang, Z., Xia, X., Yang, L., Ning, Z., ... & Qiu, G. (2022). Sulfate-accelerated photochemical oxidation of arsenopyrite in acidic systems under oxic conditions: formation and function of schwertmannite. *Journal of Hazardous Materials*, *433*, 128716.

Hoque, M. A., McArthur, J. M., & Sikdar, P. K. (2012). The palaeosol model of arsenic pollution of groundwater tested along a 32 km traverse across West Bengal, India. *Science of the Total Environment*, *431*, 157-165.

Horton, R. K. (1965). An index number system for rating water quality. *J Water Pollut Control Fed*, *37*(3), 300-306.

Hossain, D., Islam, M. S., Sultana, N., & Tusher, T. R. (2013). Assessment of iron contamination in groundwater at Tangail municipality, Bangladesh. *Journal of Environmental Science and Natural Resources*, *6*(1), 117-121.

Hou, D., O'Connor, D., Nathanail, P., Tian, L., & Ma, Y. (2017). Integrated GIS and multivariate statistical analysis for regional scale assessment of heavy metal soil contamination: A critical review. *Environmental Pollution*, *231*, 1188-1200.

Houria, B., Mahdi, K., & Zohra, T. F. (2020). Hydrochemical characterisation of groundwater quality: Merdja plain (Tebessa town, Algeria). *Civil Engineering Journal*, *6*(2), 318-325.

Hua, S., Jing, H., Yao, Y., Guo, Z., Lerner, D. N., Andrews, C. B., & Zheng, C. (2020). Can groundwater be protected from the pressure of china's urban growth?. *Environment International*, *143*, 105911.

Hua, T., Haynes, R. J., Zhou, Y. F., Boullemant, A., & Chandrawana, I. (2015). Potential for use of industrial waste materials as filter media for removal of Al, Mo, As, V and Ga from alkaline drainage in constructed wetlands–adsorption studies. *Water research*, *71*, 32-41.

Huang, J., JiLei, W. U., TieJun, L. I., XinMing, S. O. N. G., Zhang, B., Zhang, P., & Zheng, X. (2011). Effect of exposure to trace elements in the soil on the prevalence of neural tube defects in a high-risk area of China. *Biomedical and Environmental Sciences*, *24*(2), 94-101.

Huang, S. S., Liao, Q. L., Hua, M., Wu, X. M., Bi, K. S., Yan, C. Y., ... & Zhang, X. Y. (2007). Survey of heavy metal pollution and assessment of agricultural soil in Yangzhong district, Jiangsu Province, China. *Chemosphere*, *67*(11), 2148-2155.

Huang, T. C., Fung, A., & White, R. L. (1989). Recent measurements of long-wavelength x-rays using synthetic multilayers. *X-Ray Spectrometry*, *18*(2), 53-56.

Humphrey, D. G. (2002). The chemistry of chromated copper arsenate wood preservatives. *Reviews in inorganic chemistry*, *22*(1), 1-40.

Hundal, H. S., Kumar, R., Singh, K., & Singh, D. (2007). Occurrence and geochemistry of arsenic in groundwater of Punjab, Northwest India. *Communications in Soil Science and Plant Analysis*, *38*(17-18), 2257-2277.

Huq, M. E., Fahad, S., Shao, Z., Sarven, M. S., Khan, I. A., Alam, M., ... & Khan, W. U. (2020). Arsenic in a groundwater environment in Bangladesh: Occurrence and mobilization. *Journal of environmental management*, *262*, 110318.

Huq, M. E., Su, C., Li, J., & Sarven, M. S. (2018). Arsenic enrichment and mobilization in the Holocene alluvial aquifers of Prayagpur of Southwestern Bangladesh. *International Biodeterioration & Biodegradation*, *128*, 186-194.

Hussain, M. M., Bibi, I., Shahid, M., Shaheen, S. M., Shakoor, M. B., Bashir, S., ... & Niazi, N. K. (2019). Biogeochemical cycling, speciation and transformation pathways of arsenic in aquatic environments with the emphasis on algae. In *Comprehensive analytical chemistry* (Vol. 85, pp. 15-51). Elsevier.

Hutchinson, M. C. (2019). The nature of sulfate saturation in oxidized arc magmas: implications for magmatic sulfur budgets.

Huyen, D. T., Tabelin, C. B., Thuan, H. M., Dang, D. H., Truong, P. T., Vongphuthone, B., ... & Igarashi, T. (2019a). The solid-phase partitioning of arsenic in unconsolidated sediments of the Mekong Delta, Vietnam and its modes of release under various conditions. *Chemosphere*, *233*, 512-523.

Huyen, D. T., Tabelin, C. B., Thuan, H. M., Dang, D. H., Truong, P. T., Vongphuthone, B., ... & Igarashi, T. (2019b). Geological and geochemical characterizations of sediments in six borehole cores from the arsenic-contaminated aquifer of the Mekong Delta, Vietnam. *Data in brief*, *25*, 104230.

Hwang, J. Y., Park, S., Kim, H. K., Kim, M. S., Jo, H. J., Kim, J. I., ... & Kim, T. S. (2017). Hydrochemistry for the assessment of groundwater quality in Korea. *Journal of Agricultural Chemistry and Environment*, *6*(01), 1.

Iano, F. G., Ferreira, M. C., Quaggio, G. B., Fernandes, M. S., Oliveira, R. C., Ximenes, V. F., & Buzalaf, M. A. R. (2014). Effects of chronic fluoride intake on the antioxidant systems of the liver and kidney in rats. *Journal of Fluorine Chemistry*, *168*, 212-217.

ICMR (Council of Medical Research). (1975). Manual of Standards of Quality for Drinking Water Supplies, Indian. Special Report No. 44.

Inaba, T., Kobayashi, E., Suwazono, Y., Uetani, M., Oishi, M., Nakagawa, H., & Nogawa, K. (2005). Estimation of cumulative cadmium intake causing Itai–itai disease. *Toxicology letters*, *159*(2), 192-201.

Ingersoll, R. V. (1988). Tectonics of sedimentary basins. *Geological Society of America Bulletin*, *100*(11), 1704-1719.

In-Hang, S. L. (2012). *Multiple Diffraction of X-rays in Crystals* (Vol. 50). Springer Science & Business Media.

Irzon, R., Syafri, I., Ghani, A. A., Prabowo, A., Hutabarat, J., & Sendjaja, P. (2020). Petrography and geochemistry of the Pinkish Lagoi Granite, Bintan Island: Implication to magmatic differentiation, classification, and tectonic history. *Bulletin of the Geological Society of Malaysia*, *69*.

Islam, M. M., Hofstra, N., & Islam, M. (2017). The impact of environmental variables on faecal indicator bacteria in the Betna river basin, Bangladesh. *Environmental Processes*, *4*(2), 319-332.

Israil, M., Al-Hadithi, M., & Singhal, D. C. (2006). Application of a resistivity survey and geographical information system (GIS) analysis for hydrogeological zoning of a piedmont area, Himalayan foothill region, India. *Hydrogeology Journal*, *14*(5), 753-759.

Jacks, G., Bhattacharya, P., Chaudhary, V., & Singh, K. P. (2005). Controls on the genesis of some high-fluoride groundwaters in India. *Applied Geochemistry*, *20*(2), 221-228.

Jain, C. K., Sharma, S. K., & Singh, S. (2018). Physico-chemical characteristics and hydrogeological mechanisms in groundwater with special reference to arsenic contamination in Barpeta District, Assam (India). *Environmental monitoring and assessment*, *190*, 1-16.

Jang, J., Hur, H. G., Sadowsky, M. J., Byappanahalli, M. N., Yan, T., & Ishii, S. (2017). Environmental Escherichia coli: ecology and public health implications—a review. *Journal of applied microbiology*, *123*(3), 570-581.

Jelenova, H., Majzlan, J., Amoako, F. Y., & Drahota, P. (2018). Geochemical and mineralogical characterization of the arsenic-, iron-, and sulfur-rich mining waste dumps near Kaňk, Czech Republic. *Applied Geochemistry*, *97*, 247-255.

Jerzykowska, I., Majzlan, J., Michalik, M., Göttlicher, J., Steininger, R., Błachowski, A., & Ruebenbauer, K. (2014). Mineralogy and speciation of Zn and As in Fe-oxide-clay aggregates in the mining waste at the MVT Zn–Pb deposits near Olkusz, Poland. *Geochemistry*, *74*(3), 393-406.

Jeske, A. (2013). Mobility and distribution of barium and strontium in profiles of podzolic soils. *Soil Science Annual*, *64*(1), 2.

Jesubek, A., Grandel, S., & Dahmke, A. (2013). Impacts of subsurface heat storage on aquifer hydrogeochemistry. *Environmental Earth Sciences*, *69*, 1999-2012.

Jha, B. M., & Sinha, S. K. (2009). Towards better management of ground water resources in India. *QJ*, *24*(4), 1-20.

Jha, P. K., & Tripathi, P. (2021). Arsenic and fluoride contamination in groundwater: a review of global scenarios with special reference to India. *Groundwater for Sustainable Development*, *13*, 100576.

Jha, V., Garcia-Garcia, G., Iseki, K., Li, Z., Naicker, S., Plattner, B., ... & Yang, C. W. (2013). Chronic kidney disease: global dimension and perspectives. *The Lancet*, *382*(9888), 260-272.

Jia, X., O'Connor, D., Hou, D., Jin, Y., Li, G., Zheng, C., ... & Luo, J. (2019). Groundwater depletion and contamination: Spatial distribution of groundwater resources sustainability in China. *Science of the Total Environment*, *672*, 551-562.

Jia, Y., Xi, B., Jiang, Y., Guo, H., Yang, Y., Lian, X., & Han, S. (2018). Distribution, formation and human-induced evolution of geogenic contaminated groundwater in China: A review. *Science of the total environment*, *643*, 967-993.

Jiang, J. Q. (2001). Development of coagulation theory and pre-polymerized coagulants for water treatment. *Separation and Purification Methods*, *30*(1), 127-141.

Jin, Y., O'Connor, D., Ok, Y. S., Tsang, D. C., Liu, A., & Hou, D. (2019). Assessment of sources of heavy metals in soil and dust at children's playgrounds in Beijing using GIS and multivariate statistical analysis. *Environment international*, *124*, 320-328.

Johnson, C. D., Nandi, A., Joyner, T. A., & Luffman, I. (2018). Iron and manganese in groundwater: Using Kriging and GIS to locate high concentrations in Buncombe County, North Carolina. *Groundwater*, *56*(1), 87-95.

Johnson, S. (2001). Gradual micronutrient accumulation and depletion in Alzheimer's disease. *Medical hypotheses*, *56*(6), 595-597.

Johnson, S. E., Song, W. J., Cook, A. C., Vel, S. S., & Gerbi, C. C. (2021). The quartz α↔ β phase transition: Does it drive damage and reaction in continental crust?. *Earth and Planetary Science Letters*, *553*, 116622.

Johnston, K., Ver Hoef, J. M., Krivoruchko, K., & Lucas, N. (2001). *Using ArcGIS geostatistical analyst* (Vol. 380). Redlands: Esri.

Jones, M. E., Nico, P. S., Ying, S., Regier, T., Thieme, J., & Keiluweit, M. (2018). Manganese-driven carbon oxidation at oxic–anoxic interfaces. *Environmental science & technology*, *52*(21), 12349-12357.

Jordán, G., Meijninger, B. M. L., Van Hinsbergen, D. J. J., Meulenkamp, J. E., & Van Dijk, P. M. (2005). Extraction of morphotectonic features from DEMs: Development and applications for study areas in Hungary and NW Greece. *International journal of applied earth observation and geoinformation*, *7*(3), 163-182.

Jose, A., & Ray, J. G. (2018). Toxic heavy metals in human blood in relation to certain food and environmental samples in Kerala, South India. *Environmental Science and Pollution Research*, *25*(8), 7946-7953.

Joseph, D. (2021). Introductory Chapter: Tracelement Effects in Biological Applications Using Photon Induced (EDXRF), Proton Induced (PIXE) and Synchrotron Induced (EXAFS) X-Ray Spectrometry. In *Trace Elements and Their Effects on Human Health and Diseases*. In tech Open.

Juncher Jørgensen, C., Jacobsen, O. S., Elberling, B., & Aamand, J. (2009). Microbial oxidation of pyrite coupled to nitrate reduction in anoxic groundwater sediment. *Environmental science & technology*, *43*(13), 4851-4857.

Jung, S. M., Sohn, I., & Min, D. J. (2010). Chemical analysis of argon–oxygen decarburization slags in stainless steelmaking process by X-ray fluorescence spectrometry. *X-Ray Spectrometry*, *39*(5), 311-317.

Kadam, A., Wagh, V., Jacobs, J., Patil, S., Pawar, N., Umrikar, B., ... & Kumar, S. (2021). Integrated approach for the evaluation of groundwater quality through hydro geochemistry and human health risk from Shivganga river basin, Pune, Maharashtra, India. *Environmental Science and Pollution Research*, 1-23.

Kakonyi, G., & Ahmed, I. A. (2020). Cadmium and Lead: Contamination. In *Managing Global Resources and Universal Processes* (pp. 417-426). CRC Press.

Kale, S. S., Kadam, A. K., Kumar, S., & Pawar, N. J. (2010). Evaluating pollution potential of leachate from landfill site, from the Pune metropolitan city and its impact on shallow basaltic aquifers. *Environmental monitoring and assessment*, *162*(1), 327-346.

Kalnicky, D. J., & Singhvi, R. (2001). Field portable XRF analysis of environmental samples. *Journal of hazardous materials*, *83*(1-2), 93-122.

Kalugin, V., Gusev, V., Tolstykh, N., Lavrenchuk, A., & Nigmatulina, E. (2021). Origin of the Pd-Rich Pentlandite in the Massive Sulfide Ores of the Talnakh Deposit, Norilsk Region, Russia. *Minerals*, *11*(11), 1258.

Kang, D., Yu, X., Tong, S., Ge, M., Zuo, J., Cao, C., & Song, W. (2013). Performance and mechanism of Mg/Fe layered double hydroxides for fluoride and arsenate removal from aqueous solution. *Chemical Engineering Journal*, *228*, 731-740.

Kang, J., Zhang, Z., & Wang, J. J. (2011). Influence of humic substances on bioavailability of Cu and Zn during sewage sludge composting. *Bioresource Technology*, *102*(17), 8022-8026.

Kannan, N., & Joseph, S. (2009). Quality of groundwater in the shallow aquifers of a paddy dominated agricultural river basin, Kerala, India. *International Journal of Agricultural and Biosystems Engineering*, *3*(4), 223-241.

Kannan, N., Joseph, S., & Sheela, A. M. (2021). Characterization of Groundwater in the Shallow and Deep Aquifers of an Agriculture-Dominated Tropical Subhumid to Semiarid Region, India: a Multivariate and GIS Approach. *Journal of the Indian Society of Remote Sensing*, *49*(8), 1853-1868.

Kanwar, V. S., Sharma, A., Srivastav, A. L., & Rani, L. (2020). Phytoremediation of toxic metals present in soil and water environment: a critical review. *Environmental Science and Pollution Research*, *27*(36), 44835-44860.

Kapaj, S., Peterson, H., Liber, K., & Bhattacharya, P. (2006). Human health effects from chronic arsenic poisoning–a review. *Journal of Environmental Science and Health, Part A*, *41*(10), 2399-2428.

Kaper, J. B., Nataro, J. P., & Mobley, H. L. (2004). Pathogenic escherichia coli. *Nature reviews microbiology*, *2*(2), 123-140.

Karayigit, A. I., Bircan, C., Oskay, R. G., Türkmen, İ., & Querol, X. (2020). The geology, mineralogy, petrography, and geochemistry of the Miocene Dursunbey coal within fluvio-lacustrine deposits, Balıkesir (Western Turkey). *International Journal of Coal Geology*, *228*, 103548.

Karlovic, I., Posavec, K., Larva, O., & Marković, T. (2022). Numerical groundwater flow and nitrate transport assessment in alluvial aquifer of Varaždin region, NW Croatia. *Journal of Hydrology: Regional Studies*, *41*, 101084.

Karunanidhi, D., Aravinthasamy, P., Deepali, M., Subramani, T., & Roy, P. D. (2020). The effects of geochemical processes on groundwater chemistry and the health risks associated with fluoride intake in a semi-arid region of South India. *RSC Advances*, *10*(8), 4840-4859.

Karydas, A. G. (2007). Application of a portable XRF spectrometer for the non-invasive analysis of museum metal artefacts. *Annali di Chimica: Journal of Analytical, Environmental and Cultural Heritage Chemistry*, *97*(7), 419-432.

Kasprzak, K. S., Sunderman Jr, F. W., & Salnikow, K. (2003). Nickel carcinogenesis. *Mutation Research/Fundamental and Molecular Mechanisms of Mutagenesis*, *533*(1-2), 67-97.

Kato, M., Kumasaka, M. Y., Ohnuma, S., Furuta, A., Kato, Y., Shekhar, H. U., ... & Yajima, I. (2013). Comparison of barium and arsenic concentrations in well drinking water and in human body samples and a novel remediation system for these elements in well drinking water. *PloS one*, *8*(6), e66681.

Kaulich, B., Gianoncelli, A., Beran, A., Eichert, D., Kreft, I., Pongrac, P., ... & Kiskinova, M. (2009). Low-energy X-ray fluorescence microscopy opening new opportunities for bio-related research. *Journal of the Royal Society interface*, *6*(suppl_5), S641-S647.

Kaur, L., Rishi, M. S., Sharma, S., Sharma, B., Lata, R., & Singh, G. (2019). Hydrogeochemical characterization of groundwater in alluvial plains of River Yamuna in Northern India: an insight of controlling processes. *Journal of King Saud university-science*, *31*(4), 1245-1253.

Kavusi, M., Khashei Siuki, A., & Dastourani, M. (2020). Optimal design of groundwater monitoring network using the combined Election-Kriging method. *Water Resources Management*, *34*, 2503-2516.

Kazemi, H., Sarukkalige, R., & Shao, Q. (2021). Evaluation of non-uniform groundwater level data using spatiotemporal modeling. *Groundwater for Sustainable Development*, *15*, 100659.

Keen, C. L., Ensunsa, J. L., & Clegg, M. S. (2000). Manganese metabolism in animals and humans including the toxicity of manganese. *Met Ions Biol Syst*, *37*(2), 89-121.

Kern, M. L., Vieiro, A. P., & Machado, G. (2008). The fluoride in the groundwater of Guarani Aquifer System: the origin associated with black shales of Paraná Basin. *Environmental Geology*, *55*(6), 1219-1233.

Khairul, I., Wang, Q. Q., Jiang, Y. H., Wang, C., & Naranmandura, H. (2017). Metabolism, toxicity and anticancer activities of arsenic compounds. *Oncotarget*, *8*(14), 23905.

Khan, F., Krishnaraj, S., Raja, P., Selvaraj, G., & Cheelil, R. (2021). Impact of hydrogeochemical processes and its evolution in controlling groundwater chemistry along the east coast of Tamil Nadu and Puducherry, India. *Environmental Science and Pollution Research*, *28*(15), 18567-18588.

Khan, M. M. A., Umar, R., & Lateh, H. (2010). Study of trace elements in groundwater of Western Uttar Pradesh, India. *Scientific Research and Essays*, *5*(20), 3175-3182.

Khan, R., & Jhariya, D. C. (2017). Groundwater quality assessment for drinking purpose in Raipur city, Chhattisgarh using water quality index and geographic information system. *Journal of the geological society of India*, *90*(1), 69-76.

Khan, S. J., Deere, D., Leusch, F. D., Humpage, A., Jenkins, M., & Cunliffe, D. (2015). Extreme weather events: Should drinking water quality management systems adapt to changing risk profiles?. *Water research*, *85*, 124-136.

Khatri, N., & Tyagi, S. (2015). Influences of natural and anthropogenic factors on surface and groundwater quality in rural and urban areas. Front Life Sci 8 (1): 23–39.

Kim, K. W., Chanpiwat, P., Hanh, H. T., Phan, K., & Sthiannopkao, S. (2011). Arsenic geochemistry of groundwater in Southeast Asia. *Frontiers of medicine*, *5*(4), 420-433.

Kimambo, V., Bhattacharya, P., Mtalo, F., Mtamba, J., & Ahmad, A. (2019). Fluoride occurrence in groundwater systems at global scale and status of defluoridation–state of the art. *Groundwater for Sustainable Development*, *9*, 100223.

Kimura, T. (1998). Relationships between inorganic elements and minerals in coals from the Ashibetsu district, Ishikari coal field, Japan. *Fuel processing technology*, *56*(1-2), 1-19.

Kisa, P. T., & Arslan, N. (2021). Inborn errors of immunity and metabolic disorders: current understanding, diagnosis, and treatment approaches. *Journal of Pediatric Endocrinology and Metabolism*, *34*(3), 277-294.

Klein, B., Jura, M., Koester, D., Zuckerman, B., & Melis, C. (2010). Chemical abundances in the externally polluted white dwarf GD 40: evidence of a rocky extrasolar minor planet. *The Astrophysical Journal*, *709*(2), 950.

Klein, C. B., & Costa, M. A. X. (2022). Nickel. In *Handbook on the Toxicology of Metals* (pp. 615-637). Academic Press.

Knutsson, H., Westin, C. F., & Andersson, M. (2012). Structure tensor estimation: introducing monomial quadrature filter sets. In *New Developments in the Visualization and Processing of Tensor Fields* (pp. 3-28). Springer, Berlin, Heidelberg.

Knutsson, H., Westin, C. F., & Granlund, G. (1994, November). Local multiscale frequency and bandwidth estimation. In *Proceedings of 1st international conference on image processing* (Vol. 1, pp. 36-40). IEEE.

Koehler, W. C., Wollan, E. O., & Wilkinson, M. K. (1960). Neutron diffraction study of the magnetic properties of rare-earth-iron perovskites. *Physical Review*, *118*(1), 58.

Kourakos, G., Dahlke, H. E., & Harter, T. (2019). Increasing groundwater availability and seasonal base flow through agricultural managed aquifer recharge in an irrigated basin. *Water Resources Research*, *55*(9), 7464-7492.

Kraynov, S. R., Merkov, A. N., Petrova, N. G., Baturins. IV, & Zharikov. VM. (1969). Highly alkaline (pH-12) fluosilicate waters in deeper zones of lovozero massif. *Geochemistry International USSR*, *6*(4), 635.

Krishan, G., Taloor, A. K., Sudarsan, N., Bhattacharya, P., Kumar, S., Ghosh, N. C., ... & Kour, R. (2021). Occurrences of potentially toxic trace metals in groundwater of the state of Punjab in northern India. Groundwater for Sustainable Development, 15, 100655.

Krishna, S., Jaiswal, A. K., Gupta, M., Sharma, D. K., & Ali, Z. (2020). Barium poisoning with analytical aspects and its management. *International Journal of Advanced Research in Medicinal Chemistry*, *2*(1), 20-27.

Krishnan, R., Ramesh, M., & Chalakkal, P. (2015). Prevalence and characteristics of MIH in school children residing in an endemic fluorosis area of India: an epidemiological study. *European Archives of Paediatric Dentistry*, *16*(6), 455-460.

Kshetrimayum, K. S., & Hegeu, H. (2016). The state of toxicity and cause of elevated Iron and Manganese concentrations in surface water and groundwater around Naga Thrust of Assam-Arakan basin, Northeastern India. *Environmental Earth Sciences*, *75*(7), 1-14.

Kubier, A., Wilkin, R. T., & Pichler, T. (2019). Cadmium in soils and groundwater: a review. *Applied Geochemistry*, *108*, 104388.

Kukillaya, J. P., & Narayanan, T. (2014). Role of weathering of ferromagnesian minerals and surface water irrigation in evolving and modifying chemistry of groundwater in Palakkad district, Kerala, with special reference to its fluoride content. *Journal of the Geological Society of India*, *84*(5), 579-589.

Kularatne, K. U. K. S., & Pitawala, H. M. T. G. A. (2012). Leaching of fluoride from biotite mica in soil: implications for fluoride in shallow groundwater. *International Scholarly Research Notices*, *2012*.

Kulmatov, R. A., Adilov, S. A., & Khasanov, S. (2020). Evaluation of the spatial and temporal changes in groundwater level and mineralization in agricultural lands under climate change in the Syrdarya province, Uzbekistan. In *IOP Conference Series: Earth and Environmental Science* (Vol. 614, No. 1, p. 012149). IOP Publishing.

Kumar, A., & Ghosh, A. K. (2021). Assessment of arsenic contamination in groundwater and affected population of Bihar. In *Arsenic Toxicity: Challenges and Solutions* (pp. 165-191). Springer, Singapore.

Kumar, A., & Singh, C. K. (2020). Arsenic enrichment in groundwater and associated health risk in Bari doab region of Indus basin, Punjab, India. *Environmental Pollution*, *256*, 113324.

Kumar, A., Rahman, M., Ali, M., Kumar, R., Niraj, P. K., Akhouri, V., ... & Ghosh, A. K. (2021a). Assessment of arsenic exposure and its mitigation intervention in severely exposed population of Buxar district of Bihar, India. *Toxicology and Environmental Health Sciences*, *13*(3), 287-297.

Kumar, C. P., & Seethapathi, P. V. (2002). Assessment of natural groundwater recharge in Upper Ganga Canal command area. *Journal of Applied Hydrology*, *15*(4), 13-20.

Kumar, D., & Ahmed, S. (2003). Seasonal behaviour of spatial variability of groundwater level in a granitic aquifer in monsoon climate. *Current Science*, 188-196.

Kumar, M., & Puri, A. (2012). A review of permissible limits of drinking water. *Indian journal of occupational and environmental medicine*, *16*(1), 40.

Kumar, M., Das, A., Das, N., Goswami, R., & Singh, U. K. (2016a). Co-occurrence perspective of arsenic and fluoride in the groundwater of Diphu, Assam, Northeastern India. *Chemosphere*, *150*, 227-238.

Kumar, M., Goswami, R., Patel, A. K., Srivastava, M., & Das, N. (2020). Scenario, perspectives and mechanism of arsenic and fluoride co-occurrence in the groundwater: a review. *Chemosphere*, *249*, 126126.

Kumar, M., Patel, A. K., & Singh, A. (2022). Anthropogenic dominance on geogenic arsenic problem of the groundwater in the Ganga-Brahmaputra floodplain: A paradox of origin and mobilization. *Science of The Total Environment*, *807*, 151461.

Kumar, M., Ramanathan, A. L., Rahman, M. M., & Naidu, R. (2016b). Concentrations of inorganic arsenic in groundwater, agricultural soils and subsurface sediments from the middle Gangetic plain of Bihar, India. *Science of the Total Environment*, *573*, 1103-1114.

Kumar, P. S. (2013). Interpretation of groundwater chemistry using piper and Chadha's diagrams: a comparative study from Perambalur Taluk. *Elixir Geosci*, *54*, 12208-12211.

Kumar, P. S., & James, E. J. (2019). Geostatistical and geochemical model-assisted hydrogeochemical pattern recognition along the groundwater flow paths in Coimbatore district, South India. Environment, Development and Sustainability, 21(1), 369-384.

Kumar, P. S., Elango, L., & James, E. J. (2014a). Assessment of hydrochemistry and groundwater quality in the coastal area of South Chennai, India. *Arabian Journal of Geosciences*, *7*(7), 2641-2653.

Kumar, P. S., Jegathambal, P., Nair, S., & James, E. J. (2015). Temperature and pH dependent geochemical modeling of fluoride mobilization in the groundwater of a crystalline aquifer in southern India. *Journal of Geochemical Exploration*, *156*, 1-9.

Kumar, P., Mahajan, A. K., & Kumar, A. (2019). Groundwater geochemical facie: implications of rock-water interaction at the Chamba city (HP), northwest Himalaya, India. *Environmental Science and Pollution Research*, 1-15.

Kumar, P., Singh, C. K., Saraswat, C., Mishra, B., & Sharma, T. (2017). Evaluation of aqueous geochemistry of fluoride enriched groundwater: a case study of the Patan district, Gujarat, Western India. *Water Science*, *31*(2), 215-229.

Kumar, R. B., & Divya, M. P. (2012). Spatial evaluation of groundwater quality in Kazhakuttam block, Thiruvananthapuram district, Kerala. *Journal of the Geological Society of India*, *80*(1), 48-56.

Kumar, S. K., Rammohan, V., Sahayam, J. D., & Jeevanandam, M. (2009). Assessment of groundwater quality and hydrogeochemistry of Manimuktha River basin, Tamil Nadu, India. *Environmental Monitoring and Assessment*, *159*(1), 341-351.

Kumar, S., & Saxena, A. (2011). Chemical weathering of the Indo-Gangetic Alluvium with special reference to release of fluoride in the groundwater, Unnao district, Uttar Pradesh. *Journal of the Geological Society of India*, *77*, 459-477.

Kumar, S., Nair, R. R., Pillai, P. B., Gupta, S. N., Iyengar, M. A. R., & Sood, A. K. (2014b). Graphene oxide–MnFe2O4 magnetic nanohybrids for efficient removal of lead and arsenic from water. *ACS applied materials & interfaces*, *6*(20), 17426-17436.

Kumar, S., Venkatesh, A. S., Singh, R., Udayabhanu, G., & Saha, D. (2018). Geochemical signatures and isotopic systematics constraining dynamics of fluoride contamination in groundwater across Jamui district, Indo-Gangetic alluvial plains, India. *Chemosphere*, *205*, 493-505

Kumar, V. S., Amarender, B., Dhakate, R., Sankaran, S., & Kumar, K. R. (2016c). Assessment of groundwater quality for drinking and irrigation use in shallow hard rock aquifer of Pudunagaram, Palakkad District Kerala. *Applied Water Science*, *6*(2), 149-167.

Kumar, V., Pandita, S., Sidhu, G. P. S., Sharma, A., Khanna, K., Kaur, P., ... & Setia, R. (2021b). Copper bioavailability, uptake, toxicity and tolerance in plants: A comprehensive review. *Chemosphere*, *262*, 127810.

Kumarathilaka, P., Seneweera, S., Meharg, A., & Bundschuh, J. (2018). Arsenic speciation dynamics in paddy rice soil-water environment: sources, physico-chemical, and biological factors-a review. *Water research*, *140*, 403-414.

Kumari, M., & Rai, S. C. (2020). Hydrogeochemical evaluation of groundwater quality for drinking and irrigation purposes using water quality index in semiarid region of India. *Journal of the Geological Society of India*, *95*(2), 159-168.

Kundu, H., Basavaraj, P., Singla, A., Gupta, R., Singh, K., & Jain, S. (2015). Effect of fluoride in drinking water on children's intelligence in high and low fluoride areas of Delhi. *Journal of Indian Association of Public Health Dentistry*, *13*(2), 116.

Kundu, M. C., & Mandal, B. (2009). Assessment of potential hazards of fluoride contamination in drinking groundwater of an intensively cultivated district in West Bengal, India. *Environmental monitoring and assessment*, *152*(1), 97-103.

Kurwadkar, S., Kanel, S. R., & Nakarmi, A. (2020). Groundwater pollution: Occurrence, detection, and remediation of organic and inorganic pollutants. *Water Environment Research*, *92*(10), 1659-1668.

Kushawaha, J., & Aithani, D. (2021). Geogenic Pollutants in Groundwater and Their Removal Techniques. *Groundwater Geochemistry: Pollution and Remediation Methods*, 1-21.

Kuzmina, T. G., Troneva, M. A., & Romashova, T. V. (2022). Factors Affecting the Determination of Fluorine in Rocks by X-Ray Fluorescence Spectrometry Using Pressed Pellets. *Journal of Analytical Chemistry*, *77*(7), 874-881.

Lage, O. M., Soares, H. M. V. M., Vasconcelos, M. T. S. D., Parente, A. M., & Salema, R. (1996). Toxicity effects of copper (II) on the marine dinoflagellate Amphidinium carterae: influence of metal speciation. *European Journal of Phycology*, *31*(4), 341-348.

Lakshmanan, E., Kannan, R., & Kumar, M. S. (2003). Major ion chemistry and identification of hydrogeochemical processes of ground water in a part of Kancheepuram district, Tamil Nadu, India. *Environmental geosciences*, *10*(4), 157-166.

Lal, K., Sehgal, M., Gupta, V., Sharma, A., John, O., Gummidi, B., ... & Kumari, A. (2020). Assessment of groundwater quality of CKDu affected Uddanam region in Srikakulam district and across Andhra Pradesh, India. *Groundwater for Sustainable Development*, *11*, 100432.

Lalla, E. A., Cote, K., Hickson, D., Garnitschnig, S., Konstantinidis, M., Such, P., ... & Groemer, G. (2020). Laboratory analysis of returned samples from the AMADEE-18 Mars analog mission. *Astrobiology*, *20*(11), 1303-1320.

Laluraj, C. M., & Gopinath, G. (2006). Assessment on seasonal variation of groundwater quality of phreatic aquifers–a river basin system. *Environmental Monitoring and Assessment*, *117*(1), 45-57.

Lazarchick, J. (2012). Update on anemia and neutropenia in copper deficiency. *Current opinion in hematology*, *19*(1), 58-60.

Lee, J. J., Jang, C. S., Wang, S. W., & Liu, C. W. (2007). Evaluation of potential health risk of arsenic-affected groundwater using indicator kriging and dose response model. *Science of the Total Environment*, *384*(1-3), 151-162.

Lee, J. S., Chon, H. T., & Kim, K. W. (2005). Human risk assessment of As, Cd, Cu and Zn in the abandoned metal mine site. *Environmental geochemistry and health*, *27*(2), 185-191.

Leff, T., Stemmer, P., Tyrrell, J., & Jog, R. (2018). Diabetes and exposure to environmental lead (Pb). *Toxics*, *6*(3), 54.

Lengke, M. F., Sanpawanitchakit, C., & Tempel, R. N. (2009). The oxidation and dissolution of arsenic-bearing sulfides. *The Canadian Mineralogist*, *47*(3), 593-613.

Leoni, L., Menichini, M., & Saitta, M. (1982). Determination of S, Cl and F in silicate rocks by X-Ray fluorescence analyses. *X-Ray Spectrometry*, *11*(4), 156-158.

Levin, R., Vieira, C. L. Z., Rosenbaum, M. H., Bischoff, K., Mordarski, D. C., & Brown, M. J. (2021). The urban lead (Pb) burden in humans, animals and the natural environment. *Environmental research*, *193*, 110377.

Li, C., Gao, X., Zhang, X., Wang, Y., & Howard, K. (2022). Groundwater fluoride and arsenic mobilization in a typical deep aquifer system within a semi-arid basin. *Journal of Hydrology*, *609*, 127767.

Li, H., Shi, A., Li, M., & Zhang, X. (2013). Effect of pH, temperature, dissolved oxygen, and flow rate of overlying water on heavy metals release from storm sewer sediments. *Journal of Chemistry, 2013*.

Li, Y., Jiang, H., & Yang, X. (2017). Fluorine follows water: Effect on electrical conductivity of silicate minerals by experimental constraints from phlogopite. *Geochimica et Cosmochimica Acta*, *217*, 16-27.

Li, Y., Li, H., Liu, Z., & Miao, C. (2016). Spatial Assessment of Cancer Incidences and the Risks of Industrial Wastewater Emission in China. *Sustainability*, *8*(5), 480.

Liang, X., Zang, Y., Xu, Y., Tan, X., Hou, W., Wang, L., & Sun, Y. (2013). Sorption of metal cations on layered double hydroxides. *Colloids and surfaces A: physicochemical and engineering aspects*, *433*, 122-131.

Lightfoot, P. C. (2016). *Nickel sulfide ores and impact melts: Origin of the Sudbury Igneous Complex*. Elsevier.

Lin, Q., Bian, F., Wei, Z., Wang, S., & Duan, Y. (2017). A hydrogel-based solidification method for the direct analysis of liquid samples by laser-induced breakdown spectroscopy. *Journal of Analytical Atomic Spectrometry*, *32*(7), 1412-1419.

Litasov, K. D., Kagi, H., & Bekker, T. B. (2019). Enigmatic super-reduced phases in corundum from natural rocks: Possible contamination from artificial abrasive materials or metallurgical slags. *Lithos*, *340*, 181-190.

Liu, C., Yu, H. Y., Liu, C., Li, F., Xu, X., & Wang, Q. (2015a). Arsenic availability in rice from a mining area: is amorphous iron oxide-bound arsenic a source or sink?. *Environmental Pollution*, *199*, 95-101.

Liu, H., Li, P., Wang, H., Qing, C., Tan, T., Shi, B., ... & Hasan, S. Z. (2020). Arsenic mobilization affected by extracellular polymeric substances (EPS) of the dissimilatory iron reducing bacteria isolated from high arsenic groundwater. *Science of the Total Environment*, *735*, 139501.

Liu, S. A., Li, D., Li, S., Teng, F. Z., Ke, S., He, Y., & Lu, Y. (2014). High-precision copper and iron isotope analysis of igneous rock standards by MC-ICP-MS. *Journal of Analytical Atomic Spectrometry*, *29*(1), 122-133.

Liu, Y., Mao, X. A., Liu, M., & Jiang, L. (2015b). Beryllium fluoride exchange rate accelerated by Mg2+ as discovered by 19F NMR. *The Journal of Physical Chemistry A*, *119*(1), 24-28

Liu, Z., Chen, D., Zhang, J., Lü, X., Wang, Z., Liao, W., ... & Xie, G. (2019). Pyrite morphology as an indicator of paleoredox conditions and shale gas content of the Longmaxi and Wufeng shales in the middle Yangtze area, South China. *Minerals*, *9*(7), 428.

Lodh, A., Thool, K., & Samajdar, I. (2022). X-ray diffraction for the determination of residual stress of crystalline material: An overview. *Transactions of the Indian Institute of Metals*, *75*(4), 983-995.

Loganathan, P., Hedley, M. J., Wallace, G. C., & Roberts, A. H. C. (2001). Fluoride accumulation in pasture forages and soils following long-term applications of phosphorus fertilisers. *Environmental pollution*, *115*(2), 275-282.

Logeshkumaran, A., Magesh, N. S., Godson, P. S., & Chandrasekar, N. (2015). Hydro-geochemistry and application of water quality index (WQI) for groundwater quality assessment, Anna Nagar, part of Chennai City, Tamil Nadu, India. *Applied Water Science*, *5*(4), 335-343.

Lone, K. A., & Mir, R. A. (2021). A preliminary study on aquifers and its possible geometry in parts of Kashmir valley, India. *Journal of the Geological Society of India*, *97*(7), 772-780.

Lu, H., Wang, C., Liu, X., Zhang, J., Lin, Z., Hao, Z., & Pan, G. (2021). PH-dependent photochemical transformation of arsenic sulfide sludge catalyzed by Fe ions under visible light irradiation. *Applied Catalysis B: Environmental*, *293*, 120186.

Ludington, S., Hammarstrom, J., & Piatak, N. (2009). Low-fluorine stockwork molybdenite deposits. *US Geological Survey open-file report*, *1211*(9).

Luke, C. L. (1968). Determination of traces of fluorine or sulfur by x-ray analysis. *Analytica Chimica Acta*, *43*, 245-252.

Lukeenkämper, R., & Von Bohlen, A. (2001). Total-reflection X-ray fluorescence moving towards nanoanalysis: a survey. *Spectrochimica Acta Part B: Atomic Spectroscopy*, *56*(11), 2005-2018.

Lumb, A., Sharma, T. C., & Bibeault, J. F. (2011). A review of genesis and evolution of water quality index (WQI) and some future directions. *Water Quality, Exposure and Health*, *3*(1), 11-24.

Luo, Y., Xiao, Y., Hao, Q., Zhang, Y., Zhao, Z., Wang, S., & Dong, G. (2021). Groundwater geochemical signatures and implication for sustainable development in a typical endorheic watershed on Tibetan plateau. *Environmental science and pollution research*, *28*(35), 48312-48329.

Lytvynov, L. (2019). Aluminum oxide. In *Single Crystals of Electronic Materials* (pp. 447-485). Woodhead Publishing.

Lyulko, I., Ambalova, T., & Vasiljeva, T. (2001). To integrated water quality assessment in Latvia. MTM (Monitoring Tailor-Made) III. In *Proceedings of international workshop on information for sustainable water management. Netherlands* (pp. 449-452).

Ma, Q. Y., Logan, T. J., & Traina, S. J. (1995). Lead immobilization from aqueous solutions and contaminated soils using phosphate rocks. *Environmental Science & Technology*, *29*(4), 1118-1126.

Ma, Y., Liu, Z. H., Xi, B. D., Li, W. T., Xu, Y. Q., Zhao, H. Z., ... & Xing, B. (2021). Molecular structure and evolution characteristics of dissolved organic matter in

groundwater near landfill: Implications of the identification of leachate leakage. *Science of The Total Environment*, *787*, 147649.

Madhav, S., Ahamad, A., Singh, A. K., Kushawaha, J., Chauhan, J. S., Sharma, S., & Singh, P. (2020). Water pollutants: sources and impact on the environment and human health. *Sensors in Water Pollutants Monitoring: Role of Material*, 43-62.

Magesh, N. S., Chandrasekar, N., & Elango, L. (2017). Trace element concentrations in the groundwater of the Tamiraparani river basin, South India: insights from human health risk and multivariate statistical techniques. *Chemosphere*, *185*, 468-479.

Magnall, J. M., Gleeson, S. A., Creaser, R. A., Paradis, S., Glodny, J., & Richard Kyle, J. (2020). The mineralogical evolution of the clastic dominant-type Zn-Pb±Ba deposits at Macmillan Pass (Yukon, Canada)—tracing subseafloor barite replacement in the layered mineralization. *Economic Geology*, *115*(5), 961-979.

Mahanta, N., Mishra, I., Hatui, A., Mahanta, P. S., Sahoo, H. K., & Goswami, S. (2020). Geochemical appraisal of groundwater qualities and its uses in and around Maneswar Block of Sambalpur District, Odisha, India. Environmental Earth Sciences, 79, 1-13.

Mahanta, R., Chowdhury, J., & Nath, H. K. (2016). Health costs of arsenic contamination of drinking water in Assam, India. *Economic Analysis and Policy*, *49*, 30-42.

Mahato, M. K., Singh, P. K., Tiwari, A. K., & Singh, A. K. (2016). Risk assessment due to intake of metals in groundwater of East Bokaro Coalfield, Jharkhand, India. *Exposure and health*, *8*(2), 265-275.

Maheshwari, B., Varua, M., Ward, J., Packham, R., Chinnasamy, P., Dashora, Y., ... & Rao, P. (2014). The role of transdisciplinary approach and community participation in village scale groundwater management: insights from Gujarat and Rajasthan, India. *Water*, *6*(11), 3386-3408.

Maiti, S. K., De, S., Hazra, T., Debsarkar, A., & Dutta, A. (2016). Characterization of leachate and its impact on surface and groundwater quality of a closed dumpsite–a case study at Dhapa, Kolkata, India. *Procedia Environmental Sciences*, *35*, 391-399.

Makubalo, S. S., & Diamond, R. E. (2020). Hydrochemical evolution of high uranium, fluoride and nitrate groundwaters of Namakwaland, South Africa. *Journal of African Earth Sciences*, *172*, 104002.

Malakootian, M., Mansoorian, H. J., & Moosazadeh, M. (2010). Performance evaluation of electrocoagulation process using iron-rod electrodes for removing hardness from drinking water. *Desalination*, *255*(1-3), 67-71.

Malleshwaram, Y. (2014). Occurrence of groundwater in the Ponnaiyar river catchment covering eastern parts of Bangalore city, Karnataka, India. *CURRENT SCIENCE*, *106*(10), 1353.

Malyan, S. K., Singh, R., Rawat, M., Kumar, M., Pugazhendhi, A., Kumar, A., ... & Kumar, S. S. (2019). An overview of carcinogenic pollutants in groundwater of India. *Biocatalysis and Agricultural Biotechnology*, *21*, 101288.

Mamabolo, M. C., Meyer, J. A., & Casey, N. H. (2009). Effects of total dissolved solids on the accumulation of Br, As and Pb from drinking water in tissues of selected organs in broilers. *South African Journal of Animal Science*, *39*(1), 169-172.

Mamatha, P., & Rao, S. M. (2010). Geochemistry of fluoride rich groundwater in Kolar and Tumkur Districts of Karnataka. *Environmental Earth Sciences*, *61*(1), 131-142.

Mandal, A. K. (2019). Modern technologies for diagnosis and prognosis of salt-affected soils and poor-quality waters. In *Research Developments in Saline Agriculture* (pp. 95-152). Springer, Singapore.

Mandal, B. K., & Suzuki, K. T. (2002). Arsenic round the world: a review. *Talanta*, *58*(1), 201-235.

Mandal, J., & Sanyal, S. (2019). Geospatial analysis of fluoride concentration in groundwater in puruliya district, west bengal. *Space and Culture, India*, *6*(5), 71-86.

Mandal, S. U. B. H. A. S. I. S., Raju, R., Kumar, A., Kumar, P., & Sharma, P. C. (2018). Current status of research, technology response and policy needs of salt-affected soils in India—A review. *J. Indian Soc. Coast. Agric. Res*, *36*, 40-53.

Mandel, S. (2012). Groundwater resources: investigation and development. Elsevier.

Manikandan, S., Chidambaram, S., Prasanna, M. V., & Ganayat, R. R. (2019). Assessment of heavy metals pollution and stable isotopic signatures in hard rock aquifers of Krishnagiri District, South India. Geosciences, 9(5), 200.

Manikandan, S., Chidambaram, S., Ramanathan, A. L., Prasanna, M. V., Karmegam, U., Paramaguru, P., & Jainab, I. (2014). A study on the high fluoride concentration in the magnesium-rich waters of hard rock aquifer in Krishnagiri district, Tamilnadu, India. *Arabian Journal of Geosciences*, *7*(1), 273-285.

Manjula, P., & Warrier, C. U. (2019). Evaluation of water quality of Thuthapuzha Sub-basin of Bharathapuzha, Kerala, India. *Applied water science*, *9*(4), 1-13.

Mann, A. W., & Deutscher, R. L. (1980). Solution geochemistry of lead and zinc in water containing carbonate, sulphate and chloride ions. *Chemical Geology*, *29*(1-4), 293-311.

Manoj, B., Vineethkumar, V., & Prakash, V. (2020). Drinking water quality assessment in the water around a clay mine in Kannur district, Kerala. *Radiation Protection and Environment*, *43*(2), 88.

Mao, H., Wang, G., Liao, F., Shi, Z., Huang, X., Li, B., & Yan, X. (2022). Geochemical evolution of groundwater under the influence of human activities: A case study in the southwest of Poyang Lake Basin. *Applied Geochemistry*, *140*, 105299.

Marc, B., Amélie, J., Jean-Pascal, R., Manoj, D., Guillaume, M., & Delphine, C. (2018). Local environment of arsenic in sulfide minerals: insights from high-resolution X-ray spectroscopies, and first-principles calculations at the As K-edge. *Journal of Analytical Atomic Spectrometry*, *33*(12), 2070-2082.

Margat, J., & Van der Gun, J. (2013). *Groundwater around the world: a geographic synopsis*. Crc

Marghade, D., Malpe, D. B., Subba Rao, N., & Sunitha, B. (2020). Geochemical assessment of fluoride enriched groundwater and health implications from a part of Yavtmal District, India. *Human and Ecological Risk Assessment: An International Journal*, *26*(3), 673-694.

Marghade, D., Malpe, D., Duraisamy, K., Patil, P. D., & Li, P. (2021). Hydrogeochemical evaluation, suitability, and health risk assessment of groundwater in the watershed of Godavari basin, Maharashtra, Central India. *Environmental Science and Pollution Research*, *28*(15), 18471-18494.

Marguí, E., Zawisza, B., Skorek, R., Theato, T., Queralt, I., Hidalgo, M., & Sitko, R. (2013). Analytical possibilities of different X-ray fluorescence systems for determination of trace elements in aqueous samples pre-concentrated with carbon nanotubes. *Spectrochimica Acta Part B: Atomic Spectroscopy*, *88*, 192-197.

María, G. G., & Laura, B. (2015). Fluoride in the Context of the Environment. Food and Nutritional Components in Focus No. 6 Fluorine: Chemistry, Analysis, Function and Effects, edited by Victor R Preedy. *The Royal Society of Chemistry*.

Markowicz, A. A. (2008). Quantification and correction procedures. *Portable X-ray fluorescence spectrometry: capabilities for in situ analysis. The Royal Society of Chemistry, Cambridge*, 13-38.

Martin, E., González-Horta, C., Rager, J., Bailey, K. A., Sánchez-Ramírez, B., Ballinas-Casarrubias, L., ... & Fry, R. (2015). Metabolomic characteristics of arsenic-associated diabetes in a prospective cohort in Chihuahua, Mexico. *Toxicological Sciences*, *144*(2), 338-346.

Martínez-Santos, P. (2017). Does 91% of the world's population really have "sustainable access to safe drinking water"?. *International Journal of Water Resources Development*, *33*(4), 514-533.

Martz, L. W., & Garbrecht, J. (1992). Numerical definition of drainage network and subcatchment areas from digital elevation models. *Computers & Geosciences*, *18*(6), 747-761.

Matović, V., Buha, A., Đukić-Ćosić, D., & Bulat, Z. (2015). Insight into the oxidative stress induced by lead and/or cadmium in blood, liver and kidneys. *Food and Chemical Toxicology*, *78*, 130-140.

Mbonimpa, M., Aubertin, M., Chapuis, R. P., & Bussière, B. (2002). Practical pedotransfer functions for estimating the saturated hydraulic conductivity. *Geotechnical & Geological Engineering*, *20*(3), 235-259.

McCann, H. G. (1968). The solubility of fluorapatite and its relationship to that of calcium fluoride. *Archives of oral biology*, *13*(8), 987-1001.

McCormick, A. L. (2018). *Aluminum*. Enslow Publishing, LLC.

McDermott, S., Salzberg, D. C., Anderson, A. P., Shaw, T., & Lead, J. (2015). Systematic review of chromium and nickel exposure during pregnancy and impact on child outcomes. *Journal of Toxicology and Environmental Health, Part A*, *78*(21-22), 1348-1368.

McLaughlin, M. J., Maier, N. A., Freeman, K., Tiller, K. G., Williams, C. M. J., & Smart, M. K. (1995). Effect of potassic and phosphatic fertilizer type, fertilizer Cd concentration and zinc rate on cadmium uptake by potatoes. *Fertilizer research*, *40*(1), 63-70.

McQuillan, D. (2004). Ground-water quality impacts from on-site septic systems. In *Proceedings, National Onsite Wastewater Recycling Association, 13th Annual Conference, Albuquerque, NM* (pp. 6-18).

Mehta, B. C., & Srivastava, K. K. (2012). Iron in ground water in India and its geochemistry. *Mem. Ind. Soc. Anal. Geochem*, (1), 209-225.

Meira, L. A., Almeida, J. S., Dias, F. D. S., & Teixeira, L. S. (2019). Combination of extraction induced by microemulsion-breaking and pre-concentration using magnetic nanoparticles for multi-element determination of Cd, Cr, Cu and Pb in gasoline samples using energy dispersive X-ray fluorescence spectrometry. *Microchemical Journal*, *147*, 660-665.

Mejia, L. T. (2015). Lead Contamination: Environmental Geochemistry of Gold Mining Villages in Northwest Nigeria.

Melamed, D. (2005). Monitoring arsenic in the environment: a review of science and technologies with the potential for field measurements. *Analytica Chimica Acta*, *532*(1), 1-13.

Melquiades, F. L., & Appoloni, C. R. (2004). Application of XRF and field portable XRF for environmental analysis. *Journal of radioanalytical and nuclear chemistry*, *262*(2), 533-541.

Mercer, C. N., Watts, K. E., & Gross, J. (2020). Apatite trace element geochemistry and cathodoluminescent textures—A comparison between regional magmatism and the Pea Ridge IOAREE and Boss IOCG deposits, southeastern Missouri iron metallogenic province, USA. *Ore Geology Reviews*, *116*, 103129.

Milivojević, J., Krstić, D., Šmit, B., & Djekić, V. (2016). Assessment of heavy metal contamination and calculation of its pollution index for Uglješnica River, Serbia. *Bulletin of environmental contamination and toxicology*, *97*(5), 737-742.

Mirzaei, R., & Sakizadeh, M. (2016). Comparison of interpolation methods for the estimation of groundwater contamination in Andimeshk-Shush Plain, Southwest of Iran. *Environmental Science and Pollution Research*, *23*(3), 2758-2769.

Mishra, P., Pandey, C. M., Singh, U., Gupta, A., Sahu, C., & Keshri, A. (2019). Descriptive statistics and normality tests for statistical data. *Annals of cardiac anaesthesia*, *22*(1), 67.

Mladenov, N., Zheng, Y., Miller, M. P., Nemergut, D. R., Legg, T., Simone, B., ... & McKnight, D. M. (2010). Dissolved organic matter sources and consequences for iron and arsenic mobilization in Bangladesh aquifers. *Environmental science & technology*, *44*(1), 123-128.

Mobarra, N., Shanaki, M., Ehteram, H., Nasiri, H., Sahmani, M., Saeidi, M., ... & Azad, M. (2016). A review on iron chelators in treatment of iron overload

syndromes. *International journal of hematology-oncology and stem cell research*, *10*(4), 239.

Moghtaderi, T., Alamdar, R., Rodríguez-Seijo, A., Naghibi, S. J., & Kumar, V. (2020). Ecological risk assessment and source apportionment of heavy metal contamination in urban soils in Shiraz, Southwest Iran. *Arabian Journal of Geosciences*, *13*(16), 1-12.

Mohammed, I., Al Shehri, D., Mahmoud, M., Kamal, M. S., & Alade, O. S. (2021). Impact of Iron Minerals in Promoting Wettability Alterations in Reservoir Formations. *ACS omega*, *6*(5), 4022-4033.

Mohan, K. R., Krishna, A. K., Manohar, K., & Murthy, N. N. (2012a). Spatial Distribution of Arsenic in Ground Water from Nuggihalli Mining Area and its Surroundings, Southern Karnataka, India. *Journal of Applicable Chemistry*, *1*(1), 11-21.

Mohan, M., Augustine, T., Jayasooryan, K. K., Chandran, M. S., & Ramasamy, E. V. (2012b). Fractionation of selected metals in the sediments of Cochin estuary and Periyar River, southwest coast of India. *The Environmentalist*, *32*(4), 383-393.

Mohan, S. V., Nithila, P., & Reddy, S. J. (1996). Estimation of heavy metals in drinking water and development of heavy metal pollution index. *Journal of Environmental Science & Health Part A*, *31*(2), 283-289.

Mohana, P., & Velmurugan, P. M. (2020). Geochemical Characterization and Water Quality Assessment of Groundwater in Arani Taluk of Tamil Nadu, South India. *Geochemistry International*, *58*(5), 598-612.

Mohanty, A. K., & Rao, V. G. (2019). Hydrogeochemical, seawater intrusion and oxygen isotope studies on a coastal region in the Puri District of Odisha, India. *Catena*, *172*, 558-571.

Montazeri, B., Koba-Ucun, O., Arslan-Alaton, I., & Olmez-Hanci, T. (2021). Iprodione removal by UV-light-, zero-valent iron-and zero-valent aluminium-activated persulfate oxidation processes in pure water and simulated tertiary treated urban wastewater. *Water*, *13*(12), 1679.

Mooney, R. C. L. (1950). X-ray diffraction study of cerous phosphate and related crystals. I. Hexagonal modification. *Acta Crystallographica*, *3*(5), 337-340.

Mora, A., Mahlknecht, J., Ledesma-Ruiz, R., Sanford, W. E., & Lesser, L. E. (2020). Dynamics of major and trace elements during seawater intrusion in a coastal sedimentary aquifer impacted by anthropogenic activities. *Journal of Contaminant Hydrology*, *232*, 103653.

Morais, S., Costa, F. G., & Pereira, M. D. L. (2012). Heavy metals and human health. *Environmental health–emerging issues and practice*, *10*(1), 227-245.

Mudipalli, A. (2007). Lead hepatotoxicity & potential health effects. *Indian Journal of Medical Research*, *126*(6), 518.

Mueller, B., & Hug, S. J. (2018). Climatic variations and de-coupling between arsenic and iron in arsenic contaminated ground water in the lowlands of Nepal. *Chemosphere*, *210*, 347-358.

Mukherjee, A., Gupta, S., Coomar, P., Fryar, A. E., Guillot, S., Verma, S., ... & Charlet, L. (2019). Plate tectonics influence on geogenic arsenic cycling: From primary sources to global groundwater enrichment. *Science of the total environment*, *683*, 793-807.

Mukherjee, A., Verma, S., Gupta, S., Henke, K. R., & Bhattacharya, P. (2014). Influence of tectonics, sedimentation and aqueous flow cycles on the origin of global groundwater arsenic: paradigms from three continents. *Journal of hydrology*, *518*, 284-299.

Mukherjee, I., & Singh, U. K. (2018). Groundwater fluoride contamination, probable release, and containment mechanisms: a review on Indian context. *Environmental geochemistry and health*, *40*(6), 2259-2301.

Mukherjee, I., & Singh, U. K. (2020). Fluoride abundance and their release mechanisms in groundwater along with associated human health risks in a geologically heterogeneous semi-arid region of east India. *Microchemical journal*, *152*, 104304.

Mukherjee, I., & Singh, U. K. (2022). Exploring a variance decomposition approach integrated with the Monte Carlo method to evaluate groundwater fluoride exposure on the residents of a typical fluorosis endemic semi-arid tract of India. *Environmental Research*, *203*, 111697.

Müller, T., Osenbrück, K., Strauch, G., Pavetich, S., Al-Mashaikhi, K. S., Herb, C., ... & Sanford, W. (2016). Use of multiple age tracers to estimate groundwater residence times and long-term recharge rates in arid southern Oman. *Applied Geochemistry*, *74*, 67-83.

Munna, K., Guhey, R., & Vishwakarma, N. (2020). Mechanism of fluoride enrichment in groundwater of hard-rock terrain in bhopalpatnam area, Bijapur-District, Chhattisgarh, India. *Journal of Applied Geochemistry*, *22*(1), 72-85.

Murdock, C. C. (1930). The form of the X-ray diffraction bands for regular crystals of colloidal size. *Physical review*, *35*(1), 8.

Mushtaq, N., Younas, A., Mashiatullah, A., Javed, T., Ahmad, A., & Farooqi, A. (2018). Hydrogeochemical and isotopic evaluation of groundwater with elevated arsenic in alkaline aquifers in Eastern Punjab, Pakistan. *Chemosphere*, *200*, 576-586.

Muthulakshmi, L., Ramu, A., & Kannan, N. (2012). Seasonal distribution of some heavy metal concentrations in ground water of Virudhunagar district, Tamilnadu, South India. *Electronic Journal of Environmental, Agricultural and Food Chemistry*, *11*(2), 32-37.

Nadeau, O., & Harris, J. (2019). Remobilization and adsorption of colloidal gold on nano-particulate chlorite at the Hardrock Archean orogenic gold deposits: A new tool for gold exploration. *Journal of Geochemical Exploration*, *204*, 181-205.

Naderi, M., Jahanshahi, R., & Dehbandi, R. (2020). Two distinct mechanisms of fluoride enrichment and associated health risk in springs' water near an inactive volcano, southeast Iran. *Ecotoxicology and environmental safety*, *195*, 110503.

Nagaraju, A., Balaji, E., Sun, L. H., & Thejaswi, A. (2018). Processes controlling groundwater chemistry from Mulakalacheruvu area, Chittoor district, Andhra

Pradesh, South India: a statistical approach based on hydrochemistry. *Journal of the Geological Society of India*, *91*(4), 425-430.

Nagaraju, A., Sunil Kumar, K., & Thejaswi, A. (2014). Assessment of groundwater quality for irrigation: a case study from Bandalamottu lead mining area, Guntur District, Andhra Pradesh, South India. *Applied Water Science*, *4*(4), 385-396.

Nagendra Rao, C. (2003, December). Fluoride and environment—a review. In Proceedings of the third international conference on environment and health, Chennai, India (pp. 15-17).

Nair, H. C., Padmalal, D., Joseph, A., & Vinod, P. G. (2017). Delineation of groundwater potential zones in river basins using geospatial tools—an example from southern Western Ghats, Kerala, India. *Journal of Geovisualization and Spatial Analysis*, *1*(1), 1-16.

Nakamoto, T., & Rawls, H. R. (2018). Fluoride exposure in early life as the possible root cause of disease in later life. *Journal of Clinical Pediatric Dentistry*, *42*(5), 325-330.

Namaghi, H. H., Karami, G. H., & Saadat, S. (2011). A study on chemical properties of groundwater and soil in ophiolitic rocks in Firuzabad, east of Shahrood, Iran: with emphasis to heavy metal contamination. *Environmental monitoring and assessment*, *174*(1), 573-583.

Namrata, P., Alok, L., Mehrotra, S., & Srivastava, J. B. (2015). Arsenic pollution scenario in Eastern UP, India: A review. *International Research Journal of Environment Sciences*, *4*(11), 83-86.

Nandakumaran, P., & Balakrishnan, K. (2020). Groundwater quality variations in Precambrian hard rock aquifers: a case study from Kerala, India. *Applied Water Science*, *10*(1), 1-13.

Narayanamoorthy, A. (2011). Development and composition of irrigation in India: Temporal trends and regional patterns. *Irrigation and Drainage*, *60*(4), 431-445.

Narsimha, A., & Rajitha, S. (2018). Spatial distribution and seasonal variation in fluoride enrichment in groundwater and its associated human health risk assessment in Telangana State, South India. *Human and Ecological Risk Assessment: An International Journal*, *24*(8), 2119-2132.

Narsimha, A., & Sudarshan, V. (2017). Contamination of fluoride in groundwater and its effect on human health: a case study in hard rock aquifers of Siddipet, Telangana State, India. *Applied Water Science*, *7*(5), 2501-2512.

Narsimha, A., & Sudarshan, V. (2018). Data on fluoride concentration levels in semi-arid region of Medak, Telangana, South India. *Data in brief*, *16*, 717.

NASA (2020) Distribution of Water on the Earth's Surface, https://www.e-education.psu.edu/earth 103/node/701. (Accessed 4 August 2020).

Nasher, N. R., & Ahmed, M. H. (2021). Groundwater geochemistry and hydrogeochemical processes in the Lower Ganges-Brahmaputra-Meghna River Basin areas, Bangladesh. *Journal of Asian Earth Sciences: X*, *6*, 100062.

Nath, A. V., Selvam, S., Reghunath, R., & Jesuraja, K. (2021a). Groundwater quality assessment based on groundwater pollution index using Geographic Information System at Thettiyar watershed, Thiruvananthapuram district, Kerala, India. *Arabian Journal of Geosciences*, *14*(7), 1-26.

Nath, A., Samanta, S., Banerjee, S., Danda, A. A., & Hazra, S. (2021b). Threat of arsenic contamination, salinity and water pollution in agricultural practices of Sundarban Delta, India, and mitigation strategies. *SN Applied Sciences*, *3*(5), 1-15.

Nayak, B., Das, B., Chandra Mukherjee, S., Pal, A., Ahamed, S., Amir Hossain, M., ... & Chakraborti, D. (2008). Groundwater arsenic contamination in the Sahibganj district of Jharkhand state, India in the middle Ganga plain and adverse health effects. *Toxicological & Environmental Chemistry*, *90*(4), 673-694.

Nazir, M. A., Yasar, A., Bashir, M. A., Siyal, S. H., Najam, T., Javed, M. S., ... & Rehman, A. U. (2020). Quality assessment of the noncarbonated-bottled drinking water: comparison of their treatment techniques. *International journal of environmental analytical chemistry*, 1-12.

Nedobukh, T. A., & Semenishchev, V. S. (2020). Strontium: source, occurrence, properties, and detection. *Strontium Contamination in the Environment*, 1-23.

Négrel, P., Millot, R., Roy, S., Guerrot, C., & Pauwels, H. (2010). Lead isotopes in groundwater as an indicator of water–rock interaction (Masheshwaram catchment, Andhra Pradesh, India). *Chemical Geology*, *274*(3-4), 136-148.

Neumann, R. B., Ashfaque, K. N., Badruzzaman, A. B. M., Ashraf Ali, M., Shoemaker, J. K., & Harvey, C. F. (2010). Anthropogenic influences on groundwater arsenic concentrations in Bangladesh. *Nature geoscience*, *3*(1), 46-52.

Newton, R. C., Aranovich, L. Y., & Touret, J. L. (2019). Streaming of saline fluids through Archean crust: Another view of charnockite-granite relations in southern India. *Lithos*, *346*, 105157.

Ngah, S. A., & Nwankwoala, H. O. (2013). Iron (Fe2+) occurrence and distribution in groundwater sources in different geomorphologic zones of Eastern Niger Delta. *Appl Sci Res*, *5*(2), 266-272.

Nganje, T. N., Adamu, C. I., Ekwere, A. S., Ibe, K. A., Edet, A., & Hursthouse, A. S. (2021). Environmental geochemical signature of shale in pollution assessment of trace metals in soil and water in parts of southern Benue trough, southeastern Nigeria. *International Journal of Environmental Analytical Chemistry*, 1-21.

Nicolli, H. B., Bundschuh, J., García, J. W., Falcón, C. M., & Jean, J. S. (2010). Sources and controls for the mobility of arsenic in oxidizing groundwaters from loess-type sediments in arid/semi-arid dry climates–Evidence from the Chaco–Pampean plain (Argentina). *Water research*, *44*(19), 5589-5604.

Nisa, K. G., & Sujatha, C. H. (2020). Distribution pattern of trace metals in selected surface soils of Palakkad district, South India. *Environmental Forensics*, 1-11.

Nizam, S., Virk, H. S., & Sen, I. S. (2022). High levels of fluoride in groundwater from Northern parts of Indo-Gangetic plains reveals detrimental fluorosis health risks. *Environmental Advances*, *8*, 100200.

Njogu, P. M., Keriko, J. M., & Kitetu, R. W. J. (2021). Distribution of heavy metals in various lake matrices; water, soil, fish and sediments: A case study of the lake Naivasha Basin, Kenya.

Noor, S., Rashid, A., Javed, A., Khattak, J. A., & Farooqi, A. (2022). Hydrogeological properties, sources provenance, and health risk exposure of fluoride in the groundwater of Batkhela, Pakistan. *Environmental Technology & Innovation*, *25*, 102239.

Norgard, J., & Best, G. L. (2017). The electromagnetic spectrum. In *National Association of Broadcasters Engineering Handbook* (pp. 3-10). Routledge.

Norrish, K., & Hutton, J. T. (1969). An accurate X-ray spectrographic method for the analysis of a wide range of geological samples. *Geochimica et cosmochimica acta*, *33*(4), 431-453.

Novoselov, A. A., Hodson, M. E., Tapia-Gatica, J., Dovletyarova, E. A., Yáñez, C., & Neaman, A. (2022). The effect of rock lithology on the background concentrations of trace elements in alluvial soils: Implications for environmental regulation. *Applied Geochemistry*, *146*, 105440.

Nowak, B., & Lawniczak-Malińska, A. E. (2019). The influence of hydrometeorological conditions on changes in littoral and riparian vegetation of a meromictic lake in the last half-century. *Water*, *11*(12), 2651.

Nowicki, S., deLaurent, Z. R., de Villiers, E. P., Githinji, G., & Charles, K. J. (2021). The utility of Escherichia coli as a contamination indicator for rural drinking water: Evidence from whole genome sequencing. *PLoS One*, *16*(1), e0245910.

Noyan, I. C., & Cohen, J. B. (2013). *Residual stress: measurement by diffraction and interpretation*. Springer.

Nuamah Daniel, O. B., Tandoh Kingsley, K., & Brako, A. B. (2019). Geochemistry of minor and trace elements in soils of Akuse area, Southeastern Ghana. *Geosciences*, *9*(1), 8-17.

O'Neal, S. L., & Zheng, W. (2015). Manganese toxicity upon overexposure: a decade in review. *Current environmental health reports*, *2*(3), 315-328.

O'Day, P. A. (2006). Chemistry and mineralogy of arsenic. *Elements*, *2*(2), 77-83.

Odika, P. O., Anike, O. L., Onwuemesi, A. G., Odika, N. F., & Ejeckam, R. B. (2020). Assessment of environmental geochemistry of lead-zinc mining at Ishiagu area, lower Benue trough, southeastern Nigeria. *Earth Science Research*, *9*(1), 1-31.

Odika, P. O., Anike, O. L., Onwuemesi, A. G., Odika, N. F., & Ejeckam, R. B. (2020). Assessment of environmental geochemistry of lead-zinc mining at Ishiagu area, lower Benue trough, southeastern Nigeria.

Oinam, J. D., Ramanathan, A. L., Linda, A., & Singh, G. (2011). A study of arsenic, iron and other dissolved ion variations in the groundwater of Bishnupur District, Manipur, India. *Environmental Earth Sciences*, *62*(6), 1183-1195.

Okuda, B., Iwamoto, Y., Tachibana, H., & Sugita, M. (1998). Parkinsonism after acute cadmium poisoning. *Occupational Health and Industrial Medicine*, *5*(38), 232.

Olivares, M., & Uauy, R. (1996). Copper as an essential nutrient. *The American journal of clinical nutrition*, *63*(5), 791S-796S.

Olivares, M., Araya, M., & Uauy, R. (2000). Copper homeostasis in infant nutrition: deficit and excess. *Journal of pediatric gastroenterology and nutrition*, *31*(2), 102-111.

Onipe, T. A. (2018). *Geogenic fluoride source in groundwater: a case study of Siloam Village, Limpopo Province, South Africa* (Doctoral dissertation).

Osiemo, M. M., Ogendi, G. M., & M'Erimba, C. (2019). Microbial quality of drinking water and prevalence of water-related diseases in Marigat Urban Centre, Kenya. *Environmental health insights*, *13*, 1178630219836988.

Osono, A., & Katoh, M. (2021). Characteristics of the immobilization process of arsenic depending on the size fraction released from excavated rock/sediment after the addition of immobilization materials. *Journal of Environmental Management*, *298*, 113534.

O'Sullivan, G. J., Chew, D. M., Morton, A. C., Mark, C., & Henrichs, I. A. (2018). An integrated apatite geochronology and geochemistry tool for sedimentary provenance analysis. *Geochemistry, Geophysics, Geosystems*, *19*(4), 1309-1326.

Otel, I., Dias, K., Pereira, R., Fonseca, M., Jesus, A. P., Mata, A., ... & Pessanha, S. (2022). Investigation of the protective suitability of a dental fluorinated varnish by means of X Ray fluorescence and Raman spectroscopy. *Journal of Trace Elements in Medicine and Biology*, *71*, 126938.

Otero, X. L., Ferreira, T. O., Huerta-Díaz, M. A., Partiti, C. D. M., Souza Jr, V., Vidal-Torrado, P., & Macías, F. (2009). Geochemistry of iron and manganese in soils and sediments of a mangrove system, Island of Pai Matos (Cananeia—SP, Brazil). *Geoderma*, *148*(3-4), 318-335.

Oyebanjo, O. O. (2020). *Mineralogy and geochemistry of kaolins in oxidic soils developed from different parent rocks in Limpopo Province, South Africa* (Doctoral dissertation).

Ozdemir, H., & Bird, D. (2009). Evaluation of morphometric parameters of drainage networks derived from topographic maps and DEM in point of floods. *Environmental geology*, *56*(7), 1405-1415.

Oze, C., Bird, D. K., & Fendorf, S. (2007). Genesis of hexavalent chromium from natural sources in soil and groundwater. *Proceedings of the National Academy of Sciences*, *104*(16), 6544-6549.

Ozsvath, D. L. (2006). Fluoride concentrations in a crystalline bedrock aquifer Marathon County, Wisconsin. *Environmental Geology*, *50*(1), 132-138.

Ozsvath, D. L. (2009). Fluoride and environmental health: a review. *Reviews in Environmental Science and Bio/Technology*, *8*(1), 59-79.

Pabis-Mazgaj, E., Gawenda, T., Pichniarczyk, P., & Stempkowska, A. (2021). Mineral composition and structural characterization of the clinoptilolite powders obtained from zeolite-rich tuffs. *Minerals*, *11*(10), 1030.

Pai, D. S., & Nair, R. M. (2009). Summer monsoon onset over Kerala: New definition and prediction. *Journal of Earth System Science*, *118*(2), 123-135.

Pais, I., & Jones Jr, J. B. (1997). *The handbook of trace elements*. Crc Press.

Paktunc, D. (2008). *Speciation of arsenic in pyrite by micro-X-ray absorption fine-structure spectroscopy (XAFS)*. Argonne National Lab.(ANL), Argonne, IL (United States). Advanced Photon Source (APS).

Palit, S., Misra, K., & Mishra, J. (2019). Arsenic Contamination in South Asian Regions: the difficulties, challenges and vision for the future. In *Separation science and technology* (Vol. 11, pp. 113-123). Academic press.

Palmer, P. T., Jacobs, R., Baker, P. E., Ferguson, K., & Webber, S. (2009). Use of field-portable XRF analyzers for rapid screening of toxic elements in FDA-regulated products. *Journal of agricultural and food chemistry*, *57*(7), 2605-2613.

Palmer, W. C., Vishnu, P., Sanchez, W., Aqel, B., Riegert-Johnson, D., Seaman, L. A. K., ... & Rivera, C. E. (2018). Diagnosis and management of genetic iron overload disorders. *Journal of general internal medicine*, *33*(12), 2230-2236.

Pan, L. C., Hu, R. Z., Oyebamiji, A., Wu, H. Y., Li, J. W., & Li, J. X. (2021). Contrasting magma compositions between Cu and Au mineralized granodiorite intrusions in the Tongling ore district in South China using apatite chemical composition and Sr-Nd isotopes. *American Mineralogist: Journal of Earth and Planetary Materials*, *106*(12), 1873-1889.

Panayi, A. E., Spyrou, N. M., Iversen, B. S., White, M. A., & Part, P. (2002). Determination of cadmium and zinc in Alzheimer's brain tissue using inductively coupled plasma mass spectrometry. *Journal of the neurological sciences*, *195*(1), 1-10.

Panda, D. K., & Wahr, J. (2016). Spatiotemporal evolution of water storage changes in I ndia from the updated GRACE-derived gravity records. *Water Resources Research*, *52*(1), 135-149.

Panda, D. K., Mishra, A., Jena, S. K., James, B. K., & Kumar, A. (2007). The influence of drought and anthropogenic effects on groundwater levels in Orissa, India. *Journal of hydrology*, *343*(3-4), 140-153.

Pandey, P. K., Kass, P. H., Soupir, M. L., Biswas, S., & Singh, V. P. (2014). Contamination of water resources by pathogenic bacteria. *Amb Express*, *4*(1), 1-16.

Parameswari, K., & Mudgal, B. V. (2014). Geochemical investigation of groundwater contamination in Perungudi dumpsite, South India. *Arabian Journal of Geosciences*, *7*(4), 1363-1371.

Parrone, D., Ghergo, S., Frollini, E., Rossi, D., & Preziosi, E. (2020). Arsenic-fluoride co-contamination in groundwater: Background and anomalies in a volcanic-sedimentary aquifer in central Italy. *Journal of Geochemical Exploration*, *217*, 106590.

Parsons, C., Grabulosa, E. M., Pili, E., Floor, G. H., Roman-Ross, G., & Charlet, L. (2013). Quantification of trace arsenic in soils by field-portable X-ray fluorescence spectrometry: considerations for sample preparation and measurement conditions. *Journal of Hazardous Materials*, *262*, 1213-1222.

Parveen, R., & Kumar, U. (2012). Integrated approach of universal soil loss equation (USLE) and geographical information system (GIS) for soil loss risk assessment in Upper South Koel Basin, Jharkhand.

Pashkova, G. V., & Revenko, A. G. (2015). A review of application of total reflection X-ray fluorescence spectrometry to water analysis. *Applied Spectroscopy Reviews*, *50*(6), 443-472.

Patel, A. K., Das, N., Goswami, R., & Kumar, M. (2019). Arsenic mobility and potential co-leaching of fluoride from the sediments of three tributaries of the Upper Brahmaputra floodplain, Lakhimpur, Assam, India. *Journal of Geochemical Exploration*, *203*, 45-58.

Patel, D. K., Rahman, A., & Singh, M. (2022). Occurrences of Rare Earth Element (REE) Bearing Minerals in Migmatitic Gneiss and Granitoids of Chhotanagpur Granite Gneissic Complex, Bihar, India. *Journal of the Geological Society of India*, *98*(10), 1343-1355.

Patel, K. S., Sahu, B. L., Dahariya, N. S., Bhatia, A., Patel, R. K., Matini, L., ... & Bhattacharya, P. (2017). Groundwater arsenic and fluoride in Rajnandgaon District, Chhattisgarh, northeastern India. *Applied water science*, *7*(4), 1817-1826.

Patel, K. S., Shrivas, K., Hoffmann, P., & Jakubowski, N. (2006). A survey of lead pollution in Chhattisgarh State, central India. *Environmental geochemistry and health*, *28*(1), 11-17.

Pathak, P., Dwivedi, S. B., & Kumar, R. R. (2022). Geochemistry and Phase equilibrium modelling of garnet-biotite gneiss from Mauranipur, Bundelkhand Craton, Northern India; implication for tectonic setting and metamorphism. *Journal of Geosciences Research. Under Review*.

Patil, S. S., Barfield, B. J., & Wilber, G. G. (2011). Turbidity modeling based on the concentration of total suspended solids for stormwater runoff from construction and development sites. In *World Environmental and Water Resources Congress 2011: Bearing Knowledge for Sustainability* (pp. 477-486).

Patočka, J., & Černý, K. (2003). Inorganic lead toxicology. *Acta Medica (Hradec Kralove)*, *46*(2), 65-72.

Patolia, P., & Sinha, A. (2017). Fluoride contamination in Gharbar Village of Dhanbad District, Jharkhand, India: source identification and management. *Arabian Journal of Geosciences*, *10*(17), 1-10.

Patra, S., Sahoo, S., Mishra, P., & Mahapatra, S. C. (2018). Impacts of urbanization on land use/cover changes and its probable implications on local climate and groundwater level. Journal of urban management, 7(2), 70-84.

Paudyal, H., Inoue, K., Kawakita, H., Ohto, K., Kamata, H., & Alam, S. (2018). Removal of fluoride by effectively using spent cation exchange resin. *Journal of Material Cycles and Waste Management*, *20*, 975-984.

Paul, R., Prasanna, M. V., Gantayat, R. R., & Singh, M. K. (2019). Groundwater quality assessment in Jirania Block, west district of Tripura, India, using hydrogeochemical fingerprints. *SN Applied Sciences*, *1*(9), 1-14.

Penke, Y. K., Yadav, A. K., Sinha, P., Malik, I., Ramkumar, J., & Kar, K. K. (2020). Arsenic remediation onto redox and photo-catalytic/electrocatalytic Mn-Al-Fe impregnated rGO: Sustainable aspects of sludge as supercapacitor. *Chemical Engineering Journal*, *390*, 124000.

Pharoe, B. K., Evdokimov, A. N., & Bushuev, Y. Y. (2020). Mineral composition and reconstruction of the source areas of manganese-bearing alluvial deposits in the Ventersdorp area, South Africa. *Journal of African Earth Sciences*, *168*, 103841.

Pi, K., Wang, Y., Xie, X., Su, C., Ma, T., Li, J., & Liu, Y. (2015). Hydrogeochemistry of co-occurring geogenic arsenic, fluoride and iodine in groundwater at Datong Basin, northern China. *Journal of hazardous materials*, *300*, 652-661.

Piccoli, P. M., & Candela, P. A. (2002). Apatite in igneous systems. *Reviews in Mineralogy and Geochemistry*, *48*(1), 255-292.

Pickard, H., Palk, E., Schönbächler, M., Moore, R. E., Coles, B. J., Kreissig, K., ... & Rehkämper, M. (2022). The cadmium and zinc isotope compositions of the silicate Earth–Implications for terrestrial volatile accretion. *Geochimica et Cosmochimica Acta*, *338*, 165-180.

Pillai, A. V. S., Sabarathinam, C., Keesari, T., Chandrasekar, T., Rajendiran, T., Senapathi, V., ... & Samayamanthu, D. R. (2020). Seasonal changes in groundwater quality deterioration and chemometric analysis of pollution source identification in South India. *Environmental Science and Pollution Research*, *27*(16), 20037-20054.

Piper AM (1944). A graphic procedure in geochemical interpretation of water analyses. Trans Am Geophys Union 25: 914– 923

Planer-Friedrich, B., Armienta, M., & Merkel, B. (2001). Origin of arsenic in the groundwater of the Rioverde basin, Mexico. *Environmental Geology*, *40*(10), 1290-1298.

Plebow, A. (2013). X-ray-induced alteration of specimens as crucial obstacle in XRF spectrometry of fluorine in rocks and soils. *X-Ray Spectrometry*, *42*(1), 19-32.

Pophare, A. M., Lamsoge, B. R., Katpatal, Y. B., & Nawale, V. P. (2014). Impact of over-exploitation on groundwater quality: a case study from WR-2 Watershed, India. *Journal of earth system science*, *123*(7), 1541-1566.

Pothiraj, P., & Rajagopalan, B. (2013). A GIS and remote sensing based evaluation of groundwater potential zones in a hard rock terrain of Vaigai sub-basin, India. *Arabian Journal of Geosciences*, *6*(7), 2391-2407.

Pouzar, M., Černohorský, T., & Krejčová, A. (2001). Determination of metals in lubricating oils by X-ray fluorescence spectrometry. *Talanta*, *54*(5), 829-835.

Prabhakar, A., Mishra, S., & Das, A. P. (2019). Isolation and identification of lead (Pb) solubilizing bacteria from automobile waste and its potential for recovery of lead from end of life waste batteries. *Geomicrobiology Journal*, *36*(10), 894-903.

Prasad, A. S. (2004). Zinc deficiency: its characterization and treatment. *Metal ions in biological systems*, *41*, 103-138.

Prasanna, M. V., Chidambaram, S., Kumar, G. S., Ramanathan, A. L., & Nainwal, H. C. (2011). Hydrogeochemical assessment of groundwater in Neyveli Basin, Cuddalore district, South India. *Arabian Journal of Geosciences*, *4*(1), 319-330.

Prasanna, M. V., Praveena, S. M., Chidambaram, S., Nagarajan, R., & Elayaraja, A. (2012). Evaluation of water quality pollution indices for heavy metal contamination monitoring: a case study from Curtin Lake, Miri City, East Malaysia. *Environmental Earth Sciences*, *67*(7), 1987-2001.

Prasanth, S. S., Magesh, N. S., Jitheshlal, K. V., Chandrasekar, N., & Gangadhar, K. (2012). Evaluation of groundwater quality and its suitability for drinking and agricultural use in the coastal stretch of Alappuzha District, Kerala, India. *Applied Water Science*, *2*(3), 165-175.

Priju, C. P., Athira, S. G., Neerajamol, T. P., Madhavan, K., & Narasimha Prasad, N. B. (2012). Groundwater quality with special reference to salinity intrusion in Cochin area, Kerala. In *Proceedings of fifth international groundwater conference (IGWC-2012) on the assessment and management of groundwater resources in hard rock systems with special reference to basaltic terrain* (pp. 152-179).

Purushotham, D., Lone, M. A., Rashid, M., Rao, A. N., & Ahmed, S. (2012). Deciphering heavy metal contamination zones in soils of a granitic terrain of southern India using factor analysis and GIS. *Journal of earth system science*, *121*(4), 1059-1070.

Pytlakowska, K., Kozik, V., Matussek, M., Pilch, M., Hachuła, B., & Kocot, K. (2016). Glycine modified graphene oxide as a novel sorbent for preconcentration of chromium, copper, and zinc ions from water samples prior to energy dispersive X-ray fluorescence spectrometric determination. *RSC advances*, *6*(49), 42836-42844.

Qasemi, M., Shams, M., Sajjadi, S. A., Farhang, M., Erfanpoor, S., Yousefi, M., ... & Afsharnia, M. (2019). Cadmium in groundwater consumed in the rural areas of Gonabad and Bajestan, Iran: occurrence and health risk assessment. *Biological trace element research*, *192*(2), 106-115.

Qian, Q. (2018). Salt, water and nephron: mechanisms of action and link to hypertension and chronic kidney disease. *Nephrology*, *23*, 44-49.

Qiao, W., Cao, W., Gao, Z., Pan, D., Ren, Y., Li, Z., & Zhang, Z. (2022). Contrasting behaviors of groundwater arsenic and fluoride in the lower reaches of the Yellow River basin, China: Geochemical and modeling evidences. *Science of The Total Environment*, *851*, 158134.

Quina, M. J., Bordado, J. C., & Quinta-Ferreira, R. M. (2009). The influence of pH on the leaching behaviour of inorganic components from municipal solid waste APC residues. Waste Management, 29(9), 2483-2493.

Quiniou, T., & Laperche, V. (2014). An assessment of field-portable X-ray fluorescence analysis for nickel and iron in laterite ore (New Caledonia). *Geochemistry: Exploration, Environment, Analysis*, *14*(3), 245-255.

Radtke, M., Reinholz, U., & Gebhard, R. (2017). Synchrotron Radiation–Induced X-Ray Fluorescence (SRXRF) Analyses Of The Bernstorf Gold. *Archaeometry*, *59*(5), 891-899.

Radu, T., & Diamond, D. (2009). Comparison of soil pollution concentrations determined using AAS and portable XRF techniques. *Journal of hazardous materials*, *171*(1-3), 1168-1171.

Rae, I. D. (2020). Arsenic: its chemistry, its occurrence in the earth and its release into industry and the environment. *ChemTexts*, *6*(4), 1-11.

Raessler, M. (2018). The arsenic contamination of drinking and groundwaters in Bangladesh: featuring biogeochemical aspects and implications on public health. *Archives of environmental contamination and toxicology*, *75*(1), 1-7.

Raghav, S., Nair, M., & Kumar, D. (2019). Tetragonal prism shaped Ni-Al bimetallic adsorbent for study of adsorptive removal of fluoride and role of ion-exchange. *Applied Surface Science*, *498*, 143785.

Rahimzadeh, M. R., Rahimzadeh, M. R., Kazemi, S., & Moghadamnia, A. A. (2017). Cadmium toxicity and treatment: An update. *Caspian journal of internal medicine*, *8*(3), 135.

Rahman, A., Mondal, N. C., & Fauzia, F. (2021). Arsenic enrichment and its natural background in groundwater at the proximity of active floodplains of Ganga River, northern India. *Chemosphere*, *265*, 129096.

Rahman, M. M., Naidu, R., & Bhattacharya, P. (2009). Arsenic contamination in groundwater in the Southeast Asia region. *Environmental geochemistry and health*, *31*(1), 9-21.

Rahman, S. F., & Umamahesh, M. (2018). A Physicochemical Investigation of Potable Water in Adoni, Kurnool District, AP, India. *J. Chem. Chem. Sci.*, *8*, 519-523.

Raizada, A., Adhikari, R. N., Kumar, S., Patil, S. L., Ramajayam, D., Prabhavathi, M., ... & Muralidhar, W. (2018). Impact assessment of watershed interventions under low rainfall situations in semi-arid Karnataka. *Indian Journal of Soil Conservation*, *46*(2), 261-271.

Raj, D., & Shaji, E. (2017). Fluoride contamination in groundwater resources of Alleppey, southern India. *Geoscience Frontiers*, *8*(1), 117-124.

Raja, V., Lakshmi, R. V., Sekar, C. P., Chidambaram, S., & Neelakantan, M. A. (2021). Health risk assessment of heavy metals in groundwater of industrial township virudhunagar, Tamil Nadu, India. *Archives of Environmental Contamination and Toxicology*, *80*(1), 144-163.

Rajappa, B., Manjappa, S., & Puttaiah, E. T. (2010). Monitoring of heavy metal concentration in groundwater of Hakinaka Taluk, India. *Contemporary Engineering Sciences*, *3*(4), 183-190.

Rajendiran, S., Dotaniya, M. L., Coumar, M. V., Panwar, N. R., & Saha, J. K. (2015). Heavy metal polluted soils in India: status and countermeasures. *JNKVV Res J*, *49*(3), 320-337.

Rajmohan, N., & Elango, L. J. E. M. (2005). Distribution of iron, manganese, zinc and atrazine in groundwater in parts of Palar and Cheyyar river basins, South India. *Environmental Monitoring and Assessment*, *107*(1), 115-131.

Raju, N. J. (2006). Iron contamination in groundwater: A case from Tirumala-Tirupati environs, India. *The Researcher*, *1*(1), 28-31.

Raju, N. J. (2017). Prevalence of fluorosis in the fluoride enriched groundwater in semi-arid parts of eastern India: Geochemistry and health implications. *Quaternary International*, *443*, 265-278.

Raju, N. J. (2022). Arsenic in the geo-environment: A review of sources, geochemical processes, toxicity and removal technologies. *Environmental research*, *203*, 111782.

Ram, A., Tiwari, S. K., Pandey, H. K., Chaurasia, A. K., Singh, S., & Singh, Y. V. (2021). Groundwater quality assessment using water quality index (WQI) under GIS framework. *Applied Water Science*, *11*, 1-20.

Ramamohana Rao, N. V., Rao, N., Surya Prakash Rao, K., & Schuiling, R. D. (1993). Fluorine distribution in waters of Nalgonda district, Andhra Pradesh, India. *Environmental Geology*, *21*(1), 84-89.

Ramesh, K., & Elango, L. (2012). Groundwater quality and its suitability for domestic and agricultural use in Tondiar river basin, Tamil Nadu, India. Environmental monitoring and assessment, 184(6), 3887-3899.

Ramesh, M., Shankar, R., Krishnan, R., Malathi, N., & Aruna, R. M. (2014). Prevalence of dental fluorosis in the district of Salem, Tamil Nadu, South India: A pilot study. *Journal of Orofacial Sciences*, *6*(1), 37.

Ramteke, L. P., Sahayam, A. C., Ghosh, A., Rambabu, U., Reddy, M. R. P., Popat, K. M., ... & Ghosh, P. K. (2018). Study of fluoride content in some commercial phosphate fertilizers. *Journal of Fluorine Chemistry*, *210*, 149-155.

Rango, T., Bianchini, G., Beccaluva, L., & Tassinari, R. (2010). Geochemistry and water quality assessment of central Main Ethiopian Rift natural waters with emphasis on source and occurrence of fluoride and arsenic. *Journal of African Earth Sciences*, *57*(5), 479-491.

Rani, A., Kumar, A., Lal, A., & Pant, M. (2014). Cellular mechanisms of cadmium-induced toxicity: a review. *International journal of environmental health research*, *24*(4), 378-399.

Ranjan, S. P., Kazama, S., & Sawamoto, M. (2006). Effects of climate and land use changes on groundwater resources in coastal aquifers. *Journal of Environmental Management*, *80*(1), 25-35.

Ranjan, S., & Yasmin, S. (2019). Geological source of fluoride in fluoride endemic region of Gaya district, Bihar, India. *Bioscience Biotechnology Research Communications*, *12*(4), 1165-1172.

Rao, K. N., & Latha, P. S. (2019). Groundwater quality assessment using water quality index with a special focus on vulnerable tribal region of Eastern Ghats hard rock terrain, Southern India. *Arabian Journal of Geosciences*, *12*(8), 1-16.

Rao, N. S. (2018). Groundwater quality from a part of Prakasam district, Andhra Pradesh, India. *Applied water science*, *8*(1), 1-18.

Rao, N. S., & Chaudhary, M. (2019). Hydrogeochemical processes regulating the spatial distribution of groundwater contamination, using pollution index of groundwater (PIG) and hierarchical cluster analysis (HCA): a case study. *Groundwater for Sustainable Development*, *9*, 100238.

Rao, N. S., Sunitha, B., Sun, L., Spandana, B. D., & Chaudhary, M. (2020). Mechanisms controlling groundwater chemistry and assessment of potential health risk: a case study from South India. *Geochemistry*, *80*(4), 125568.

Rashid, A., Khattak, S. A., Ali, L., Zaib, M., Jehan, S., Ayub, M., & Ullah, S. (2019). Geochemical profile and source identification of surface and groundwater pollution of District Chitral, Northern Pakistan. *Microchemical Journal*, *145*, 1058-1065.

Ratnaike, R. N. (2003). Acute and chronic arsenic toxicity. *Postgraduate medical journal*, *79*(933), 391-396.

Raudsepp, M. J., Wilson, S., Morgan, B., Patel, A., Johnston, S. G., Gagen, E. J., & Fallon, S. J. (2022). Non-classical crystallization of very high magnesium calcite and magnesite in the Coorong Lakes, Australia. *Sedimentology*, *69*(5), 2246-2266.

Raval, N. P., Shah, P. U., & Shah, N. K. (2016). Adsorptive removal of nickel (II) ions from aqueous environment: A review. *Journal of Environmental Management*, *179*, 1-20.

Raychowdhury, N., Mukherjee, A., Bhattacharya, P., Johannesson, K., Bundschuh, J., Sifuentes, G. B., ... & del Rosario Storniolo, A. (2014). Provenance and fate of arsenic and other solutes in the Chaco-Pampean Plain of the Andean foreland, Argentina: From perspectives of hydrogeochemical modeling and regional tectonic setting. *Journal of Hydrology*, *518*, 300-316.

Raymahashay, B. C., Rao, K. S., Mehta, V. K., & Bhavana, P. R. (1987). Mineralogy and geochemistry of lateritic soil profiles in Kerala, India. *Chemical geology*, *60*(1-4), 327-330.

Reddy, A. G. S., Reddy, D. V., & Kumar, M. S. (2016). Hydrogeochemical processes of fluoride enrichment in Chimakurthy pluton, Prakasam district, Andhra Pradesh, India. *Environmental Earth Sciences*, *75*, 1-17.

Reddy, B. M., Sunitha, V., Prasad, M., Reddy, Y. S., & Reddy, M. R. (2019). Evaluation of groundwater suitability for domestic and agricultural utility in semi-arid region of Anantapur, Andhra Pradesh State, South India. *Groundwater for Sustainable Development*, *9*, 100262.

Reddy, K. S., Puppala, R., Kethineni, B., Reddy, H., Reddy, A., & Kalyan, V. S. (2017). Prevalence of Dental Fluorosis Among 6–12-Year-Old School Children of Mahabubnagar District, Telangana State, India− A Cross-Sectional Study. *Journal of Indian Association of Public Health Dentistry*, *15*(1), 42.

Refsgaard, J. C., Christensen, T. H., & Ammentorp, H. C. (1991). A model for oxygen transport and consumption in the unsaturated zone. *Journal of Hydrology*, *129*(1-4), 349-369.

Rehman, K., Fatima, F., Waheed, I., & Akash, M. S. H. (2018). Prevalence of exposure of heavy metals and their impact on health consequences. *Journal of cellular biochemistry*, *119*(1), 157-184.

Reig, P., Maddocks, A., & Gassert, F. (2013). World's 36 most water-stressed countries, wri.org

Rejith, P. G., Jeeva, S. P., Vijith, H., Sowmya, M., & Hatha, A. M. (2009). Determination of groundwater quality index of a highland village of Kerala (India) using geographical information system. *Journal of Environmental Health*, *71*(10), 51-61.

Rejith, R. G., Sundararajan, M., Gowtham, B., Balasubramanian, A., & Lawrence, J. F. (2021). Characterization of weathering profile and quality of groundwater over hard rock terrain. *Arabian Journal of Geosciences*, *14*(3), 1-12.

Ren, Y., & Zuo, X. (2018). Synchrotron X-ray and neutron diffraction, total scattering, and small-angle scattering techniques for rechargeable battery research. *Small Methods*, *2*(8), 1800064.

Richards, L. A., Kumari, R., Parashar, N., Kumar, A., Lu, C., Wilson, G., ... & Gooddy, D. C. (2022). Environmental tracers and groundwater residence time indicators reveal controls of arsenic accumulation rates beneath a rapidly developing urban area in Patna, India. *Journal of Contaminant Hydrology*, *249*, 104043.

Richts, A., & Vrba, J. (2016). Groundwater resources and hydroclimatic extremes: mapping global groundwater vulnerability to floods and droughts. *Environmental Earth Sciences*, *75*(10), 926.

Riedel, T. (2019). Temperature-associated changes in groundwater quality. *Journal of hydrology*, *572*, 206-212.

Rietveld, H. M. (1988). The Rietveld method? A historical perspective. *Australian Journal of Physics*, *41*(2), 113-116.

Ringwood, A. E. (1955). The principles governing trace element distribution during magmatic crystallization Part I: The influence of electronegativity. *Geochimica et Cosmochimica Acta*, *7*(3-4), 189-202.

Roberts, A. L., Lyall, K., Hart, J. E., Laden, F., Just, A. C., Bobb, J. F., ... & Weisskopf, M. G. (2013). Perinatal air pollutant exposures and autism spectrum disorder in the children of Nurses' Health Study II participants. *Environmental health perspectives*, *121*(8), 978-984.

Roberts, T. L. (2014). Cadmium and phosphorous fertilizers: the issues and the science. *Procedia Engineering*, *83*, 52-59.

Rocchini, R., & Swain, L. G. (1995). The British Columbia water quality index. *Water Quality Branch, EP Department, BC, Ministry of Environment, Land and Park, Victoria, BC, Canada*, *13*.

Rocha-Amador, D., Navarro, M. E., Carrizales, L., Morales, R., & Calderón, J. (2007). Decreased intelligence in children and exposure to fluoride and arsenic in drinking water. *Cadernos de saúde pública*, *23*, S579-S587.

Rochelle-Newall, E., Nguyen, T. M. H., Le, T. P. Q., Sengtaheuanghoung, O., & Ribolzi, O. (2015). A short review of fecal indicator bacteria in tropical aquatic ecosystems: knowledge gaps and future directions. *Frontiers in microbiology*, *6*, 308.

Rodell, M., Velicogna, I., & Famiglietti, J. S. (2009). Satellite-based estimates of groundwater depletion in India. *Nature*, *460*(7258), 999-1002.

Roshni, V., & Harikumar, V. S. (2021). Fluoride contamination in wetlands of Kuttanad, India: Predisposing edaphic factors. *Eurasian Journal of Soil Science*, *10*(1), 61-68.

Rout, D., Krishnamurthi, R., & Sinha, D. K. (2022). Mineralogy and Paragenesis of the Meso-Proterozoic Rohil Uranium Deposit, North Delhi Fold Belt, Rajasthan, India. *Ore Geology Reviews*, 105204.

Rubio, E. (2021). *Understanding and Using X-rays*. Enslow Publishing, LLC.

Rull, F., Veneranda, M., Manrique-Martinez, J. A., Sanz-Arranz, A., Saiz, J., Medina, J., ... & Lopez-Reyes, G. (2022). Spectroscopic study of terrestrial analogues to support rover missions to Mars–A Raman-centred review. *Analytica Chimica Acta*, *1209*, 339003.

Russell, A., McDermott, F., McGrory, E., Cooper, M., Henry, T., & Morrison, L. (2021). As–Co–Ni sulfarsenides in Palaeogene basaltic cone sheets as sources of groundwater arsenic contamination in co. Louth, Ireland. *Applied Geochemistry*, *127*, 104914.

Rusydi, A. F., Onodera, S. I., Saito, M., Ioka, S., Maria, R., Ridwansyah, I., & Delinom, R. M. (2021). Vulnerability of groundwater to iron and manganese contamination in the coastal alluvial plain of a developing Indonesian city. *SN Applied Sciences*, *3*(4), 1-12.

Rutchik, J. S., Zheng, W., Jiang, Y., & Mo, X. (2012). How does an occupational neurologist assess welders and steelworkers for a manganese-induced movement disorder? An international team's experiences in Guanxi, China, part I. *Journal of occupational and environmental medicine/American College of Occupational and Environmental Medicine*, *54*(11), 1432.

Ryan, J. G., Shervais, J. W., Li, Y., Reagan, M. K., Li, H. Y., Heaton, D., ... & IODP Expedition 352 Scientific Team. (2017). Application of a handheld X-ray fluorescence spectrometer for real-time, high-density quantitative analysis of drilled igneous rocks and sediments during IODP Expedition 352. *Chemical Geology*, *451*, 55-66.

Ryu, J. Y., Lee, J. M., Van Nghia, N., Lee, K. M., Lee, S., Lee, M. H., ... & Lee, J. (2018). Supramolecular Pt (II) and Ru (II) Trigonal Prismatic Cages Constructed with a Tris (pyridyl) borane Donor. *Inorganic chemistry*, *57*(18), 11696-11703.

Sadiq, M. (1990). Arsenic chemistry in marine environments: a comparison between theoretical and field observations. *Marine Chemistry*, *31*(1-3), 285-297.

Saha, D. (2009). Arsenic groundwater contamination in parts of middle Ganga plain, Bihar. *Curr Sci*, *97*(6), 753-755.

Saha, D., & Sahu, S. (2016). A decade of investigations on groundwater arsenic contamination in Middle Ganga Plain, India. *Environmental geochemistry and health*, *38*(2), 315-337.

Saha, J. C., Dikshit, A. K., Bandyopadhyay, M., & Saha, K. C. (1999). A review of arsenic poisoning and its effects on human health. *Critical reviews in environmental science and technology*, *29*(3), 281-313.

Saha, N., & Rahman, M. S. (2020). Groundwater hydrogeochemistry and probabilistic health risk assessment through exposure to arsenic-contaminated groundwater of Meghna floodplain, central-east Bangladesh. *Ecotoxicology and Environmental Safety*, *206*, 111349.

Sahoo, P. K., Ray, S. B., Kerketta, A., Behera, P., Neogi, G., & Sahoo, H. B. (2022). Geogenic enrichment of fluoride in groundwater of hard rock aquifer in fluorosis prevalent area of Balangir district, Odisha, India. *Groundwater for Sustainable Development*, *19*, 100830.

Sahoo, S., & Khaoash, S. (2020). Impact assessment of coal mining on groundwater chemistry and its quality from Brajrajnagar coal mining area using indexing models. *Journal of geochemical exploration*, *215*, 106559.

Sahu, B. L., Banjare, G. R., Ramteke, S., Patel, K. S., & Matini, L. (2017). Fluoride contamination of groundwater and toxicities in dongargaon block, Chhattisgarh, India. *Exposure and Health*, *9*, 143-156.

Sahu, S., Gogoi, U., & Nayak, N. C. (2021). Groundwater solute chemistry, hydrogeochemical processes and fluoride contamination in phreatic aquifer of Odisha, India. *Geoscience Frontiers*, *12*(3), 101093.

Sailo, L., & Mahanta, C. (2014). Arsenic mobilization in the Brahmaputra plains of Assam: groundwater and sedimentary controls. *Environmental monitoring and assessment*, *186*(10), 6805-6820.

Saini, A., & Ratan, J. K. (2022). Formulation and evaluation of surface-fluorinated microsized-TiO2 based self-cleaning cement: characterization, self-cleaning, depollution and antimicrobial study. *Chemical Papers*, *76*(5), 3201-3214.

Sajeev, S., Sekar, S., Kumar, B., Senapathi, V., Chung, S. Y., & Gopalakrishnan, G. (2020). Variations of water quality deterioration based on GIS techniques in surface and groundwater resources in and around Vembanad Lake, Kerala, India. *Geochemistry*, *80*(4), 125626.

Sajil Kumar, P. J., Davis Delson, P., & Thomas Babu, P. (2012). Appraisal of heavy metals in groundwater in Chennai city using a HPI model. *Bulletin of environmental contamination and toxicology*, *89*(4), 793-798.

Sajil Kumar, P. J., Jegathambal, P., & James, E. J. (2014). Chemometric evaluation of nitrate contamination in the groundwater of a hard rock area in Dharapuram, south India. *Applied Water Science*, *4*(4), 397-405.

Samarghandi, M. R., Khiadani, M., Foroughi, M., & Zolghadr Nasab, H. (2016). Defluoridation of water using activated alumina in presence of natural organic matter via response surface methodology. *Environmental Science and Pollution Research*, 23(1), 887–897. https://doi.org/10.1007/s11356-015-5293-x.

Sanaei, F., Amin, M. M., Alavijeh, Z. P., Esfahani, R. A., Sadeghi, M., Bandarrig, N. S., ... & Rezakazemi, M. (2021). Health risk assessment of potentially toxic elements intake via food crops consumption: Monte Carlo simulation-based probabilistic and heavy metal pollution index. *Environmental Science and Pollution Research*, *28*(2), 1479-1490.

Sánchez, M., Sabio, L., Gálvez, N., Capdevila, M., & Dominguez-Vera, J. M. (2017). Iron chemistry at the service of life. *IUBMB life*, *69*(6), 382-388.

Sandoval, M. A., Fuentes, R., Nava, J. L., Coreño, O., Li, Y., & Hernández, J. H. (2019). Simultaneous removal of fluoride and arsenic from groundwater by electrocoagulation using a filter-press flow reactor with a three-cell stack. *Separation and Purification Technology*, *208*, 208-216.

Sappa, G., Ergul, S., Ferranti, F., Sweya, L. N., & Luciani, G. (2015). Effects of seasonal change and seawater intrusion on water quality for drinking and irrigation purposes, in coastal aquifers of Dar es Salaam, Tanzania. *Journal of African Earth Sciences*, *105*, 64-84.

Saraf, A. K., & Choudhury, P. R. (1998). Integrated remote sensing and GIS for groundwater exploration and identification of artificial recharge sites. *International journal of Remote sensing*, *19*(10), 1825-1841.

Sargaonkar, A., & Deshpande, V. (2003). Development of an overall index of pollution for surface water based on a general classification scheme in Indian context. *Environmental monitoring and assessment*, *89*(1), 43-67.

Sarkar, A., & Paul, B. (2016). The global menace of arsenic and its conventional remediation-A critical review. *Chemosphere*, *158*, 37-49.

Sarvi, M., & Masoum, M. A. (2008). A neural network model for Ni-Cd batteries. In *2008 43rd International Universities Power Engineering Conference* (pp. 1-5). IEEE.

Sasidharan, S., & Jaya, D. S. (2021). Metal Contamination of Groundwater Sources in the Environs of a Tropical Estuary in South India. *Bulletin of Environmental Contamination and Toxicology*, *106*(2), 342-348.

Satish Kumar, V., Amarender, B., Dhakate, R., Sankaran, S., & Raj Kumar, K. (2016). Assessment of groundwater quality for drinking and irrigation use in shallow hard rock aquifer of Pudunagaram, Palakkad District Kerala. *Applied Water Science*, *6*(2), 149-167.

Sato, K., Tanaka, I., & Otsuki, T. (1979). X-Ray fluorescence analysis in the X-ray region of 0.4 to 7 nm: Application to determination of fluorine in slags. *X-Ray Spectrometry*, *8*(2), 68-72.

Satoh, M., Koyama, H., Kaji, T., Kito, H., & Tohyama, C. (2002). Perspectives on cadmium toxicity research. *The Tohoku journal of experimental medicine*, *196*(1), 23-32.

Saunders, J. A., Lee, M. K., Dhakal, P., Ghandehari, S. S., Wilson, T., Billor, M. Z., & Uddin, A. (2018). Bioremediation of arsenic-contaminated groundwater by sequestration of arsenic in biogenic pyrite. *Applied geochemistry*, *96*, 233-243.

Savage, K. S., Tingle, T. N., O'Day, P. A., Waychunas, G. A., & Bird, D. K. (2000). Arsenic speciation in pyrite and secondary weathering phases, Mother Lode gold district, Tuolumne County, California. *Applied Geochemistry*, *15*(8), 1219-1244.

Saxena, V., & Ahmed, S. (2001). Dissolution of fluoride in groundwater: a water-rock interaction study. *Environmental geology*, *40*(9), 1084-1087.

Saxena, V., & Ahmed, S. (2003). Inferring the chemical parameters for the dissolution of fluoride in groundwater. *Environmental Geology*, *43*(6), 731-736.

Scanlon, B. R., Longuevergne, L., & Long, D. (2012). Ground referencing GRACE satellite estimates of groundwater storage changes in the California Central Valley, USA. *Water Resources Research*, *48*(4).

Schellmann, W. (1994). Geochemical differentiation in laterite and bauxite formation. *Catena*, *21*(2-3), 131-143.

Schilling, K. E., Zhang, Y. K., Hill, D. R., Jones, C. S., & Wolter, C. F. (2009). Temporal variations of Escherichia coli concentrations in a large Midwestern river. *Journal of Hydrology*, *365*(1-2), 79-85.

Schlesinger, W. H., Klein, E. M., & Vengosh, A. (2017). Global biogeochemical cycle of vanadium. *Proceedings of the National Academy of Sciences*, *114*(52), E11092-E11100.

Schmitz Jr, J. A. (2005). What determines productivity? Lessons from the dramatic recovery of the US and Canadian iron ore industries following their early 1980s crisis. *Journal of political Economy*, *113*(3), 582-625.

Schuh, C. E., Jamieson, H. E., Palmer, M. J., Martin, A. J., & Blais, J. M. (2019). Controls governing the spatial distribution of sediment arsenic concentrations and solid-phase speciation in a lake impacted by legacy mining pollution. *Science of the Total Environment*, *654*, 563-575.

Schwartz, M. O. (2000). Cadmium in zinc deposits: economic geology of a polluting element. *International Geology Review*, *42*(5), 445-469.

Seema, K., Ranjan Sen, M., Upadhyay, S., & Bhattacharjee, A. (2011). Dissemination of the New Delhi metallo-β-lactamase-1 (NDM-1) among Enterobacteriaceae in a tertiary referral hospital in north India. *Journal of antimicrobial chemotherapy*, *66*(7), 1646-1647.

Sekabira, K., Origa, H. O., Basamba, T. A., Mutumba, G., & Kakudidi, E. (2010). Assessment of heavy metal pollution in the urban stream sediments and its tributaries. *International journal of environmental science & technology*, *7*(3), 435-446.

Şener, Ş., Şener, E., & Davraz, A. (2017). Evaluation of water quality using water quality index (WQI) method and GIS in Aksu River (SW-Turkey). *Science of the Total Environment*, *584*, 131-144.

Senthilkumar, S., Gowtham, B., Sundararajan, M., Chidambaram, S., Lawrence, J. F., & Prasanna, M. V. (2018). Impact of landuse on the groundwater quality along coastal aquifer of Thiruvallur district, South India. *Sustainable Water Resources Management*, *4*(4), 849-873.

Seraj, B., Shahrabi, M., Shadfar, M., Ahmadi, R., Fallahzadeh, M., Eslamlu, H. F., & Kharazifard, M. J. (2012). Effect of high water fluoride concentration on the intellectual development of children in makoo/iran. *Journal of Dentistry (Tehran, Iran)*, *9*(3), 221.

Shah, B. A. (2010). Arsenic-contaminated groundwater in Holocene sediments from parts of middle Ganga plain, Uttar Pradesh, India. *Current Science(Bangalore)*, *98*(10), 1359-1365.

Shah, B. A. (2012). Role of Quaternary stratigraphy on arsenic-contaminated groundwater from parts of Barak Valley, Assam, North–East India. *Environmental earth sciences*, *66*(8), 2491-2501.

Shah, B. A. (2015). Status of groundwater arsenic contamination in the states of North-east India: a review. *Indian Groundwater*, *5*, 32-37.

Shah, T. (2008). India's master plan for groundwater recharge: an assessment and some suggestions for revision. *Economic and political weekly*, 41-49.

Shah, T. (2010). *Taming the anarchy: Groundwater governance in South Asia*. Routledge.

Shaharoona, B., Al-Ismaily, S., Al-Mayahi, A., Al-Harrasi, N., Al-Kindi, R., Al-Sulaimi, A., ... & Al-Abri, M. (2019). The role of urbanization in soil and groundwater contamination by heavy metals and pathogenic bacteria: A case study from Oman. *Heliyon*, *5*(5), e01771.

Shahid, M., Javed, H. M. A., Ahmad, M. I., Qureshi, A. A., Khan, M. I., Alnuwaiser, M. A., ... & Rafique, A. (2022). A brief assessment on recent developments in efficient electrocatalytic Nitrogen reduction with 2D non-metallic nanomaterials. *Nanomaterials*, *12*(19), 3413.

Shahin, M. (2002). Groundwater resources of Africa. *Hydrology and Water Resources of Africa*, 509-563.

Shaji, E., Gómez-Alday, J. J., Hussein, S., Deepu, T. R., & Anilkumar, Y. (2018). Salinization and deterioration of groundwater quality by nitrate and fluoride in the Chittur block, Palakkad, Kerala. *Journal of the Geological Society of India*, *92*(3), 337-345.

Shaji, E., Santosh, M., Sarath, K. V., Prakash, P., Deepchand, V., & Divya, B. V. (2021). Arsenic contamination of groundwater: A global synopsis with focus on the Indian Peninsula. *Geoscience frontiers*, *12*(3), 101079.

Shaji, E., Viju, J., & Thambi, D. S. (2007). High fluoride in groundwater of Palghat District, Kerala. *Current Science*, 240-245.

Shaji, E., Vinayachandran, N., & Thambi, D. S. (2009). Hydrogeochemical characteristics of groundwater in coastal phreatic aquifers of Alleppey district, Kerala. *Journal of the Geological Society of India*, *74*(5), 585.

Shakerkhatibi, M., Mosaferi, M., Pourakbar, M., Ahmadnejad, M., Safavi, N., & Banitorab, F. (2019). Comprehensive investigation of groundwater quality in the north-west of Iran: Physicochemical and heavy metal analysis. *Groundwater for Sustainable Development*, *8*, 156-168.

Shalini, T. A., Pandey, A. C., & Nathawat, M. S. (2012). Groundwater level and rainfall variability trend analysis using GIS in parts of Jharkhand state (India) for sustainable management of water resources. *International Research Journal of Environment Sciences*, *1*(4), 24-31.

Shammi, M., Rahman, M. M., Bondad, S. E., & Bodrud-Doza, M. (2019, March). Impacts of salinity intrusion in community health: a review of experiences on drinking water sodium from coastal areas of Bangladesh. In *Healthcare* (Vol. 7, No. 1, p. 50). MDPI.

Shamrukh, M., & Abdel-Wahab, A. (2011). Water pollution and riverbank filtration for water supply along river Nile, Egypt. In *Riverbank filtration for water security in desert countries* (pp. 5-28). Springer, Dordrecht.

Shankar, P. V., Kulkarni, H., & Krishnan, S. (2011). India's groundwater challenge and the way forward. *Economic and political Weekly*, 37-45.

Sharma, M. K., & Kumar, M. (2020). Sulphate contamination in groundwater and its remediation: an overview. *Environmental Monitoring and Assessment*, *192*(2), 1-10.

Sharma, S., & Chhipa, R. C. (2016). Seasonal variations of ground water quality and its agglomerates by water quality index. *Global Journal of Environmental Science and Management*, *2*(1), 79-86.

Sharma, V. S. S., & Sharma, S. (2004). Toxicity of fluoride on living beings. *Environmental contamination and bioreclamation. APH Publishing, New Delhi*, 392-411.

Sharpe, R. T., & Livesey, C. T. (2005). Surveillance of suspect animal toxicoses with potential food safety implications in England and Wales between 1990 and 2002. *Veterinary Record*, *157*(16), 465-469.

Shehab, H., Desouza, E. D., O'Meara, J., Pejović-Milić, A., Chettle, D. R., Fleming, D. E. B., & McNeill, F. E. (2015). Feasibility of measuring arsenic and selenium in human skin using in vivo x-ray fluorescence (XRF)—a comparison of methods. *Physiological measurement*, *37*(1), 145.

Shekhar, S. (2006). An approximate projection of availability of the fresh groundwater resources in the South West district of NCT Delhi, India: a case study. *Hydrogeology Journal*, *14*(7), 1330-1338.

Shiklomanov, I. A. (1993). World fresh water resources In: Gleick PH, editor. Water in crisis: a guide to the world's freshwater resources.

Shirke, K. D., & Pawar, N. J. (2015). Enrichment of arsenic in the Quaternary sediments from Ankaleshwar industrial area, Gujarat, India: an anthropogenic influence. *Environmental monitoring and assessment*, *187*(9), 1-11.

Shirke, K. D., Kadam, A. K., & Pawar, N. J. (2020). Temporal variations in hydro-geochemistry and potential health risk assessment of groundwater from lithological diversity of semi-arid region, Western Gujarat, India. *Applied Water Science*, *10*(6), 1-20.

Shukla, D. P., Dubey, C. S., Singh, N. P., Tajbakhsh, M., & Chaudhry, M. (2010). Sources and controls of Arsenic contamination in groundwater of Rajnandgaon and Kanker District, Chattisgarh Central India. *Journal of Hydrology*, *395*(1-2), 49-66.

Silin, I., Gürsel, D., Kremer, D., Hahn, K. M., & Wotruba, H. (2020). Production of vanadium concentrate from a small-scale lead vanadate deposit by gravity concentration: a pilot plant study. *Minerals*, *10*(11), 957.

Silva, C. S., Moutinho, C., Ferreira da Vinha, A., & Matos, C. (2019). Trace minerals in human health: Iron, zinc, copper, manganese and fluorine. *International Journal of Science and Research Methodology*, *13*(3), 57-80.

Simonsson, M., Hillier, S., & Öborn, I. (2009). Changes in clay minerals and potassium fixation capacity as a result of release and fixation of potassium in long-term field experiments. *Geoderma*, *151*(3-4), 109-120.

Singh, A. K. (2004). Arsenic contamination in groundwater of North Eastern India. In *Proceedings of 11th national symposium on hydrology with focal theme on water quality, National Institute of Hydrology, Roorkee* (pp. 255-262).

Singh, A. L., & Singh, V. K. (2018). Assessment of groundwater quality of Ballia district, Uttar Pradesh, India, with reference to arsenic contamination using multivariate statistical analysis. *Applied Water Science*, *8*, 1-18.

Singh, A. P., Goel, R. K., & Kaur, T. (2011a). Mechanisms pertaining to arsenic toxicity. *Toxicology international*, *18*(2), 87.

Singh, C. K., Shashtri, S., & Mukherjee, S. (2011b). Integrating multivariate statistical analysis with GIS for geochemical assessment of groundwater quality in Shiwaliks of Punjab, India. *Environmental Earth Sciences*, *62*(7), 1387-1405.

Singh, D. K., & Singh, A. K. (2002). Groundwater situation in India: Problems and perspective. *International Journal of Water Resources Development*, *18*(4), 563-580.

Singh, G. (2009). Salinity-related desertification and management strategies: Indian experience. *Land Degradation & Development*, *20*(4), 367-385.

Singh, G., Rishi, M. S., Herojeet, R., Kaur, L., & Sharma, K. (2020). Multivariate analysis and geochemical signatures of groundwater in the agricultural dominated taluks of Jalandhar district, Punjab, India. *Journal of geochemical exploration*, *208*, 106395.

Singh, P. K., Rajak, P. K., Singh, M. P., Singh, V. K., & Naik, A. S. (2016). Geochemistry of kasnau-matasukh lignites, Nagaur basin, Rajasthan (India). *International Journal of Coal Science & Technology*, *3*(2), 104-122.

Singh, P., Gupta, N. D., & Bey, A. (2014a). Dental fluorosis and periodontium: A game of shadows? *Journal of oral biology and craniofacial research*, *4*(1), 47-48.

Singh, P., Saharan, J. P., Sharma, K., & Saharan, S. (2010). Physio-chemical & EDXRF analysis of groundwater of Ambala, Haryana, India. *Researcher*, *2*(1), 68-75.

Singh, R. P., & Agrawal, M. (2008). Potential benefits and risks of land application of sewage sludge. *Waste management*, *28*(2), 347-358.

Singh, S. K., Ghosh, A. K., Kumar, A., Kislay, K., Kumar, C., Tiwari, R. R., ... & Imam, M. D. (2014b). Groundwater arsenic contamination and associated health risks in Bihar, India. *International Journal of Environmental Research*, *8*(1), 49-60.

Singh, S., Deolia, D. K., & Tignath, S. (2020). Alarming Danger of Arsenic in Groundwater of Jabalpur, Madhya Pradesh, India. *International Journal of Research in Engineering, Science and Management*, *3*(8), 172-175.

Singh, S., Sharma, P., Mudhulkar, R., Chakravorty, B., & Singh, A. (2022). Assessment of hydrogeochemistry and arsenic contamination in groundwater of Bahraich District, Uttar Pradesh, India. *Arabian Journal of Geosciences*, *15*(1), 1-18.

Singh, U. K., Ramanathan, A. L., & Subramanian, V. (2018). Groundwater chemistry and human health risk assessment in the mining region of East Singhbhum, Jharkhand, India. *Chemosphere*, *204*, 501-513.

Singh, V. K., Bikundia, D. S., Sarswat, A., & Mohan, D. (2012). Groundwater quality assessment in the village of Lutfullapur Nawada, Loni, District Ghaziabad, Uttar Pradesh, India. *Environmental monitoring and assessment*, *184*(7), 4473-4488.

Sitko, R., Janik, P., Zawisza, B., Talik, E., Margui, E., & Queralt, I. (2015). Green approach for ultratrace determination of divalent metal ions and arsenic species using total-reflection X-ray fluorescence spectrometry and mercapto-modified graphene oxide nanosheets as a novel adsorbent. *Analytical chemistry*, *87*(6), 3535-3542.

Sivakarun, N., Udayaganesan, P., Chidambaram, S., Venkatramanan, S., Prasanna, M. V., Pradeep, K., & Panda, B. (2020). Factors determining the hydrogeochemical processes occurring in shallow groundwater of coastal alluvial aquifer, India. *Geochemistry*, *80*(4), 125623.

Sjoqvist, A. S., Cornell, D. H., Andersen, T., Christensson, U. I., & Berg, J. T. (2017). Magmatic age of rare-earth element and zirconium mineralisation at the Norra Kärr alkaline complex, southern Sweden, determined by U–Pb and Lu–Hf isotope analyses of metasomatic zircon and eudialyte. *Lithos*, *294*, 73-86.

Slavík, R., Julinová, M., & Labudíková, M. (2012). Screening of the spatial distribution of risk metals in topsoil from an industrial complex. *Ecological Chemistry and Engineering S-Chemia I Inzynieria Ekologiczna S*.

Sloan, C. E. (1972). *Ground-water hydrology of prairie potholes in North Dakota* (No. 585). US Government Printing Office.

Smedley, P. L., & Kinniburgh, D. G. (2002). A review of the source, behaviour and distribution of arsenic in natural waters. *Applied geochemistry*, *17*(5), 517-568.

Smedley, P. L., Kinniburgh, D. G., Macdonald, D. M. J., Nicolli, H. B., Barros, A. J., Tullio, J. O., ... & Alonso, M. S. (2005). Arsenic associations in sediments from the loess aquifer of La Pampa, Argentina. *Applied geochemistry*, *20*(5), 989-1016.

Smil, V. (2000). Phosphorus in the environment: natural flows and human interferences. *Annual review of energy and the environment*, *25*(1), 53-88.

Snyder, B. E., Bols, M. L., Schoonheydt, R. A., Sels, B. F., & Solomon, E. I. (2017). Iron and copper active sites in zeolites and their correlation to metalloenzymes. *Chemical reviews*, *118*(5), 2718-2768.

Soares, L. E. S., & De Carvalho Filho, A. C. B. (2015). Protective effect of fluoride varnish and fluoride gel on enamel erosion: roughness, SEM-EDS, and μ-EDXRF studies. *Microscopy research and technique*, *78*(3), 240-248.

Soloviev, S. G., Kryazhev, S. G., Dvurechenskaya, S. S., Vasyukov, V. E., Shumilin, D. A., & Voskresensky, K. I. (2019). The superlarge Malmyzh porphyry Cu-Au deposit, Sikhote-Alin, eastern Russia: Igneous geochemistry, hydrothermal alteration, mineralization, and fluid inclusion characteristics. *Ore Geology Reviews*, *113*, 103112.

Soman, K. (1997). Geology of Kerala, published by Geological Society of India, Bangalore, India-560019, 280.

Song, X., Wang, P., Van Zwieten, L., Bolan, N., Wang, H., Li, X., ... & Li, F. (2022). Towards a better understanding of the role of Fe cycling in soil for carbon stabilization and degradation. *Carbon Research*, *1*(1), 5.

Spangler, A. H., & Spangler, J. G. (2009). Groundwater manganese and infant mortality rate by county in North Carolina: an ecological analysis. *Ecohealth*, *6*(4), 596-600.

Sparrow, L. A., & Uren, N. C. (2014). Manganese oxidation and reduction in soils: effects of temperature, water potential, pH and their interactions. *Soil Research*, *52*(5), 483-494.

Spencer, H., Osis, D., & Wiatrowski, E. (1975). Retention of fluoride with time in man. *Clinical chemistry*, *21*(4), 613-618.

Sponsler, O. L. (1925). X-ray diffraction patterns from plant fibers. *The Journal of General Physiology*, *9*(2), 221-233.

Sreekanth, P. D., Geethanjali, N., Sreedevi, P. D., Ahmed, S., Kumar, N. R., & Jayanthi, P. K. (2009). Forecasting groundwater level using artificial neural networks. *Current science*, 933-939.

Sreekumar, S., & Aslam, A. (2010). Spatio-temporal distribution of slope failures in the Western Ghats of Kerala, India. *Risk Analysis*, *43*(2010), 417-427.

Sridharan, M., & Nathan, D. S. (2018). Chemometric tool to study the mechanism of arsenic contamination in groundwater of Puducherry Region, South East Coast of India. *Chemosphere*, *208*, 303-315.

Srinivas, Y., Hudson, O. D., Stanley, R. A., & Chandrasekar, N. (2014). Quality assessment and hydrogeochemical characteristics of groundwater in Agastheeswaram taluk,

Kanyakumari district, Tamil Nadu, India. *Chinese Journal of Geochemistry*, *33*(3), 221-235.

Srinivas, Y., Hudson, O. D., Stanley, R. A., & Chandrasekar, N. (2014). Quality assessment and hydrogeochemical characteristics of groundwater in Agastheeswaram taluk, Kanyakumari district, Tamil Nadu, India. *Chinese Journal of Geochemistry*, *33*(3), 221-235.

Srinivasan, V., Seto, K. C., Emerson, R., & Gorelick, S. M. (2013). The impact of urbanization on water vulnerability: A coupled human–environment system approach for Chennai, India. *Global Environmental Change*, *23*(1), 229-239.

Srivastava, P. K., & Bhattacharya, A. K. (2006). Groundwater assessment through an integrated approach using remote sensing, GIS and resistivity techniques: a case study from a hard rock terrain. *International Journal of Remote Sensing*, *27*(20), 4599-4620.

Srivastava, P. K., Mukherjee, S., Gupta, M., & Singh, S. K. (2011). Characterizing monsoonal variation on water quality index of River Mahi in India using geographical information system. *Water Quality, Exposure and Health*, *2*(3), 193-203.

Srivastava, P. K., Pandey, P. C., Petropoulos, G. P., Kourgialas, N. N., Pandey, V., & Singh, U. (2019). GIS and remote sensing aided information for soil moisture estimation: A comparative study of interpolation techniques. *Resources*, *8*(2), 70.

Srivastava, S., & Sharma, Y. K. (2013). Arsenic occurrence and accumulation in soil and water of eastern districts of Uttar Pradesh, India. *Environmental monitoring and assessment*, *185*(6), 4995-5002.

Stefanidou, M., Maravelias, C., Dona, A., & Spiliopoulou, C. (2006). Zinc: a multipurpose trace element. *Archives of toxicology*, *80*(1), 1-9.

Steinhart, C. E., Schierow, L. J., & Sonzogni, W. C. (1982). An environmental quality index for The Great Lakes 1. *JAWRA Journal of the American Water Resources Association*, *18*(6), 1025-1031.

Stigter, T. Y., Van Ooijen, S. P. J., Post, V. E. A., Appelo, C. A. J., & Dill, A. C. (1998). A hydrogeological and hydrochemical explanation of the groundwater composition under irrigated land in a Mediterranean environment, Algarve, Portugal. *Journal of Hydrology*, *208*(3-4), 262-279.

Strahler, A. N. (1964). Part II. Quantitative geomorphology of drainage basins and channel networks. *Handbook of Applied Hydrology: McGraw-Hill, New York*, 4-39.

Su, H., Wang, J., & Liu, J. (2019). Geochemical factors controlling the occurrence of high-fluoride groundwater in the western region of the Ordos basin, northwestern China. *Environmental Pollution*, *252*, 1154-1162.

Su, Z., Wu, J., He, X., & Elumalai, V. (2020). Temporal changes of groundwater quality within the groundwater depression cone and prediction of confined groundwater salinity using Grey Markov model in Yinchuan area of northwest China. *Exposure and Health*, *12*(3), 447-468.

Subba Rao, N. (2006). Groundwater potential index in a crystalline terrain using remote sensing data. *Environmental Geology*, *50*(7), 1067-1076.

Subba Rao, N. (2008). Iron content in groundwaters of Visakhapatnam environs, Andhra Pradesh, India. *Environmental monitoring and assessment*, *136*(1), 437-447.

Subba Rao, N. (2021). Spatial distribution of quality of groundwater and probabilistic non-carcinogenic risk from a rural dry climatic region of South India. *Environmental geochemistry and health*, *43*(2), 971-993.

Subba Rao, N., Ravindra, B., & Wu, J. (2020). Geochemical and health risk evaluation of fluoride rich groundwater in Sattenapalle Region, Guntur district, Andhra Pradesh, India. *Human and ecological risk assessment: An international journal*, *26*(9), 2316-2348.

Subba Rao, N., Subrahmanyam, A., & Babu Rao, G. (2013). Fluoride-bearing groundwater in Gummanampadu sub-basin, Guntur district, Andhra Pradesh, India. *Environmental earth sciences*, *70*(2), 575-586.

Sudheer Kumar, M., Dhakate, R., Yadagiri, G., & Srinivasa Reddy, K. (2017). Principal component and multivariate statistical approach for evaluation of hydrochemical characterization of fluoride-rich groundwater of Shaslar Vagu watershed, Nalgonda District, India. *Arabian Journal of Geosciences*, *10*, 1-17.

Sudicky, E. A., Illman, W. A., Goltz, I. K., Adams, J. J., & McLaren, R. G. (2010). Heterogeneity in hydraulic conductivity and its role on the macroscale transport of a solute plume: From measurements to a practical application of stochastic flow and transport theory. *Water Resources Research*, *46*(1).

Suhag, R. (2016). Overview of ground water in India. *PRS Legislative Research Standing Committee on Water Resources: Delhi, India*.

Suiekpayev, Y. S., Sapargaliyev, Y. M., Dolgopolova, A. V., Pirajno, F., Seltmann, R., Khromykh, S. V., ... & Azelkhanov, A. Z. (2021). Mineralogy, geochemistry and U-Pb zircon age of the Karaotkel Ti-Zr placer deposit, Eastern Kazakhstan and its genetic link to the Karaotkel-Preobrazhenka intrusion. *Ore Geology Reviews*, *131*, 104015.

Sujana, M. G., Soma, G., Vasumathi, N., & Anand, S. (2009). Studies on fluoride adsorption capacities of amorphous Fe/Al mixed hydroxides from aqueous solutions. *Journal of Fluorine Chemistry*, *130*(8), 749-754.

Sujatha, D., & Reddy, B. R. (2003). Quality characterization of groundwater in the south-eastern part of the Ranga Reddy district, Andhra Pradesh, India. *Environmental Geology*, *44*(5), 579-586.

Sultana, S. S. P., Kishore, D. H. V., Kuniyil, M., Khan, M., Siddiqui, M. R. H., Alwarthan, A., ... & Adil, S. F. (2017). Promoting effects of thoria on the nickel-manganese mixed oxide catalysts for the aerobic oxidation of benzyl alcohol. *Arabian Journal of Chemistry*, *10*(4), 448-457.

Sun, F., Dempsey, B. A., & Osseo-Asare, K. A. (2012). As (V) and As (III) reactions on pristine pyrite and on surface-oxidized pyrite. *Journal of colloid and interface science*, *388*(1), 170-175.

Sunitha, V., & Reddy, Y. S. (2019). Hydrogeochemical evaluation of groundwater in and around Lakkireddipalli and Ramapuram, YSR District, Andhra Pradesh, India. *HydroResearch*, *2*, 85-96.

Sutadian, A. D., Muttil, N., Yilmaz, A. G., & Perera, B. J. C. (2016). Development of river water quality indices—a review. *Environmental monitoring and assessment*, *188*(1), 1-29.

Suthar, S., Bishnoi, P., Singh, S., Mutiyar, P. K., Nema, A. K., & Patil, N. S. (2009). Nitrate contamination in groundwater of some rural areas of Rajasthan, India. *Journal of hazardous materials*, *171*(1-3), 189-199.

Swaziland Water Service Corporation (SWSC), 2014. Swaziland Water Services Corporation Annual report for 2014, Zulwini, Swaziland. (Unpublished).

Symonds, R. B., Rose, W. I., & Reed, M. H. (1988). Contribution of C1-and F-bearing gases to the atmosphere by volcanoes. *Nature*, *334*(6181), 415-418.

Tabelin, C. B., Corpuz, R. D., Igarashi, T., Villacorte-Tabelin, M., Alorro, R. D., Yoo, K., ... & Hiroyoshi, N. (2020). Acid mine drainage formation and arsenic mobility under strongly acidic conditions: Importance of soluble phases, iron oxyhydroxides/oxides and nature of oxidation layer on pyrite. *Journal of Hazardous Materials*, *399*, 122844.

Tabelin, C. B., Igarashi, T., Villacorte-Tabelin, M., Park, I., Opiso, E. M., Ito, M., & Hiroyoshi, N. (2018). Arsenic, selenium, boron, lead, cadmium, copper, and zinc in naturally contaminated rocks: A review of their sources, modes of enrichment, mechanisms of release, and mitigation strategies. *Science of the Total Environment*, *645*, 1522-1553.

Takem, G. E., Kuitcha, D., Ako, A. A., Mafany, G. T., Takounjou-Fouepe, A., Ndjama, J., ... & Ayonghe, S. N. (2015). Acidification of shallow groundwater in the unconfined sandy aquifer of the city of Douala, Cameroon, Western Africa: implications for groundwater quality and use. *Environmental Earth Sciences*, *74*(9), 6831-6846.

Tamasi, G., & Cini, R. (2004). Heavy metals in drinking waters from Mount Amiata (Tuscany, Italy). Possible risks from arsenic for public health in the Province of Siena. *Science of the total environment*, *327*(1-3), 41-51.

Tang, C., Azuma, K., Iwami, Y., Ohji, B., & Sakura, Y. (2004). Nitrate behaviour in the groundwater of a headwater wetland, Chiba, Japan. *Hydrological Processes*, *18*(16), 3159-3168.

Tapia, J., Mukherjee, A., Rodríguez, M. P., Murray, J., & Bhattacharya, P. (2022). Role of tectonics and climate on elevated arsenic in fluvial systems: Insights from surface water and sediments along regional transects of Chile. *Environmental Pollution*, *314*, 120151.

Tarnopolskaia, M., Nikolaeva, I., Bychkov, A., & Lubkova, T. (2021). Experimental study of ZrF 6 2-and HfF 6 2-stability in hydrothermal solutions. *Goldschmidt2021• Virtual• 4-9 July*.

Taylor, C. A., & Stefan, H. G. (2009). Shallow groundwater temperature response to climate change and urbanization. *Journal of Hydrology*, *375*(3-4), 601-612.

Thakur, B. K., & Gupta, V. (2019). Valuing health damages due to groundwater arsenic contamination in Bihar, India. *Economics & Human Biology*, *35*, 123-132.

Thakuria, D., & Godboley, B. J. (2016). Contamination and removal of iron and flouride from groundwater by adsorption and filtration: A review. *International Journal of Science Technology & Engineering*, *2*(7), 80-85.

Thapa, R., Gupta, S., Kaur, H., & Baski, R. (2019). Assessment of groundwater quality scenario in respect of fluoride and nitrate contamination in and around Gharbar village, Jharkhand, India. *HydroResearch*, *2*, 60-68.

Thatcher, J. W., & Campbell, W. J. (1965). *Instrumentation for Primary and Secondary Excitation of Low-Energy X-ray Spectral Lines* (Vol. 6689). US Department of the Interior, Bureau of Mines.

Thivya, C., Chidambaram, S., Rao, M. S., Thilagavathi, R., Prasanna, M. V., & Manikandan, S. J. A. W. S. (2017). Assessment of fluoride contaminations in groundwater of hard rock aquifers in Madurai district, Tamil Nadu (India). *Applied Water Science*, *7*(2), 1011-1023.

Thivya, C., Chidambaram, S., Singaraja, C., Thilagavathi, R., Prasanna, M. V., Anandhan, P., & Jainab, I. (2013). A study on the significance of lithology in groundwater quality of Madurai district, Tamil Nadu (India). *Environment, development and sustainability*, *15*(5), 1365-1387.

Thomas, B. F., & Famiglietti, J. S. (2019). Identifying climate-induced groundwater depletion in GRACE observations. *Scientific reports*, *9*(1), 1-9.

Thomsen, V. (2006). A timeline of atomic spectroscopy. *SPECTROSCOPY-SPRINGFIELD THEN EUGENE THEN DULUTH-*, *21*(10), 32.

Thornton, I. (1986). Geochemistry of cadmium. In *Cadmium in the Environment* (pp. 7-12). Birkhäuser Basel.

Tian, H., Gao, J., Lu, L., Zhao, D., Cheng, K., & Qiu, P. (2012). Temporal trends and spatial variation characteristics of hazardous air pollutant emission inventory from municipal solid waste incineration in China. *Environmental science & technology*, *46*(18), 10364-10371.

Tian, Y., Wu, M., Lin, X., Huang, P., & Huang, Y. (2011). Synthesis of magnetic wheat straw for arsenic adsorption. *Journal of hazardous materials*, *193*, 10-16.

Tiefenthaler, L. L., Stein, E. D., & Lyon, G. S. (2009). Fecal indicator bacteria (FIB) levels during dry weather from Southern California reference streams. *Environmental monitoring and assessment*, *155*(1), 477-492.

Tirumalesh, K., Shivanna, K., & Jalihal, A. A. (2007). Isotope hydrochemical approach to understand fluoride release into groundwaters of Ilkal area, Bagalkot District, Karnataka, India. *Hydrogeology Journal*, *15*(3), 589-598.

Tiwari, A. K., & Pal, D. B. (2021). Recent Trends in Groundwater Conservation and Management. *Groundwater Geochemistry: Pollution and Remediation Methods*, 379-391.

Tiwari, A. K., Singh, P. K., Chandra, S., & Ghosh, A. (2016a). Assessment of groundwater level fluctuation by using remote sensing and GIS in West Bokaro coalfield, Jharkhand, India. *ISH Journal of Hydraulic Engineering*, *22*(1), 59-67.

Tiwari, A. K., Singh, P. K., Singh, A. K., & De Maio, M. (2016b). Estimation of heavy metal contamination in groundwater and development of a heavy metal pollution index by using GIS technique. *Bulletin of environmental contamination and toxicology*, *96*(4), 508-515.

Tiwari, K. K., Krishan, G., Prasad, G., Mondal, N. C., & Bhardwaj, V. (2020). Evaluation of fluoride contamination in groundwater in a semi-arid region, Dausa District, Rajasthan, India. *Groundwater for Sustainable Development*, *11*, 100465.

Tm, M., Joseph, S., Petitta, M., & Thomas, J. (2017). Integrated approach for identifying the factors controlling groundwater quality of a tropical coastal zone in Kerala, India. *Environmental Earth Sciences*, *76*(14).

Todd, D. K., & Mays, L. W. (1980). Groundwater Hydrology. John Willey & Sons. *Inc., New York*, *535*.

Tomasek, I., Mouri, H., Dille, A., Bennett, G., Bhattacharya, P., Brion, N., ... & Kervyn, M. (2022). Naturally occurring potentially toxic elements in groundwater from the volcanic landscape around Mount Meru, Arusha, Tanzania and their potential health hazard. *Science of the Total Environment*, *807*, 150487.

Tossou, Y. Y. J., Yessoufou, S., Orban, P., Vander Auwera, J., Boukari, M., & Brouyère, S. (2021). Bedrock petrology controls on hydrogeochemistry and fluoride concentrations in Precambrian aquifers of central Benin, Western Africa. *Journal of African Earth Sciences*, *182*, 104301.

Trenberth, K. E., Smith, L., Qian, T., Dai, A., & Fasullo, J. (2007). Estimates of the global water budget and its annual cycle using observational and model data. *Journal of Hydrometeorology*, *8*(4), 758-769.

Trivedi, M. H., Verma, R. J., Chinoy, N. J., Patel, R. S., & Sathawara, N. G. (2007). Effect of high fluoride water on intelligence of school children in India. *Fluoride*, *40*(3), 178-183.

Tumuklu, A., Sunkari, E. D., Yalcin, F., & Ozer Atakoglu, O. (2022). Data analysis of the Gumusler Dam Lake Reservoir soils using multivariate statistical methods (Nigde, Türkiye). *International Journal of Environmental Science and Technology*, 1-14.

Tunstall, B. R. (2005). Dryland salinity implications of interactions between clay, organic matter, salt and water in soils. *URL: www. eric. com. au/docs/research/dryland/matte r_interactions. pdf*.

Turner, B. D., Binning, P., & Stipp, S. L. S. (2005). Fluoride removal by calcite: evidence for fluorite precipitation and surface adsorption. *Environmental science & technology*, *39*(24), 9561-9568.

Tuschl, K., Mills, P. B., & Clayton, P. T. (2013). Manganese and the brain. *International review of neurobiology*, *110*, 277-312.

Tutmez, B., Hatipoglu, Z., & Kaymak, U. (2006). Modelling electrical conductivity of groundwater using an adaptive neuro-fuzzy inference system. *Computers & geosciences*, *32*(4), 421-433.

Uchimiya, M., & Bannon, D. I. (2013). Solubility of lead and copper in biochar-amended small arms range soils: influence of soil organic carbon and pH. *Journal of agricultural and food chemistry*, *61*(32), 7679-7688.

Uddin, M. G., Nash, S., & Olbert, A. I. (2021). A review of water quality index models and their use for assessing surface water quality. *Ecological Indicators*, *122*, 107218.

Udeshani, W. A. C., Dissanayake, H. M. K. P., Gunatilake, S. K., & Chandrajith, R. (2020). Assessment of groundwater quality using water quality index (WQI): A case study of a hard rock terrain in Sri Lanka. *Groundwater for Sustainable Development*, *11*, 100421.

Ullah, N., Mansha, M., Khan, I., & Qurashi, A. (2018). Nanomaterial-based optical chemical sensors for the detection of heavy metals in water: Recent advances and challenges. *TrAC Trends in Analytical Chemistry*, *100*, 155-166.

Umar, M., Waseem, A., Sabir, M. A., Kassi, A. M., & Khan, A. S. (2013). The impact of geology of recharge areas on groundwater quality: a case study of Zhob River Basin, Pakistan. *Clean–Soil, Air, Water*, *41*(2), 119-127.

Umbugadu, A. A., & Igwe, O. (2019). Mineralogical and major oxide characterization of Panyam clays, North-Central Nigeria. *International Journal of Physical Sciences*, *14*(11), 108-115.

Uriu-Adams, J. Y., & Keen, C. L. (2005). Copper, oxidative stress, and human health. *Molecular aspects of medicine*, *26*(4-5), 268-298.

Urrutia, J., Herrera, C., Custodio, E., Jódar, J., & Medina, A. (2019). Groundwater recharge and hydrodynamics of complex volcanic aquifers with a shallow saline lake: Laguna Tuyajto, Andean Cordillera of northern Chile. *Science of the Total Environment*, *697*, 134116.

USDA (1954) Diagnosis and improvement of saline and alkali soils. U.S. Salinity Laboratory Staff, Government Printing Office, Washington, DC

USEPA (1986) *Ambient Water Quality Criteria for Bacteria*. Washington, DC: USEPA.

USGS (2020) How Much Water is There on Earth? https://www.usgs.gov/specialtopic/water-science-school/science/how-much-water-there-earth?qt-science_center_objects=0#qt-cience_center_objects. (Accessed 4 August 2020).

USGS, N. (2005). Available online at http://water. usgs. gov/nawqa. *Accessed September*, *30*, 2005.

Usham, A. L., Dubey, C. S., Shukla, D. P., Mishra, B. K., & Bhartiya, G. P. (2018). Sources of fluoride contamination in Singrauli with special reference to Rihand reservoir and its surrounding. *Journal of the Geological Society of India*, *91*(4), 441-448.

Uvarova, Y. A., Tassios, S., Francis, N., LeGras, M., Cleverley, J. S., & Baensch, A. (2020). Top-of-holes sensing techniques: developments within Deep Exploration Technologies Cooperative Research Centre. *Australian Journal of Earth Sciences*, 1-13.

Valdez-Alegría, C. J., Fuentes-Rivas, R. M., García-Rivas, J. L., Fonseca-Montes de Oca, R. M. G., & García-Gaitán, B. (2019). Presence and distribution of fluoride ions in groundwater for human in a semiconfined volcanic aquifer. *Resources*, *8*(2), 116.

Valdez-Jiménez, L., Fregozo, C. S., Beltrán, M. M., Coronado, O. G., & Vega, M. P. (2011). Effects of the fluoride on the central nervous system. *Neurología (English Edition)*, *26*(5), 297-300.

Valenzuela-Vasquez, L., Ramirez-Hernandez, J., Reyes-Lopez, J., Sol-Uribe, A., & Lazaro-Mancilla, O. (2006). The origin of fluoride in groundwater supply to Hermosillo City, Sonora, Mexico. *Environmental Geology*, *51*(1), 17-27.

Van der Aa, M. (2003). Classification of mineral water types and comparison with drinking water standards. *Environmental geology*, *44*(5), 554-563.

Van Herreweghe, S., Swennen, R., Vandecasteele, C., & Cappuyns, V. (2003). Solid phase speciation of arsenic by sequential extraction in standard reference materials and industrially contaminated soil samples. *Environmental pollution*, *122*(3), 323-342.

Vardhan, K. H., Kumar, P. S., & Panda, R. C. (2019). A review on heavy metal pollution, toxicity and remedial measures: Current trends and future perspectives. *Journal of Molecular Liquids*, *290*, 111197.

Varghese, J., & Jaya, D. S. (2014). Metal pollution of groundwater in the vicinity of Valiathura sewage farm in Kerala, South India. *Bulletin of environmental contamination and toxicology*, *93*(6), 694-698.

Varma, A. (2017). Groundwater resource and governance in Kerala: Status, issues and prospects. Forum for Policy Dialogue on Water Conflicts in India.

Varua, M. E., Ward, J., Maheshwari, B., Oza, S., Purohit, R., & Chinnasamy, P. (2016). Assisting community management of groundwater: irrigator attitudes in two watersheds in Rajasthan and Gujarat, India. *Journal of Hydrology*, *537*, 171-186.

Velusamy, S., Roy, A., Sundaram, S., & Kumar Mallick, T. (2021). A review on heavy metal ions and containing dyes removal through graphene oxide-based adsorption strategies for textile wastewater treatment. *The Chemical Record*, *21*(7), 1570-1610.

Veneranda, M., Lopez-Reyes, G., Manrique-Martinez, J. A., Sanz-Arranz, A., Lalla, E., Konstantinidis, M., ... & Rull, F. (2020). ExoMars Raman Laser Spectrometer (RLS): Development of chemometric tools to classify ultramafic igneous rocks on Mars. *Scientific Reports*, *10*(1), 1-14.

Venkatesan, G., & Swaminathan, G. (2009). Review of chloride and sulphate attenuation in ground water nearby solid-waste landfill sites. *Journal of environmental engineering and landscape management*, *17*(1), 1-7.

Venkatesan, G., Subramani, T., Sathya, U., & Roy, P. D. (2020). Seasonal changes in groundwater composition in an industrial center of south India and quality evaluation for consumption and health risk using geospatial methods. *Geochemistry*, *80*(4), 125651.

Verma, S., Mukherjee, A., Mahanta, C., Choudhury, R., & Mitra, K. (2016). Influence of geology on groundwater–sediment interactions in arsenic enriched tectono-morphic aquifers of the Himalayan Brahmaputra river basin. *Journal of Hydrology*, *540*, 176-195.

Vermeulen, L. C., & Hofstra, N. (2014). Influence of climate variables on the concentration of Escherichia coli in the Rhine, Meuse, and Drentse Aa during 1985–2010. *Regional Environmental Change*, *14*(1), 307-319.

Verschoor, M. J., & Molot, L. A. (2013). A comparison of three colorimetric methods of ferrous and total reactive iron measurement in freshwaters. *Limnology and Oceanography: Methods*, *11*(3), 113-125.

Veter, M., Foley, S. F., Mertz-Kraus, R., & Groschopf, N. (2017). Trace elements in olivine of ultramafic lamprophyres controlled by phlogopite-rich mineral assemblages in the mantle source. *Lithos*, *292*, 81-95.

Vetrimurugan, E., Brindha, K., Elango, L., & Ndwandwe, O. M. (2017). Human exposure risk to heavy metals through groundwater used for drinking in an intensively irrigated river delta. *Applied Water Science*, *7*(6), 3267-3280.

Viero, A. P., Roisenberg, C., Roisenberg, A., & Vigo, A. (2009). The origin of fluoride in the granitic aquifer of Porto Alegre, Southern Brazil. *Environmental geology*, *56*(8), 1707-1719.

Vincy, M. V., Brilliant, R., & Pradeepkumar, A. P. (2015). Hydrochemical characterization and quality assessment of groundwater for drinking and irrigation purposes: a case study of Meenachil River Basin, Western Ghats, Kerala, India. *Environmental monitoring and assessment*, *187*(1), 1-19.

Vinnarasi, F., Srinivasamoorthy, K., Saravanan, K., Gopinath, S., Prakash, R., Ponnumani, G., & Babu, C. (2021). Chemical weathering and atmospheric carbon dioxide (CO 2) consumption in Shanmuganadhi, South India: Evidences from groundwater geochemistry. *Environmental Geochemistry and Health*, *43*, 771-790.

Vinnarasi, F., Srinivasamoorthy, K., Saravanan, K., Gopinath, S., Prakash, R., Ponnumani, G., & Babu, C. (2020). Rare earth elements geochemistry of groundwater from Shanmuganadhi, Tamilnadu, India: Chemical weathering implications using geochemical mass-balance calculations. *Geochemistry*, *80*(4), 125668.

Vinnarasi, F., Srinivasamoorthy, K., Saravanan, K., Kanna, A. R., Gopinath, S., Prakash, R., ... & Babu, C. (2022). Hydrogeochemical characteristics and risk evaluation of potential toxic elements in groundwater from Shanmughanadhi, Tamilnadu, India. *Environmental Research*, *204*, 112199.

Virk, H. S. (2019). Groundwater Contamination of Amritsar District of Punjab due to Heavy Metals Iron and Arsenic and its Mitigation. *Res Rev: J Toxicol*, *9*(2), 18-27p.

Vishnu, C. L., Rani, V. R., Sajinkumar, K. S., Oommen, T., Bonali, F. L., Pareeth, S., ... & Rajaneesh, A. (2020). Catastrophic flood of August 2018, Kerala, India: Study of partitioning role of lineaments in modulating flood level using remote sensing data. *Remote Sensing Applications: Society and Environment*, *20*, 100426.

Vithanage, M., & Bhattacharya, P. (2015). Fluoride in the environment: sources, distribution and defluoridation. *Environmental Chemistry Letters*, *13*(2), 131-147.

Vithanage, M., Jayarathna, L., Rajapaksha, A. U., Dissanayake, C. B., Bootharaju, M. S., & Pradeep, T. (2012). Modeling sorption of fluoride on to iron rich laterite. *Colloids and Surfaces A: Physicochemical and Engineering Aspects*, *398*, 69-75.

Vithanage, M., Kumarathilaka, P., Oze, C., Karunatilake, S., Seneviratne, M., Hseu, Z. Y., ... & Rinklebe, J. (2019). Occurrence and cycling of trace elements in ultramafic soils and their impacts on human health: A critical review. *Environment International*, *131*, 104974.

Vodyanitskii, Y. N. (2009). Mineralogy and geochemistry of manganese: a review of publications. *Eurasian Soil Science*, *42*(10), 1170-1178.

Voute, F., Hagemann, S. G., Evans, N. J., & Villanes, C. (2019). Sulfur isotopes, trace element, and textural analyses of pyrite, arsenopyrite and base metal sulfides associated with gold mineralization in the Pataz-Parcoy district, Peru: Implication for paragenesis, fluid source, and gold deposition mechanisms. *Mineralium Deposita*, *54*, 1077-1100.

Voutsis, N., Kelepertzis, E., Tziritis, E., & Kelepertsis, A. (2015). Assessing the hydrogeochemistry of groundwaters in ophiolite areas of Euboea Island, Greece, using multivariate statistical methods. *Journal of Geochemical Exploration*, *159*, 79-92.

Vural, A., & Gundogdu, A. (2020). High-fluoride risk and toxicity in surface waters in Gumushane-Gokdere valley drainage network (NE Turkey). *Journal of Engineering Research and Applied Science*, *9*(1), 1323-1334.

Wada, Y., Van Beek, L. P. H., & Bierkens, M. F. (2011). Modelling global water stress of the recent past: on the relative importance of trends in water demand and climate variability. *Hydrology and Earth System Sciences*, *15*(12), 3785-3808.

Wada, Y., Van Beek, L. P., Van Kempen, C. M., Reckman, J. W., Vasak, S., & Bierkens, M. F. (2010). Global depletion of groundwater resources. *Geophysical research letters*, *37*(20).

Wagh, V. M., Mukate, S. V., Panaskar, D. B., Muley, A. A., & Sahu, U. L. (2019). Study of groundwater hydrochemistry and drinking suitability through Water Quality Index (WQI) modelling in Kadava river basin, India. *SN Applied Sciences*, *1*(10), 1-16.

Wagh, V. M., Panaskar, D. B., Varade, A. M., Mukate, S. V., Gaikwad, S. K., Pawar, R. S., ... & Aamalawar, M. L. (2016). Major ion chemistry and quality assessment of the groundwater resources of Nanded tehsil, a part of southeast Deccan Volcanic Province, Maharashtra, India. *Environmental Earth Sciences*, *75*(21), 1-26.

Wagner, B. J. (1995). Recent advances in simulation-optimization groundwater management modeling. *Reviews of Geophysics*, *33*(S2), 1021-1028.

Wali, S. U., Alias, N., & Harun, S. B. (2020). Quality reassessment using water quality indices and hydrochemistry of groundwater from the Basement Complex section of Kaduna Basin, NW Nigeria. *SN Applied Sciences*, *2*(10), 1-21.

Walker, D. B., Baumgartner, D. J., Gerba, C. P., & Fitzsimmons, K. (2019). Surface water pollution. In *Environmental and pollution science* (pp. 261-292). Academic Press.

Wang, A., Duan, L., Huang, H., Ma, J., Zhang, Y., Ma, Q., ... & Ba, Y. (2022). Association between fluoride exposure and behavioural outcomes of school-age children: a pilot study in China. *International journal of environmental health research*, *32*(1), 232-241.

Wang, C., Gao, Y., Wang, W., Zhao, L., Zhang, W., Han, H., ... & Sun, D. (2012). A national cross-sectional study on effects of fluoride-safe water supply on the prevalence of fluorosis in China. *BMJ open*, *2*(5), e001564.

Wang, J. S., & Wai, C. M. (2004). Arsenic in drinking water—a global environmental problem. *Journal of Chemical Education*, *81*(2), 207.

Wang, J., Zheng, N., Liu, H., Cao, X., Teng, Y., & Zhai, Y. (2021a). Distribution, formation and human health risk of fluorine in groundwater in Songnen Plain, NE China. *Water*, *13*(22), 3236.

Wang, L., Ma, L., & Yang, Z. (2018). Spatial variation and risk assessment of heavy metals in paddy rice from Hunan Province, Southern China. *International Journal of Environmental Science and Technology*, *15*(7), 1561-1572.

Wang, L., Shi, C., Pan, L., Zhang, X., & Zou, J. J. (2020a). Rational design, synthesis, adsorption principles and applications of metal oxide adsorbents: a review. *Nanoscale*, *12*(8), 4790-4815.

Wang, S. X., Wang, Z. H., Cheng, X. T., Li, J., Sang, Z. P., Zhang, X. D., ... & Wang, Z. Q. (2007). Arsenic and fluoride exposure in drinking water: children's IQ and growth in Shanyin county, Shanxi province, China. *Environmental health perspectives*, *115*(4), 643-647.

Wang, T., Yang, Q., Wang, Y., Wang, J., Zhang, Y., & Pan, W. P. (2020b). Arsenic release and transformation in co-combustion of biomass and coal: Effect of mineral elements and volatile matter in biomass. *Bioresource technology*, *297*, 122388.

Wang, W., Zhang, C., Shan, J., & He, M. (2020c). Comparison of the reaction kinetics and mechanisms of Sb (III) oxidation by reactive oxygen species from pristine and surface-oxidized pyrite. *Chemical Geology*, *552*, 119790.

Wang, X., Chen, C., & Wang, J. (2017). Phytoremediation of strontium contaminated soil by Sorghum bicolor (L.) Moench and soil microbial community-level physiological profiles (CLPPs). *Environmental Science and Pollution Research*, *24*, 7668-7678.

Wang, X., Han, Z., Wang, W., Zhang, B., Wu, H., Nie, L., ... & Liu, Q. (2019a). Continental-scale geochemical survey of lead (Pb) in mainland China's pedosphere:

Concentration, spatial distribution and influences. *Applied geochemistry*, *100*, 55-63.

Wang, Y., Li, J., Ma, T., Xie, X., Deng, Y., & Gan, Y. (2021b). Genesis of geogenic contaminated groundwater: As, F and I. *Critical Reviews in Environmental Science and Technology*, *51*(24), 2895-2933.

Wang, Y., Pi, K., Fendorf, S., Deng, Y., & Xie, X. (2019b). Sedimentogenesis and hydrobiogeochemistry of high arsenic Late Pleistocene-Holocene aquifer systems. *Earth-Science Reviews*, *189*, 79-98.

Wang, Y., Zhang, G., Wang, H., Cheng, Y., Liu, H., Jiang, Z., ... & Wang, Y. (2021c). Effects of different dissolved organic matter on microbial communities and arsenic mobilization in aquifers. *Journal of hazardous materials*, *411*, 125146.

Wang, Z., Chai, L., Wang, Y., Yang, Z., Wang, H., & Wu, X. (2011). Potential health risk of arsenic and cadmium in groundwater near Xiangjiang River, China: a case study for risk assessment and management of toxic substances. *Environmental monitoring and assessment*, *175*(1), 167-173.

Wang, Z., Laurenz, V., Petitgirard, S., & Becker, H. (2016). Earth's moderately volatile element composition may not be chondritic: Evidence from In, Cd and Zn. *Earth and Planetary Science Letters*, *435*, 136-146.

Wang, Z., Su, J., Hu, X., Ali, A., & Wu, Z. (2021d). Isolation of biosynthetic crystals by microbially induced calcium carbonate precipitation and their utilization for fluoride removal from groundwater. *Journal of Hazardous Materials*, *406*, 124748.

Ward, C. R. (2016). Analysis, origin and significance of mineral matter in coal: An updated review. *International Journal of Coal Geology*, *165*, 1-27.

Warren, B. E. (1940). X-ray Diffraction Study of the Structure of Glass. *Chemical Reviews*, *26*(2), 237-255.

Wasana, H., Perera, G. D., Gunawardena, P. D. S., Fernando, P. S., & Bandara, J. (2017). WHO water quality standards Vs Synergic effect (s) of fluoride, heavy metals and hardness in drinking water on kidney tissues. *Scientific Reports*, *7*(1), 1-6.

Wasserman, G. A., Liu, X., Parvez, F., Factor-Litvak, P., Ahsan, H., Levy, D., ... & Graziano, J. H. (2011). Arsenic and manganese exposure and children's intellectual function. *Neurotoxicology*, *32*(4), 450-457.

Wasserman, L. (2006). *All of nonparametric statistics*. Springer Science & Business Media.

Webb, J. A., & Nash, D. J. (2020). Reassessing southern African silcrete geochemistry: implications for silcrete origin and sourcing of silcrete artefacts. *Earth Surface Processes and Landforms*, *45*(13), 3396-3413.

Webster, J. D., Thomas, R., Rhede, D., Förster, H. J., & Seltmann, R. (1997). Melt inclusions in quartz from an evolved peraluminous pegmatite: Geochemical evidence for strong tin enrichment in fluorine-rich and phosphorus-rich residual liquids. *Geochimica et Cosmochimica Acta*, *61*(13), 2589-2604.

Wedepohl, K. H. (1995). The composition of the continental crust. *Geochimica et cosmochimica Acta*, *59*(7), 1217-1232.

Weinstein, L. H., & Davison, A. (2004). *Fluorides in the environment: effects on plants and animals*. Cabi.

Wen, Y. (2012). Impacts of road de-icing salts on manganese transport to groundwater in roadside soils.

White, A. F., & Yee, A. (1985). Aqueous oxidation-reduction kinetics associated with coupled electron-cation transfer from iron-containing silicates at 25 C. *Geochimica et Cosmochimica Acta*, *49*(5), 1263-1275.

Whitford, G. M. (1996). *The metabolism and toxicity of fluoride*. Karger Publishers.Whitford GM (1994) Intake and metabolism of fluoride. Adv Dent Res 8(1):5–14

Whittington, B. I., & Muir*, D. (2000). Pressure acid leaching of nickel laterites: a review. *Mineral Processing and Extractive Metullargy Review*, *21*(6), 527-599.

Widdowson, M. (2009). Evolution of laterite in Goa. *Natural Resources of Goa: A geological perspective*, 35-68.

Wiesner-Friedman, C., Beattie, R. E., Stewart, J. R., Hristova, K. R., & Serre, M. L. (2022). Characterizing Differences in Sources of and Contributions to Fecal Contamination of Sediment and Surface Water with the Microbial FIT Framework. *Environmental Science & Technology*, *56*(7), 4231-4240.

Wilberforce, O. J. O. (2016). Review of principles and application of AAS, PIXE and XRF and their usefulness in environmental analysis of heavy metals. *IOSR-JAC*, *9*(6), 15-17.

Wilcox, L. (1955). *Classification and use of irrigation waters* (No. 969). US Department of Agriculture.

Wilcox, L. V. (1948). The quality of water for irrigation use (No. 1488-2016-124600).

Wilkinson, J. J., Chang, Z., Cooke, D. R., Baker, M. J., Wilkinson, C. C., Inglis, S., ... & Gemmell, J. B. (2015). The chlorite proximitor: A new tool for detecting porphyry ore deposits. *Journal of Geochemical Exploration*, *152*, 10-26.

Williams, J. A., Billington, R. W., & Pearson, G. J. (1999). The influence of sample dimensions on fluoride ion release from a glass ionomer restorative cement. *Biomaterials*, *20*(14), 1327-1337.

Williams-Jones, A. E., Migdisov, A. A., & Samson, I. M. (2012). Hydrothermal mobilisation of the rare earth elements–a tale of "ceria" and "yttria". *Elements*, *8*(5), 355-360.

Winfield, M. D., & Groisman, E. A. (2003). Role of nonhost environments in the lifestyles of Salmonella and Escherichia coli. *Applied and environmental microbiology*, *69*(7), 3687-3694.

World Bank. (2012). India groundwater: A valuable but diminishing resource. https://www.worldbank.org/en/news/feature/2012/03/06/india-groundwater-critical-diminishing

World Health Organization, & WHO. (2017). *Guidelines for drinking-water quality*: fourth edition incorporating the first addendum. World Health Organization, Geneva

World Health Organization, WHO., & World Health Organisation Staff. (2004). *Guidelines for drinking-water quality* (Vol. 1). World Health Organization.

World Health Organization. (2008). *Guidelines for drinking-water quality: second addendum. Vol. 1, Recommendations*. World Health Organization.

World Health Organization. (2009). *Calcium and magnesium in drinking water: public health significance*. World Health Organization

Wrye, L. A. (2008). *Distinguishing between natural and anthropogenic sources of arsenic in soils from the Giant mine, Northwest Territories and the North Brookfield mine, Nova Scotia* (Doctoral dissertation).

Wu, H., Chen, J., Qian, H., & Zhang, X. (2015a). Chemical characteristics and quality assessment of groundwater of exploited aquifers in Beijiao water source of Yinchuan, China: a case study for drinking, irrigation, and industrial purposes. *Journal of Chemistry*, *2015*.

Wu, H., Liao, Q., Chillrud, S. N., Yang, Q., Huang, L., Bi, J., & Yan, B. (2016). Environmental exposure to cadmium: health risk assessment and its associations with hypertension and impaired kidney function. *Scientific reports*, *6*(1), 1-9.

Wu, J., Li, P., & Qian, H. (2015b). Hydrochemical characterization of drinking groundwater with special reference to fluoride in an arid area of China and the control of aquifer leakage on its concentrations. *Environmental Earth Sciences*, *73*, 8575-8588.

Wu, L., Xie, Z., Lu, L., Zhao, J., Wang, Y., Jiang, X., ... & Zhang, H. (2018). Few-layer tin sulfide: a promising black-phosphorus-analogue 2D material with exceptionally large nonlinear optical response, high stability, and applications in all-optical switching and wavelength conversion. *Advanced Optical Materials*, *6*(2), 1700985.

Wu, M., Samson, I. M., Qiu, K., & Zhang, D. (2023). Multi-stage metasomatic Zr mineralization in the world-class Baerzhe rare earth element Nb-Zr-Be deposit, China. *American Mineralogist: Journal of Earth and Planetary Materials*, *108*(2), 389-405.

Wu, R., Podgorski, J., Berg, M., & Polya, D. A. (2021). Geostatistical model of the spatial distribution of arsenic in groundwaters in Gujarat State, India. *Environmental geochemistry and health*, *43*(7), 2649-2664.

Wuana, R. A., & Okieimen, F. E. (2011). Heavy metals in contaminated soils: a review of sources, chemistry, risks and best available strategies for remediation. *International Scholarly Research Notices*, *2011*.

Wurts, W. A. (2002). Alkalinity and hardness in production ponds. *WORLD AQUACULTURE-BATON ROUGE-*, *33*(1), 16-17.

Wyckoff, W. G., Greig, J. W., & Bowen, N. L. (1926). X-ray diffraction patterns; mullite and sillimanite. *American Journal of Science*, *5*(66), 459-472.

Xiang, Q., Liang, Y., Chen, L., Wang, C., Chen, B., Chen, X., ... & Shanghai, P. R. (2003). Effect of fluoride in drinking water on children's intelligence. *Fluoride*, *36*(2), 84-94.

Xie, X., Wang, Y., Li, J., Yu, Q., Wu, Y., Su, C., & Duan, M. (2015). Effect of irrigation on Fe (III)–SO42− redox cycling and arsenic mobilization in shallow groundwater from the Datong basin, China: evidence from hydrochemical monitoring and modeling. *Journal of Hydrology*, *523*, 128-138.

Xie, X., Wang, Y., Su, C., Li, J., & Li, M. (2012). Influence of irrigation practices on arsenic mobilization: evidence from isotope composition and Cl/Br ratios in groundwater from Datong Basin, northern China. *Journal of Hydrology*, *424*, 37-47.

Xing, W., Liu, H., Banet, T., Wang, H., Ippolito, J. A., & Li, L. (2020). Cadmium, copper, lead and zinc accumulation in wild plant species near a lead smelter. *Ecotoxicology and Environmental Safety*, *198*, 110683.

Xing, Y., Brugger, J., Tomkins, A., & Shvarov, Y. (2019). Arsenic evolution as a tool for understanding formation of pyritic gold ores. *Geology*, *47*(4), 335-338.

Xiong, W., Deng, H., Moore, J., Crandall, D., Hakala, J. A., & Lopano, C. (2021). Influence of Flow Pathway Geometry on Barite Scale Deposition in Marcellus Shale during Hydraulic Fracturing. Energy & Fuels, 35(15), 11947-11957.

Xu, C., Zhang, H., Han, L., & Zhai, L. (2014). Characteristic monitoring of groundwater-salt transportation and input-output in inland arid irrigation area. *Journal of Environmental Biology*, *35*(6), 1181.

Xu, J., Cook, N. J., Ciobanu, C. L., Li, X., Kontonikas-Charos, A., Gilbert, S., & Lv, Y. (2021). Indium distribution in sphalerite from sulfide–oxide–silicate skarn assemblages: a case study of the Dulong Zn–Sn–In deposit, Southwest China. *Mineralium Deposita*, *56*, 307-324.

Yadav, A., Nanda, A., Sahu, B. L., Sahu, Y. K., Patel, K. S., Pervez, S., ... & Bhattacharya, P. (2020a). Groundwater hydrochemistry of Rajnandgaon district, Chhattisgarh, central India. *Groundwater for sustainable development*, *11*, 100352.

Yadav, K. K., Gupta, N., Kumar, V., Choudhary, P., & Khan, S. A. (2018). GIS-based evaluation of groundwater geochemistry and statistical determination of the fate of contaminants in shallow aquifers from different functional areas of Agra city, India: levels and spatial distributions. *RSC advances*, *8*(29), 15876-15889.

Yadav, P., Garg, V. K., Singh, B., & Mor, S. (2020b). Assessment of Arsenic in Groundwater of Southwestern Haryana, India and Chemical Body Burden Caused by its Ingestion. *Journal of the Geological Society of India*, *96*(5), 521-525.

Yadav, S., Kumbhar, N., Jan, R., Roy, R., & Satsangi, P. G. (2019). Ge-notoxic effects of PM10 and PM2. 5 bound metals: metal bioaccessibility, free radical generation, and role of iron. *Environmental geochemistry and health*, *41*(3), 1163-1186.

Yan, Q., Zhu, Y., Feng, G., Zhu, Z., Zhang, L., Liu, J., & He, H. (2020). Characterization, dissolution and solubility of lead fluorapatite at 25-45° C. *Applied Geochemistry*, *120*, 104659.

Yang, D., Sasaki, A., & Endo, M. (2018). Solidification/stabilization of arsenic in red mud upon addition of Fe (III) or Fe (III) and Al (III) dissolved in H2SO4. *Journal of Water and Environment Technology*, *16*(2), 115-126.

Yang, J., Chen, L., Liu, L. Z., Shi, W. L., & Meng, X. Z. (2014). Comprehensive risk assessment of heavy metals in lake sediment from public parks in Shanghai. *Ecotoxicology and environmental safety*, *102*, 129-135.

Yang, K., Liang, X. (2011). Fluoride in drinking water: effect on liver and kidney function. In: Nriagu Jerome O (ed) Encyclopedia of Environmental Health. Elsevier, Amsterdam, pp 769–775.

Yang, Q., Li, Z., Lu, X., Duan, Q., Huang, L., & Bi, J. (2018). A review of soil heavy metal pollution from industrial and agricultural regions in China: Pollution and risk assessment. *Science of the total environment*, *642*, 690-700.

Yang, W., Li, F., Zhao, Y., Lu, X., Yang, S., & Zhu, P. (2022). Quantitative analysis of heavy metals in soil by X-ray fluorescence with PCA–ANOVA and support vector regression. *Analytical Methods*, *14*(40), 3944-3952.

Yang, Z., Cheng, H., Xi, X., & Liu, A. (2005). Regional ecological geochemical assessment: ideas and prospects: ideas and prospects. *Geological Bulletin of China*, *24*(8), 687-693.

Yao, W., Tsang, M. Y., & Wortmann, U. G. (2022). Oxidation of pyrite during barite extraction. *Chemical Geology*, *607*, 121011.

Yarincik, K. M., Murray, R. W., Lyons, T. W., Peterson, L. C., & Haug, G. H. (2000). Oxygenation history of bottom waters in the Cariaco Basin, Venezuela, over the past 578,000 years: Results from redox-sensitive metals (Mo, V, Mn, and Fe). *Paleoceanography*, *15*(6), 593-604.

Yarmohammadi, S., & Wood, D. A. (2022). Integrated microfacies interpretations of large natural gas reservoirs combining qualitative and quantitative image analysis. In *Sustainable Geoscience for Natural Gas Subsurface Systems* (pp. 93-127). Gulf Professional Publishing.

Yasunori, Y., Kenichi, I., Akihiko, K., Koichiro, S., Shigeki, T., Mitsuhiro, S., & Hiroshi, Y. (2012). Arsenic polluted groundwater and its countermeasures in the middle basin of the Ganges, Uttar Pradesh State, India. *Journal of Environmental Protection*, *2012*.

Ye, L., Cook, N. J., Liu, T., Ciobanu, C. L., Gao, W., & Yang, Y. (2012). The Niujiaotang Cd-rich zinc deposit, Duyun, Guizhou province, southwest China: ore genesis and mechanisms of cadmium concentration. *Mineralium Deposita*, *47*(6), 683-700.

Yeganeh, M., Afyuni, M., Khoshgoftarmanesh, A. H., Khodakarami, L., Amini, M., Soffyanian, A. R., & Schulin, R. (2013). Mapping of human health risks arising from soil nickel and mercury contamination. *Journal of hazardous materials*, *244*, 225-239.

Yetişsin, F., & Kardeş, İ. (2021). Could acetone O-(4-chlorophenylsulfonyl) oxime be a copper chelating and antioxidative molecule on maize seedlings?. *International Journal of Phytoremediation*, 1-9.

Yin, S., Yang, L., Wen, Q., & Wei, B. (2022). Temporal variation and mechanism of the geogenic arsenic concentrations in global groundwater. *Applied Geochemistry*, 105475.

Younas, A., Mushtaq, N., Khattak, J. A., Javed, T., Rehman, H. U., & Farooqi, A. (2019). High levels of fluoride contamination in groundwater of the semi-arid alluvial aquifers, Pakistan: evaluating the recharge sources and geochemical identification via stable isotopes and other major elemental data. *Environmental Science and Pollution Research*, *26*, 35728-35741.

Young, N. J., Coley, M. D., & Greenaway, A. M. (2019). Mineralogical investigations of Jamaican hematite-rich and goethite-rich bauxites using XRD and solid state 27Al and 31P MAS NMR spectroscopy. *Journal of Geochemical Exploration*, *200*, 54-76.

Zabala, M. E., Manzano, M., & Vives, L. (2016). Assessment of processes controlling the regional distribution of fluoride and arsenic in groundwater of the Pampeano Aquifer in the Del Azul Creek basin (Argentina). *Journal of hydrology*, *541*, 1067-1087.

Zandbergen, P. A., & Hall, K. J. (1998). Analysis of the British Columbia water quality index for watershed managers: a case study of two small watersheds. *Water Quality Research Journal*, *33*(4), 519-550.

Zango, M. S., Pelig-Ba, K. B., Anim-Gyampo, M., Gibrilla, A., & Sunkari, E. D. (2021). Hydrogeochemical and isotopic controls on the source of fluoride in groundwater within the Vea catchment, northeastern Ghana. *Groundwater for Sustainable Development*, *12*, 100526.

Zango, M. S., Sunkari, E. D., Abu, M., & Lermi, A. (2019). Hydrogeochemical controls and human health risk assessment of groundwater fluoride and boron in the semi-arid North East region of Ghana. *Journal of Geochemical Exploration*, *207*, 106363.

Zelazny, L. W., Jackson, M. L., & Lim, C. H. (1986). Oxides, hydroxides, and aluminosilicates. *Methods of Soil Analysis: Part 1 Physical and Mineralogical Methods*, *5*, 101-150.

Zhang, G., Liu, Y., Wang, J., & Li, H. (2020). Efficient arsenic (III) removal from aqueous solution by a novel nanostructured iron-copper-manganese trimetal oxide. *Journal of Molecular Liquids*, *309*, 112993.

Zhang, H., Zhang, X., Liu, W., Yeh, P. J. F., Ye, P., & He, X. (2022). Impacts of active tectonics on geogenic arsenic enrichment in groundwater in the Hetao Plain, Inner Mongolia. *Quaternary Science Reviews*, *278*, 107343.

Zhang, J., Brutus, T. E., Cheng, J., & Meng, X. (2017). Fluoride removal by Al, Ti, and Fe hydroxides and coexisting ion effect. *Journal of environmental sciences*, *57*, 190-195.

Zhang, L., Qin, X., Tang, J., Liu, W., & Yang, H. (2017). Review of arsenic geochemical characteristics and its significance on arsenic pollution studies in karst groundwater, Southwest China. *Applied geochemistry*, *77*, 80-88.

Zhang, X., Gao, X., Li, C., Luo, X., & Wang, Y. (2019). Fluoride contributes to the shaping of microbial community in high fluoride groundwater in Qiji County, Yuncheng City, China. *Scientific reports*, *9*(1), 1-10.

Zhao, M. (2020). An indirect interpolation model and its application for digital elevation model generation. *Earth Science Informatics*, *13*(4), 1251-1264.

Zhou, J., Wang, H., Cravotta III, C. A., Dong, Q., & Xiang, X. (2017). Dissolution of fluorapatite by Pseudomonas fluorescens P35 resulting in fluorine release. *Geomicrobiology Journal*, *34*(5), 421-433.

Zhou, Y., Zeng, Y., Zhou, J., Guo, H., Li, Q., Jia, R., ... & Zhao, J. (2017). Distribution of groundwater arsenic in Xinjiang, PR China. *Applied geochemistry*, *77*, 116-125.

Zhu, G., Wu, X., Ge, J., Liu, F., Zhao, W., & Wu, C. (2020). Influence of mining activities on groundwater hydrochemistry and heavy metal migration using a self-organizing map (SOM). *Journal of Cleaner Production*, *257*, 120664.

Zhu, J., Zhao, H., & Ni, J. (2007). Fluoride distribution in electrocoagulation defluoridation process. *Separation and Purification Technology*, *56*(2), 184-191.

Zolekar, R. B., Todmal, R. S., Bhagat, V. S., Bhailume, S. A., Korade, M. S., & Das, S. (2021). Hydro-chemical characterization and geospatial analysis of groundwater for drinking and agricultural usage in Nashik district in Maharashtra, India. *Environment, Development and Sustainability*, *23*, 4433-4452.

Zoni, S., Albini, E., & Lucchini, R. (2007). Neuropsychological testing for the assessment of manganese neurotoxicity: a review and a proposal. *American journal of industrial medicine*, *50*(11), 812-830.

ANNEXURE

Annexure 1: The average and standard deviation of pH of samples collected from Palakkad and Malappuram during the Pr, Mo, and Po seasons.

Palakkad district				Malappuram district			
sample	Pr	Mo	Po	Sample	Pr	Mo	Po
	Mean ± SD	Mean ± SD	Mean ± SD		Mean ± SD	Mean ± SD	Mean ± SD
P01	7.18 ± 0.04	7.57 ± 0.57	7.34 ± 0.25	M01	5.91 ± 0.01	6.98 ± 0.29	6.94 ± 0.07
P02	6.39 ± 0.26	6.74 ± 0.39	6.51 ± 0.16	M02	5.19 ± 0.29	5.56 ± 0.05	5.76 ± 0.28
P03	6.06 ± 0.04	6.53 ± 0.04	6.29 ± 0.13	M03	5.72 ± 0.69	5.92 ± 1.26	5.54 ± 0.53
P04	5.85 ± 0.06	5.64 ± 0.06	5.1 ± 0.17	M04	4.91 ± 0.38	5.08 ± 0.04	5.68 ± 0.23
P05	6.76 ± 0.06	8.18 ± 0.28	6.83 ± 0.21	M05	5.36 ± 0.47	4.96 ± 0.04	5.36 ± 0.45
P06	5.83 ± 0.18	4.92 ± 0.05	5.47 ± 0.57	M06	5.86 ± 0.03	5.73 ± 0.38	6.53 ± 0.44
P07	5.77 ± 0.55	5.18 ± 0.25	5.64 ± 0.45	M07	7.45 ± 1.36	8.34 ± 0.44	8.31 ± 0.21
P08	6.65 ± 0.47	5.98 ± 0.18	6.08 ± 0.67	M08	5.96 ± 1.61	7.43 ± 0.4	7.3 ± 0.06
P09	6.01 ± 1.31	4.48 ± 0.25	5.33 ± 0.01	M09	5.08 ± 0.04	5.22 ± 0.08	5.18 ± 0.3
P10	6.06 ± 0.93	4.6 ± 0.14	4.95 ± 0.28	M10	6.02 ± 0.31	5.2 ± 0.28	4.62 ± 0.48
P11	5.68 ± 1.17	6.52 ± 0.24	6.41 ± 0.18	M11	5.14 ± 0.38	5.13 ± 0.04	5.38 ± 0.45
P12	6.72 ± 0.59	6.75 ± 0.01	7.18 ± 0.33	M12	5.34 ± 0.41	5.08 ± 0.04	5.53 ± 0.4
P13	7.02 ± 0.45	6.62 ± 0.12	6.92 ± 0.3	M13	5.44 ± 0.08	5.63 ± 0.25	5.73 ± 0.21
P14	6.65 ± 0.05	6.48 ± 0.29	6.75 ± 0.45	M14	5.01 ± 0.58	4.82 ± 0.18	5.02 ± 0.23
P15	7.48 ± 0.25	7.85 ± 0.41	8 ± 0.11	M15	6 ± 0.42	5.98 ± 0.21	5.74 ± 0.25
P16	7.37 ± 0.86	7.75 ± 0.57	7.71 ± 0.25	M16	5.67 ± 0.3	5.72 ± 0.13	6 ± 0.9
P17	6.32 ± 0.34	6.25 ± 0.07	5.99 ± 0.28	M17	5.94 ± 0.21	4.95 ± 2.24	6.45 ± 0.21
P18	7.03 ± 0.27	7.51 ± 0.3	7.8 ± 0.54	M18	5.81 ± 0.16	4.82 ± 0.1	5.99 ± 0.22
P19	6.54 ± 0.2	6.9 ± 0.42	7.58 ± 0.99	M19	5.87 ± 0.33	5.58 ± 0.16	5.87 ± 0.46
P20	5.61 ± 0.2	5.84 ± 0.01	5.88 ± 0.44	M20	5.26 ± 1.33	6.06 ± 0.08	5.89 ± 0.3
P21	6.92 ± 0.02	7.44 ± 0.43	7.83 ± 0.79	M21	5.81 ± 0.86	5.13 ± 0.16	5.2 ± 0.66
P22	8.32 ± 0.3	8.29 ± 0.16	8.09 ± 0.03	M22	5.15 ± 0.29	5.59 ± 0.13	5.54 ± 0.28
P23	6.52 ± 0.29	7.26 ± 0.04	7.63 ± 0.65	M23	5.11 ± 0.11	6.3 ± 0.23	5.91 ± 0.04
P24	6.92 ± 0.35	6.93 ± 0.4	7.27 ± 0.78	M24	5.87 ± 0.1	5.6 ± 0.23	5.61 ± 0.3
P25	8.13 ± 0.11	7.95 ± 0.28	8 ± 0.32	M25	6.98 ± 0.23	7.16 ± 0.3	7.47 ± 0.47
P26	7.64 ± 0.36	7.52 ± 0.12	8.22 ± 0.66	M26	6.04 ± 0.91	5.43 ± 0.16	5.67 ± 0.4
P27	6.51 ± 0.11	6.78 ± 0.33	7.45 ± 1.27	M27	6.32 ± 0.34	6.05 ± 0.05	5.95 ± 0.47
P28	7.09 ± 0.4	7.42 ± 0.42	7.71 ± 0.73	M28	5.55 ± 0.26	5 ± 0.06	5.33 ± 0.95
P29	7.57 ± 0.05	7.46 ± 0.49	7.94 ± 0.25	M29	6.2 ± 0.3	6.19 ± 0.16	6.09 ± 0.35
P30	7.32 ± 0.11	7.92 ± 0.86	7.99 ± 0.32	M30	6.54 ± 0.2	6.71 ± 0.28	6.77 ± 0.2
P31	7.09 ± 0.66	6.91 ± 0.54	7.32 ± 0.77	M31	5.38 ± 0.14	4.71 ± 0.11	4.93 ± 0.44
P32	8.01 ± 0.25	8.2 ± 0.31	7.81 ± 0.25	M32	7.05 ± 0.18	6.74 ± 0.34	4.87 ± 2.49
P33	7.78 ± 0.91	7.34 ± 1.24	6.66 ± 0.25	M33	6.19 ± 0.13	5.65 ± 1.33	6.57 ± 0.24

Annexure 2: The average and standard deviation of temperature (°C) of samples collected from Palakkad and Malappuram during the Pr, Mo, and Po seasons.

Palakkad district				**Malappuram district**			
Sample	**Pr**	**Mo**	**Po**		**Pr**	**Mo**	**Po**
	Mean ± SD	**Mean ± SD**	**Mean ± SD**	**Sample**	**Mean ± SD**	**Mean ± SD**	**Mean ± SD**
P01	31.5 ± 2.1	27.4 ± 0.8	28.5 ± 0.7	M01	30.7 ± 2.4	27.5 ± 1.1	27.3 ± 0.4
P02	31.4 ± 2	27.8 ± 1.1	27.5 ± 0	M02	30.9 ± 3.3	27.3 ± 1	27.8 ± 1.1
P03	30.8 ± 2.5	27.8 ± 1	28.3 ± 1.1	M03	31.1 ± 2.9	27.3 ± 1.1	27.5 ± 0.7
P04	31.7 ± 2.4	27.5 ± 0.7	28.5 ± 1.4	M04	31.3 1.8	27.6 1.3	28 0
P05	30.4 ± 3.4	28.8 ± 0.4	28.4 ± 0.2	M05	31.2 ± 1.7	27.4 ± 1.5	27.5 ± 0
P06	29.3 ± 3.2	27.9 ± 0.6	27.6 ± 0.8	M06	31.7 ± 1.6	27.3 ± 1.1	27.3 ± 0.4
P07	30 ± 4.2	28.1 ± 0.1	28.1 ± 0.1	M07	30.7 ± 1.6	27.2 ± 1.1	27.8 ± 0.4
P08	30.7 ± 1.7	28.3 ± 0.4	28.2 ± 0.2	M08	30.8 ± 1.1	28.8 ± 0.2	27.5 ± 0
P09	30.9 ± 2.7	28.1 ± 0.1	28.1 ± 0.1	M09	30.3 ± 1.8	27.9 ± 1.4	28.3 ± 1.8
P10	31.3 ± 2.5	27.5 ± 0.8	28.6 ± 0.1	M10	30.5 ± 2.1	27.8 ± 1.3	27.8 ± 0.4
P11	31.2 ± 1.6	28.1 ± 1.8	28.6 ± 0.6	M11	31.4 ± 2.6	27.5 ± 1.5	28.3 ± 0.4
P12	30.8 ± 3.3	28.4 ± 0.2	28.6 ± 0.6	M12	30.5 ± 2.1	27.2 ± 0.5	27.8 ± 1.1
P13	30.4 ± 3.4	28.6 ± 0.4	29 ± 0.8	M13	31.3 ± 1.8	27.6 ± 1.1	27.3 ± 0.4
P14	29.4 ± 3.4	28.3 ± 0.4	27.8 ± 0.4	M14	31.8 2.5	27.2 1.8	28.8 0.4
P15	30.7 ± 1.7	28.1 ± 0.1	28.4 ± 0.2	M15	31 ± 2.8	27.7 ± 1.2	28.7 ± 0.3
P16	31 ± 2.1	28.2 ± 0.2	28 ± 0	M16	30.6 ± 2.3	27.1 ± 1.3	28.3 ± 0.4
P17	30.6 ± 3.7	28.4 ± 0.2	28.3 ± 0.4	M17	30.1 ± 3.6	27.2 ± 1.2	28 ± 0
P18	30.5 ± 2.8	28.7 ± 0.6	28.4 ± 0.1	M18	31.6 ± 2.3	27.5 ± 1.5	27.9 ± 0.6
P19	30 ± 2.8	28.4 ± 0.1	28.3 ± 0.4	M19	30.5 ± 2.1	27.5 ± 1.4	27.6 ± 0.8
P20	31.4 ± 2.6	28.8 ± 0.8	28.5 ± 0.7	M20	30.7 ± 2.3	28.9 ± 0.5	28 ± 0.7
P21	30.8 ± 2.5	28.9 ± 0.8	28.3 ± 0	M21	31.8 ± 2.5	27.6 ± 1.2	28 ± 0.7
P22	32.3 ± 1.8	28.7 ± 0.6	28.7 ± 0.2	M22	31 ± 2.8	27.2 ± 1.1	28.8 ± 1.1
P23	30.7 ± 3.8	28.6 ± 0.6	28.5 ± 0	M23	31.1 ± 2.9	27.3 ± 1.3	28.3 ± 0.4
P24	30.7 ± 3.7	24.5 ± 5.7	28.8 ± 1.1	M24	31.2 ± 1.7	27.7 ± 1.2	28.1 ± 0.8
P25	30.5 ± 2.1	28.3 ± 0.3	28 ± 0	M25	31.5 ± 2.1	28 ± 1.5	28.8 ± 0.4
P26	30 ± 2.8	28 ± 0.7	28 ± 0	M26	31.7 ± 2.3	27.4 ± 1.6	28.7 ± 0.2
P27	30.1 ± 2.9	28.3 ± 0.4	28.1 ± 0.1	M27	31 ± 2.8	28 ± 0.6	28.5 ± 0.7
P28	30.7 ± 3	28.6 ± 0.6	28 ± 0	M28	31.2 ± 2.3	27.4 ± 0.8	28 ± 1.4
P29	31.5 ± 2.1	28.7 ± 0.4	28.9 ± 0.5	M29	30.8 ± 2.5	27.8 ± 1.6	28 ± 0
P30	31.7 ± 0.9	28.1 ± 0.6	28.4 ± 0.2	M30	31.6 ± 2.3	27.7 ± 0.8	28.6 ± 0.1
P31	31.5 ± 2.1	28.2 ± 0.5	28.3 ± 0.4	M31	31.4 ± 2.6	28 ± 1.1	28.3 ± 0.4
P32	30.3 ± 3.2	28 ± 0.7	28.8 ± 0.4	M32	31.5 ± 2.1	28.3 ± 0.4	28.7 ± 0.2
P33	31.8 ± 1.1	28.4 ± 0.9	28.8 ± 0.4	M33	31 ± 2.1	27.9 ± 0.8	28.4 ± 0.5

Annexure 3: The average and standard deviation of EC (µS) of samples collected from Palakkad and Malappuram during the Pr, Mo, and Po seasons.

Palakkad district				**Malappuram district**			
Sample	**Pr**	**Mo**	**Po**	**Sample**	**Pr**	**Mo**	**Po**
	Mean ± SD	**Mean ± SD**	**Mean ± SD**		**Mean ± SD**	**Mean ± SD**	**Mean ± SD**
P01	1232 ± 123	1524 ± 372	1475 ± 372	M01	313 ± 35	1096 ± 422	802 ± 422
P02	239 ± 131	468 ± 14	532 ± 14	M02	149 ± 23	171 ± 1	189 ± 1
P03	206 ± 13	232 ± 13	284 ± 13	M03	54 ± 2	73 ± 8	66 ± 8
P04	239 ± 30	266 ± 26	269 ± 26	M04	110 ± 6	118 ± 9	106 ± 9
P05	278 ± 30	284 ± 67	422 ± 67	M05	178 ± 4	235 ± 21	217 ± 21
P06	151 ± 10	103 ± 37	144 ± 37	M06	44 ± 4	56 ± 2	76 ± 2
P07	180 ± 9	208 ± 5	213 ± 5	M07	424 ± 56	535 ± 26	533 ± 26
P08	246 ± 44	198 ± 48	197 ± 48	M08	274 ± 34	368 ± 44	375 ± 44
P09	132 ± 37	196 ± 9	183 ± 9	M09	62 ± 4	75 ± 1	79 ± 1
P10	183 ± 37	291 ± 15	87 ± 15	M10	76 ± 4	103 ± 8	86 ± 8
P11	106 73	193 ± 32	177 ± 32	M11	71 ± 20	132 ± 57	161 ± 57
P12	448 ± 50	353 ± 25	431 ± 25	M12	116 ± 13	128 ± 5	126 ± 5
P13	181 ± 122	120 ± 9	150 ± 9	M13	137 ± 19	117 ± 7	120 ± 7
P14	448 ± 9	371 ± 53	449 ± 53	M14	66 ± 15	114 ± 4	126 ± 4
P15	465 ± 46	584 ± 55	579 ± 55	M15	111 ± 56	101 ± 7	110 ± 7
P16	429 ± 14	558 ± 10	552 ± 10	M16	195 ± 23	284 ± 36	258 ± 36
P17	441 ± 20	386 ± 67	401 ± 67	M17	384 ± 150	347 ± 58	564 ± 58
P18	712 ± 69	825 ± 38	819 ± 38	M18	72 ± 24	93 ± 10	79 ± 10
P19	691 ± 73	905 ± 37	847 ± 37	M19	212 ± 25	173 ± 42	119 ± 42
P20	272 ± 2	468 ± 12	320 ± 12	M20	276 ± 174	139 ± 0	96 ± 0
P21	1295 ± 278	1412 ± 7	1697 ± 7	M21	137 ± 13	90 ± 1	74 ± 1
P22	1928 ± 86	2215 ± 34	2087 ± 34	M22	78 ± 1	137 ± 0	86 ± 0
P23	637 ± 77	753 ± 106	817 ± 106	M23	261 ± 17	378 ± 53	186 ± 53
P24	740 ± 101	1006 ± 14	863 ± 14	M24	106 ± 8	237 ± 18	140 ± 18
P25	537 ± 371	738 ± 63	764 ± 63	M25	299 ± 178	599 ± 15	597 ± 15
P26	1078 ± 404	980 ± 65	1017 ± 65	M26	161 ± 21	138 ± 21	142 ± 21
P27	371 ± 156	778 ± 433	665 ± 433	M27	561 ± 41	355 ± 19	306 ± 19
P28	1366 ± 79	1528 ± 47	1420 ± 47	M28	85 ± 32	99 ± 353	336 ± 353
P29	888 ± 33	1133 ± 96	1068 ± 96	M29	230 ± 7	362 ± 10	386 ± 10
P30	782 ± 256	1057 ± 2	946 ± 2	M30	329 ± 80	569 ± 29	662 ± 29
P31	752 ± 284	1109 ± 7	1052 ± 7	M31	514 ± 548	114 ± 132	181 ± 132
P32	758 ± 254	656 ± 49	611 ± 49	M32	416 ± 47	325 ± 124	404 ± 124
P33	386 ± 25	286 ± 272	349 ± 272	M33	573 ± 583	131 ± 1	186 ± 1

Annexure 4: The average and standard deviation of salinity (mg/L) of samples collected from Palakkad and Malappuram during the Pr, Mo, and Po seasons.

Palakkad district				**Malappuram district**			
Sample	**Pr**	**Mo**	**Po**	**Sample**	**Pr**	**Mo**	**Po**
	Mean ± SD	**Mean ± SD**	**Mean ± SD**		**Mean ± SD**	**Mean ± SD**	**Mean ± SD**
P01	670 ± 10	706 ± 148	689 ± 177	M01	235 ± 100	501 ± 13	366 ± 198
P02	180 ± 10	208 ± 19	241 ± 7	M02	81 ± 4	78 ± 3	87 ± 0
P03	111 ± 3	111 ± 14	129 ± 7	M03	25 ± 16	38 ± 10	36 ± 3
P04	128 ± 4	119 ± 5	122 ± 11	M04	62 ± 2	56 ± 3	51 ± 5
P05	163 ± 23	131 ± 7	269 ± 42	M05	96 ± 6	104 ± 3	98 ± 10
P06	82 ± 2	47 ± 17	67 ± 15	M06	31 ± 0	32 ± 5	39 ± 1
P07	95 ± 8	93 ± 6	97 ± 3	M07	225 ± 11	239 ± 28	239 ± 11
P08	132 ± 11	89 ± 13	91 ± 22	M08	148 ± 4	165 ± 14	168 ± 19
P09	71 ± 15	88 ± 2	84 ± 4	M09	37 ± 2	39 ± 2	40 ± 1
P10	101 ± 28	27 ± 21	44 ± 6	M10	44 ± 2	50 ± 0	43 ± 5
P11	63 ± 41	88 ± 1	74 ± 24	M11	49 ± 1	62 ± 4	75 ± 24
P12	227 ± 23	153 ± 18	195 ± 13	M12	65 ± 4	60 ± 1	60 ± 2
P13	97 ± 54	47 ± 21	70 ± 4	M13	75 ± 3	56 ± 4	58 ± 3
P14	226 ± 9	166 ± 44	201 ± 24	M14	40 ± 9	55 ± 1	60 ± 2
P15	233 ± 23	259 ± 42	262 ± 23	M15	51 ± 11	51 ± 3	54 ± 3
P16	230 ± 30	244 ± 9	251 ± 0	M16	105 ± 2	127 ± 2	117 ± 15
P17	236 ± 34	168 ± 31	181 ± 31	M17	200 ± 60	155 ± 59	255 ± 28
P18	384 ± 3	366 ± 46	374 ± 16	M18	51 ± 4	46 ± 10	41 ± 5
P19	380 ± 2	401 ± 76	385 ± 15	M19	116 ± 0	79 ± 28	57 ± 17
P20	137 ± 0	203 ± 115	145 ± 5	M20	90 ± 15	65 ± 7	48 ± 0
P21	705 ± 88	639 ± 101	796 ± 5	M21	65 ± 16	45 ± 6	39 ± 1
P22	995 ± 6	1014 ± 74	990 ± 20	M22	45 ± 1	64 ± 6	44 ± 0
P23	321 ± 42	332 ± 4	373 ± 52	M23	141 ± 6	169 ± 52	86 ± 23
P24	274 ± 200	405 ± 82	395 ± 6	M24	59 ± 1	107 ± 23	66 ± 8
P25	325 ± 264	326 ± 43	364 ± 2	M25	216 ± 39	270 ± 3	271 ± 7
P26	555 ± 220	438 ± 125	471 ± 32	M26	88 ± 4	64 ± 0	67 ± 9
P27	185 ± 76	349 ± 55	300 ± 208	M27	393 ± 136	205 ± 36	138 ± 7
P28	706 ± 39	697 ± 37	678 ± 8	M28	50 ± 18	71 ± 10	44 ± 1
P29	450 ± 16	507 ± 51	496 ± 45	M29	123 ± 9	163 ± 8	175 ± 5
P30	397 ± 128	475 ± 33	430 ± 0	M30	174 ± 27	255 ± 44	303 ± 12
P31	382 ± 150	503 ± 158	482 ± 2	M31	59 ± 11	55 ± 4	85 ± 57
P32	384 ± 129	293 ± 23	287 ± 37	M32	224 ± 9	149 ± 6	183 ± 55
P33	192 ± 13	128 ± 87	158 ± 120	M33	55 ± 4	74 ± 10	86 ± 1

Annexure 5: The average and standard deviation of TDS (mg/L) of samples collected from Palakkad and Malappuram during the Pr, Mo, and Po seasons.

Palakkad district				**Malappuram district**			
Pr		**Mo**	**Po**		**Pr**	**Mo**	**Po**
Sample	**Mean ± SD**	**Mean ± SD**	**Mean ± SD**	**Sample**	**Mean ± SD**	**Mean ± SD**	**Mean ± SD**
P01	669 ± 8	916 ± 190	895 ± 224	M01	170 ± 3	658 ± 13	485 ± 255
P02	186 ± 10	281 ± 23	323 ± 9	M02	82 ± 4	103 ± 4	115 ± 0
P03	112 ± 4	132 ± 41	173 ± 8	M03	33 ± 7	44 ± 16	40 ± 5
P04	133 ± 7	160 ± 7	163 ± 16	M04	62 ± 4	71 ± 5	66 ± 3
P05	166 ± 28	147 ± 10	302 ± 81	M05	97 ± 7	138 ± 5	131 ± 13
P06	83 ± 2	68 ± 30	87 ± 22	M06	29 ± 7	35 ± 9	46 ± 1
P07	99 ± 14	110 ± 27	129 ± 3	M07	230 ± 10	321 ± 37	323 ± 15
P08	134 ± 12	102 ± 4	119 ± 29	M08	151 ± 4	221 ± 20	227 ± 27
P09	90 ± 11	103 ± 21	125 ± 28	M09	36 ± 4	45 ± 2	48 ± 1
P10	101 ± 30	50 ± 0	52 ± 8	M10	42 ± 1	134 ± 103	52 ± 6
P11	60 ± 45	116 ± 1	162 ± 57	M11	49 ± 6	79 ± 6	97 ± 35
P12	238 ± 9	182 ± 9	261 ± 15	M12	64 ± 0	77 ± 2	76 ± 3
P13	98 ± 53	65 ± 19	91 ± 5	M13	76 ± 2	70 ± 6	73 ± 5
P14	229 ± 5	200 ± 91	272 ± 32	M14	38 ± 14	69 ± 0	76 ± 2
P15	238 ± 23	312 ± 101	373 ± 2	M15	118 ± 103	57 ± 3	67 ± 5
P16	235 ± 30	295 ± 57	336 ± 3	M16	107 ± 1	170 ± 4	156 ± 22
P17	240 ± 30	198 ± 3	243 ± 40	M17	206 ± 63	209 ± 81	372 ± 8
P18	388 ± 2	440 ± 129	496 ± 22	M18	50 ± 9	56 ± 14	49 ± 7
P19	382 ± 3	450 ± 209	512 ± 20	M19	118 ± 2	103 ± 40	72 ± 25
P20	139 ± 2	231 ± 96	194 ± 7	M20	158 ± 113	84 ± 10	58 ± 0
P21	704 ± 83	752 ± 239	1479 ± 633	M21	76 ± 0	54 ± 9	45 ± 0
P22	984 ± 39	1153 ± 120	1264 ± 18	M22	44 ± 6	82 ± 9	52 ± 0
P23	326 ± 39	394 ± 70	494 ± 63	M23	145 ± 7	227 ± 70	113 ± 32
P24	379 ± 52	486 ± 173	524 ± 10	M24	59 ± 3	143 ± 31	85 ± 11
P25	335 ± 276	392 ± 115	484 ± 8	M25	220 ± 43	360 ± 8	362 ± 9
P26	560 ± 219	497 ± 44	616 ± 39	M26	73 ± 18	83 ± 1	86 ± 12
P27	190 ± 80	415 ± 143	403 ± 262	M27	397 ± 134	277 ± 49	186 ± 11
P28	710 ± 41	805 ± 182	865 ± 23	M28	48 ± 23	54 ± 0	48 ± 7
P29	453 ± 19	597 ± 27	648 ± 57	M29	126 ± 9	217 ± 11	234 ± 6
P30	401 ± 130	550 ± 65	573 ± 1	M30	178 ± 27	342 ± 56	402 ± 16
P31	385 ± 147	568 ± 70	637 ± 3	M31	58 ± 9	79 ± 19	110 ± 80
P32	387 ± 130	342 ± 42	368 ± 26	M32	226 ± 4	202 ± 5	246 ± 77
P33	198 ± 13	139 ± 76	212 ± 166	M33	55 ± 4	97 ± 14	113 ± 0

Annexure 6: The average and standard deviation of TSS (mg/L) of samples collected from Palakkad and Malappuram during the Pr, Mo, and Po seasons.

Palakkad district				Malappuram district			
Sample	**Pr**	**Mo**	**Po**		**Pr**	**Mo**	**Po**
	Mean ± SD	**Mean ± SD**	**Mean ± SD**	**Sample**	**Mean ± SD**	**Mean ± SD**	**Mean ± SD**
P01	221 ± 277	94.2 ± 62.4	95.4 ± 68.4	M01	80 ± 101.6	181.7 ± 13.2	34.8 ± 28.9
P02	94.2 ± 10.5	29.4 ± 37.3	127.5 ± 90.2	M02	68.2 ± 74.3	257.5 ± 343.2	5.2 ± 0
P03	138.3 ± 102.7	107.8 ± 69.6	57.4 ± 34.2	M03	36.9 ± 6.7	66 ± 58.4	119.8 ± 164.9
P04	77.5 ± 106.3	320.5 ± 162.7	117.2 ± 44.3	M04	184.1 ± 88.9	48.8 ± 61.2	63.9 ± 10.9
P05	44 ± 43.1	22.9 ± 24.3	92.9 ± 67.7	M05	512.9 ± 417	62 ± 23.3	118.5 ± 111.9
P06	48.6 ± 66.7	151.9 ± 115.1	112.7 ± 34.3	M06	11.2 ± 7	54.6 ± 51.3	13.9 ± 1.4
P07	170.8 ± 57.1	90.2 ± 111.5	91.1 ± 59.5	M07	310.1 ± 94.5	39.3 ± 8.4	57.4 ± 13
P08	96.4 ± 82.7	7.9 ± 10	120.8 ± 27.1	M08	88.7 ± 116.7	79.2 ± 19.5	72.7 ± 1.6
P09	72.3 ± 64	47 ± 63.4	94.5 ± 29.1	M09	14 ± 9.7	55 ± 30.5	12.4 ± 0.5
P10	49.1 ± 12.9	39.6 ± 42	77.7 ± 78.9	M10	16.7 ± 3.9	75.8 ± 88.8	37.9 ± 19.7
P11	99.9 ± 124.5	74 ± 43.8	88.3 ± 99.6	M11	41 ± 36.4	10.8 ± 8.2	32.7 ± 36.1
P12	91.6 ± 108.3	47.9 ± 23.1	78.9 ± 99.9	M12	25.7 ± 14.5	113.5 ± 44.2	73.6 ± 73.6
P13	152.3 ± 17.5	15.1 ± 9.6	79 ± 37	M13	4.5 ± 1.8	29.8 ± 22.4	97 ± 75.5
P14	221.4 ± 75.2	169.9 ± 77.3	97.8 ± 74.4	M14	111.8 ± 56.4	10.8 ± 0.4	113.7 ± 101.2
P15	202 ± 175.3	98.4 ± 1.6	86.7 ± 1.6	M15	112.1 ± 80.8	212.5 ± 300.4	33.3 ± 33
P16	205 ± 58	65.4 ± 29.2	173.8 ± 130.2	M16	113.3 ± 140.6	79.7 ± 95.1	113.9 ± 133.7
P17	10.1 ± 12.2	52.4 ± 17.5	376.7 ± 270.8	M17	163.8 ± 218.1	31.5 ± 24	7.5 ± 8.3
P18	321.6 ± 181.8	170.3 ± 86.5	334.1 ± 302.8	M18	80.1 ± 89.8	194.2 ± 254.3	61.5 ± 63.8
P19	108.1 ± 17.1	109.7 ± 152.6	118.4 ± 22.2	M19	82.2 ± 58.1	46.7 ± 58.9	27.9 ± 3
P20	180.6 ± 86.7	99.2 ± 59.7	45.9 ± 49.4	M20	2.1 ± 0.1	76.1 ± 103	41.7 ± 0.2
P21	136.1 ± 111.1	77.8 ± 26.5	701.5 ± 413.7	M21	33.2 ± 40.7	65.8 ± 76.3	25.1 ± 14.5
P22	636.3 ± 293.5	317.5 ± 275.1	136 ± 75	M22	185.6 ± 121.4	68.1 ± 80.2	57.6 ± 14
P23	4.4 ± 3.2	75.7 ± 56.1	325.6 ± 445.7	M23	95.3 ± 78.3	113.1 ± 15.3	77.4 ± 38.5
P24	101.5 ± 137.2	44.1 ± 45.8	115.9 ± 123.2	M24	11.5 ± 16.2	37.5 ± 30.9	75 ± 73.7
P25	44.6 ± 6.9	47.9 ± 58.3	195.5 ± 49	M25	170 ± 84.4	20 ± 20.8	58.5 ± 65.5
P26	159.6 ± 6.9	82.6 ± 97.2	13.6 ± 3.3	M26	87.4 ± 123.5	67.3 ± 71.3	24.2 ± 30
P27	10.1 ± 5.2	95 ± 128.9	87.8 ± 23.1	M27	353.3 ± 389.3	133.4 ± 6.2	64.4 ± 87.5
P28	300.4 ± 111.7	84.7 ± 111.4	290.4 ± 397.3	M28	11.9 ± 5	156.3 ± 14.2	87.5 ± 28.1
P29	366.9 ± 500.2	123.4 ± 168.4	52 ± 55.9	M29	334.4 ± 217.3	192.6 ± 24.7	105.6 ± 119.4
P30	128.9 ± 58.9	310.3 ± 319.5	96.9 ± 97.6	M30	132.3 ± 13.2	37.8 ± 28.6	7.8 ± 1.8
P31	204.9 ± 37	162.3 ± 198.3	152.8 ± 158.8	M31	56.5 ± 55.1	51.2 ± 51.5	30.2 ± 23.1
P32	2.6 ± 2.5	208.3 ± 226.2	42.2 ± 12.1	M32	53.6 ± 60.8	117.7 ± 23.6	63.8 ± 63
P33	205.2 ± 10.2	121 ± 150.5	38.1 ± 9.9	M33	74 ± 104.3	193.2 ± 28.6	127.1 ± 85

Annexure 7: The average and standard deviation of TS (mg/L) of samples collected from Palakkad and Malappuram during the Pr, Mo, and Po seasons.

Palakkad district				Malappuram district			
Sample	**Pr**	**Mo**	**Po**	**Sample**	**Pr**	**Mo**	**Po**
	Mean ± SD	**Mean ± SD**	**Mean ± SD**		**Mean ± SD**	**Mean ± SD**	**Mean ± SD**
P01	890 ± 268.7	1010 ± 127.3	990 ± 155.6	M01	250 ± 99	840 ± 0	520 ± 226.3
P02	280 ± 0	310 ± 14.1	450 ± 99	M02	150 ± 70.7	360 ± 339.4	120 ± 0
P03	250 ± 99	240 ± 28.3	230 ± 42.4	M03	70 ± 14.1	110 ± 42.4	160 ± 169.7
P04	210 ± 99	480 ± 169.7	280 ± 28.3	M04	246 ± 93.3	120 ± 56.6	130 ± 14.1
P05	210 ± 70.7	170 ± 14.1	395 ± 148.5	M05	610 ± 410.1	200 ± 28.3	250 ± 99
P06	130 ± 70.7	220 ± 84.9	200 ± 56.6	M06	40 ± 0	90 ± 42.4	60 ± 0
P07	270 ± 70.7	200 ± 84.9	220 ± 56.6	M07	540 ± 84.9	360 ± 28.3	380 ± 28.3
P08	230 ± 70.7	110 ± 14.1	240 ± 56.6	M08	240 ± 113.1	300 ± 0	300 ± 28.3
P09	162.5 ± 53	150 ± 42.4	220 ± 56.6	M09	50 ± 14.1	100 ± 28.3	60 ± 0
P10	150 ± 42.4	90 ± 42.4	130 ± 70.7	M10	250 ± 268.7	210 ± 14.1	90 ± 14.1
P11	160 ± 169.7	190 ± 42.4	250 ± 42.4	M11	90 ± 42.4	90 ± 14.1	130 ± 70.7
P12	330 ± 99	230 ± 14.1	340 ± 84.9	M12	90 ± 14.1	190 ± 42.4	150 ± 70.7
P13	250 ± 70.7	80 ± 28.3	170 ± 42.4	M13	80 ± 0	100 ± 28.3	170 ± 70.7
P14	450 ± 70.7	370 ± 14.1	370 ± 42.4	M14	150 ± 70.7	80 ± 0	190 ± 99
P15	440 ± 198	410 ± 99	460 ± 0	M15	230 ± 183.8	270 ± 297	100 ± 28.3
P16	440 ± 28.3	360 ± 28.3	510 ± 127.3	M16	220 ± 141.4	250 ± 99	270 ± 155.6
P17	250 ± 42.4	250 ± 14.1	620 ± 311.1	M17	370 ± 155.6	240 ± 56.6	380 ± 0
P18	710 ± 183.8	610 ± 42.4	830 ± 325.3	M18	130 ± 99	250 ± 268.7	110 ± 70.7
P19	490 ± 14.1	560 ± 56.6	630 ± 42.4	M19	200 ± 56.6	150 ± 99	100 ± 28.3
P20	320 ± 84.9	330 ± 155.6	240 ± 56.6	M20	160 ± 113.1	160 ± 113.1	100 ± 0
P21	840 ± 28.3	830 ± 212.1	2180 ± 1046.5	M21	450 ± 523.3	120 ± 84.9	70 ± 14.1
P22	1620 ± 254.6	1470 ± 155.6	1400 ± 56.6	M22	230 ± 127.3	150 ± 70.7	110 ± 14.1
P23	330 ± 42.4	470 ± 14.1	820 ± 509.1	M23	240 ± 84.9	340 ± 84.9	190 ± 70.7
P24	480 ± 84.9	530 ± 127.3	640 ± 113.1	M24	240 ± 226.3	180 ± 0	160 ± 84.9
P25	380 ± 282.8	440 ± 56.6	680 ± 56.6	M25	390 ± 127.3	380 ± 28.3	420 ± 56.6
P26	620 ± 84.9	580 ± 141.4	630 ± 42.4	M26	160 ± 141.4	150 ± 70.7	110 ± 42.4
P27	200 ± 84.9	510 ± 14.1	491 ± 239	M27	750 ± 523.3	410 ± 42.4	250 ± 99
P28	1010 ± 70.7	890 ± 70.7	1155 ± 374.8	M28	60 ± 28.3	210 ± 14.1	330 ± 240.4
P29	820 ± 480.8	720 ± 141.4	700 ± 113.1	M29	460 ± 226.3	410 ± 14.1	340 ± 113.1
P30	530 ± 70.7	860 ± 254.6	670 ± 99	M30	310 ± 14.1	380 ± 84.9	410 ± 14.1
P31	590 ± 183.8	730 ± 268.7	790 ± 155.6	M31	350 ± 268.7	130 ± 70.7	140 ± 56.6
P32	390 ± 127.3	550 ± 183.8	410 ± 14.1	M32	280 ± 56.6	320 ± 28.3	310 ± 14.1
P33	404 ± 22.6	260 ± 226.3	250 ± 155.6	M33	390 ± 268.7	290 ± 42.4	240 ± 84.9

Annexure 8: The average and standard deviation of turbidity (NTU) of samples collected from Palakkad and Malappuram during the Pr, Mo, and Po seasons.

Palakkad district				**Malappuram district**			
Sample	**Pr**	**Mo**	**Po**	**Sample**	**Pr**	**Mo**	**Po**
	Mean ± SD	**Mean ± SD**	**Mean ± SD**		**Mean ± SD**	**Mean ± SD**	**Mean ± SD**
P01	1.85 ± 1.06	5.95 ± 4.74	1.5 ± 0.14	M01	2 ± 2.12	3.64 ± 5.01	0.3 ± 0.14
P02	0.3 ± 0.14	2.4 ± 3.11	0.35 ± 0.07	M02	0.8 ± 0.28	2.77 ± 3.92	0.4 ± 0
P03	8 ± 2.12	15.05 ± 6.58	17.95 ± 12.8	M03	1.15 ± 0.49	2.87 ± 3.06	0.2 ± 0.28
P04	0.2 ± 0	2.15 ± 3.04	0.2 ± 0	M04	1.05 ± 1.34	3.3 ± 2.55	1.2 ± 1.27
P05	0.96 ± 1.2	2.55 ± 3.18	1.55 ± 1.77	M05	1.3 ± 0.99	2.47 ± 3.49	0.35 ± 0.35
P06	0.7 ± 0.57	2.9 ± 4.1	0.75 ± 0.64	M06	0.65 ± 0.49	2.73 ± 3.86	0.85 ± 0.78
P07	1.75 ± 1.2	3.55 ± 2.19	0.55 ± 0.21	M07	0.15 ± 0.21	4.33 ± 6.12	0.4 ± 0.28
P08	7.7 ± 0.71	5.6 ± 2.26	6.1 ± 6.36	M08	3.05 ± 3.32	4.01 ± 5.24	3.25 ± 3.04
P09	0.8 ± 0	2.6 ± 2.83	0.25 ± 0.07	M09	0.8 ± 0.14	2.63 ± 3.58	0.7 ± 0.14
P10	0.2 ± 0.14	2.1 ± 2.97	0.2 ± 0.14	M10	3.15 ± 3.46	2.7 ± 3.82	0.15 ± 0.07
P11	0.85 ± 0.07	2.85 ± 2.76	2.65 ± 1.77	M11	0.9 0.85	8.63 4.91	0.35 0.21
P12	0.45 ± 0.64	1.85 ± 1.2	0.5 ± 0.71	M12	1.3 ± 1.13	2.55 ± 3.61	0.2 ± 0
P13	1.75 ± 1.06	4.25 ± 1.77	1.5 ± 0.85	M13	1.25 ± 1.2	3.11 ± 3.83	0.3 ± 0.14
P14	1.5 ± 2.12	2.2 ± 3.11	0.2 ± 0	M14	3.8 ± 4.38	2.57 ± 3.35	0.1 ± 0
P15	9.8 ± 11.6	1.2 ± 1.7	0.7 ± 0.28	M15	6.05 ± 8.41	6.92 ± 1.53	5.75 ± 6.86
P16	0.55 ± 0.35	1.95 ± 0.21	0.75 ± 0.21	M16	0.3 ± 0.14	2.96 ± 4.04	0.15 ± 0.07
P17	0.9 ± 0.57	2.35 ± 2.9	0.15 ± 0.07	M17	1.2 ± 0.42	8.07 ± 2.17	0.3 ± 0.28
P18	2.7 ± 1.13	2.3 ± 0.57	2.1 ± 1.13	M18	4.65 ± 1.77	2.45 ± 3.46	0.15 ± 0.07
P19	8.4 ± 2.69	14.95 ± 6.58	4.85 ± 0.07	M19	13.6 ± 18.1	3.09 ± 3.37	0.2 ± 0.28
P20	0.15 ± 0.07	2.15 ± 2.9	0.95 ± 0.21	M20	1 ± 0.85	3.05 ± 4.17	0.45 ± 0.49
P21	3.85 ± 4.03	4.65 ± 2.9	0.6 ± 0.57	M21	2.85 ± 3.61	3.12 ± 3	0.25 ± 0.07
P22	2.3 ± 0.85	1.45 ± 0.78	3.05 ± 1.77	M22	0.95 ± 0.78	2.94 ± 3.73	1 ± 0.71
P23	2.25 ± 3.18	1.45 ± 2.05	2.85 ± 2.33	M23	1.05 ± 1.06	3.28 ± 4.5	0.3 ± 0.28
P24	0.1 ± 0.14	2.25 ± 3.18	0.45 ± 0.49	M24	2.1 ± 0.99	3.73 ± 2.87	0.3 ± 0.14
P25	0.25 ± 0.21	1 ± 1.41	0.25 ± 0.07	M25	9 ± 0.14	29.34 ± 31.06	26.9 ± 30.55
P26	0.65 ± 0.35	1.3 ± 1.27	0.55 ± 0.21	M26	3.1 ± 1.27	3.92 ± 2.29	3.05 ± 2.19
P27	1.25 ± 1.06	2.35 ± 0.49	7.5 ± 9.48	M27	2.3 ± 2.55	3.49 ± 3.66	0.6 ± 0
P28	2 ± 0.71	1.3 ± 1.56	0.05 ± 0.07	M28	2.95 ± 3.46	2.9 ± 4.09	1.75 ± 1.06
P29	0.45 ± 0.21	1.15 ± 0.78	0.45 ± 0.21	M29	2.5 ± 2.26	3.15 ± 4.45	0.15 ± 0.07
P30	0.65 ± 0.35	1.15 ± 1.06	0.3 ± 0.14	M30	4.2 ± 3.54	3.76 ± 4.46	12.25 ± 15.77
P31	7.45 ± 9.12	10.95 ± 4.17	7.85 ± 1.2	M31	0.9 ± 0.85	2.4 ± 3.39	0.3 ± 0.14
P32	2.6 ± 1.98	4.05 ± 0.07	1.75 ± 0.49	M32	1.35 ± 1.06	5.09 ± 2.67	0.1 ± 0.14
P33	0.45 ± 0.07	1.8 ± 1.98	1.1 ± 0.28	M33	6.45 ± 2.9	3.7 ± 4.09	26.05 ± 8.56

Annexure 9: The average and standard deviation of TAc. (mg/L) of samples collected in Palakkad and Malappuram during the Pr, Mo, and Po seasons.

Palakkad district				**Malappuram district**			
Sample	**Pr**	**Mo**	**Po**	**Sample**	**Pr**	**Mo**	**Po**
	Mean ± SD	**Mean ± SD**	**Mean ± SD**		**Mean ± SD**	**Mean ± SD**	**Mean ± SD**
P01	7 ± 9.9	12 ± 16.97	14 ± 19.8	M01	31.85 ± 17.18	12 ± 16.97	32 ± 5.66
P02	23.85 ± 5.87	16 ± 0	30 ± 8.49	M02	25.76 ± 8.15	48 ± 0	72 ± 5.66
P03	65.28 ± 41.41	34 ± 2.83	46 ± 19.8	M03	26.79 ± 1.12	46 ± 19.8	62 ± 8.49
P04	102.95 ± 49.43	24 ± 11.31	38 ± 14.14	M04	26.79 ± 1.12	60 ± 16.97	60 ± 22.63
P05	0 ± 0	8 ± 11.31	15 ± 9.9	M05	23.79 ± 5.36	58 ± 2.83	56 ± 16.97
P06	41.73 ± 8.87	26 ± 2.83	56 ± 22.63	M06	7.94 ± 0.08	22 ± 2.83	14 ± 8.49
P07	71.49 ± 6.38	48 ± 11.31	52 ± 33.94	M07	2 ± 2.83	0 ± 0	0 ± 0
P08	13.91 ± 2.96	6 ± 2.83	48 ± 0	M08	17.82 ± 8.23	1 ± 1.41	8 ± 11.31
P09	359 ± 49.5	46 ± 2.83	44 ± 45.25	M09	33.61 ± 24.9	36 ± 16.97	60 ± 5.66
P10	24.76 ± 9.56	80 ± 56.57	112 ± 67.88	M10	11.94 ± 5.74	30 ± 2.83	44 ± 5.66
P11	15.82 ± 11.06	18 ± 8.49	34 ± 25.46	M11	17.85 ± 2.62	32 ± 5.66	52 ± 11.31
P12	11.88 ± 5.49	7 ± 1.41	12 ± 16.97	M12	27.82 ± 5.91	58 ± 14.14	60 ± 11.31
P13	17.94 ± 14.23	5 ± 1.41	16 ± 5.66	M13	21.82 ± 2.57	52 ± 16.97	46 ± 8.49
P14	13.79 ± 19.5	18 ± 14.14	62 ± 53.74	M14	60.34 ± 37.25	56 ± 0	40 ± 5.66
P15	3.94 ± 5.57	0 ± 0	0 ± 0	M15	21.82 ± 2.57	10 ± 14.14	42 ± 2.83
P16	3.94 ± 5.57	7.2 ± 1.13	0 ± 0	M16	55.34 ± 44.32	26 ± 2.83	28 ± 28.28
P17	29.85 ± 14.35	5 ± 4.24	54 ± 2.83	M17	23.76 ± 10.97	28 ± 16.97	82 ± 19.8
P18	7.88 ± 11.14	3 ± 4.24	0 ± 0	M18	61.79 ± 48.38	42 ± 14.14	36 ± 5.66
P19	9.91 ± 2.7	19 ± 15.56	0 ± 0	M19	80.95 ± 80.54	44 ± 5.66	42 ± 8.49
P20	29.82 ± 8.74	30 ± 2.83	100 ± 56.57	M20	51.49 ± 21.91	14 ± 19.8	44 ± 5.66
P21	15.76 ± 22.29	1 ± 1.41	0 ± 0	M21	21.88 ± 8.65	32 ± 11.31	56 ± 5.66
P22	0 ± 0	0 ± 0	0 ± 0	M22	27.76 ± 5.32	56 ± 22.63	38 ± 53.74
P23	7.91 ± 5.53	3 ± 1.41	0 ± 0	M23	22.88 ± 10.07	30 ± 2.83	48 ± 28.28
P24	15.76 ± 22.29	2 ± 2.83	30 ± 31.11	M24	15.82 ± 11.06	34 ± 2.83	64 ± 11.31
P25	0 ± 0	3 ± 4.24	0 ± 0	M25	9.94 ± 2.91	14 ± 19.8	28 ± 5.66
P26	0 ± 0	0 ± 0	0 ± 0	M26	31.76 ± 0.34	66 ± 2.83	62 ± 19.8
P27	27.79 ± 0.3	9 ± 1.41	32 ± 45.25	M27	17.82 ± 8.23	42 ± 8.49	14 ± 2.83
P28	9.85 ± 13.93	10 ± 2.83	0 ± 0	M28	19.85 ± 0.21	18 ± 2.83	22 ± 31.11
P29	3.94 ± 5.57	8 ± 2.83	0 ± 0	M29	6.96 ± 1.48	36 ± 5.66	50 ± 19.8
P30	13.85 ± 8.27	2 ± 2.83	0 ± 0	M30	25.94 ± 25.54	18 ± 25.46	74 ± 2.83
P31	15.76 ± 22.29	17 ± 9.9	30 ± 42.43	M31	14.96 ± 12.79	38 ± 14.14	50 ± 2.83
P32	0 ± 0	0 ± 0	0 ± 0	M32	9.97 ± 8.53	22 ± 2.83	38 ± 8.49
P33	3.94 ± 5.57	4 ± 5.66	22 ± 2.83	M33	13.94 ± 8.57	28 ± 5.66	56 ± 11.31

Annexure 10: The average and standard deviation of TA (mg/L) of samples collected from Palakkad and Malappuram during the Pr, Mo, and Po seasons.

Palakkad district				**Malappuram district**			
Sample	**Pr**	**Mo**	**Po**	**Sample**	**Pr**	**Mo**	**Po**
	Mean ± SD	**Mean ± SD**	**Mean ± SD**		**Mean ± SD**	**Mean ± SD**	**Mean ± SD**
P01	427 ± 103	293 ± 168	604 ± 447	M01	47 ± 27	114 ± 139	250 ± 8
P02	94 ± 48	80 ± 28	120 ± 11	M02	18 ± 3	20 ± 6	40 ± 23
P03	97 ± 33	65 ± 27	122 ± 59	M03	13 ± 10	11 ± 4	30 ± 25
P04	10 ± 3	8 ± 1	16 ± 11	M04	14 ± 3	14 ± 11	22 ± 8
P05	99 ± 58	101 ± 78	72 ± 57	M05	8 ± 11	8 ± 0	30 ± 20
P06	40 ± 0	7 ± 1	36 ± 28	M06	20 ± 0	11 ± 4	48 ± 17
P07	42 ± 8	13 ± 10	52 ± 57	M07	190 ± 8	132 ± 57	320 ± 215
P08	88 ± 23	33 ± 27	94 ± 105	M08	128 ± 6	104 ± 51	194 ± 110
P09	14 ± 3	10 ± 3	14 ± 3	M09	16 ± 6	7 ± 1	18 ± 8
P10	43 ± 21	7 ± 1	14 ± 8	M10	8 ± 0	7 ± 1	8 ± 6
P11	22 ± 25	59 ± 30	84 ± 17	M11	12 ± 0	4 ± 0	20 ± 0
P12	127 ± 81	50 ± 48	224 ± 141	M12	18 ± 8	7 ± 1	20 ± 6
P13	89 ± 1	25 ± 16	70 ± 48	M13	28 ± 0	15 ± 4	42 ± 20
P14	86 ± 59	79 ± 47	184 ± 102	M14	13 ± 1	6 ± 3	6 ± 3
P15	126 ± 20	124 ± 28	204 ± 85	M15	6 ± 8	10 ± 14	40 ± 17
P16	182 ± 14	170 ± 42	356 ± 175	M16	60 ± 34	17 ± 1	44 ± 34
P17	52 ± 11	30 ± 8	74 ± 59	M17	89 ± 27	25 ± 13	162 ± 99
P18	215 ± 35	165 ± 66	324 ± 147	M18	17 ± 4	9 ± 4	18 ± 8
P19	224 ± 28	180 ± 96	342 ± 178	M19	121 ± 75	20 ± 11	44 ± 23
P20	59 ± 13	31 ± 13	62 ± 31	M20	4 ± 6	4 ± 6	22 ± 8
P21	358± 25	182 ± 48	432 ± 204	M21	30 ± 8	8 ± 6	28 ± 11
P22	402 ± 3	240 ± 136	502 ± 206	M22	11 ± 1	12 ± 6	12 ± 11
P23	198 ± 20	142 ± 48	288 ± 124	M23	14 ± 8	30 ± 25	20 ± 0
P24	247 ± 10	210 ± 105	342 ± 178	M24	19 ± 7	15 ± 7	34 ± 8
P25	237 ± 177	140 ± 74	264 ± 124	M25	146 ± 42	151 ± 64	304 ± 124
P26	288 ± 62	221 ± 66	320 ± 6	M26	38 ± 3	18 ± 8	38 ± 31
P27	96 ± 17	106 ± 76	168 ± 40	M27	103 ± 21	11 ± 7	46 ± 14
P28	327 ± 98	249 ± 100	470 ± 150	M28	32 ± 17	14 ± 14	14 ± 14
P29	329 ± 10	158 ± 14	454 ± 190	M29	44 ± 6	41 ± 10	78 ± 42
P30	166 ± 31	231 ± 105	247 ± 89	M30	80 ± 62	133 ± 66	266 ± 122
P31	163 ± 16	147 ± 58	230 ± 93	M31	15 ± 1	4 ± 0	12 ± 6
P32	144 ± 34	107 ± 41	142 ± 8	M32	74 ± 3	41 ± 33	88 ± 45
P33	145 ± 4	46 ± 3	26 ± 8	M33	60 ± 17	34 ± 42	110 ± 65

Annexure 11: The average and standard deviation of TH (mg/L) of samples collected from Palakkad and Malappuram during the Pr, Mo, and Po seasons.

Palakkad district				**Malappuram district**			
Sample	**Pr**	**Mo**	**Po**	**Sample**	**Pr**	**Mo**	**Po**
	Mean ± SD	**Mean ± SD**	**Mean ± SD**		**Mean ± SD**	**Mean ± SD**	**Mean ± SD**
P01	475 ± 273	252 ± 31	252 ± 17	M01	142 ± 76	240 ± 14	175 ± 98
P02	102 ± 93	129 ± 27	169 ± 1	M02	36 ± 51	36 ± 3	39 ± 7
P03	140 ± 85	130 ± 48	87 ± 10	M03	24 ± 34	31 ± 16	20 ± 8
P04	83 ± 47	41 ± 10	48 ± 6	M04	26 ± 37	28 ± 6	18 ± 3
P05	182 ± 76	75 ± 41	152 ± 28	M05	72 ± 102	58 ± 17	45 ± 4
P06	75 ± 35	13 ± 10	31 ± 4	M06	41 ± 4	25 ± 10	30 ± 0
P07	55 ± 21	31 ± 10	39 ± 4	M07	227 ± 126	172 ± 8	66 ± 17
P08	142 ± 76	35 ± 4	56 ± 34	M08	174 ± 144	150 ± 3	143 ± 13
P09	41 ± 16	26 ± 0	25 ± 1	M09	23 ± 18	14 ± 3	15 ± 4
P10	74 ± 8	6 ± 8	16 ± 3	M10	46 ± 48	19 ± 1	16 ± 6
P11	50 ± 25	45 ± 21	62 ± 11	M11	22 ± 31	26 ± 8	27 ± 10
P12	270 ± 144	129 ± 21	177 ± 16	M12	22 ± 31	19 ± 16	24 ± 0
P13	70 ± 65	33 ± 7	49 ± 10	M13	52 ± 74	19 ± 16	34 ± 0
P14	182 ± 133	105 ± 30	135 ± 21	M14	39 ± 13	10 ± 14	15 ± 1
P15	228 ± 136	208 ± 37	210 ± 28	M15	54 ± 31	28 ± 6	27 ± 4
P16	304 ± 113	220 ± 3	232 ± 17	M16	90 ± 42	50 ± 6	47 ± 4
P17	280 ± 141	65 ± 16	91 ± 16	M17	185 ± 134	81 ± 30	146 ± 23
P18	466 ± 246	328 ± 17	288 ± 45	M18	28 ± 40	23 ± 7	16 ± 3
P19	431 ± 199	304 ± 37	294 ± 8	M19	127 ± 69	57 ± 44	28 ± 8
P20	82 ± 88	110 ± 68	65 ± 35	M20	20 ± 28	23 ± 4	24 ± 3
P21	596 ± 396	362 ± 34	438 ± 3	M21	48 ± 23	25 ± 7	16 ± 6
P22	892 ± 458	474 ± 42	500 ± 6	M22	30 ± 20	35 ± 10	20 ± 0
P23	432 ± 255	247 ± 1	264 ± 37	M23	123 ± 81	112 ± 34	48 ± 20
P24	404 ± 175	247 ± 35	257 ± 1	M24	39 ± 13	18 ± 3	14 ± 3
P25	419 ± 267	208 ± 3	213 ± 4	M25	300 ± 181	226 ± 20	202 ± 57
P26	368 ± 91	276 ± 51	283 ± 24	M26	70 ± 37	31 ± 1	30 ± 11
P27	147 ± 13	208 ± 31	171 ± 126	M27	245 ± 100	96 ± 23	61 ± 10
P28	568 ± 288	407 ± 7	357 ± 72	M28	29 ± 10	19 ± 1	18 ± 8
P29	343 ± 239	311 ± 86	304 ± 31	M29	91 ± 47	65 ± 41	99 ± 1
P30	419 ± 75	411 ± 78	363 ± 33	M30	130 ± 71	114 ± 59	182 ± 23
P31	287 ± 10	354 ± 91	298 ± 3	M31	41 ± 16	56 ± 51	9 ± 4
P32	420 ± 136	236 ± 20	219 ± 4	M32	171 ± 52	177 ± 10	85 ± 18
P33	190 ± 127	116 ± 57	130 ± 122	M33	76 ± 107	38 ± 25	53 ± 4

Annexure 12: The average and standard deviation of Ca (mg/L) of samples collected from Palakkad and Malappuram during the Pr, Mo, and Po seasons

Palakkad district				**Malappuram district**			
Sample	**Pr**	**Mo**	**Po**		**Pr**	**Mo**	**Po**
	Mean ± SD	**Mean ± SD**	**Mean ± SD**	**Sample**	**Mean ± SD**	**Mean ± SD**	**Mean ± SD**
P01	75 ± 7	97 ± 10	58 ± 6	M01	12 ± 0	5 ± 7	7 ± 1
P02	79 ± 106	81 ± 24	58 ± 8	M02	20 ± 28	9 ± 4	12 ± 0
P03	69 ± 21	87 ± 33	106 ± 34	M03	20 ± 28	10 ± 8	17 ± 4
P04	43 ± 13	46 ± 23	113 ± 109	M04	29 ± 7	34 ± 6	28 ± 6
P05	101 ± 13	140 ± 99	110 ± 57	M05	17 ± 16	14 ± 3	11 ± 1
P06	33 ± 13	156 ± 20	100 ± 14	M06	124 ± 113	42 ± 14	62 ± 28
P07	27 ± 33	157 ± 10	26 ± 6	M07	10 ± 14	8 ± 0	7 ± 1
P08	37 ± 16	100 ± 42	28 ± 3	M08	51 ± 18	19 ± 10	14 ± 6
P09	15 ± 10	85 ± 7	117 ± 38	M09	89 ± 38	92 ± 8	30 ± 0
P10	48 ± 6	92 ± 20	135 ± 7	M10	99 ± 52	71 ± 10	59 ± 13
P11	18 ± 20	84 ± 28	50 ± 0	M11	6 ± 8	12 ± 0	14 ± 3
P12	101 ± 4	80 ± 14	60 ± 14	M12	40 ± 57	25 ± 1	21 ± 1
P13	36 ± 23	62 ± 37	36 ± 3	M13	17 ± 4	16 ± 8	21 ± 4
P14	65 ± 7	175 ± 21	52 ± 14	M14	8 ± 11	16 ± 8	11 ± 1
P15	124 ± 0	116 ± 8	199 ± 4	M15	12 ± 17	13 ± 1	11 ± 1
P16	106 ± 37	160 ± 82	96 ± 65	M16	10 ± 14	13 ± 16	22 ± 3
P17	125 ± 72	33 ± 4	80 ± 14	M17	69 ± 49	112 ± 40	101 ± 66
P18	103 ± 10	91 ± 18	127 ± 18	M18	13 ± 10	8 ± 3	6 ± 3
P19	114 ± 8	128 ± 37	149 ± 58	M19	8 ± 6	4 ± 0	7 ± 1
P20	25 ± 10	62 ± 0	125 ± 18	M20	20 ± 6	10 ± 3	5 ± 1
P21	99 ± 61	17 ± 10	38 ± 17	M21	6 ± 8	15 ± 4	10 ± 0
P22	123 ± 75	69 ± 1	90 ± 0	M22	16 ± 11	19 ± 1	15 ± 1
P23	100 ± 11	45 ± 30	66 ± 62	M23	80 ± 40	95 ± 33	41 ± 13
P24	123 ± 47	8 ± 8	10 ± 0	M24	17 ± 4	11 ± 4	7 ± 1
P25	79 ± 10	15 ± 1	12 ± 8	M25	31 ± 18	17 ± 1	14 ± 3
P26	92 ± 14	18 ± 3	22 ± 3	M26	217 ± 151	181 ± 41	105 ± 21
P27	90 ± 37	17 ± 1	26 ± 3	M27	60 ± 34	88 ± 37	70 ± 0
P28	117 ± 95	25 ± 1	24 ± 3	M28	16 ± 6	36 ± 31	5 ± 1
P29	65 ± 21	66 ± 6	40 ± 40	M29	44 ± 6	33 ± 33	51 ± 1
P30	109 ± 27	76 ± 8	35 ± 21	M30	115 ± 58	98 ± 20	68 ± 17
P31	103 ± 47	71 ± 13	39 ± 24	M31	38 ± 54	18 ± 11	26 ± 0
P32	139 ± 13	3 ± 4	9 ± 1	M32	159 ± 92	64 ± 17	33 ± 4
P33	66 ± 25	19 ± 4	47 ± 16	M33	12 ± 0	8 ± 0	8 ± 3

Annexure 13: The average and standard deviation of Mg (mg/L) of samples collected from Palakkad and Malappuram during the Pr, Mo, and Po seasons

Palakkad district				Malappuram district			
Sample	**Pr**	**Mo**	**Po**	**Sample**	**Pr**	**Mo**	**Po**
	Mean ± SD	**Mean ± SD**	**Mean ± SD**		**Mean ± SD**	**Mean ± SD**	**Mean ± SD**
P01	400 ± 266	176 ± 40	217 ± 4	M01	73 ± 27	128 ± 54	74 ± 31
P02	23 ± 13	58 ± 40	130 ± 25	M02	26 ± 37	23 ± 18	17 ± 4
P03	71 ± 64	64 ± 42	47 ± 49	M03	16 ± 23	15 ± 7	9 ± 7
P04	40 ± 34	16 ± 8	24 ± 8	M04	14 ± 20	15 ± 4	7 ± 1
P05	81 ± 89	30 ± 11	33 ± 41	M05	32 ± 45	33 ± 16	24 ± 3
P06	42 ± 48	5 ± 1	21 ± 4	M06	24 ± 0	9 ± 1	9 ± 4
P07	28 ± 11	13 ± 13	17 ± 1	M07	138 ± 88	80 ± 0	36 ± 17
P08	105 ± 61	18 ± 3	30 ± 31	M08	75 ± 92	79 ± 7	84 ± 25
P09	26 ± 25	11 ± 1	13 ± 10	M09	15 ± 13	10 ± 3	8 ± 3
P10	26 ± 14	3 ± 4	7 ± 4	M10	33 ± 38	11 ± 1	10 ± 3
P11	32 ± 6	26 ± 17	15 ± 4	M11	16 ± 23	14 ± 8	13 ± 7
P12	169 ± 140	67 ± 21	52 ± 34	M12	2 ± 3	10 ± 11	12 ± 0
P13	34 ± 42	16 ± 3	11 ± 7	M13	32 ± 45	9 ± 7	17 ± 4
P14	117 ± 140	36 ± 31	45 ± 21	M14	27 ± 13	5 ± 7	8 ± 3
P15	104 ± 136	80 ± 0	61 ± 30	M15	37 ± 16	16 ± 6	16 ± 3
P16	198 ± 150	129 ± 21	105 ± 1	M16	61 ± 49	16 ± 0	19 ± 1
P17	155 ± 69	32 ± 11	11 ± 1	M17	61 ± 21	39 ± 16	84 ± 6
P18	363 ± 256	168 ± 65	192 ± 110	M18	18 ± 25	15 ± 7	9 ± 1
P19	317 ± 208	188 ± 45	95 ± 13	M19	76 ± 51	38 ± 34	14 ± 3
P20	57 ± 78	48 ± 31	29 ± 33	M20	14 ± 20	8 ± 0	14 ± 3
P21	497 ± 457	187 ± 13	386 ± 17	M21	29 ± 16	15 ± 10	11 ± 7
P22	769 ± 383	394 ± 57	440 ± 20	M22	14 ± 8	16 ± 8	5 ± 1
P23	332 ± 243	163 ± 30	214 ± 37	M23	43 ± 41	17 ± 1	7 ± 7
P24	281 ± 129	162 ± 42	140 ± 37	M24	22 ± 8	7 ± 1	7 ± 1
P25	340 ± 277	116 ± 17	78 ± 3	M25	83 ± 30	45 ± 21	97 ± 78
P26	276 ± 105	179 ± 41	225 ± 30	M26	39 ± 18	14 ± 3	16 ± 8
P27	57 ± 49	127 ± 55	113 ± 117	M27	86 ± 8	32 ± 6	28 ± 14
P28	451 ± 194	250 ± 3	331 ± 78	M28	17 ± 10	11 ± 1	10 ± 6
P29	278 ± 218	211 ± 44	276 ± 28	M29	47 ± 41	32 ± 8	48 ± 0
P30	310 ± 48	271 ± 21	253 ± 89	M30	70 ± 37	26 ± 23	112 ± 23
P31	184 ± 57	198 ± 71	198 ± 17	M31	25 ± 10	20 ± 20	4 ± 3
P32	281 ± 123	149 ± 13	113 ± 30	M32	56 ± 6	79 ± 10	17 ± 1
P33	124 ± 153	70 ± 34	17 ± 13	M33	38 ± 54	20 ± 14	27 ± 4

Annexure 14: The average and standard deviation of Na (mg/L) of samples collected from Palakkad and Malappuram during the Pr, Mo, and Po seasons

Palakkad district				Malappuram district			
Sample	**Pr**	**Mo**	**Po**	**Sample**	**Pr**	**Mo**	**Po**
	Mean ± SD	**Mean ± SD**	**Mean ± SD**		**Mean ± SD**	**Mean ± SD**	**Mean ± SD**
P01	242.9 ± 7.4	292.1 ± 70.6	357.3 ± 86.5	M01	56.5 ± 0.2	136.4 ± 2.8	112.4 ± 51.
P02	48.1 ± 1.4	61.5 ± 5.9	68 ± 3.8	M02	40.5 ± 1.2	36.5 ± 3.7	42.1 ± 1.1
P03	11.5 ± 0.1	18.9 ± 12.8	23.7 ± 1.1	M03	3.7 ± 0.5	6.3 ± 2.6	6.2 ± 0.7
P04	50.2 ± 0.8	49.1 ± 11	57.1 ± 2.8	M04	21.4 ± 4.9	21.7 ± 1.1	20.7 ± 0.9
P05	19.6 ± 5.6	27.7 ± 6.2	47.1 ± 22.5	M05	17.6 ± 2.8	32.4 ± 6.7	35.9 ± 6.3
P06	17.1 ± 0.6	15.2 ± 7.5	39.5 ± 27.7	M06	10.9 ± 0.8	2.8 ± 2.5	1.4 ± 1
P07	35 ± 0.2	47.8 ± 4.9	45.8 ± 0.8	M07	95.5 ± 0.4	78.2 ± 15.6	141.5 ± 8.5
P08	17.5 ± 6.5	42 ± 4	24.9 ± 11	M08	20.1 ± 0.3	27.1 ± 6.4	26.8 ± 2.1
P09	27.9 ± 10.5	46.1 ± 0.4	45.7 ± 3	M09	5.5 ± 4.3	14.9 ± 5.7	17.1 ± 1.3
P10	33.2 ± 9.1	19.6 ± 4.9	19.9 ± 1.6	M10	5.7 ± 5.8	27.1 ± 4.2	19.9 ± 0.6
P11	9 9.5	23 4.8	25.2 6.8	M11	13.9 ± 1.7	28.1 ± 1.5	21.2 ± 4.6
P12	21.7 ± 0.9	18.7 ± 5.4	26.8 ± 0	M12	24.8 ± 19.6	22.7 ± 7.2	21.2 ± 0.9
P13	20.5 ± 9.2	6.4 ± 0.7	15.9 ± 1	M13	16.2 ± 5.2	14.2 ± 4.6	13.5 ± 1.3
P14	68 ± 0.4	47 ± 14.4	61.4 ± 5.4	M14	4.2 ± 0.1	24.1 ± 4.2	34.2 ± 3
P15	42.5 ± 7.3	45.9 ± 7.4	51.2 ± 1.6	M15	19.2 ± 12.6	17.6 ± 3.4	12.6 ± 0.9
P16	18.5 ± 2	16.1 ± 9.9	25.1 ± 1.3	M16	29.4 ± 1.8	55.2 ± 5.8	49.1 ± 13.8
P17	90.4 ± 13.6	83.7 ± 19.8	73.7 ± 6.4	M17	66.7 ± 26.9	65.8 ± 24.7	92.7 ± 2.1
P18	50.7 ± 3	62 ± 12.3	60.2 ± 9.3	M18	26.4 ± 23.2	13 ± 1.3	9.2 ± 2.1
P19	79.5 ± 1.8	95 ± 20.2	84.9 ± 9.4	M19	13.8 ± 6.2	24.3 ± 2.5	18.8 ± 3.3
P20	24.6 ± 23.3	71.5 ± 41.3	292.5 ± 210	M20	51.8 ± 13	20.9 ± 3.2	31.4 ± 20.2
P21	205.4 ± 27	208.5 ± 41.2	268.8 ± 44.2	M21	90 ± 8.9	7.8 ± 4.6	10.4 ± 0.5
P22	319.8 ± 97.9	348.3 ± 95	193.6 ± 205.7	M22	9.8 ± 0.4	17.4 ± 0	8 ± 0.8
P23	88 ± 7.4	86.5 ± 8.1	102.4 ± 11	M23	46.8 ± 4.2	53.5 ± 15.1	27.1 ± 11
P24	97.7 ± 30.4	120.9 ± 19.3	119.5 ± 2.5	M24	23 ± 0.7	74.2 ± 11.3	41.1 ± 6.4
P25	76.9 ± 74.4	115 ± 18	126.4 ± 10.1	M25	53.9 ± 6	60.4 ± 12.4	64.9 ± 9.6
P26	173.7 ± 157.5	114.6 ± 16.1	154.5 ± 29.6	M26	31.6 ± 2.4	25.3 ± 4	28.5 ± 2.3
P27	52.2 ± 22.7	107 ± 23.7	94.8 ± 50.5	M27	113 ± 11.7	88.5 ± 8.1	58.9 ± 3.9
P28	236.1 ± 10.5	156 ± 81.5	246.5 ± 25.4	M28	23.5 ± 32.2	17.7 ± 7.7	19 ± 3.5
P29	171.5 ± 5.7	174.2 ± 12.5	178 ± 0.6	M29	30.6 ± 12.1	58.5 ± 8.8	62.8 ± 2.1
P30	75.4 ± 26	77 ± 3.9	75.2 ± 1.4	M30	70.8 ± 13.4	89.5 ± 16.6	103.5 ± 6.7
P31	144.6 ± 14.3	126.4 ± 22.8	128.1 ± 2	M31	29.9 ± 9.8	27.3 ± 9	20.3 ± 0.2
P32	80.9 ± 31.5	59.5 ± 5.9	59.3 ± 2.8	M32	99.2 ± 2.8	69.4 ± 5.4	78.8 ± 21.1
P33	29.3 ± 1.1	23.1 ± 4.7	31 ± 9	M33	14.7 ± 5.4	27.4 ± 6.4	20.6 ± 1.8

Annexure 15: The average and standard deviation of K (mg/L) of samples collected from Palakkad and Malappuram during the Pr, Mo, and Po seasons

Palakkad district				Malappuram district			
Sample	**Pr**	**Mo**	**Po**	**Sample**	**Pr**	**Mo**	**Po**
	Mean ± SD	**Mean ± SD**	**Mean ± SD**		**Mean ± SD**	**Mean ± SD**	**Mean ± SD**
P01	38.1 ± 0.85	16.45 ± 9.4	24.6 ± 5.52	M01	11.7 ± 0.14	125.6 ± 11.6	97.3 ± 62.5
P02	8.6 ± 6.65	3.95 ± 1.63	4.1 ± 0.42	M02	14.6 ± 0.42	1.4 ± 1.56	0.9 ± 1.27
P03	11.05 ± 0.35	8.6 ± 0.57	13.4 ± 0.28	M03	7.55 ± 8.7	0.9 ± 0.28	1.35 ± 0.35
P04	11.65 ± 0.49	10.65 ± 2.05	13.9 ± 3.82	M04	14.15 ± 0.21	1.9 ± 0.71	1.4 ± 1.41
P05	9.2 ± 4.24	6.4 ± 1.13	12 ± 0.14	M05	13.7 ± 0	0.75 ± 1.06	1.2 ± 0.57
P06	12.95 ± 0.07	2.9 ± 2.69	13.55 ± 14.1	M06	14.4 ± 0.14	2 ± 0.99	1.4 ± 0.99
P07	12.4 ± 0	6.35 ± 0.49	6.65 ± 0.49	M07	13.3 ± 0.14	1.95 ± 1.2	1.25 ± 0.92
P08	12.6 ± 0.14	5.65 ± 1.48	3.4 ± 0.71	M08	12.65 ± 0.35	3.8 ± 1.13	3.65 ± 0.92
P09	11.1 ± 1.84	5.15 ± 0.07	4.25 ± 0.07	M09	14.25 ± 0.07	2.25 ± 1.34	1.8 ± 1.13
P10	8.9 ± 1.7	1.4 ± 0.99	1.35 ± 0.78	M10	14.2 ± 0.14	1.5 ± 1.41	0.7 ± 0.57
P11	13.2 ± 1.13	5.15 ± 1.34	6.55 ± 2.05	M11	14.15 ± 0.07	0.75 ± 0.07	0.35 ± 0.07
P12	9.25 ± 5.02	2.35 ± 1.34	4.75 ± 0.78	M12	13.05 ± 0.64	3 ± 0.99	2.85 ± 0.64
P13	7.2 ± 5.37	1.3 ± 0.57	2.2 ± 0.99	M13	13.55 ± 0.49	1 ± 1.13	0.75 ± 0.92
P14	12.3 ± 0.57	15.85 ± 10.8	16.35 ± 5.87	M14	12.55 ± 0.92	0.6 ± 0.85	0.6 ± 0.28
P15	10.3 ± 1.98	7.95 ± 0.35	9.9 ± 0.71	M15	12 ± 1.98	3.4 ± 4.81	0.55 ± 0.64
P16	11.9 ± 0.14	6.15 ± 1.06	7.55 ± 0.07	M16	12.5 ± 0	14.9 ± 1.56	12 ± 6.79
P17	15.1 ± 3.82	1.05 ± 0.21	2.3 ± 1.56	M17	13.25 ± 0.92	3.1 ± 0.57	5.25 ± 1.34
P18	9.9 ± 0	14.4 ± 0.57	14.75 ± 1.1	M18	12.3 ± 2.26	2.85 ± 0.07	3.65 ± 2.19
P19	10 ± 0.28	18.35 ± 2.9	16.35 ± 0.64	M19	12.75 ± 1.48	7.2 ± 8.34	10.3 ± 1.27
P20	13.1 ± 0.28	2.15 ± 1.06	18.5 ± 12.59	M20	9.35 ± 1.06	0.9 ± 0.71	5.3 ± 5.94
P21	27.15 ± 21.8	10.65 ± 12.1	9.6 ± 3.82	M21	13.65 ± 2.19	4.4 ± 1.7	4.05 ± 1.06
P22	40.9 ± 27.01	13.35 ± 6.15	13.6 ± 15.6	M22	13.3 ± 0.14	3.15 ± 0.78	0.75 ± 0.21
P23	13.55 ± 0.07	0.85 ± 0.21	0.6 ± 0.85	M23	10.65 ± 0.35	13.1 ± 4.81	5.3 ± 1.41
P24	11.15 ± 0.49	11.55 ± 1.06	10.95 ± 0.78	M24	7.4 ± 8.63	0.9 ± 0.28	0.85 ± 0.92
P25	16.5 ± 5.37	20.6 ± 13.86	19.9 ± 4.81	M25	12.9 ± 0	4.4 ± 2.12	4.6 ± 1.13
P26	14.25 ± 5.02	46.25 ± 10.7	51.9 ± 2.97	M26	12.55 ± 1.63	2.85 ± 1.34	3.65 ± 1.77
P27	9.35 ± 1.34	42.05 ± 16.6	24.2 ± 13.3	M27	4.9 ± 4.67	14.75 ± 0.35	10.9 ± 0.57
P28	25.75 ± 21.7	2.85 ± 2.33	12 ± 1.41	M28	12.75 ± 1.34	2.15 ± 1.48	6.19 ± 8.51
P29	11.65 ± 0.21	2.7 ± 3.82	8.3 ± 1.56	M29	12.4 ± 0.28	7.05 ± 1.34	7.2 ± 1.56
P30	10.85 ± 0.21	11.15 ± 0.07	10.8 ± 1.27	M30	12.3 ± 0.14	19.35 ± 2.47	9.6 ± 3.68
P31	11.3 ± 0.57	12.3 ± 0.57	11.35 ± 0.1	M31	12.15 ± 0.35	1.65 ± 2.33	1.55 ± 0.78
P32	12.7 ± 0.28	3.9 ± 0.85	5.6 ± 2.26	M32	8.3 ± 0.42	9.1 ± 2.97	16.9 ± 9.19
P33	12.5 ± 0.28	3.4 ± 1.56	2.9 ± 3.82	M33	12 ± 0.28	3.7 ± 3.96	5.9 ± 0.85

Annexure 16: The average and standard deviation of Cl (mg/L) of samples collected from Palakkad and Malappuram during the Pr, Mo, and Po seasons

Palakkad district				Malappuram district			
Sample	**Pr**	**Mo**	**Po**	**Sample**	**Pr**	**Mo**	**Po**
	Mean ± SD	**Mean ± SD**	**Mean ± SD**		**Mean ± SD**	**Mean ± SD**	**Mean ± SD**
P01	108.6 ± 31.9	161.7 ± 1.1	133 ± 41	M01	82.5 ± 58.8	131.2 ± 37.1	77 ± 43.8
P02	36.8 ± 23.1	46.2 ± 5.3	42 ± 2.8	M02	31.8 ± 10.2	18.7 ± 8.8	25 ± 1.4
P03	30.6 ± 3.1	24 ± 8.5	26 ± 2.8	M03	11.5 ± 1.2	10 ± 0	11 ± 1.4
P04	72.9 ± 12.8	59 ± 8.5	47 ± 7.1	M04	20.6 ± 6	20.7 ± 2.5	19 ± 1.4
P05	124.2 ± 50.3	60.7 ± 2.5	100 ± 8.5	M05	26.2 ± 8.1	40 ± 7.1	31 ± 1.4
P06	33.8 ± 7.3	21.5 ± 12	30 ± 5.7	M06	7.4 ± 4.6	7.7 ± 0.4	7 ± 1.4
P07	32.6 ± 6	37.4 ± 1.9	33 ± 1.4	M07	18.6 ± 8.9	23 ± 4.2	10 ± 0
P08	28.8 ± 5.6	33.2 ± 13.1	36 ± 8.5	M08	3.8 ± 0.4	6.5 ± 2.1	11 ± 1.4
P09	53.8 ± 10.9	43.7 ± 5.3	40 ± 0	M09	13 ± 6.7	20.2 ± 3.2	17 ± 1.4
P10	24.4 ± 5.6	20 ± 0	18 ± 5.7	M10	15 ± 3.8	21 ± 1.4	18.5 ± 3.5
P11	15 ± 3.8	17.5 ± 3.5	15 ± 1.4	M11	22.7 ± 3.1	25.2 ± 3.2	20 ± 0
P12	16.8 ± 6.3	20.7 ± 2.5	19 ± 1.4	M12	22.7 ± 3.1	16.7 ± 8.1	22 ± 0
P13	46.2 ± 24.8	17 ± 4.2	14 ± 0	M13	22.4 ± 8.5	16.2 ± 1.8	18 ± 0
P14	51.2 ± 2.8	37.5 ± 10.6	44 ± 8.5	M14	19.4 7.4	25.2 3.2	21 1.4
P15	69.3 ± 17.8	63.5 ± 2.1	55 ± 4.2	M15	27.6 ± 19	16.2 ± 8.8	34 ± 25.4
P16	26.8 ± 2.7	21.7 ± 1.1	23 ± 1.4	M16	28.2 ± 5.2	50 ± 7.1	37 ± 12.7
P17	92.8 ± 44.3	81 ± 33.9	45 ± 32.5	M17	62.4 ± 7.1	64.2 ± 4.6	68 ± 2.8
P18	93.2 ± 1.5	95.2 ± 3.2	81 ± 15.6	M18	20.6 ± 6	19.5 ± 7.8	18 ± 2.8
P19	88.3 ± 20.5	109.2 ± 2.5	91 ± 4.2	M19	24.4 ± 5.6	22.5 ± 10.6	19 ± 1.4
P20	56.8 ± 4.9	78.2 ± 41.4	60 ± 2.8	M20	40.5 ± 12.2	37 ± 11.3	26 ± 11.3
P21	262 ± 5.4	254.2 ± 2.5	290.9 ± 7.1	M21	17.1 ± 0.9	15 ± 0	10 ± 0
P22	250.6 ± 6.6	287.7 ± 98.6	235.9 ± 22.6	M22	20.3 ± 11.4	20.5 ± 6.4	16 ± 2.8
P23	70.9 ± 25	91.7 ± 22.3	90 ± 28.3	M23	37.7 ± 6.9	42.2 ± 14.5	12 ± 11.3
P24	61.9 ± 52.8	92.7 ± 14.5	76 ± 2.8	M24	34.4 ± 3.5	64.2 ± 25.8	29 ± 4.2
P25	150.8 ± 12.7	67.5 ± 10.6	50 ± 19.8	M25	50.1 ± 24.4	45 ± 0	38 ± 8.5
P26	100.3 ± 8.6	47.5 ± 31.8	39 ± 1.4	M26	47 ± 26.3	26.5 ± 4.9	23 ± 4.2
P27	41.2 ± 11.9	122.7 ± 13.8	89 ± 83.4	M27	90.6 ± 12.2	82.2 ± 21.6	47 ± 1.4
P28	399.8 ± 136.5	187.2 ± 42.8	142 ± 5.7	M28	9.4 ± 1.7	23.7 ± 1.8	12 ± 5.7
P29	45.6 ± 0.7	82 ± 25.4	103 ± 63.6	M29	26.5 ± 2.7	47.5 ± 3.5	44 ± 5.7
P30	41.5 ± 6.5	44.7 ± 3.9	31 ± 12.7	M30	34.1 ± 1.9	34.5 ± 7.8	45 ± 12.7
P31	122.9 ± 86.9	309.9 ± 21.1	182.9 ± 1.4	M31	18.8 ± 3.4	26.2 ± 1.8	35 ± 12.7
P32	43 ± 14.4	42.7 ± 6.7	43 ± 9.9	M32	58.8 ± 2	34 ± 1.4	48 ± 19.8
P33	20.6 ± 6	21 ± 12.7	15 ± 4.2	M33	31.4 ± 19.3	21 ± 12.7	11 ± 4.2

Annexure 17: The average and standard deviation of SO_4 (mg/L) of samples collected from Palakkad and Malappuram during the Pr, Mo, and Po seasons

Palakkad district				Malappuram district			
Sample	Pr	Mo	Po	Sample	Pr	Mo	Po
	Mean ± SD	Mean ± SD	Mean ± SD		Mean ± SD	Mean ± SD	Mean ± SD
P01	1.11 ± 1.29	0.53 ± 0.24	0.28 ± 0.08	M01	2.88 ± 1.1	2.93 ± 0.55	3.64 ± 0.29
P02	3.47 ± 0.59	4.75 ± 0.04	6.65 ± 0.41	M02	2.28 ± 0.21	2.66 ± 0.07	2.51 ± 0.03
P03	0.3 ± 0.11	0.35 ± 0.5	0.28 ± 0.17	M03	2.18 ± 0.16	0.53 ± 0.12	0.81 ± 0.12
P04	5.54 ± 0.35	5.42 ± 0.53	6.46 ± 0.08	M04	3.48 ± 0.28	5.31 ± 0.6	4.74 ± 1.37
P05	0.2 ± 0.21	1.51 ± 0.04	0.89 ± 0.92	M05	0.9 ± 0.14	3.1 ± 3.19	0.58 ± 0.06
P06	0.95 ± 0.41	0.96 ± 0.16	1.42 ± 0.35	M06	5.06 ± 0.15	1.46 ± 1.24	4.96 ± 0.68
P07	2.83 ± 0.64	4.07 ± 0.65	4.38 ± 0.2	M07	1.09 ± 0.28	1.7 ± 0.58	1.16 ± 0.14
P08	0.8 ± 0.42	2.21 ± 0.12	1.24 ± 1.04	M08	2.56 ± 0.11	1.62 ± 0.52	1.48 ± 0.38
P09	3.17 ± 1.6	4.19 ± 0.13	2.77 ± 0.65	M09	0.07 ± 0	0.26 ± 0.28	0.22 ± 0.17
P10	0.49 ± 0.22	0.81 ± 0.23	0.74 ± 0.13	M10	0.19 ± 0.02	0.24 ± 0.07	1.7 ± 1.79
P11	0.54 ± 0.44	0.44 ± 0.29	0.42 ± 0.12	M11	1.83 ± 0.27	3.89 ± 0.55	2.52 ± 1.78
P12	0.11 ± 0.02	0.88 ± 0.14	0.2 ± 0.08	M12	6.46 ± 0.32	6.77 ± 0.21	6.56 ± 0.94
P13	5.21 ± 0.92	7.5 ± 0	6.2 ± 0.28	M13	0.23 ± 0	0.39 ± 0.11	0.44 ± 0.14
P14	3.08 ± 0.11	1.17 ± 0.71	2.25 ± 0.66	M14	0.65 ± 0	0.59 ± 0.22	1.85 ± 1.9
P15	0.1 ± 0.1	2.09 ± 2.7	0.15 ± 0.08	M15	2.63 ± 0.18	3.09 ± 0.2	1.64 ± 2.31
P16	0.07 ± 0.02	0.09 ± 0	0.05 ± 0.01	M16	2.98 ± 0.44	3.42 ± 0.36	3.8 ± 1.46
P17	6.74 ± 0	3.99 ± 0.05	7.65 ± 2.25	M17	2.58 ± 0.03	7.16 ± 1.56	3.63 ± 1.53
P18	0.21 ± 0.02	0.29 ± 0.05	0.08 ± 0.12	M18	1.93 ± 0.19	1.92 ± 0.48	2.36 ± 0.6
P19	0.12 ± 0.16	0.17 ± 0.03	0.31 ± 0.08	M19	0.18 ± 0.01	0.9 ± 0.95	0.17 ± 0.07
P20	0.84 ± 0.03	4.77 ± 5.71	0.9 ± 0.2	M20	5.45 ± 0.79	2.28 ± 0.15	1.76 ± 0.29
P21	0.51 ± 0.14	1.74 ± 1.71	0.25 ± 0.01	M21	5.7 ± 0.39	6.4 ± 0.07	5.31 ± 0.02
P22	0.25 ± 0.06	0.5 ± 0.41	0.34 ± 0	M22	0.74 ± 0.14	0.65 ± 0.19	0.62 ± 0.1
P23	0.8 ± 0.38	1.57 ± 0.27	1.22 ± 0.5	M23	7.66 ± 0.02	5.95 ± 3.33	1.82 ± 0.08
P24	1.24 ± 0.01	2.5 ± 1.94	2.32 ± 0.29	M24	0.55 ± 0.38	0.28 ± 0.14	0.12 ± 0.03
P25	1.98 ± 0.31	4.02 ± 2.98	5.83 ± 2.39	M25	0.73 ± 0.11	0.66 ± 0.02	0.87 ± 0.03
P26	0.19 ± 0.02	0.75 ± 0.14	0.26 ± 0.12	M26	2.36 ± 0.28	2.83 ± 0.03	1.28 ± 0.84
P27	0.4 ± 0.31	1.36 ± 0.76	0.37 ± 0.21	M27	0.77 ± 0.07	0.21 ± 0.05	1.02 ± 0.75
P28	3.28 ± 0.11	2.33 ± 0.3	3.35 ± 0.38	M28	3.04 ± 0.57	1.71 ± 0.11	1.34 ± 0.53
P29	0.13 ± 0.01	0.47 ± 0.47	0.65 ± 0.38	M29	4.95 ± 0.21	5.57 ± 0.42	6.87 ± 1.6
P30	0.13 ± 0.12	0.07 ± 0.03	0.04 ± 0.01	M30	2.43 ± 3.34	4.07 ± 0.51	5.36 ± 0.41
P31	0.53 ± 0.16	0.46 ± 0.18	0.35 ± 0.07	M31	0.24 ± 0.25	0.26 ± 0.24	0.45 ± 0.41
P32	0.38 ± 0.14	0.19 ± 0.19	0.23 ± 0.15	M32	2.38 ± 1.22	5.39 ± 0.57	6.96 ± 1.5
P33	0.13 ± 0.05	0.2 ± 0.16	0.1 ± 0.11	M33	1.16 ± 0.29	2.84 ± 0.22	1.67 ± 2.22

Annexure 18: The average and standard deviation of NO_3 (mg/L) of samples collected from Palakkad and Malappuram during the Pr, Mo, and Po seasons.

Palakkad district				Malappuram district			
Sample	**Pr**	**Mo**	**Po**	**Sample**	**Pr**	**Mo**	**Po**
	Mean ± SD	**Mean ± SD**	**Mean ± SD**		**Mean ± SD**	**Mean ± SD**	**Mean ± SD**
P01	1.11 ± 1.29	0.53 ± 0.24	0.28 ± 0.08	M01	2.58 ± 0.03	7.16 ± 1.56	3.63 ± 1.53
P02	3.47 ± 0.59	4.75 ± 0.04	6.65 ± 0.41	M02	2.98 ± 0.44	3.42 ± 0.36	3.8 ± 1.46
P03	0.3 ± 0.11	0.35 ± 0.5	0.28 ± 0.17	M03	0.65 ± 0	0.59 ± 0.22	1.85 ± 1.9
P04	5.54 ± 0.35	5.42 ± 0.53	6.46 ± 0.08	M04	2.63 ± 0.18	3.09 ± 0.2	1.64 ± 2.31
P05	0.2 ± 0.21	1.51 ± 0.04	0.89 ± 0.92	M05	6.46 ± 0.32	6.77 ± 0.21	6.56 ± 0.94
P06	0.95 ± 0.41	0.96 ± 0.16	1.42 ± 0.35	M06	0.23 ± 0	0.39 ± 0.11	0.44 ± 0.14
P07	2.83 ± 0.64	4.07 ± 0.65	4.38 ± 0.2	M07	0.07 ± 0	0.26 ± 0.28	0.22 ± 0.17
P08	0.8 ± 0.42	2.21 ± 0.12	1.24 ± 1.04	M08	0.19 ± 0.02	0.24 ± 0.07	1.7 ± 1.79
P09	3.17 ± 1.6	4.19 ± 0.13	2.77 ± 0.65	M09	0.18 ± 0.01	0.9 ± 0.95	0.17 ± 0.07
P10	0.49 ± 0.22	0.81 ± 0.23	0.74 ± 0.13	M10	1.93 ± 0.19	1.92 ± 0.48	2.36 ± 0.6
P11	0.54 0.44	0.44 0.29	0.42 0.12	M11	1.83 ± 0.27	3.89 ± 0.55	2.52 ± 1.78
P12	0.11 ± 0.02	0.88 ± 0.14	0.2 ± 0.08	M12	2.28 ± 0.21	2.66 ± 0.07	2.51 ± 0.03
P13	5.21 ± 0.92	7.5 ± 0	6.2 ± 0.28	M13	2.18 ± 0.16	0.53 ± 0.12	0.81 ± 0.12
P14	3.08 ± 0.11	1.17 ± 0.71	2.25 ± 0.66	M14	2.88 ± 1.1	2.93 ± 0.55	3.64 ± 0.29
P15	0.1 ± 0.1	2.09 ± 2.7	0.15 ± 0.08	M15	0.9 ± 0.14	3.1 ± 3.19	0.58 ± 0.06
P16	0.07 ± 0.02	0.09 ± 0	0.05 ± 0.01	M16	3.48 ± 0.28	5.31 ± 0.6	4.74 ± 1.37
P17	6.74 ± 0	3.99 ± 0.05	7.65 ± 2.25	M17	5.06 ± 0.15	1.46 ± 1.24	4.96 ± 0.68
P18	0.21 ± 0.02	0.29 ± 0.05	0.08 ± 0.12	M18	1.09 ± 0.28	1.7 ± 0.58	1.16 ± 0.14
P19	0.12 ± 0.16	0.17 ± 0.03	0.31 ± 0.08	M19	2.56 ± 0.11	1.62 ± 0.52	1.48 ± 0.38
P20	0.84 ± 0.03	4.77 ± 5.71	0.9 ± 0.2	M20	5.7 ± 0.39	6.4 ± 0.07	5.31 ± 0.02
P21	0.51 ± 0.14	1.74 ± 1.71	0.25 ± 0.01	M21	5.45 ± 0.79	2.28 ± 0.15	1.76 ± 0.29
P22	0.25 ± 0.06	0.5 ± 0.41	0.34 ± 0	M22	0.74 ± 0.14	0.65 ± 0.19	0.62 ± 0.1
P23	0.8 ± 0.38	1.57 ± 0.27	1.22 ± 0.5	M23	7.66 ± 0.02	5.95 ± 3.33	1.82 ± 0.08
P24	1.24 ± 0.01	2.5 ± 1.94	2.32 ± 0.29	M24	0.55 ± 0.38	0.28 ± 0.14	0.12 ± 0.03
P25	1.98 ± 0.31	4.02 ± 2.98	5.83 ± 2.39	M25	2.36 ± 0.28	2.83 ± 0.03	1.28 ± 0.84
P26	0.19 ± 0.02	0.75 ± 0.14	0.26 ± 0.12	M26	0.73 ± 0.11	0.66 ± 0.02	0.87 ± 0.03
P27	0.4 ± 0.31	1.36 ± 0.76	0.37 ± 0.21	M27	2.38 ± 1.22	5.39 ± 0.57	6.96 ± 1.5
P28	3.28 ± 0.11	2.33 ± 0.3	3.35 ± 0.38	M28	1.16 ± 0.29	2.84 ± 0.22	1.67 ± 2.22
P29	0.13 ± 0.01	0.47 ± 0.47	0.65 ± 0.38	M29	4.95 ± 0.21	5.57 ± 0.42	6.87 ± 1.6
P30	0.13 ± 0.12	0.07 ± 0.03	0.04 ± 0.01	M30	0.77 ± 0.07	0.21 ± 0.05	1.02 ± 0.75
P31	0.53 ± 0.16	0.46 ± 0.18	0.35 ± 0.07	M31	3.04 ± 0.57	1.71 ± 0.11	1.34 ± 0.53
P32	0.38 ± 0.14	0.19 ± 0.19	0.23 ± 0.15	M32	2.43 ± 3.34	4.07 ± 0.51	5.36 ± 0.41
P33	0.13 ± 0.05	0.2 ± 0.16	0.1 ± 0.11	M33	0.24 ± 0.25	0.26 ± 0.24	0.45 ± 0.41

Annexure 19: The average and standard deviation of PO_4 (mg/L) of samples collected from Palakkad and Malappuram during the Pr, Mo, and Po seasons.

Palakkad district				Malappuram district			
Sample	**Pr**	**Mo**	**Po**	**Sample**	**Pr**	**Mo**	**Po**
	Mean ± SD	**Mean ± SD**	**Mean ± SD**		**Mean ± SD**	**Mean ± SD**	**Mean ± SD**
P01	0.08 ± 0.02	0 ± 0.01	0.05 ± 0.02	M01	0.08 ± 0.01	0.05 ± 0.05	0.1 ± 0.05
P02	0.15 ± 0.07	0.39 ± 0.54	0.09 ± 0.04	M02	0.07 ± 0.01	0.02 ± 0.02	0.02 ± 0.01
P03	0.07 ± 0.02	0.03 ± 0.03	0.04 ± 0.02	M03	0.07 ± 0.02	0.02 ± 0.02	0.03 ± 0.01
P04	0.09 ± 0.04	0 ± 0	0.02 ± 0.02	M04	0.06 ± 0.02	0.01 ± 0.01	0.04 ± 0.01
P05	0.07 ± 0.01	0.02 ± 0.02	0.04 ± 0.02	M05	0.05 ± 0.01	0.01 ± 0	0.06 ± 0
P06	0.13 ± 0.06	0 ± 0	0.03 ± 0.04	M06	0.05 ± 0	0 ± 0	0.04 ± 0.02
P07	0.05 ± 0.05	0 ± 0	0.08 ± 0.06	M07	0.08 ± 0.03	0 ± 0.01	0.05 ± 0.02
P08	0.06 ± 0.03	0 ± 0	0.03 ± 0	M08	0.05 ± 0.08	0.02 ± 0.02	0.06 ± 0.01
P09	0.05 ± 0.02	0.01 ± 0.01	0.03 ± 0.01	M09	0.06 ± 0.01	0 ± 0	0.03 ± 0
P10	0.05 ± 0	0 ± 0	0.03 ± 0.01	M10	0.05 ± 0	0.01 ± 0	0.03 ± 0.01
P11	0.13 ± 0.05	0.02 ± 0.01	0.14 ± 0.02	M11	0.04 ± 0.05	0.04 ± 0.02	0.03 ± 0
P12	0.06 ± 0.01	0.02 ± 0.01	0.04 ± 0.01	M12	0.08 ± 0.05	0.03 ± 0.03	0.03 ± 0
P13	0.16 ± 0.15	0.02 ± 0.03	0.03 ± 0.01	M13	0.09 ± 0	0 ± 0	0.03 ± 0.01
P14	0.1 ± 0.01	0.03 ± 0.03	0.1 ± 0	M14	0.22 ± 0.24	0.03 ± 0.04	0.02 ± 0
P15	0.07 ± 0.05	0.02 ± 0.02	0.06 ± 0	M15	0.09 ± 0.03	0 ± 0	0.02 ± 0.01
P16	0.06 ± 0.01	0.02 ± 0.02	0.05 ± 0.02	M16	0.06 ± 0.02	0.01 ± 0.02	0.04 ± 0
P17	0.06 ± 0	0.01 ± 0.01	0.02 ± 0.02	M17	0.2 ± 0.15	0 ± 0	0.04 ± 0.01
P18	0.06 ± 0.01	0.01 ± 0.01	0.03 ± 0.01	M18	0.19 ± 0.02	0.01 ± 0	0.08 ± 0.04
P19	0.13 ± 0.07	0.07 ± 0.09	0.05 ± 0.01	M19	0.08 ± 0.01	0.01 ± 0	0.03 ± 0.01
P20	0.1 ± 0.02	0.04 ± 0.05	0.07 ± 0.02	M20	0.05 ± 0.01	0.05 ± 0.06	0.03 ± 0.01
P21	0.25 ± 0.11	0.01 ± 0	0.2 ± 0.02	M21	0.14 ± 0.03	0.04 ± 0.05	0.04 ± 0
P22	0.04 ± 0	0.05 ± 0.06	0.05 ± 0.01	M22	0.06 ± 0.01	0.07 ± 0.08	0.03 ± 0
P23	0.08 ± 0.01	0.06 ± 0.06	0.06 ± 0.02	M23	0.05 ± 0.01	0.08 ± 0.11	0.06 ± 0.03
P24	0.06 ± 0.01	0.06 ± 0.07	0.1 ± 0.07	M24	0.03 ± 0	0.13 ± 0.15	0.03 ± 0
P25	0.08 ± 0.03	0.1 ± 0.12	0.05 ± 0.04	M25	0.05 ± 0.01	0.14 ± 0.19	0.07 ± 0.01
P26	0.07 ± 0.05	0.06 ± 0.07	0.07 ± 0	M26	0.08 ± 0.01	0.03 ± 0.04	0.09 ± 0.01
P27	0.22 ± 0.16	0.16 ± 0.18	0.37 ± 0.06	M27	0.07 ± 0.01	0.06 ± 0.08	0.03 ± 0
P28	0.05 ± 0	0.05 ± 0.06	0.04 ± 0.01	M28	0.16 ± 0.13	0.05 ± 0.06	0.83 ± 1.04
P29	0.06 ± 0.02	0.05 ± 0.06	0.05 ± 0.03	M29	0.07 ± 0	0.06 ± 0.08	0.03 ± 0
P30	0.03 ± 0.01	0.01 ± 0.01	0.05 ± 0.01	M30	0.2 ± 0.08	0.07 ± 0.09	0.17 ± 0.09
P31	0.08 ± 0.04	0.06 ± 0.08	0.07 ± 0.01	M31	0.37 ± 0.41	0.1 ± 0.14	0.04 ± 0
P32	0.07 ± 0	0.01 ± 0.01	0.06 ± 0.01	M32	0.17 ± 0.01	0.05 ± 0.04	0.11 ± 0.15
P33	0.05 ± 0.01	0.03 ± 0.03	0.05 ± 0.03	M33	0.21 ± 0.07	0.04 ± 0.01	0.31 ± 0.09

Annexure 20: The average and standard deviation of DO (mg/L) of samples collected from Palakkad and Malappuram during the Pr, Mo, and Po seasons.

Palakkad district				Malappuram district			
Sample	Pr	Mo	Po	Sample	Pr	Mo	Po
	Mean ± SD	Mean ± SD	Mean ± SD		Mean ± SD	Mean ± SD	Mean ± SD
P01	1.62 ± 0	2.84 ± 2.3	3.03 ± 2.01	M01	3.65 ± 2.87	6.08 ± 0	3.24 ± 1.15
P02	2.63 ± 0.86	2.64 ± 3.15	1.23 ± 0.59	M02	2.43 ± 0	4.05 ± 0	3.65 ± 0
P03	1.42 ± 1.43	4.06 ± 1.14	0.81 ± 0	M03	4.05 ± 3.44	2.84 ± 0	4.87 ± 1.15
P04	4.86 ± 0.58	3.24 ± 2.29	2.84 ± 0.57	M04	2.63 ± 0.86	1.62 ± 0	2.64 ± 2.01
P05	1.22 ± 0.57	3.04 ± 2	4.38 ± 1.31	M05	4.86 ± 2.86	4.05 ± 0	2.43 ± 0
P06	7 ± 5.31	4.05 ± 0	4.87 ± 1.15	M06	5.47 ± 0.28	8.1 ± 0	4.06 ± 2.3
P07	3.45 ± 2.01	3.65 ± 1.72	2.03 ± 1.72	M07	2.46 ± 1.1	3.24 ± 0	1.42 ± 0.86
P08	1.62 ± 1.15	3.24 ± 2.29	1.72 ± 0.15	M08	1.22 ± 0.57	1.22 ± 0	1.22 ± 0
P09	4.02 ± 2.24	3.45 ± 2.01	1.93 ± 0.72	M09	3.45 ± 0.28	4.46 ± 0	2.84 ± 1.15
P10	5.64 ± 0.62	1.62 ± 0	4.16 ± 1	M10	3.04 ± 2	4.05 ± 0.01	4.86 ± 2.29
P11	2.6 ± 3.11	0.61 ± 0.29	1.22 ± 0	M11	5.88 ± 1.44	2.43 ± 0	3.04 ± 0.28
P12	2.64 ± 0.86	4.26 ± 1.43	1.82 ± 0.86	M12	2.23 ± 0.29	3.24 ± 0	1.62 ± 1.15
P13	5.88 ± 0.86	4.26 ± 0.86	4.26 ± 1.44	M13	5.07 ± 0.29	3.24 ± 0	4.66 ± 3.15
P14	6.89 ± 4.01	3.65 ± 1.14	3.86 ± 0.29	M14	2.25 ± 0.89	4.87 ± 0	3.24 ± 1.14
P15	1.22 ± 0.57	4.86 ± 4.01	2.43 ± 1.72	M15	3.47 ± 0.25	6.48 ± 0	4.05 ± 0.57
P16	3.24 ± 2.29	3.04 ± 2.01	3.85 ± 3.73	M16	6.93 ± 0.5	4.87 ± 0	4.86 ± 2.29
P17	5.68 ± 3.43	6.89 ± 4.59	3.85 ± 0.29	M17	6.48 ± 1.14	3.65 ± 0	0.81 ± 0.57
P18	3.24 ± 2.29	0.81 ± 0	2.23 ± 2.01	M18	1.82 ± 0.86	2.03 ± 0	4.46 ± 1.72
P19	1.01 ± 0.29	1.22 ± 1.15	2.44 ± 2.3	M19	3.27 ± 0.04	3.65 ± 0	4.06 ± 0.57
P20	4.73 ± 1.52	3.85 ± 0.29	3.65 ± 1.72	M20	5.45 ± 0.83	6.04 ± 0	4.28 ± 1.4
P21	2.64 ± 2.01	4.46 ± 1.73	4.06 ± 2.3	M21	2.03 ± 1.72	0.82 ± 0	1.01 ± 0.29
P22	1.62 ± 1.15	0.61 ± 0.29	1.62 ± 1.15	M22	4.75 ± 0.41	2.43 ± 0	3.34 ± 1.02
P23	3.24 ± 0	5.68 ± 0	2.64 ± 0.29	M23	2.43 ± 1.15	5.27 ± 0	4.48 ± 1.18
P24	2.23 ± 1.44	2.23 ± 2.58	1.22 ± 0.57	M24	4.05 ± 1.15	2.84 ± 0	3.65 ± 0.57
P25	6.49 ± 2.3	4.66 ± 4.88	3.24 ± 2.87	M25	1.42 ± 0.86	0.41 ± 0.57	0.51 ± 0.43
P26	3.85 ± 0.29	2.23 ± 0.86	3.04 ± 1.43	M26	0.81 ± 0	3.24 ± 0	1.72 ± 1
P27	4.46 ± 1.72	4.87 ± 0.58	4.66 ± 3.15	M27	2.64 ± 0.86	4.43 ± 0	6.69 ± 2.58
P28	2.23 ± 0.28	1.21 ± 0.01	3.24 ± 3.44	M28	4.26 ± 0.28	4.86 ± 0	3.45 ± 2.58
P29	2.03 ± 1.72	3.65 ± 2.29	3.85 ± 0.86	M29	4.43 ± 2.28	4.43 ± 0	1.42 ± 0.86
P30	2.63 ± 0.86	3.96 ± 4.73	2.84 ± 2.29	M30	0.92 ± 0.15	2.89 ± 0	1.01 ± 0.86
P31	2.23 ± 1.43	1.32 ± 1	1.22 ± 0	M31	2.64 ± 1.43	2.03 ± 0	2.23 ± 0.29
P32	3.65 ± 2.87	6.69 ± 2.01	3.65 ± 4.59	M32	4.86 ± 1.15	4.05 ± 0	3.44 ± 1.43
P33	1.82 ± 0.86	4.87 ± 5.74	3.65 ± 4.01	M33	1.31 ± 1.05	0.82 ± 0	0.61 ± 0.29

Annexure 21: The average and standard deviation of T. coli (CFU/ml) of samples collected from Palakkad and Malappuram during the Pr, Mo, and Po seasons.

Palakkad district				Malappuram district			
Sample	Pr	Mo	Po	Sample	Pr	Mo	Po
	Mean ± SD	Mean ± SD	Mean ± SD		Mean ± SD	Mean ± SD	Mean ± SD
P01	515 ± 728	980 ± 1386	1468 ± 1941	M01	602 ± 663	1078 ± 824	2398 ± 4
P02	1750 ± 665	1005 ± 615	718 ± 329	M02	64 ± 51	720 ± 311	460 ± 177
P03	233 ± 138	13 ± 4	1500 ± 2121	M03	19 ± 16	1475 ± 346	855 ± 912
P04	988 ± 689	273 ± 343	1285 ± 1775	M04	63 ± 18	585 ± 28	338 ± 477
P05	1020 ± 1442	0 ± 0	0 ± 0	M05	167 ± 37	1000 ± 1103	313 ± 286
P06	280 ± 0	1078 ± 1276	570 ± 134	M06	63 ± 18	210 ± 184	730 ± 304
P07	573 ± 675	270 ± 184	578 ± 668	M07	69 ± 98	983 ± 1312	3 ± 4
P08	1174 ± 1607	1210 ± 891	2580 ± 3649	M08	68 ± 95	815 ± 1153	678 ± 725
P09	385 ± 516	213 ± 286	1468 ± 1884	M09	140 ± 198	165 ± 106	23 ± 32
P10	334 ± 412	1205 ± 1662	373 ± 25	M10	48 ± 67	1540 ± 679	40 ± 7
P11	1127 ± 1518	90 ± 85	18 ± 11	M11	398 ± 32	360 ± 417	700 ± 792
P12	318 ± 435	925 ± 460	3515 ± 4900	M12	160 ± 120	403 ± 569	290 ± 141
P13	1227 ± 1723	1050 ± 615	820 ± 1131	M13	1038 ± 371	1075 ± 601	195 ± 276
P14	530 ± 735	625 ± 884	835 ± 516	M14	143 ± 11	710 ± 354	235 ± 332
P15	49 ± 51	1115 ± 1223	2428 ± 3157	M15	127 ± 19	240 ± 233	250 ± 346
P16	1270 ± 1796	250 ± 198	2223 ± 3023	M16	25 ± 35	405 ± 28	650 ± 438
P17	657 ± 839	830 ± 594	3138 ± 4048	M17	119 ± 157	333 ± 442	88 ± 110
P18	672 ± 54	380 ± 523	1240 ± 1711	M18	505 ± 396	260 ± 134	473 ± 95
P19	1044 ± 1352	238 ± 223	920 ± 962	M19	258 ± 244	648 ± 803	413 ± 265
P20	275 ± 304	1003 ± 732	1118 ± 612	M20	38 ± 53	713 ± 1008	143 ± 145
P21	1214 ± 1706	520 ± 283	1565 ± 1266	M21	467 ± 443	1275 ± 1011	5 ± 7
P22	2 ± 2	1333 ± 1368	93 ± 117	M22	1070 ± 1513	628 ± 880	220 ± 113
P23	812 ± 1101	723 ± 216	1565 ± 1831	M23	357 ± 330	473 ± 435	1440 ± 2022
P24	1347 ± 1900	940 ± 1146	5990 ± 3833	M24	60 ± 85	1565 ± 898	335 ± 318
P25	1313 ± 1856	1663 ± 1015	723 ± 958	M25	1030 ± 636	148 ± 209	220 ± 57
P26	213 ± 293	1238 ± 378	1500 ± 1273	M26	1464 ± 2059	1565 ± 757	63 ± 74
P27	549 ± 765	120 ± 71	988 ± 477	M27	298 ± 315	860 ± 1216	353 ± 166
P28	577 ± 776	1670 ± 99	773 ± 576	M28	159 ± 140	113 ± 11	103 ± 25
P29	254 ± 348	1910 ± 693	1513 ± 1906	M29	98 ± 32	1125 ± 1591	18 ± 11
P30	647 ± 613	1068 ± 1488	1213 ± 1679	M30	2025 ± 955	275 ± 389	523 ± 117
P31	597 ± 839	1358 ± 484	2270 ± 410	M31	1225 ± 35	1313 ± 1679	35 ± 35
P32	1280 ± 1810	43 ± 60	2275 ± 1025	M32	470 ± 665	993 ± 718	365 ± 516
P33	877 ± 1235	553 ± 534	1685 ± 1153	M33	8 ± 11	260 ± 255	450 ± 636

Annexure 22: The average and standard deviation of *E.coli* (CFU/ml) of samples collected from Palakkad and Malappuram during the Pr, Mo, and Po seasons.

Palakkad district				Malappuram district			
Sample	Pr	Mo	Po	Sample	Pr	Mo	Po
	Mean ± SD	Mean ± SD	Mean ± SD		Mean ± SD	Mean ± SD	Mean ± SD
P01	0 ± 0	65 ± 92	1425 ± 2001	M01	544 ± 716	0 ± 0	765 ± 106
P02	0 ± 0	0 ± 0	503 ± 633	M02	38 ± 53	30 ± 28	28 ± 39
P03	63 ± 88	0 ± 0	1500 ± 2121	M03	14 ± 8	0 ± 0	33 ± 39
P04	7 ± 5	13 ± 4	1283 ± 1778	M04	49 ± 23	10 ± 14	30 ± 42
P05	5 ± 7	0 ± 0	0 ± 0	M05	50 ± 71	35 ± 35	55 ± 78
P06	42 ± 40	0 ± 0	203 ± 223	M06	32 ± 2	30 ± 21	195 ± 255
P07	145 ± 205	38 ± 32	450 ± 636	M07	30 ± 42	103 ± 145	3 ± 4
P08	0 ± 0	438 ± 81	140 ± 198	M08	63 ± 88	0 ± 0	635 ± 785
P09	225 ± 318	5 ± 7	100 ± 141	M09	105 ± 148	73 ± 39	23 ± 32
P10	188 ± 265	240 ± 339	135 ± 191	M10	5 ± 7	223 ± 67	15 ± 14
P11	0 ± 0	23 ± 18	0 ± 0	M11	182 ± 238	148 ± 194	178 ± 81
P12	98 ± 138	0 ± 0	0 ± 0	M12	20 ± 28	98 ± 138	83 ± 110
P13	0 ± 0	138 ± 18	10 ± 14	M13	253 ± 357	135 ± 170	88 ± 124
P14	149 ± 199	20 ± 28	628 ± 527	M14	24 ± 20	48 ± 39	20 ± 28
P15	39 ± 51	48 ± 67	20 ± 28	M15	13 ± 18	15 ± 7	115 ± 156
P16	15 ± 21	0 ± 0	13 ± 18	M16	4 ± 6	293 ± 152	170 ± 240
P17	314 ± 440	188 ± 265	115 ± 163	M17	104 ± 143	3 ± 4	5 ± 7
P18	128 ± 166	35 ± 35	10 ± 14	M18	185 ± 262	43 ± 46	28 ± 11
P19	0 ± 0	33 ± 46	155 ± 78	M19	0 ± 0	5 ± 7	343 ± 237
P20	237 ± 260	75 ± 85	268 ± 286	M20	19 ± 27	5 ± 7	88 ± 88
P21	15 ± 21	35 ± 49	288 ± 131	M21	15 ± 21	303 ± 378	5 ± 7
P22	20 ± 28	13 ± 18	878 ± 1241	M22	0 ± 0	13 ± 18	33 ± 18
P23	143 ± 202	115 ± 85	685 ± 841	M23	3 ± 4	18 ± 25	55 ± 21
P24	0 ± 0	248 ± 350	1683 ± 2259	M24	23 ± 32	48 ± 67	23 ± 25
P25	875 ± 1237	43 ± 18	700 ± 990	M25	32 ± 45	83 ± 53	60 ± 7
P26	10 ± 14	98 ± 131	340 ± 332	M26	0 ± 0	115 ± 64	18 ± 18
P27	10 ± 14	13 ± 4	390 ± 177	M27	32 ± 9	3 ± 4	200 ± 7
P28	0 ± 0	328 ± 230	75 ± 106	M28	9 ± 8	55 ± 78	18 ± 2
P29	0 ± 0	0 ± 0	723 ± 788	M29	10 ± 14	33 ± 46	43 ± 46
P30	8 ± 11	115 ± 148	55 ± 42	M30	175 ± 247	80 ± 113	195 ± 170
P31	38 ± 53	620 ± 559	1115 ± 1223	M31	10 ± 14	215 ± 64	30 ± 21
P32	0 ± 0	5 ± 7	15 ± 7	M32	200 ± 283	3 ± 4	365 ± 516
P33	0 ± 0	185 ± 247	425 ± 516	M33	0 ± 0	23 ± 11	5 ± 7

Annexure 23: The bimonthly concentration of F and its mean and standard deviation of samples collected from Palakkad and Malappuram during the Pr, Mo, and Po seasons.

Palakkad district										Malappuram district									
Sample	Pr			Mo			Po			Sample	Pr			Mo			Po		
	Feb-Mar	Apr-May	Avg ± SD	Jun-Jul	Aug-Sep	Avg ± SD	Oct-Nov	Dec-Jan	Avg ± SD		Feb-Mar	Apr-May	Avg ± SD	Jun-Jul	Aug-Sep	Avg ± SD	Oct-Nov	Dec-Jan	Avg ± SD
P01	**1.6**	**1.8**	**1.7 ± 0.1**	1.2	1.5	1.4 ± 0.2	**1.8**	**1.6**	**1.7 ± 0.1**	M01	1	1.3	1.2 ± 0.2	0.9	0.7	0.8 ± 0.1	1.2	1.1	1.1 ± 0.1
P02	1.2	1.2	1.2 ± 0	0.6	1.2	0.9 ± 0.4	1.4	1.3	1.3 ± 0.1	M02	1.3	1.3	1.3 ± 0	1.0	0.7	0.9 ± 0.2	1.3	1.1	1.2 ± 0.1
P03	1.1	1.2	1.2 ± 0.1	1.2	0.8	1 ± 0.3	1.5	1.2	1.3 ± 0.2	M03	1.3	1.2	1.3 ± 0	0.9	0.6	0.7 ± 0.2	1.1	1.2	1.1 ± 0.1
P04	1	1.4	1.2 ± 0.3	0.9	0.6	0.8 ± 0.2	1.2	1.1	1.1 ± 0.1	M04	1.1	1.1	1.1 ± 0	0.9	0.4	0.6 ± 0.4	1.1	1.1	1.1 ± 0
P05	1.4	1.1	1.3 ± 0.2	0.8	0.9	0.8 ± 0.1	1.2	1.0	1.1 ± 0.1	M05	1.2	1.1	1.2 ± 0	1.0	0.8	0.9 ± 0.1	1.3	1.1	1.2 ± 0.1
P06	1.1	1.2	1.2 ± 0.1	0.9	0.9	0.9 ± 0	1.5	1.2	1.3 ± 0.2	M06	1.2	1.2	1.2 ± 0	0.9	0.7	0.8 ± 0.1	1.1	1.1	1.1 ± 0
P07	1.2	1.3	1.2 ± 0	0.9	1.2	1.1 ± 0.2	1.1	1.0	1 ± 0.1	M07	1.2	1.4	1.3 ± 0.1	0.9	1.0	1 ± 0.1	1.1	**1.9**	**1.5 ± 0.5**
P08	1.3	1.3	1.3 ± 0	1.0	0.9	1 ± 0.1	1.1	1.2	1.2 ± 0	M08	1.2	1.2	1.2 ± 0	1.0	0.8	0.9 ± 0.2	1.5	1.1	1.3 ± 0.3
P09	1.4	1.3	1.3 ± 0.1	1.2	**1.6**	1.4 ± 0.3	1.1	1.2	1.2 ± 0.1	M09	1.1	1.4	1.2 ± 0.2	0.9	0.7	0.8 ± 0.1	1.2	1.2	1.2 ± 0.1
P10	1.2	1.0	1.1 ± 0.1	1.1	0.8	0.9 ± 0.2	1.4	1.0	1.2 ± 0.3	M10	1.1	1.1	1.1 ± 0	0.9	0.8	0.8 ± 0	1.2	1.3	1.3 ± 0
P11	1.2	1.3	1.3 ± 0	1.1	1.2	1.1 ± 0.1	1.4	1.0	1.2 ± 0.3	M11	1	1.1	1 ± 0	0.9	0.7	0.8 ± 0.1	1	1.1	1 ± 0.1
P12	1.2	1.5	1.3 ± 0.2	1.0	1.2	1.1 ± 0.1	1.2	1.2	1.2 ± 0	M12	1	1.2	1.1 ± 0.1	0.9	0.5	0.7 ± 0.3	1.2	0.9	1.1 ± 0.2
P13	0.7	1.2	0.9 ± 0.4	1.0	1.0	1 ± 0	1.5	1.0	1.3 ± 0.3	M13	1.2	1.1	1.2 ± 0	0.0	**1.2**	0.6 ± 0.8	1.1	1	1.1 ± 0.1
P14	1	1.2	1.1 ± 0.2	0.8	1.0	0.9 ± 0.2	1.2	1.0	1.1 ± 0.1	M14	1	1.3	1.1 ± 0.2	0.9	0.9	0.9 ± 0	1.2	1.1	1.1 ± 0.1
P15	1.3	0.6	0.9 ± 0.5	1.0	1.0	1 ± 0.1	1.3	1.1	1.2 ± 0.1	M15	1.1	1.1	1.1 ± 0.1	0.9	1.1	1 ± 0.1	1	1.2	1.1 ± 0.1
P16	1.2	1.3	1.2 ± 0.1	1.0	1.0	1 ± 0	1.3	1.1	1.2 ± 0.2	M16	0.9	1	1 ± 0.1	0.8	0.9	0.8 ± 0	1.2	1	1.1 ± 0.1
P17	0.8	1.1	0.9 ± 0.2	0.7	0.8	0.8 ± 0.1	1.3	1.0	1.1 ± 0.2	M17	1.1	1	1.1 ± 0	1.0	0.7	0.9 ± 0.2	1.4	0.9	1.2 ± 0.3
P18	1.4	1.5	1.4 ± 0.1	1.3	1.0	1.1 ± 0.2	1.4	1.2	1.3 ± 0.1	M18	1	1.1	1.1 ± 0.1	0.9	0.9	0.9 ± 0.1	1.1	1.1	1.1 ± 0
P19	1.2	0.8	1 ± 0.2	1.1	1.1	1.1 ± 0	1.4	1.1	1.2 ± 0.2	M19	1.2	1.3	1.3 ± 0.1	0.9	0.7	0.8 ± 0.2	1.1	1.1	1.1 ± 0
P20	1.3	1.2	1.2 ± 0.1	0.8	1.0	0.9 ± 0.1	0.3	1.1	0.7 ± 0.6	M20	1.1	1.4	1.2 ± 0.3	1.0	1.1	1 ± 0.1	1.3	1.1	1.2 ± 0.1
P21	1.5	1.5	1.5 ± 0	1.2	0.9	1 ± 0.2	1.5	1.4	1.5 ± 0.1	M21	1.1	1.6	1.3 ± 0.4	0.9	1.2	1.1 ± 0.2	1.2	0.9	1.1 ± 0.2
P22	**1.7**	**1.7**	**1.7 ± 0**	**1.8**	**1.5**	**1.6 ± 0.2**	**2.2**	**1.5**	**1.8 ± 0.5**	M22	1	1.3	1.2 ± 0.2	0.9	0.7	0.8 ± 0.2	1.2	1	1.1 ± 0.2
P23	1.3	1.5	1.4 ± 0.1	1.3	1.1	1.2 ± 0.2	1.5	1.5	1.5 ± 0	M23	1.1	1.3	1.2 ± 0.1	0.9	0.7	0.8 ± 0.1	1.2	1.1	1.2 ± 0.1
P24	1.4	1.5	1.5 ± 0.1	1.2	1.1	1.2 ± 0.1	1.4	1.2	1.3 ± 0.2	M24	1.1	1.3	1.2 ± 0.1	1.1	0.8	0.9 ± 0.2	1.2	1	1.1 ± 0.2
P25	1.4	1.5	1.4 ± 0.1	1.1	1.2	1.2 ± 0	1.4	1.1	1.2 ± 0.2	M25	1	1.4	1.2 ± 0.2	1.0	1.0	1 ± 0	1.3	1.2	1.3 ± 0.1
P26	1.4	1.3	1.4 ± 0.1	1.4	1.0	1.2 ± 0.2	1.5	1.5	1.5 ± 0	M26	1	1.5	1.2 ± 0.3	1.1	0.6	0.9 ± 0.3	1.4	0.2	0.8 ± 0.9
P27	1	1.2	1.1 ± 0.1	0.9	1.0	1 ± 0.1	1.2	1.4	1.3 ± 0.1	M27	1.3	**1.8**	**1.5 ± 0.3**	0.9	0.9	0.9 ± 0	1.4	1.1	1.2 ± 0.2
P28	**1.6**	1.5	1.5 ± 0	1.3	1.3	1.3 ± 0	**1.9**	**1.6**	**1.8 ± 0.3**	M28	1.3	1.1	1.2 ± 0.2	1.0	0.9	0.9 ± 0.1	**1.6**	**1.5**	**1.5 ± 0.1**
P29	**1.7**	**1.6**	**1.7 ± 0.1**	1.4	1.4	1.4 ± 0	**1.8**	**1.5**	**1.7 ± 0.2**	M29	1.2	1.4	1.3 ± 0.1	1.0	1.0	1 ± 0	1.2	1.2	1.2 ± 0.1
P30	1.4	1.4	1.4 ± 0	1.2	1.2	1.2 ± 0	1.4	1.3	1.3 ± 0.1	M30	1.3	1.2	1.2 ± 0.1	1.0	0.6	0.8 ± 0.2	1.4	1.4	1.4 ± 0
P31	1.2	1.4	1.3 ± 0.2	1.2	1.1	1.1 ± 0.1	1.4	1.3	1.4 ± 0.1	M31	1.2	1.3	1.2 ± 0.1	1.0	0.8	0.9 ± 0.1	1.3	1.1	1.2 ± 0.2
P32	1.3	1.3	1.3 ± 0.1	1.1	1.1	1.1 ± 0	1.5	1.4	1.4 ± 0	M32	1.1	1.4	1.2 ± 0.2	1.1	0.9	1 ± 0.2	1.3	1.2	1.2 ± 0.1
P33	1.2	1.2	1.2 ± 0	1.0	1.0	1 ± 0	1.1	1.1	1.1 ± 0	M33	1.4	**1.7**	**1.5 ± 0.2**	1.1	1.0	1.1 ± 0.1	1.2	1.2	1.2 ± 0

Annexure 24: The bimonthly concentration of As and its average and standard deviation of samples collected from Palakkad and Malappuram during the Pr, Mo, and Po seasons.

Palakkad district										Malappuram district									
Sample	Pr			Mo			Po			Sample	Pr			Mo			Po		
	Feb-Mar	Apr-May	Avg ± SD	Jun-Jul	Aug-Sep	Avg ± SD	Oct-Nov	Dec-Jan	Avg ± SD		Feb-Mar	Apr-May	Avg ± SD	Jun-Jul	Aug-Sep	Avg ± SD	Oct-Nov	Dec-Jan	Avg ± SD
P01	0.000	0.010	0.005 ± 0.007	0.050	0.010	0.03 ± 0.028	0.050	0.000	0.025 ± 0.035	M01	0.010	0.005	0.008 ± 0.004	0.050	0.050	0.05 ± 0	0.050	0.050	0.05 ± 0
P02	0.050	0.010	0.03 ± 0.028	0.010	0.005	0.008 ± 0.004	0.010	0.000	0.005 ± 0.007	M02	0.010	0.010	0.01 ± 0	0.010	0.010	0.01 ± 0	0.050	0.050	0.05 ± 0
P03	0.050	0.000	0.025 ± 0.035	0.010	0.000	0.005 ± 0.007	0.010	0.010	0.01 ± 0	M03	0.000	0.010	0.005 ± 0.007	0.010	0.010	0.01 ± 0	0.050	0.010	0.03 ± 0.028
P04	0.010	0.015	0.013 ± 0.004	0.050	0.010	0.03 ± 0.028	0.010	0.010	0.01 ± 0	M04	0.020	0.000	0.01 ± 0.014	0.010	0.000	0.005 ± 0.007	0.050	0.010	0.03 ± 0.028
P05	0.000	0.000	0 ± 0	0.000	0.000	0 ± 0	0.000	0.000	0 ± 0	M05	0.000	0.000	0 ± 0	0.010	0.000	0.005 ± 0.007	0.010	0.050	0.03 ± 0.028
P06	0.005	0.005	0.005 ± 0	0.050	0.005	0.028 ± 0.032	0.010	0.050	0.03 ± 0.028	M06	0.010	0.000	0.005 ± 0.007	0.010	0.050	0.03 ± 0.028	0.010	0.050	0.03 ± 0.028
P07	0.010	0.000	0.005 ± 0.007	0.100	0.050	**0.075 ± 0.035**	0.010	0.050	0.03 ± 0.028	M07	0.050	0.005	0.028 ± 0.032	0.010	0.000	0.005 ± 0.007	0.050	0.050	0.05 ± 0
P08	0.000	0.005	0.003 ± 0.004	0.010	0.050	0.03 ± 0.028	0.010	0.050	0.03 ± 0.028	M08	0.000	0.010	0.005 ± 0.007	0.050	0.000	0.025 ± 0.035	0.010	0.010	0.01 ± 0
P09	0.050	0.000	0.025 ± 0.035	0.100	0.050	**0.075 ± 0.035**	0.100	0.050	**0.075 ± 0.035**	M09	0.010	0.000	0.005 ± 0.007	0.010	0.000	0.005 ± 0.007	0.050	0.000	0.025 ± 0.035
P10	0.000	0.005	0.003 ± 0.004	0.050	0.010	0.03 ± 0.028	0.005	0.000	0.003 ± 0.004	M10	0.005	0.000	0.003 ± 0.004	0.010	0.000	0.005 ± 0.007	0.010	0.010	0.01 ± 0
P11	0.010	0.005	0.008 ± 0.004	0.050	0.010	0.03 ± 0.028	0.030	0.000	0.015 ± 0.021	M11	0.020	0.000	0.01 ± 0.014	0.010	0.000	0.005 ± 0.007	0.005	0.050	0.028 ± 0.032
P12	0.010	0.010	0.01 ± 0	0.050	0.000	0.025 ± 0.035	0.000	0.010	0.005 ± 0.007	M12	0.005	0.000	0.003 ± 0.004	0.050	0.050	0.05 ± 0	0.010	0.000	0.005 ± 0.007
P13	0.000	0.010	0.005 ± 0.007	0.100	0.050	**0.075 ± 0.035**	0.010	0.050	0.03 ± 0.028	M13	0.000	0.000	0 ± 0	0.010	0.000	0.005 ± 0.007	0.010	0.010	0.01 ± 0
P14	0.000	0.010	0.005 ± 0.007	0.010	0.005	0.008 ± 0.004	0.010	0.000	0.005 ± 0.007	M14	0.000	0.010	0.005 ± 0.007	0.010	0.010	0.01 ± 0	0.010	0.010	0.01 ± 0
P15	0.050	0.000	0.025 ± 0.035	0.010	0.000	0.005 ± 0.007	0.050	0.010	0.03 ± 0.028	M15	0.005	0.005	0.005 ± 0	0.050	0.000	0.025 ± 0.035	0.010	0.050	0.03 ± 0.028
P16	0.010	0.010	0.01 ± 0	0.005	0.005	0.005 ± 0	0.010	0.010	0.01 ± 0	M16	0.050	0.010	0.03 ± 0.028	0.010	0.000	0.005 ± 0.007	0.010	0.000	0.005 ± 0.007
P17	0.050	0.000	0.025 ± 0.035	0.005	0.005	0.005 ± 0	0.010	0.100	**0.055 ± 0.064**	M17	0.000	0.000	0 ± 0	0.050	0.000	0.025 ± 0.035	0.050	0.010	0.03 ± 0.028
P18	0.000	0.010	0.005 ± 0.007	0.010	0.050	0.03 ± 0.028	0.010	0.010	0.01 ± 0	M18	0.010	0.005	0.008 ± 0.004	0.010	0.050	0.03 ± 0.028	0.010	0.010	0.01 ± 0
P19	0.010	0.005	0.008 ± 0.004	0.100	0.010	**0.055 ± 0.064**	0.005	0.010	0.008 ± 0.004	M19	0.010	0.005	0.008 ± 0.004	0.010	0.050	0.03 ± 0.028	0.010	0.010	0.01 ± 0
P20	0.050	0.010	0.03 ± 0.028	0.010	0.010	0.01 ± 0	0.010	0.050	0.03 ± 0.028	M20	0.000	0.000	0 ± 0	0.010	0.000	0.005 ± 0.007	0.050	0.000	0.025 ± 0.035
P21	0.050	0.005	0.028 ± 0.032	0.100	0.050	**0.075 ± 0.035**	0.005	0.050	0.028 ± 0.032	M21	0.000	0.000	0 ± 0	0.010	0.000	0.005 ± 0.007	0.005	0.010	0.008 ± 0.004
P22	0.050	0.030	0.04 ± 0.014	0.050	0.050	0.05 ± 0	0.010	0.050	0.03 ± 0.028	M22	0.000	0.000	0 ± 0	0.050	0.000	0.025 ± 0.035	0.010	0.005	0.008 ± 0.004
P23	0.010	0.050	0.03 ± 0.028	0.050	0.050	0.05 ± 0	0.050	0.050	0.05 ± 0	M23	0.000	0.005	0.003 ± 0.004	0.050	0.000	0.025 ± 0.035	0.050	0.010	0.03 ± 0.028
P24	0.050	0.000	0.025 ± 0.035	0.010	0.010	0.01 ± 0	0.000	0.050	0.025 ± 0.035	M24	0.000	0.000	0 ± 0	0.000	0.000	0 ± 0	0.010	0.010	0.01 ± 0
P25	0.050	0.000	0.025 ± 0.035	0.010	0.010	0.01 ± 0	0.050	0.050	0.05 ± 0	M25	0.000	0.010	0.005 ± 0.007	0.050	0.000	0.025 ± 0.035	0.050	0.050	0.05 ± 0
P26	0.010	0.005	0.008 ± 0.004	0.005	0.050	0.028 ± 0.032	0.005	0.010	0.008 ± 0.004	M26	0.000	0.005	0.003 ± 0.004	0.010	0.050	0.03 ± 0.028	0.010	0.010	0.01 ± 0
P27	0.010	0.010	0.01 ± 0	0.005	0.050	0.028 ± 0.032	0.005	0.100	**0.053 ± 0.067**	M27	0.010	0.000	0.005 ± 0.007	0.020	0.000	0.01 ± 0.014	0.005	0.010	0.008 ± 0.004
P28	0.010	0.005	0.008 ± 0.004	0.005	0.010	0.008 ± 0.004	0.010	0.005	0.008 ± 0.004	M28	0.005	0.005	0.005 ± 0	0.050	0.000	0.025 ± 0.035	0.010	0.010	0.01 ± 0
P29	0.010	0.005	0.008 ± 0.004	0.010	0.050	0.03 ± 0.028	0.000	0.000	0 ± 0	M29	0.010	0.010	0.01 ± 0	0.010	0.000	0.005 ± 0.007	0.050	0.050	0.05 ± 0
P30	0.050	0.000	0.025 ± 0.035	0.010	0.010	0.01 ± 0	0.010	0.050	0.03 ± 0.028	M30	0.010	0.010	0.01 ± 0	0.010	0.000	0.005 ± 0.007	0.050	0.050	0.05 ± 0
P31	0.005	0.000	0.003 ± 0.004	0.000	0.005	0.003 ± 0.004	0.010	0.010	0.01 ± 0	M31	0.010	0.001	0.006 ± 0.006	0.050	0.050	0.05 ± 0	0.050	0.050	0.05 ± 0
P32	0.000	0.005	0.003 ± 0.004	0.005	0.005	0.005 ± 0	0.005	0.010	0.008 ± 0.004	M32	0.010	0.000	0.005 ± 0.007	0.010	0.000	0.005 ± 0.007	0.010	0.010	0.01 ± 0
P33	0.000	0.010	0.005 ± 0.007	0.050	0.010	0.03 ± 0.028	0.005	0.050	0.028 ± 0.032	M33	0.000	0.020	0.01 ± 0.014	0.010	0.000	0.005 ± 0.007	0.050	0.050	0.05 ± 0

Annexure 25: The bimonthly concentration of Fe and its average and standard deviation of samples collected from Palakkad and Malappuram during the Pr, Mo, and Po seasons.

Palakkad district										Malappuram district									
Sample	Pr			Mo			Po			Sample	Pr			Mo			Po		
	Feb-Mar	Apr-May	Avg ± SD	Jun-Jul	Aug-Sep	Avg ± SD	Oct-Nov	Dec-Jan	Avg ± SD		Feb-Mar	Apr-May	Avg ± SD	Jun-Jul	Aug-Sep	Avg ± SD	Oct-Nov	Dec-Jan	Avg ± SD
P01	0.770	0.357	0.6 ± 0.3	0.923	1.245	1.1 ± 0.2	0.37	0.531	0.5 ± 0.1	M01	0.067	0.134	0.1 ± 0	0.051	0.07	0.1 ± 0	0.059	0.121	0.1 ± 0
P02	0.328	0.098	0.2 ± 0.2	0.059	0.150	0.1 ± 0.1	0.07	0.132	0.1 ± 0	M02	0.07	0.108	0.1 ± 0	0.051	0.084	0.1 ± 0	0.070	0.081	0.1 ± 0
P03	2.950	1.033	2 ± 1.4	1.845	1.797	1.8 ± 0	1.662	3.639	2.7 ± 1.4	M03	0.298	0.21	0.3 ± 0.1	0.201	0.124	0.2 ± 0.1	0.106	0.092	0.1 ± 0
P04	0.034	0.078	0.1 ± 0	0.168	0.084	0.1 ± 0.1	0.066	0.092	0.1 ± 0	M04	0.086	0.194	0.1 ± 0.1	0.242	0.403	0.3 ± 0.1	0.172	0.414	0.3 ± 0.2
P05	0.604	0.491	0.5 ± 0.1	0.562	0.600	0.6 ± 0	0.63	0.574	0.6 ± 0	M05	0.051	0.082	0.1 ± 0	0.029	0.092	0.1 ± 0	0.033	0.048	0 ± 0
P06	0.127	0.399	0.3 ± 0.2	0.443	0.055	0.2 ± 0.3	0.176	0.096	0.1 ± 0.1	M06	0.2	0.09	0.1 ± 0.1	0.088	0.106	0.1 ± 0	0.073	0.124	0.1 ± 0
P07	0.103	0.694	0.4 ± 0.4	0.355	0.092	0.2 ± 0.2	0.088	0.168	0.1 ± 0.1	M07	0.059	0.09	0.1 ± 0	0.04	0.088	0.1 ± 0	0.037	0.062	0 ± 0
P08	3.370	4.450	3.9 ± 0.8	3.370	0.770	2.1 ± 1.8	1.13	3.046	2.1 ± 1.4	M08	0.35	0.469	0.4 ± 0.1	0.549	0.604	0.6 ± 0	0.597	0.513	0.6 ± 0.1
P09	0.119	0.049	0.1 ± 0	0.084	0.062	0.1 ± 0	0.055	0.095	0.1 ± 0	M09	0.067	0.005	0 ± 0	0.121	0.179	0.2 ± 0	0.253	0.095	0.2 ± 0.1
P10	0.084	0.055	0.1 ± 0	0.048	0.062	0.1 ± 0	0.055	0.044	0 ± 0	M10	0.088	0.064	0.1 ± 0	0.044	0.073	0.1 ± 0	0.037	0.051	0 ± 0
P11	0.390	0.482	0.4 ± 0.1	0.238	0.121	0.2 ± 0.1	0.802	0.143	0.5 ± 0.5	M11	0.058	0.1	0.1 ± 0	0.915	0.073	0.5 ± 0.6	0.051	0.062	0.1 ± 0
P12	0.306	0.168	0.2 ± 0.1	0.077	0.106	0.1 ± 0	0.022	0.037	0 ± 0	M12	0.046	0.161	0.1 ± 0.1	0.029	0.117	0.1 ± 0.1	0.029	0.081	0.1 ± 0
P13	0.680	1.268	1 ± 0.4	0.150	0.198	0.2 ± 0	0.483	0.362	0.4 ± 0.1	M13	0.112	0.355	0.2 ± 0.2	0.015	0.146	0.1 ± 0.1	0.040	0.117	0.1 ± 0.1
P14	0.343	0.090	0.2 ± 0.2	0.212	0.059	0.1 ± 0.1	0.095	0.113	0.1 ± 0	M14	0.072	0.171	0.1 ± 0.1	0.059	0.095	0.1 ± 0	0.066	0.040	0.1 ± 0
P15	0.086	0.054	0.1 ± 0	0.165	0.242	0.2 ± 0.1	0.183	0.117	0.2 ± 0	M15	0.189	0.143	0.2 ± 0	0.373	0.033	0.2 ± 0.2	0.059	0.062	0.1 ± 0
P16	0.118	0.151	0.1 ± 0	0.286	0.143	0.2 ± 0.1	0.157	0.454	0.3 ± 0.2	M16	0.131	0.109	0.1 ± 0	0.037	0.081	0.1 ± 0	0.040	0.044	0 ± 0
P17	0.344	0.092	0.2 ± 0.2	0.124	0.146	0.1 ± 0	0.029	0.084	0.1 ± 0	M17	0.333	0.72	0.5 ± 0.3	0.608	0.286	0.4 ± 0.2	0.121	0.150	0.1 ± 0
P18	0.308	0.110	0.2 ± 0.1	0.326	0.399	0.4 ± 0.1	0.373	0.384	0.4 ± 0	M18	0.822	0.92	0.9 ± 0.1	0.092	0.084	0.1 ± 0	0.044	0.084	0.1 ± 0
P19	1.770	0.939	1.4 ± 0.6	0.930	0.128	0.5 ± 0.6	0.655	0.403	0.5 ± 0.2	M19	0.173	0.373	0.3 ± 0.1	0.139	0.143	0.1 ± 0	0.055	0.399	0.2 ± 0.2
P20	0.109	0.153	0.1 ± 0	0.117	0.216	0.2 ± 0.1	0.066	0.139	0.1 ± 0.1	M20	0.146	0.117	0.1 ± 0	0.062	0.135	0.1 ± 0.1	0.092	0.040	0.1 ± 0
P21	0.386	0.542	0.5 ± 0.1	0.633	0.139	0.4 ± 0.3	0.106	0.135	0.1 ± 0	M21	0.065	0.135	0.1 ± 0	0.249	0.417	0.3 ± 0.1	0.077	0.150	0.1 ± 0.1
P22	0.376	0.231	0.3 ± 0.1	0.070	0.073	0.1 ± 0	0.205	0.578	0.4 ± 0.3	M22	0.084	0.036	0.1 ± 0	0.066	0.19	0.1 ± 0.1	0.106	0.037	0.1 ± 0
P23	0.365	0.064	0.2 ± 0.2	0.015	0.117	0.1 ± 0.1	0.121	0.282	0.2 ± 0.1	M23	0.065	0.121	0.1 ± 0	0.033	0.135	0.1 ± 0.1	0.099	0.414	0.3 ± 0.2
P24	0.049	0.031	0 ± 0	0.110	0.238	0.2 ± 0.1	0.113	0.055	0.1 ± 0	M24	0.197	0.291	0.2 ± 0.1	0.135	0.179	0.2 ± 0	0.165	0.157	0.2 ± 0
P25	0.337	0.860	0.6 ± 0.4	0.513	0.103	0.3 ± 0.3	0.696	0.787	0.7 ± 0.1	M25	4.45	5.579	5 ± 0.8	6.582	2.746	4.7 ± 2.7	4.741	5.139	4.9 ± 0.3
P26	0.298	0.289	0.3 ± 0	0.220	0.124	0.2 ± 0.1	0.055	0.106	0.1 ± 0	M26	1.107	0.57	0.8 ± 0.4	0.249	0.3	0.3 ± 0	0.593	0.670	0.6 ± 0.1
P27	0.377	0.311	0.3 ± 0	0.143	0.073	0.1 ± 0	0.139	0.838	0.5 ± 0.5	M27	0.079	0.064	0.1 ± 0	0.249	0.245	0.2 ± 0	0.088	0.033	0.1 ± 0
P28	0.374	0.842	0.6 ± 0.3	0.106	0.077	0.1 ± 0	0.132	0.436	0.3 ± 0.2	M28	0.128	0.161	0.1 ± 0	0.549	0.275	0.4 ± 0.2	2.400	0.205	1.3 ± 1.6
P29	0.375	0.105	0.2 ± 0.2	0.092	0.044	0.1 ± 0	0.805	0.351	0.6 ± 0.3	M29	0.091	0.021	0.1 ± 0	0.04	0.103	0.1 ± 0	0.088	0.048	0.1 ± 0
P30	0.326	0.097	0.2 ± 0.2	0.018	0.157	0.1 ± 0.1	0.11	0.626	0.4 ± 0.4	M30	1.047	1.461	1.3 ± 0.3	0.106	0.161	0.1 ± 0	0.176	1.757	1 ± 1.1
P31	0.900	1.180	1 ± 0.2	1.095	1.216	1.2 ± 0.1	1.296	1.739	1.5 ± 0.3	M31	0.041	0.049	0 ± 0	0.051	0.07	0.1 ± 0	0.055	0.040	0 ± 0
P32	0.379	0.929	0.7 ± 0.4	0.604	0.421	0.5 ± 0.1	0.45	0.633	0.5 ± 0.1	M32	0.182	0.068	0.1 ± 0.1	0.037	0.048	0 ± 0	0.048	0.026	0 ± 0
P33	0.185	0.131	0.2 ± 0	0.099	0.267	0.2 ± 0.1	0.187	0.355	0.3 ± 0.1	M33	1.647	1.56	1.6 ± 0.1	0.98	1.904	1.4 ± 0.7	2.006	1.882	1.9 ± 0.1

Annexure 26: The bimonthly concentration of Cd and its average and standard deviation of samples collected from Palakkad and Malappuram during the Pr, Mo, and Po seasons.

Palakkad district										Malappuram district									
Sample	Pr			Mo			Po			Sample	Pr			Mo			Po		
	Feb-Mar	Apr-May	Avg ± SD	Jun-Jul	Aug-Sep	Avg ± SD	Oct-Nov	Dec-Jan	Avg ± SD		Feb-Mar	Apr-May	Avg ± SD	Jun-Jul	Aug-Sep	Avg ± SD	Oct-Nov	Dec-Jan	Avg ± SD
P01	0.0031	0.0037	0.0034 ± 0.0004	0.0021	0.0013	0.0017 ± 0.0006	0.0013	0.0038	0.0026 ± 0.0018	M01	0.0060	0.0049	0.0055 ± 0.0008	0.0048	0.0049	0.0049 ± 0.0001	0.0021	0.0039	0.003 ± 0.0013
P02	0.0039	0.0044	0.0042 ± 0.0004	0.0026	0.0042	0.0034 ± 0.0011	0.0029	0.0036	0.0033 ± 0.0005	M02	0.0045	0.0040	0.0043 ± 0.0004	0.0039	0.0042	0.0041 ± 0.0002	0.0004	0.0036	0.002 ± 0.0023
P03	0.0056	0.0064	0.006 ± 0.0006	0.0050	0.0040	0.0045 ± 0.0007	0.0050	0.0054	0.0052 ± 0.0003	M03	0.0040	0.0031	0.0036 ± 0.0006	0.0038	0.0022	0.003 ± 0.0011	0.0000	0.0039	0.002 ± 0.0028
P04	0.0070	0.0061	0.0066 ± 0.0006	0.0060	0.0031	0.0046 ± 0.0021	0.0025	0.0048	0.0037 ± 0.0016	M04	0.0020	0.0025	0.0023 ± 0.0004	0.0028	0.0021	0.0025 ± 0.0005	0.0000	0.0024	0.0012 ± 0.0017
P05	0.0014	0.0013	0.0014 ± 0.0001	0.0004	0.0007	0.0006 ± 0.0002	0.0000	0.0006	0.0003 ± 0.0004	M05	0.0007	0.0009	0.0008 ± 0.0001	0.0008	0.0010	0.0009 ± 0.0001	0.0000	0.0006	0.0003 ± 0.0004
P06	0.0036	0.0039	0.0038 ± 0.0002	0.0030	0.0029	0.003 ± 0.0001	0.0017	0.0045	0.0031 ± 0.002	M06	0.0035	0.0030	0.0033 ± 0.0004	0.0016	0.0011	0.0014 ± 0.0004	0.0000	0.0033	0.0017 ± 0.0023
P07	0.0040	0.0052	0.0046 ± 0.0008	0.0031	0.0047	0.0039 ± 0.0011	0.0037	0.0060	0.0049 ± 0.0016	M07	0.0031	0.0026	0.0029 ± 0.0004	0.0021	0.0029	0.0025 ± 0.0006	0.0017	0.004	0.0029 ± 0.0016
P08	0.0051	0.0061	0.0056 ± 0.0007	0.0046	0.0052	0.0049 ± 0.0004	0.0046	0.0068	0.0057 ± 0.0016	M08	0.0064	0.0056	0.006 ± 0.0006	0.0042	0.0052	0.0047 ± 0.0007	0.0046	0.0051	0.0049 ± 0.0004
P09	0.0042	0.0048	0.0045 ± 0.0004	0.0036	0.0044	0.004 ± 0.0006	0.0025	0.0051	0.0038 ± 0.0018	M09	0.0007	0.0010	0.0009 ± 0.0002	0.0020	0.0024	0.0022 ± 0.0003	0.0000	0.0028	0.0014 ± 0.002
P10	0.0024	0.0030	0.0027 ± 0.0004	0.0026	0.0043	0.0035 ± 0.0012	0.0000	0.0030	0.0015 ± 0.0021	M10	0.0006	0.0007	0.0007 ± 0.0001	0.0010	0.0020	0.0015 ± 0.0007	0.0000	0.0028	0.0014 ± 0.002
P11	0.0029	0.0030	0.003 ± 0.0001	0.0025	0.0026	0.0026 ± 0.0001	0.0029	0.0030	0.003 ± 0.0001	M11	0.0049	0.0031	0.004 ± 0.0013	0.0050	0.0040	0.0045 ± 0.0007	0.0017	0.003	0.0024 ± 0.0009
P12	0.0050	0.0036	0.0043 ± 0.001	0.0027	0.0051	0.0039 ± 0.0017	0.0033	0.0040	0.0037 ± 0.0005	M12	0.0024	0.0026	0.0025 ± 0.0001	0.0028	0.0026	0.0027 ± 0.0001	0.0008	0.0025	0.0017 ± 0.0012
P13	0.0009	0.0010	0.001 ± 0.0001	0.0007	0.0005	0.0006 ± 0.0001	0.0017	0.0026	0.0022 ± 0.0006	M13	0.0026	0.0024	0.0025 ± 0.0001	0.0008	0.0009	0.0009 ± 0.0001	0.0000	0.0006	0.0003 ± 0.0004
P14	0.0021	0.0027	0.0024 ± 0.0004	0.0005	0.0004	0.0005 ± 0.0001	0.0000	0.0004	0.0002 ± 0.0003	M14	0.0040	0.0030	0.0035 ± 0.0007	0.0039	0.0021	0.003 ± 0.0013	0.0035	0.0005	0.002 ± 0.0021
P15	0.0029	0.0031	0.003 ± 0.0001	0.0027	0.0024	0.0026 ± 0.0002	0.0013	0.0035	0.0024 ± 0.0016	M15	0.0051	0.0044	0.0048 ± 0.0005	0.0049	0.0520	0.0285 ± 0.0333	0.0035	0.0048	0.0042 ± 0.0009
P16	0.0035	0.0039	0.0037 ± 0.0003	0.0027	0.0020	0.0024 ± 0.0005	0.0000	0.0031	0.0016 ± 0.0022	M16	0.0036	0.0029	0.0033 ± 0.0005	0.0025	0.0039	0.0032 ± 0.001	0.0004	0.0006	0.0005 ± 0.0001
P17	0.0029	0.0034	0.0032 ± 0.0004	0.0006	0.0008	0.0007 ± 0.0001	0.0000	0.0020	0.001 ± 0.0014	M17	0.0060	0.0049	0.0055 ± 0.0008	0.0048	0.0061	0.0055 ± 0.0009	0.0025	0.0045	0.0035 ± 0.0014
P18	0.0041	0.0036	0.0039 ± 0.0004	0.0037	0.0044	0.0041 ± 0.0005	0.0025	0.0045	0.0035 ± 0.0014	M18	0.0051	0.0046	0.0049 ± 0.0004	0.0042	0.0052	0.0047 ± 0.0007	0.0025	0.0048	0.0037 ± 0.0016

P19	0.0039	0.0042	0.0041 ± 0.0002	0.0047	0.0026	0.0037 ± 0.0015	0.0029	0.0037	0.0033 ± 0.0006	M19	0.0026	0.0029	0.0028 ± 0.0002	0.0021	0.0000	0.0011 ± 0.0015	0.0021	0.0035	0.0028 ± 0.001
P20	0.0026	0.0031	0.0029 ± 0.0004	0.0021	0.0013	0.0017 ± 0.0006	0.0000	0.0031	0.0016 ± 0.0022	M20	0.0012	0.0014	0.0013 ± 0.0001	0.0025	0.0010	0.0018 ± 0.0011	0.0000	0.0021	0.0011 ± 0.0015
P21	0.0038	0.0043	0.0041 ± 0.0004	0.0036	0.0048	0.0042 ± 0.0008	0.0029	0.0039	0.0034 ± 0.0007	M21	0.0018	0.0020	0.0019 ± 0.0001	0.0031	0.0025	0.0028 ± 0.0004	0.0000	0.0026	0.0013 ± 0.0018
P22	0.0005	0.0007	0.0006 ± 0.0001	0.0006	0.0008	0.0007 ± 0.0001	0.0000	0.0030	0.0015 ± 0.0021	M22	0.0031	0.0024	0.0028 ± 0.0005	0.0031	0.0026	0.0029 ± 0.0004	0.0000	0.024	0.012 ± 0.017
P23	0.0031	0.0029	0.003 ± 0.0001	0.0006	0.0005	0.0006 ± 0.0001	0.0000	0.0004	0.0002 ± 0.0003	M23	0.0028	0.0034	0.0031 ± 0.0004	0.0022	0.0030	0.0026 ± 0.0006	0.0004	0.0018	0.0011 ± 0.001
P24	0.0025	0.0030	0.0028 ± 0.0004	0.0018	0.0027	0.0023 ± 0.0006	0.0000	0.0036	0.0018 ± 0.0025	M24	0.0006	0.0004	0.0005 ± 0.0001	0.0004	0.0006	0.0005 ± 0.0001	0.0000	0.0022	0.0011 ± 0.0016
P25	0.0009	0.0010	0.0009 ± 0.000	0.0006	0.0005	0.0006 ± 0.0001	0.0000	0.0008	0.0004 ± 0.0006	M25	0.0008	0.0007	0.0008 ± 0.0001	0.0023	0.0022	0.0023 ± 0.0001	0.0000	0.0011	0.0006 ± 0.0008
P26	0.0036	0.0046	0.0041 ± 0.0007	0.0039	0.0042	0.0041 ± 0.0002	0.0035	0.0025	0.003 ± 0.0007	M26	0.0031	0.0027	0.0029 ± 0.0003	0.0039	0.0032	0.0036 ± 0.0005	0.0000	0.0048	0.0024 ± 0.0034
P27	0.0041	0.0024	0.0033 ± 0.0012	0.0025	0.0049	0.0037 ± 0.0017	0.0035	0.0020	0.0028 ± 0.0011	M27	0.0034	0.0038	0.0036 ± 0.0003	0.0026	0.0037	0.0032 ± 0.0008	0.0023	0.0024	0.0024 ± 0.0001
P28	0.0029	0.0026	0.0028 ± 0.0002	0.0030	0.0010	0.002 ± 0.0014	0.0000	0.0008	0.0004 ± 0.0006	M28	0.0025	0.0024	0.0025 ± 0.0001	0.0005	0.0013	0.0009 ± 0.0006	0.0000	0.0026	0.0013 ± 0.0018
P29	0.0028	0.0038	0.0033 ± 0.0007	0.0016	0.0031	0.0024 ± 0.0011	0.0000	0.0028	0.0014 ± 0.002	M29	0.0036	0.0026	0.0031 ± 0.0007	0.0029	0.0022	0.0026 ± 0.0005	0.0025	0.0027	0.0026 ± 0.0001
P30	0.0026	0.0014	0.002 ± 0.0008	0.0017	0.0012	0.0015 ± 0.0004	0.0000	0.0020	0.001 ± 0.0014	M30	0.0032	0.0028	0.003 ± 0.0003	0.0015	0.0012	0.0014 ± 0.0002	0.0009	0.0031	0.002 ± 0.0016
P31	0.0013	0.0014	0.0014 ± 0.0001	0.0018	0.0027	0.0023 ± 0.0006	0.0000	0.0008	0.0004 ± 0.0006	M31	0.0036	0.0040	0.0038 ± 0.0003	0.0030	0.0036	0.0033 ± 0.0004	0.0000	0.0048	0.0024 ± 0.0034
P32	0.0031	0.0027	0.0029 ± 0.0003	0.0026	0.0038	0.0032 ± 0.0008	0.0025	0.0040	0.0033 ± 0.0011	M32	0.0009	0.0006	0.0008 ± 0.0002	0.0008	0.0007	0.0008 ± 0.0001	0.0004	0.0008	0.0006 ± 0.0003
P33	0.0006	0.0013	0.001 ± 0.0005	0.0006	0.0007	0.0007 ± 0.0001	0.0000	0.0025	0.0013 ± 0.0018	M33	0.0012	0.0013	0.0013 ± 0.0001	0.0006	0.0007	0.0007 ± 0.0001	0.0010	0.0014	0.0012 ± 0.0003

Annexure 27: The bimonthly concentration of Pb and its average and standard deviation of samples collected from Palakkad and Malappuram during the Pr, Mo, and Po seasons.

Palakkad district										Malappuram district									
Sample	Pr			Mo			Po			Sample	Pr			Mo			Po		
	Feb-Mar	Apr-May	Avg ± SD	Jun-Jul	Aug-Sep	Avg ± SD	Oct-Nov	Dec-Jan	Avg ± SD		Feb-Mar	Apr-May	Avg ± SD	Jun-Jul	Aug-Sep	Avg ± SD	Oct-Nov	Dec-Jan	Avg ± SD
P01	0.013	0.010	0.012 ± 0.002	0.000	0.003	0.002 ± 0.002	0.005	0.016	0.011 ± 0.008	M01	0.020	0.010	0.015 ± 0.007	0.000	0.017	0.009 ± 0.012	0.015	0.010	0.013 ± 0.004
P02	0.003	0.013	0.008 ± 0.007	0.000	0.010	0.005 ± 0.007	0.004	0.016	0.01 ± 0.009	M02	0.030	0.017	0.023 ± 0.009	0.000	0.031	0.016 ± 0.022	0.055	0.029	0.042 ± 0.019
P03	0.010	0.013	0.012 ± 0.002	0.004	0.006	0.005 ± 0.001	0.009	0.000	0.004 ± 0.006	M03	0.020	0.013	0.017 ± 0.005	0.000	0.017	0.009 ± 0.012	0.024	0.014	0.019 ± 0.007
P04	0.013	0.003	0.008 ± 0.007	0.000	0.003	0.002 ± 0.002	0.005	0.012	0.009 ± 0.005	M04	0.017	0.020	0.018 ± 0.002	0.000	0.017	0.009 ± 0.012	0.026	0.035	0.031 ± 0.006
P05	0.010	0.013	0.012 ± 0.002	0.004	0.010	0.007 ± 0.004	0.024	0.013	0.019 ± 0.007	M05	0.010	0.020	0.015 ± 0.007	0.000	0.010	0.005 ± 0.007	0.005	0.012	0.009 ± 0.005
P06	0.010	0.020	0.015 ± 0.007	0.000	0.031	0.016 ± 0.022	0.032	0.000	0.016 ± 0.023	M06	0.007	0.000	0.003 ± 0.005	0.000	0.003	0.002 ± 0.002	0.006	0.008	0.007 ± 0.001
P07	0.023	0.013	0.018 ± 0.007	0.004	0.052	0.028 ± 0.034	0.032	0.008	0.02 ± 0.017	M07	0.023	0.020	0.022 ± 0.002	0.000	0.003	0.002 ± 0.002	0.006	0.016	0.011 ± 0.007
P08	0.007	0.020	0.013 ± 0.009	0.000	0.037	0.019 ± 0.026	0.006	0.027	0.016 ± 0.015	M08	0.007	0.002	0.004 ± 0.003	0.010	0.003	0.007 ± 0.004	0.003	0.006	0.005 ± 0.002
P09	0.007	0.010	0.008 ± 0.002	0.000	0.045	0.022 ± 0.032	0.038	0.002	0.02 ± 0.025	M09	0.013	0.010	0.012 ± 0.002	0.000	0.006	0.003 ± 0.004	0.005	0.013	0.009 ± 0.005
P10	0.017	0.017	0.017 ± 0	0.000	0.003	0.002 ± 0.002	0.004	0.008	0.006 ± 0.003	M10	0.007	0.027	0.017 ± 0.014	0.000	0.038	0.019 ± 0.027	0.054	0.016	0.035 ± 0.026
P11	0.020	0.007	0.013 ± 0.009	0.004	0.024	0.014 ± 0.014	0.005	0.012	0.009 ± 0.005	M11	0.013	0.013	0.013 ± 0	0.000	0.017	0.009 ± 0.012	0.018	0.010	0.014 ± 0.005
P12	0.007	0.020	0.013 ± 0.009	0.004	0.010	0.007 ± 0.004	0.004	0.010	0.007 ± 0.004	M12	0.010	0.017	0.013 ± 0.005	0.000	0.005	0.003 ± 0.004	0.006	0.008	0.007 ± 0.002
P13	0.020	0.010	0.015 ± 0.007	0.000	0.017	0.009 ± 0.012	0.004	0.025	0.014 ± 0.014	M13	0.023	0.010	0.017 ± 0.009	0.000	0.038	0.019 ± 0.027	0.038	0.016	0.027 ± 0.015
P14	0.017	0.010	0.013 ± 0.005	0.000	0.017	0.009 ± 0.012	0.005	0.008	0.007 ± 0.002	M14	0.000	0.010	0.005 ± 0.007	0.000	0.010	0.005 ± 0.007	0.032	0.012	0.022 ± 0.014
P15	0.007	0.027	0.017 ± 0.014	0.010	0.010	0.01 ± 0	0.004	0.004	0.004 ± 0	M15	0.007	0.007	0.007 ± 0	0.000	0.007	0.003 ± 0.005	0.006	0.004	0.005 ± 0.001
P16	0.003	0.003	0.003 ± 0	0.004	0.009	0.006 ± 0.003	0.006	0.010	0.008 ± 0.003	M16	0.020	0.020	0.02 ± 0	0.000	0.052	0.026 ± 0.037	0.065	0.006	0.035 ± 0.041

P17	0.030	0.020	0.025 ± 0.007	0.000	0.007	0.003 ± 0.005	0.006	0.006	0.006 ± 0	M17	0.010	0.013	0.012 ± 0.002	0.000	0.006	0.003 ± 0.004	0.005	0.006	0.006 ± 0.001
P18	0.023	0.007	0.015 ± 0.012	0.000	0.038	0.019 ± 0.027	0.005	0.002	0.004 ± 0.002	M18	0.013	0.017	0.015 ± 0.002	0.000	0.007	0.004 ± 0.005	0.005	0.006	0.006 ± 0.001
P19	0.020	0.007	0.013 ± 0.009	0.000	0.017	0.009 ± 0.012	0.005	0.002	0.003 ± 0.002	M19	0.010	0.017	0.013 ± 0.005	0.000	0.007	0.003 ± 0.005	0.011	0.004	0.008 ± 0.005
P20	0.010	0.020	0.015 ± 0.007	0.000	0.024	0.012 ± 0.017	0.005	0.012	0.009 ± 0.005	M20	0.003	0.017	0.01 ± 0.009	0.000	0.006	0.003 ± 0.004	0.006	0.002	0.004 ± 0.003
P21	0.017	0.027	0.022 ± 0.007	0.000	0.005	0.003 ± 0.004	0.006	0.002	0.004 ± 0.003	M21	0.013	0.027	0.02 ± 0.009	0.000	0.045	0.022 ± 0.032	0.059	0.019	0.039 ± 0.029
P22	0.013	0.033	0.023 ± 0.014	0.000	0.024	0.012 ± 0.017	0.005	0.016	0.01 ± 0.008	M22	0.020	0.013	0.017 ± 0.005	0.000	0.008	0.004 ± 0.006	0.006	0.004	0.005 ± 0.002
P23	0.007	0.017	0.012 ± 0.007	0.000	0.017	0.009 ± 0.012	0.005	0.012	0.009 ± 0.005	M23	0.017	0.027	0.022 ± 0.007	0.000	0.007	0.004 ± 0.005	0.006	0.014	0.01 ± 0.006
P24	0.010	0.020	0.015 ± 0.007	0.000	0.005	0.003 ± 0.004	0.004	0.005	0.005 ± 0	M24	0.020	0.020	0.02 ± 0	0.000	0.007	0.003 ± 0.005	0.004	0.000	0.002 ± 0.003
P25	0.007	0.017	0.012 ± 0.007	0.000	0.004	0.002 ± 0.003	0.006	0.000	0.003 ± 0.005	M25	0.010	0.017	0.013 ± 0.005	0.000	0.010	0.005 ± 0.007	0.010	0.033	0.021 ± 0.016
P26	0.010	0.030	0.02 ± 0.014	0.064	0.086	0.075 ± 0.015	0.048	0.023	0.036 ± 0.018	M26	0.007	0.013	0.01 ± 0.005	0.000	0.009	0.005 ± 0.007	0.003	0.012	0.008 ± 0.006
P27	0.007	0.023	0.015 ± 0.012	0.000	0.121	0.06 ± 0.085	0.043	0.000	0.022 ± 0.03	M27	0.010	0.013	0.012 ± 0.002	0.004	0.003	0.004 ± 0	0.027	0.006	0.017 ± 0.015
P28	0.017	0.037	0.027 ± 0.014	0.000	0.031	0.016 ± 0.022	0.038	0.004	0.021 ± 0.024	M28	0.007	0.010	0.008 ± 0.002	0.000	0.017	0.009 ± 0.012	0.005	0.006	0.006 ± 0.001
P29	0.027	0.013	0.02 ± 0.009	0.004	0.010	0.007 ± 0.004	0.048	0.000	0.024 ± 0.034	M29	0.000	0.013	0.007 ± 0.009	0.000	0.012	0.006 ± 0.008	0.004	0.002	0.003 ± 0.002
P30	0.010	0.037	0.023 ± 0.019	0.000	0.024	0.012 ± 0.017	0.043	0.000	0.022 ± 0.03	M30	0.013	0.023	0.018 ± 0.007	0.000	0.009	0.004 ± 0.006	0.006	0.021	0.013 ± 0.01
P31	0.010	0.033	0.022 ± 0.016	0.004	0.024	0.014 ± 0.014	0.027	0.023	0.025 ± 0.003	M31	0.007	0.017	0.012 ± 0.007	0.000	0.011	0.005 ± 0.007	0.004	0.008	0.006 ± 0.003
P32	0.017	0.033	0.025 ± 0.012	0.004	0.048	0.026 ± 0.031	0.043	0.025	0.034 ± 0.013	M32	0.010	0.030	0.02 ± 0.014	0.000	0.011	0.006 ± 0.008	0.048	0.012	0.03 ± 0.026
P33	0.020	0.020	0.02 ± 0	0.000	0.031	0.016 ± 0.022	0.048	0.000	0.024 ± 0.034	M33	0.017	0.003	0.01 ± 0.009	0.000	0.003	0.002 ± 0.002	0.004	0.004	0.004 ± 0

Table 28: The bimonthly concentration of Ni and its average and standard deviation of samples collected from Palakkad and Malappuram during the Pr, Mo, and Po seasons.

Palakkad district										Malappuram district									
Sample	Pr			Mo			Po			Sample	Pr			Mo			Po		
	Feb-Mar	Apr-May	Avg ± SD	Jun-Jul	Aug-Sep	Avg ± SD	Oct-Nov	Dec-Jan	Avg ± SD		Feb-Mar	Apr-May	Avg ± SD	Jun-Jul	Aug-Sep	Avg ± SD	Oct-Nov	Dec-Jan	Avg ± SD
P01	0.018	0.003	0.011 ± 0.01	0.020	0.024	0.022 ± 0.002	0.013	0.019	0.016 ± 0.004	M01	0.03	0.023	0.026 ± 0.005	0.009	0.014	0.011 ± 0.003	0.024	0.017	0.021 ± 0.005
P02	0.027	0.009	0.018 ± 0.013	0.021	0.005	0.013 ± 0.011	0.021	0.025	0.023 ± 0.003	M02	0.009	0.018	0.013 ± 0.007	0.019	0.014	0.017 ± 0.004	0.029	0.011	0.02 ± 0.013
P03	0.031	0.003	0.017 ± 0.02	0.023	0.016	0.02 ± 0.005	0.025	0.022	0.024 ± 0.002	M03	0.009	0.014	0.011 ± 0.004	0.025	0.007	0.016 ± 0.012	0.021	0.015	0.018 ± 0.004
P04	0.015	0.023	0.019 ± 0.006	0.020	0.004	0.012 ± 0.012	0.007	0.010	0.008 ± 0.002	M04	0.02	0.03	0.025 ± 0.007	0.017	0.007	0.012 ± 0.007	0.005	0.012	0.009 ± 0.005
P05	0.019	0.026	0.022 ± 0.005	0.014	0.007	0.011 ± 0.004	0.017	0.018	0.017 ± 0.001	M05	0.03	0.011	0.02 ± 0.013	0.012	0.003	0.007 ± 0.007	0.01	0.014	0.012 ± 0.003
P06	0.035	0.030	0.032 ± 0.004	0.027	0.009	0.018 ± 0.013	0.025	0.029	0.027 ± 0.003	M06	0.027	0.015	0.021 ± 0.008	0.027	0.012	0.02 ± 0.01	0.023	0.025	0.024 ± 0.001
P07	0.003	0.026	0.015 ± 0.016	0.028	0.006	0.017 ± 0.015	0.015	0.011	0.013 ± 0.003	M07	0.043	0.024	0.034 ± 0.013	0.026	0.015	0.02 ± 0.008	0.015	0.019	0.017 ± 0.003
P08	0.022	0.015	0.018 ± 0.005	0.017	0.000	0.009 ± 0.012	0.006	0.017	0.012 ± 0.008	M08	0.022	0.02	0.021 ± 0.001	0.022	0.007	0.015 ± 0.01	0.006	0.019	0.012 ± 0.009
P09	0.007	0.006	0.007 ± 0.001	0.033	0.005	0.019 ± 0.02	0.029	0.023	0.026 ± 0.004	M09	0.026	0.007	0.016 ± 0.013	0.019	0.026	0.022 ± 0.005	0.019	0.019	0.019 ± 0
P10	0.047	0.005	0.026 ± 0.03	0.023	0.022	0.023 ± 0.001	0.012	0.018	0.015 ± 0.004	M10	0.023	0.005	0.014 ± 0.013	0.02	0.011	0.016 ± 0.006	0.028	0.03	0.029 ± 0.002
P11	0.020	0.002	0.011 ± 0.013	0.023	0.015	0.019 ± 0.006	0.017	0.016	0.017 ± 0.001	M11	0.023	0.015	0.019 ± 0.006	0.024	0.001	0.013 ± 0.016	0.013	0.018	0.015 ± 0.003
P12	0.023	0.020	0.022 ± 0.002	0.015	0.010	0.012 ± 0.004	0.030	0.022	0.026 ± 0.006	M12	0.028	0.018	0.023 ± 0.007	0.022	0.028	0.025 ± 0.004	0.01	0.013	0.012 ± 0.002
P13	0.003	0.024	0.014 ± 0.015	0.016	0.005	0.01 ± 0.008	0.015	0.015	0.015 ± 0	M13	0.009	0.016	0.013 ± 0.006	0.019	0.024	0.021 ± 0.003	0.014	0.015	0.014 ± 0.001
P14	0.010	0.038	0.024 ± 0.02	0.022	0.019	0.02 ± 0.003	0.007	0.023	0.015 ± 0.011	M14	0.022	0.034	0.028 ± 0.008	0.026	0.025	0.025 ± 0.001	0.013	0.017	0.015 ± 0.002
P15	0.023	0.034	0.028 ± 0.007	0.010	0.004	0.007 ± 0.004	0.010	0.019	0.015 ± 0.006	M15	0.019	0.015	0.017 ± 0.003	0.018	0.005	0.011 ± 0.009	0.015	0.022	0.018 ± 0.005
P16	0.015	0.019	0.017 ± 0.003	0.017	0.001	0.009 ± 0.011	0.026	0.011	0.019 ± 0.01	M16	0.003	0.011	0.007 ± 0.006	0.019	0.015	0.017 ± 0.003	0.024	0.024	0.024 ± 0

P17	0.006	0.027	0.016 ± 0.015	0.013	0.015	0.014 ± 0.001	0.010	0.023	0.016 ± 0.01	M17	0.03	0.049	0.039 ± 0.014	0.015	0.011	0.013 ± 0.003	0.018	0.025	0.022 ± 0.005
P18	0.013	0.020	0.016 ± 0.006	0.018	0.025	0.021 ± 0.005	0.016	0.022	0.019 ± 0.005	M18	0.013	0.006	0.009 ± 0.005	0.03	0.019	0.024 ± 0.008	0.01	0.024	0.017 ± 0.01
P19	0.019	0.018	0.018 ± 0.001	0.019	0.010	0.015 ± 0.007	0.025	0.019	0.022 ± 0.004	M19	0.013	0.011	0.012 ± 0.001	0.018	0.009	0.013 ± 0.007	0.023	0.01	0.016 ± 0.009
P20	0.024	0.041	0.033 ± 0.012	0.018	0.015	0.016 ± 0.002	0.017	0.018	0.018 ± 0	M20	0.009	0	0.004 ± 0.006	0.024	0.007	0.016 ± 0.012	0.022	0.025	0.023 ± 0.003
P21	0.035	0.032	0.034 ± 0.002	0.014	0.004	0.009 ± 0.007	0.018	0.017	0.017 ± 0.001	M21	0.038	0.024	0.031 ± 0.009	0.02	0.02	0.02 ± 0	0.015	0.007	0.011 ± 0.005
P22	0.027	0.007	0.017 ± 0.014	0.019	0.010	0.014 ± 0.006	0.025	0.019	0.022 ± 0.004	M22	0.019	0.022	0.02 ± 0.002	0.022	0.01	0.016 ± 0.008	0.024	0.019	0.022 ± 0.003
P23	0.014	0.023	0.018 ± 0.007	0.022	0.027	0.024 ± 0.004	0.011	0.019	0.015 ± 0.005	M23	0.023	0.022	0.022 ± 0.001	0.025	0.015	0.02 ± 0.007	0.028	0.022	0.025 ± 0.004
P24	0.015	0.014	0.014 ± 0.001	0.038	0.005	0.021 ± 0.023	0.026	0.023	0.025 ± 0.002	M24	0.031	0.026	0.028 ± 0.004	0.019	0.017	0.018 ± 0.001	0.025	0.023	0.024 ± 0.001
P25	0.006	0.032	0.019 ± 0.019	0.040	0.009	0.024 ± 0.022	0.010	0.011	0.01 ± 0.001	M25	0.002	0.031	0.016 ± 0.02	0.024	0.001	0.013 ± 0.016	0.018	0.017	0.018 ± 0.001
P26	0.018	0.014	0.016 ± 0.003	0.017	0.019	0.018 ± 0.001	0.014	0.022	0.018 ± 0.006	M26	0.016	0.011	0.014 ± 0.004	0.019	0.019	0.019 ± 0.001	0.021	0.022	0.021 ± 0.001
P27	0.007	0.013	0.01 ± 0.004	0.025	0.011	0.018 ± 0.01	0.022	0.022	0.022 ± 0	M27	0.02	0.016	0.018 ± 0.003	0.019	0.024	0.021 ± 0.003	0.017	0.017	0.017 ± 0
P28	0.016	0.019	0.018 ± 0.002	0.046	0.019	0.032 ± 0.019	0.012	0.012	0.012 ± 0	M28	0.015	0.002	0.009 ± 0.009	0.014	0.015	0.015 ± 0	0.005	0.013	0.009 ± 0.005
P29	0.035	0.014	0.024 ± 0.015	0.031	0.012	0.022 ± 0.013	0.020	0.027	0.023 ± 0.005	M29	0.019	0.016	0.018 ± 0.002	0.023	0.005	0.014 ± 0.013	0.018	0.017	0.018 ± 0.001
P30	0.011	0.013	0.012 ± 0.001	0.025	0.031	0.028 ± 0.004	0.014	0.009	0.012 ± 0.003	M30	0.018	0.018	0.018 ± 0	0.017	0.017	0.017 ± 0.001	0.03	0.026	0.028 ± 0.003
P31	0.016	0.006	0.011 ± 0.007	0.026	0.012	0.019 ± 0.01	0.024	0.015	0.02 ± 0.007	M31	0.034	0.005	0.019 ± 0.021	0.019	0.012	0.016 ± 0.005	0.011	0.014	0.013 ± 0.002
P32	0.016	0.016	0.016 ± 0	0.029	0.003	0.016 ± 0.019	0.023	0.029	0.026 ± 0.004	M32	0	0.036	0.018 ± 0.026	0.026	0.003	0.014 ± 0.017	0.008	0.012	0.01 ± 0.003
P33	0.010	0.009	0.009 ± 0.001	0.040	0.007	0.024 ± 0.023	0.017	0.019	0.018 ± 0.002	M33	0.018	0.026	0.022 ± 0.006	0.02	0.028	0.024 ± 0.006	0.025	0.012	0.019 ± 0.009

Annexure 29: The bimonthly concentration of Mn and its average and standard deviation of samples collected from Palakkad and Malappuram during the Pr, Mo, and Po seasons.

Palakkad district										Malappuram district									
Sample	Pr			Mo			Po			Sample	Pr			Mo			Po		
	Feb-Mar	Apr-May	Avg ± SD	Jun-Jul	Aug-Sep	Avg ± SD	Oct-Nov	Dec-Jan	Avg ± SD		Feb-Mar	Apr-May	Avg ± SD	Jun-Jul	Aug-Sep	Avg ± SD	Oct-Nov	Dec-Jan	Avg ± SD
P01	0.04	0.06	0.05 ± 0.02	0.08	0.05	0.06 ± 0.02	0.01	0.08	0.04 ± 0.05	M01	0	0	0 ± 0	0.01	0.01	0.01 ± 0	0.02	0.01	0.02 ± 0.01
P02	0.04	0.00	0.02 ± 0.03	0.01	0.01	0.01 ± 0	0.01	0.02	0.02 ± 0.01	M02	0.01	0.04	0.02 ± 0.02	0.02	0.01	0.02 ± 0	0.01	0.03	0.02 ± 0.01
P03	0.14	0.08	0.11 ± 0.04	0.18	0.17	0.17 ± 0.01	0.07	0.24	0.16 ± 0.12	M03	0.03	0.01	0.02 ± 0.01	0.03	0.02	0.02 ± 0.01	0.01	0.04	0.03 ± 0.02
P04	0.04	0.20	0.12 ± 0.12	0.09	0.1	0.09 ± 0	0.19	0.12	0.15 ± 0.05	M04	0.03	0.01	0.02 ± 0.01	0.02	0.01	0.01 ± 0.01	0.02	0.02	0.02 ± 0.01
P05	0.17	0.19	0.18 ± 0.01	0.01	0.01	0.01 ± 0.01	0.01	0.01	0.01 ± 0	M05	0.01	0.05	0.03 ± 0.03	0.07	0.07	0.07 ± 0	0.01	0.07	0.04 ± 0.04
P06	0.02	0.02	0.02 ± 0	0.02	0.01	0.02 ± 0.01	0.02	0.02	0.02 ± 0	M06	0.03	0.03	0.03 ± 0	0.02	0.01	0.01 ± 0.01	0.02	0.01	0.02 ± 0.01
P07	0.03	0.07	0.05 ± 0.02	0.04	0.02	0.03 ± 0.02	0.02	0.03	0.02 ± 0.01	M07	0	0	0 ± 0	0.01	0.01	0.01 ± 0	0.05	0.1	0.08 ± 0.03
P08	0.01	0.10	0.06 ± 0.06	0.03	0.01	0.02 ± 0.01	0.1	0.09	0.1 ± 0.01	M08	0.01	0.04	0.02 ± 0.02	0.04	0.05	0.04 ± 0	0.02	0.04	0.03 ± 0.02
P09	0.04	0.05	0.04 ± 0.01	0.01	0.03	0.02 ± 0.02	0.03	0.04	0.03 ± 0.01	M09	0.03	0	0.01 ± 0.02	0.01	0.01	0.01 ± 0	0.02	0.02	0.02 ± 0
P10	0.01	0.02	0.01 ± 0.01	0.02	0.01	0.01 ± 0.01	0.03	0.02	0.02 ± 0.01	M10	0.05	0.01	0.03 ± 0.03	0.02	0.02	0.02 ± 0	0.01	0.02	0.02 ± 0.01
P11	0.01	0.03	0.02 ± 0.01	0.02	0.02	0.02 ± 0	0.01	0.02	0.02 ± 0	M11	0.01	0.01	0.01 ± 0	0.02	0.02	0.02 ± 0	0.09	0.02	0.06 ± 0.05
P12	0.11	0.19	0.15 ± 0.05	0.01	0.23	0.12 ± 0.15	0.02	0.03	0.03 ± 0.01	M12	0.02	0	0.01 ± 0.01	0.02	0.01	0.01 ± 0	0.01	0.02	0.01 ± 0
P13	0.10	0.11	0.1 ± 0.01	0.04	0.01	0.02 ± 0.02	0.03	0.02	0.02 ± 0	M13	0.01	0.01	0.01 ± 0	0.01	0.01	0.01 ± 0	0.05	0.02	0.03 ± 0.02
P14	0.01	0.02	0.01 ± 0.01	0.01	0.03	0.02 ± 0.01	0.02	0.02	0.02 ± 0	M14	0	0.01	0 ± 0	0.02	0.01	0.02 ± 0	0.01	0.02	0.02 ± 0
P15	0.00	0.01	0 ± 0	0.01	0.01	0.01 ± 0	0.01	0.01	0.01 ± 0	M15	0.01	0.02	0.01 ± 0.01	0.02	0.02	0.02 ± 0	0.12	0.01	0.07 ± 0.08
P16	0.25	0.03	0.14 ± 0.15	0.02	0.01	0.02 ± 0.01	0.04	0.01	0.03 ± 0.02	M16	0.04	0.01	0.02 ± 0.02	0.02	0.03	0.03 ± 0.01	0.14	0.02	0.08 ± 0.09

P17	0.02	0.03	0.03 ± 0.01	0.01	0.01	0.01 ± 0	0.02	0.02	0.02 ± 0	M17	0.06	0.16	0.11 ± 0.07	0.18	0.23	0.2 ± 0.04	0.02	0.16	0.09 ± 0.1
P18	0.07	0.08	0.07 ± 0.01	0.05	0.09	0.07 ± 0.03	0.07	0.07	0.07 ± 0	M18	0.04	0.08	0.06 ± 0.03	0.03	0.01	0.02 ± 0.01	0.01	0.02	0.01 ± 0.01
P19	0.10	0.15	0.12 ± 0.03	0.16	0.12	0.14 ± 0.03	0.08	0.11	0.1 ± 0.02	M19	0.02	0.06	0.04 ± 0.03	0.02	0.01	0.02 ± 0.01	0.01	0.01	0.01 ± 0
P20	0.02	0.09	0.05 ± 0.05	0.03	0.06	0.04 ± 0.02	0.01	0.06	0.03 ± 0.04	M20	0	0.03	0.02 ± 0.02	0.01	0.01	0.01 ± 0	0.02	0.01	0.02 ± 0.01
P21	0.05	0.78	0.42 ± 0.52	0.21	0.02	0.12 ± 0.14	0.03	0.08	0.05 ± 0.04	M21	0	0	0 ± 0	0.02	0.02	0.02 ± 0	0.03	0.04	0.03 ± 0.01
P22	0.02	0.02	0.02 ± 0.01	0.01	0.01	0.01 ± 0	0.01	0.02	0.02 ± 0.01	M22	0.02	0.05	0.04 ± 0.03	0.03	0.04	0.03 ± 0.01	0.05	0.02	0.04 ± 0.02
P23	0.19	0.19	0.19 ± 0.01	0.02	0.09	0.06 ± 0.05	0.27	0.64	0.46 ± 0.26	M23	0.02	0.03	0.02 ± 0.01	0.03	0.02	0.02 ± 0.01	0.03	0.03	0.03 ± 0
P24	0.07	0.06	0.07 ± 0	0.04	0.18	0.11 ± 0.1	0.06	0.04	0.05 ± 0.01	M24	0	0.02	0.01 ± 0.01	0.02	0.01	0.02 ± 0	0.05	0.03	0.04 ± 0.01
P25	0.09	0.10	0.09 ± 0.01	0.02	0.01	0.01 ± 0.01	0.01	0.11	0.06 ± 0.07	M25	0.05	0.03	0.04 ± 0.01	0.18	0.14	0.16 ± 0.03	0.05	0.05	0.05 ± 0
P26	0.01	0.01	0.01 ± 0	0.01	0.02	0.01 ± 0	0.02	0.02	0.02 ± 0	M26	0.01	0.02	0.01 ± 0	0.03	0.04	0.03 ± 0.01	0.14	0.02	0.08 ± 0.09
P27	0.06	0.24	0.15 ± 0.13	0.05	0.04	0.04 ± 0.01	0.13	0.03	0.08 ± 0.07	M27	0.03	0	0.02 ± 0.02	0.1	0.55	0.33 ± 0.32	0.02	0.07	0.04 ± 0.04
P28	0.04	0.03	0.03 ± 0.01	0.10	0.05	0.08 ± 0.04	0.07	0.03	0.05 ± 0.03	M28	0.03	0.05	0.04 ± 0.01	0.02	0.01	0.02 ± 0.01	0.02	0.03	0.02 ± 0.01
P29	0.00	0.01	0 ± 0.01	0.05	0.01	0.03 ± 0.03	0.02	0.01	0.01 ± 0	M29	0.03	0.03	0.03 ± 0	0.02	0.01	0.01 ± 0.01	0.01	0.02	0.02 ± 0.01
P30	0.02	0.03	0.02 ± 0.01	0.04	0.02	0.03 ± 0.01	0.02	0.02	0.02 ± 0	M30	0.02	0.01	0.01 ± 0	0.02	0.03	0.02 ± 0.01	0.02	0.1	0.06 ± 0.05
P31	0.21	0.28	0.25 ± 0.04	0.56	0.04	0.3 ± 0.36	0.38	0.2	0.29 ± 0.12	M31	0.02	0.04	0.03 ± 0.01	0.02	0.02	0.02 ± 0	0.1	0.12	0.11 ± 0.02
P32	0.02	0.06	0.04 ± 0.03	0.07	0.04	0.06 ± 0.02	0.06	0.04	0.05 ± 0.01	M32	0.04	0	0.02 ± 0.02	0.01	0.01	0.01 ± 0	0.06	0.04	0.05 ± 0.01
P33	0.01	0.01	0.01 ± 0	0.01	0.01	0.01 ± 0	0.01	0.04	0.02 ± 0.02	M33	0	0	0 ± 0	0.03	0.06	0.04 ± 0.02	0.07	0.01	0.04 ± 0.04

Annexure 30: The bimonthly concentration of Cu and its average and standard deviation of samples collected from Palakkad and Malappuram during the Pr, Mo, and Po seasons.

Palakkad district										Malappuram district									
Sample	Pr			Mo			Po			Sample	Pr			Mo			Po		
	Feb-Mar	Apr-May	Avg ± SD	Jun-Jul	Aug-Sep	Avg ± SD	Oct-Nov	Dec-Jan	Avg ± SD		Feb-Mar	Apr-May	Avg ± SD	Jun-Jul	Aug-Sep	Avg ± SD	Oct-Nov	Dec-Jan	Avg ± SD
P01	0.022	0.024	0.023 ± 0.001	0.018	0.037	0.027 ± 0.013	0.02	0.005	0.012 ± 0.01	M01	0.02	0.024	0.022 ± 0.003	0.018	0.028	0.023 ± 0.007	0.018	0.006	0.012 ± 0.009
P02	0.023	0.022	0.023 ± 0.001	0.014	0.042	0.028 ± 0.019	0.022	0.003	0.012 ± 0.014	M02	0.02	0.021	0.021 ± 0.001	0.018	0.027	0.022 ± 0.006	0.021	0.012	0.016 ± 0.006
P03	0.019	0.021	0.02 ± 0.002	0.018	0.045	0.032 ± 0.019	0.017	0.003	0.01 ± 0.009	M03	0.018	0.022	0.02 ± 0.003	0.018	0.03	0.024 ± 0.008	0.023	0.043	0.033 ± 0.014
P04	0.024	0.023	0.024 ± 0.001	0.03	0.036	0.033 ± 0.004	0.028	0.017	0.022 ± 0.008	M04	0.019	0.023	0.021 ± 0.003	0.016	0.027	0.021 ± 0.007	0.066	0.013	0.039 ± 0.037
P05	0.018	0.022	0.02 ± 0.003	0.014	0.025	0.019 ± 0.008	0.024	0.003	0.014 ± 0.014	M05	0.019	0.021	0.02 ± 0.002	0.017	0.032	0.025 ± 0.011	0.021	0.021	0.021 ± 0
P06	0.016	0.023	0.02 ± 0.005	0.013	0.027	0.02 ± 0.01	0.025	0.004	0.015 ± 0.015	M06	0.021	0.022	0.021 ± 0.001	0.017	0.032	0.024 ± 0.01	0.025	0.014	0.019 ± 0.007
P07	0.017	0.024	0.02 ± 0.005	0.018	0.029	0.023 ± 0.008	0.018	0.008	0.013 ± 0.007	M07	0.02	0.022	0.021 ± 0.001	0.016	0.032	0.024 ± 0.011	0.024	0.011	0.017 ± 0.009
P08	0.019	0.022	0.02 ± 0.002	0.017	0.029	0.023 ± 0.009	0.021	0.007	0.014 ± 0.01	M08	0.025	0.022	0.024 ± 0.002	0.014	0.031	0.023 ± 0.012	0.028	0.016	0.022 ± 0.008
P09	0.02	0.02	0.02 ± 0	0.013	0.027	0.02 ± 0.01	0.02	0.001	0.01 ± 0.013	M09	0.022	0.023	0.022 ± 0.001	0.02	0.027	0.023 ± 0.005	0.021	0.012	0.016 ± 0.006
P10	0.02	0.02	0.02 ± 0	0.016	0.037	0.026 ± 0.014	0.018	0.003	0.01 ± 0.011	M10	0.019	0.024	0.022 ± 0.003	0.016	0.027	0.021 ± 0.007	0.021	0.016	0.018 ± 0.003
P11	0.022	0.022	0.022 ± 0	0.018	0.033	0.026 ± 0.01	0.019	0.008	0.013 ± 0.008	M11	0.021	0.027	0.024 ± 0.004	0.026	0.033	0.029 ± 0.005	0.017	0.011	0.014 ± 0.005
P12	0.02	0.02	0.02 ± 0	0.015	0.029	0.022 ± 0.01	0.026	0.004	0.015 ± 0.016	M12	0.018	0.024	0.021 ± 0.004	0.016	0.037	0.027 ± 0.015	0.003	0.003	0.003 ± 0
P13	0.025	0.027	0.026 ± 0.001	0.018	0.028	0.023 ± 0.007	0.032	0.018	0.025 ± 0.01	M13	0.021	0.022	0.021 ± 0.001	0.011	0.034	0.023 ± 0.016	0.021	0.006	0.014 ± 0.011
P14	0.023	0.023	0.023 ± 0	0.018	0.027	0.022 ± 0.006	0.021	0.006	0.013 ± 0.01	M14	0.019	0.029	0.024 ± 0.007	0.02	0.036	0.028 ± 0.011	0.017	0.003	0.01 ± 0.01
P15	0.019	0.021	0.02 ± 0.001	0.018	0.029	0.024 ± 0.007	0.009	0.003	0.006 ± 0.004	M15	0.023	0.025	0.024 ± 0.001	0.018	0.036	0.027 ± 0.012	0.037	0.085	0.061 ± 0.034
P16	0.023	0.027	0.025 ± 0.003	0.016	0.028	0.022 ± 0.009	0.013	0.003	0.008 ± 0.007	M16	0.034	0.036	0.035 ± 0.001	0.024	0.037	0.03 ± 0.009	0.034	0.009	0.021 ± 0.017

P17	0.023	0.025	0.024 ± 0.001	0.015	0.031	0.023 ± 0.011	0.021	0.003	0.012 ± 0.012	M17	0.023	0.041	0.032 ± 0.013	0.017	0.032	0.025 ± 0.011	0.022	0.01	0.016 ± 0.009
P18	0.021	0.023	0.022 ± 0.002	0.016	0.027	0.022 ± 0.008	0.025	0.001	0.013 ± 0.017	M18	0.019	0.022	0.021 ± 0.002	0.018	0.027	0.022 ± 0.007	0.028	0.013	0.021 ± 0.01
P19	0.028	0.023	0.026 ± 0.004	0.016	0.027	0.022 ± 0.008	0.02	0.004	0.012 ± 0.011	M19	0.021	0.029	0.025 ± 0.006	0.031	0.03	0.03 ± 0	0.022	0.006	0.014 ± 0.012
P20	0.023	0.02	0.021 ± 0.002	0.014	0.03	0.022 ± 0.011	0.004	0.009	0.007 ± 0.004	M20	0.022	0.02	0.021 ± 0.002	0.02	0.027	0.024 ± 0.005	0.022	1.796	0.909 ± 1.255
P21	0.027	0.021	0.024 ± 0.005	0.023	0.03	0.026 ± 0.005	0.03	0.008	0.019 ± 0.015	M21	0.021	0.025	0.023 ± 0.003	0.019	0.03	0.025 ± 0.008	0	0.016	0.008 ± 0.011
P22	0.023	0.03	0.027 ± 0.004	0.017	0.032	0.024 ± 0.01	0.021	0.02	0.021 ± 0.001	M22	0.019	0.021	0.02 ± 0.001	0.018	0.027	0.022 ± 0.006	0.019	0.002	0.01 ± 0.012
P23	0.023	0.025	0.024 ± 0.002	0.015	0.025	0.02 ± 0.007	0.022	0.012	0.017 ± 0.007	M23	0.019	0.025	0.022 ± 0.004	0.018	0.03	0.024 ± 0.008	0.019	0.007	0.013 ± 0.009
P24	0.016	0.023	0.02 ± 0.005	0.014	0.027	0.02 ± 0.009	0.019	0.006	0.012 ± 0.009	M24	0.017	0.022	0.019 ± 0.003	0.02	0.012	0.016 ± 0.006	0.025	0.013	0.019 ± 0.008
P25	0.019	0.021	0.02 ± 0.002	0.017	0.025	0.021 ± 0.006	0.019	0.005	0.012 ± 0.01	M25	0.018	0.021	0.019 ± 0.002	0.018	0.024	0.021 ± 0.004	0.025	0.006	0.016 ± 0.014
P26	0.027	0.031	0.029 ± 0.003	0.03	0.029	0.029 ± 0.001	0.026	0.008	0.017 ± 0.013	M26	0.019	0.022	0.02 ± 0.003	0.018	0.026	0.022 ± 0.006	0.02	0.008	0.014 ± 0.009
P27	0.02	0.027	0.023 ± 0.005	0.023	0.031	0.027 ± 0.006	0.013	0.029	0.021 ± 0.012	M27	0.02	0.028	0.024 ± 0.005	0.025	0.028	0.027 ± 0.002	0.017	0.006	0.012 ± 0.008
P28	0.02	0.028	0.024 ± 0.006	0.019	0.032	0.026 ± 0.009	0.021	0.012	0.016 ± 0.006	M28	0.02	0.025	0.022 ± 0.003	0.022	0.03	0.026 ± 0.006	0.028	0	0.014 ± 0.02
P29	0.041	0.02	0.031 ± 0.015	0.027	0.025	0.026 ± 0.001	0.021	0.007	0.014 ± 0.01	M29	0.042	0.033	0.037 ± 0.007	0.132	0.026	0.079 ± 0.075	0.034	0.01	0.022 ± 0.017
P30	0.023	0.022	0.023 ± 0.001	0.016	0.027	0.022 ± 0.008	0.021	0.006	0.014 ± 0.011	M30	0.02	0.023	0.022 ± 0.002	0.018	0.027	0.022 ± 0.006	0.019	0.007	0.013 ± 0.009
P31	0.023	0.022	0.023 ± 0	0.022	0.057	0.04 ± 0.025	0.022	0.011	0.017 ± 0.008	M31	0.035	0.022	0.029 ± 0.009	0.018	0.025	0.022 ± 0.005	0.019	0.009	0.014 ± 0.007
P32	0.016	0.023	0.02 ± 0.005	0.015	0.027	0.021 ± 0.009	0.013	0	0.006 ± 0.009	M32	0.026	0.025	0.026 ± 0	0.016	0.029	0.023 ± 0.009	0.025	0.008	0.017 ± 0.011
P33	0.021	0.022	0.022 ± 0.001	0.014	0.027	0.02 ± 0.009	0.017	0.004	0.011 ± 0.009	M33	0.016	0.026	0.021 ± 0.007	0.031	0.062	0.046 ± 0.022	0.019	0.008	0.013 ± 0.008

Annexure 31: The bimonthly concentration of Zn and its average and standard deviation of samples collected from Palakkad and Malappuram during the Pr, Mo, and Po seasons.

Palakkad district										Malappuram district									
Sample	Pr			Mo			Po			Sample	Pr			Mo			Po		
	Feb-Mar	Apr-May	Avg ± SD	Jun-Jul	Aug-Sep	Avg ± SD	Oct-Nov	Dec-Jan	Avg ± SD		Feb-Mar	Apr-May	Avg ± SD	Jun-Jul	Aug-Sep	Avg ± SD	Oct-Nov	Dec-Jan	Avg ± SD
P01	0.00	0.00	0 ± 0	0.02	0.01	0.01 ± 0	0.02	0.01	0.01 ± 0.01	M01	0.06	0.00	0.03 ± 0.04	0.05	0.05	0.05 ± 0	0.02	0.02	0.02 ± 0
P02	0.00	0.00	0 ± 0	0.01	0.01	0.01 ± 0	0.01	0.01	0.01 ± 0	M02	0.54	1.24	0.89 ± 0.5	0.52	0.32	0.42 ± 0.14	0.36	0.37	0.36 ± 0
P03	0.00	0.00	0 ± 0	0.02	0.01	0.01 ± 0.01	0.03	0.02	0.03 ± 0	M03	0.00	0.00	0 ± 0	0.06	0.00	0.03 ± 0.04	0.02	0.01	0.02 ± 0
P04	0.07	0.00	0.03 ± 0.05	0.04	0.04	0.04 ± 0	0.03	0.04	0.03 ± 0.01	M04	0.00	0.00	0 ± 0	0.02	0.01	0.02 ± 0.01	0.01	0.05	0.03 ± 0.02
P05	0.00	0.00	0 ± 0	0.01	0.01	0.01 ± 0	0.01	0.01	0.01 ± 0	M05	0.00	0.00	0 ± 0	0.02	0.01	0.01 ± 0	0.01	0.02	0.02 ± 0
P06	0.25	0.28	0.26 ± 0.02	0.11	0.31	0.21 ± 0.14	0.10	0.43	0.27 ± 0.23	M06	0.19	0.13	0.16 ± 0.04	0.05	0.05	0.05 ± 0	0.05	0.10	0.07 ± 0.04
P07	0.00	0.01	0 ± 0	0.02	0.01	0.01 ± 0.01	0.01	0.03	0.02 ± 0.01	M07	0.00	0.00	0 ± 0	0.01	0.00	0.01 ± 0.01	0.03	0.01	0.02 ± 0.01
P08	0.00	0.00	0 ± 0	0.02	0.01	0.02 ± 0	0.01	0.01	0.01 ± 0	M08	0.00	0.00	0 ± 0	0.02	0.05	0.04 ± 0.02	0.03	0.04	0.03 ± 0.01
P09	0.00	0.00	0 ± 0	0.08	0.01	0.05 ± 0.04	0.02	0.02	0.02 ± 0	M09	0.00	0.00	0 ± 0	0.02	0.01	0.01 ± 0.01	0.03	0.02	0.02 ± 0.01
P10	0.02	0.00	0.01 ± 0.02	0.03	0.01	0.02 ± 0.01	0.01	0.01	0.01 ± 0	M10	0.00	0.01	0.01 ± 0.01	0.01	0.00	0 ± 0.01	0.02	0.01	0.01 ± 0
P11	0.00	0.00	0 ± 0	0.04	0.10	0.07 ± 0.04	0.01	0.01	0.01 ± 0.01	M11	0.00	0.00	0 ± 0	0.03	0.00	0.02 ± 0.02	0.02	0.01	0.02 ± 0.01
P12	0.00	0.00	0 ± 0	0.09	0.05	0.07 ± 0.03	0.06	0.02	0.04 ± 0.03	M12	0.00	0.00	0 ± 0	0.03	0.01	0.02 ± 0.01	0.01	0.02	0.01 ± 0
P13	0.01	0.33	0.17 ± 0.23	0.10	0.19	0.15 ± 0.06	0.13	0.88	0.51 ± 0.53	M13	0.03	0.04	0.04 ± 0.01	0.01	0.22	0.11 ± 0.15	0.01	0.02	0.01 ± 0.01
P14	0.04	0.01	0.02 ± 0.02	0.02	0.05	0.04 ± 0.02	0.05	0.01	0.03 ± 0.03	M14	0.00	0.00	0 ± 0	0.01	0.01	0.01 ± 0	0.01	0.01	0.01 ± 0
P15	0.00	0.00	0 ± 0	0.01	0.01	0.01 ± 0	0.02	0.01	0.01 ± 0	M15	0.00	0.00	0 ± 0	0.02	0.02	0.02 ± 0	0.02	0.01	0.02 ± 0.01
P16	0.00	0.00	0 ± 0	0.01	0.00	0.01 ± 0.01	0.01	0.02	0.01 ± 0	M16	0.07	0.05	0.06 ± 0.01	0.04	0.06	0.05 ± 0.01	0.03	0.09	0.06 ± 0.04
P17	0.00	0.04	0.02 ±	0.04	0.02	0.03 ±	0.02	0.02	0.02 ± 0	M17	0.36	1.03	0.7 ±	0.05	0.26	0.16 ±	0.09	0.03	0.06 ±

			0.03			0.01							0.47			0.15			0.05
P18	0.00	0.00	0 ± 0	0.01	0.00	0.01 ± 0.01	0.01	0.01	0.01 ± 0	M18	0.57	0.05	0.31 ± 0.37	0.36	0.18	0.27 ± 0.13	0.08	0.07	0.08 ± 0.01
P19	0.00	0.00	0 ± 0	0.01	0.00	0.01 ± 0.01	0.01	0.01	0.01 ± 0	M19	0.29	0.11	0.2 ± 0.12	0.07	0.34	0.21 ± 0.19	0.02	0.01	0.01 ± 0.01
P20	0.00	0.58	0.29 ± 0.4	0.18	0.38	0.28 ± 0.14	0.02	0.34	0.18 ± 0.23	M20	0.00	0.25	0.12 ± 0.18	0.03	0.00	0.02 ± 0.02	0.03	0.01	0.02 ± 0.01
P21	0.01	0.00	0 ± 0	0.01	0.01	0.01 ± 0.01	0.03	0.02	0.02 ± 0.01	M21	0.00	0.00	0 ± 0	0.02	0.00	0.01 ± 0.01	0.02	0.03	0.02 ± 0.01
P22	0.04	0.75	0.39 ± 0.5	0.03	0.19	0.11 ± 0.11	0.05	0.03	0.04 ± 0.02	M22	0.00	0.00	0 ± 0	0.02	0.01	0.02 ± 0.01	0.03	0.03	0.03 ± 0
P23	0.03	0.06	0.04 ± 0.02	0.01	0.02	0.02 ± 0.01	0.02	0.03	0.03 ± 0.01	M23	0.87	0.74	0.81 ± 0.09	0.22	0.18	0.2 ± 0.03	0.10	0.37	0.23 ± 0.19
P24	0.03	0.00	0.02 ± 0.02	0.01	0.01	0.01 ± 0	0.01	0.01	0.01 ± 0	M24	0.01	0.04	0.02 ± 0.03	0.07	0.11	0.09 ± 0.03	0.05	0.11	0.08 ± 0.04
P25	0.00	0.00	0 ± 0	0.01	0.00	0.01 ± 0.01	0.01	0.02	0.02 ± 0.01	M25	0.00	0.00	0 ± 0	0.01	0.00	0.01 ± 0.01	0.02	0.01	0.01 ± 0
P26	0.02	0.01	0.02 ± 0.01	0.01	0.00	0.01 ± 0.01	0.02	0.03	0.02 ± 0.01	M26	0.35	0.01	0.18 ± 0.24	0.07	0.07	0.07 ± 0	0.06	0.06	0.06 ± 0.01
P27	0.05	0.06	0.06 ± 0	0.02	0.02	0.02 ± 0	0.02	0.03	0.02 ± 0.01	M27	0.13	0.09	0.11 ± 0.03	0.03	0.01	0.02 ± 0.01	0.02	0.02	0.02 ± 0
P28	0.10	0.00	0.05 ± 0.07	0.01	0.00	0.01 ± 0.01	0.01	0.02	0.02 ± 0.01	M28	0.22	0.06	0.14 ± 0.11	0.02	0.01	0.01 ± 0	0.20	0.16	0.18 ± 0.03
P29	0.36	0.04	0.2 ± 0.23	1.09	1.26	1.18 ± 0.12	0.32	0.66	0.49 ± 0.24	M29	0.05	0.00	0.02 ± 0.03	0.02	0.02	0.02 ± 0	0.02	0.02	0.02 ± 0
P30	0.00	0.00	0 ± 0	0.03	0.00	0.02 ± 0.02	0.02	0.01	0.01 ± 0	M30	0.00	0.00	0 ± 0	0.01	0.00	0.01 ± 0.01	0.02	0.01	0.02 ± 0
P31	0.13	0.00	0.07 ± 0.09	0.02	0.00	0.01 ± 0.01	0.01	0.02	0.01 ± 0	M31	0.03	0.11	0.07 ± 0.06	0.01	0.00	0.01 ± 0.01	0.04	0.06	0.05 ± 0.02
P32	0.00	0.00	0 ± 0	0.01	0.00	0.01 ± 0.01	0.01	0.01	0.01 ± 0	M32	0.02	0.00	0.01 ± 0.01	0.02	0.01	0.02 ± 0	0.03	0.01	0.02 ± 0.01
P33	0.00	0.00	0 ± 0	0.02	0.04	0.03 ± 0.01	0.02	0.02	0.02 ± 0	M33	0.00	0.00	0 ± 0	0.02	0.00	0.01 ± 0.01	0.02	0.01	0.02 ± 0

Research Publications and Presentations from the Research work

1. **M. Sheeja and C. C. Harilal (2022**) Spatial distribution and seasonal variation of heavy metal contaminants and pollution indices in a coastal landmass of Kerala, Peninsular India, Chemistry and Ecology, Taylor & Francis DOI: 10.1080/02757540.2022.2036729

2. **M. Sheeja and C. C. Harilal (2021**) Ionic flux and geological release of fluoride in groundwater sources of a semi-arid tropical region in south India, International Journal of Environmental Analytical Chemistry, Taylor & Francis DOI: 10.1080/03067319.2021.1901281

Paper presentations in seminars

1. **Sheeja K. M. and C.C. Harilal (2020)** A paper entitled 'Variation in groundwater with respect to changing monsoonal patterns in Malappuram and Palakkad districts of Kerala' was presented in the UGC-sponsored national seminar on Role of community in water conservation: A milestone towards sustainable development conducted by the Centre for Futures Studies, The Gandhigram Rural Institute, Deemed University on February 6 and 7, 2020.

2. **Sheeja K. M. and C.C. Harilal (2019)** A paper entitled 'Surveillance of Fluoride Contamination in the Groundwater Sources of Palakkad District, Kerala' was presented in the International Conference on Recent Innovations in Bio-sustainability and Environmental Research-2019, conducted by the Department of Zoology, Annamalai University, February 20–22, 2019.

3. **Sheeja K. M. and C.C. Harilal (2018**) A paper entitled 'Seasonal changes in the groundwater table of Malappuram and Palakkad districts of Kerala with respect to Changing Monsoonal Patterns' was presented in a National seminar on 'Recent Trends in Climate Change and Carbon Research', organized by the Department of Botany, the University of Calicut, from February 26–28, 2018.